NASA Reference Publication 1078

THE LANDSAT TUTORIAL WORKBOOK

BASICS OF SATELLITE REMOTE SENSING

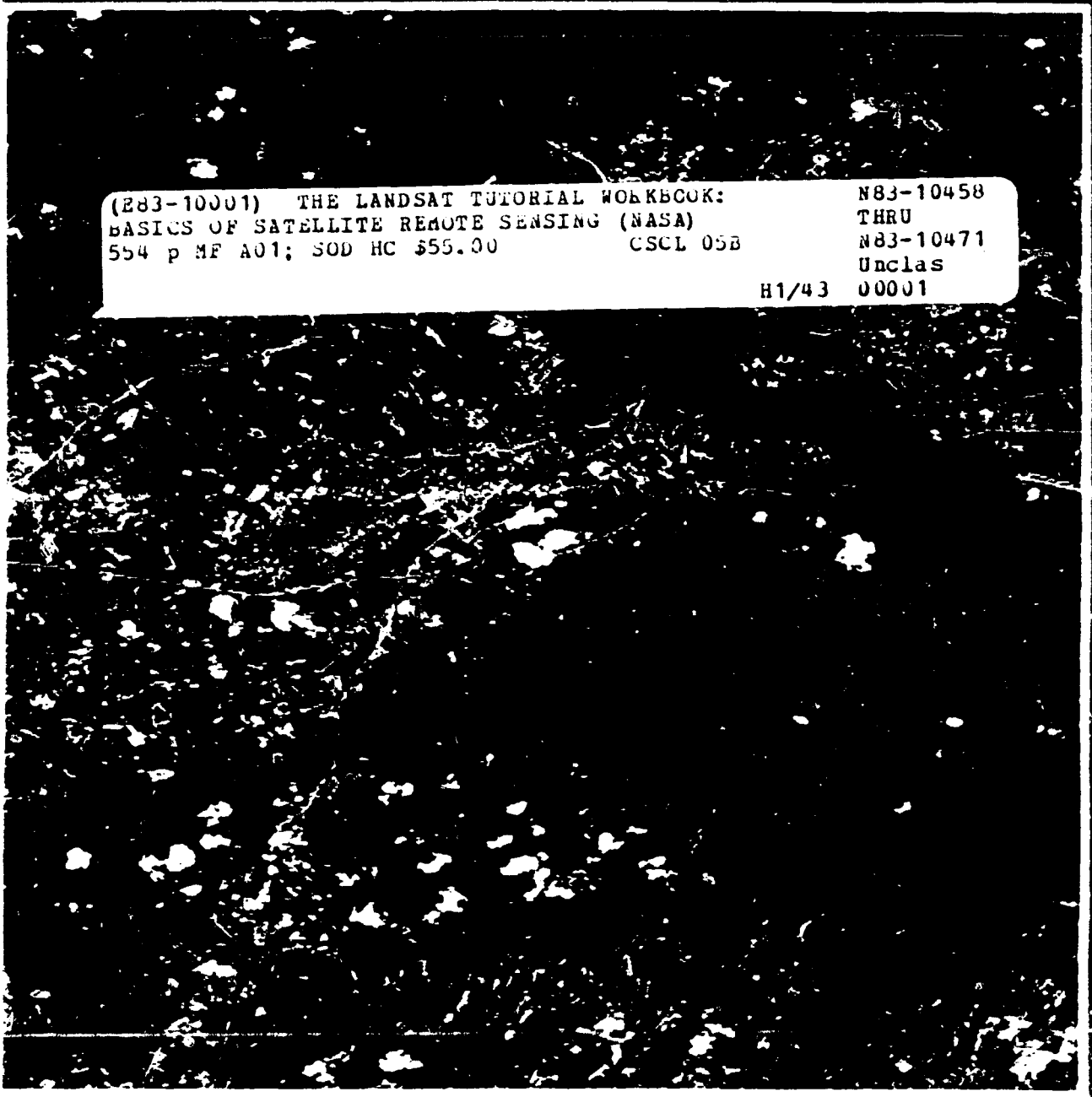

NASA Reference Publication 1078

THE LANDSAT TUTORIAL WORKBOOK

BASICS OF SATELLITE REMOTE SENSING

Nicholas M. Short
Goddard Space Flight Center

Prepared under the auspices of the Eastern Regional Remote Sensing Applications Center, with sections contributed by W. Campbell, S. Cox, H. Ramapriyan, J. Robinson, and J. Rose, ERRSAC, and N. H. MacLeod

NASA Scientific and Technical Information Branch 1982
National Aeronautics and Space Administration
Washington, DC

Front Cover: Harrisburg, Pennsylvania, and environs as imaged by Landsat 2 on July 14, 1977. Digital data from the Multispectral Scanner was used to computer-enhance this 512 × 512 pixel image. The scene covers approximately 24 km (15 miles) on a side. Compare this with Figure 5-30 in the Workbook and note that the cover version has not been aspect-corrected.

Library of Congress Catalog Card No. 81-600117

For sale by the Superintendent of Documents
U.S. Government Printing Office, Washington, D.C. 20402

FOREWORD

Early in the development of what is now the Eastern Regional Remote Sensing Applications Center (ERRSAC) came a brief flirtation with the name "Eastern Earth Resources Training Center." While the name fortunately passed into obscurity, it correctly emphasized the most essential element of NASA's efforts to extend the use of its satellite remote sensing technology—training. People who do not at present know how to use satellite remote sensing data in their environmental and resource management jobs must learn how to do so. However, experience has pointed out several impediments to this learning process.

The problems of selection, motivation, availability and travel costs of potential trainees restricts the number of people who can come to a central or regional facility for training. The same factors also restrict the length of time these personnel can spend at such a facility. Turnover of personnel, technological developments, new legislative requirements, and organizational decisions or mandates also produce a continuing need for new training.

This workbook will help people who cannot get away for training, or who can only get away for a limited period, to acquire a fundamental understanding of the technology on which they can build. It will serve as a primer for use by trainees before coming to a central training facility, to give those with a variety of backgrounds a common and substantial base, thus enabling them to use precious training time more effectively. This workbook will assist in the introduction of remote sensing concepts into college courses, which will help prepare young people to use this technology in the resource management jobs they will hold.

So there is a need, especially for those who must learn on their own, for a remote sensing primer. The "Landsat Tutorial Workbook" is a response to that need. Many scientists contributed their expertise, as writers or reviewers; they are acknowledged elsewhere. All the contributors, and especially Dr. Nicholas Short, the author, should be pleased with the result.

An ancient parable tells us that if you give a man a fish, you feed him for a day; if you teach a man to fish, you feed him for a lifetime.

Welcome to the "Compleat Angler" of satellite remote sensing.

Dr. Philip J. Cressy
Chief, ERRSAC
Goddard Space Flight Center
Greenbelt, Md.

PREFACE

Remote sensing from satellites came of age in the 1970's. As we move into the 1980's, many signs point to the reassuring conclusion that remote sensing from space is here to stay, not only as a useful adjunct to remote sensing from aircraft but as a valuable technique in its own right. Just two indicators will validate that statement. One is the record of the Landsats—the three Earth resources satellites successfully launched in the 1970's by the National Aeronautics and Space Administration (NASA).[1] Each of the first two performed superbly for more than five years; the third, launched in 1978, has functioned through mid-1981. Together, these satellites have radioed back images of more than 800,000 scenes (often cloud-covered) of the Earth; these images are of such quality that an abundance of new uses and applications has been spawned from the information they contain. Confidence in the future of Earth-observing satellites is demonstrated by the advent of a new generation of Landsats for the current decade, as well as plans by France, Japan, and possibly other countries to design and launch their own satellites for monitoring the Earth's surface. The other indicator is provided by Presidential Directive No. 54, signed by President Carter on November 20, 1979, which charges the National Oceanic and Atmospheric Administration (NOAA) with the task of formulating and implementing a federal program to establish and manage an *operational* remote sensing/Earth resources system. This action will provide timely data from satellites to a wide community of users in the United States and any other nations interested in sharing in the benefits of this new technology.

Thus, the spate of activity over the last few years has turned remote sensing from an esoteric specialty pursued by a small cadre of pioneers to a fully-fledged field practiced by many thousands throughout the world. The remote sensing community now consists not only of physicists, photogrammetrists, and instrument technologists, but also of an increasing number of discipline scientists, nontechnical managers, and even line workers, most of whom have limited schooling in the scientific/technical foundation on which remote sensing has developed. A remote sensing symposium today attracts a variety of professionals, such as foresters, land use planners, geographers, environmentalists, hydrologists, agronomists, architects, geologists, and meteorologists. In most cases their education did not include any formal training in remote sensing. That subject, as it has since evolved, was not taught in many universities or technical schools before the late 1960's and even now is available only at a few colleges. The situation will surely change as a burgeoning job market creates demand. However, meanwhile, how is the existing workforce to be given enough background and skills in applied remote sensing to "take up the baton and run" until joined by a new team?

[1] Most of the acronyms used in this workbook are identified at the end of Appendix D.

NASA recognized almost as soon as it defined its Earth resources and remote sensing programs in the late 1960's that most of the potential user community lacked detailed understanding of this new technology. In 1971, a NASA-initiated study group, on which the author of this workbook served, was convened to recommend needs and means for assisting the user community, through various types of training and educational programs, to develop sufficient expertise to eventually apply remote sensing in its ongoing functions and operations. Many of the ideas resulting from this study have been used in the design and implementation of a series of training courses for state and local government agency personnel and university faculty given at the Eastern Regional Remote Sensing Applications Center (ERRSAC) at NASA's Goddard Space Flight Center.

This workbook is a compendium of much that is presented in these courses, supplemented by even more material that would be taught but for lack of time. The impetus for writing the workbook is derived from two unrelated objectives. First, there is a pragmatic reason. We at ERRSAC believe that much of the information from the course can be given before a trainee comes to Goddard for formal instruction; this frees up considerable time for working there (with computers and other processing equipment) on the data from Landsat and other types of remote sensing products. The workbook is conceived to do precisely this task by covering most of the subject matter of a full training course in a self-teaching mode, even to simulating some of the "hands-on" computer analysis the trainee will do at Goddard. Secondly, and on a more personal note, the workbook reflects the author's background and interest in academia stemming from his experiences in teaching. From numerous conversations with faculty contacted in connection with the author's duties as University Programs coordinator for ERRSAC, he has noticed a persistent gap in the instructional resources available for remote sensing education both on and off campus. Although there are now a number of good texts on remote sensing, there is still no "how to do it" training manual that combines a review of basics, a survey of systems, and a treatment of the principles and mechanics of image analysis by computer, with a laboratory approach for learning to utilize the data through practical experiences with the applications. This workbook should accomplish this amalgamation. Furthermore, it is intended to let you, the user, achieve this on your own by guiding you to complete the exercises and questions at your pace and in your own surroundings at home or in the office. The workbook is completely self-contained except for a few standard items such as rulers and colored pencils. The workbook, then, is your classroom, with you in the dual role of teacher and student.

This book has been almost three years in preparation, having been started as a simple hand-out to accompany a forty-five minute verbal overview of Landsat during a one-day workshop for state legislators in 1978. Many individuals have since made contributions of various sorts to its development and testing. Specific acknowledgments of a debt of gratitude are directed to Dr. Philip Cressy, Chief of ERRSAC, and Dr. E.K. Ramapriyan of ERRSAC for their intensive reviews, and to W. Campbell and S. Cox of ERRSAC for their written contributions as well as reviews. Other members of ERRSAC provided useful suggestions along with reviews of sections of the workbook. Personnel from Computer Sciences Corporation (CSC), supporting ERRSAC, assisted in preparation of the review copies: particular thanks goes to Dr. F. Gunther for helpful comments on several sections, to J. Rose for writing a section on microprocessors, and to M. Tarlton for much of the artwork. Reviews of the first version were carried out by several university faculty during a Summer 1979 fellowship program at Goddard. Detailed reviews of the final manuscript were supplied by staff at NASA's Earth Resources Laboratory (Bay St. Louis, Miss.), at the Western Regional Applications Program Center (NASA Ames Research Center, Moffett Field, Calif.) and at the Department of the Interior's EROS Data Center (Sioux Falls, S. Dak.). A similar review was undertaken by Ms. Shirley Davis and staff at Purdue's Laboratory for Applied Remote Sensing (LARS). Special thanks are directed to Dr. Norman MacLeod for his invaluable technical review at the galley proof stage which led to some important corrections and additions.

Some users of this workbook may become so intrigued with their newly acquired knowledge and skills as to feel ambitious and challenged enough to want to do more practical exercises or to answer still different types of questions dealing with remote sensing. Such zealots should be aware of several other workbooks that have recently appeared in the marketplace. Two remote sensing laboratory manuals are now available. The Laboratory Manual for *Introduction to Remote Sensing of the Environment*, edited by Benjamin F. Richason, Jr., was published in 1978 by Kendall/Hunt (Dubuque, Iowa) to accompany his textbook of the same title (see reference in Appendix G). This manual stresses aerial photointerpretation but includes sections covering other aspects of remote sensing. In 1981, Floyd F. Sabins, Jr. distributed a Remote Sensing Laboratory Manual (obtained from Remote Sensing Enterprises, P.O. Box 2893, La Habra, Calif. 90631) as a companion to his book entitled *Remote Sensing: Principles and Interpretation* (Appendix G). Both that book and the manual highlight geological examples but include discussion and questions covering some other disciplines. The USDI/Geological Survey EROS Data Center (Sioux Falls, S. Dak. 57198) has developed a series of individual workshop exercises that can be purchased. Many of these treat geological topics but other application areas are included in several of the exercises. Finally, various basic concepts are presented through questions and simple exercises in the Study Guides that are part of the slide/audiotape sets in a Minicourse Series on the Fundamentals of Remote Sensing produced at the Laboratory for Applications of Remote Sensing (LARS), Purdue University (West Lafayette, Ind. 47907).

So in summary, the moment to start has arrived. Enjoy your endeavors. Avoid feelings of frustration when you do not know the answer, or more likely, do not understand a question because of the author's wording or other ambiguities. The end result in completing the questions in the workbook, be it primarily from your own efforts to respond or from having looked at the answers in Appendix H, will be strong awareness of what remote sensing is, what it is used for, and what you must resolve to do next to master the field.

In general, the activities are best undertaken the sequence (see Table of Contents) in which :y are presented. Each activity starts with a state- nt of learning objectives; these are the informa- n and skills you are expected to master before)gressing to the next section. After completing tivity 1, and before starting Activities 2 and 3, would be wise to consult one or more of the 'erences on remote sensing principles listed in pendix G. Before beginning the second activity, d through Appendix A, which reviews the ndsat system. You may want to refer to the ssary in Appendix E whenever unfamiliar terms presented in any activity. We strongly advise to read through Appendix B, a nonmathemat- l review of processing by computer, at least once ore attempting Activity 5 unless you are one of few with in-depth knowledge of image pro- sing by computer. Activities 6 and 7 are straight- ward but presuppose completion of the preced- activities. Activity 8, a case study of applications New Jersey, asks you to evaluate what you have rned by surveying an actual state-conducted gram leading to practical applications. Consid- tion of other remote sensing systems—past, sent, and future—is deferred until Activity 9, several references to individual systems, and ir products, occur in earlier activities. The ac- ity ends with a quick look at several future ASA programs and missions in remote sensing that now under consideration. The main text closes h a summary that includes a brief resume of the antages (including selected cost benefits) of ng Landsat-centered data to solve practical blems in Earth resources and environmental nagement.

The figures and tables are placed near the first evant activity task; however, some illustrations also referred to at several other places in the t. Most of the black-and-white (half-tone) prints arranged in logical groupings (for example, four ds of one scene; images to be compared) on gle or facing pages. Sometimes, several color ditions are combined on single pages. Within the t, each specific Landsat image is referred to by gure number, or in many instances by its unique ntification number (see page 32), or date of ge acquisition (overpass), interchangeably. The ginal annotation provided with Landsat images been preserved wherever appropriate.

Whenever possible, images and maps are reproduced at the same scales as the originals. Special materials such as transparent overlays, image transparencies, and maps, are contained in the pocket mounted inside the back cover. The overlays are matched as closely as practical to the corresponding imagery, but you should exercise some judgment in looking for small features located at the end of the keyed arrows.

You must furnish certain materials needed for the activities. These include:

1. Pencils (standard lead and multicolor set),
2. Clear mounting tape,
3. Rulers, dividers, other measuring tools,
4. Magnifying glass or hand lens,
5. Pocket stereoscope,
6. Light table (optional).

Most questions require an answer; some do not, having been posed simply to stimulate your thinking. In the original test version of the workbook, space was provided to answer the questions much in the manner of a laboratory manual in a physics or earth science course. For several practical reasons we have dispensed with that approach in this published volume except for a few questions where sketches or plots are called for. We suggest two options in your response to the questions. One alternative is to answer the questions *in your head.* Many learners would prefer this mental action as it allows one to proceed more rapidly by avoiding the time-consuming writing of a sentence or paragraph. The other alternative is to record your written answers on separate paper or in a notebook. Some people think better when a response must be organized and written down and some will wish to document their thinking in a permanent form. Regardless of which course you choose to follow, be encouraged to cross-check frequently with the answers section to assure yourself of being "on-track" and to partake of certain discussion or added thoughts developed in many answers that you might otherwise miss. Depending on your skills, experience, and attention span, you will probably finish the workbook reading and activities in about thirty-six to forty hours. This estimate is based on the time needed by volunteer testers to finish the next-to-final version of the workbook.

Guidelines for Effective Use of This Workbook

This workbook was initially conceived and developed as a teaching aid for the training programs conducted by the staff of the Eastern Regional Remote Sensing Applications Center (ERRSAC) at NASA's Goddard Space Flight Center. Two groups of trainees have used and tested the workbook in its formative stages: (1) personnel from state agencies such as departments of natural resources, environmental protection, and regional planning, and (2) university professors from departments of geography, geology, oceanography, forestry, biology, and engineering. Each group displayed a diversity of backgrounds and skills, which are probably representative of those possessed by most users of this workbook. In other words, we expect users to have some previous scientific or technical training. Many of them will come from federal and state agencies, private firms, and universities, where their relevant work emphasis is on obtaining information to monitor, inventory, explore for, and manage the Earth's surficial resources and environments. We have "pitched" the baseline level of the activities to the skills and experience of an upper division college student in one of the natural science or technology fields.

Two valuable attributes that should be possessed by most users are, *first*, a broad understanding of the identifying characteristics of the major natural and man-made features found in various land and marine environments, and *second*, familiarity with the appearance of these features as seen from above (i.e., from aircraft or in aerial photos). In many instances, a user will almost certainly not have a specific background in some of the disciplines (cartography, geography, geology, hydrology, agriculture, forestry, land use, ecology, environmental science, resources management) now routinely employing Landsat data. In such cases, the user may lack the direct experience to deduce or otherwise obtain the answers to certain questions or observations within the workbook activities.

If this applies to you, we still urge you to try as much of each activity as your skills permit by responding whenever you can to the numbered questions. However, feel free to omit any beyond your expertise or interest. In Appendix H, you will find the author's suggested answers to nearly all the questions. These answers are considered to be valid although not always uniquely correct. Many answers are accompanied by brief explanations or discussions of the author's intent or of the information conveyed. As you proceed through the activities, you are encouraged to look up an answer whenever you are uncertain of your response, lack the requisite knowledge to respond, or find the question unclear. But hold this "peeking" to a minimum. In this way, you will be following some of the procedures underlying the "programmed learning" technique of self-teaching, in which the learner moves on only after mastering each new unit of study by giving "correct" answers for each step.

This workbook is constructed primarily around just two scenes in the eastern United States. This allows you to concentrate on a typical region in which you might conduct some practical applications in an operational mode. If you are personally familiar with eastern Pennsylvania and New Jersey, or at least with similar areas in the eastern United States, you have a distinct advantage. If not, you may wish to read through some reference books on regional geography or physiography (for example, Hunt, C.B., *Natural Regions of the United States and Canada*, W.H. Freeman and Co., San Francisco, 1974; *National Atlas of the United States*, U.S. Geological Survey, 1970) to expand your background.

It would have been possible to organize the study units around a variety of Landsat scenes from across the country or worldwide. This would allow better choices of representative examples of certain topics covered in several activities, but would likewise have required an individual to have a broader range of location-dependent knowledge. The scenes used in the workbook were ultimately chosen to optimize the variety of terrain and cultural types present in several eastern states within the regions serviced by the ERRSAC program. However, to give wider scope, or universality, to the potential applicability of this book, twelve selected Landsat scenes from other parts of the world are included in Appendix C, along with some general questions pertinent to each scene. By working through that appendix after completion of the activities, you should gain a fuller set of skills in handling Landsat data from many regions.

SYNOPSIS

The tutorial workbook has been conceived as a "user-friendly" document. Its underlying philosophy is to present the reader with a straightforward opportunity to learn about remote sensing by *doing* something with data-derived information rather than just reading about it as one usually does in a textbook. Thus, we have called this a workbook simply because you, the reader—or, better, the student—must commit your mind and your time to actually do much of the *work* in the overall learning process by answering innumerable thought-provoking and instructive questions and by solving simple problems or completing exercises.

Moreover, since the workbook is not meant to be a textbook, many topics in remote sensing normally found in a text are instead treated cursorily, or in a nonconventional manner, or are not covered at all in the workbook. The emphasis in the workbook is therefore not on completeness or detail but on practicality and applicability. The book endeavors to concentrate on the concepts, techniques, and skills needed to get started and then get the job done, without being distracted by too much theory or too many excursions into academic or peripheral subjects. To a large extent, the workbook proceeds along much the same course followed during the one-week training program at the Eastern Regional Remote Sensing Applications Center (ERRSAC) at NASA's Goddard Space Flight Center, in which stress is placed on what must be learned and understood to become functional in remote sensing operations with a minimum of pedagogy and a maximum of hands-on activities.

This workbook is designed to assist you to learn, on your own, the answers to the following basic questions:

- What is remote sensing?
- What is Landsat and how does it operate?
- How is Landsat-based technology applied effectively to mapping, inventory, and management of the Earth's resources and man's activities?
- What makes the multispectral approach to data acquisition and analysis work?
- How does one "read" a Landsat image?
- How can you interpret and extract useful information from Landsat data by visual inspection?
- Why does digital (computer) processing improve results?
- What other remote sensing systems are providing useful data complimentary to Landsat?
- How is Landsat-derived information integrated with information of other kinds and sources?
- What are the cost benefits (economic payoff) in using Landsat and other remote sensing data?

You should proceed through the workbook at your own pace. All relevant image products are contained in this volume. You should be able to complete the activities, depending on your skills and experience, in thirty-six to forty hours.

INTRODUCTION

A new era in space applications that focus on the Earth itself was opened on July 26, 1972 with the launch of the first Earth Resources Technology Satellite (ERTS) (Figure I-1). It has since been renamed Landsat and has been joined by two other vehicles in orbit. This family of satellites has proved an invaluable component of a new approach to locating, monitoring, and managing many of the natural and man-made resources used by all peoples of the world. To appreciate the significance of this approach, you are encouraged to read, or at least browse through, the book that best summarizes the achievements of Landsat for the general public:

Mission to Earth: Landsat Views the World[1]
(Short, Lowman, Freden, and Finch)

In particular, you should examine the review of applications included in pp. 1-26ff of that book under the title "Survey of the Landsat Program" before you start this workbook. For those without access to *Mission to Earth*, the section (Appendix A) on the Landsat system in that book (describing spacecraft characteristics, orbital parameters, payload and the data processing and products) is reproduced in Appendix A of this workbook. A summary of the Landsat system is also provided in Table I-1.

After perusing *Mission to Earth*, you are likely to agree with the worldwide community of Earth resources specialists that the Landsats are among the most sophisticated and productive satellites ever orbited by NASA. Numerous applications of data acquired by these satellites have been developed and verified, as summarized in Table I-2.

[1]NASA SP-360; for sale by the Government Printing Office @ $14.00.

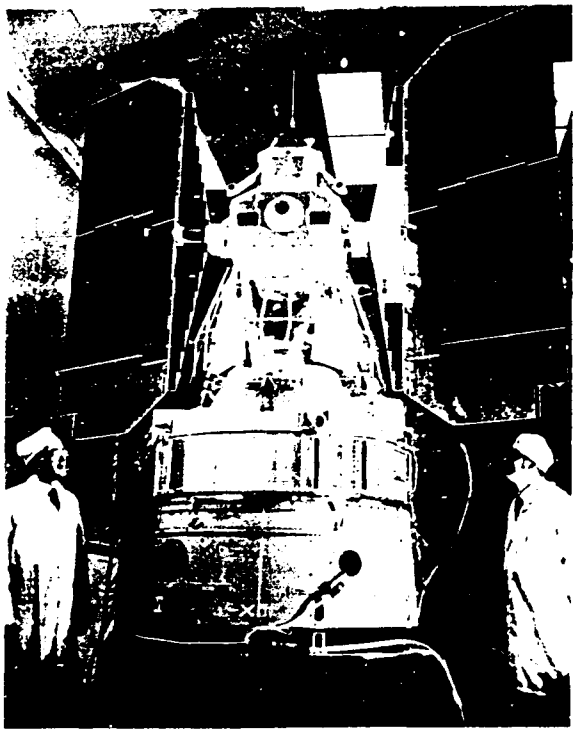

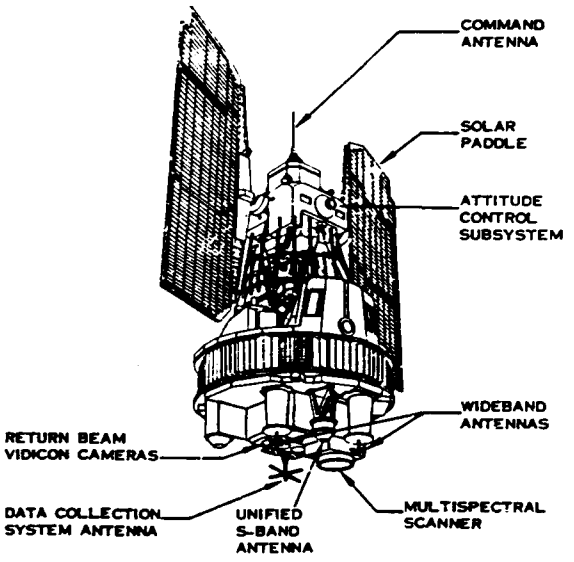

Figure I-1. Left: Landsat-1 spacecraft undergoing fabrication at General Electric's Space Sciences Facility at Valley Forge, Pa. Right: Schematic showing control and sensor systems on Landsat-1.

Table 1-1
The Landsat System†

- Coverage of nearly the entire land surface and selected ocean areas of the Earth
- Spacecraft altitude: 917 km (570 nautical miles)
- 14 revolutions/day; repetitive 18-day cycle; multiseasonal
- Sun-synchronous near polar orbit; fixed time (*ca.* 9:30 a.m. local Sun time at Equator) of pass over imaged scene
- 185 km X 185 km (115 statute mile X 115 statute mile) ground scene in each image; orthographic; standard image scale in 9-in format: 1:1,000,000
- Stereo sidelap viewing: 85% near polar to 14% equatorial
- Effective ground resolution of image: 79 m (260 ft); 0.45 hectare or 1.1 acre
- Sensor Systems:

  * Multispectral Scanner (MSS)
    Band 4: 0.5-0.6 μm (green)
    5: 0.6-0.7 μm (red)
    6: 0.7-0.8 μm (near IR)
    7: 0.8-1.1 μm (near IR)
    8: 10.4-12.6 μm (thermal IR) (Landsat-3 only)

  * Return Beam Vidicon (RBV)
    Band 1: 0.48-0.57 μm (green)
    2: 0.58-0.68 μm (red)
    3: 0.69-0.83 μm (IR)

    (RBV on Landsat 3: 0.50-0.75 μm)

- Onboard digitization of data; recording on tape of data collected when the satellite is beyond the line-of-sight of any Landsat Ground Receiving Station
- Principal data products:

  * Black-and-white and color prints and transparencies
  * Computer-compatible tapes (CCT's); 7 and 9 track; 800 and 1600 bits per inch (bpi)
  * Computer-processed data bases:
    -- Statistical evaluation of radiometric parameters
    — Density-sliced images or printouts
    — Contrast-stretched images
    — Edge-enhanced (band pass filtered) images
    — Band ratio images or printouts
    — Classification (thematic) printouts or images ("maps")

† Landsat-1 launched on July 23, 1972 and ceased operation on January 6, 1978; Landsat-2 launched on January 22, 1975, stopped on January 22, 1980 but resumed operation on May 27, 1980; Landsat-3 launched on March 5, 1978, MSS turned off on December 17, 1980, reactivated April 13, 1981.

Table I-2
Summary of Applications of Landsat Data in the Various Earth Resources Disciplines

Agriculture, Forestry and Range Resources	Land Use and Mapping	Geology	Water Resources	Oceanography and Marine Resources	Environment
Discrimination of vegetative types: Crop types Timber types Range vegetation	Classification land uses	Recognition of rock types	Determination of water boundaries and surface water area and volume	Detection of living marine organisms	Monitoring surface mining and reclamation
Measurement of crop acreage by species	Cartographic mapping and map updating	Mapping of major geologic units	Mapping of floods and flood plains	Determination of turbidity patterns and circulation	Mapping and monitoring of water pollution
Measurement of timber acreage and volume by species	Categorization of land capability	Revising geologic maps	Determination of areal extent of snow and snow boundaries	Mapping shoreline changes	Detection of air pollution and its effects
Determination of range readiness and biomass	Separation of urban and and rural categories	Delineation of unconsolidated rock and soils	Measurement of glacial features	Mapping of shoals and shallow areas	Determination of effects of natural disasters
Determination of vegetation vigor	Regional planning	Mapping igneous intrusions	Measurement of sediment and turbidity patterns	Mapping of ice for shipping	Monitoring environmental effects of man's activities (lake eutrophication, defoliation, etc.)
Determination of vegetation stress	Mapping of transportation networks	Mapping recent volcanic surface deposits	Determination of water depth	Study of eddies and waves	
Determination of soil conditions	Mapping of land-water boundaries	Mapping landforms	Delineation of irrigated fields		
Determination of soil associations	Mapping of (fractures)	Search for surface guides to mineralization	Inventory of lakes		
Assessment of grass and forest fire damage		Determination of regional structures			
		Mapping linears			

The main purpose of this tutorial workbook is to convince you of this last statement by giving you some direct "hands-on" experience with Landsat imagery and computer products. To accomplish this, you must proceed through the tutorial activities 1–9, preferably in that order.

Our minimal goal in leading you through these activities is to provide you with an appreciation of the Landsat system and an ability to apply Landsat images to your work and everyday life. For example, you can expect to see your home state from the new vantage point of space. However, you need not be in orbit to see the Earth in this way. Try using a Landsat image as a map during your next air trip. You will be surprised and delighted to learn how easy it is to locate and orient yourself as you look out and to predict what will shortly appear along the flight line. However, ask yourself about the information you lose by relying on the image alone. How well can you identify and classify the ground features—especially crops and land cover—that you spot in the image even as your plane passes over? How can you keep track of the thousands of individual features encountered during the flight? How do you retrieve data on the characteristics of objects in the scene—in particular those that change with time over the seasons? As you seek answers to these and similar questions, you will begin to appreciate the advantages of computer processing in handling the huge quantities of information supplied by the Landsats. This is the broader goal addressed in this tutorial workbook.

On completing these activities, you can expect to have gained considerable understanding and skills that will enable you to interpret Landsat data, develop your own applications, and solve practical problems with remote sensing techniques. However, you will not become a certified expert; that is, you will not be ready to set up a remote sensing facility or establish a utilization program within your organization. That will require much more experience on your part through extensive reading, formal training, attendance at workshops and symposia, and more effort with actual production work on relevant projects of your own choosing.

Now, before you begin these activities, review the advice and instructions in the next section, which provides a set of guidelines for effective use of this workbook through the self-teaching or tutorial approach.

CONTENTS

N83
10459

UNCLAS

ACTIVITY I

SOME FUNDAMENTAL CONCEPTS IN REMOTE SENSING

LEARNING OBJECTIVES:

- *Develop a working definition of the term remote sensing and understand the significance of the key ideas in this definition.*
- *Become familiar with the electromagnetic spectrum, especially those wavelength regions available to remote sensing.*
- *Examine energy and wave propagation laws for relevance to remote sensing.*
- *Investigate the characteristics of emitted and reflected radiation and its detection by remote sensors.*
- *Understand the meaning of classes and their identification by spectral signatures.*
- *Appreciate the multispectral approach—a keystone of remote sensing.*
- *Survey the principal types of sensors and platforms used in remote sensing.*

INTRODUCTION

The professional in the field of remote sensing needs a broad background to be an effective practitioner. Such an individual will probably have a minimum of one (college) degree in science, engineering, or technology and will have developed an acquaintance with, and some mastery of, physics (with emphasis on optics and radiation), mathematics (particularly statistical methods), aspects of electronics, digital data processing, and possibly aerial photogrammetry. He or she, as well, will probably be a natural resources specialist (a geographer, forester, agronomist, hydrologist, geologist, or environmental analyst), or will, as a resources manager or decision maker, have developed a strong working knowledge of these fields.

You just might fit closely into the above model of a professional in remote sensing, in which case you are probably not using this tutorial workbook as a learning tool. However, it is more likely that you are a resources program manager or technician, a decision maker in a legislative or executive position, a college professor or student, or a member of the general public. Your present objective is to obtain rather quickly some understanding of and practical skills in satellite remote sensing without recourse to an intensive study of textbooks, a plethora of journal papers, or a semester-full of lectures. This workbook should help you to accomplish that end.

However, you will also realize—after you have tried some of the exercises or at least scanned this book—that the theoretical foundation of remote sensing is a complex subject that requires some technical awareness to apply it effectively as a problem-solving approach. One aspect of the technology not covered in depth in this workbook is a comprehensive review of the basic principles of remote sensing, both in theory and in practice. If you wish to become proficient in the field and want to delve further into the literature, an appreciation of these principles should be your goal.

To aid you in planning for further self-study, we have devised a checklist of the main concepts that together provide a foundation in the principles of remote sensing. These are presented in Table 1-1 as key phrase topics, arranged logically in a sequence that might be followed in a formal course.

If, after perusing this list, you decide that you already have a firm understanding of these principles, or if you wish to avoid becoming enmeshed in what might appear to be "heavy" theoretical considerations, then *skip* this activity and proceed to Activity 2. However, you are more likely to want to refresh or enlarge your background in some of these fundamental ideas, or may need to build almost from scratch, and are therefore urged to *read on*. Be reassured that the treatment of basic principles of remote sensing in Activity 1, which touch upon some but not all topics listed in Table 1-1, is presented largely from a nonmathematical approach (except for some key formulas). Another inducement for reading (and thinking) through this chapter is simply that some important terms used frequently in the workbook will be defined or otherwise evaluated here.

REMOTE SENSING DEFINED

If your time is not at a premium, you might best master the concepts of Activity 1 by careful reading of the relevant chapters in the prime references (Appendix G). However, since this is likely to be inconvenient, we shall instead try to give you a quick grasp of the bare essentials of remote sensing principles[1] by having you review some important concepts and terms embodied in (or derived from) the following working definition of *remote sensing* itself.

Remote sensing is the acquisition of data and derivative information about objects or materials (targets) located at the Earth's surface or in its atmosphere by using sensors mounted on platforms located at a distance from the targets to make

[1]Much of the material covered on pp. 14 through 38 was extracted from Chapters 3 and 4 of the *Manual of Remote Sensing* (see Appendix G).

Table 1-1
Basic Principles of Remote Sensing: Key Phrases

Nature and definition of remote sensing
Definition and review of the electromagnetic spectrum
Nature of light and color
Principles (laws) and practices of optics
Energy/brightness/intensity relations
Radiance/radiometry/irradiance/excitance
Emittance/reflectance/absorptance/transmittance/scattering/albedo
Look angle/aspect/bidirectional reflectance
Units of measurement
Solar illumination
Photographic images/filters/films
Aerial photography, photogrammetry, and photointerpretation
Stereoscopy
Resolution/resolving power/spatial and spectral resolution
Production and manipulation of photo-images; role of photo-contrast
Spectral signatures (response curves)/sources of variation
Spectral properties of materials
Role of atmosphere/attenuation/windows/corrections
Multispectral sensing/multibands
Thermal concepts: blackbody radiation; radiation laws - Wien's Displacement; Stefan-Boltzmann; Planck; Kirchhoff Laws
Nature, function, and design of sensors/detectors; scanners/radiometers/spectrometers
Sensitivity/detectability/signal-to-noise ratio
Active/passive systems; imaging/nonimaging systems
UV/visible-near IR/thermal IR/microwave/radar systems
Limitations of remote sensing

measurements (usually multispectral) of interactions between the targets and electromagnetic radiation.[2]

#1-1: Make note of (or underline) the key words in the definition of remote sensing

[2] Some definitions include certain force fields (e.g., magnetic) or even mechanical waves (e.g., sonic) as part of remote sensing. These more properly belong to geophysics. Others consider remote sensing to be a geophysical technique itself.

MATERIALS AND OBJECTS—SOME PHILOSOPHICAL MUSINGS

Before we begin to dissect and analyze this definition of remote sensing, we need to ponder and expand upon some fundamental meanings and concepts dealing with such ideas as "matter," "class," "feature," "identification," and "measurement." The acquired data consist primarily of measured variations in intensity of radiation reflected or emitted from the sensed surface. These data, to be useful, must be translated into meaningful information about surface materials and objects, and must also be spatially and geographically specific.

#1-2: Suggest several types of information about natural or man-made objects that can be derived from the data (for example, shape).

Most remote sensing devices provide data on surface features or classes in their correct spatial relations. But, as we shall see later, the parameters really being measured by remote sensors are spectral characteristics resulting from the interaction between radiation and matter. Moreover, the materials consist of individual atoms or molecules making up substances or aggregates of substances. Much like a fundamental concept in Aristotelian philosophy, a *substance* is initially an abstraction without shape and location until it becomes partitioned into distinct objects with discrete boundaries and distribution by taking on *form*. Substance or matter thus becomes individualized: wood becomes door or plank or statue or table, or more precisely *this* table (door, etc.) found *here*. Shape and location and finiteness give a material some degree of particularity.

We note therefore that material objects can consist of discrete items (such as a tree, a house, a lake) or their component parts (leaves, windows, waves), or a mixture of entities (a forest with different tree species and a littered soil-covered floor; a group of buildings in a housing development with roads and lawns; a body of water containing suspended silt, with a shoreline, scattered islands). A set of related objects is collectively grouped into a discrete unit called a *class*. A class, in this sense, is an arbitrarily defined aggregate of one or more object types having common attributes, to which some cognitive name or description is assigned.

The Nature of "Class"

Like matter, a class may be referred to as either *general* or *specific*. When considered as a concept without regard to location, shape, and size, a class is a general notion. Thus, we can image the class *ocean* and visualize an expanse of sea lacking a tangible boundary and particular locality. However, as soon as we recall a real section of some sea, such as the one along the East Coast of the United States, we begin to specify a *part* of the ocean with a geographical location (the Western Atlantic). We place the ocean in a particular context relative to its surroundings (other classes such as wetlands and lagoons), and to discrete boundaries (the adjacent classes, such as a beach). Every part of the Earth's surface may be classified (mapped) in this way. Individual sections of the surface, whether continuous or (more usually) separated, become specific manifestations of the general class. Each section, then, is individualized by its own bounded areas, but all sections together are members identified by the same class name (and a symbol or pattern on a map). The name assigned is affected by the scale at which the class is established. At different scales, different components tend to dominate our awareness of certain class characteristics. At one scale, we can readily comprehend the entity "Shopping Center." At another scale, that entity is resolved into stores, walkways, parking lots, storage and loading areas, etc. At a very fine scale, the entities appear as assemblages of atoms in crystal structures, but such detail obscures the nature of "Shopping Center."

We see then that classes may usually be subdivided into hierarchical levels according to the relative significance of their components. Thus, "hills" or "plains" can themselves be considered as *terrain* classes, or might better be treated as subclasses of the general class *topography*. Likewise, the term *cropland* connotes a field, with some distinct shape, comprising soil with contained moisture, and one or more distinct vegetation types grown as foodstuff, along with other essential or extraneous entities (access roads, barns, houses, etc.). The general class "cropland" normally consists of several components familiar to us but may in some instances be limited to a single, or dominant, component, such as a dry, barren field or a continuous wheat cover. Each characteristic specifies certain conditions applicable to the class; these are described by adjectives such as "tilled" field. In a hierarchical classification, a tilled field is one of a subclass of fields (others might include nontilled or irrigated), and level or rolling tilled fields represent even further subdivision.

#1-3: Consider the class urban. Subdivide it into a set of its essential components and arrange these in some hierarchy from general to specific (an analog would be the orderly taxonomy of plants and animals, from phylum through family to species).

Even though any class may be a collection of different objects composed of different materials, the assemblage comprises some coherent and interrelated notion that one may recognize as unique to that class, to which is assigned some descriptive and identifying name. Thus, such mutually exclusive classes (types) as *city*, *cornfield*, and *cemetery* are each made up of somewhat diverse elemental components (differing in composition, size, shape, proportions, and distribution) but are nevertheless each specified by defining characteristics (features) and allowable variants. One such characteristic is represented by the spectral properties of these components or objects; when emphasis is placed on these parameters, the class can properly be referred to as a spectral class.

Other Terms for Surface Units

Terms related to or synonymous with class are frequently encountered in remote sensing. They may have similar meanings, but there may be important shades of difference. Some are defined precisely, others more loosely or vaguely. We shall briefly touch upon the most common of these terms since they appear many times in this workbook and in the open literature on remote sensing. Consult the glossary in Appendix D for working definitions of some of the following terms.

The term *category* is often used synonymously with class. Both terms refer in the material sense to assemblages of interrelated objects. Ideas may also be categorized by organizing related concepts dealing with aspects of knowledge. *Type*, according to Webster's Dictionary, is defined as "qualities common to a number of individuals that distinguish them as an identifiable class" and furthermore may connote a taxonomic category; it is most commonly used to imply "strong and clearly marked similarity throughout the items.... typical of the group"; "kind," "sort," "nature," "character," and "description" are acceptable synonyms but with subtle differences. *Ground* or *land cover type* is a geographer's term which denotes a class describing the "vegetational (natural) and artificial constructions covering the land surface" (Burley, 1961)[3] in contrast to *land use type*, which refers to "man's activities on land which are directly related to the land" (Clawson and Stewart, 1965).[4] *Group* is occasionally used in the sense of class, but a group can be just an assemblage of objects that need not be interrelated. Dictionaries describe a *theme* as a subject or topic, which fits its use in remote sensing. The word *theme* has come to mean an aggregate of classes which properly belong to the same hierarchical rank, such as a vegetation map—combining all vegetation classes—as for example, crops, forests, grasslands. The Thematic Mapper sensor being devel-

[3]Burley, T. M., *Land Use or Land Utilization?*, Prof. Geographer, Vol 3, No. 13, pp. 18-20, 1961.

[4]Clawson, M., and C. L. Stewart, *Land Use Information: A Critical Survey of U.S. Statistics, Including Possibilities for Greater Uniformity*, Johns Hopkins Press, 402, 6, 1965.

oped for Landsat-D is supposed to invoke the idea of identifying classes and determining their distribution.

The term *pattern* alludes to the spatial and/or temporal arrangement or configuration of "things" as well as to the idea of a model used to replicate the arrangement. In remote sensing, pattern describes the notion of spatial or geometrical characteristics that can be measured. Texture, an attribute of spatial patterns, relates to the frequency of tonal change as determined by variations in size, shape, orientation, and radiation properties of different classes. *Pattern Recognition* refers to a process (usually automated, as on a computer but often performed better by trained analysts) by which measurement patterns may be used to classify a scene into some number of recognizable classes.

Another widely applied term, *feature*, may have three distinct meanings. First, in common linguistic usage, feature is defined as "overall appearance," "mark," "structure," or "part," but this conveys little meaning of the term as applied to remote sensing. Secondly, in the context of remote sensing, feature relates to one of a set of *measurable* properties (for example, reflectance, temperature or hardness) that are diagnostic of a class or material. In this sense, reflectance, composition, and hardness are examples of a substance endowed with form that can be used to identify an object, localize its distribution, and assign it to a class. The mathematical process of converting measurements of one or more features into information about the class is called *feature extraction*. A third meaning is one now in technical usage but with a special sense. Although commonplace in texts, articles, and reports dealing with remote sensing, the term "surface feature" as such is seldom defined. In this usage, *surface feature* is a composite term that may refer to a geometrical or geomorphic entity such as a hill, a stream, a rock outcrop, a lawn, or almost anything found on a natural or man-made surface. Such usage connotes a sense of "parts." The term may describe a statistical class in one instance and a particular object or specific landform in another. To the degree that these objects or landforms are measurable attributes of a general surface, for example, a given terrain characterized by low hills, deep valleys, and dissected plateaus, the landforms themselves become the features that may best classify the surface.

All of these terms have something else in common besides their synonymity with class: they all describe the general nature of the information shown on *maps*. A map consists of classes (categories, types, features) defined in the legend that depict at some useful scale what is found on a surface (the Earth or other planet's exterior [solid/liquid] boundary, or even an underground reference plane as in a tunnel). Maps themselves consist of patterns coincident with arbitrarily defined classes. Elements of location, shape, and other attributes of classes in the specific sense, are implicit in the concept of "map." When remote sensing data are "mapped," a classification of surface features, stated in familiar categorical terms, is the desired end product.

ELECTROMAGNETIC RADIATION

Returning to our task of analyzing the definition of remote sensing, we can now appreciate that remote sensing is broadly concerned with all matter (arranged in classes) present on the entire surface of a planetary body (stellar bodies are excluded, even though similar methods may be applied to most astronomical objects) and in its gaseous envelope or atmosphere if extant. For convenience, the term remote sensing as considered in this workbook will be associated primarily with the Earth's land and sea surface and any outer layers (e.g., clear water) from which radiation can be sensed. In this context, the atmosphere is excluded from consideration and is treated as noise or interference; however, meteorologists consider the air and its associated constituents as their "object of interest" and thus apply various remote sensing instruments and techniques to measure radiation effects on the gaseous and particulate materials.

1-4: Suggest four parameters of the atmosphere amenable to remote sensing observations.

Remote sensing involves measuring (sampling) radiation within the electromagnetic (EM) spectrum; the spectrum is a designation or chart of the distribution of radiant energy as a function of wavelength (or frequency). A diagram illustrating the EM spectrum scale in units of either wavelength (A) or frequency (B) is shown at the top of Figure 1-1. The spectrum has been divided into a number of intervals or regions, each defined to include all radiation assigned some characteristic name.

Electromagnetic radiation (EMR) is dynamic radiant energy made evident by its interaction with matter and is the consequence of changes in force fields. Thus, this question of what EMR is cannot be separated from the question of what matter itself is. Specifically, EMR may be thought of as energy consisting of linked electric and magnetic fields and transmitted in packets, or *quanta*, in some form of wave motion. The term *photon*, proposed by Einstein in 1905 for light quanta,[5] is now widely used for other short wavelength EMR in general. Quanta, or photons, may be considered crudely as particles of pure energy having zero mass at rest. The demonstration by Planck in 1901, and more specifically by Einstein in 1905, that electromagnetic waves consist of individual packets of energy was in essence a revival of Newton's then discarded corpuscular theory of light. But is radiation in fact merely a stream of particles, as Newton suggested, or is it wave motion? The answer is that light, and all other forms of EMR, behaves both as waves and particles. This is the famous "wave-particle duality" enunciated by de Broglie, Heisenberg, Born, Schroedinger, and others in the 1920's. Atomic particles, such as electrons, can display wave behavior, such as diffraction, under certain conditions, and can be treated mathematically as waves. Another aspect of the fundamental interrelation between waves and particles, discovered by Einstein in 1905-1907, is that energy is convertible to mass and that, conversely, mass is equivalent to energy as expressed by the famous equation $E = mc^2$, in which m is the mass in grams, c is the speed of EMR radiation in a vacuum, in centimeters per second (3×10^{10} cm/s), and E, the energy in ergs.

[5]Visible light refers to EM radiation within a narrow wavelength interval that causes a sensed reaction or response in the human eye within its functional range of *ca.* 0.33 to 0.75 μm.

Once again, EMR represents energy transfer by means of wave motion. The waves oscillate in harmonic patterns, of which one common form is the sinusoidal (∿) wave. Waves of this type are also known as transverse waves because particles within a physical medium are set into vibrational motion *normal* (at right angles) to the direction of propagation. However, EMR can also move through empty space (a vacuum) lacking particulates in the carrier medium so that the photons are the only physical entities. Each photon is surrounded by an electric field and magnetic field represented by vectors E and H oriented at right angles to each other as well as to the direction of propagation. The behavior of the E and H fields with respect to time is expressed by Maxwell's equations that include the terms μ_0 (permeability of the electric field in a vacuum; μ applies to nonconductive media) and ϵ_0 (permittivity of the magnetic field). The fields oscillate systematically as described by covarying sine waves having the same wavelength λ (distance between two crests on a waveform) and frequency υ (number of oscillations per unit time). The vibrational directions of the electric and magnetic force fields may be in any orientation within 360° and may shift to other orientations during wave propagation. When the electric field direction is made to line up and remain in one direction, the radiation is said to be plane polarized.[6] The wave amplitudes of the two fields are also coincident in time and are a measure of radiation intensity (brightness).

Units for λ are specified in the metric system and are dependent on the particular region of the EM spectrum being considered. Familiar wavelength units include the nanometer, micrometer (micron now obsolete), and the Angstrom.

#1-5: Given that 1 nanometer (nm) = 10^{-9} m; 1 micrometer (μm) = 10^{-6} m; and 1 Angstrom (Å) = 10^{-10} m, how many nanometers in a micrometer? How many Angstrom units in a micrometer? Note that frequencies are expressed in cycles per second; 1 cycle/s is termed a hertz; kilohertz,

[6]Remote sensing devices generally do not distinguish between unpolarized and polarized radiation, although depolarizing filters may be a part of some instruments. The exception is radar, in which polarization plays an important role. Although radiation can be polarized during reflection, that modification does not influence the measurements normally made for practical applications.

megahertz, and gigahertz are respectively 10^3, 10^6, and 10^9 cycles/s.

A fixed quantum of energy E (in units of ergs, joules, or electron volts) is characteristic of any photon transmitted at some discrete frequency, according to Planck's quantum hypothesis, stated as: $E = \nu h = hc/\lambda$, where h is the Planck constant ($h = 6.62 \times 10^{-34}$ joule sec), ν is frequency, and c is radiation (light) speed. (The equation relating radiation speed,[7] wavelength, and frequency is $c = \lambda\nu$; note that ν varies inversely with λ.) From the Planck equation it is evident that waves representing different (photon) energies will oscillate at different frequencies. It follows, too, that the shorter the wavelength, the greater the energy of the photons.

How is EMR produced? Essentially, EMR may be generated when an electric charge is accelerated or, more generally, whenever the size and/or direction of the electric (E) or magnetic (H) field is varied with time at its source. A radio wave, for example, is produced by a rapidly oscillating electric current in a conductor (the antenna). At the high frequency (highest energy) end of the EM spectrum, gamma rays result from decay within the atomic nucleus. X-rays emanate from atoms in which electrons experience transitions from an outer orbit to one further in. Radiation of successively lower energy involves other atomic motions, as follows: UV, Visible—outer shell electron shifts; Infrared—inter- or intra-molecular vibrations and rotations; Microwave—molecular rotations and field fluctuations; Radio, and AC current—fluctuations in the electric and magnetic fields of the waveform.

Interactions Between Matter and Radiation

Just as there is a dualistic nature to EMR, as expressed by the "wave-particle" aspects of radiation, so also can the mechanisms of interactions between matter and radiant energy be described from two seemingly different, but actually interrelated, approaches. One follows the framework provided by optical physics; this perspective depends on the *macroscopic* view of the ways in which radiation impinges upon and is affected by matter. This view of matter-energy interactions, governed by the laws of optics familiar to most readers from introductory physics courses, will dominate the concepts examined in the remaining sections of this activity and elsewhere in the workbook.

But, a more fundamental, exact, and intrinsic approach treats the interactions as a *microscopic*, or more properly, atomic or molecular phenomenon. Some of the principles underlying this approach were already considered in the preceding section. However, only a broad sketch of the quantum mechanical nature of photons, the structure of radiant waves, and the generation of EMR was constructed and a further in-depth consideration is beyond the scope of this workbook. On the other hand, an insight into the essentials of the microscopic, or atomic-molecular, approach should prove invaluable to anyone wishing to delve deeply into the real nature of matter-energy interactions. A detailed analytical examination of this second, sometimes complex approach, requires a firm and somewhat specialized background within physics not possessed by many readers. The inquisitive reader is urged to consult an appropriate text on the subject. A superlative review of pertinent concepts underlying the interactions is given by G.R. Hunt in Chapter 2 of the recently published *Remote Sensing in Geology* (Siegal and Gillespie, editors) (see reference in Appendix G). From that source a simplified synopsis is presented in the next nine paragraphs, primarily to provide a brief look at the types of concepts and terms needed to master this avenue to understanding the phenomenology of radiation from the atomic view.

The basis for predicting how atoms will respond to EMR is found in the Schroedinger wave equation which derives a specific wave function ψ for an atom or atomic system of mass m. This equation (not stated here because of its complexity) is the quantum mechanical analog to the Newtonian force equation ($F = ma$) in classical mechanics. A key term in the Schroedinger equation is E,

[7] Velocity in a vacuum is just the speed of light; that velocity is slowed in a material medium by an amount indicated by the index of refraction of the material.

a characteristic energy value (also known as eigenvalue). For any atomic species, there are a number of possible energy states (eigenstates) or levels within that system; for different species, the characteristic states are different and possess unique values diagnostic of the particular element. There are, therefore, certain allowable levels for each atomic species; their discrete eigenvalues satisfy the Schroedinger equation to permit acceptable solutions for determination of the wave function.

Under the influence of external EM radiation, the atom may undergo a transition from one stationary state or energy level to another. This occurs whenever the oscillating EMR field (normally, but not necessarily, the electric field) disturbs the potential energy of the system by just the right amount to produce an allowable transition to a new eigenstate. The change in eigenvalue is given by $E_2 - E_1 = h\nu$, the expression for Planck's law. This transition to the new energy state brought about by interaction with EMR is thus evidenced by a consequent output of radiation that oscillates sinusoidally at a frequency ν determined by the exact change in energy (ΔE) associated with the permissible transition.

The above description is simplified to apply to atoms of a single species (element) in some characteristic atomic structure. The situation becomes much more complex when polyatomic structures are considered and only approximate solutions to the Schroedinger equation are obtained. Other factors also enter in: the nature of the bonding, the coordination of the atoms in molecules or ionic compounds, the distribution of valency electrons in certain orbitals or conduction bands, to mention a few. Without further pursuing these important considerations, we shall concentrate on still another aspect. The transition can be related to three types of energy—electronic, vibrational, and rotational—the sum of which equals the total energy of the system.

Electronic energy transitions involve shifts of electrons from one quantum level to another (to different quantized orbits) according to precise rules. Any allowable transfer is determined from four quantities called the quantum numbers for that atomic system. These are (1) the principal quantum number n, (2) the angular momentum quantum number L, (3) the magnetic quantum number m, and (4) (for polyelectronic atoms), the spin quantum number m_s. Electronic transitions occur within atoms in all familiar states of matter (solid, liquid, gas). The wavelengths (reciprocals of frequency) at which these transitions proceed will depend on the particular behavior of the constituent elements in a material experiencing excitement by EMR. For example, elements such as iron (also Ni, Co, Cr, V and others) can undergo many transitions, each controlled by valence state (degree of oxidation), location in the crystal structure, symmetry of atomic groups containing the iron, and so forth. For compounds dominated by ionic bonding, the calculations of permissible transitions are influenced by crystal field theory. Organic compounds, which usually are held by covalent bonds, must be studied with a different approach. Electronic transitions are especially ubiquitous in the ultraviolet and visible light and near infrared parts of the spectrum which correspond to those regions where higher excitation energies (and larger frequency values) are needed to effect the changes in energy levels.

Vibrational energy is associated with relative displacements between equilibrium center positions within diatomic and polyatomic molecules. These translational motions may be linear and unidirectional or more complex (as analyzed in a 3-axis coordinate system). Specific transitions are produced by distortions of bonds between atoms, as described by such terms as stretching and bending modes. There is one fundamental energy level for a given vibrational transition, and a series of secondary vibrations or overtones at different, mathematically related frequencies, as well as combination tones (composed of two or more superimposed fundamental or overtone frequencies). A tonal group of related frequencies comprises a *band*. Again, vibrational energy changes are characteristic of all states of matter; because these changes require less energy to initiate, the resulting ΔE's tend to occur at lower frequencies located at longer wavelengths in the infrared and beyond. Rotations of molecules also are accompanied by specific transitions. These take place only in molecules in the gaseous state and can be described in terms of three axes of rotation about a molecular center and the moments of inertia determined by the moving atomic masses. This type of shift is

relevant to the action of EMR on atmospheric gases involved as the interspersed medium between sensor and surface. Being a lower order energy transition, the energy levels are characterized by somewhat longer wavelengths. During excitation of gas molecules, both vibrational and rotational energy changes occur simultaneously.

The net energy detected as evidence of a series of electronic, vibrational, and rotational transitions over a range of wavelengths is, in another sense, a function of the manner in which energy is partitioned between the EMR source and subsequent interactions with atoms in a material. The radiation may be transmitted through the material, or absorbed within it, or reflected from atoms near the surface, or scattered by molecules or particulates composed of groups of atoms, or reradiated through emission, or, as is common, by some combination of all these processes. A plot of wavelength-dependent energy intensities comprising a spectrum can be treated in terms of the particular process being considered. Thus, there are three prevalent types of spectra associated with a material/object—absorption (or its inverse, transmission), reflection, and emission spectra—depending on the nature and location of the radiation source, the dominant interaction being measured, and the mode of detector response. For absorption spectra, the object lies between source and detector; for reflection spectra, the source and detector are positioned on the outside of the reflecting surface at an angle between them of less than 180°; for emission spectra, the immediate source is located within the material/object although an external activating source may initiate or change the emission.

Spectra can be obtained from pure substances (single phases), as from a metal, a silicate mineral, or an organic compound, or from multiphase systems (mixtures), as from soil, or a mud slurry, or such macroscopic classes as were discussed in preceding sections. Examples of reflectance spectra are given in Figures 1-4, 3-5, and 6-18 of this workbook. The field of spectroscopy is concerned with analysis of spectra to determine the nature (identity) of the materials and their internal structures, the characteristics of transitions and other atomic (microscopic) phenomena, the interaction processes, and the quantities of substances present. The appearance of a spectrum representing a single or multicomponent object or class is a combination of microscopic and macroscopic interactions, modified by "environmental" factors including density (atomic packing), thermal gradients, surface state, and geometry of the source-object-detector arrangement. For a discontinuous spectrum, as recorded in a spectrogram made by dispersing composite radiation with a prism or diffraction grating into discrete wavelengths, individual spectral lines[8] correlate with shifts in energy levels within individual atomic species; each precise wavelength indicates an energy state transition associated with some element species. The detection of that species is disclosed in a spectrogram by presence of one or more (often many) characteristic spectral lines whose densities in a photo plate provide a measure of concentration (amount). Emission spectra result from thermally- or electrically-excited (often ionized) atoms and molecules, whereas absorption spectra occur when radiation from these atomic species passes through gases of the same composition.

Continuous spectra are produced by excitation of atoms and molecules in solids, liquids, or gases into a broad range of energy states. A continuous spectrum consists of a curve connecting values of relative intensities of reflected, absorbed, or emitted radiation over the wavelengths associated with the interactive processes. This curve or line contains relatively straight segments that vary in slope from wavelength to wavelength, on which are superimposed various diagnostic features (defined in the second sense discussed on page 29). These features may be numerous local "wiggles" (small upturns and downturns of the line) or larger "spikes" consisting of "peaks" and "troughs" (prominent deflections and reversals of slope direction associated with sudden increases or decreases in intensity). The peaks and troughs represent absorption/emission/reflection maxima and minima centered at some wavelength or wavelength interval (band). These maxima and minima correspond to frequencies at which some characteristic interaction such as a transition or eigenstate change occurs within atomic/molecular constituents. This usually happens at a resonance frequency for the EMR-atomic interaction: a special case is

[8] The lines, as recorded on a photographic plate, are multiple images of a linear aperture; each line represents some refracted or diffracted set of waves having a specific wavelength.

described by the Christiansen frequency in which one or more maxima for emission or transmission processes (or a minimum for absorption) result from scattering of radiation at those frequencies in which the refractive index of the material coincides with its enclosing medium.

Depending on the depth of interaction between EMR and the material, and the type of interactive process, a spectral feature may appear as a sharp to broad, strong to weak maximum (peak) or minimum (trough). Thus, a smooth surface may produce an absorption or emission minimum feature at some wavelength, whereas a maximum at this wavelength develops for reflection from this surface. Objects or surfaces made up of thin to thick layers of particulate materials will produce still different patterns of maxima and minima, e.g., a thin layer gives rise to an emission maximum while a thick layer brings about an emission minimum at the same resonant frequency. Particle size also exerts an influence; for strongly absorbing materials, reflections decrease with diminishing particle dimensions. Some materials give spectra marked by abrupt changes in slope, or absorption edges, over a narrow wavelength interval. Many of the features in a spectral curve can be tied to interactions with specific element or molecular species. Chief among these in many inorganic solids are electronic and bending or stretching vibrational transitions relatable to ferrous or ferric iron, oxides, CO_2, OH^-, and molecular or surface-absorbed water, or more generally to color center effects.

The Meaning of Color

The properties of visible color depend in part on the electronic processes that relate to transmission and absorption of radiation (light) within materials. For an in-depth review of these processes, the reader is referred to "The Causes of Color" by K. Nassau, in *Scientific American*, V 243, #4, pp. 124-154, October, 1980. The particular colors perceived at or above the Earth's surface by the eye (through a psychophysical process controlled by the brain's recognition mechanism), or by a sensor capable of detecting in the visible spectral range, are essentially the consequence of certain dominant (more intense) reflected radiation in one (e.g., green) or more (e.g., purple—a blend of red and blue) narrow wavelength intervals. Other colors within the visible range have been absorbed and/or transmitted and are therefore diminished or absent in the reflected component. Colors can also be produced by emission as in a neon light, during discrete electronic transitions. Radiation reflected or emitted at shorter or longer wavelengths beyond the visible will also show variations in intensities at different wavelengths. This "unseeable" radiation is measurable by sensors commonly containing several detectors that respond over different spectral ranges. Various techniques exist by which the invisible radiation can be expressed in color patterns by systematically assigning certain colors to image patterns brought about by radiation outside the visible wavelength region (see, for example, the production of a false color composite described on page 94).

Insofar as the eye is concerned, color can be described rigorously in several ways (see also the discussion on pages 92 to 97). The trichromaticity theory states that the three primary colors (red, green, and blue) can be combined to produce themselves and all other colors by varying the intensity of light representing one or more of the primaries. The physiological effects of color in terms of purity, shades, and brightness can be induced by variations of the three parameters specified in the tristimulus theory of color, namely, hue, saturation, and intensity. Hue refers to the dominant or average wavelength of light contributing to the color; a color may be pure (red, yellow, green, blue) or mixed (purple, magenta). Saturation specifies the spread of wavelengths over the spectral regions contributing to the color; this is indicated by the amount of hue in a color (thus, crimson is strongly red but pink expresses a low saturation) Pastel colors represent unsaturated hues. Intensity is determined by the total quantity of reflected energy, independent of wavelength; the degree of "brightness" relates to intensity. In the Munsell system of color description, the saturation is replaced by the term "chroma" and intensity is replaced by "value,"

a measure of lightness or darkness as determined by a scale ranging from white through grays to black. Pink in this system is a bluish-red hue with low chroma and high (light) value. In still another system, a color triangle diagram is produced in which colors (both primary and secondary) occupy one angle, black a second angle, and white a third. *Grays* are produced by mixes of black and white; *shades* result from varying the mix between black and a color; *tints* develop by mixes of color and white; and *tones* occur when color is blended with different grays. Thus, red mixed with white yields a pink tint; red combined with black forms a maroon shade; and red joined with gray results in a rose tone. Other aspects of color specification are considered in Activity 3.

Radiation Terms and Units

The paths followed by EM waves are directional and may be represented by rays. The rays proceed along straight lines unless refracted (direction changes on passing from one medium into another) or diffracted (direction changes as waves encounter opaque edges, small apertures, or narrow lines). These rays may be visualized as flow lines that constitute a *radiation flux*. The flux is defined as the rate at which radiant energy passes a reference position. A flux is considered to be composed of photons released in short bursts of quantized energy from the source and dispersed within the wave train; flux characterized by visible light frequencies is called a luminous flux.

Radiant energy (Q) is a measure of the capacity of radiation to do work (1) as changes in motion of particles acted upon by force fields, (2) through heating, or (3) by a change of state. The radiant flux is just the rate of change of radiant energy with time, dQ/dt. Radiant power Φ (in watts, W) is a measure of the rate of doing work and in effect is synonymous with the definition of radiant flux.

The flux from a point source spreads out directionally. Consider a sphere (or hemisphere) of reference surrounding the source. Areas on a sphere of any radius (R) may be specified in terms of conical solid angles measured in steradians (cone angle = $A R^{-2}$; there are 4π steradians [sr] in a sphere). Radiant intensity (I) is defined as the radiant flux per unit solid angle (W sr) emanating in some direction from a *point* source. In this context, intensity is associated with the flow of energy through a reference area related to a solid angle. The passage through some specified planar surface area intercepting the solid angle at a distance R from the source gives rise to a radiant flux density. That flux density is in turn proportional to the squares of the amplitudes of the component waves. In this way, a relation between radiant intensity and wave amplitude is established.

Irradiance (E) refers to the incident radiant flux from one or more external sources onto a plane surface. Solar irradiation includes both the direct fluxes from the Sun and secondary radiation from excited atmospheric constituents. The general term for the flux leaving a plane surface is exitance (M). This is usually a composite of reflected external radiation and internal radiation such as from interior heat and reradiated absorbed irradiance. Emittance is used interchangeably with the somewhat more general term exitance. Both E and M are given in units of watts per square meter ($W m^{-2}$).

Radiance (L) is a frequently used radiometric quantity, defined as the radiant flux per unit solid angle Ω coming from an *extended* surface. The units are watts per square meters per steradian ($W m^{-2} sr^{-1}$). The source area is a projected one, that is, for any viewing position is the apparent area as calculated by $A \cos \theta$, where A is the reference area and θ is the perspective angle between the normal to the area surface and any viewing position. In a sketch, this is:

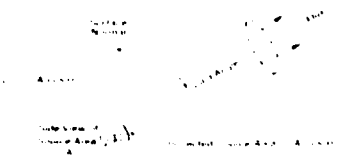

When not specified further, the radiance may consist of either reflectance or exitance contributions, or, from most natural surfaces, a combination of both. The solid angle Ω determines the surface of acceptance, namely, the area through

which the flux passes; in a sensor, the area seen is dependent on the optics and detector geometry of the system.

The radiometric quantities Q, I, E, M, and L apply to the entire EM spectrum, that is, they are the integrated total of photon fluxes at all wavelengths involved in the radiation. In practice, the variation of the radiant flux (and the derivative radiometric quantities) depends mainly on the nature and properties of both the primary source and the intercepting surface material. Thus, a composite wave will consist of numerous sinusoidal component waves, each associated with its characteristic wavelength (or frequency), amplitude, and phase. Each discrete waveform is then one spectral component of the composite or complex wave. The waveform of the complex wave is governed by the principle of superposition of wave motion, which states that the resultant amplitude of the complex wave is the sum of the amplitudes of the component waves. Any complex wave may be analyzed by Fourier analysis. This analysis involves the definition of a series of simple harmonic or sinusoidal waves differing in frequency, amplitude and phase, which, when combined in a proper sequence, reproduce the initial complex wave. If two waves of different wavelengths combine to develop a regular and systematic relationship between their amplitudes, the resultant radiation (e.g., radio waves) is said to be coherent. However, if the amplitudes are irregular or randomly related, the radiation (e.g., polychromatic light) is incoherent.

When the radiant flux is specified for a discrete wavelength or, more commonly, a continuous interval or band of wavelengths in the EM spectrum, the radiometric quantity for that wavelength or band becomes a spectral radiometric quantity, as for example, the spectral radiance in the 0.6 to 0.7 μm band. A spectral radiometric quantity is indicated by a subscript λ, as E_λ or I_λ. The value of λ may be given as a single wavelength or may denote a band interval ($\lambda_2 - \lambda_1$) through which variations in the flux are integrated. A plot of variations of radiances with wavelength throughout the spectrum defines the distribution of spectroradiances for the source material, or an excited surface or target, yielding some type of spectral response curve (see p. 91).

SPECTRAL REGIONS

In remote sensing, the sensed (detected and measured) radiation usually extends over narrow or broad regions (bands) of the spectrum. Depending on the detector used, the quantity measured may be *energy*, *power*, or *intensity at specified wavelengths* or *frequencies*. Several of the regions are also further subdivided into more specific segments (Figure 1-1A). Thus, the ultraviolet (UV) region is often broken into near (shorter wavelengths) and far (longer wavelengths) UV, the visible (light-producing) region into distinctive colors ranging from blue (shorter wavelength), green, yellow, orange, to red (longer wavelength), and the infrared into reflective IR (0.7 to 3.0 μm), and emissive or thermal IR (3.0 to 300.0 μm) (or, together, more or less synonymous with near and far IR). Parts of the IR are also known as the photographic IR (0.7 to 0.9 μm), limited to the response range of film exposed to radiation just beyond the visible red; the solar IR (0.7 to 4.0 μm), a region in which radiation from the Sun is reflected; NIR, for near infrared, as applied to the wavelength interval between 0.7 and 1.3 μm (essentially equivalent to bands 6 and 7 on the Landsat MSS); SWIR, for shortwave infrared, referring to the interval 1.5 to 2.5 μm; the mid IR (3.0 to 5.0 μm), an interval in the thermal IR (TIR) in which weak emissive energy is detectable through the atmosphere; and another detectable TIR interval (8.0 to 14.0 μm) commonly, but not exclusively, referred to as the "thermal IR."[9]

[9] The term "thermal infrared," as used in remote sensing, normally refers to the spectral region (8 to 14 μm) representing emitted radiant energy from the Earth's outer layer (at temperatures in the range -20 to +40°C), that results from internal terrestrial and external solar heating. The term does not imply a feeling of "hot," as experienced with a glowing ember or a hot plate; such objects produce strong sensible radiation that extends from the visible through wavelengths even longer than 14 μm. As a corollary, the terms "near infrared" and "shortwave infrared" should in no way be confused with "hot" or "heat effects"; they largely represent the contribution of reflected solar radiant energy in the 0.7 to 3.0 μm interval.

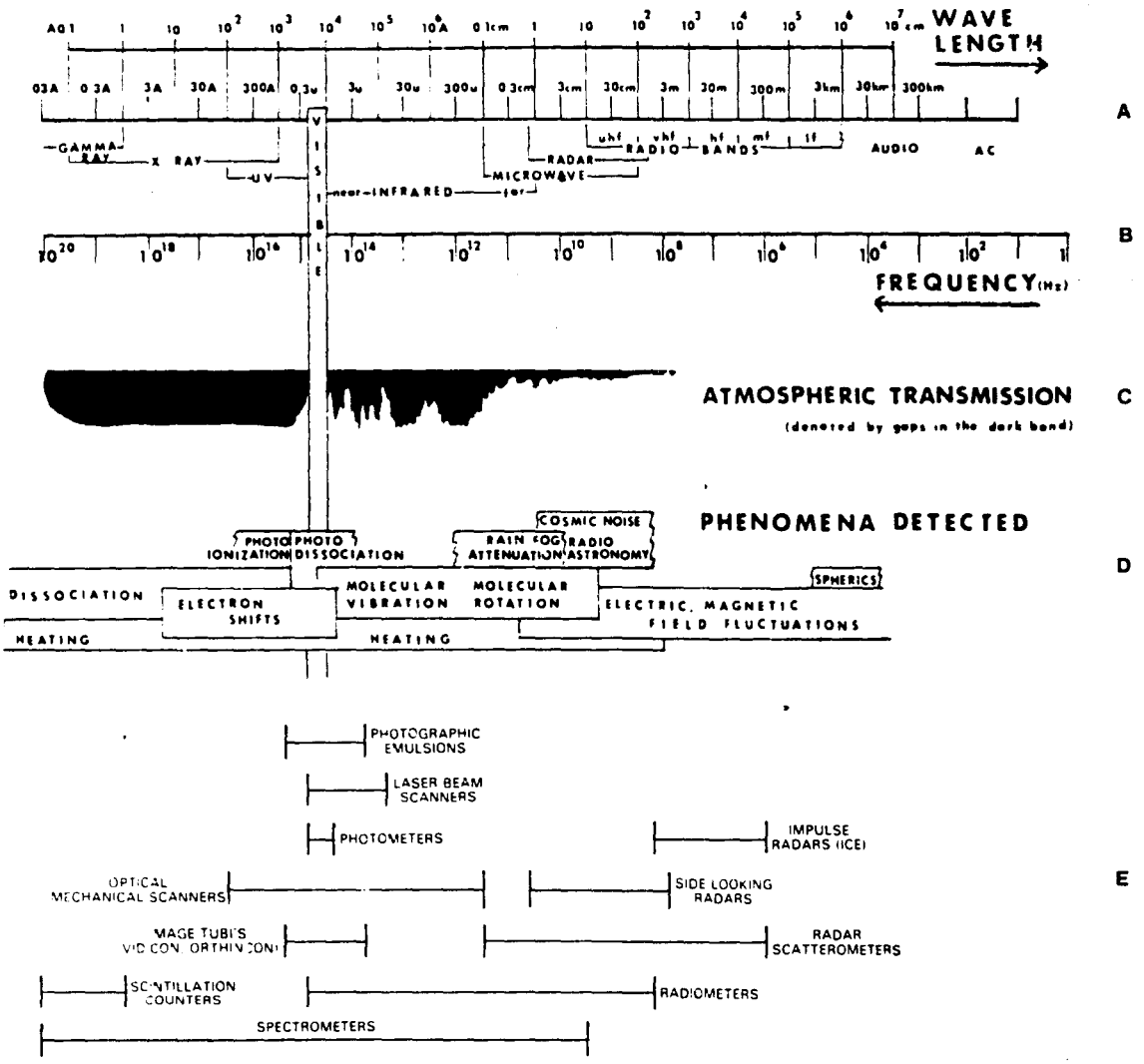

Figure 1-1. The electromagnetic spectrum, atmospheric windows, and the spectral operating range of sensors. Modified from R. Colwell (upper diagram), and from *Remote Sensing of Environment*, J. Lintz, Jr. and D. S. Simonett (Editors), with permission of the Publisher, Addison–Wesley, Reading, Mass. (lower diagram, E).

INFLUENCE OF THE ATMOSPHERE

The spectrum of incoming solar radiation (insolation) at the top of the Earth's atmosphere is shown in the upper curve of Figure 1-2. Some of the solar radiant flux will be transmitted through the atmosphere, some will be absorbed by the air's constituents, and the remainder will be reflected

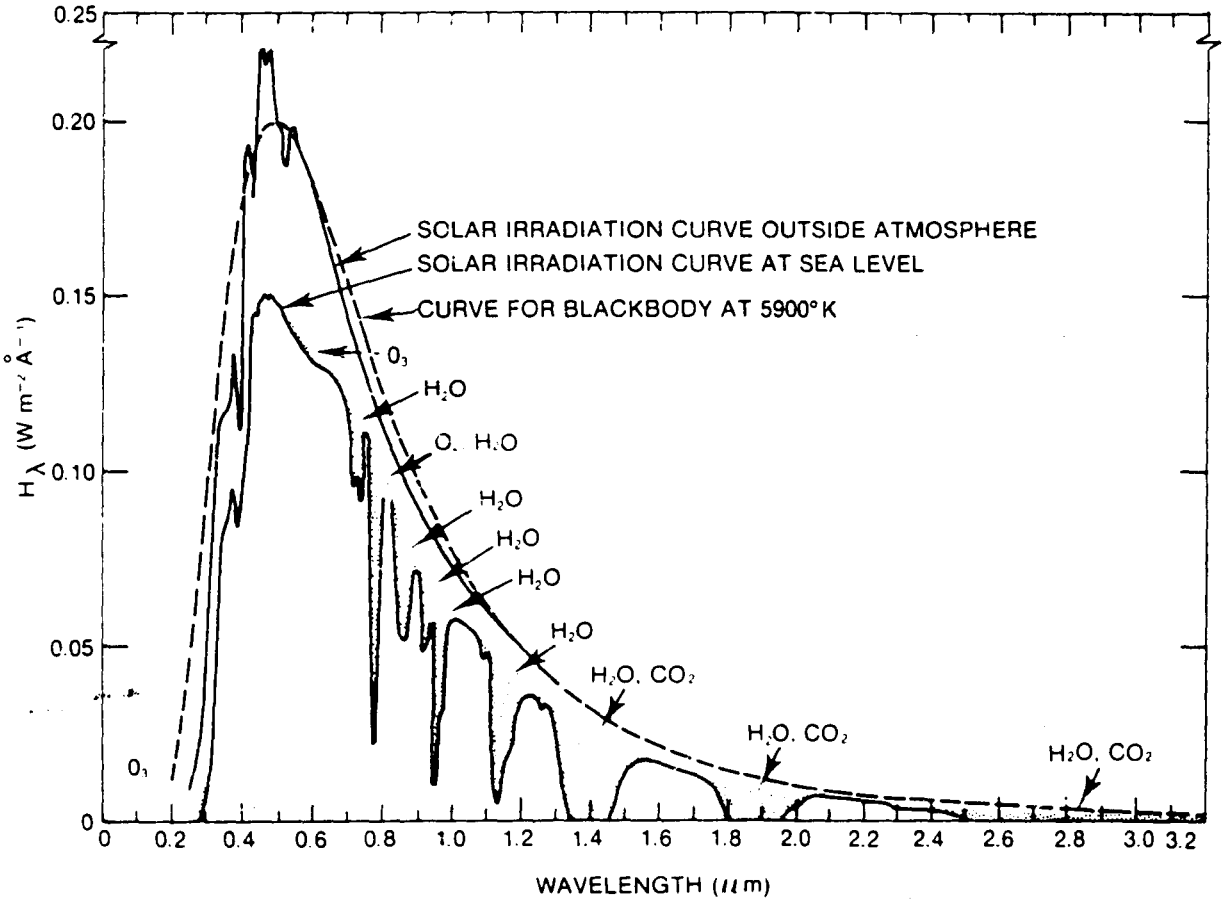

Figure 1-2. Solar irradiation curves, showing location of atmospheric absorption bands, from *Handbook of Geophysics and Space Environments*, S. Valley (Editor), copyright © 1965 McGraw–Hill. Published with permission of McGraw–Hill Book Company.

from gaseous molecules and particles.[10] Radiant energy that is converted to heat during interaction will be reradiated as emitted radiation. This interaction reduces the energy passed through the atmosphere, as shown by the lower curve of Figure 1-2. The downward spikes, or troughs, in the curve represent energy losses through absorption over specific wavelength intervals. These absorption bands are related to specific molecular interactions, mainly with water vapor, oxygen, and carbon dioxide.

Interactions of atmospheric gases with radiation are particularly prominent in certain regions of the EM spectrum. Absorption and other interactions occur over many of the shorter wavelength regions, so that only a fraction of the incoming radiation reaches the surface.[11] The atmosphere is much more transparent (transmissive) in the visible

[10] Mie scattering refers to reflection and refraction of radiation by atmospheric constituents (e.g., smoke) whose dimensions are of the order of the radiation wavelengths. Rayleigh scattering results from constituents (e.g., molecular gases, such as water vapor) that are much smaller than the radiation wavelengths. Such scattering increases with decreasing (shorter) wavelengths (blue sky effect). Particles much larger (e.g., dust) than the wavelengths give rise to nonselective (wavelength-independent) scattering.

[11] Atmospheric backscatter can, under certain conditions, account for 80 to 90 percent of the radiant energy observed by a spacecraft sensor. The backscattered radiation experiences polarization that varies in intensity and direction. This effect may be reduced by designing sensors to have minimal polarization sensitivity.

region, in parts of the infrared, and in microwave and longer wavelength regions. These intervals of efficient transmission are called "atmospheric windows" (see Figure 1-1C). Significant reductions in transmission occur around 1.5, 1.9, 2.5 to 3.0, 4.3, and 5.2 to 7.9 μm in the infrared. These are, therefore "forbidden" intervals for practical remote sensing of the surface.

#1-6: Using Figure 1-1C, list the four principal "windows" (by wavelength) open to effective remote sensing from above the atmosphere.

#1-7: What is likely to happen further to radiation that first experiences energy loss (say 25 percent) in passing down through the atmosphere, then interacts with the surface, and is finally sensed from a spacecraft above the atmosphere?

MACROSCOPIC INTERACTIONS

As implied earlier, remote sensing techniques depend mainly on the detection of emitted and reflected radiation resulting from the *interaction* between *matter* at or above the Earth's surface and *energy* from internal and or external sources (the principal source is the Sun). For any material, internal EMR must be considered in terms of absorbed, transmitted, and scattered components, whereas external EMR influenced by the material consists of incident, reflected, and emitted components. Any incident radiant energy acting on a surface will obey the law of conservation of energy such that $\tau + \alpha + \rho = 1$, where τ, α, and ρ are the transmittance, absorptance, and reflectance respectively, defined as the ratios of transmitted, absorbed, and reflected radiation to the incident radiation.[12]

The total radiance or radiant flux emanating from surface features varies with wavelength. As measured by a spaceborne or airborne sensor system, that radiance is the sum of three contributing components: (1) a reflected component, (2) an emitted component, and (3) an atmospheric component (emitted and scattered radiation).

Reflectance and Related Concepts

There are two general types of reflecting surfaces that interact with radiation: specular (smooth) and diffuse (rough). These terms are defined geometrically, not physically. A surface may appear to be perfectly smooth in the physical sense (i.e., it appears and feels smooth), but at a scale on the order of the wavelength of light, many irregularities might occur throughout that surface. Again, a concrete roadway may look smooth and flat from a distance but feels rough when a finger passes over it; on close inspection that surface shows grooves, pits, and granular protuberances, which in effect produce a miniature topography with widely varying slopes. Radiation impinging on such a diffuse surface is likely to be reflected or scattered in many directions. The Rayleigh criterion is used to determine surface roughness with respect to radiation. That criterion is expressed as

$$h \sim \lambda / 8 \cos \theta,$$

where h is an average height, in some unit of wavelength λ (e.g., Angstroms), of irregularities above the base plane of the surface and θ is the angle of incidence (measured from the normal to the surface). If $\lambda \sim h$, the surface acts as a *diffuse* reflector; $\lambda > h$ designates a *smooth* or *specular* surface.

The radiometric parameter most frequently measured by remote sensors operating in the 0.4 to 2.5 μm range is *reflectance*. Reflectance, and the

[12] The terms transmissivity, absorptivity, and reflectivity refer to intrinsic properties of a substance and are measures of the capacity of a substance to transmit, absorb, and reflect incident radiation, without regard to the nature or source of that radiation. Measurements are made on samples of *unit thickness* in which the incident radiation strikes a *smooth* (specular) surficial interface. Throughout this workbook, terms ending in "ance" are used in preference to those ending in "ivity" when specific materials irradiated by the Sun are being considered.

companion terms transmittance and absorptance, are dimensionless numbers (from ratios). Reflectance from a material surface is defined as the ratio of reflected radiant energy to the irradiant energy and is commonly expressed as a percentage. Alternatively, the energy terms can be replaced by power terms, in watts per square meter per steradian ($W\ m^{-2}\ sr^{-1}$).

A specular surface reflects radiation according to Snell's Law, which states that the angle of incidence θ_i is equal to the angle of reflection θ_r, where the angles are measured from the normal to the surface and within the principal plane containing both incident and reflected rays. Actual values of specular reflectance depend on the type of specular surface involved. Specular reflectances within the visible wavelength range vary from as high as 0.99 for a very good mirror to values of 0.02 to 0.04 for a smooth water surface. In general, natural surfaces depart significantly from specular at shorter wavelengths (into the infrared) and may still be diffuse in the microwave region.

The behavior of a perfectly diffuse, or Lambertian, surface is depicted in Figure 1-3A. In this case, incident rays from a single distant source S lying at an incident angle θ_0 (measured from a zenith or vertical direction Z) and an azimuth angle ϕ_0 (relative to north N) strike a horizontal surface (equatorial plane within a sphere). If that plane is rough or diffuse at the wavelengths of a bundle of rays, a ray at any point Q will be reflected in some direction depending on the slope at the point of contact. That direction R may be represented by a characteristic vector fixed (in polar coordinates) on the upper hemisphere by its angle of reflectance θ (or scattering angle β) and its azimuth angle ϕ. At other points, the direction of R will probably differ according to the orientation of the slope at the immediate irregularity in the surface. Thus, a large number of incoming rays meeting the surface at other irregularities (most probably with randomly oriented slopes) will be redirected (diverge) in all possible directions extending through the upper hemisphere of reference. The radiance at any one direction is, on average, the same as any other; in other words, radiance is constant at any viewing position on the hemisphere and is therefore independent of θ_0 (but remember that radiance does depend on the projected area viewed). However, the radiant intensity measured at any position will vary according to the relation: $I_\theta = I_0 \cos \theta$, which states that as the angle of incident radiation is varied, the intensity of incoming radiation also changes. This equation applies to the special case of *directional reflectance*, in which the incident and reflected rays lie in the same principal plane. For radiation impinging the surface along the zenith direction (i.e., normal to the surface), $\theta = 0$ and $\cos \theta = 1$, and therefore $I_\theta = I_0$.[13] At any other angle of θ, $\cos \theta < 1$ and I_0 is reduced. Although a surface viewed from any position will seem to be uniformly illuminated (constant radiance), that surface will become less bright as the source is moved from a vertical (overhead) position towards the plane itself (horizon). The term *bidirectional reflectance*[14] describes the common observational condition (such as in remote sensing) in which the viewing angle ϕ differs from the angle θ incident on a diffuse surface, and the rays are not in the same principal plane. In the general case, the expression relating the bidirectional reflectance ρ to the irradiance E is:

$$\rho_R (\theta_0, \phi_0, \theta, \phi) = \frac{1}{\pi} \rho (\theta_0, \phi_0, \theta, \phi) \cos \theta \, | E \cos \theta_0 |,$$

where ρ_R is measured reflectance along a direction R from a scattering plane.

Nearly all natural surfaces tend to be combinations, to varying degrees, of specular and diffuse reflectors. Figure 1-3B[15] is a plot of directional reflectances within a principal plane of the hemisphere for (1) a perfectly diffuse reflector

[13] In the usual case for space observations, solar irradiation comes in at various angles (daily and seasonal changes in elevation and azimuth) non-normal to the Earth's reflective surfaces, whereas those surfaces are viewed almost at a normal to the surface through a small scan angle (±0.88° for the Landsat MSS).

[14] Another term, albedo, refers to the fraction of the total incident energy reflected from a diffuse *natural* planetary surface. It is, in effect, the averaged reflected radiances integrated over a hemisphere of reference.

[15] Adapted from Bartman, F. L., *The Reflectance and Scattering of Solar Radiation by the Earth*, Technical Report 05863-11-T, College of Engineering, University of Michigan, Ann Arbor, 196[illegible].

(symmetrical envelope associated with ray D; the envelope remains the same for all other angles of incidence), and (2) an imperfectly diffuse (specular component) reflector (envelopes vary with incident angles A, B, and C). For other scattering angles β, the bidirectional reflectances will integrate into irregular three-dimensional envelopes within the reference hemisphere. Since reflectances vary with wavelength, envelopes of spectral bidirectional reflectance must be produced for each wavelength in the range considered.

#1-8: Why does the general outdoor scene seemingly brighten from dawn to noon and then darken towards sunset? Why can you still see objects after the Sun has dipped below the horizon? What conditions cause the Sun glint effect—a bright glare coming from an area within a lake as you look down from a hillside?

#1-9: With the ideas in the preceding paragraphs in mind, explain the phenomenon of progressive darkening towards the edges that is commonly observed in low-altitude aerial photos.

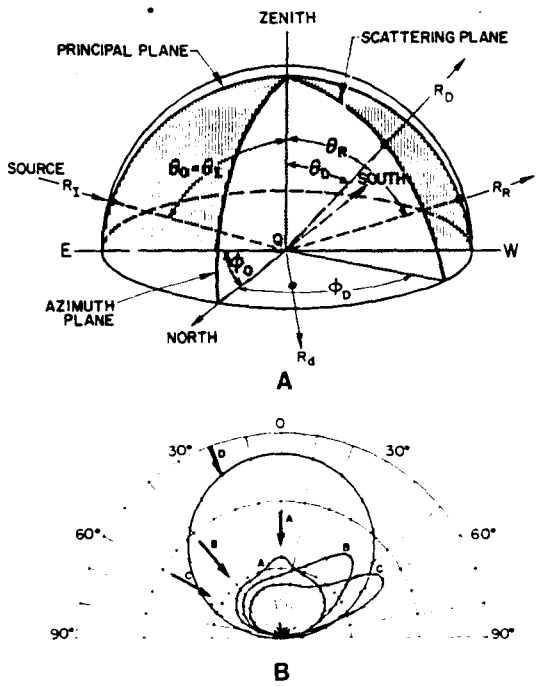

Figure 1-3. Schematic diagrams showing distribution of reflected radiation from diffuse reflectors.

#1-10: What other effect (geometrical) is likely to be present in such photos?

Various ideas developed in the last few pages can be brought together at this stage by considering the radiances measured by sensors on an orbiting satellite such as Landsat. For a given spectral band, specified as $\lambda = \lambda_1$ to λ_2, the MSS on Landsat-1 will measure a total radiance L as the sum of reflected solar EMR from the surface, L_s and the EMR scattered by the atmosphere, L_A. A general expression[16] for this is:

$$L = \frac{1}{\pi} \int_{\lambda_1}^{\lambda_2} [E(\lambda) R(\lambda)] \tau_\beta(\lambda) \tau_2(\lambda) \rho(\lambda) \sin\beta + \rho'_\beta(\lambda)] \, d\lambda \, .$$

where

- $E(\lambda)$ = spectral solar irradiance normal to the top of the atmosphere,
- $R(\lambda)$ = spectral responsivity of the instrument,
- $\tau_\beta(\lambda)$ = monochromatic slant path transmissivity of the atmosphere for Sun elevation angle β (measured from the ground to the path of the solar ray to the nadir point),
- $\tau_2(\lambda)$ = monochromatic transmissivity of the atmosphere through the zenith (nadir) direction,
- $\rho(\lambda)$ = spectral reflectance of the surface,
- $\rho'_\beta(\lambda)$ = atmospheric reflectance as a function of the Sun elevation angle β.

A plot of L or ρ versus λ produces a spectral response curve, as discussed on pages 28 and 91. Another useful plot, that of radiance versus Sun elevation angle for any material, may be constructed for each spectral band. This serves as a set of criteria allowing identification (and separation) of materials by using radiance values obtained under different incident angles and a constant (vertical) viewing angle.

[16] Equation 4-26, p. 91, in the *Manual of Remote Sensing*.

EMITTANCE AND THERMAL PROPERTIES

For the Earth's surface as irradiated by the Sun, the amount of reflected radiation begins to drop off gradually above *ca.* 1.0 μm. Above *ca.* 4.5 μm, the radiation from the surface becomes predominantly emissive. This radiation results from changes in the kinetic states of vibrating atoms and molecules in the excited materials and is therefore thermal in nature. All substances at temperatures above absolute zero (0° K [Kelvin])[17] emit energy over various regions of the EM spectrum, depending on their specific temperature. Materials at the Earth's surface receive some internal heat (largely from radioactive elements in the crust) and are therefore continually emitting thermal energy. In addition, a large part of the incident EM energy irradiated from the Sun is absorbed and transformed into re-radiated thermal energy. Thus, most of the sensed surface heat results from solar irradiation, which adds a variable (diurnal and seasonal changing) amount of thermal energy to the constant small heat flux from the interior.

At infrared wavelengths longer than *ca.* 3.0 μm, and especially in the 3-5 μm and 8-14 μm atmospheric windows, remote sensing is concerned with the effects of heat and the measurement of temperatures. In making measurements and calculations, an ideal thermal state—that of a perfect blackbody—is adopted as a reference condition. A blackbody is defined as an ideal emitter at all wavelengths, absorbing and emitting radiant energy with the maximum possible intensity and maximum possible flux rate per unit area. Thus, such a body absorbs[18] and converts all incident radiation into heat, regardless of spectral composition of incident EMR. For any wavelength, the spectral radiant exitance M_λ (in units of W m^{-2} $Å^{-1}$), is given by:

$$M_\lambda = \frac{2\pi hc^2}{\lambda^5} \left(\frac{1}{e^{hc/\lambda kT} - 1} \right)$$

an expression known as Planck's spectral distribution law; h (Plank's constant) = 6.62 X 10^{-34} joule sec, k (Boltzmann's constant) = 1.38 X 10^{-23} joule per °K and c = speed of light. This equation indicates that, at any given wavelength, the exitance (and hence total energy) of emitted blackbody radiation increases as temperatures rise. It likewise states that the intensity distribution of the radiation varies with wavelength (depending on the relative contributions of λ^5 and $e^{1/\lambda}$ terms) through minima at high and low wavelengths to a maximum value at some intermediate wavelength characteristic of the particular temperature prevailing at thermal equilibrium.

Only a few natural materials approach the behavior of a theoretical blackbody. Real materials are gray bodies, that is, ones whose emissive power at given temperatures is decreased by the multiplicative factor ϵ, or the emissivity (ratio of emittance of a real body to that of an ideal blackbody) characteristic of each material. The emissivity of gray bodies is constant at all wavelengths. A selective radiator describes natural materials whose emissivities vary with wavelength.

Experimental conditions simulating a blackbody state may be approximated by directing radiation into a closed cavity with opaque walls coated with some absorbing material, and maintaining the walls at a uniform temperature. One commonly used cavity is the Hovis sphere, made of metal with the inner lining covered with black paint. Thermal radiation characteristic of the interior temperature is sampled through a small hole; the measured radiant exitance (emittance) at any wavelength should conform to the value calculated from the Planck equation.

According to the Stefan-Boltzmann Law, the radiant flux F_B from a blackbody is related to its kinetic temperature T_k by $F_B = \sigma T_k^4$, where the constant σ = 5.67 X 10^{-12} W cm^{-2} $°K^{-4}$. This equation shows that the total energy (over all wavelengths) emitted from a blackbody increases with increasing temperatures. The flux F_R for a real body is $F_R = \epsilon\sigma T_k^4$, from which the radiant temperature T_R for that body may be derived by using the expression $T_R = \epsilon^{1/4} T_k$. The variable T_R is the parameter most conveniently measured by thermal

[17] Degrees Kelvin = Degrees Celsius (°C) + 273.

[18] Black as a "color" results when all visible incident radiation is absorbed and the blackbody is not sufficiently heated to induce reradiation discernible to the eye's response range (ca 0.4-0.7 μm). Humans perceive black objects by their contrast to colored surroundings.

radiometers. Note that the emissivity ϵ may also be calculated as the ratio of F_R to F_B. When the fluxes are referenced to some unit area (giving then, by definition, the emittance) at any wavelength, $\epsilon_\lambda = M_R(\lambda)/M_B(\lambda)$, which indicates some dependence on wavelength.

At thermal equilibrium, spectral emissivity ϵ_λ is equal (in magnitude) to spectral absorptance (α_λ), a statement of Kirchhoff's Law. Since a blackbody is a perfect absorber, its emissivity must be 1 (for a perfect reflector, $\epsilon = 0$). From the relation $\tau + \alpha + \rho = 1$ (see p. 24), for an opaque material with $\tau = 0$, and substituting ϵ for α, the relation $\epsilon + \rho = 1$, or $\epsilon = 1 - \rho$, is derived; emissivity may thus be calculated from reflectance measurements for any wavelength or wave band.

Most natural materials, as gray bodies, have values of ϵ between 0 and 1. Rocks and many other inorganic materials have emissivities between 0.80 and 0.95; ϵ for water is about 0.98. Variations in ϵ are smaller in the 8 to 14 μm range than in the 3 to 5 μm range, so that common materials are more spectrally similar at the longer wavelengths.

Thus, the temperature of a material measured remotely by a sensor is just its blackbody temperature reduced by the factor ϵ for that material. Thermal data collected by the sensor must also be corrected for atmospheric attenuation and meteorological effects, and for the sensor responsivity R, a constant of the instrument calculated as $R = S/\phi$ (λ_1 to λ_2), where S is the signal value, ϕ is the incident flux, and (λ_1 to λ_2) is the wave band of interest. The measured temperature is known as apparent temperature (or brightness temperature when applied to the microwave region).

For any body, the wavelength of maximum thermal emission λ_{max} (in micrometers) is given by Wien's Displacement Law:

$$\lambda_{max} = \frac{2.987 \times 10^3}{T_{rad}} \ \mu m\ ^\circ K$$

From this expression one can deduce that increasingly hotter bodies radiate their maximum energy at progressively shorter wavelengths (the peak defines the characteristic radiation "color" at the specific temperature).

#1-11: Using Wien's Displacement Law, calculate the peak wavelength for thermal radiation from (1) the Sun's photosphere at 6000 °K, (2) a forest fire at a temperature of 600°C, and (3) the Earth's surface at a local temperature of 17°C.

#1-12: What part of the EM spectrum should be used to sense the thermal state of (1) the Sun's exterior, (2) the Earth's surface, and (3) a forest fire detected through obscuring smoke?

At longer wavelengths (microwave-radio regions) the measured temperature is customarily referred to as the brightness temperature, T_B, a function of integrated spectral power as determined by the Rayleigh-Jeans approximation for radiance: $L = 2kT/\lambda^2 = 2f^2\ kT/c^2$ where k = the Boltzmann constant (1.38×10^{-23} J/°K), f = frequency in hertz (Hz), c = speed of light and L is in units of watts per square meter per hertz per steradian ($W\ m^{-2}\ Hz^{-1}\ sr^{-1}$). In the microwave region, variations in the dielectric constants for different materials become important in determining the emissivity effect. Although the emissive character of a material is of principal interest from the thermal to microwave regions, emitted radiation at these wavelengths is itself capable of being transmitted, absorbed, or reflected.

THE MULTISPECTRAL APPROACH

From the previous discussions on reflected and emitted radiation, it should be evident that materials will respond in different, generally distinctive ways in different parts of the EM spectrum. Moreover, within any limited region of the spectrum, a particular material will exhibit a diagnostic spectral radiance pattern (i.e., characteristic intensities of reflected or emitted radiation that vary with wavelength), which generally differs from that of another material. Thus, every individual substance or class of related substances has its own specific *spectral signature* or spectral response curve (see p. 91). Each class of substances or features shows some dominant signature or pattern by which members of a class can be identified. The signatures of these members (as, for

example, different crop types or different soils) share some common traits (such as certain absorption bands or other fine structure) but often show enough variation to allow identification of individual types.

In the current practice of remote sensing techniques, the *multispectral* approach has proved most effective. This involves either measurement of the spectral signatures over one or more regions of the spectrum, as with a spectrometer, or sampling of the radiation intensities (or some related parameter, such as power or reflectance) as single values integrated through specific intervals or wavebands, as with a spectroradiometer. This is illustrated in Figure 1-4, (see also Figure 3-5 and related questions), which shows typical curves making up the spectral signatures for three common classes of materials, generalized from spectrometer measurements by omitting most of the fine structure.

This fine structure within a spectral response curve can be important in identifying specific materials. For example, many individual mineral species have diagnostic narrow absorption bands (transmission minima) centered at certain, well-established wave lengths. Laboratory techniques using spectrometers are commonly sensitive enough to distinguish between closely related minerals or other materials with similar compositions and/or crystal structures by measuring the precise location of the band centers. The spectral curves for a series of generally different rock types from Wyoming, shown in Figure 6-18, demonstrate this point. In the interval from 0.4-2.5 μm, distinctive absorption troughs provide significant data on the presence of ferrous iron (band centers around 0.9 μm), OH^- (around 1.4 μm and in the 2.1-2.3 μm interval), water (1.4 and 1.9 μm), and $CO_3^=$ (mainly, near 2.35 and 2.55 μm). Shifts in the band centers may disclose the precise type of clay or carbonate mineral present in sedimentary rocks, or make evident the nature of characteristic rock alteration products (e.g., iron-rich or iron-poor secondary minerals); the band amplitudes relate to the amounts present. Additional information as to composition resides in the thermal IR intervals, within which the reststrahlen effect (see p. 338) is sensitive to silica content of assemblages of the silicate minerals that make up most rocks and soils. Even in the field, the somewhat smoother curves for rocks and soils obtained with a spectrometer may show sufficient details to permit identification of groups of related materials. (Figure 6-19B).

There is also fine structure in spectral reflectance curves of vegetation (see Figure 6-23). As indicated in that figure (and also Figure 6-21), the influence of chlorophyll and other pigments, leading to absorption in the blue and red regions (but not strongly affecting the green region – hence, the typical colors of green vegetation) controls the response to irradiation in the visible. The distinctively high reflectance of vegetation in the 0.7 to 1.2 μm region is dominated by the internal structure (cell walls) of the vegetative materials; water absorption bands occur at various wavelengths throughout this region and in the continuation of the spectrum out to 2.5μm. Variations in water content in the vegetation further influence the overall heights of response curves beyond the chlorophyll absorption band at 0.65 μm.

Ideally, one would wish to operate a spectrometer from an aircraft or spacecraft platform in order to acquire spectral curves having the details just described. For most such instruments, this cannot be done practically because of the need for the spectrometer to dwell on the ground target long enough to run through all the spectral regions of interest. Even for fast spectrometers that complete their measurements in 2-3 seconds, the field of view distance (see p. 33) traversed along the ground track would be many kilometers from an orbiting spacecraft (thus, very poor spatial resolution). Of course, the spectrometer could be sighted manually on a target, as was done by the astronauts on Skylab. Or, a large number of individual detectors, each of narrow bandwidth, can measure the dispersed spectroradiance, but the number of photons counted by each detector (amount of energy sensed) would likely produce too low a signal to noise ratio (see p. 37). At the time that Landsat-1 was designed and launched, the state of the art in sensor technology required use of multiband radiometers which instantaneously measure spectroradiances, over broad spectral intervals. Thus, we shall confine our attention here to a consideration of sampling discrete wavelengths as center points of individual (broader) wavebands.

#1-13: Which regions of the spectrum show the largest reflectance for these materials: (a) Water, (b) Rock, (c) Vegetation?

#1-14: Which material has the highest emittance; the lowest?

#1-15. Which material is "brighest" (most reflective) in the visible range?

#1-16: Calculate the ratio of reflectances of vegetation and rock at: (a) 0.6 μm, (b) 0.9 μm, (c) 1.6 μm.

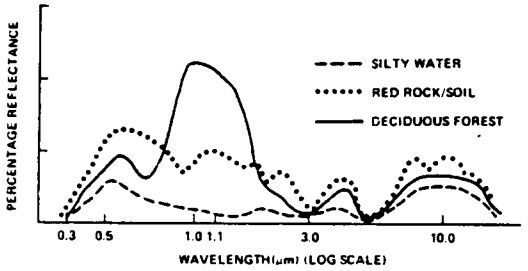

Figure 1-4. Typical spectral curves (generalized) for three common surface cover types, from *Remote Sensing: The Quantitative Approach* by P. Swain and S. Davis. Copyright © 1978 McGraw–Hill. Used with permission of McGraw–Hill Book Company.

At which wavelength is separation (distinction) based on intensity differences most likely to be achieved (see p. 163 for a review of the usefulness of ratioing)?

#1-17: From the curves in Figure 1-4, you should now measure the reflectance of each class at two discrete (very narrow) wavelength intervals, centered at 0.5 and 1.1 μm. Make a table like the one below.

Reflectance (%)
(Class)

	○ Water	▲ Rock	+ Vegetation
λ_1 = 0.5 μm			
λ_2 = 1.1 μm			

Plot these values on the diagram below, in which the 0.5 μm values are plotted on the X-axis and 1.1 values on the Y-axis.

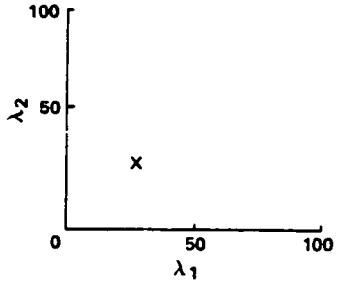

#1-18: Suppose that an unknown material or class is characterized by spectral values that plot at x. What is this object most likely to be? How might you test for the identity of this object, assuming that you have an instrument capable of measuring any part of the spectral region covered by these signatures? Consider, too, that this might be from a new class.

#1-19: If you plot values measured at three discrete wavelengths (λ_1, λ_2, λ_3), sketch one type of diagram that would help to visualize the distribution of the values.

#1-20: What if four or more wavelengths are measured? Can these be conveniently plotted? Comment on what might be done instead.

#1-21: Let us presume that two surface features, a forest and a dense field crop, are measured for their spectral responses and both display similar values for wavelengths λ_1, λ_2, and λ_3, and possibly for other wavelengths not measured. How might these be separated and identified (assume the multispectral data are used to construct images of the ground containing these features)?

The multispectral approach, then, is carried out by using cameras (with filters), scanning radiometers, or spectrometers to measure radiation intensities continually through a spectral region or discontinuously in discrete intervals (wavebands) within the region or even at specific wavelengths. For analysis, spectral data may be plotted in multidimensional space (N dimensions: special plotting techniques or mathematical analysis are required for N>3) by using the discrete bands or wavelengths as axes. Measurements of the same class or surface feature will vary (why?), so that plotted points will scatter, as shown in Figure 1-5 for the two-dimensional case.

Each class consists of a population of variable characteristics, such as spectral properties, giving rise to a distribution or cluster of values. Hence, this type of plot is often referred to as a cluster diagram. There is some single value, calculated as an average or mean (shown as ○), representative of the population of values in each class. The variation or spread of values may be numerically expressed as a standard deviation σ or a variance σ^2. A number of statistical tests (for instance, analysis of variance, Chi-square) may be applied to the data to characterize and distinguish different class populations. These tests also apply to data values

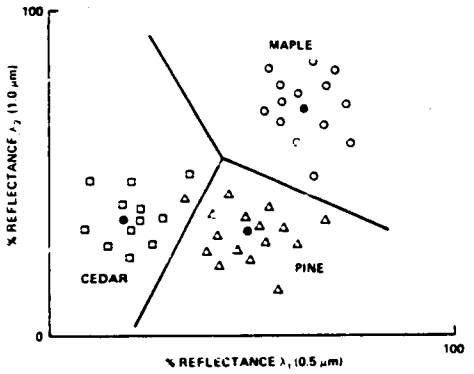

Figure 1-5. Two band cluster diagram, with decision boundaries for three common types of trees, from *Remote Sensing: The Quantitative Approach* by P. Swain and S. Davis. Copyright © 1978 McGraw–Hill. Used with permission of McGraw–Hill Book Company.

for unknown objects. Special tests are performed to determine the population, if any, to which an unknown belongs. These statistical procedures are at the heart of the process of classification (class identification) described in Activity 5. If classes are truly distinct with regard to spectral characteristics, they can be separated, as shown in Figure 1-5, by linear or multidimensional boundaries determined by some appropriate discriminant function.

Multispectral Imagery

Perhaps the easiest way to gain a quick insight into the multispectral approach is to examine a set of multispectral images. When displayed as photographs, these images record the variations in radiance from band to band (wavelength intervals) as gray shades or levels within a gray scale. Thus, the highest intensities, or brightness levels, of radiation reflected or emitted from a surface are rendered in light shades and the lowest levels in dark shades. This relationship is simply the expression of a basic equation underlying the characteristics of a film negative. The equation, $D = \gamma \log E$, states that the increase in film density D (or opacity) (proportional to gray level) is a function of the logarithm of the exposure E (a time-dependent measure of luminous flux or the quantity of photons impinging on a unit area over a stated time interval). Density is also influenced by γ (gamma), the slope (given by $\tan \theta$), of the familiar characteristic curve produced by plotting corresponding D and log E values. For a range of exposures, this plot (the Hurter-Driffield, or H-D curve) will be a straight line but becomes nonlinear at higher and lower exposure values. The rate of change of densities or contrast with respect to varying exposure is determined primarily by the value of gamma. The intrinsic scene brightness initially determines the slope of the curve and the intercept of the extrapolated straight line portion with the exposure axis. Important factors modifying both contrast and brightness include film characteristics and developing conditions.

When a multicolored scene is photographed on panchromatic black and white film through an unfiltered lens, different objects in the scene will be imaged in different gray shades depending on their color composition and radiance or brightness levels. It is usually difficult to deduce the actual color of each object since its brightness also contributes to the level of gray recorded in a positive print and represented by the film density in a negative. However, suppose the multicolored scene is photographed through a series of colored filters, each selected to pass a narrow range of wavelengths centered at some dominant wavelength. Consider Figure 1-6. The upper left panel shows a colored geologic map of southeastern Pennsylvania. (See Figure 4-9B for a larger version of the same map.) This map was photographed on standard black and white film through three narrow bandpass filters, centered on segments of the visible spectrum in the blue, green, and red, respectively. Now, look first at the resulting black and white photo made with a blue filter (upper right). Light reflected from the bluer patterns in the map will pass through the blue filter with only moderate absorption (or, said another way, with high transmission); the film negative receiving such light is strongly exposed (high dens. /) and a positive print made therefrom will show the blue areas as light shades. Conversely, the red and orange reflected light is highly absorbed by the blue filter, causing only slight densities in the negative and very dark shades in the print. Greens in the map will show up as intermediate gray shades in this blue band print.

As you might predict, a comparable situation

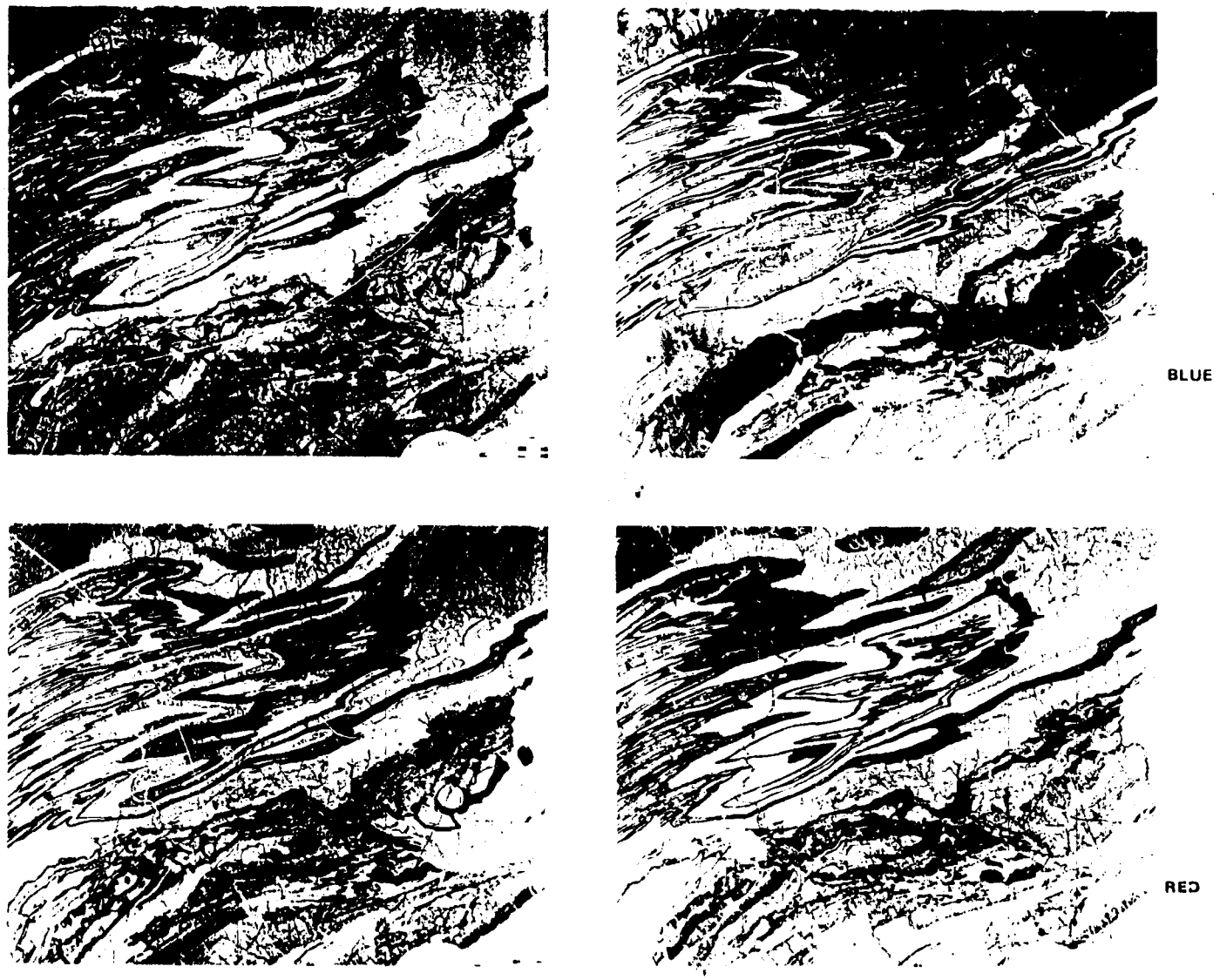

Figure 1-6. Examples of the use of color filters to simulate multispectral photographs. Geological map of southeastern Pennsylvania (see Figure 4-9B) is photographed on panchromatic film using blue, green, and red filters.

may be derived from analysis of the prints produced through use of the green (lower left) and red (lower right) filters in exposing the intermediate negatives. Thus, the green filter nearly completely absorbs the red light, so that reddish patterns appear very dark in the print. Likewise, colors located towards the red end of the visible spectrum will give rise to shades of gray with varying degrees of lightness in the red filter print whereas the original blue tones appear as dark shades. Note also that some colors tend to produce generally dark (or light) shades in all three filter prints, as for example the dark reddish-brown zig-zag pattern prevalent in the left side of the colored map. This results in part from the inherent darkness (level of saturation; see p. 19) of this particular color and also from the nature of brown itself (a mix of red and yellow with black).

It should now be obvious that one can deduce the approximate color of an object or pattern by measurements (or, often, simple visual inspection) of the varying levels of gray in a set of multispectral images or photos made from different bandpass filters, provided the brightness levels are also taken into account. It is also possible to recombine several (usually three) different multiband images through a color additive technique (page 93) to generate a color photo-image. The specific colors thus regenerated depend on the gray level patterns in each multiband image and on the color filters used in the additive process, among other factors. Those color renditions that simulate the original scene colors are called natural color images; those consisting of significantly different colors (e.g., red for green) than their original counterparts are referred to as false color images. Much of Activity 3 is devoted to expounding upon these concepts just introduced here, with emphasis placed on the interrelations between spectral signatures, multiband sampling of radiation, color-brightness characteristics, gray levels, and formation of color products. Examples of multispectral images, mainly those created from data acquired by Landsat sensors, recur throughout this workbook, and especially in Activities 2 and 4.

SPATIAL RESOLUTION

As will become increasingly clear in other parts of this workbook, successful identification of individual classes within an image depends on both *spectral* and *spatial* characteristics of the ground features making up the classes. The role of "spatial" cannot be overstressed. Photointerpretation of conventional aerial photographs relies more heavily on spatial attributes (especially shape, size, and context) than on color or tone properties. In multispectral imagery, this same dependence on pattern, in the geometrical sense, is involved in classification, but the spectral characteristics are often equally important. In fact, some classes may be accurately identified solely by their spectral responses. In remote sensing, the use of pattern recognition in image analysis involves sets of measurements of diagnostic properties that relate to sampling points at specific locations $x_1, x_2, \ldots, x_n$. Because a measured property usually has varying magnitudes, the array of values in measurement space may be represented by measurement vectors.

In the spatial realm, *resolution* is a key parameter which influences the ability to extract useful information. It is important, therefore, to have a clear understanding of the meaning of "resolution."[19]

In the vernacular, 'spatial resolution' defines the fineness of detail depicted in an image. This translates into a measure of the smallness of objects on the ground that can be distinguished as separate entities. This is not a rigorous definition of spatial resolution and lacks an intrinsic quantitative aspect. One problem in understanding resolution is that different definitions have been proposed. Four ways of categorizing spatial resolution are considered here, namely determination based on (1) geometrical properties of imaging systems, (2) ability to distinguish between point targets, (3) ability to measure periodicity of repetitive targets, and (4) ability to measure spectral properties of small finite targets.

In the first category, resolution is determined by sensor characteristics or, more specifically, by certain optical and electronic parameters. Consider a sensor mounted on a platform orbiting the Earth. The portion of the ground scene that is effectively imaged is called the (total) field of view or FOV. The FOV may be quantified as twice the solid angle of viewing, β, measured between a line to the

[19] This treatment of spatial resolution is adapted from an unpublished review by John R.G. Townshend, prepared at Goddard Space Flight Center.

scene center (along the optical axis) and another to the scene edge. Thus, FOV is not necessarily equivalent to the diameter of a lens at the front of a telescope since diffraction, aberrations, and geometrical factors can decrease the sharpness at the edges and might degrade the image to an unusable condition. For a single camera system, the size of the FOV depends on the aperture setting, the focal length of the lens and its light gathering power, and the distance between the camera and a planar target (e.g., the ground).[20] For a scanning system such as the MSS, the geometry of the detector and the sampling rate become the critical factors. A second measure, called the instantaneous field of view or IFOV, must be considered for scanners. Thus, IFOV = Hd/f, where H is the height above the surface, d is the detector size, and f is the focal length of the optics. In essence, IFOV encloses the small section of the scene or surface area that is reflecting or emitting radiation during the instant of sampling (see "pixel," on p. 82.)

The IFOV for Landsat is controlled by the focal length of the optical telescope, the dimensions of the optical fiber pipe (square cross section) leading to the detectors located at the focal plane, and the height of the spacecraft above the Earth. At an altitude of 917 km, a resolution of 79 m quoted for Landsat is just the IFOV of the MSS (equivalent to the base diameter of a narrow cone whose solid angle is 0.086 mrad). This simply implies that, in theory, radiation reflected from a ground area 79 m on a side is recorded as a discrete signal at the detector and is represented by a measurement vector (a spectroradiance value) associated with a picture element or "pixel." In actual fact, the pixel itself has different dimensions, as explained on p. 82. A Landsat scene is constructed from the array of all pixels, built up from sequential IFOV inputs gathered during a single scan across track (the ground "footprint" of the orbiting platform), and repeated through some number of scan lines taken successively along track. The swath width of this scene (as a data array of an image) is set by the ±2.88° angle through which the scanning mirror of the MSS oscillates. This, coupled with the optical parameters of the telescope, gives rise to a viewing angle of 11.56°, defined by the lines projected from the orbiting scanner to the edges of the ground corresponding to the ends of each scan line. The image itself does not occupy the full FOV of the MSS optical telescope, so that some of the aberrations and other distortions introduced by lens edge effects are minimized.

The second category concerns a property of an imaging lens that recreates the image of a single *point* on a target as a diffraction (Airy) pattern in the image plane. The pattern consists of a bright central disc surrounded by light and dark rings. Two point targets become resolved when their angular separation allows the central bright spot of the first point to be on the outermost dark ring of the second. This criterion specifies the absolute achievable resolution for a perfect lens of given aperture and wavelength.

The third case concerns parallel repeating linear patterns in which there is a radiance-level contrast between line pairs and the space separating them (as a light background between two adjacent dark lines). Resolution is measured by the separation at which the contrast between lines becomes too small to permit visual distinction of each as an individual. In practice, one or more groupings of parallel lines are inscribed on a resolution target viewed by the sensor. Sets of lines with different spacings are examined and/or the distance between target and sensor is varied until some narrowly spaced sets blur or merge. This allows resolution to be stated in units of line pairs/mm or cycles/mm. Contrast is measured by a Modulation (M) function, defined as $M = I_{max} - I_{min} / I_{max} + I_{min}$, in which I is a radiant intensity parameter. In turn, the ratio of image to object (target) modulations produces a value between 0 and 1.0, termed the modulation transfer factor. This factor varies with spatial frequency, that is to say, is dependent on the spacing between periodic linear targets. A standard measure of resolution is the FIFOV or Effective Instantaneous Field of View, which is determined as the ground distance corresponding to the number of pairs/mm at the 0.5 (50 percent) modulation transfer factor point. The plot of transfer factor with respect to spatial frequency produces a curve that describes the modulation transfer function, or MTF. In photography, different films have different MTF's, according to their speed or graininess. Thus, when calibrated by a target of contrasting linear objects imaged at some altitude, the resolving power of an aerial film will depend on its MTF and on a line-spread function,

[20] The size of a picture, however, is also governed by frame sizes,

For the MSS, each component of the imaging system has its own characteristic MTF. The resultant MTF of the total system is the product of the individual component MTF's as multiplied; a photo-image of a Landsat scene would include the contribution of the scanner and the film MTF.

In the fourth category, resolution is defined in terms of the effective resolution element (ERE). This element is considered to be a single homogeneous object (normally circular) surrounded by a larger homogeneous object field whose radiance is just 50 percent of the full-scale capability of the measuring sensor. ERE is the minimum area of the central object whose spectral properties may be distinguished from the surrounding field with a 95 percent confidence that the recorded value differs from the actual value by no greater than 5 percent of the sensor full scale value. This approach requires knowledge of the probability distribution of the signal power and takes noise effects into account. Such a measure, based on radiometric as well as spatial characteristics of the signal source (target object), provides a realistic indication of spatial resolution, but difficulties in conducting the measurement on the Earth's surface make it an impractical method.

From the previous paragraphs, we see that different values of spatial resolution will result from the different ways in which this property is measured. Both the IFOV and MTF approaches are most often cited for space-acquired imagery.

Perhaps the easiest way to gain a qualitative insight into the meaning and importance of spatial resolution would be to examine the same scene as imaged at one time under conditions that are identical except for varying resolution. This obviously could be done by mounting several electro-optical scanners, each with a different IFOV (usually accomplished by adjusting detector size), or several photo-cameras, each with different optics and/or film MTF's, on an airplane or spacecraft. Such an experiment is impractical and unnecessary. A simple alternative uses a computer program to progressively "degrade" a high resolution scanner image (acquired in a digital mode) through a sequence of lower resolutions. The initial IFOV (pixel size, in this instance) is combined through resampling (see p. 152) in increments of 2, 3, 4, 8, or other convenient whole numbers. Each newly created larger pixel (lower resolution) represents a radiance averaged from some number of initial pixels. Examine the effect of this technique for deriving resolutions of 20, 30, 40, and 80 meters from original 10-meter IFOV data obtained by a multispectral scanner operated from an aircraft over a test site in Tennessee (Figure 1-7). Note in particular the gradual loss of detail in the street patterns of the town of Maryville, several factory complexes, groups of homes, and the nearby airport. With decreasing resolution (from 10 to 80 m), the ability to identify these classes or features progressively diminishes so that few if any can be recognized by spatial characteristics alone at 80 m. The larger, more homogeneous fields and forest stands retain their identities through the 40-meter rendition but become ambiguous at 80 m. However, both urban features and the field-forest classes display some distinguishing spectral characteristics even at this lowest resolution.

SENSOR SYSTEMS

Let us now resume our analysis of the definition of remote sensing. Sensor systems today are often sophisticated instruments consisting of optical, mechanical, and electronic subsystems. The four components of a typical sensor are (1) Collector (such as a telescope, lens, or antenna), (2) Detector (film, photomultiplier, diode), (3) Signal processor (amplifier, modulator), and (4) Recording unit (photographs, tape recorders, digitizer, strip chart, display system such as TV monitor or CRT [cathode ray tube]) (see Figure 1-1E).

An airborne multispectral scanner (Figure 1-8) is one such typical system. The scanning element is usually a rotating or oscillating mirror that sweeps across a scene in a direction usually normal to a flight path, so that the forward motion of the aircraft is responsible for the advance from one scan line to the next. Radiation from a source or target is collected through a telescopic optical system having either a fixed or an adjustable FOV that defines the scan line width. This radiation must be directed along definite pathways and focused by using lenses, prisms, mirrors, and collimators as required. The multispectral radiation may be subdivided into discrete wavelengths by means of diffracting prisms or gratings, or into wavebands

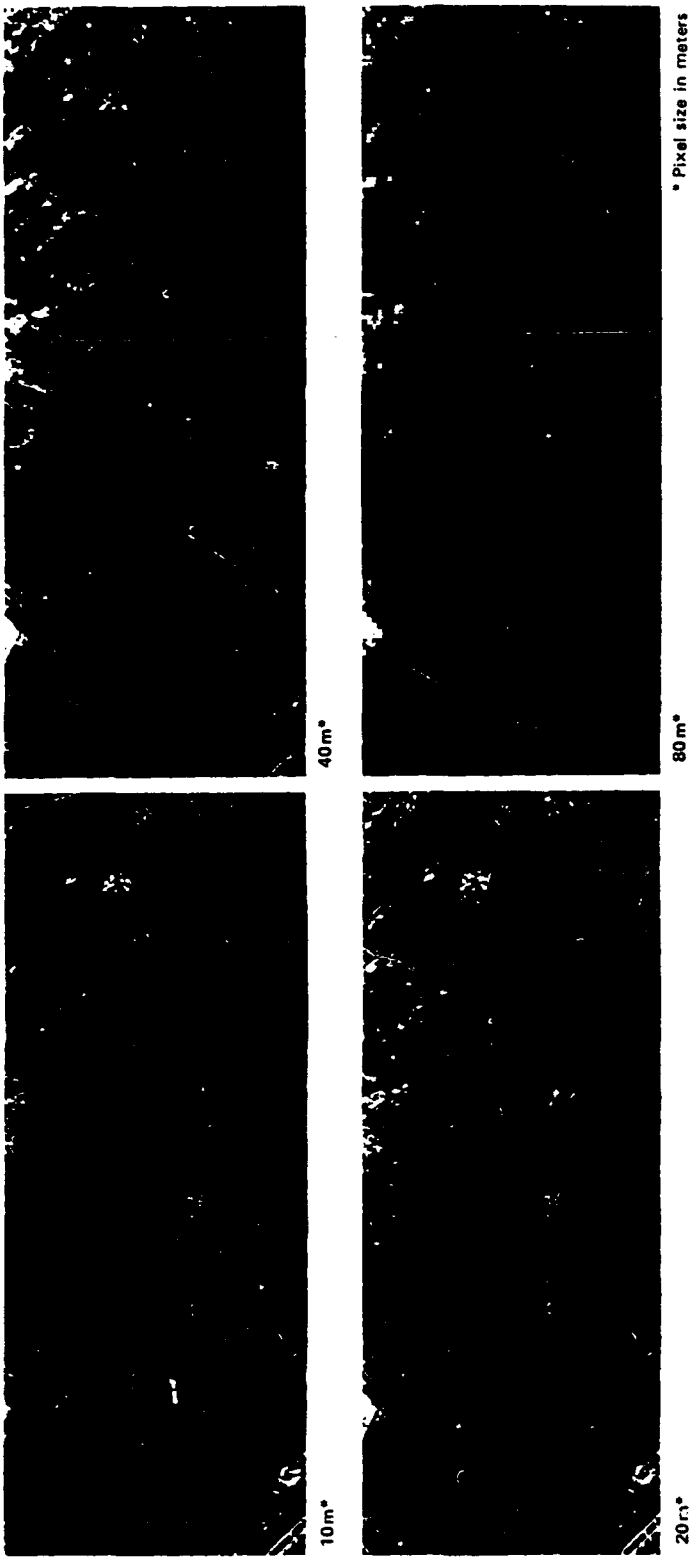

Figure 1-7. The Maryville, Tenn. urban area imaged at five different spatial resolutions. (Produced for the EROS Data Center by Geospectra, Inc.)

by variable or fixed wavelength-interval (band pass) transmission or absorption filters. Some scanners use rotating filter wheels containing one or more interference filters. In one mode, each of several filters samples only one specific wave band. In another mode, a circularly variable filter (CVF) produces different wave bands as a function of changing thickness of the dielectric elements in the interference filter. Each band contains those wavelengths passed through a particular thickness range in the rotating filter as radiation is admitted through a chopper (which alternately transmits or stops the beam). In one setup, the radiation in each band is channeled (e.g., through optical fibers) to a detector sensitive to radiation in that band region. The usually weak signals are intensified by some amplifying (gain) device. These analog signals (as voltages or currents) may be recorded directly or indirectly from within the sensor or transmitted as analog or digital pulses to a receiver elsewhere. The signals are then decoded, if necessary, and played back on an imaging device (for example, an electron beam or laser beam recorder), a strip chart recorder, or, when digitized, within a computer processing system. One component often inserted in the optical train is a chopper, which permits the incoming radiation to be split or interrupted and a second radiation source (usually an internal radiation source for calibration) sampled alternately.

Various detectors may be used in the sensor. For photo-cameras, panchromatic, color, and infrared-sensitive films serve both as detectors and recorders. Most electronic detecters are sensitive to incoming photons or other particles over a limited range. Some typical detectors are photomultipliers (0.3 to 0.9 μm), silicon photodiodes (0.9 to 2.5 μm), and mercury-cadmium-telluride detectors (8 to 14 μm range). For longer wavelengths, particularly, in the thermal region, the detectors must operate at low temperatures (well below 0° C) and are therefore cooled passively (for instance by normal heat dissipation to space, as with the Landsat-3 thermal band) or by some refrigerant in a vacuum bottle or by enclosure in a closed cycle mechanical cooler. This cooling suppresses electronic noise (small, spurious transient signals that make up the background continuum) caused by molecular or electronic motions in the detector. A detector's performance is measured by its signal-to-noise ratio (S/N), which specifies the smallest external signal that can be detected above the noise. For reflected radiation (ρ), this sensitivity measurement is expressed as NE$\Delta\rho$, or the noise-equivalent reflectance (where $\Delta\rho = \rho_s - \rho_n$); for thermal radiation, the parameter is NEΔT.

Remote sensors are classed or named according to how they function. Most are passive systems that measure radiation originating at or reflected from targets illuminated by natural means. A few are active systems that generate their own radiation output (for example, radar waves) beamed to irradiate the target and then sensed as a return signal. Among the principal sensor classes are (1) Radiometer (measures radiation in a single wavelength interval or band, such as microwave), (2) Photometer (measures intensity of light [photon counter] in all or part of the visible spectrum), (3) Spectroradiometer (measures more than one spectral interval; multiband or multichannel instrument), (4) Spectrometer (measures continuous spectral radiances [at discrete wavelengths] over some wavelength interval), (5) Radiation Counter (measures quantity or intensity of radiation by some integrating or discriminating device), (6) Scanner (measures spatial distribution of radiances by scanning across a target or object, usually by means of a rotating or oscillating mirror), and (7) Camera (measures light or other radiation that can be recorded on film; also provides a spatial distribution pattern or image of varying radiation intensities).

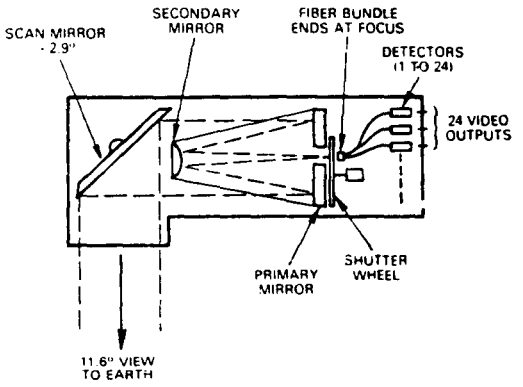

Figure 1-8. Schematic engineering cutaway drawing of the Landsat Multispectral Scanner (MSS).

SENSOR PLATFORMS

To be used efficiently, a sensor must be mounted on a stable platform. The simplest of these is the familiar tripod holding a camera that produces still photographs or movies. Cameras, radiometers, spectrometers, and other sensors can be mounted on mobile platforms attached by jointed booms ("cherry picker") to trucks for variable distance near-surface operation. In remote sensing, most practical uses of sensors require them to be in motion well above the ground so as to accommodate large fields of view and to cover extended areas during a single mission. Balloons, either tethered or free, provide one such platform. The best known platforms are aircraft of various kinds; they include low (less than 20000 ft), medium (20000 to 40000 ft) and high (more than 40000 ft) altitude airplanes (both piston and jet engines), helicopters and other hovercraft, sailplanes (gliders), dirigibles, and drones. From these platforms come numerous types of aerial photographs which, until recently, were the most common remote sensing products in terms of numbers of individual scenes acquired per annum. Other sensors, including radiometers, scanners, and radar units, are also flown on airborne platforms. One disadvantage experienced by some sensors is the influence during air flight of irregular movements (pitch, roll, and yaw effects, and changes in altitude) on time-dependent (not instantaneous) measurements, such as are made by scanners. These introduce distortions into the data sets; images from a flight strip will often display elongation or shortening, and discontinuities.

Since the advent of the space era, platforms have moved into outer space, above the disturbing (wind prone) air masses. Earliest uses of space systems included sounding rockets or probes with mounted cameras and hand-held cameras operated by astronauts during the Mercury and Gemini missions. The Apollo astronauts used multispectral cameras during Earth-orbiting missions as well as lunar excursions. Several new sensor systems, designed for space operations, were tested during the Skylab missions from 1973 into early 1974. Included were multispectral cameras, an Earth terrain camera (high resolution, large area), a continual sweep multispectral scanner, an infrared spectrometer, a microwave scatterometer, and a microwave radiometer.

Various sensors, including infrared radiometers, scanners and television imagers, have flown on some unmanned satellites. Metsats, or satellites used to make meteorological observations, have carried such instruments since the early 1960's. The Nimbus and TIROS series of satellites offered frequent surveys of large areas of the terrain as a by-product of meteorological data gathering. These programs provided some early insight into the value of synoptic observations of land surfaces, with applications to Earth resources in mind.

The present Landsat program evolved from such programs as Nimbus, Gemini, and the S0-65 experiment on Apollo-9. Landsat is a dedicated platform (see Figure I-1) hosting sensors designed specifically for Earth resources observations. Landsat-1 was launched on July 23, 1972, Landsat-2 was orbited on January 22, 1975, and Landsat-3 on March 5, 1978.

This activity can now be closed. However, before proceeding to the next activity, you should once more consider the working definition of remote sensing on page 10. Ask yourself what you learned and can better appreciate about each of the key words you underlined at the outset, now that you have explored some of the details and implications developed for these terms in the exposition that followed. Then, in your mind or in your notebook, record for posterity your own definition of remote sensing in as few words as possible make it a "one-liner."

N83
10460

UNCLAS

ACTIVITY 2

FAMILIARIZATION WITH LANDSAT IMAGERY

LEARNING OBJECTIVES:

- *Know how to read the annotation on a Landsat image.*
- *Become acquainted with characteristics of 1:1,000,000 scale transparencies and prints of Landsat Multispectral Scanner (MSS) images.*
- *Take note of the general information visible in these Landsat photo products.*
- *Be aware of the changes of appearance of any ground feature or class in the black-and-white images made from the four MSS bands and note the characteristic color of each class in color composites.*
- *Determine the degree to which a Landsat image meets map accuracy standards and can be fitted to map projections.*
- *Assess the effects of Landsat enlargements and scale changes and of the limitations of Landsat resolution relative to aerial photos.*
- *Observe the influence of time of acquisition (season) on a Landsat scene.*
- *Get a feel for image quality as dependent on processing and photo reproduction.*
- *Appreciate the unique characteristics of the Return Beam Vidicon (RBV) and thermal band imagery obtained from Landsat-3.*
- *Be familiar with certain attributes of adjacent Landsat images which permit them to be joined in mosaics and to be viewed in stereo.*

This activity effectively serves to introduce you to what can be learned in general from a Landsat image. We shall work mainly with a well-known scene imaged by Landsat during exceptional viewing conditions on October 10, 1972. This image shows most of New Jersey and nearby New York City and Philadelphia.

READING LANDSAT IMAGE ANNOTATION

To open this activity, let us learn to "translate" the information that appears in the annotation header at the bottom of any Landsat frame. (See Figure 2-1, a color composite image of the New York City/Philadelphia/New Jersey area taken during the October 10, 1972 overpass.) Entries in the annotation and along the image margin provide a quick way to locate any Landsat scene in its proper geographical context. The most important points are marked by lettered arrows at the bottom of Overlay 1 (tied to the annotation on this scene). These are explained as follows:

a. The Landsat frame identification (ID) number. The first four numbers are coded to *days* (last three digits) after launch of Landsat-1 (1000 and 5000 series) and Landsat-2 (2000 and 6000 series). For Landsat-3, five numbers (30000 series) are used. Following a dash, the second five numbers for each Landsat represent the hour (digit positions 1 and 2), minute (digit positions 3 and 4), and tens of seconds (digit position 5) relative to Greenwich Mean Time (GMT) at the time of observation. For example, if the MSS scans a midwestern United States scene between 23 and 48 s (a full frame takes 25 s to acquire) after 9:45 a.m. (standard time in that zone), the orbit would be recorded as acquired at 15:45:3 (where 3 indicates the nadir point time at 35 s, in the third set of tens), the corresponding time at the Greenwich Observatory outside London, six time zones to the east. If this image is acquired by Landsat-1, 183 days after launch, its ID number is 1183-15453.
b. The calendar date of Landsat frame data acquisition.
c. The latitude-longitude coordinates of the principal point (format center) of the scene.
d. The latitude-longitude coordinates of the nadir point.
e. The specific sensor band (1,2,3 = RBV for Landsats 1 and 2; A and B for pair of RBV's on Landsat-3); (4,5,6,7 = MSS reflectance bands); (8 = MSS thermal channel on Landsat-3), also indicated to right of second dash in notation A.
f. The elevation (EL) and azimuth or compass bearing (AZ), in degrees, of the Sun at the time of acquisition.

Additional details on this annotation, especially as it has been modified since early in 1977, are presented in the summaries prepared by the EROS Data Center and reproduced as Tables 2-1A and 2-1B.

#2-1: Examine the annotation at the bottom of Figure 2-1. Record its (a) scene ID, (b) nadir point coordinates, (c) Sun elevation, (d) date of acquisition, (e) sensor band.

The foregoing annotation system provides immediate information pertinent to an image already in hand. However, in many instances, the prospective user needs to know whether a region or a smaller area has been imaged by Landsat on some given date or within a particular time period. The percentage cloud cover at those times and the quality of the imagery are also important factors in choosing suitable scenes. From 1972 through early 1979 this basic information was recorded in U.S. and Foreign Catalogs prepared and issued quarterly by Goddard Space Flight Center. Since 1979 this function has been assumed by the EROS Data Center (EDC), at Sioux Falls, S.D.

The EDC also publishes sets of maps, each consisting of an index to Landsat coverage of a broad region over some specified period (usually a year). These maps specify nominal-scene coverage for data acquired at receiving stations in the United States (Landsat data obtained at foreign stations are cataloged by and available from the operating country). These nominal (named) scenes are located on a path-row coordinate system implemented initially by the Canada Center for Remote Sensing, then adopted by EDC for all of North America, and later extended into a Worldwide Reference System. The map sheets (1:18,000,000) make up the World Plotting Series (North America; South America; Eurasia; Africa; Oceania; Arctic Ocean; Antarctica).

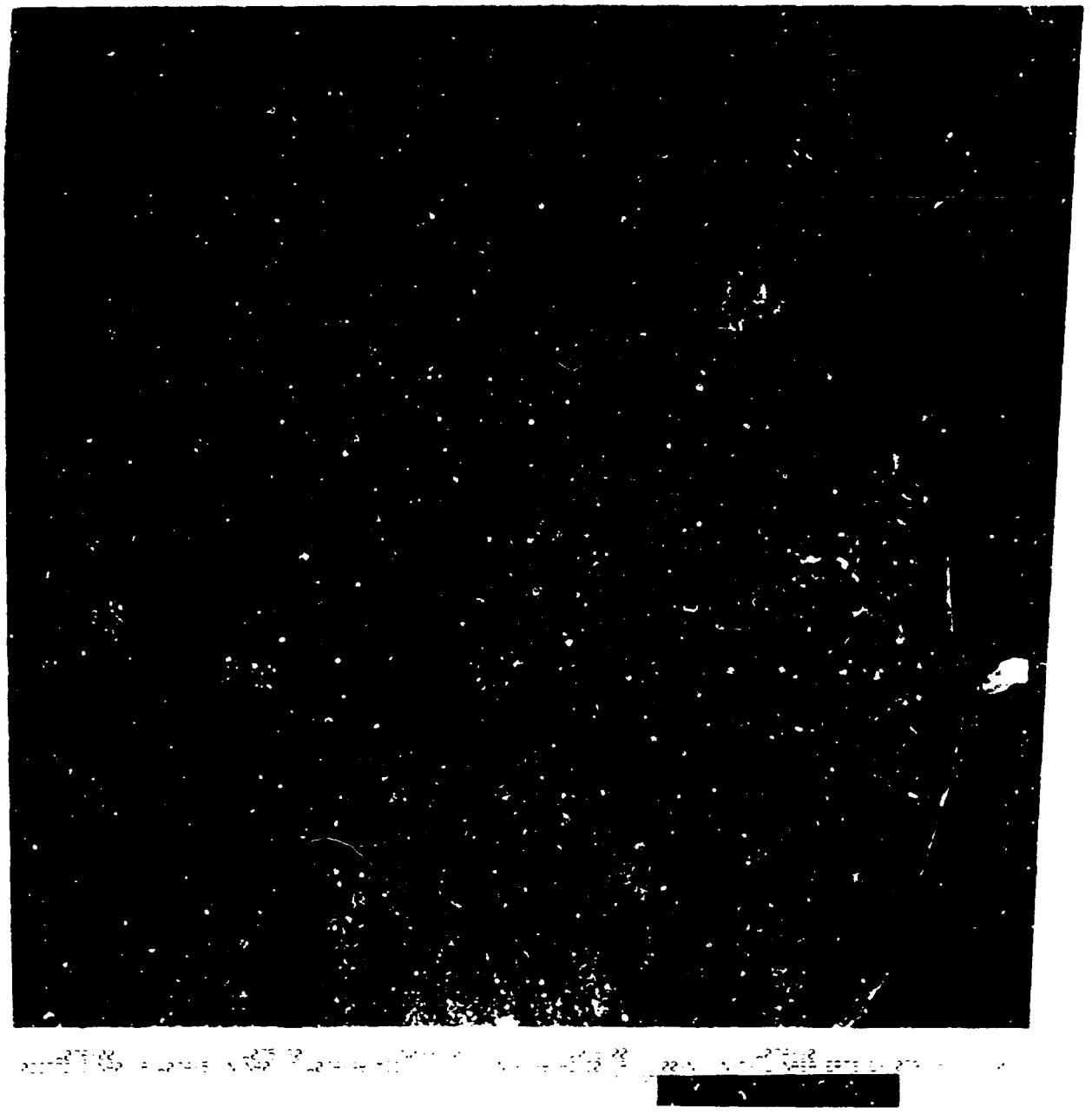

Figure 2-1. False color image of the New York City - New Jersey - Philadelphia scene obtained by Landsat on October 10, 1972.

Table 2-1A
Explanation of the Alphanumeric Annotation of Landsat Imagery

Original annotation in use from July 23, 1972 to Feb. 17, 1977

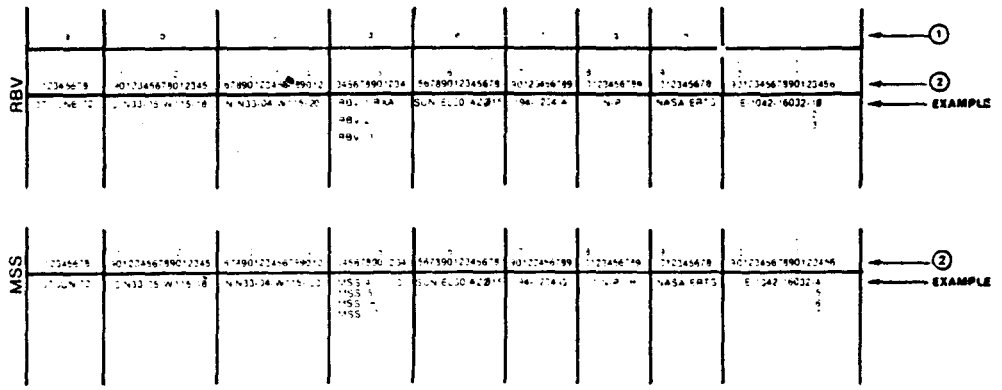

a. Character Positions 01-08.
#7 JUN 72 Day, month and year of picture exposure.

b. Character Positions 09-25.
CN33-#5/W115-18
Format Center — latitude and longitude at the center of the RBV and MSS image format is indicated in degrees and minutes. MSS and RBV format centers are identical. Format center is the geometric extension of the spacecraft yaw axis to the earth's surface.

c. Character Positions 26-42
N 33-#4/W115-2#
Latitude and longitude of the nadir, the intersection with the earth's surface of a perpendicular line from the spacecraft to the earth ellipsoid, is indicated in degrees and minutes. The NASA Ellipsoid is the Earth model.

d. Character Positions 43-54
RBV - DXA
Characters in this group are sensor and spectral band specific.

For RBV images:

(3) 43-49 Sensor and NDPF spectral band identification code.

50 — "D" indicates direct transmission.
"R" indicates stored data played back from the satellite WBVT recorder.

51-52 RBV Shutter Duration Code. "XA" means the shutter for Camera 1 was set for 4.0 milliseconds, Camera 2 for 4.8 ms., and Camera 3 for 6.4 ms. "XB" would indicate the shutter setting for Camera 1 is 5.6 ms, Camera 2 is 6.4 ms and Camera 3 is 7.2 ms.

Alpha-betic Code	Camera 1	Camera 2	Camera 3
A	4.0	4.8	6.4
B	5.6	6.4	7.2
C	8.0	9.8	9.8
D	12.0	12.0	12.0
E	16.0	16.0	16.0

53-54 Aperture Correction Indicator
"#" — Aperture correction in.
"0#" — Aperture correction out.
"#" — blank

For MSS images:

43-51 Sensor and NDPF spectral band identification code.

50 — "D" indicates direct transmission.
"R" indicates stored data played back from the satellite WBVT recorder.

e. Character Positions 55-68.
SUN EL 3# AZ# 15
Sun Angles — Sun elevation angle and sun azimuth angle measured clockwise from true North at the time of RBV exposure or midpoint of MSS frame is specified to nearest degree.

f. Character Positions 69-79
194-1234-A

Character Positions 69-71
Spacecraft heading to nearest degree, measured clockwise from true North at its orbital path plus spacecraft yaw. Heading relative to an image is always toward the image annotation block.

Character Positions 73-76.
Four digit orbit revolution. Rev "0001" starts with the first ascending node (south to north equator crossing) after launch.

Character Position 78.
Ground recording station: G-Goldstone, A-Alaska, N-NTTF.

g. Character Positions 80-89.
N-N-P-1H

Character position 81 indicates image is full size.

Character position 83 indicates type of processing procedures used.
N = Normal
A = Abnormal

Character position 85 indicates ephemeris data used to compute image center.
P = predicted orbit
D = definitive or best

Character position 87 indicates mode of MSS signal processing prior to transmission from satellite to ground station.
(4) 1 = linear mode
2 = companded mode

Character position 88 indicates gain.
"H" = high gain
"L" = low gain (for Bands 4 and 5 only which have a commandable gain option.)

h. Character Positions 90-98.
NASA ERTS.

Identifies the Agency and the Project.

i. Character Positions 99-114
E-1#42-16#32-1#
Frame Identification Number — each image or frame has a unique identification number whose format is E-ADDD-HHMMS-BCRR where:

E — Encoded Project Identifier
A — Landsat Mission
1 = Landsat 1
2 = Landsat 2
DDD — Day number relative to launch at time of observation
HH — Hour at time of observation
MM — Minute at time of observation.
S — Tens of seconds at time of observation
B — NDPF Identification Code (RBV 1, 2, 3. MSS: 4, 5, 6, 7).
C — Blank for earth images. Either #, 1 or 2 for RBV radiometric calibration images indicating lowest to highest exposure level respectively.
RR — Regeneration number indicates the re-run of a video tape in the event of a malfunction in the prior run.

NOTES: (1) THE LETTERS "a" THROUGH "i" REFER TO PARAGRAPHS IN THIS DOCUMENT THAT EXPLAIN THE ANNOTATION BLOCK.

(2) CHARACTER "POSITION" IN THE ANNOTATION BLOCK.

(3) SPECTRAL IDENTIFICATION CODE NUMBERS ARE STAGGERED TO PERMIT IDENTIFICATION OF THE SPECTRAL IMAGES USED TO MAKE A COLOR COMPOSITE TRANSPARENCY.

(4) COMPRESSED DATA WILL BE DECOMPRESSED DURING PROCESSING.

ORIGINAL PAGE IS
OF POOR QUALITY

Table 2-1B
Explanation of the Alphanumeric Annotation of Landsat Imagery

Annotation in use for NDPF-produced imagery from Feb. 18, 1977 to Jan. 15, 1978

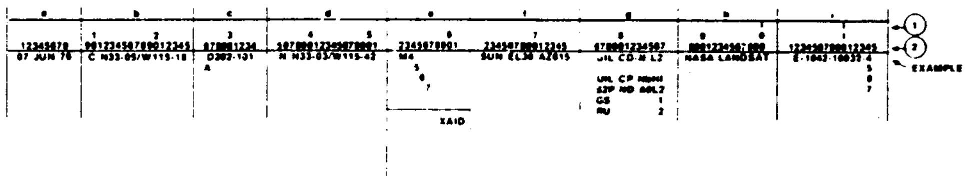

Annotation in use for NDPF-produced imagery from Jan. 16, 1978 to mid-1978

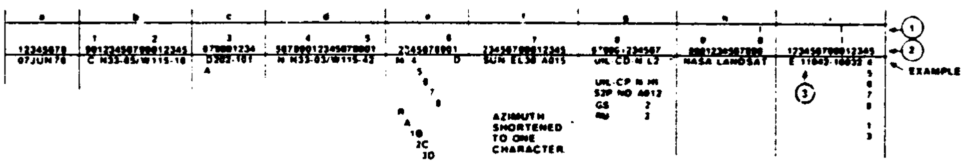

Annotation in use for IPF/EDIPS-produced imagery after mid-1978

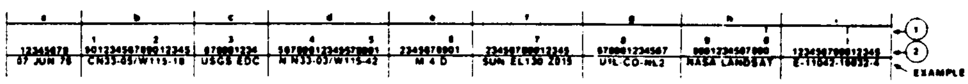

a Character Positions 01-08
(4) → Ø7 JUN 76Ø Day, month and year of picture exposure

b Character Positions 09-25
CØN33-Ø5 W115-18Ø
Format Center — latitude and longitude at the center of the RBV and MSS image format is indicated in degrees and minutes

c For NDPF-produced imagery
Character Position 26-34
D202-101Ø
The D indicates spacecraft is descending, an A indicates spacecraft is ascending. Nominal path and row identifier. The 202 is path number and 101 is row number.
For IPF EDIPS-produced imagery
USGS-EDC Image produced by U.S. Geological Survey EROS Data Center

d Character Positions 35-51
NØN33-Ø3 W115-42Ø
Nominal latitude and longitude

e Character Positions 52-61
Characters in this group are sensor and spectral band specific

For RBV images

52-56 Sensor spectral band or Landsat 3 RBV subscene ID designation

57-58 RBV Shutter Duration Code. For Landsat 1 and 2 it is the same as [illegible]

59 Aperture Correction Indicator
I - Aperture correction in
O - Aperture correction out

60 D indicates direct transmission
R indicates stored data played back from the satellite WBVT recorder

61 Blank

For MSS images

52-58 The sensor spectral band identification code

60 D indicates direct transmission
R indicates stored data played back from the satellite WBVT recorder

61 Blank

f Character Positions 62-75
SUNØEL3ØØ AØ15Ø
Sun Angles — the sun elevation angle and sun azimuth angle measured clockwise from true North at the time of midpoint of MSS frame is specified to the nearest degree. Blank for ascending mode coverage.

g Character position 76 defines the type of geometric correction applied to the data
U uncorrected
S system level
G geometrically corrected based on geometric GCP's
R geometrically corrected based on relative GCP's

Character position 77 indicates the scale of the image
1 185 km x 185 km (100 nm x 100 nm)
2 92.5 km x 92.5 km (50 nm x 50 nm)
3 185 km x 170 km [illegible]

Character position 78 defines the projection
L Lambert projection
P Polar Stereo projection
H Hotine Oblique projection
S Space Oblique Mercator projection
U UTM projection
N Natural perspective

Character position 80 indicates the resampling algorithm
C cubic
N nearest neighbor

Character position 81 indicates the type of ephemeris data used to compute the image center
P predictive
D definitive (for system level correction only)

Character position 83 gives the processing procedure
N normal processing procedure
A abnormal processing procedure

Character position 84 defines whether an Earth image or RBV calibration image has been processed
blank Earth image
Either Ø, 1 or 2 RBV Radiometric calibration images indicating lowest to highest exposure level respectively

Character position 85 indicates the sensor gain options
H = high gain
L = low gain

Character position 86 shows the type of MSS transmission
1 = linear mode
2 compressed mode

h Character Positions 88-100
NASAØLANDSATØ
Identifies the agency and the project

i Character Positions 101-115
E-11Ø42-16Ø32-4
Each scene has a unique identification number whose format is E-ADDD-HHMMS where
E Encoded Project Identifier
A Landsat Mission
1 Landsat 1
2 Landsat 2
3 Landsat 3
DDDD Day number relative to launch at time of observation
HH Hour at time of observation
MM Minute at time of observation
S Tens of seconds at time of observation
Each image or subscene is identified by a number or letter separated from the scene ID by a dash representing the spectral band or subscene (RBV 1, 2, 3, MSS 4, 5, 6, 7, 8, RBV A, B, C, D).

NOTES (1) THE LETTERS "a" THROUGH "i" REFER TO PARAGRAPHS IN THIS DOCUMENT THAT EXPLAIN THE ANNOTATION BLOCK
(2) CHARACTER "POSITION" IN THE ANNOTATION BLOCK
(3) CHARACTER ADDED TO ACCOMMODATE DAY — 1000 AND GREATER RELATIVE TO LAUNCH
(4) Ø BLANK

A larger-scale coverage map for the United States that illustrates the path-row system is reproduced in Figure 2-2. Each individual Landsat scene for any particular pass (date) tends to have its principal point located near some geographical location. Principal points for a series of repetitive passes over time will cluster around that location (usually within 10 km) owing to orbital perturbations. Some combination of three-digit path and row values specifies each nominal scene as, for example, path 024-row 031 for Chicago, in Figure 2-?.

#2-2: Referring to Figure 2-2, determine the path-row numbers for the closest nominal scene for the following locations: (a) Philadelphia, Pa. (b) Waco, Tex., (c) Boise, Idaho.

#2-3: What is the upper limit of different nominal scenes (both along an orbital path and an adjacent one) which can image the same locality (say, a town)?

As an example of a location outside the United States, the path-row coordinates for Perth, Australia, are 120-083.

The path-row index number for any nominal scene does not uniquely select any given image (which has exclusively one frame identification number). To order an image from EDC (see Appendix E), one must indicate desired date(s) and maximum acceptable cloud cover along with the path-row number. Information on all passes over the nominal scene that meet these conditions can be provided by EDC to aid in the final selection. If feasible, it is best to visit some nearby Landsat Browse Facility (Appendix E) to inspect the images on file before making a choice.

PINPOINTING FEATURES IN AN IMAGE

If you are well-traveled and have developed some geographical "savvy," you will probably recognize certain landmarks and regions in many Landsat images just by looking. Others will be less familiar and must often be identified by consulting some reference. You no doubt reacted to your first glance at Figure 2-1 by easily recognizing several well-known features. Let us see what else you can locate in this image. A grid extracted from the one used throughout *Mission to Earth* has been drawn on Overlay 1 in the back pocket.

#2-4: Using the grid coordinates (e.g., L-13) list any major geographical features that you recognize from your experience. Then, referring as needed to the National Geographic Atlas (or other atlases as convenient), locate by grid coordinates these less obvious places:

a. Paterson, N.J.
b. Schuylkill River
c. Sandy Hook, N.J.
d. Reading, Pa.
e. Delaware Water Gap
f. Staten Island, N.Y.
g. Wilmington, Del.
h. Pocono Mountains
i. Barnegat Bay
j. Allentown, Pa.

CHARACTERISTICS OF EACH BAND

Next, refer to the four black-and-white images in Figures 2-3A and B. These images are arranged in the order of bands 4 through 7, the four channels on the Landsat multispectral scanner (MSS) that sense reflected radiation.

#2-5: Which band is the darkest overall?

#2-6: Which is lightest in tone?

#2-7: Which band shows the greatest photo contrast (range of light and dark gray tones)?

#2-8: Speculate on why band 4 appears somewhat "washed out." (Hint: think "atmospheric.")

#2-9: In which bands are urban areas best picked out? In which bands are these areas dark?

#2-10: In which bands are lakes and river drainage patterns most easily outlined?

#2-11: Can you guess why most of the land surface in band 6 and 7 images appears light in tone? (Hints: check the spectral range of these bands [Table I-1] and also examine the spectrometer curves shown on page 91.)

#2-12: Which band best shows mountain ridge patterns? Speculate on the reason.

#2-13: Is Atlantic City, N.J., in this scene?

#2-14: Can you find segments of the Pennsylvania Turnpike (give coordinates)? The New Jersey Turnpike? Is (are) any band(s) better than others for discerning these roadways? Why?

#2-15: Carefully look over the metropolitan region centered around New York City as displayed in any or all of the black-and-white and color renditions. Use a magnifying glass or hand lens if necessary. From your general knowledge of this well-known region, locate any recognizable major geographical points of interest (such as Central Park) and describe how you recognized them. Now, compare your observations with those on a map (see a suitable atlas) of the region. How well did you do? Can you broadly zone the main urban and suburban sections; if so, on what basis?

SYNOPTIC CHARACTER OF LANDSAT IMAGERY

Returning to the full New Jersey scene (Figures 2-1 and 2-3) the *synoptic* (expansive area) view afforded by Landsat embraces an extensive piece of "real estate" extending through the northern two-thirds of New Jersey, part of eastern Pennsylvania, and sections of New York and Delaware. This scene includes six *land regions* or *physiographical provinces* of major significance to geographers and geologists, namely the following:

1. *Appalachian Plateau*: The region is characterized by flat and moderately dipping (folded) sedimentary rocks. However, recent uplift has increased the stream gradients so that erosion has produced strong relief, giving rise to mountainous terrain (e.g., Pocono Mountains).

2. *Appalachian Ridge and Valley*: This province runs continuously from New York to Alabama and is characterized by narrow linear or arcuate ridges (for example, Kittatinny Mountains) of resistant rocks (sandstones) and broad valleys of weaker rocks (shales, carbonates). These rock units are strongly folded.

3. *New Jersey Highlands*: This upland region is underlain by gneiss and other igneous and metamorphic units and is marked by flat-topped mountains and numerous lakes. The province is narrow in this scene but widens to the north and east to form the Hudson Highlands in New York and the Berkshires, Taconic Mountains, and Green Mountains in western New England.

4. *Piedmont*: The region is underlain by crystalline rocks (granitic intrusions, metamorphic belts) that tend to form rolling hills and weathered, soil covered lowlands which often reflect the structural lineations within these strongly deformed units.

5. *Triassic Lowlands*: In places, the Piedmont province has been involved in later geological events that formed distinct lowlands (usually fault-bounded grabens) invaded by igneous intrusions. In this scene, the major event was confined to intrusion of basalt dikes and sills, which are expressed as distinct ridges and hills (for example, the Palisades and the Watchung Mountains).

6. *Atlantic Coastal Plain*: This region is marked by gentle lowlands and nearly flat areas underlain by almost horizontal shallow marine sedimentary rocks dipping eastward. The western surface is given to extensive agriculture. To the east, forests, salt marshes,

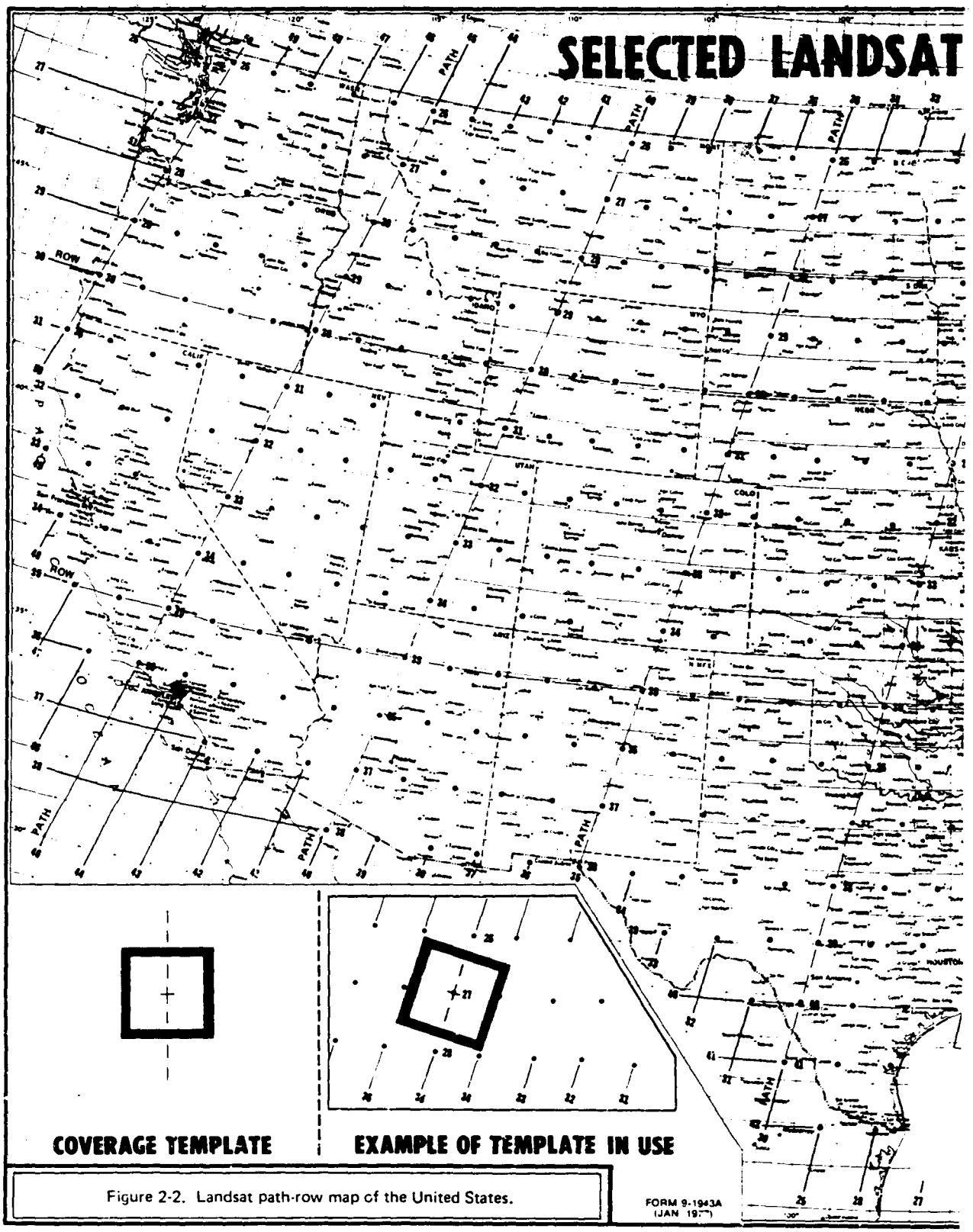

Figure 2-2. Landsat path-row map of the United States.

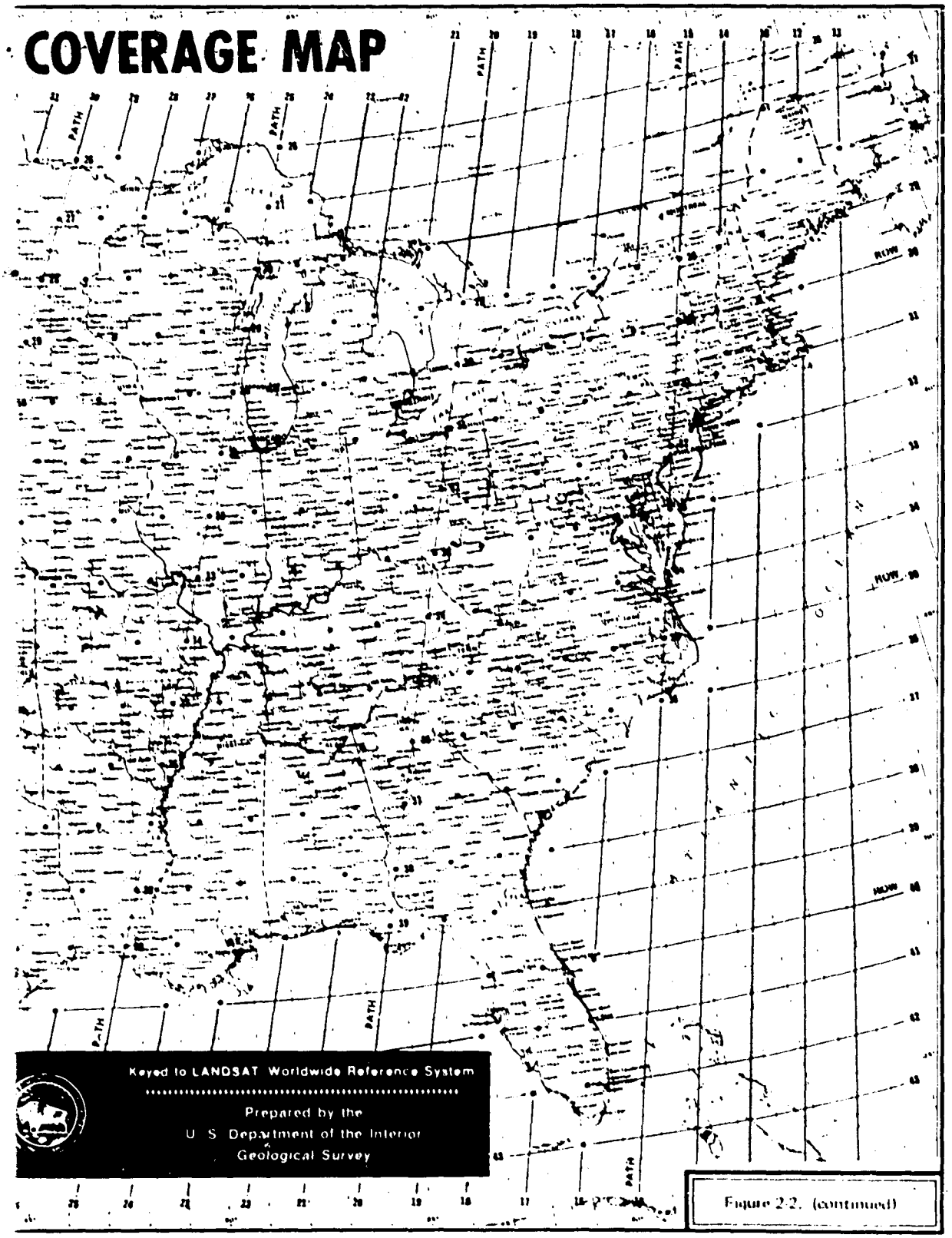

Figure 2-2. (continued)

Figure 2-3A. Band 4, October 10, 1972 scene.

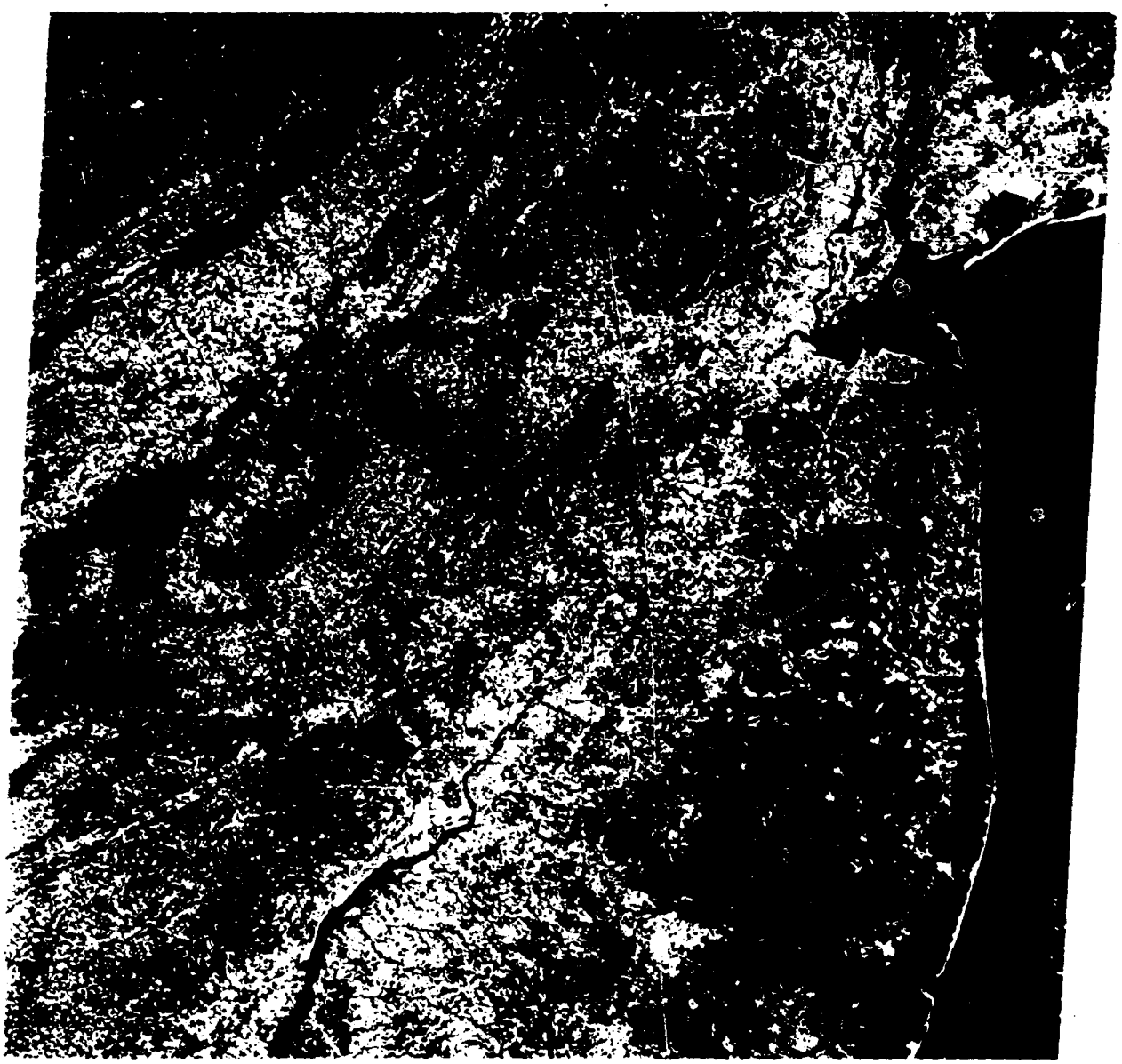

Figure 2-3B. Band 5.

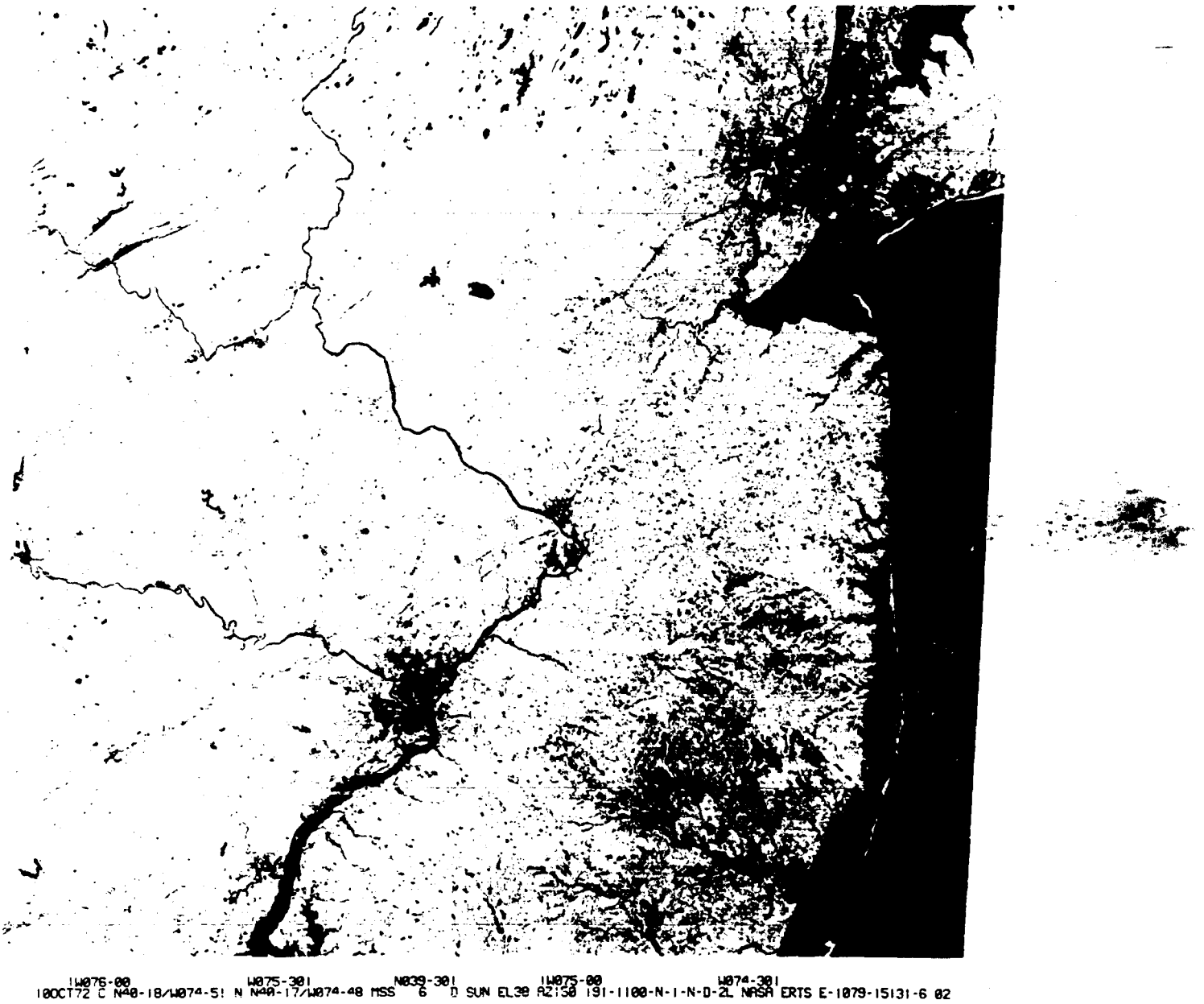

Figure 2-3C. Band 6.

ORIGINAL PAGE
BLACK AND WHITE PHOTOGRAPH

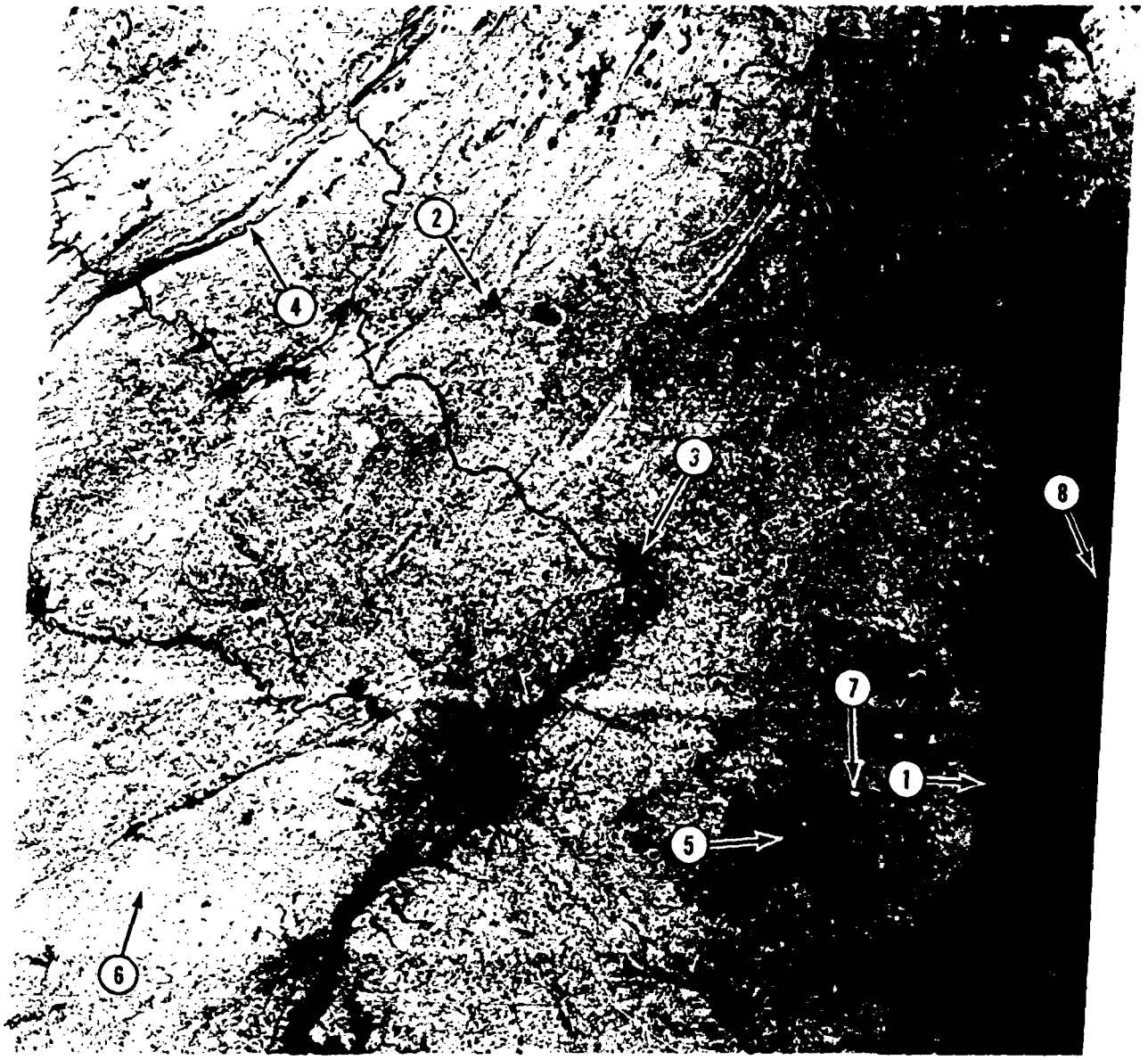

Figure 2-3D. Band 7. (Numbers relate to Figure 3-4.)

and meadows grade into brackish water bays and lagoons enclosed by barrier islands that make up a distinctive coastline, in a sense a distinct province of its own.

#2-16: With these descriptive guidelines, try to recognize each province in the fall scene. You should mark with a grease pencil the estimated boundary separating each province on Overlay 1 (back pocket). After completing the task, compare your choice with some appropriate physiographical map such as those drawn by Raisz, Strahler, or others, as reproduced in many general geography or geology texts.

GEOMETRICAL FIDELITY

One of the most desirable attributes of a Landsat MSS image is that it can be used "as received" as an effective base map on which data acquired in the field or transferred from other maps may be plotted or sketched. In fact, geometrically corrected Landsat images now meet national map accuracy standards for 1:250,000 scale maps.

After undergoing geometrical corrections (see pp 425 to 431) at the Goddard Image Processing Facility (IPF), the images are nearly orthogonal (i.e., distortions due to oblique viewing beyond the nadir point have been minimized). By means of ground control points the images can then be transformed to a specific cartographic projection. Initially, the IPF fitted images to the Universal Transverse Mercator (UTM) projection. In 1978, this projection was replaced by the Hotine Oblique Mercator Projection, an approximation to the Space Oblique Mercator Projection. Landsat images can be presented in still other projections most easily accomplished by computer-assisted transformations.

Overlay 2 (back pocket) is a transparent copy of a map of sections of New York, New Jersey, and Pennsylvania, as reproduced from part of the 1:1,000,000 Albers Conical Equal-Area Projection appearing in the National Geographic Society Atlas (1963 edition). The New Jersey scene imaged in 1079-15131 is situated in this map. Try your hand at matching the map with any of the bands in Figure 2-3 by moving it into position and then fixing it with mounting tape. You can also attempt to match the overlay with the band 5 transparency of this scene (see back pocket) by placing them on a light table or a viewgraph projector, or by simply holding them against a daylight window.

#2-17: How well does the map fit the image? Where are the largest discrepancies?

Note that true (geographical) north is not perpendicular to the upper horizontal edge of a frame but meets it at a high angle slanted left. Also, the side edges (swath boundaries) of a frame are nonvertical this results from progressive westward shifts of the scan lines after adjustment to correct for the rotation of the Earth under the spacecraft while it moves along its orbital path on the daylight side.

Effects of Scale Changes

Useful information can be cross-correlated between Landsat images and maps drawn or reproduced over a wide range of scales (typically, from 1:24,000 to 1:10,000,000). As an example, obtain a copy of the 1:250,000 AMS map of part of New Jersey and Pennsylvania (NK 18-11; Newark) sold for $2.00 by the U.S. Geological Survey (see Appendix E). Locate common features on the map and the Landsat scene in Figures 2-1 and 2-3, and thereby familiarize yourself with interrelating the features in an image and their counterparts on a map at a different scale.

There are several convenient ways to facilitate this comparison for more practical purposes such as map updating, detection of changes, or interpretation. One way is to enlarge (or reduce) part of a Landsat image to the scale of the map. This is demonstrated in Figure 2-4, in which a section of a Landsat scene covering New York City and Philadelphia in the spring of 1975 (30044-

Figure 2-4. Enlargement of part of Landsat scene 30044-15011, band 7, April 1978 to a scale of approximately 1:250,000.

15011, band 7; see Figure 2-11B) has been enlarged by standard darkroom methods to *ca.* 1:250,000.

#2-18: Locate this subscene on the map by using the city locations and the river patterns as guides. Comment on the changes in image quality introduced into this enlargement.

#2-19: Estimate the scale of the maximum enlargement you might achieve photographically, beyond which "fuzziness" would severely hamper your ability to extract useful information.

Another way to match a Landsat image at one scale with a map at another scale is to use an optical device such as the Zoom Transfer Scope (ZTS) (Figure 2-5A) manufactured by Bausch and Lomb, Inc. The ZTS will permit registration (superposition) of and comparisons between images and maps that differ in scale by factors of 14 or less. If you have access to a ZTS-type device, try to register the band 5 image in Figure 2-3 or the band 5 transparency (back pocket) of this same scene (1079-15131) with the corresponding areas in the AMS map. The ZTS can be equipped with a 35-mm or a polaroid camera mounted along the viewing axis to allow the registered image pair to be photographed.[1] Since most readers will not have a ZTS available, the photographic results of combining the 1:1,000,000

[1]When a ZTS or an equivalent device are not at hand, a simple way to fit a Landsat image at one scale to a map at another scale is to produce a 35-mm slide of the image (some distortion will probably result) and project in a darkened room onto a map mounted on a wall. A scale fit is achieved by moving the projector back and forth.

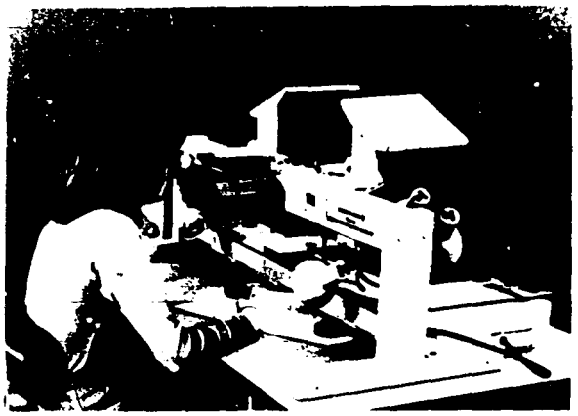

Figure 2-5A. The Zoom Transfer Scope (ZTS) in use.

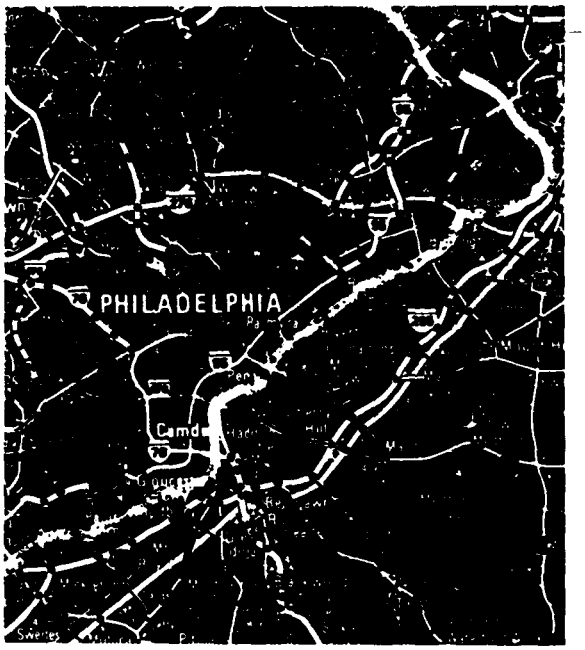

Figure 2-5B. Photo taken through ZTS showing superposition and registration of 1:500,000 road map (rephotographed in white) on October 10, 1972 1:1,000,000 Landsat scene.

color image from Figure 2-1 with a 1:500,000 AAA road map, as would be seen looking through the binocular viewer of the ZTS, are presented here as Figure 2-5B. At any scale full image dimensions are equivalent to a scene whose outline is about 185 km (115 statute miles; 100 nautical miles) on a side.

#2-20: Approximately how many square miles are enclosed in a Landsat frame? Square kilometers? Acres? (Note: there are approximately 640 acres in a square mile.)

Effective resolution (at optimum contrast) of ground features is about 79 m (255 ft) across a scan line. This resolution is also related to pixel size, which depends on the instantaneous field of view (IFOV), detector geometry, sensor optics and signal sampling rates.[2] It is almost achievable in the best computer-generated images but is poorer in standard contact prints.

Comparison with Aerial Photos

It will be instructive at this point to gain a feeling for just how well Landsat represents some smaller area within its images. Let us look at higher resolution (*ca.* 5 m) aerial photography of an area in 1079-15131. Examine Figure 2-6, reproduced from a 1:130,000 scale color IR photograph obtained on February 5, 1974, by a camera mounted on a NASA RB-57 aircraft flown at 17,000 m (55,000 ft).

#2-21: Can you locate the area encompassed by this aerial photo on any band image of 1079-15131? Using Overlay 1 as a base, outline in grease pencil or tracing pen the borders of the photo in relation to the Landsat scene. Is any part of the photo not represented in the Landsat scene? Use Overlay 2 to familiarize yourself with specific localities common to the photo and the Landsat image.

[2] A pixel (or picture element) is a discrete geometrical representation in some image display of the averaged radiance (reflected or emitted) or brightness level sensed from the smallest resolvable area of the surface (ground) under observation. This area usually corresponds to the IFOV of the sensor. Thus, the size of the ground area as represented by pixel dimensions is a controlling factor in the stated resolution of images produced from scanner observation. See p 74 for a full discussion of the characteristics of a pixel.

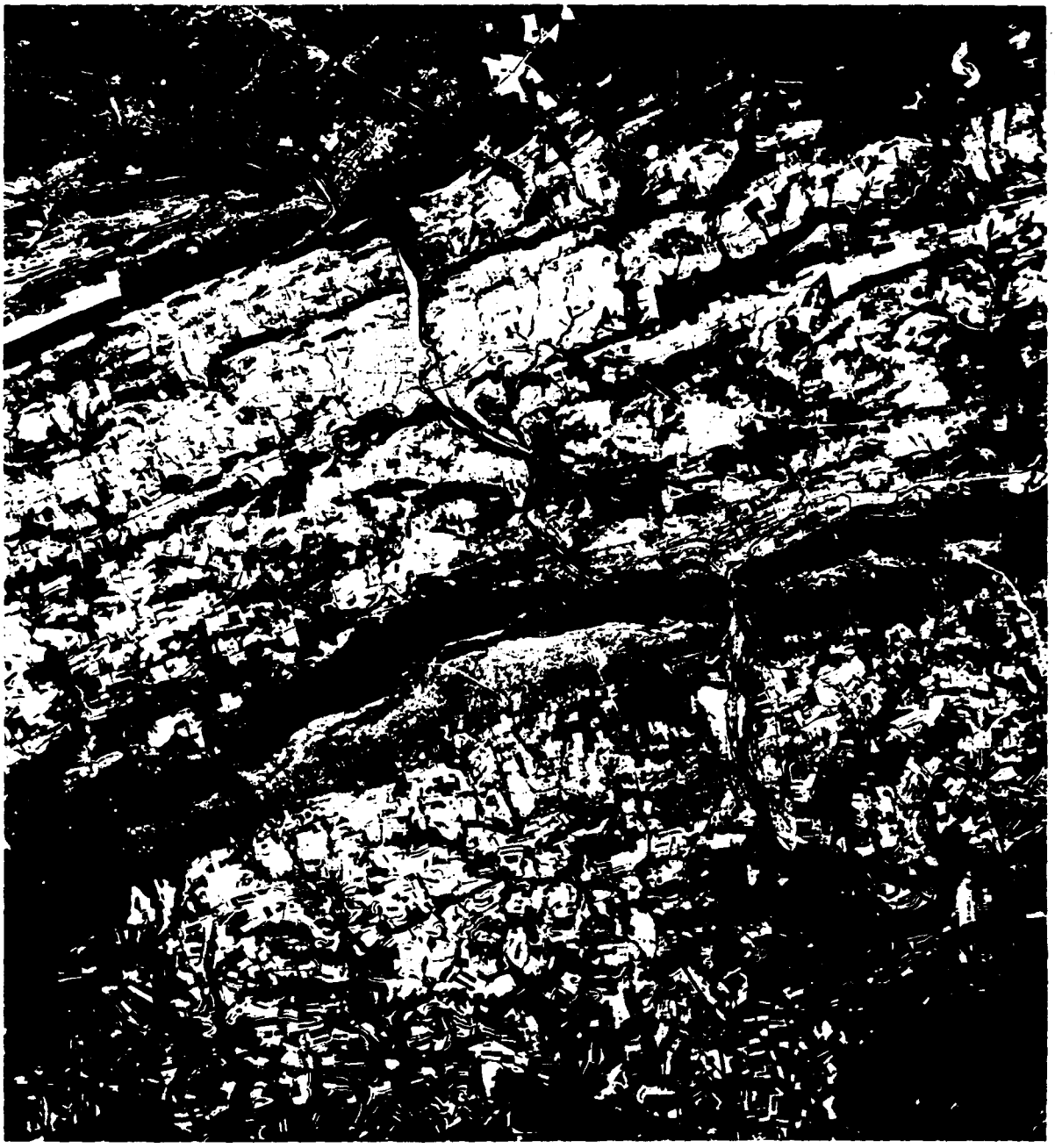

Figure 2-6. High altitude colcr IR aerial photo of Lehigh River area.

#2-22: Can you spot the towns of Slatington-Walnutport, Lehighton, and Jim Thorpe (Mauch Chunk) (see atlas) – readily seen in the aerial photo along the Lehigh River–in the Landsat imagery? Which town(s) show up best?

#2-23: What features within the towns, obvious on the aerial photo, cannot be made out in the Landsat version?

#2-24: What Landsat renditions (bands, color) are best for picking out these towns?

#2-25: Can you find the northern extension of the Pennsylvania Turnpike on the Landsat image as it runs through the hills northeast of Jim Thorpe? In which band is the longest stretch visible? Why does the roadway appear light in band 5 and dark in band 7?

#2-26: Some smaller drainage channels, such as the streams in both lowlands and hills east and northeast of Jim Thorpe (around the reservoir), are evident in the aerial photo. Try to locate and trace these on the corresponding area in the October 10, 1972, (see Figure 2-1) image. Did you find the longer of the streams that eventually flow into the Lehigh River? The smaller ones? Which band(s) show the drainage best?

#2-27: Compare the agricultural field patterns visible in the Landsat images with those in the aerial photo. Keeping in mind the seasonal influences between the two dates of acquisition, discuss briefly the similarities and differences in extractable information about these fields from the two data sources–Landsat and the aerial photo. Make a rough percentage estimate of the number of separate fields that can be distinguished in Landsat relative to the aerial photo.

Perhaps a better way to assess the relative information content in Landsat and aerial photography should involve a comparison of areas within a large metropolitan region containing many familiar urban and industrial features. At this point, work with bands 5 and 7 in Figures 2-3 or 2-11 and the single photos in Figures 2-7A and 2-7B, and also Figure 2-8. The Figure 2-7A product is a red band black-and-white photo (scale 1:108,300) of the Philadelphia environs taken on February 5, 1974, from a NASA U-2 aircraft at an altitude of *ca.* 18,000 m (59,000 ft). Locate this scene within the Landsat image. The Figure 2-7B photo was acquired on March 13, 1973 from a low-altitude aircraft and is reproduced at a scale of 1:24,000. Figure 2-8 is a photo enlargement, to approximately 1:80,000, of a small section of 30044-15011, band 5. Fit the low-altitude aircraft scene into the U-2 photo and, as well as you can, within the Landsat images. Inspection of equivalent areas at the four scales will enable you to appreciate the scales at which surface objects can be recognized (spotted, but with insufficient details to be identified) and, often, properly identified (i.e., named, or classed), as well as those objects that cannot be resolved and/or identified in the smaller scale Landsat imagery.

#2-28: Using the numbered landmarks in Figure 2-7A as a guide, indicate in the table on the facing page your ability to recognize or identify in the 1:1,000,000 or 1:80,000 Landsat scenes any of these landmarks evident in the Figure 2-7A and Figure 2-7B photos. Pencil in a "+" if you can pick out the equivalent landmark in either Landsat scene, a "–" if you cannot, and a "?" if you are uncertain.

#2-29: Note the dark diffuse "patch" visible in the central part of Philadelphia. Find this area in the aerial photos. Explain its presence. (Hint: form a mental picture of "row houses.")

#2-30: Judging from the aerial photos, the density of buildings in central Philadelphia appears similar in magnitude (probably greater, though) to the built-up area in New Jersey just south of the Delaware River. However, the Landsat color renditions do not display the characteristic blue tones in much of this Jerseyside area. Why? (Examine band 7, in particular, for one clue and then consider the nature of "outlying" sections of a large metropolitan district.)

#2-31: Remembering that the Landsat images were taken from an orbital altitude some 50 to 200 times higher than high- or low-altitude aerial photos, summarize in a paragraph your thoughts on the relative information content of the several rendi-

tions (Landsat images and photos). Include statements on the effects of scale and resolution, the types of information lost in one or the other, the expression of vegetation, water bodies, and cultural features in each, and any advantages you might find for the Landsat images over the aerial photos.

You will work again with the urban features discernible in the Philadelphia area as you consider, at the end of Activity 5, how a computer-produced classification might be used by the Bureau of the Census in demographic (population) studies.

Aerial Photo Landmark	*Landsat Image*	
	Recognize	*Identify*
(1) Mouth of Schuylkill River	*(1)* _____	_____
(2) Philadelphia International Airport	*(2)* _____	_____
(3) Walt Whitman Bridge	*(3)* _____	_____
(4) Oil farms along Schuylkill River	*(4)* _____	_____
(5) Veterans Stadium/JFK Stadium Complex	*(5)* _____	_____
(6) Lake in Franklin D. Roosevelt Park	*(6)* _____	_____
(7) Ship wharves in the Delaware River	*(7)* _____	_____
(8) Tall buildings in Central City (near Independence Hall)	*(8)* _____	_____
(9) Residential area near Woodbury	*(9)* _____	_____
(10) Interstate 95 along river	*(10)* _____	_____
(11) Rail yards near the Delaware River	*(11)* _____	_____
(12) Intersection of New Jersey Turnpike and the North-South Freeway (Interstate 76)	*(12)* _____	_____

IMPORTANCE OF RESOLUTION

You have now examined in some detail the same area in one part of the world by means of images and photos at three very different scales and resolutions obtained from combinations of aerial and satellite platforms. Let us next look at the effect of going to a larger scale and higher resolution by employing another sensor from the same satellite platform. On Landsat-3, the Return Beam Vidicon (RBV, essentially a TV camera) provides simultaneous coverage of the same frame being imaged by the MSS.[3] However, the MSS equivalent area is imaged by four individual RBV pictures. Two RBV cameras (A and B), mounted side by side, take simultaneous pictures that together cover the upper left and right quadrants of an MSS scene. Some 11 s later, the camera pair takes pictures that closely coincide with the lower left and right quadrants of the scene.

Figure 2-9 is a single RBV frame taken on April 18, 1978 over New York City and nearby New Jersey. Figure 2-10A is a band 5 rendition of frame 30044-15011 imaged by Landsat on that date. The best estimate of equivalent ground resolution for standard-processed Landsat-3 RBV images is about 30 m.

Carefully examine this RBV image of New York City with a magnifying glass. The crosses within the image are reseau marks (etched on the vidicon plate) used in precision geometrical correction of the RBV data. Fit Overlay 1 on the full-scene band 5 image (Figure 2-17A), and then trace with a grease pencil the approximate boundaries of the RBV frame.

=2-32: The RBV frame is produced at the same picture dimensions as the MSS image of the full scene. What is the corresponding scale of a single RBV frame?

[3] The RBV system on Landsat-1 and Landsat-2 differs from that on Landsat-3 in being multispectral and having lower spatial resolution (see Appendix A). Because of an electronic failure soon after launch of Landsat-1, this RBV system has not been operated since then on either spacecraft.

Figure 2-7A. High altitude red band aerial photo of Philadelphia environs; scale 1:108,300.

#2-33: Visually compare the RBV image content with its equivalent area in the MSS scene for April 18, 1978 (use your tracing on Overlay 1 as a guide). Describe any additional ground details (including new features now visible or identifiable) that you note in the RBV scene, relative to the MSS subscene, for the following geographical categories (refer to an atlas as needed): (a) Manhattan, (b) Newark-Jersey City, (c) Lakewood, N.J.-Pine Barrens, (d) Lake Hopatcong (Morris-Passaic Counties), and (e) farm country east of Princeton.

Figure 2-7B. Low altitude panchromatic aerial photo of central Philadelphia; scale 1:24,000.

The RBV's on Landsat-3, unlike those on Landsat-1 and Landsat-2 which used filters to provide multispectral data, integrate light over a spectral range from 0.505 μm to 0.750 μm -- approximately equivalent to panchromatic black-and-white film.

=2-34: Look at both the RBV frame containing New York City and the same area in the bands 5 and 7 images of the 30044-15011 scene (Figures 2-10A and 2-10B). Ignoring spatial resolution differences, summarize your observations about the relative merits and disadvantages of panchromatic versus multiband imagery for a given scene by comparing specific land cover categories such as urban areas, transportation patterns, and farmlands.

Figure 2-8. Enlargement of part of Landsat scene 30044-15011, band 5 to a scale of approximately 1:80,000.

MULTITEMPORAL IMAGES

At this point it will be interesting to look at three other Landsat scenes covering the New Jersey area at different times of the year. Refer to Figures 2-10B, 2-11, and 2-12, spring, winter, and summer, band 7 scenes, respectively, and Figure 2-13, a color composite for the same spring scene.

ORIGINAL PAGE
BLACK AND WHITE PHOTOGRAPH

APR78 C N40-23/W074-19 D815-832 N N40-11/W074-54 R B DXBI SUN EL58 AI38 S2S- P-N L2 NASA LANDSAT E-30044-15011-B

Figure 2-9. New Jersey scene, April 18, 1978 imaged by Landsat-3 RBV.

#2-35: Compare the area located around Thorpe as depicted in the color IR aerial photo gure 2-6) with the same area appearing in these ltitemporal Landsat scenes (disregard differ- es between color and black-and-white rendi- ns). Do you wish to modify any of your answers to questions 2-22 through 2-27, particularly with regard to the relative expressions of drainage, agriculture, and towns in these scenes?

#2-36: Which Landsat scene (by ID and date) best displays the geological and topographical

Figure 2-10A. April 18, 1978 scene, band 5, taken by Landsat-3 MSS.

features observed in the aerial photo? Assuming that there are no stereo pairs, do any of the Landsat scenes or the aerial photo appear to better describe the minor topographical irregularities in the valleys between the ridges? What factor(s) influence the improved expression of these irregularities?

#2-37: When the four temporal scenes (February 1973 [winter], April 1978 [spring], June 1977 [summer], and October 1972 [fall]) are

ORIGINAL PAGE
BLACK AND WHITE PHOTOGRAPH

Figure 2-10B. April 18, 1978 scene, band 7.

compared overall, for the same band 7, the differences are striking. Cultural changes no doubt occur, but other factors account for most of the differences. Mention three factors.

=2-38: Choose any three subscenes within the New Jersey fall scene—pick these areas to be at least 255 km^2 (100 square miles) in area. Outline, with key words, notable differences (at least three) you observe in the same (equivalent) subscene within each of the other temporal images (winter, spring, summer).

Figure 2-11. New Jersey scene acquired by Landsat-1 on February 13, 1973, band 7.

THE CLOUD FACTOR

These multidate images and, for that matter, most other Landsat images in this workbook were chosen because of their photographic quality, information content and cloud-free status. If one has never browsed through a stack of Landsat images produced as routine output by the NASA

Figure 2-12. View of New Jersey, band 7, taken by Landsat-3 on June 11, 1973.

IPF, the impression given in this workbook, in *Mission to Earth*, and in other publications featuring Landsat, is that either most scenes are taken only on clear days or there has been a remarkable worldwide improvement in climate such that a typical Arizona day is now the norm. Your common sense tells you that the latter conclusion is false. Familiarity with IPF products discounts the former observation; the majority of Landsat scenes are in fact compromised by extensive cloud cover, even though the spacecraft sensors are frequently not turned on over regions outside the United States

ORIGINAL PAGE
COLOR PHOTOGRAPH

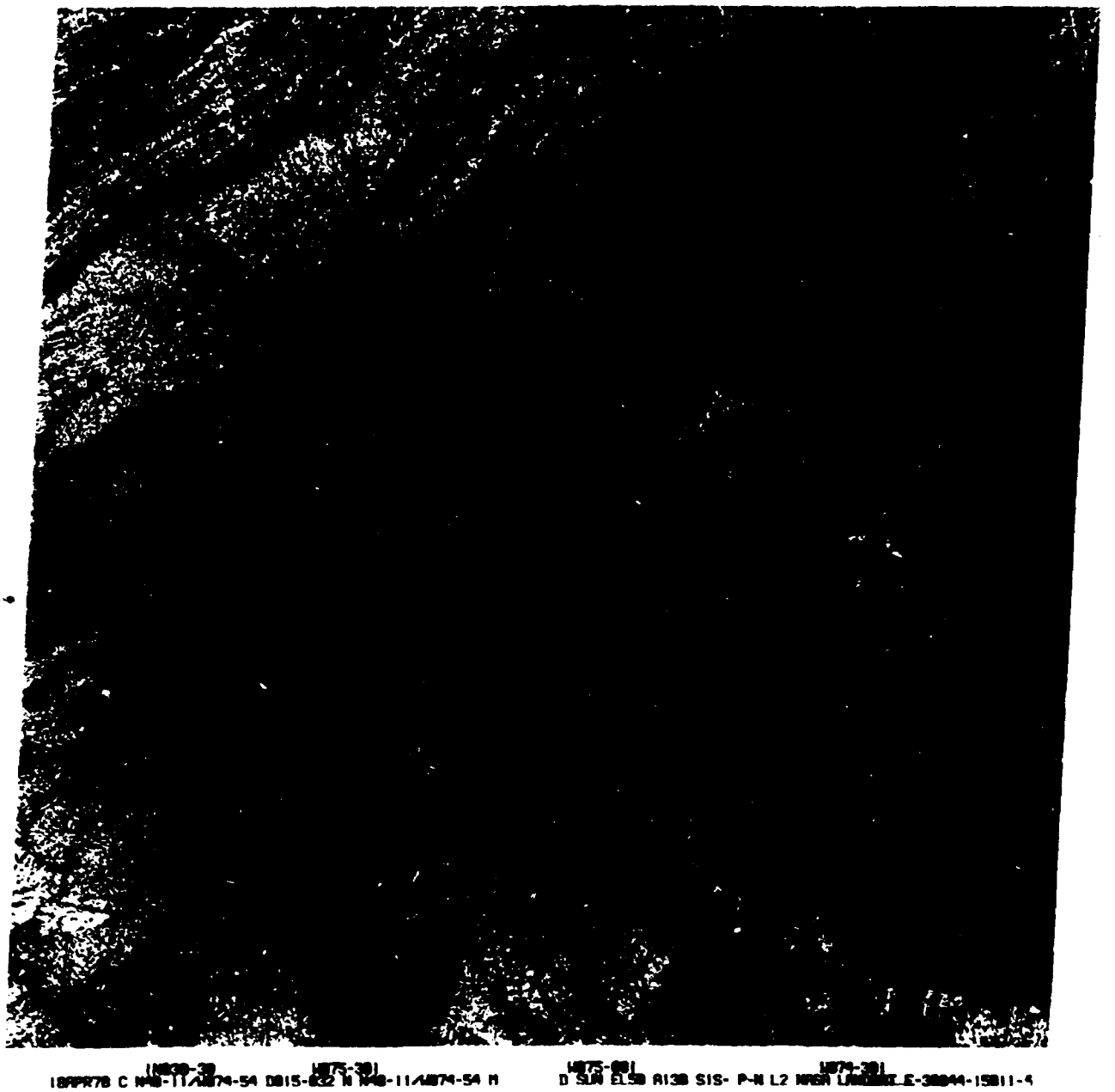

Figure 2-13. False color composite made from bands 4, 5, and 7 of April 18, 1978 Landsat-3 images.

when weather forecasts are obviously unfavorable.

What is the likelihood of getting a cloud-free (here defined as 10 percent or less of surface-obscuring clouds) Landsat image? That, of course, depends on location, time of year (fall and winter are generally best in much of the United States), time of day (in summer, mornings are better because of thermal convection buildup by afternoon), and luck. Various studies based on climatological data for given regions, viewing experience with Nimbus and other meteorological satellites, and now Landsat itself, have led to charts and maps that quanti-

tatively assess or predict likelihood of cloud cover on a seasonal basis.

A recent study made at the Jet Propulsion Laboratory in California inserts data from several sources to generate a percentage probability map (Figure 2-14) by which one can estimate the chances of a clear look (0 to 10 percent cloud cover) on any given pass. As expected, the maximum likelihood region centers in the desert southwest, where two of every five passes (40 percent) result in a nearly cloud-free scene. Least likely regions are the Pacific and Gulf Coast zones and parts of the coastal and inland northeast.

#2-39: Look at Figure 2-14 to locate your town and/or any regions of the United States for which your organization has operational activities. Estimate the number of times per year (on average) that you might expect to obtain essentially cloud-free (less than 10 percent cloud) Landsat images from a single Landsat spacecraft; from two Landsats orbiting over the same area on a 9-day time separation from one another.

IMAGE VARIABILITY FROM PROCESSING

Now that you have some feeling for the characteristics of each band and the appearance of major ground features in these bands, we shall consider the relative variations in extractable information due to differences in the processing leading to the photo negative and in the quality of photo reproduction. First, we shall compare two renditions of the New Jersey scene made under different conditions. Switch back and forth between the bands 5 and 7 images in Figures 2-3 and 2-15. Examine details with a magnifying glass.

Figure 2-15A and B are standard products

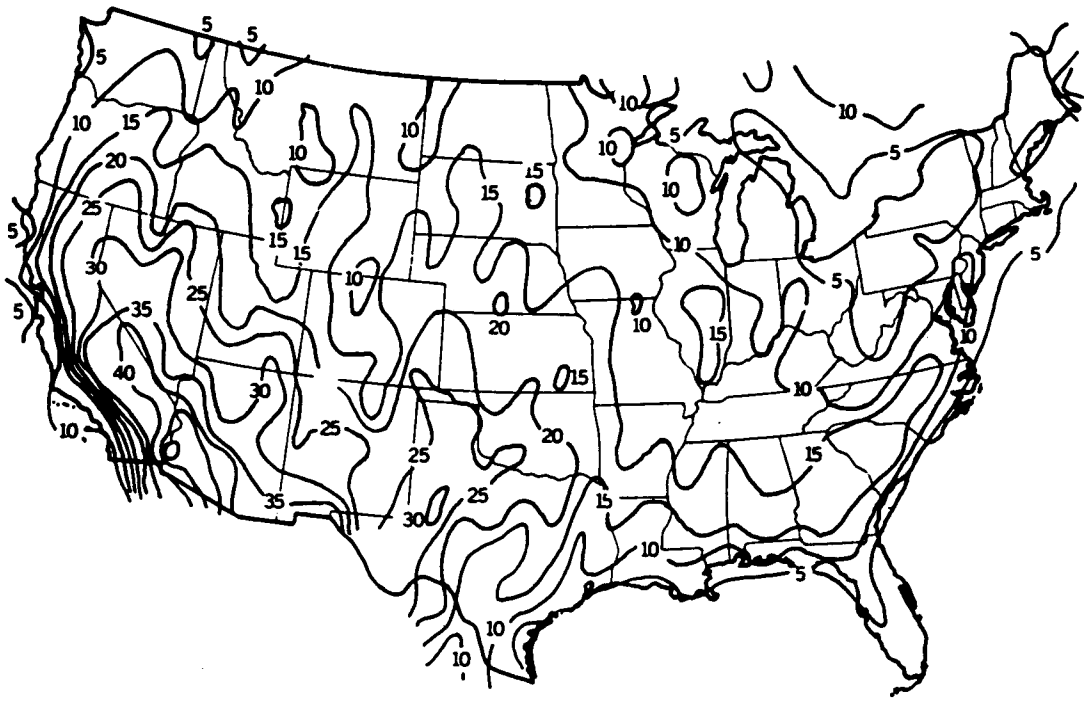

Figure 2-14. Percent probability of 0 to 10 percent cloud cover for any overflight (based on EDC Landsat statistics).

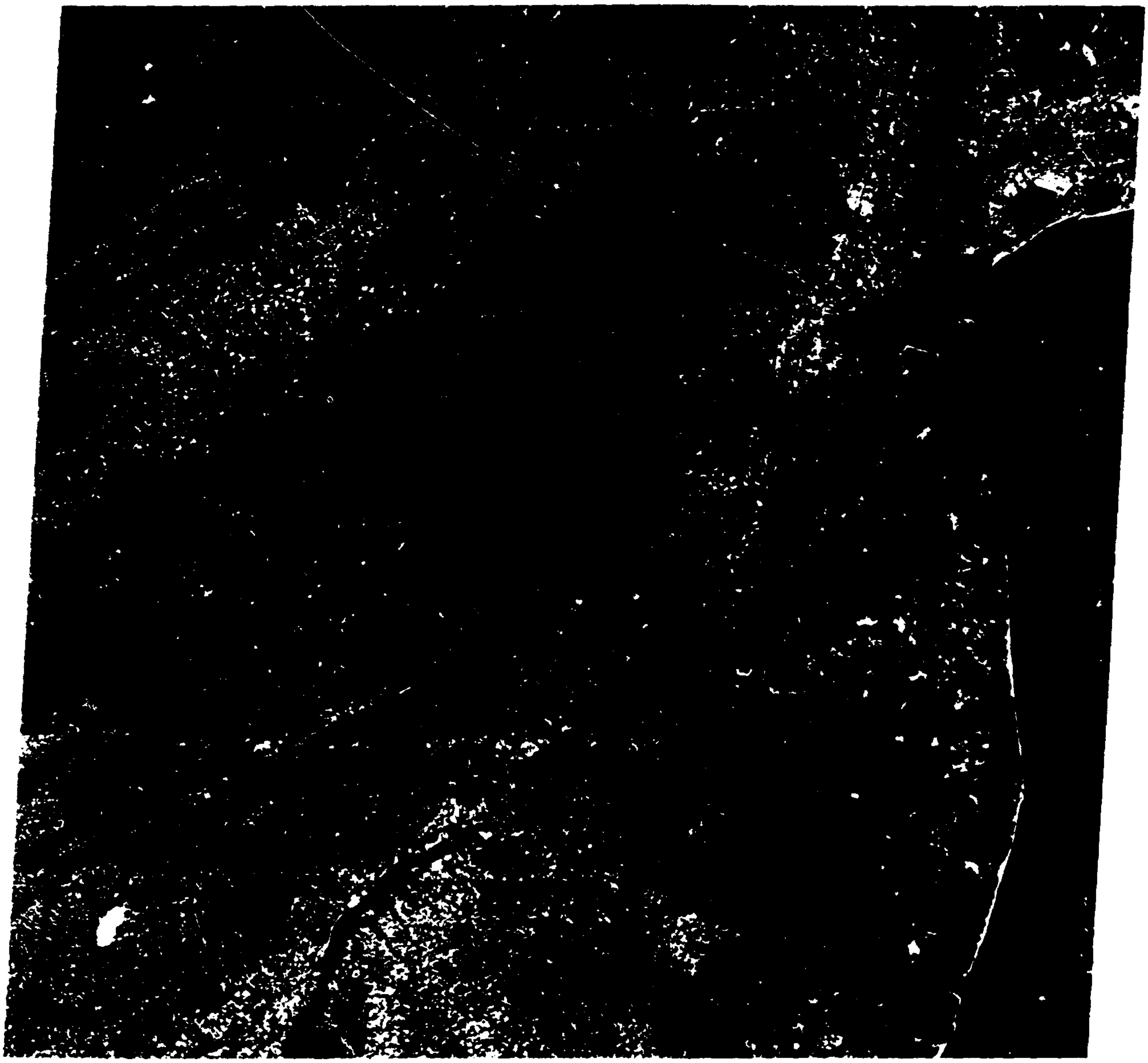

Figure 2-5A. Standard band 5 rendition of Landsat-1 October 10, 1972 scene.

available from most federal outlets and private suppliers. The images used here were ordered routinely from the Goddard IPF and are typical of the product received by the Landsat user community before 1979.[4] Generally, this product is made from third, or even fourth generation negatives. In this

[4] In 1979 the EROS Data Center became the sole supplier of Landsat data acquired by United States receiving stations. All imagery for scenes obtained after February 1, 1979, are produced from the EDIPS processing routine which significantly enhances visual quality (see Figure 4-3 for an EDIPS example).

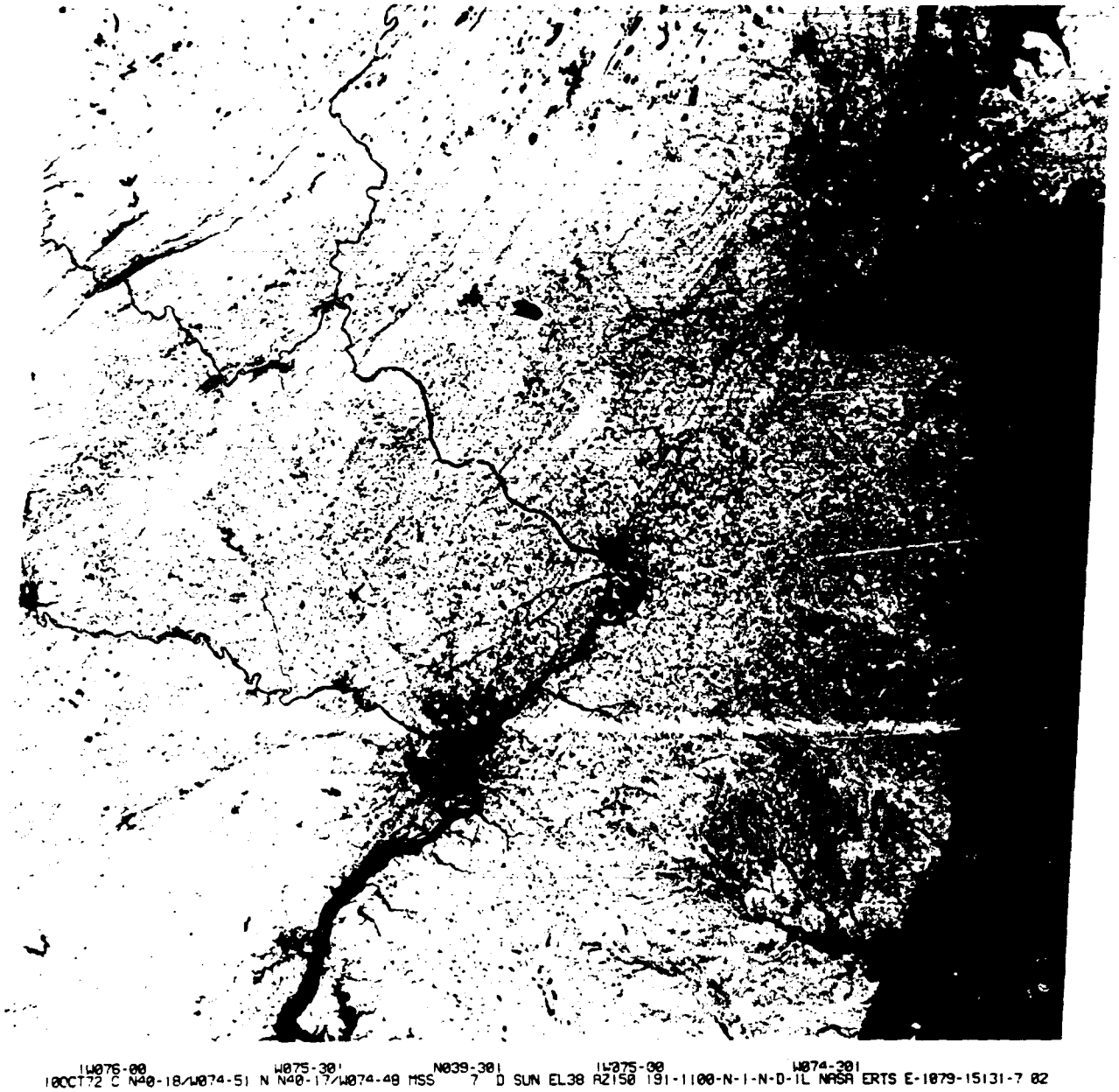

Figure 2-15B. Standard band 7 rendition.

example, the paper print was produced by the Goddard Image Processing Facility, using a third generation negative and a flat finish. The gray scale at the bottom shows low contrast but follows the density step relations that correspond to the radiometric intensity differences sensed by the MSS on Landsat. In other words, the changes in the gray level over most of the density range should effectively represent the changes in brightness values or radiances measured by the scanner sensors.

The Figure 2-3 images, which we looked at earlier to form a first impression of the appearance

of the Earth as seen in the four Landsat MSS bands, were printed in the Still Photography Laboratory at the Goddard Space Flight Center in an effort to get a near-optimum rendition. A special dark negative supplied by the Goddard IPF was used. Exposure times, paper types, and developing conditions were varied empirically to obtain a high contrast (derived from the slope [γ] of the density/exposure time curve) print.

#2-40: Compare the band 5 and 7 images of the two renditions (Figures 2-3 and 2-15). Look at each in toto and again at equivalent spots you select. Examine also the gray scale strips at the bottom of each rendition. Which rendition seems sharper and appears to contain more readily accessible information?

#2-41: Which do you think may be more important in determining image quality: the particular generation of negative used to make the print, or the contrast (range of densities or gray shades)?

#2-42: We have included a transparency version of the band 5 image from Figure 2-3 in the back pocket of this workbook. If you have access to a light table (or just a bright lamp), go over this transparency, once again looking at the equivalent spots picked out in #2-40. Which product type seems superior in quality and extractability of information: print or transparency? Try to think of the reason.

Now, consider both images in Figure 2-16A and B. These are prints of bands 5 and 7 of the October 1972 New Jersey scene made from a first-generation negative derived from a computer-enhanced version produced by Dr. Ralph Bernstein of the IBM Corporation at Gaithersburg, Md. Preparation of this computer version involved geometrical and radiometric corrections, destriping (reduction of scan line differences due to variations in response of the detectors), and band pass filtering (Activity 5 and Appendix B). The effect is to "clean up" the image by sharpening the boundaries and giving a clearer rendering of subtle shadings of gray tones (in effect, a broadening of the contrast range).

#2-43: How do you rate this computer version with respect to the standard EBR-produced images shown in Figures 2-3 and 2-15?

In Activity 5 you will learn much more about the benefits of computer processing to improve image quality.

It is becoming obvious from the above comparisons that the information content in a Landsat photo product is strongly dependent on the approach and care taken in photo processing. The nature of the input (for instance, the method used in producing the negative) is also a vital factor.

Experience also shows that false color renditions of Landsat images will show a wider variability depending again on both input and processing techniques.[5] The specific color processing system used by a particular photo lab is usually both critical and distinctive. Usually, a color product may be identified with the source (producer) by its characteristic color balance (relative contribution of reds, blues, etc.). Obviously, some versions are better, more informative and/or more pleasing to the eye than others. We can test this conclusion by comparing three color versions of the New Jersey scene. You have already seen one (Figure 2-1) that was prepared by a commercial photo lab (General Electric Space Sciences, Inc., Beltsville, Md). Figure 2-17 is a typical color product made at Goddard's IPF. Figure 2-18 is the color version prepared by IBM from its computer-enhanced transparencies of bands 4, 5, and 7 of the same October 1972 scene.

#2-44: Summarize your impressions of the relative quality and usefulness of these two color versions.

#2-45: For a typical summer scene in the eastern United States, what characteristic(s) of a Landsat color image would you conclude to be most detrimental to effective interpretation?

[5] The manner in which false color composite images are made from individual black-and-white bands and the association of specific colors with correlative ground features are considered in Activity 3 (p. 91 - 98).

THE THERMAL BAND

Landsat-3, launched in March 1978, was the first Earth resources satellite to carry a sensor that operates in the thermal (emitted) IR. (See pp 27 to 28 for a review of some basic concepts of interpreting data acquired in the thermal infrared.) The multispectral scanner differs from those on the first two Landsats in having a fifth channel (band 8) designed to sense heat effects in the 10.4 to 12.6 μm region of the electromagnetic spectrum. The detectors for this channel are capable of sensing a temperature difference (NEΔT) of 1.5°K within a response range of 260 to 340°K.[6] The IFOV and signal sampling rates provide an effective resolution of 240 m (790 ft). Normally, the thermal sensor acquires daytime data during the local mid-morning passes but can also be activated on the nighttime side of each orbit.

The thermal channel on Landsat-3 experienced difficulties soon after launch. One of the two detectors failed within a few months and the second detector degraded to a thermal sensitivity of ±3°K. For later data, alternate missing lines were filled in with repeats of adjacent lines; this is comparable to increasing pixel size to 240 m × 480 m.

In spite of these problems, some useful thermal data have been collected and are still undergoing analysis and appraisal. Figure 2-19 is an excellent example of the type of thermal imagery produced by band 8. The area imaged is the same April 18, 1978, scene shown in Figures 2-10A and 2-10B.

Overall, this image shows noticeable differences in relation to the reflected light images formed from bands 4 to 7 of the MSS, but there are some aspects that appear similar. In the thermal image, the coolest surfaces are depicted as dark gray or blackish tones, whereas the warmest surfaces appear as light gray tones. Note that the gray scale at the bottom is reversed relative to the scale on MSS images, with the densest step on the left representing the lowest temperatures and successively lighter steps to the right representing progressively higher temperatures. There are fourteen steps in this rendition that can readily be distinguished by eye. Actual temperature values are not yet available for these steps and would require processing of calibration data.

Although the image shown in Figure 2-19 is photographically "flat" compared with the other MSS bands (eventually, computer processing will be able to increase or expand the tonal contrast and hence highlight subtle differences), it is still possible to recognize some of the major land and ocean features by their distinctive thermal characteristics.

#2-46: Compare the following features already identified in 1079-15131 (Figure 2-3) with their equivalent areas on the thermal image. Indicate for each its approximate gray level with respect to the closest step density shown at the bottom of the thermal image (number the distinguishable steps from 1 through 10 going from left [darkest] to right).

a. New York City	*e. Pocono Mountains*
b. Philadelphia	*f. Barnegat Bay*
c. Lake Hopatcong	*g. Delaware River*
d. Pine Barrens	*h. Offshore clouds*

In general, what are the coolest features in the thermal scene? The warmest?

Like the reflectance data, the thermal channel data are acquired in the digital mode. However, very few of the data were converted to computer compatible tapes so that only a few examples of reprocessing are available. One of the best so far appears in Figure 2-19B. This night scene,[7] also sensed on April 18, 1978, is the next frame to the north of that shown in Figure 2-19A. Computer processing consists of enhancement by a contrast stretch (p. 433) which broadens the narrow range of gray levels (initially 90 percent of the six bit thermal data is spread over 9 quantized levels representing an estimated temperature range of 15°C) by a factor of two. Figures 2-20A and 2-20B depict one computer-processed subscene (equivalent to about 42 km [26 miles] across the base)

[6] K refers to degrees in Kelvin units (K = °C + 273).

[7] This scene is described by J. Price, *The Contribution of Thermal Data in Landsat Multispectral Classification*, Photogram. Engnr. and Remote Sensing, V. XLVII, no. 2, Feb. 1981, pp. 229-236.

Figure 2-16A. Computer-processed band 5 image of October 10, 1972 New York - New Jersey - Pennsylvania - Delaware Landsat scene.

Figure 2-16B. Computer-processed band 7 image (IBM).

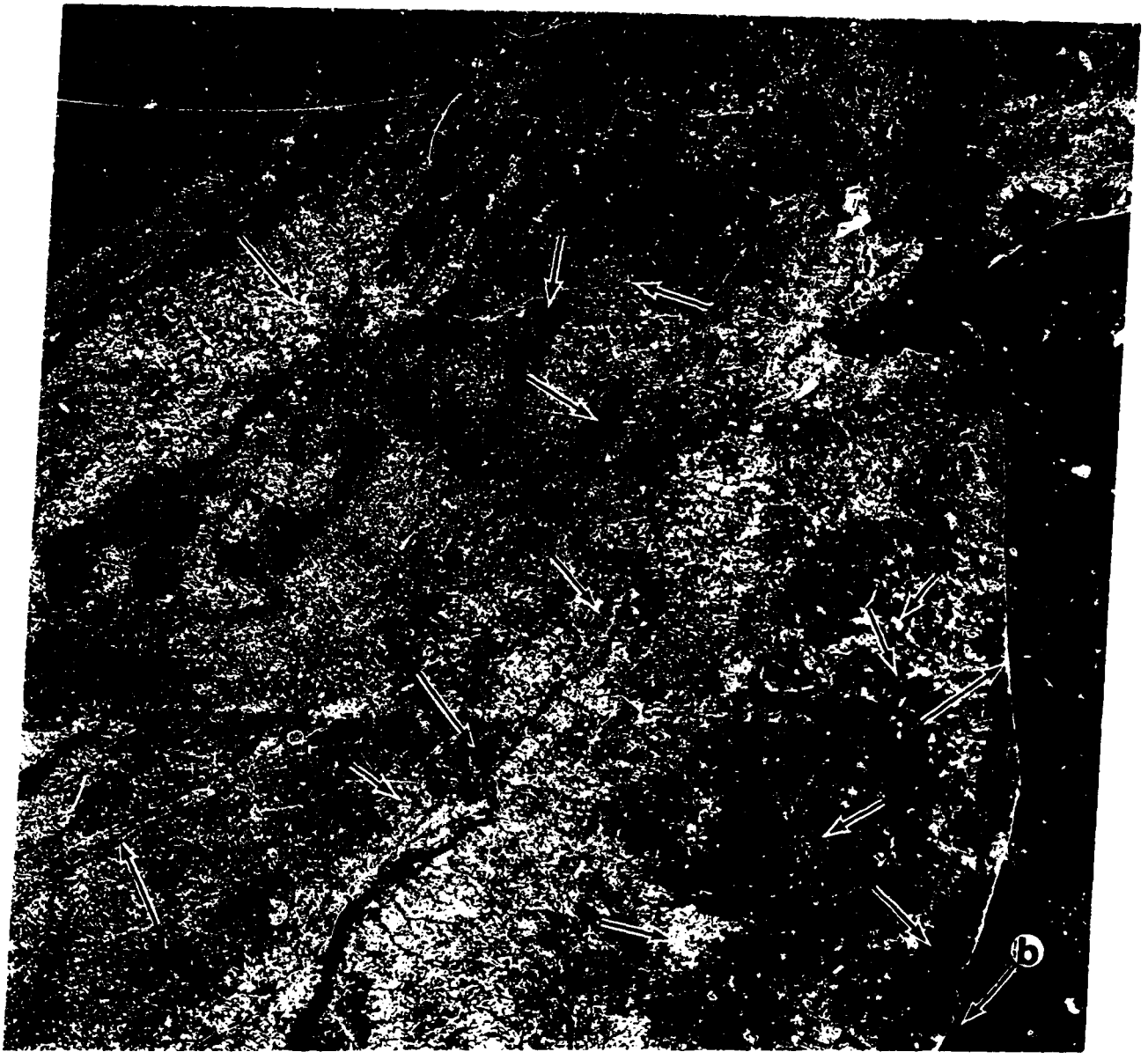

Figure 2-17. October 10, 1972 Landsat-1 image in standard false color version (letters relate to Table 3-3).

around Baltimore, Md., just south of the Harrisburg study area. The upper print (A) is a band 8 black-and-white image constructed from the thermal data. The light tones coincide with the more populated areas of Baltimore, where heat from buildings, sparse vegetation, concrete and asphalt surfaces, and restricted patterns of air circulation combine to produce the typical *Urban Heat Island* effect. To produce the lower print (B), every 240-m pixel along each scan line was subdivided into nine identical 80 m units so that each unit is repeated three times in both column and row direc-

ORIGINAL PAGE
COLOR PHOTOGRAPH

Figure 2-18. Computer-generated false color composite of the October 10, 1972 scene of New Jersey and adjacent states, as produced by R. Bernstein of IBM

Figure 2-19A. Thermal IR image of New York - Philadelphia region taken by Landsat-3 (band 8) on April 18, 1978.

tions. The subdivided thermal band pixels have been combined with reflectances from bands 5 and 7 to register corresponding pixels (all now at 80 m). The color composite in Figure 2-20B uses this band-filter combination: band 5 - blue, band 7 - green, and band 8 - red. Thus, warm areas through much of central Baltimore and at the Sparrows Point industrial (steel) complex stand out as prominent red tones. Actual temperature values corresponding to the gray levels in the band 8 image have not been calculated.

Figure 2-19B. Band 8 thermal IR image, contrast-stretched by a factor of 2, showing the Hudson Valley, Catskill and Pocono Mountains northwest of New York City; April 18, 1978.

LANDSAT MOSAICS

The ability of Landsat images to be combined in mosaics is a useful asset; its value will be demonstrated in this section. Take the series of stapled images marked "mosaic" included in the pocket at the back of this workbook. Tear out the first two images (1079-15131 and 1080-15185). Try fitting the left (west) margin of 1079-15131 to the equivalent area boundary within 1080-15185. This is made easier by trimming off the white border of the left side of 1079-15131. Then, by lining up equivalent patterns along the tie line between the pair of images, make as precise a join as practical, and affix the two prints with clear tape. By doing this you should get a feel for approximately where the overlapping subareas are in each scene.

=2-47: *How well can you fit or tie together the two images? What are the maximum joining errors (in terms of millimeters or fractions of an inch) along the fit line if you place the same points (some obvious common feature) in the two images exactly together at or near the mid-point of the*

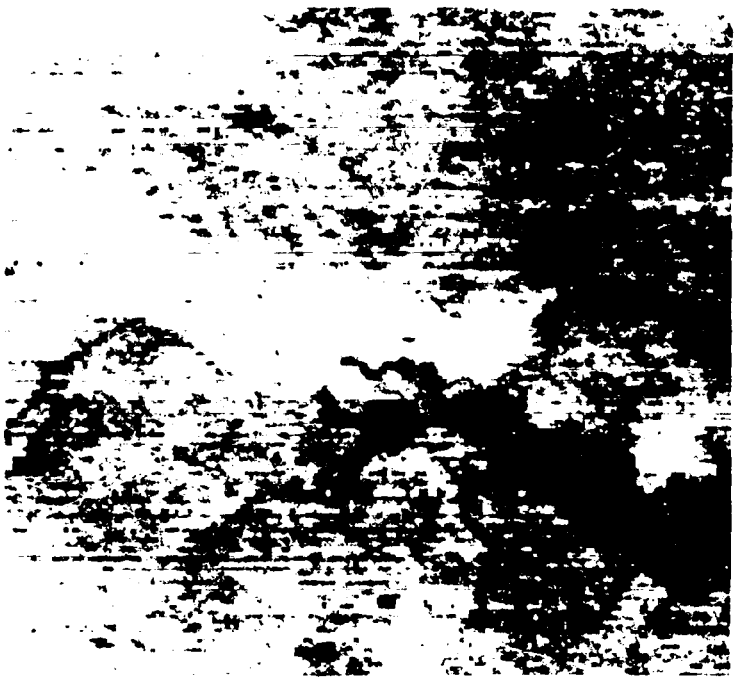

Figure 2-20A. Computer-processed band 8 image of Landsat April 18, 1978 subscene around Baltimore, Md.

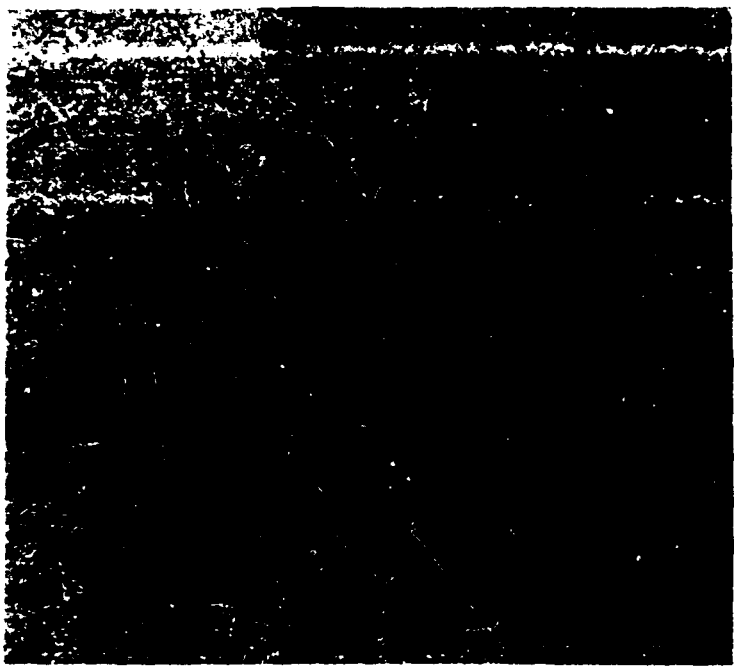

Figure 2-20B. Color composite of Baltimore subscene using bands 5 (blue), 7 (green), and 8 (red).

left margin? (Hint: look for other prominent features extending across the fit line.) Where do the largest displacements occur along the join line relative to this midpoint?

#2-48: Next, try a similar rough fit of band 7 images of a second copy of 1079-15131 and of 1350-15190, found in the mosaic sequence. Do not tape together. Briefly discuss any fitting problems you might encounter and compare the mosaic "quality" of this pairing relative to the join made above. Give reasons for differences in quality. Also, explain why adjacent Landsat images acquired at widely separated times (dates) still fit together so well. (Hint: consider both the viewing geometry of Landsat in orbit and corrections applied in processing.)

One of the more remarkable properties of Landsat images is this ability to be joined together to form mosaics that can extend over vast regions (subcontinental or even broader). The famous black-and-white (Soil Conservation Service) and color (National Geographic Society) mosaics of the contiguous forty-eight United States are perhaps the best known examples.

#2-49: Detach the additional black-and-white prints found in the mosaic package. Note that the remaining ones are all from the two orbital paths of October 10 and 11, 1972. Building up from the first pair of images (same dates) you have already joined, construct an eight-frame mosaic from the other six. What problems are likely to make production of such mosaics somewhat difficult?

#2-50: What might be done to reduce these problems?

#2-51: As an optional exercise, locate this mosaic in terms of its geographical boundaries (use an atlas or a small-scale map). Examine various terrain and cultural features that you identify in the mosaic and describe (in your mind) their characteristics and any useful information they convey to you.

#2-52: Mention several practical uses of regional small-scale mosaics.

STEREO VIEWING

Finally, we shall consider some of the stereo effects that can be observed in Landsat imagery. Complete this section only if you have access to a stereoscope (or have developed the knack of seeing in stereovision with the unaided eyes). Some knowledge of the principles of stereoscopy is desirable—see references in Appendix G.

Remove the second copy of the 1080-15185 print from the mosaic package and arrange it side by side with the still detached second copy of 1070-15131 at the appropriate separation for stereo viewing. Observe the overlap area visible in stereo.

#2-53: What fraction (as a percentage of the total) of the adjacent pairs common to both can been seen in stereo? How does this compare with typical aerial photos? This fraction varies from about 10 percent at the Equator to 85 percent at 80° latitude for Landsat data. Why does this change? Describe the three-dimensional representation of topography in the Landsat stereo version relative to your experience with aerial photo stereo versions. (Note that the base to height [B/H] ratio for Landsat stereo is about 0.2 here, compared with 1.6 in typical low-altitude aerial photos.)

The stereo effect you have just witnessed is produced essentially in the conventional manner, in that the pair is acquired along adjacent flight lines (or orbits for satellites). This takes advantage of the parallax principle, in which equivalent points in the two images are viewed from different (and opposing) look angles. There is an alternative way in which a pseudo-stereo effect may be achieved with Landsat images. This is done by examining approximately equivalent scenes obtained along about the *same* (rather than adjacent) orbital path or track at significantly different times of the year (as for example, summer and winter; not necessarily the same year). This technique has been termed "solar stereo" by V.C. Miller.[8] To experience this

[8] Miller, V.C., *Solar Stereo Landsat Imagery*, ITC Journal, No. 1, 1978, pp. 158-166.

type of stereo viewing, use the unattached band 7 images for scenes 1079-15131 and 1350-15190 taken from the mosaic package. Align them as though they were a stereo pair—with a proper lateral separation of equivalent segments—and look at them under a stereoscope.

#2-54: Describe your observations and compare the stereo effect for this arrangement with the previous results from adjacent pairs.

#2-55: Can you explain the cause of this solar stereo effect? (Hint: which factor(s) change appreciably with seasons?)

#2-56: Suggest several ways in which viewing a Landsat image in stereo can assist in extracting and interpreting information contained in the scene.

#2-57: If you were to design a Stereosat (a satellite system now under consideration for flight in the 1980's), what parameters would you choose to modify from those of Landsat to optimize the stereo viewing? (Skip this question if you are generally unfamiliar with stereoscopy.)

It is also possible to produce a stereo image pair from a single Landsat image by using topographic map data to calculate the amount of parallax shift to be applied to each pixel. This is conveniently done through a computer process, as described on p. 292. An example of such a stereo pair is included in the back pocket of this workbook.

At this stage, you should have a reasonable understanding of the nature and general characteristics of Landsat images and should appreciate the variety of ways in which they can be manipulated. In the next activity we shall consider the multispectral aspects of Landsat images, a special attribute that makes it easier to extract information about pattern identities, hence improving the ability to classify and map the features they represent.

ACTIVITY 3

SOME SPECTRAL AND SPATIAL CHARACTERISTICS OF LANDSAT DATA

LEARNING OBJECTIVES:

- *Gain some insight into the way in which the Landsat MSS produces multispectral data.*
- *Have some understanding of what a "pixel" means in a Landsat image or data set. Know the implications of the term "mixed pixel."*
- *Become familiar with the concept of spectral signatures.*
- *Be able to derive a simple signature for a class or feature by analysis of the four band images.*
- *Understand the production of false color composites.*
- *Appreciate the use of color additive techniques.*
- *Be acquainted with the preparation of Diazo images.*
- *Learn how to make quick visual identifications of major land cover types by their characteristic gray tones or colors in Landsat images.*

THE MULTISPECTRAL SCANNER

To fully appreciate the advantages of multispectral remote sensing techniques, you should consider first the performance of the multispectral scanner (MSS) and then the nature of the pixels that are produced by this sensor.

The Landsat MSS functions as a multiband spectroradiometer rather than as a spectrometer. In other words, it measures reflected radiances (actually time-dependent energy received, or power) in four discrete wavelength intervals (bands).[1] Continuous radiation is diverted by a beam splitter in the optical train through four fixed interference filters onto an array of six detectors for each waveband.[2] Variations of intensity with wavelength within the intervals are averaged over each band. The average radiances (or power) integrated within each band may be plotted as bars in a histogram (see Figure 6-17). For each band the radiances received at the MSS detectors give rise to a range of analog outputs (in volts) proportional to radiances emanating from each discrete area of the ground and modified by the atmosphere. The radiances from each area make up one data point in each band, represented by a pixel as the video signal is sampled and commutates once every 9.95 ms. To improve the signal-to-noise (S/N) ratio in bands 4, 5, and 6, the signals are compressed on board by using quasi-logarithmic amplifiers. The video signals are digitized and then multiplexed on board into a pulse amplitude-modulated stream that is then transmitted to the ground as wideband video signals. The video amplitudes are expressed by digital numbers (DN) in a 6-bit code (2^6) ranging from 0 for no detected radiance to 63 for maximum radiance. In ground processing, the DN's from bands 4, 5, and 6 (photomultiplier detectors) are decompressed to a range of 0 to 127 (2^7), but the upper DN limit for band 7 (silicon photodioxide detectors) is kept at 63, since its S/N is best matched by linear quantization.

PIXELS

Next, we shall investigate the nature of a pixel—the fundamental data point making up a Landsat image.[3] The concept of pixel is basic to one's understanding of this imagery. The term *pixel* is a contraction for picture element. In the general sense, an image is an (idealized) representation of any real scene, formed from a regular (two-dimensional in X-Y space) arrangement or array of picture elements. Each picture element corresponds to an equivalent finite area in the scene. In turn, the ground area represented by the pixel is related to the effective resolution of the sensor system. The size of this ground segment is determined by the instantaneous field of view (IFOV) established by the sensor optics (mainly the focal length of the telescope lens and the optical fiber dimensions), but its final shape may be further modified by the electronic sampling rate of the video signals from the detectors. Some varying parameter (such as radiance) within each area in the scene array is recorded as a changing magnitude (vectorial) in the third or Z-direction within the image array. This parameter is usually wavelength-dependent brightness or spectroradiance. An X-Y image is produced by expressing one or more Z-parameters in a correct array as alphanumeric characters in a printout map or by converting Z-values into vari-

[1] A fifth band (8), only on the Landsat-3 MSS, senses just emitted thermal energy over a 10.4-12.6 μm wavelength interval. This band failed shortly after launch and is not considered again in this activity. All references therein to radiance and energy imply the reflective region.

[2] The 24 detectors for the 4 reflectance bands normally operate in a low gain mode, that is to say, they respond to maximum radiances from 1.76 mW cm^{-2} sr^{-1} for band 6 to 4.60 mW cm^{-2} sr^{-1} for band 7. Some surfaces, such as water and dark rock, produce low radiances so that small (but often significant) variations may be hard to differentiate. For this condition, bands 4 and 5 may be placed in a high gain mode (activated by ground command) which uses the large dynamic range of the detectors and allows signal amplification by a factor of 3.

[3] For a good technical review of the nature of a Landsat pixel, see F. Gordon, Jr., *The Time-space Relationships of the Data Points (Pixels) of the Thematic Mapper and Multispectral Scanner, or "The Myth of Simultaneity,"* NASA Tech. Paper 1715, 1980.

able signals used by a film recorder to produce a photograph. In a photograph, the pixels are defined by clusters (with nonprecise boundaries) of varying densities of developed silver grains, all activated during film exposure. These density variations are usually recognized as gray levels (or relate to different colors in color film).

In a Landsat MSS image, the pixels are established sequentially along each scan line during scanning of the scene. For Landsat, each sharply bounded pixel records the radiances that emanate from a 79 m X 79 m (square) area on the ground. Because of the particular rate or interval in which video signals produced by incoming radiation are sampled along each scan line, each Landsat MSS pixel has effective ground dimensions of 79 m X 56 m. Since the IFOV is 79 m wide, adjacent pixels overlap, but the common practice is to ignore this overlap and consider a pixel as 56 m wide. The pixel in this case is therefore a rectangle with an area of 4424 m^2, but contains radiation inputs from an actual ground area of 6241 m^2, as determined by the 79 m X 79 m IFOV of the scanner. Any pixel can be retrieved and modified (reshaped) by appropriate computer processing.

A two-dimensional array is built up from all pixels in every single MSS scan line and those in each successive line.[4] Since these pixels are arranged in their proper relative positions with respect to the corresponding surface locations (usually through subsequent geometrical corrections), the result is a geographically accurate portrayal of that surface. Any given pixel is composed of integrated single values of reflectance collected from all the various reflecting objects, including clouds, within that segment of the surface encompassed in the IFOV. The array of DN's may be used to generate either an array of points (squares or rectangles) of different gray tones to produce a photo image, or an array of numbers in a printout map.

Mixed Pixels

The averaging of radiances from the different objects within each IFOV gives rise to the concept of mixed pixels. There are two contexts in which the effects of mixed pixels must be considered.

Consider first the imaging of such gross surface features as are shown in the typical rural setting of Figure 3-1. Each named class[5] is more or less homogeneous and some are larger than the sensor IFOV. If each resulting pixel happens to lie completely within, or fortuitously coincides with, the boundaries of a given class, then the brightness value (intensity) and its representative digital number for that pixel will be a single "pure" value characteristic of the band spectral properties of the dominant object making up that surface (for example, water body, barren soil, rock outcrop, dense forest stand). However, it is more likely that the pixel will straddle or cut across several class or feature boundaries. Owing to their natural sizes, distribution, and diversity, one might expect that parts of surfaces containing more than one class may be included in a pixel. The resulting brightness value is then a composite or weighted average of the spectral response from each, according to its proportion in the IFOV. Therefore, recognition of each feature or class becomes difficult, since there are two primary unknowns to account for—the identity of each class and its relative contribution. Various mathematical methods have been devised to solve for these unknowns, that is to say, to extract information about the individual classes contributing to the composite brightness value, but the problem remains complex. One simple improvement is to reduce pixel size (increase resolution) so that more pixels tend to fall within a given class or feature and fewer tend to cross boundaries.

Now consider an even more realistic case for Landsat. Within most 79 m X 79 m IFOV's the surface is likely to include many objects. Thus, one pixel may include soil, scattered rock outcrops, a stream, patches of grass, trees, a road, and a small house. The multiband brightness values (and their

[4] Pixels within a line are commonly called *samples* or *elements*. The two-dimensional array, then, consists of n lines (top to bottom) and s samples per line (left to right).

[5] Remember that a class may be described by its characteristics or features, but features may also be physical entities such as the trees, soils, and rocks, making up the wooded ridge in Figure 3-1.

ORIGINAL PAGE
COLOR PHOTOGRAPH

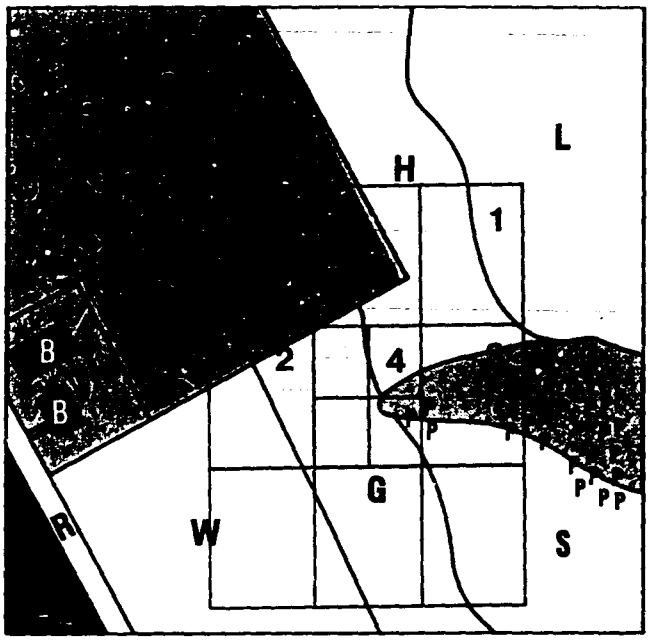

CATEGORY	BAND 5	BAND 7
L = LAKE	10	5
O = ROCK OUTCROP	30	45
H = HARDWOODS	30	55
P = PINEWOODS	15	30
G = GRASSLANDS	40	60
S = SHRUBBY MEADOWS	25	40
W = WHEAT	50	70
C = CORN	30	60
F = FALLOW FIELD	40	30
R = ROAD	70	40
B = BUILDING	40	10
Y = YARD	30	40

Figure 3-1. Hypothetical surface with typical land cover categories (classed by percent reflectances for two bands); random pixel array.

DN's) for this scene are therefore not indicative of any individual objects, unless one object tends to dominate.

In some special cases, we can make a more specific deduction of the nature of the object content in a given pixel. Identification of different crops is a good example. Plots of spectroradiances from several vegetable or grain types are generally very similar—essentially because of comparable contributions of chlorophyll absorption and cellular reflectance from the plant fibers. In cultivated fields, the shapes, sizes (both inherent and stage of growth), and spacing (affecting the relative proportion of soil and canopy or leaf area) of the different crop types become critical variables that greatly exceed the minor spectral variations. Thus, by combining knowledge of planting practices and the crop calendar, most major crop types can be separated and individually identified (usually, with 75 percent to 98 percent accuracy depending on crop characteristics, field sizes, number of observations, etc.).

The reason that we can classify and interpret Landsat images with reasonable accuracy is simply, as implied earlier, that we define our classes to be broad (large) enough to be grouped into distinct spectral and spatial patterns on a smaller scale regional (synoptic) basis. These are the so-called first and (some) second level categories that make up the land cover classifications devised by geographers (see p. 182). Thus, at Landsat resolution we can spot forests but not individual trees, cities but not houses and factories, landforms but often not exposed stratigraphic units, and field crops but not individual plantings. To recognize the smaller objects, we must use higher resolution scanners, preferably on aircraft platforms. The key rule in optimizing classification is simply to choose a resolution that approximates the sizes of the smallest specific classes whose identities are being sought.

#3-1: Are there any "pure" pixels in Figure 3-1? Name the features. Is this feature really pure? If not, why does it act as pure, i.e., have a characteristic set of spectroradiances that could be used to identify it as a distinct feature?

#3-2: Calculate the approximate percentage reflectances in bands 5 and 7 for the pixels labeled 1, 2, 3. (Hint: estimate relative areas, in decimals, of included features.)

#3-3: Estimate the relative areas of the features in the full pixel 4. Then, calculate the areas in the upper right and the lower left rectangles within pixel 4.

#3-4: From your consideration of pixel 4, draw some conclusion about the degree of "purity" as a function of pixel size.

Pixel Inhomogeneity

Let us now consider the problem of pixel inhomogeneity from the perspective of inherent class variability. As implied in a preceding paragraph, a single class (such as a field crop) will normally show some natural variation in spectral response because of differences in individual plant sizes, shapes, spacing, and vigor, as well as differences in soil clump size, moisture, and the like. Measurement values of surface reflectances for a given class made from different individual sampling points will tend to cluster around an average (mean) but will, nevertheless, show a spread or range (usually estimated as standard deviation σ). If the class is general enough, different field crops will show distinct differences evidenced as separable means and nonoverlapping spreads. However, in many instances, a Landsat classification may fail to distinguish the various crops with acceptable accuracy but can, at least, lead to a distinction between all field crops (combined) and other, possibly similar, categories or classes.

To illustrate this concept, examine Figure 3-2. This is a plot of percentage reflectance calculated from bands 5 and 7 Landsat data taken by the satellite over a county-sized area in the Piedmont of central Virginia on April 29, 1978. The two-band data (see pp. 29, - 273, and 446 for related discussions) were clustered into 50 separable spectral subclasses[6] by an unsupervised procedure (p. 446). The center of each numbered cluster (smaller ellipses and circles) denotes the statistical mean and the cluster boundary marks the spread at 1.5 σ for each spectral subclass.

[6] A spectral subclass is defined as a local cluster of similar spectral radiant values (for two or more bands) within a larger distribution of spectral radiances that characterize some given class or ground cover type; it usually, but not necessarily, corresponds to one of several physical or compositional variants within the class.

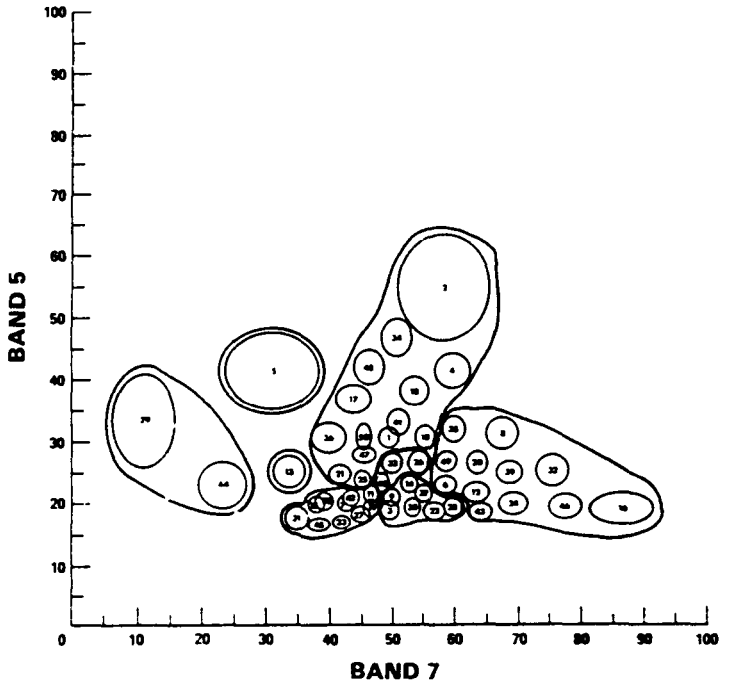

Figure 3-2. Clusters of 50 subclasses, representing 9 land cover classes in an area in Virginia, as determined by a band 5 - band 7 plot.

Just what land cover type accounts for a given cluster is not self-evident and must usually be established in the field. In this example, a painstaking ground verification study found that many seemingly different spectral subclasses actually embraced a range of variants within a single broad ground class. Thus, clusters 11, 19, 23, 27, 31, and 45 are all grouped near one another (that is, are spectrally similar in band 5 but show some variation in band 7). Field studies determined all these to be associated with stands of conifers—hence, representatives of a single ground class. However, the spectral differences within these stands express variations such as different species or, more commonly, ranges of crown cover (a function of tree density). Under some circumstances it is appropriate to set up each small cluster as a subclass, perhaps based on density, within the more general class *conifer*, but for Landsat this degree of division is often inaccurate and requires higher spatial resolution.

Field work confirmed that the other clusters are subclasses or variants that were conveniently grouped into more general classes, as shown in Table 3-1.

These classes are indicated by heavy line envelopes in Figure 3-2. Note that there is almost no overlap among the major classes (thus, efficient separability) although some subclasses experience slight to strong overlap at 1.5 σ.

Table 3-1
Classes and Subclasses of Clusters

Classes	Subclasses
Water	29, 44
Wetlands (nonforested)	13
Developed (bare ground)	5
Conifers	11, 19, 23, 27, 31, 45
Wetlands (forested)	7, 15, 38, 42
Agricultural Fields	1, 2, 4, 10, 17, 18, 21, 25, 34, 36, 41, 47, 48, 50
Fields (other)	6, 8, 12, 16, 20, 24, 32, 39, 43, 46, 49
Deciduous Forest	3, 14, 22, 28, 30, 37
Mixed Forest	9, 26, 33, 40

Pixels And Resolution

Before leaving this subject of mixed pixels, you can reach a rather startling awareness of the precise implication of pixel size (resolution) by an objective examination of Figures 3-3A through 3-3E. Figure 3-3A is a computer-generated enlargement of part of the Harrisburg, Pa., subscene in Landsat image 2904-14452 (see Figure 4-10) as photographed from the monitor of the IDIMS interactive system (pp. 194 to 211). At this scale, a few of the major features of an urban area may still be recognized (e.g., roads). The pixels making up the subscene are just beginning to appear as individuals but the array still strikes the eye more like points than discrete squares. However, in Figure 3-3B, a further enlargement (through resampling; see p. 431) of a small area (around the arrow) has now made each pixel clearly visible. The image that is still intelligible in Figure 3-3A has begun to take on an almost abstract look in Figure 3-3B because the presence of noticeable squares resembles a mosaic more than any representation of the real world. Yet a smaller subscene (again, around the arrow in Figure 3-3B) has been enlarged even further in Figures 3-3C and 3-3D. Figure 3-3C clearly shows the exact color assumed by each pixel when the same pixels from the bands 4, 5, and 7 data sets are superimposed in a false color composite (see p. 94). In Figure 3-3D, a band 7 image, each pixel is seen to have a single gray level. The blockiness is so dominant that the real world it

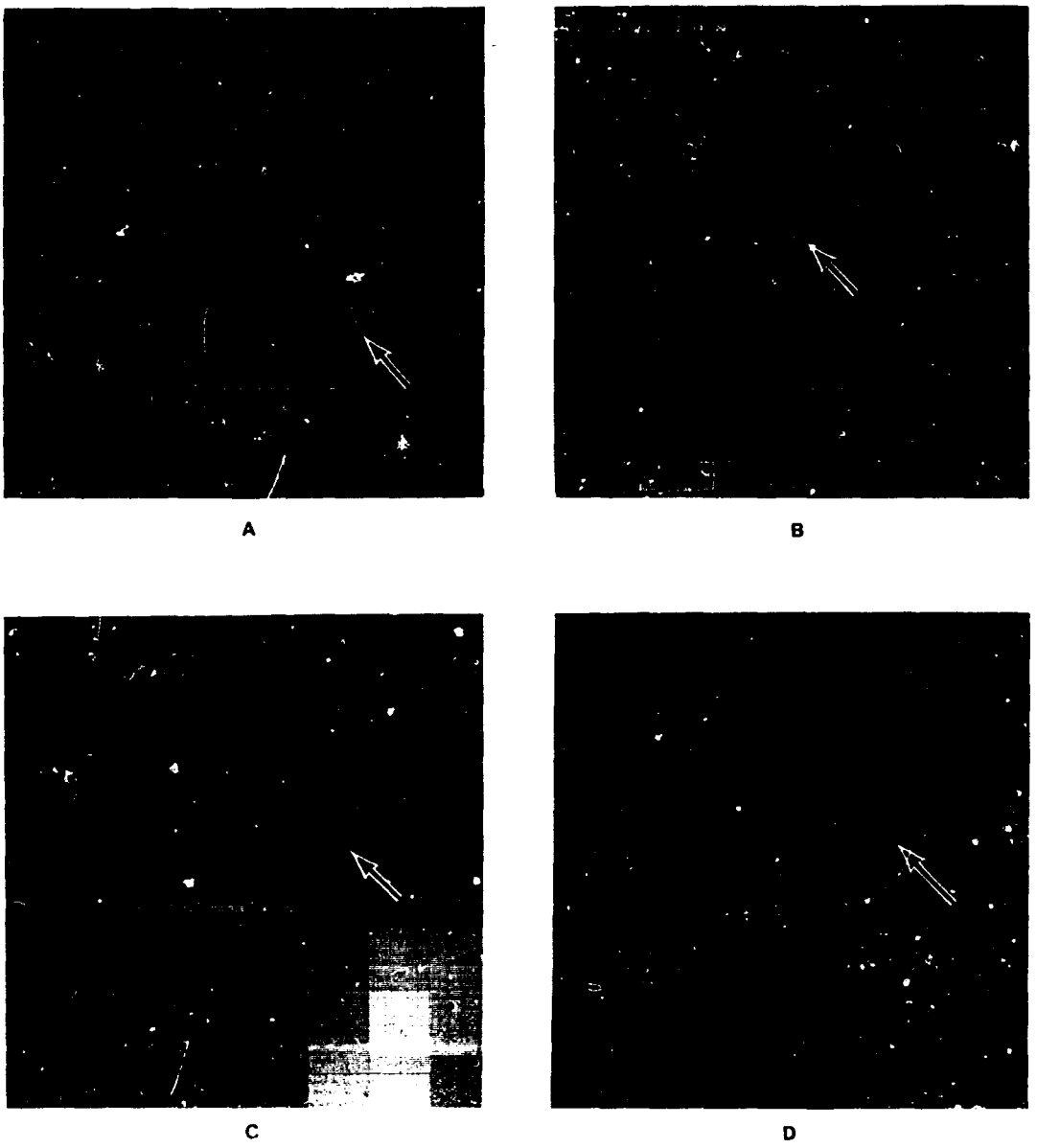

Figure 3-3A-D. Progressive enlargement (by computer) of a Landsat subscene around Harrisburg, Pa. (reference area marked by arrows [see text]).

llegedly depicts is almost totally unrecognizable. /ou are actually looking at parcels of ground 79 m n a side, in which many individual and varied bjects are contributing their own characteristic pectroradiances to the sensor. The mixing or veraging effect is responsible for the uniform ray level associated with each pixel. But now for revelation! The blocky subscene in Figures 3-3C nd 3-3D represents approximately the same round dimensions and location as the detailed ubscene in the aerial photo shown in Figure 3-3E on the following page. (It was impossible to duplicate these dimensions exactly: the Landsat subscene is about 50 percent larger than the 1:4000 scale aerial photo.) The aerial photo can display all objects in the scene larger than *ca.* 0.5 m, whereas, only discrete objects larger than 80 m are potentially identifiable in the Landsat subscene—and then only if they have some distinctive attributes such as a diagnostic shape or spectral response. One such feature in the aerial photo is the water-filled quarry (arrow). It is equivalent to about 1.5 pixels

Figure 3-3E. 1:4,000 scale aerial photo of area marked by arrows in 3-3B; lake corresponds to arrows in 3-3C and D.

(120 m) in longer dimension and is spectrally distinct from its surroundings. This "lake" does indeed dominate one pixel in Figure 3-3C, as marked by an arrow, and also influences several neighboring pixels, since it is likely that two or more pixels are superimposed over it.

#3-5: Can you correlate any other individual pixels with a feature or group of objects in the aerial photo? If so, name the feature.

#3-6: In Figure 3-3 you have been observing successively smaller areas of an image at larger and larger magnifications, in which individual components (the pixels) become bigger but their relation to their surroundings (context) becomes more obscured. Which common laboratory optical instrument does much the same thing?

#3-7: Lest you become disillusioned with Landsat images at this point in the workbook, and decide that nothing much worthwhile may be identified or learned from them, reassure yourself by writing a brief statement that specifies the kinds of information extractable from small-scale satellite imagery. In other words, why is low resolution imagery still useful for certain types of applications, even though the usual details recorded in aerial photos are not discernible?

MULTISPECTRAL REPRESENTATION OF COVER TYPES

So far in this activity, we have focused on the manner in which the Landsat MSS measures the spectroradiances from individual objects within plots of side length 79 m on the Earth's surface and integrates these reflectances into a set of values that together give a clue about the dominant cover type in each sampled plot. We shall now examine how these pixel arrays of varying spectroradiances yield different black and white photo images for each band and, conversely, how the gray levels in the band images may be analyzed to plot crude but usually diagnostic spectral curves for the major cover types.

Each cover type tends to be expressed by a characteristic gray tone in each band. The shape of each ground pattern occupied by a cover type may also serve, in some instances, as a clue to its identity. This gray tone is directly related to the percentage reflectance or brightness level of the type or class. The greater the reflectance from a cover type surface, i.e., the brighter or more radiant it appears to an energy detector, the lighter toned (toward white) will be its expression in a positive black and white photo-print. Conversely, greatly reduced reflectance, as from darker surfaces, will show up as dark (toward black) in the print.

The eight landscape cover types listed in the first column of Figure 3-4 are located within 1079-15131 (Figure 2-3D) by arrows labeled with arabic numerals. Find the cover type in each of the four black and white images in Figure 2-3, and note its gray level. The step scale at the bottom of each band frame is a guide. Count ten steps from right to left to cover the range distinguishable by eye, but combine every two adjacent steps to establish five levels from very light to very dark. In Figure 3-4, each landscape cover type is to be identified with one of the five levels of gray for each of the four MSS bands. A box for each level is placed under each band column. For each numbered cover type, note which band image has the darkest level or tone and place an X in the middle of that box. Then, plot X's under the band with the lightest tone and the two bands with appropriate intermediate levels. Fill in the area under the X in each column with pencil shading. This has been done for cover type 1 as an example.

LAND COVER TYPE	TONE	MSS				PREDICTED COLOR
		4	5	6	7	
(1) Barnegat Bay (lagoonal water)	V. Lt. Gray					
	Light Gray					
	Medium Gray					
	Dark Gray					
	V. Dk. Gray					
(2) Round Valley Reservoir (water behind dam)						
(3) Trenton, N.J. (metropolitan area)						
(4) Blue Mountain (N. of Allentown) (heavily forested ridge)						
(5) Pine Barrens N.J. (piney woods)						
(6) Large Open Area S. of Coatsville, Pa. (field crops)						
(7) Rectangle W. of Cedar Bridge, N.J. (cleared barrens)						
(8) Clouds (over ocean)						

Figure 3-4. Development of spectral signatures for eight land cover types.

Spectral Response Curves

The pencil-shaded areas resemble bars in a histogram (see Figure 6-17) and provide a graphical picture of the variation in reflectance from band to band. Now, connect the X's with a continuous line as shown in the Barnegat Bay example. The line you produce from each four plotted points is, in effect, roughly analogous to the spectroradiance curves extending across a continuum of spectral reflectances measured by a spectrometer in the field. Compare your results with the typical spectral curves for single classes on nonvegetated and vegetated land surfaces (taken from Root and Miller[7]) shown in Figure 3-5.

#3-8: Why is the width allotted to band 7 in Figure 3-4 greater than the spaces given to the three shorter wavelength bands? (Hint: Recall that the range of the photomultiplier detectors used in bands 4, 5, and 6 drops off drastically above about 1.0 μm; a photodiode detector is used for band 7.)

#3-9: What similarities do you observe among the class curves? What differences?

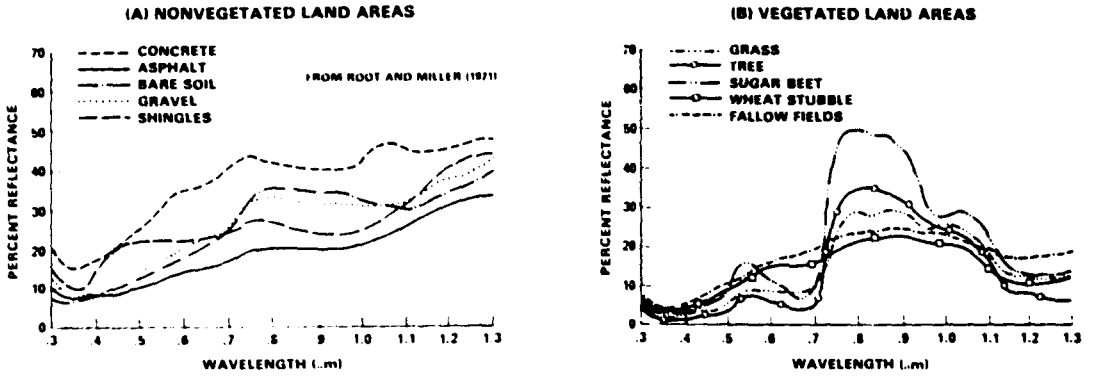

Figure 3-5. Some characteristic spectral signatures of land cover types.

Spectral Signatures

Curves representing measurements of the variation of reflected or emitted radiation intensities as a function of wavelengths in the electromagnetic spectrum are commonly referred to as *spectral signatures*.[8] Each ground cover type or class tends to have its own characteristic signature, which may be sufficient to identify it, although the shapes assumed by a type or class may also be necessary for identification.

> *This fundamental concept*, namely, that a class or object may be identified by its characteristic spectral signature, along with its distinctive shape, texture, and distribution (context) as supporting information, *is the keystone of multispectral remote sensing.*

The ability to obtain quantitative measurements of the spectral characteristics of different cover types or classes stands as one of three major advantages provided by the Landsat observing system over conventional panchromatic aerial photographic methods for monitoring the Earth's surface.

---

[7] Root, R. R., and L. D. Miller, *Identification of Urban Watershed Units Using Multispectral Remote Sensing Data*, Colorado State University, Ft. Collins, Colo., Grant #14031-001-3006, 51 p., 1971.

[8] Also known as spectral response patterns or spectral response curves. A spectral signature of a class (in reality, of the materials making up the objects that define the class) is not a unique curve but shows variations depending on the conditions of measurement, mix of objects, and other factors. See p. 30.

#3-10: Can you specify two other advantages?

#3-11: Again examine the two sets of curves in Figure 3-5. By visual inspection select and record up to three wavelengths (in practice, usually an interval or waveband) that could be used to separate or distinguish between the following combinations of two land cover classes: (a) Grass-Wheat; (b) Concrete-Asphalt; (c) Gravel-Shingles; (d) Wheat Stubble-Fallow Field; (e) Sugar Beets-Gravel; (f) Tree-Bare Soil. To do this, look for wavelengths in which differences in percentage reflectance are large (greater than 10 percent). These wavelengths, which you should designate λ_1, λ_2, and λ_3, need not, and usually will not, be the same for different pairs of classes. List two extended (greater than 0.05 μm) intervals in which most of the nonvegetation classes may be unambiguously differentiated from the vegetation classes shown.

#3-12: Obviously, a complete spectral reflectance curve, with all its fine structure, as produced with a continuously integrating spectrometer, provides more diagnostic and detailed information (absorption bands; fine structure) about the composition and other characteristics of the class or material being analyzed than does a series of single-valued waveband intensities measured by a spectroradiometer. However, at present it is technically "impractical" to operate a conventional spectrometer capable of measuring over a frequency (wavelength) continuum on unmanned satellites such as Landsat. Why? What prevents this mode of operation? (Hint: A spectrometer was used by astronauts on Skylab.)

FORMATION OF COLOR COMPOSITES

We shall now turn our attention to the ways in which Landsat color composite images are formed by combining black and white images from individual bands. One of the color versions (Figures 2-1, 2-17, or 2-18) of 1079-15131 is a typical product. To understand the production process, consider the reasoning behind the following experiment.

Look at the three squares in Figure 3-6 below. They contain four different geometrical designs, each located in the same position in all the squares.

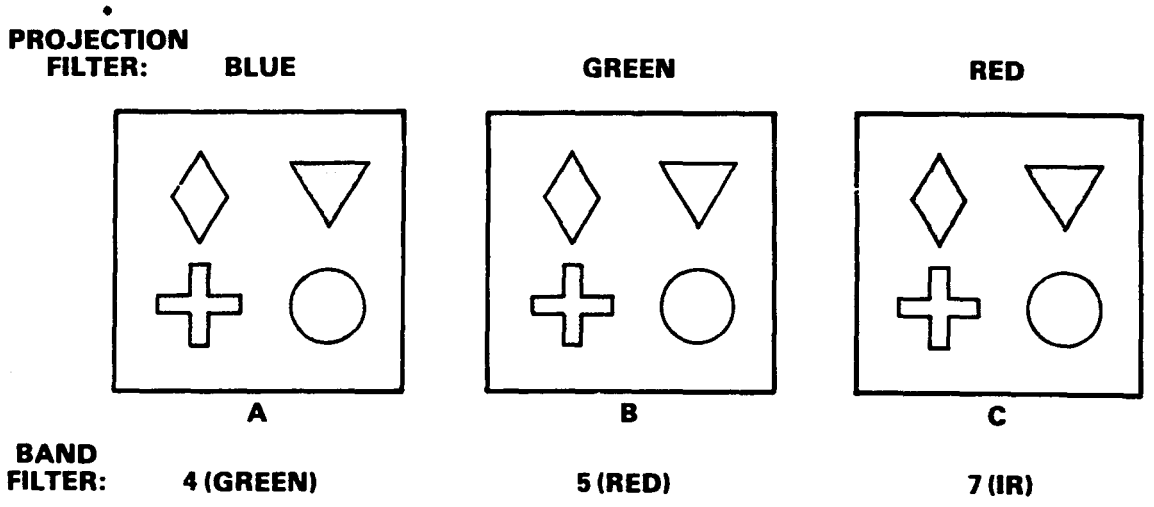

Figure 3-6. Diagram of projection filter and corresponding band filter.

The designs are openings over which light-transmitting filters are placed. Each dark (heavily shaded) design is covered by a minimum (< 10 percent) transmitting filter. Each light (clear, outlined only) design is covered by a maximum (> 90 percent) transmitting filter. The remaining area in each square will be considered opaque, that is to say, it has no effect in the experiment.[9]

The squares are now mounted each in its own light projector (for instance, 35 mm or lantern slide type). The designs projected simultaneously on a surface screen are precisely registered by moving each projector until equivalent shapes are superposed. A color filter is then placed in front of the lens of each projector: blue for square A, green for B, and red for C. Light passing through any two or three of the same clear designs and the color filters will be mixed by an additive process. The resulting colors can be easily predicted from the left-hand diagram of Figure 3-7.

This procedure, in which radiation of varying wavelengths and intensities (as through the use of variable density filters, or through patterns with different gray levels in an image transparency) from two or more independent sources is passed through color filters and mixed upon superposition, is an example of the *color additive* process. This process is used in forming primary colors and combinations thereof in color TV sets. Hues other than those indicated in Figure 3-7 (left) result when primary colors are mixed in unequal proportions.

Next, let us view the designs in Figure 3-6 in a different way. Consider now each clear design to be solid (not open) and covered by highly reflective material that is either assigned some visible color (including white) or returns radiation in the near infrared. Ignore the dark designs and, once again, pretend the material of the square between the designs is opaque, with no effect on radiation.

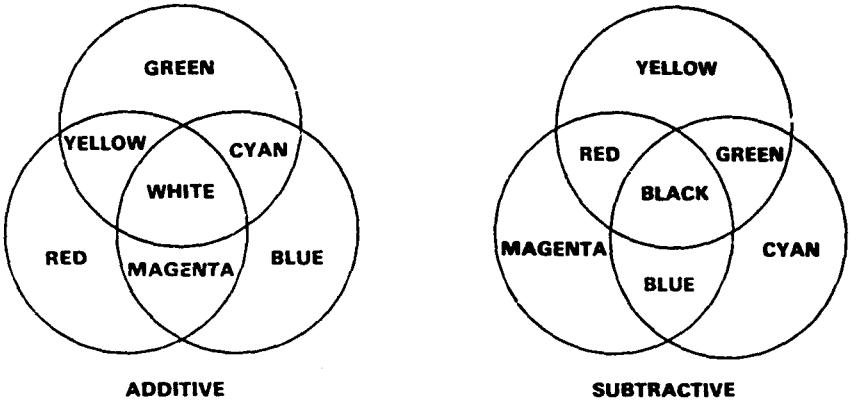

Figure 3-7. Color production by additive and subtractive processes.

The ◇ will be dominated by blue (almost no green or red contribution). The ▽ will be green, and + will show up as red. The combination of green and red for the ○ figure (in B and C) will produce yellow.

#3-13: What color would result if the + in A were clear instead of dark?

#3-14: What color would occur if ○ were clear in all these squares?

#3-15: What combination is needed to achieve a black tone? A brown tone?

The objective of this second experiment is to determine what gray level will be recorded on (visible/infrared-sensitive) film when the clear designs are (1) assigned a "color" (including IR), and then (2) viewed through some highly selective filter (one that passes only a narrow band of wavelengths).

[9] If you are so inclined, you can actually conduct the experiment at this stage. Make the squares out of cardboard, cut out the designs and cover them with exposed (dense) film and clear plastic or cellophane. However, you can just as well visualize the entire experiment and probably deduce the expected results.

If we look at the reflecting design in square A through a green band filter, we ask what colors it can have that will pass through the filter, be recorded on a film negative, and be registered on a positive black and white print as a light gray ◇. The obvious answer is green. Reflected light from a red (or blue, or other nongreen color) design would be completely absorbed so that the ◇ appears dark (blackish) on the print. However, if the design is white, that portion of the white light (all colors) consisting of green wavelengths will likewise pass through the filter to produce a similar light gray ◇. If the design is black, it will show as black on a print, regardless of filter bandpass wavelengths.

#3-16: What "colors" must be assigned to the clear designs in B to produce a corresponding light gray on a print? In C? What must we change to record a blue design as a light gray pattern? What must be used to record in like manner a yellow design? Suppose the "light" is reflected IR radiation; how does one record this as a light tone?

We have just described in an elementary way the essence of how a multispectral sensor (typically, composed of radiation-gathering optics, selective filters, detectors, and recording system) senses "colors" from features distributed in the scene, and how some color rendition of that scene may then be reconstructed photographically. A selective filter passes all radiation within its waveband and rejects other radiation, while preserving the relative positions (in the sensed scene) of each radiation source or surface feature. This results in different light and dark patterns (designs) on film that correspond to the passed or rejected (nontransmitted) radiation from the different surface features. Different gray level patterns corresponding to these features are produced by different selective filters, but each pattern is mutually coincident (registered) on film renditions of the different bands. When these patterns are recorded on positive transparencies, combinations of the transparencies may be projected (by back illumination) through color filters to reconstruct the original colors or to produce false color composite images. A ***false color composite*** is formed by using projection filters whose "colors" or radiation-passing wavebands are not the same as those used by the sensor in making each black and white band (i.: Figure 3-6, the projection filters are listed at the top and the selective filters defining the sensor band are specified at the bottom). The conditions by which the standard false color composite is produced from Landsat black and white transparencies (as for example, Figure 2-1) are given in Table 3-2.

We must use false color to depict radiation beyond the wavelength response range of the human eye (in this case, parts of the near or reflective infrared). In effect, we have shifted three consecutive intervals of radiation in the green, red, and near-infrared toward shorter wavelengths until the green is expressed in blue, the red in green, and the IR in red (other natural colors, such as yellow, will likewise assume new false colors as well). The sequence yellow, magenta, and cyan was chosen for film recording by color subtraction because

Table 3-2
Standard False Color Composite Conditions

Dominant Natural "Color" of Scene Feature	Band Number	Band Wavelength Interval	Color of Projection Filter	False Color of Scene Feature
Blue	4	0.5-0.6 μm	Blue	Faint Blue to Black
Green	5	0.6-0.7 μm	Blue	Blue
Yellow to Red	6	0.7-0.8 μm	Green	Green to Yellow
Near IR	7	0.8-1.1 μm*	Red	Red
White	4-7	0.5-1.1 μm	All	White

*Note that 0.9 μm is approximate cutoff wavelength for photographic IR negative film

only cyan dye in a photo emulsion is sensitive to infrared radiation (beyond a 0.70 μm cutoff for magenta and 0.60 for yellow). This explains why highly reflective infrared radiation from vegetation is expressed in red tones in color IR photos (see also pp. 97-98).

#3-17: Why is a false color IR image or color IR film better suited than natural color images or film for detecting different vegetation types or vegetation stress? (Hint: Examine the curves in Figure 3-5.)

In practice, any three of the four black and white positive transparencies made by film recorders from the four Landsat MSS band data may be combined into a false color composite. This is commonly done by photographic techniques (see below). Alternatively, the transparencies (usually as 70 mm "chips" rather than standard 9 in. or 1:1,000,000, products) may be inserted into a color additive viewer that enlarges and projects an image onto a viewing screen.[10] A typical viewer contains four film holders through which white light is transmitted into an optical train consisting of prisms and lenses that redirect, focus, and superpose the images onto a frosted screen. Precise superposition is accomplished by gears that allow *X-Y* translations, rotations, and up-down movements of each tray. Four filters (blue, green, red, clear) are mounted in each of four filter wheels which may be inserted into the optical train to project each image in some primary color or in black and white. The relative amount of each filter color added to the scene may be controlled by varying the intensity of the light bulb used with each image.

Thus, consider a given pattern that appears medium gray in the band 4 image transparency, dark gray in band 5, and very light gray in band 7 of a Landsat scene. When superposed in a color additive viewer, the pattern will take on a reddish color as blue, green, and red filters are coupled with the bands 4, 5, and 7 images respectively. This is the color almost exclusively associated with vegetation. A pattern of dark gray (4), light gray (5), and medium gray (7) yields a yellow (with greenish tint) color, characteristic of red soils.

#3-18: What color will a pattern assume when the combination band 4 = medium gray (red filter), band 5 = very dark gray (green filter), band 6 = medium light gray (blue filter) is used?

This last question suggests that different combinations of filters and band images can lead to interesting, often esthetically pleasing color composites and, for some features, significant enhancement (emphasis), allowing better detection and/or measurements. This is well illustrated in Figure 3-8, in which the New Jersey scene (1079-15131) has been produced by the filter-band combination of red (4), green (5), blue (6).

#3-19: Compare this with the false color composite of this scene (Figure 2-1). Describe the effect of this new combination on patterns of sediment in the Atlantic Ocean off the New Jersey coast. Are any other features easier to detect in this combination? Specify.

#3-20: Now refer again to Figure 3-4. Applying the standard combination of bands and filters (4 = blue, 5 = green, 7 = red), predict the color expected for each cover type listed in that table, using the last column to record your response.

#3-21: What colors would you expect for cover types 4 and 7 if the band/filter combinations were changed to 4 = blue, 5 = red, 7 = green?

#3-22: Why can the natural colors of many features (for example, water) not be reproduced from the combination in #3-21, which would seem to produce reds for red soils and greens for trees and other vegetation?

#3-23: What would be needed as a future MSS system to obtain natural (true) color images?

[10] Still another simple and low cost technique is to mount each of the three transparencies in one of three suitable projectors (e.g., lantern slide type), place a blue or green or red filter in the optical path of each projector, project the proper combination of film and filter onto a screen or wall, and move individual projectors until images superpose.

ORIGINAL PAGE
COLOR PHOTOGRAPH

Figure 3-8. New York Landsat scene in nonstandard false color rendition (band 4, red; 5, green; and 7, blue).

Note: A crude quasi-natural color image is sometimes obtained by combining only band 5 (red) and band 7 (green), but water bodies appear black. Projecting band 4 through blue distorts the colors of the red and green objects. Experiments by the U.S. Geological Survey and others have produced remarkably realistic natural color images through creation of a "blue band" image. This is generated from a computer program that assigns appropriate gray levels based on the spectral response of common objects in the blue wavelength region. The Thematic Mapper (TM) on Landsat-D will carry a blue channel (see p. 378).

Color composites may also be made by a subtractive process. Most positive color film transparencies and prints are generated in this way. The right-hand diagram in Figure 3-7 shows how each of the primary colors is reconstituted by superposition of the appropriate two subtractive colors,[11] each being one of the complementary colors (e.g., cyan is complementary to red and magenta to green; cyan and magenta together form blue).

In summary, the color printing process works this way. A color negative is produced by passing white light (containing the primary colors) through an emulsion that consists of layers sensitive to blue, green, and red light. The blue layer responds to blue light and retains images of blue objects in the scene. The green and red layers record green and red objects respectively. When the negative is developed, dyes are formed in each layer as follows: blue layer-yellow dye; green layer-magenta dye; red layer-cyan dye. A red object will be represented by a cyan color on the developed negative, a blue by a yellow image, and so forth. When white light is passed through this negative to make a print, each dye acts as a color filter on a primary color. The cyan-dyed image, for example, absorbs red and passes blue and green. This dye then produces the color complementary to blue and green namely red, in the final prints. This color is the same as that of the original object.

As another illustration of the subtractive process, you might seek a demonstration of the Diazo process—if not available, imagine the following. Transparent light-sensitive Diazochrome films come in a selection of ten colors including the three complementary ones—cyan, magenta, and yellow. To "burn" or expose a film sheet, a black and white positive transparency is placed in contact with the film, ultraviolet light is passed through it, and the film developed by ammonia vapors. Suppose a standard Landsat false color composite is required. For band 7, the vegetation patterns appearing as light tones in the transparency will allow light to reach a cyan film and thus expose or bleach out the cyan color. Vegetation patterns, expressed as medium dark and very dark tones in bands 4 and 5 positive transparencies, respectively, will appear as unexposed or still colored areas in the magenta (band 5) and yellow (band 4) films. When the three developed film sheets are superposed in close registration, the combination of yellow plus magenta plus clear (bands 4, 5, 7, respectively) will, as seen from the right diagram in Figure 3-7, give rise to the reds characteristic of vegetation in a false color composite. Red soil, which appears yellow in this false color composite, is represented as dark, very light, and light tones in bands 4, 5, and 7 transparencies, respectively. The yellow color remains for the soil patterns when band 4 is paired with yellow Diazo film. The magenta and cyan films, coupled with bands 5 7, become clear at the red soil patterns. When the three film sheets are superposed, only the yellow contributes at the registered patterns. Bluish silty water is produced by the combination band 4-dark yellow; band 5-medium dark magenta; band 7-light cyan.

[11] A primary color is produced by subtraction whenever white light passes through a color filter that subtracts (absorbs) all other colors.

VISUAL IDENTIFICATION OF LAND COVER TYPES

To complete this section, review the information in Table 3-3, which lists the characteristic gray tones and false colors of common land cover types appearing in black and white and false color images. Then examine Figure 2-17 (and refer also to Figure 2-3 A to D). The arrows point to examples of the land cover categories. Each arrow is labeled by a small arabic letter corresponding to

Table 3-3
Identification of Land Cover Categories

Category	Best Bands	Salient Characteristics
a. Clear Water	7	Black tone in black and white and color.
b. Silty Water	4, 7	Dark in 7; bluish in color.
c. Nonforested Coastal Wetlands	7	Dark gray tone between black water and light gray land; blocky pinks, reds, blues, blacks.
d. Deciduous Forests	5, 7	Very dark tone in 5, light in 7; dark red.
e. Coniferous Forest	5, 7	Mottled medium to dark gray in 7, very dark in 5; brownish-red and subdued tone in color.
f. Defoliated Forest	5, 7	Lighter tone in 5, darker in 7 and grayish to brownish-red in color, relative to normal vegetation.
g. Mixed Forest	4, 7	Combination of blotchy gray tones; mottled pinks, reds, and brownish-red.
h. Grasslands (in growth)	5, 7	Light tone in black and white; pinkish-red.
i. Croplands and Pasture	5, 7	Medium gray in 5, light in 7; pinkish to moderate red in color depending on growth stage.
j. Moist Ground	7	Irregular darker gray tones (broad); darker colors.
k. Soils-bare Rock—Fallow Fields	4, 5, 7	Depends on surface composition and extent of vegetative cover. If barren or exposed, may be brighter in 4 and 5 than in 7. Red soils and red rock in shades of yellow; gray soil and rock dark bluish; rock outcrops associated with large land forms and structure.
l. Faults and Fractures	5, 7	Linear (straight to curved), often discontinous; interrupts topography; sometimes vegetated.
m. Sand and Beaches	4, 5	Bright in all bands; white, bluish, to light buff.
n. Stripped Land-Pits and Quarries	4, 5	Similar to beaches—usually not near large water bodies; often mottled, depending on reclamation.
o. Urban Areas: Commercial Industrial	5, 7	Usually light toned in 5, dark in 7; mottled bluish-gray with whitish and reddish specks.
p. Urban Areas: Residential	5, 7	Mottled gray, with street patterns visible; pinkish to reddish.
q. Transportation	5, 7	Linear patterns; dirt and concrete roads light, in 5; asphalt dark in 7.

the letter for that category in Table 3-3. However, not every category is present (or identified) in the scene. You can refer to this table again in responding to questions in Activity 4, when specific land covers need to be identified.

One last comment: It might seem from Table 3-3 and other indications in this section that band 6 has only limited value. It is generally true that band 6 is largely redundant in relation to band 7. Spectral responses in each wavelength interval represented by the two bands (6 = 0.7–0.8 μm; 7 = 0.8–1.1 μm) tend to be similar for most common surface features and objects. However, there are real, often significant, differences in average spectral intensities recorded in these two bands. For example, certain rocks containing ferric iron will reflect less light (because of absorption bands) in band 7 than in 6. Silt-laden water is somewhat more reflective in band 6 than in 7. Certain vegetation types are characterized by diagnostic, but slightly different, reflectance intensities in the two bands. These differences, even though usually small, become important when computer processing depends on digital number values from both bands for feature identification and classification.

ACTIVITY 4

PHOTOINTERPRETATION OF LANDSAT IMAGES

LEARNING OBJECTIVES:

- *Develop a facility for applying conventional techniques of photointerpretation to small scale (satellite) imagery.*
- *Be able to locate, identify and interpret small natural and man-made surface features in a Landsat image.*
- *Use supporting imagery, such as aerial and space photographs, to conduct specific applications analyses.*
- *Learn to apply change detection techniques to recognize and explain transient and temporal events in individual or seasonal imagery.*
- *Produce photointerpretation maps that define major surface units, themes, or classes.*
- *Become adept at classifying or analyzing a scene for specific discipline applications in geology, agriculture, forestry, hydrology, coastal wetlands, and environmental pollution.*
- *Evaluate both advantages and shortcomings in relying on the photointerpretive approach - rather than computer-based analytical approach - for extracting information from Landsat data.*

HELPFUL RULES FOR PHOTO-INTERPRETATION

Although the trend in information extraction from Landsat is clearly toward use of computers to handle the large volumes and quantitative nature of the data, much may still be learned and accomplished by examination of images with the classical techniques of the photointerpreter. This approach—particularly favored by geologists—is also well suited to teaching others some of the basic principles by which the Earth's surface may be analyzed for practical applications. In this activity, we shall concentrate on two adjacent scenes imaged at different times in a year over a span of 5 years. Thus, the emphasis in this activity will be placed on information extraction and the resulting applications based on *change detection*. You will be concerned with several specific themes that will occupy most of the interpretive work you do during this tutorial session, but there will also be some follow-up questions and exercises presented as an additional challenge to those of you so motivated to delve deeper. Although most of the images you will use in this activity are standard or darkroom enhanced photoproducts, you will also examine several computer enhanced versions as a further aid to interpretation and as an introduction to the next activity, which deals with computer processing.

Here are some helpful rules to guide you in reaching accurate interpretations of photoimagery when performing this activity:

1. Look for differences in gray tones and/or color. Such differences are often paramount in recognizing the presence of specific surface features and defining boundaries between different classes. In many instances, each tonal or color pattern is a key to the identification of a specific feature or class, as you have just noted from Table 3-3.
2. Rely on shapes of ground features and their context (spatial relations with one another) as further clues to identify.
3. Compare two or more scenes to resolve uncertainties about some unknown features. If a feature remains similar in tone or color (after compensating for differences in atmosphere, Sun-illumination, and photoprocessing) from season to season, it is probably not related to vegetation or to transient events (river silt, smoke, etc.). Features in band 7 images that appear light during growing seasons and noticeably darker in late fall–winter–early spring scenes are almost certainly vegetation.
4. Seek out supporting information from maps, reports, and publications as aids to feature (pattern) recognition and classification. Perhaps the best single reference for interpreting Landsat images of parts of the United States is the National Atlas of the United States, published in 1970 by the U.S. Geological Survey.
5. Draw upon your own experiences, your observations of the countryside, and your knowledge of recent environmental and resources concerns as supporting sources of information for recognizing features and interpreting changes.

As you perform the various tasks in this section, you may be asked at first to look at certain specific features without being given much background information. Apply your reasoning powers and your fund of knowledge to arrive at conclusions. Don't feel discouraged if you are unable to answer every question, as you simply may not know some essential information. As you progress, the answers will more or less unfold and you will begin to see the methods and relations used by experts in photointerpretation.

THE HARRISBURG SCENE: A FIRST LOOK

We shall begin Activity 4 by becoming generally familiar with a scene covering part of southeastern Pennsylvania. It will be referred to hereafter as the Harrisburg scene. It lies to the west of the New Jersey scene we studied earlier, and, in fact, the specific rendition to be looked at first (Figure 4-1A and B, and Figure 4-2, frame 1080-15185) was acquired on the following day (October 11, 1972) from the adjacent orbit. On this day, in particular, the weather was outstanding for ob-

Figure 4-1A. Band 5 rendition of October 11, 1972 Landsat-1 scene covering east-central Pennsylvania including Harrisburg.

taining a sharp image from Landsat; a crisp cold front had advanced over the entire eastern United States after a heavy rainstorm on the previous day. Behind the front was a high pressure, low moisture, clear air mass that reduced scattering and absorption and thus caused only minimal degradation of scene radiance. On the same day, the next scene along the same orbital path covered Washington, D.C., whence was generated the image so often reproduced as an outstanding example of the quality of imagery obtainable from Landsat (see Figure 5-1). Examine the Harrisburg scene, in both its black and white and color renditions, to savor its quality.

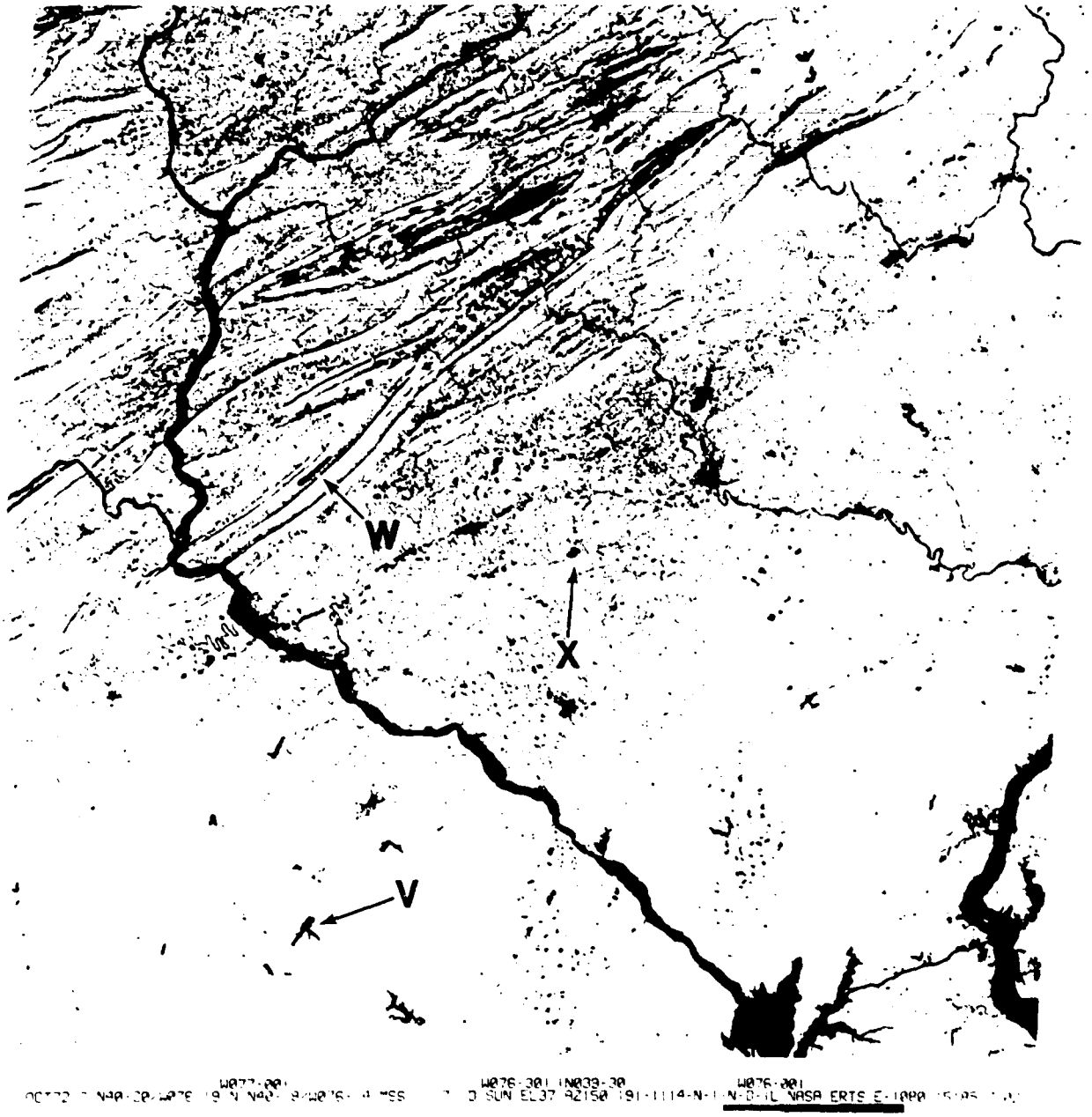

Figure 4-18. Band 7 version of October 11 Harrisburg scene.

#4-1: To develop an orientation to the geography contained in this scene, locate by grid coordinates (using Overlay 1) the following places (refer to an atlas): (a) Harrisburg, (b) Chesapeake Bay, (c) Interstate 80, (d) Allentown, Pa., (e) Juniata River, (f) Reading, Pa., (g) South Mountain, (h) Delaware River, (i) Sudbury, Pa., (j) Lycoming Creek, (k) Penn. Turnpike, (l) Gettysburg, Pa.

#4-2: List any other geographical features and points of interest you may recognize in this scene. Some of these may be singled out in subsequent parts of this activity.

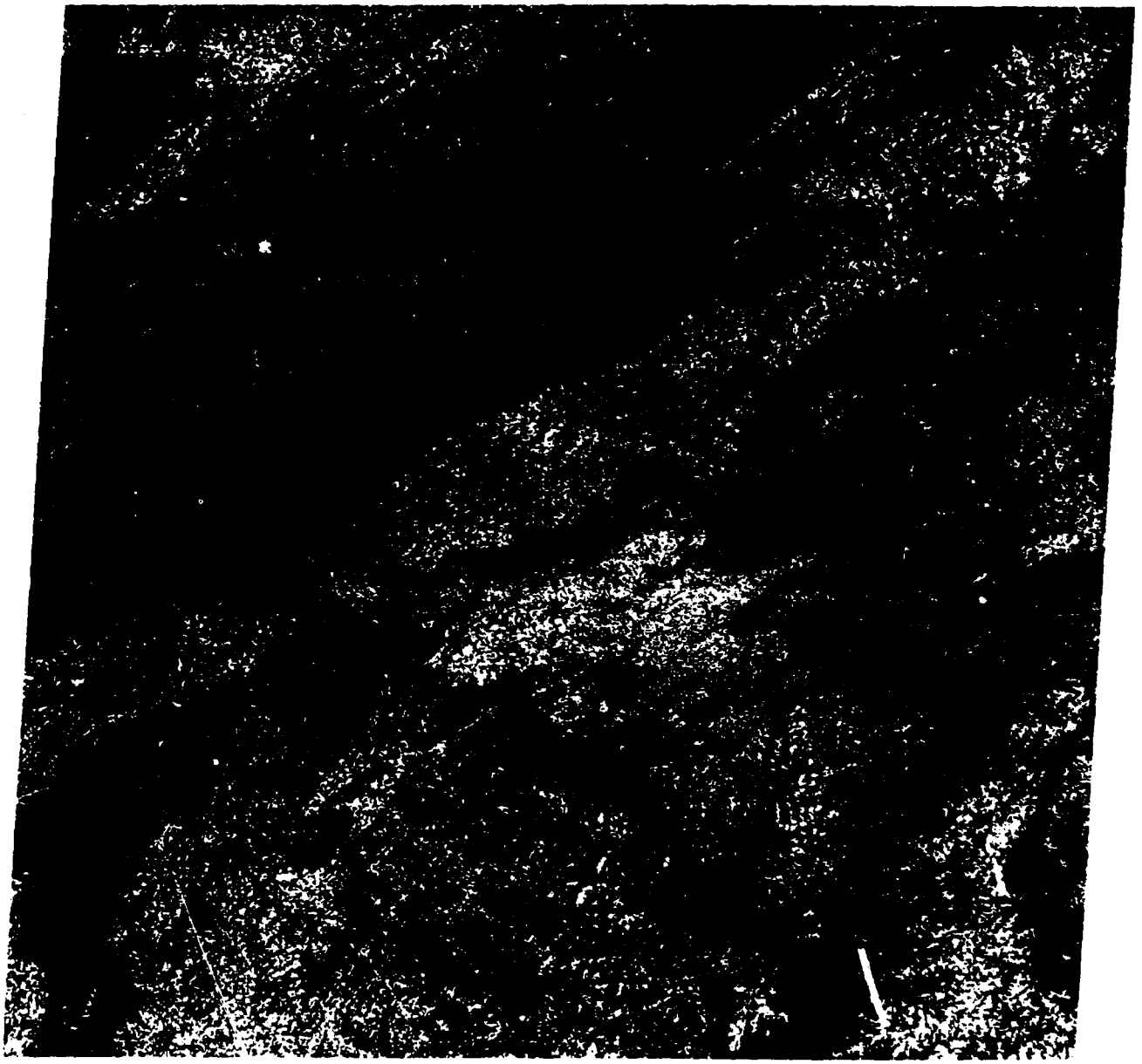

Figure 4-2. False color composite image of October 11, 1978 Harrisburg scene.

Superb as the 1972 scene is, it is actually eclipsed by those shown in Figures 4-3 and 4-4. This scene, also of the Harrisburg region and acquired during October, but in 1975 and two weeks later in the season, has been generated with the computer routine (geometrical/radiometric correction, destriping, contrast and edge enhancements) developed by the EROS Data Center (see p. 149).

#4-3: Examine both the band 7 and color renditions of this 1975 scene. To evaluate the relative merits of the two renditions, look once more for the same localities picked out in #4-1. Compare

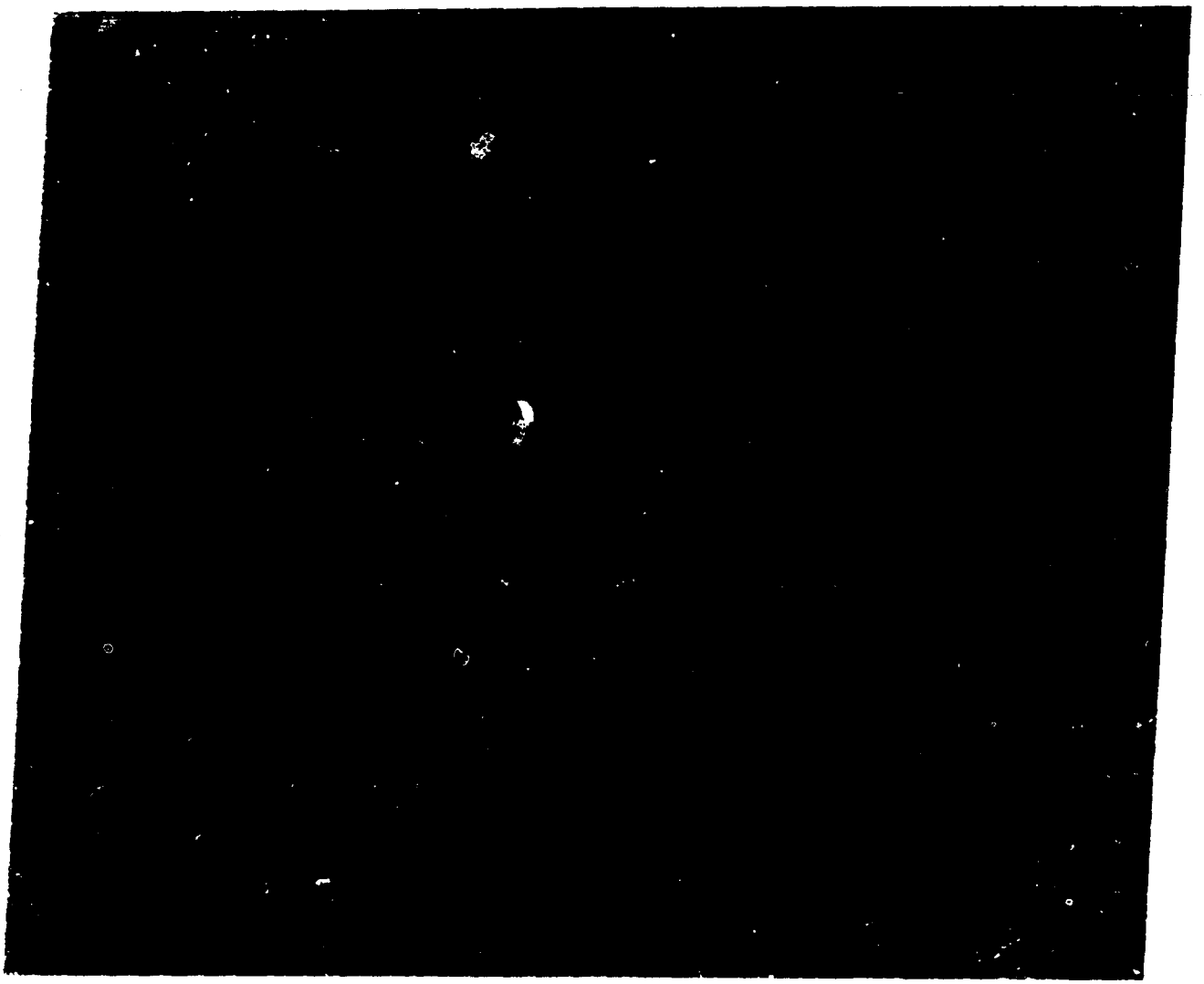

their expression in the October 1972 and 1975 scenes. Then closely scrutinize each scene for the details in and around the following areas (again, consult an atlas as required) and comment on the presumed improvements in the 1975 version: South Mountain; farmlands around Hershey, Pa.; Wilmington, Del.

#4-4: Can you spot at least one major addition to the 1975 scene of some man-made feature not evident (and presumably not completed) in 1972? (Hint: Think fluid.) Locate by Overlay 1 grid coordinates. What is it?

Figure 4-38. Band 7 image, October 23, 1975; computer-processed at EDC.

A VIEW FROM SKYLAB

Since we have focused our attention on this overall scene of the Harrisburg and eastern Pennsylvania region, let us divert for a moment to consider a characteristic product obtained by another imaging system that operated from a space platform. Figure 4-5 is a false color infrared photo taken by the astronauts with the S-190 A film camera (Itek Camera #3) from Skylab-3, at an altitude of about 431 km (268 miles). The picture was acquired on August 16, 1973. At a nominal scale of nearly 1:1,000,000, it covers a distance of approximately 130 km (80 miles)

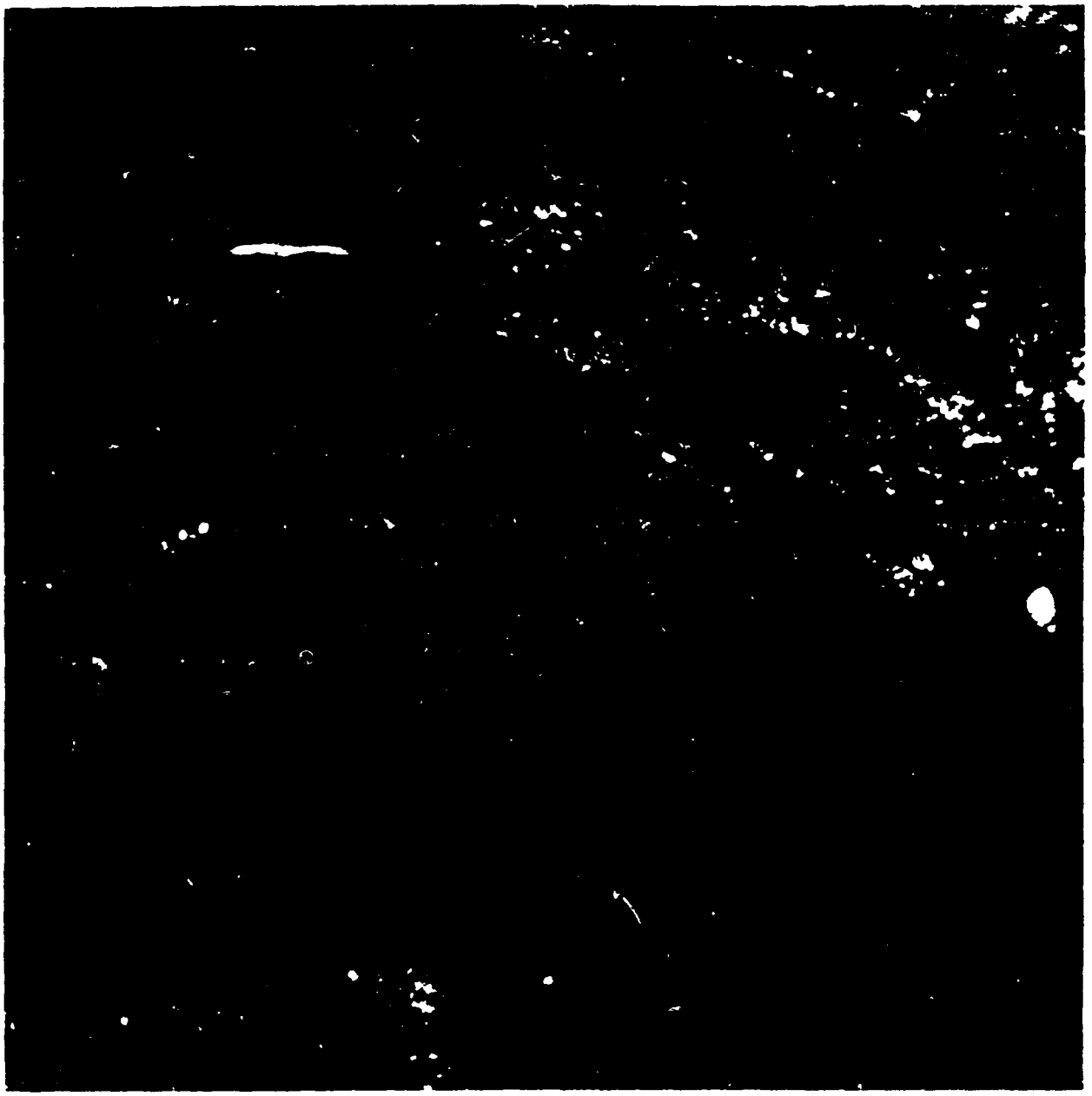

Figure 4-5. Skylab's 190A photo taken on August 16, 1973 showing part of southeastern Pennsylvania.

from left to right. This particular photo was shot at a slight angle off the vertical, and so distances and ground resolution vary somewhat with position from the nadir point (i.e., the instantaneous ground point lying vertically below the viewing platform). Under optimal conditions, a resolution of about 70 m (230 ft) has been cited for the camera/spacecraft configuration.

#4-6: The location of this Skylab scene should be obvious. You are invited to compare this rendition with the same-scale October 1972 and 1975 Landsat scenes and draw your own conclusions about relative merits. Suggest a reason for the dominant blue hue in this color IR photo, particularly since response of vegetation (as red tones) should be high in August.

Perhaps the most spectacular set of Skylab images of the eastern United States were acquired by the Earth Terrain Camera (S-190B) during a northeast pass from Louisiana to New England in September of 1973. Images taken during that orbit have been joined in an uncontrolled mosaic strip prepared at the Johnson Space Center in Houston, Texas. The mosaic that extends across southeastern Pennsylvania, from west of Harrisburg to east of Allentown, is included as a fold sheet in the back pocket of this workbook. Color processing has eliminated the blue hue which pervades Figure 4-5 but the resulting image departs somewhat from a natural color photo (especially evident in the river waters). Nevertheless, this is a striking rendition with which you should become familiar.

#4-7: The Earth Terrain Camera flown during this Skylab-3 mission has an optimal resolution of 30 m (98 ft) in natural color photos. Examine the Skylab mosaic. What new features can be identified in this 1:250,000 scale mosaic?

APPLICATIONS-ORIENTED PHOTOINTERPRETATION

Atmospheric Effects

During most of the remainder of this activity we shall also use examples of the Harrisburg scene from other dates. However, keep the splendid October 1972 and 1975 Landsat scenes and the Skylab mosaic on hand as standards of reference.

Let us continue by trying to identify some obvious features. In the black and white renditions of 1350-15190 (Figure 4-6A and B), look at the whitish feature marked by arrow A just east of Allentown, Pa. Compare this with the equivalent area in 2868-14471 (Figure 4-8A and B). Note the dates each scene was imaged.

#4-8: What is the most likely explanation?

#4-9: Do you think the same explanation holds true for the whitish feature under arrow B as shown in 2868-14471? What alternative explanation(s) can you propose?

#4-10: Examine bands 5 and 7 for each scene (Figures 4-6A and B and 4-8A and B). In which are the features A and B best displayed? Why?

#4-11: From this pair of observations, can you suggest any practical use of Landsat imagery as an environmental monitoring tool?

#4-12: What is an obvious limitation to this use?

While we are still thinking about above-surface phenomena, let us reexamine the black and white and color renditions of the 1350-15190 scene (Figures 4-6 and 4-7). Compare these with equivalent images from the October 1972 and 1975 scenes.

#4-13: What is your general assessment of the quality of the 1350-15190 scene compared with the October scenes?

#4-14: Noting the date of acquisition—July 1973—of 1350-15190 and recalling the typical summer climate in the eastern United States, offer an explanation for the seeming degradation of the image quality. Which band displays the most degradation? Why? Which band shows least effect? Why?

#4-15: What might be done to improve the quality of this image? (Some knowledge of computer processing may be necessary to answer this.)

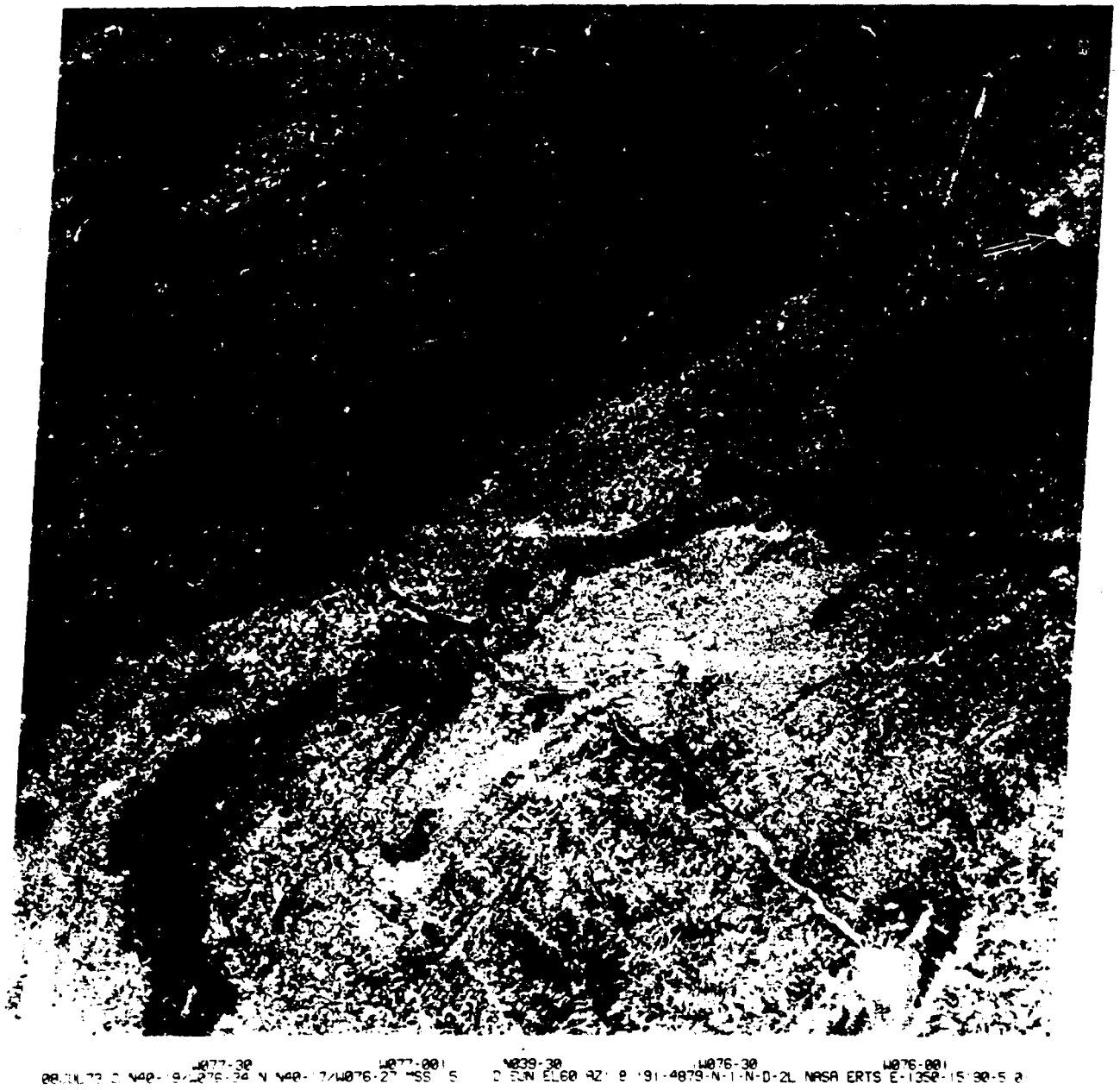

Figure 4-6A. Band 5 image of Harrisburg scene obtained by Landsat-1 on July 8, 1973.

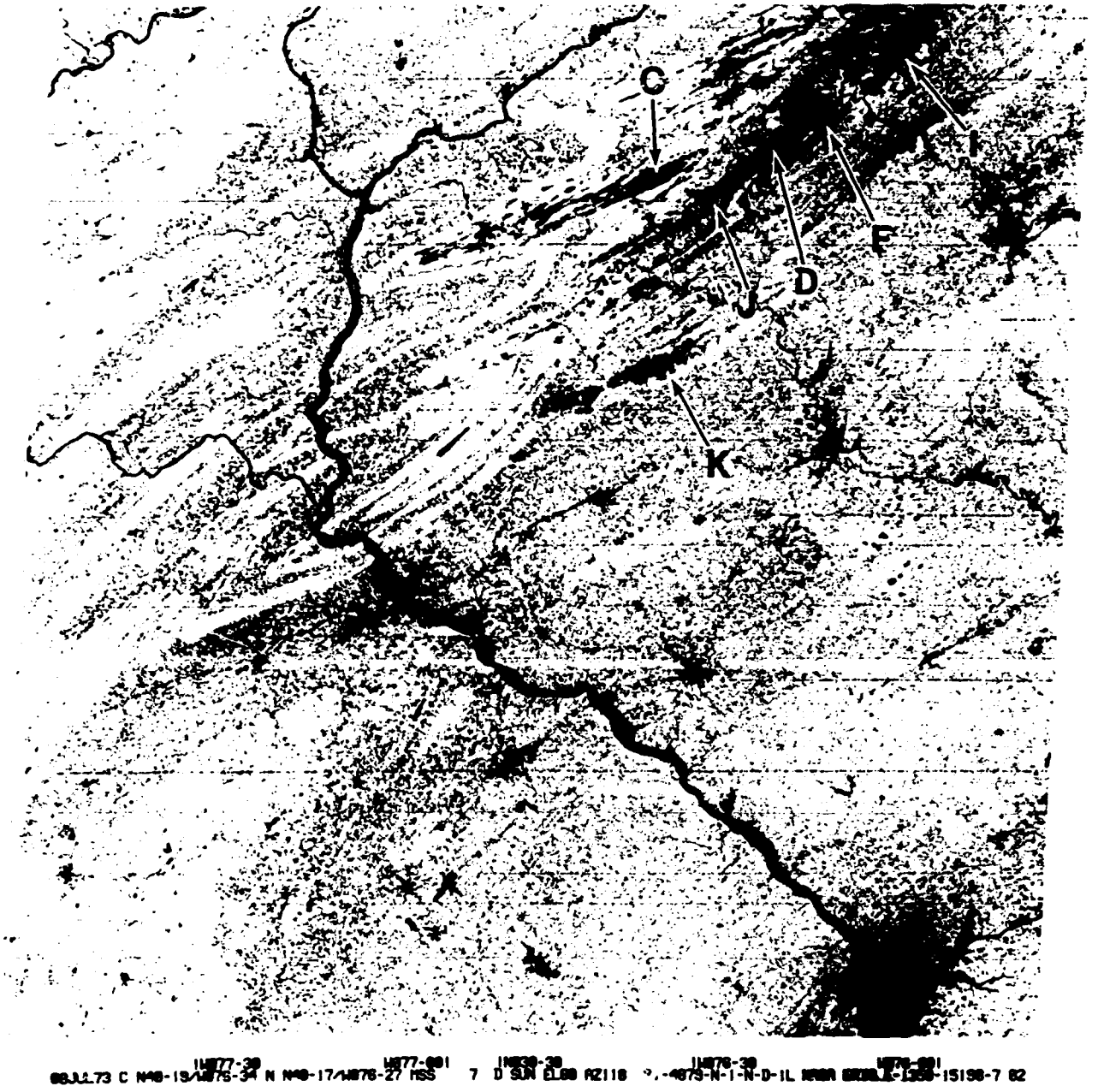

Figure 4-6B. Band 7 image at July 8, 1973 scene.

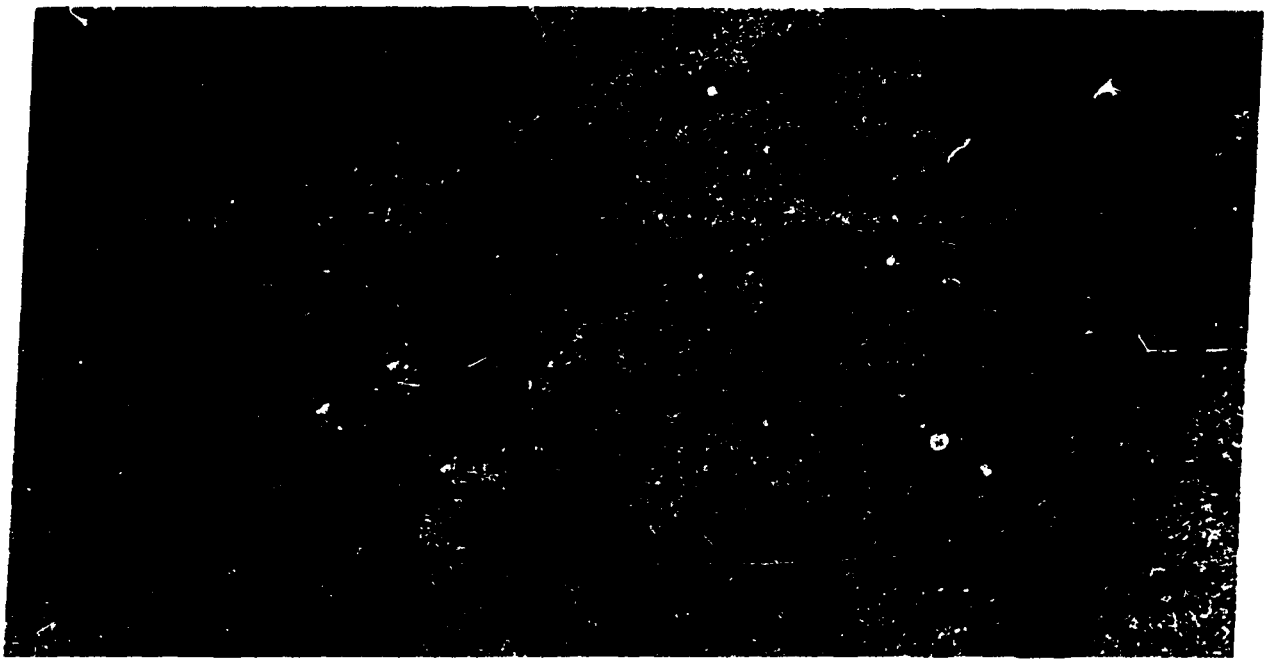

Figure 4-7. False color composite image of July 8, 1973 Landsat-1 scene of Harrisburg and southeastern Pennsylvania.

Figure 4-8A. Landsat-2, band 5 image of Harrisburg scene, June 8, 1977.

Figure 4-38. Band 7 image of June 8, 1977 scene.

Influence of Sun Angle

Now, examine scene 2688-14552 (Figure 4-9A), a band 7 winter scene covering the same region. Jot down the Sun elevation for this scene in your notebook.

#4-16: Overall, what improvements in scene definition or quality are evident in the winter scene? Why? Which features show up best?

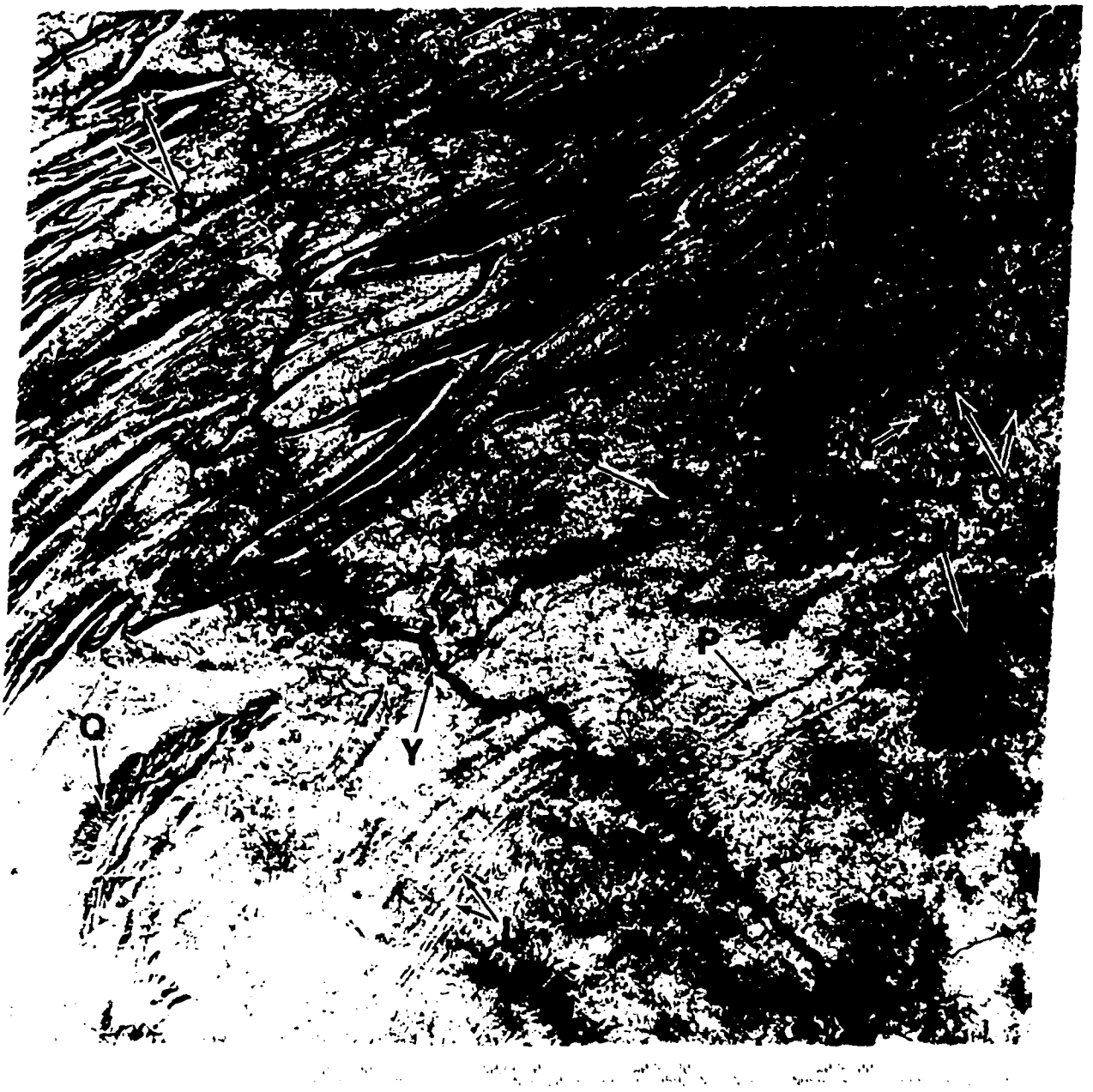

Figure 4-9A. The southeastern Pennsylvania scene, band 7, imaged by Landsat-2 on December 10, 1976.

#4-5: Look at equivalent sections of the mountain ridges (fold mountains) in the band 7 images of the October 1972 and October 1975 scenes. Noting that the gray scales for each scene have about the same level or tone for corresponding steps, describe the evident difference in tone or gray density in these mountainous areas. Can you account for this?

Figure 4-4. Computer-generated false color composite October 23, 1975 Landsat-2 image of eastern Pennsylvania.

ORIGINAL PAGE
COLOR PHOTOGRAPH

#4-17: From a radiometric viewpoint, what disadvantage is there in winter imagery? (Hint: Note the overall tone level of the image, think of this as a function of light intensity, and remember the use of spectral signatures to identify features.)

Figure 4-9B. Geological map of southeastern Pennsylvania (see text).

A Combustible Topic

Next, look at the large mottled features shown under arrows C and D in band 7 of 1350-15190 (Figure 4-6B). Check these and similar features as they appear in this, the winter scene (Figure 4-9A) and 2868-14471 (Figure 4-8B). You are looking at the Blue Mountain area of the folded Appalachian mountain belt. The largest nearby town is Hazleton, Pa.

#4-18: Can you find this town; what are its grid coordinates (Overlay 1)?

Other well-known (to natives of the region), smaller towns nearby include Pottsville, Shamokin, and Jim Thorpe (Mauch Chunk). What is this area famous for (a mining product)?

#4-19: Look closely at the area around arrow C as shown in bands 5 and 7 of 1350-15190 (locate on your own the equivalent area in 2868-14471). Describe the tones at C in Band 5; Band 7.

#4-20: How does this area appear in the color composite of 1350-15190 (Figure 4-7)? Speculate on the explanation for the darkest (blackest) spots in this and comparable areas. Also, give some explanation for the red tones in certain areas of the color composite, as at arrow E, which are marked by darker gray tones in band 7 of 1350-15190 (Hint: Think reclamation.) Afterwards (don't peek now!) read through the inserted discussion on page 120, which treats this and related points dealing with questions #4-18 through 4-23.

#4-21: Now, note the feature in band 7 of 1350-15190 (Figure 4-6B) indicated under arrow F. This is just west of the Lehigh River near Jim Thorpe. What are you looking at in this 1973 scene?

#4-22: Also, note the arrow G feature in 2868-14471 (Figure 4-8B). What is different in the 1977 scene? Are there any real and lasting changes (explain)?

#4-23: Other, very subtle, changes may be recognized in the 1977 summer scene but these require a practiced eye. Can you find any change near arrow H in band 7, 2868-14471? Then, look elsewhere throughout this scene and crosscheck to the 1973 scene if you encounter any feature that has changed, is transient, or seems new. Describe your observations.

An Entomological Challenge

You are by now becoming adept at the art of change detection, but here comes your big challenge. Look under arrows I, J, and K at the dark toned areas in band 7 of 1350-15190 (Figure 4-6B). Compare these and other areas with band 7 of 2868-14471 (Figure 4-8B), and 2904-14450 (Figure 4-10B).

#4-24: Describe the gray tones under the arrows for the 1973 scene. Locate the approximately equivalent areas in the 1977 scene. How do the gray tones differ overall?

#4-25: How do the same areas appear in the band 5 image for 1973 (Figure 4-6A)? In band 5 of 1977 (Figure 4-8A)?

#4-26: How would you describe the color of these three areas (arrows I, J, K) in 1350-15190 (Figure 4-7)?

#4-27: What color difference exists between this and other parts of the mountain ridges in 1350-15190? Do the color and gray tone of the arrow-centered feature (pattern) in band 7 of 1350-15190 (Figure 4-6B) differ from that of the coal waste areas in the same scene? In what way(s)?

#4-28: What color best depicts the equivalent areas in 2904-14552 (Figure 4-11), imaged in July 1977? Does this show the same variations as in 1350-15190 (Figure 4-6)? Comment.

ORIGINAL PAGE
BLACK AND WHITE PHOTOGRAPH

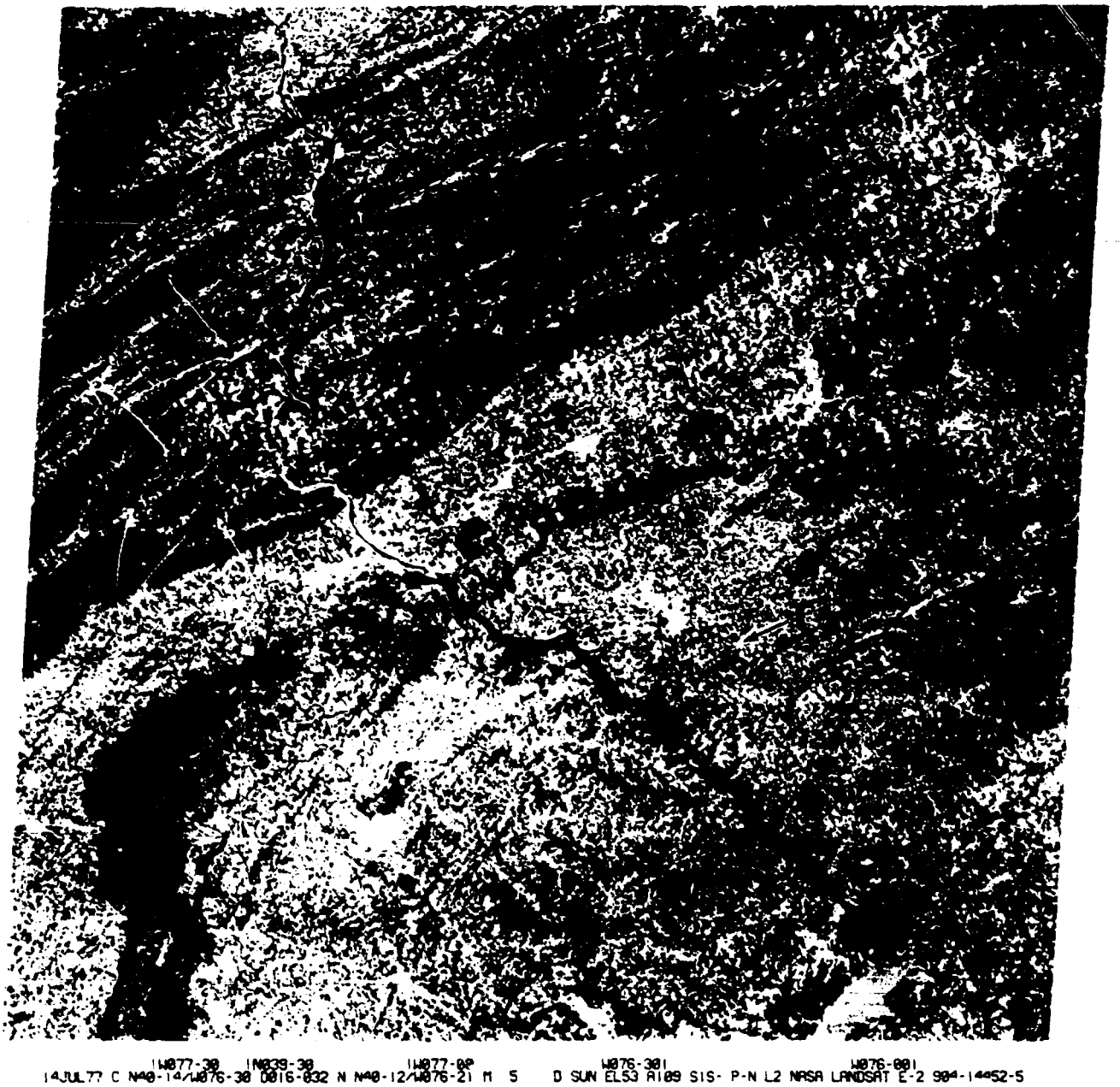

Figure 4-10A. Landsat-2, band 5 image of Harrisburg scene acquired on July 14, 1977.

Inserted Discussion for Questions 4-18 through 4-23

The areas observed as mottled patterns in both 1350-15190 and 2868-14471 (as well as 1080-15185, 2688-14552, and 2904-14452) are part of a vast belt of anthracite coal that was strip-mined to some extent in the 1940's and 1950's. Before that, predominantly underground mining had continued since the last century. Much of the coal occurs in steep-dipping seams within the ridges but the valleys also contain shallow, often flatter seams that can be stripped economically. Many of the lower areas around Wilkes-Barre and Scranton, Pa., westward through Pottsville, were laid bare by stripping before any environmental reclamation became mandatory.

Most of this area now consists of spoil pile wastes and small lakes dammed by the piles. Active stripping is currently at a minimum but many of the piles are being reworked. Some reclamation (tree planting and regrassing) is even now under way.

Many of the darkest spots, which appear lake-like in band 7, are surface deposits of coal fines (small sized particulates) obtained during the crushing and washing process applied to both surface- and underground-extracted coal. They are placed in banks or abandoned strip cuts. Some accumulate in ponds and form a water-covered coal slime.

The rate of surface stripping has almost reached a standstill in this part of Pennsylvania. To the west in Clarion, Jefferson, Clearfield, Westmoreland, Somerset counties, and elsewhere, surface stripping of individual workings advances at rates of 10 to 20 acres per year (see Figure 9-31). This is well within the detection capability of the Landsat multispectral scanner when scenes from different years are compared.

The enlarging lake west of the town of Jim Thorpe (see question #4-21) has been generated by the Deer Creek Dam. This dam was completed in 1971, so that the smaller lake detected in Landsat imagery acquired in July and August of the next year (see 1080-15185) represents early stages of filling after winter and spring precipitation and runoff.

#4-29: Look at the band 7 image of 2868-14471 to find one or more areas that show the same approximate gray tone levels as in 1350-15190. Note that similarly toned areas tend to associate with one particular landform (use shape as well). What is that landform?

#4-30: Does the anomalous gray tone pattern (found mainly with this landform) considered in questions #4-25 and #4-26 show up in the same or different places in the 1973 and 1977 scenes?

#4-31: Now, using a red grease pencil, outline on Overlay 1[1] the areas in the band for the 1973 scene (1350-15190; Figure 4-6) that are characterized by the distinctive gray tone we have been examining. Use a solid line for this outline. Do the same for either (or both) of the summer 1977 scenes (2868-14471; Figure 4-7, and 2904-14552; Figure 4-11) but mark boundary outlines with a green and a blue grease pencil respectively (or dashed and dotted lines if color markers are not available).

[1] This overlay is used several times in these activities. Remove previous markings where expedient.

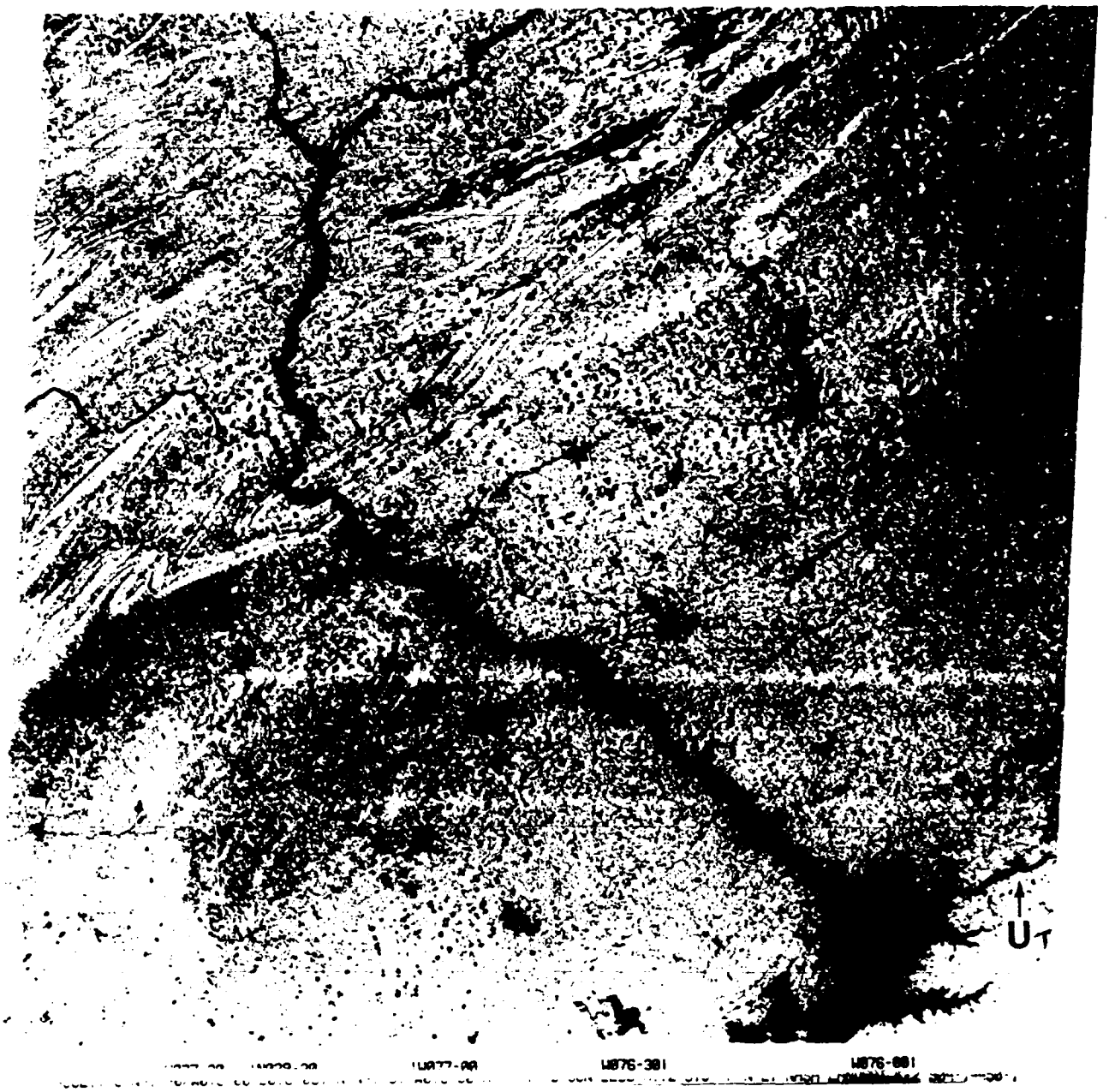

Figure 4-10B. Band 7 image of July 14, 1977 scene.

ORIGINAL PAGE
COLOR PHOTOGRAPH

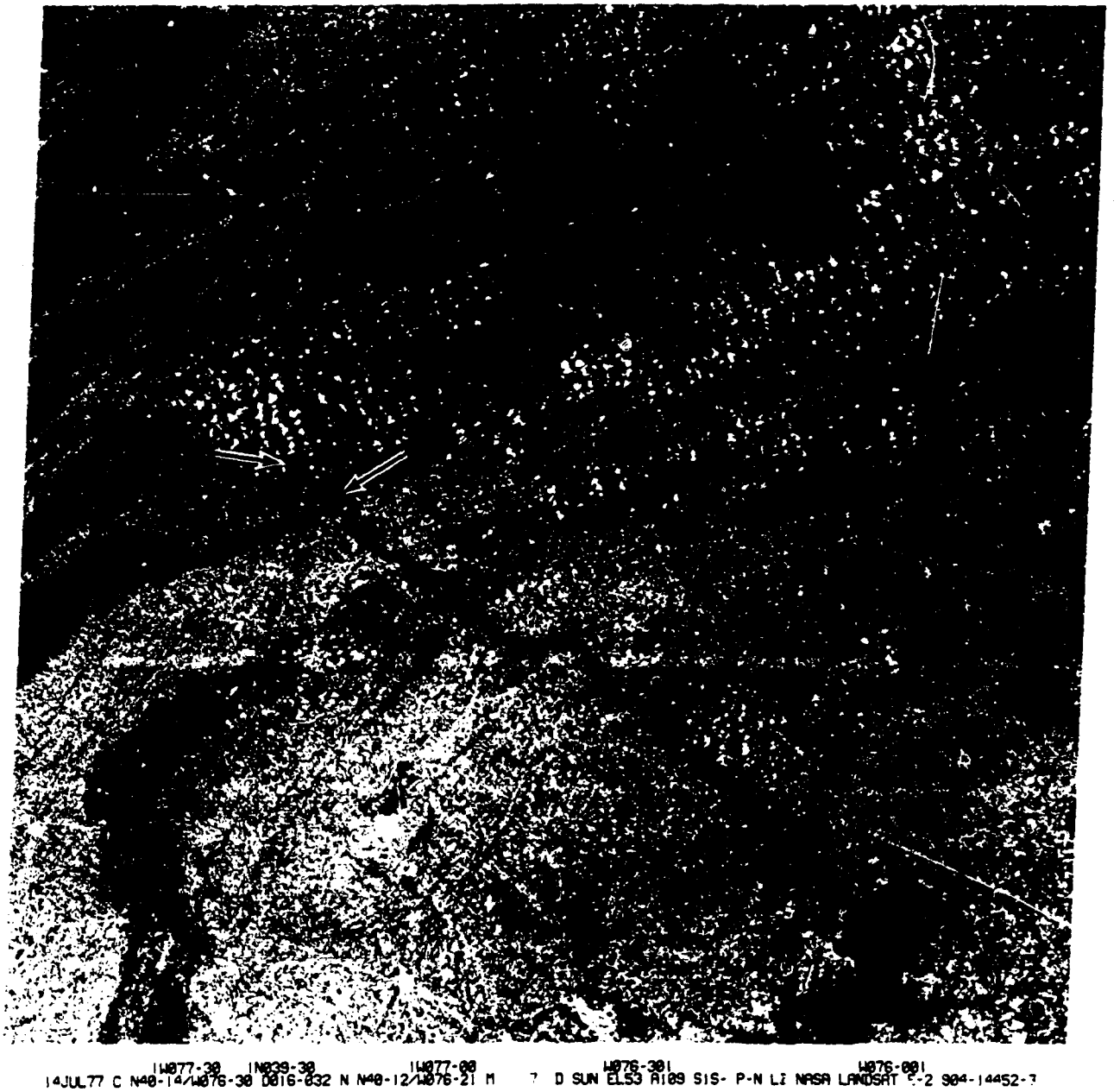

Figure 4-11. The July 14, 1977 Landsat-2 scene of southeastern Pennsylvania shown as a false color composite.

#4-32: To what extent do the outlined areas for the scenes chosen overlap?

You are now invited to speculate on the general nature of the feature you have been comparing in several scenes from different years. Refer to Table 3-3 and Rule 3 on page 102 for useful hints about its likely identity.

#4-33: List your first, second, and third choices for the identity of this feature.

#4-34: Account for any differences in areal distribution (geographical location) and characteristics of the outlined feature.

Now, turn to the top of p. 126 for a happy message!!

#4-35: If available to you, examine any other Landsat imagery for the current or most recent year that covers this eastern Pennsylvania region. Search appropriate bands for any evidence of active defoliation. Describe your observations, with special attention given to comparisons of currently and previously affected areas.

#4-36: The gypsy moth defoliation areas resemble the tonal signature of the pinewoods in the Pine Barrens of New Jersey as shown in two bands in scene 1079-15131 (Figure 2-3; see also Figure 3-4), but these areas display a distinctive difference in a third band. Which band shows this critical difference? Try to offer a reason for this.

#4-37: Before leaving the Hazleton area, try your hand at making a general purpose interpretation map showing the distribution of major classes you can identify. Use the color enlargement of the relevant section from 1350-15190 provided here as Figure 4-12. Also use the black and white aerial photo (scale 1:78,000; taken on October 12, 1976, Figure 4-13) and the 1:250,000 AMS Map NK 18-11 (Newark Sheet) as other sources of ground information. First, delineate the boundaries of this enlarged area on Overlay 1 placed over 1350-15190 (Figure 4-7) and use this sketch again to block out the same area in any other Landsat full scenes previously examined whenever more data are needed. Next, fasten a piece of thin tracing paper (or a clear plastic sheet) over Figure 4-12. Then lightly outline the boundary of the aerial photo (Figure 4-13) on this overlay. To get you started in making an interpretation map, we have selected some "training sites" for most of the common surface classes present in the scene. These have been placed on Figure 4-12 but, in common practice, would more likely have been drawn on a separate overlay. Assume that the identified class or surface feature is distributed immediately around (without boundaries being shown) each keyed letter. Complete the map by outlining the boundaries of the classes you recognize throughout the enlargement. Use the patterns shown below to indicate each class within its boundaries at the various locations in the scene where you recognize it.

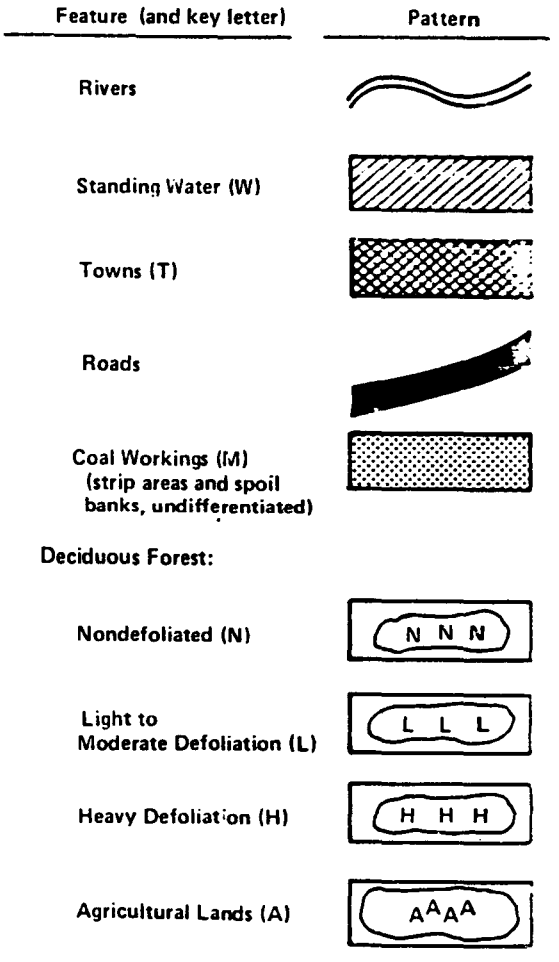

Figure 4-12. Enlargement of part of Landsat scene 1350-15190 covering Hazleton, Pa. area.

ORIGINAL PAGE
BLACK AND WHITE PHOTOGRAPH

Figure 4-13. 1:78,000 aerial photo of Hazleton, Pa. area.

Inserted Discussion for Questions 4-24 through 4-34

CONGRATULATIONS

You are now a qualified photointerpreter!

You have just done an operation in a few minutes with Landsat that could have taken weeks or even months with aerial photography and ground surveys, at a cost of tens of thousands of dollars.

You have outlined the extent of defoliation by the Gypsy Moth—a hungry scavenger that prefers hardwoods. This destructive insect has caused millions of dollars in damage to deciduous trees in the eastern United States during this decade alone. The history of gypsy moth damage and the economic implications of this defoliation—along with the value of Landsat as a damage monitoring and assessment system—are touched upon again in the Summation Chapter (pp. 389 ff.) of this workbook.

The damage shows up simply because the principal reflectors, the leaves, are almost completely removed to expose the understory below the trees. This understory consists of shrubs and brushy foliage, soil, and bare rock. The infrared reflectance from vegetation is significantly lowered in the defoliated areas; this greatly reduces the red tones as well as any blue tone input from band 4. The gray levels for all three bands are generally on the darker side. The effect on a color composite is to produce subdued reddish tones with gray to gray-brown overtones. A similar tonal signature is noted in the coal waste areas because of the naturally darker surfaces and sparse vegetation.

Fortunately, much of the damage is not permanent, and chewed or stripped trees usually refoliate in the same season or by the following year. This too can be monitored. The comparison you made between the 1973 and 1977 color composite scenes clearly shows that nearly the entire ridge suffering extensive damage in 1973 had recovered soon afterwards, but new areas were under attack in 1977. The mid-July 1977 scene (2904-14452; Figures 4-10 and 4-11) shows that while some of these new areas attacked by the moths earlier in the year had since refoliated, several newer areas were experiencing infestation as the season advanced.

Two computer-generated classification maps covering smaller sections of this Hazleton area scene are reproduced in Activity 5 as Figures 5-35 and 5-36, accompanied by a discussion on how they were produced and what they show. Compare your photointerpretation map with these computer classifications.

#4-38: How well does your map coincide with the principal classes in Figure 5-35? Where (what) are the main areas (categories) of disagreement?

To continue, let us see what other fairly obvious changes can be detected in Landsat imagery.

Geological Features

We shall next investigate the July 1973 (Figures 4-6 and 4-7) and the December 1976 (Figure 4-9A) scenes of the Harrisburg region in terms of evidence for the geological character of the Appalachians and adjacent terrain. A glance at the color composites for this region suggests that we might have considerable difficulty in recognizing rock (stratigraphic) units and certain other common geological phenomena because of the usually heavy and extensive vegetative cover. As a general rule, these units are not well expressed or even discernible in Landsat images for

regions where vegetation cover exceeds 25 to 30 percent of the surface area; in such regions, soil cover is also extensive and rock outcrops commonly cover less than 10 percent of the surface. This surface condition is largely true for much of the eastern half of the United States. Comparison of Landsat images taken over the entire United States, as shown in the NASA book, *Mission to Earth*, indicates strong differences in the content of observable geological information between typical western scenes (Wyoming, New Mexico, Utah, Oregon), where vegetative cover is often less than 30 percent, and eastern scenes (New England, North Carolina, Alabama, Ohio, Kansas), where forest and grass cover are dominant. However, with some training and experience, more can be extracted from many eastern scenes than initially meets the eye. Band 7 and winter (low Sun angle) scenes are particularly helpful.

#4-39: Why can more geological features be detected in the infrared and in winter scenes? What kinds of geological information are reasonably well revealed?

#4-40: Can you find evidence of any individual stratigraphic units (formations)? If so, locate these by grid coordinates. Otherwise, explain your failure to find any units or outcrops. What physiographical province (see page 45) is best displayed?

The Piedmont, which occupies most of the lower right diagonal half of these scenes, is a region of ancient crystalline rocks whose structural grain is well displayed by Landsat imagery. A series of volcanic dikes in the Piedmont appears at arrow L within 2688-14452 (Figure 4-9A). A linear belt of metamorphosed sedimentary rock units, some separated by faults, is touched by arrow M. Parts of these linear features are associated with higher densities of trees (forest rows), that grow preferentially because of differences in soil composition and moisture content.

The geology of a northeast-trending region running from approximately York, Lancaster, and Phoenixville to the south and Harrisburg to Reading to the north is controlled by a complex zone of somewhat metamorphosed lower Paleozoic sedimentary rocks and reddish to gravish Triassic sedimentary rocks, interspersed with old granitic rocks (arrow N) and Triassic basalt (trap rock) filling steeply dipping dikes (arrow O). Forests tend to cover the granitic and basaltic rock units, which usually form more hilly terrain.

A broad area between the previous region and the front along the folded Appalachians, including the towns of Harrisburg, Hershey, and Lebanon, is largely underlain by carbonate rocks. This lowland is generally considered a northeastern extension of the Shenandoah Valley of Virginia, and is known locally as the Great Valley. It widens and continues through the Allentown area to the northeast.

The northwest edge of the much younger coastal plains, consisting of marine sedimentary rocks deposited along the Atlantic (ocean) coastal shelf during the last 70 million years, appears in the southeast corner of all examples of this Harrisburg scene.

With this quick review of the geologic makeup of southeastern Pennsylvania you can better appreciate the level of information in the Landsat scenes in relation to the known geology. Figure 4-9B is a copy of part of the State Geologic Map of Pennsylvania, reduced to 1:1,000,000 from the original scale of 1:250,000. No legend is included in the figure but, by careful examination of this map copy, you should find the letter symbols for the different stratigraphic units. For example, S_t refers to the Tuscarora formation of Silurian age. The first letter of each symbol denotes units of the following (increasing) ages present in the map: Q=Quaternary; ℟=Triassic; P=Pennsylvanian; M=Mississippian; D=Devonian; S=Silurian; O=Ordovician; ℭ=Cambrian; X=crystalline rocks of Precambrian to early Paleozoic Age.

#4-41: Which scene—summer or winter—seems to help you to make the best match to the stratigraphic rock units depicted on the map?

#4-42: By glancing back and forth between Figures 4-9A and 4-9B, describe the geological features (without specifically identifying units as to rock type or age) at arrows P, Q, R, and S (Figure 4-9A) in terms of topographical expression, subunits present, and degree of correspondence (goodness of fit) of major boundaries.

#4-43: Then, pick out any three areas where you judge the correspondence between mapped geology and Landsat expression to be poor. Indicate these by grid coordinates (Overlay 1).

For most of the eastern United States, the lack of good rock exposures (owing to thick soils and extensive vegetation cover) has prevented wide use of Landsat for mapping geological units or alteration effects around ore bodies. However, as just shown, much can be learned about some aspects of the regional geology in terrains where tectonic disturbances are mirrored in topography. Areas of moderate or high relief generally correspond to structurally controlled differential erosion. Folds, faults, and joints affect the patterns of landforms in distinctive ways that are frequently revealed—and sometimes exclusively—in the synoptic views of Earth from space.

#4-44: Some of the geological features in the Harrisburg area are distinguished by a distinctive linearity (for example, dikes located at arrow L, Figure 4-9A). Over much of the Piedmont, sets of steeply dipping, narrow Triassic dikes occur as isolated individuals or swarms that trend generally North 30° East. These are shown as thin red lines on the geological map. Look at bands 5 and 7 of 1350-15190 (Figure 4-6) and 2688-14552 (Figure 4-9A). Can you find a trace of any of these dikes, especially in the areas corresponding to the lower third of the geological map? Which band seems best to show any detected dikes? Why? Did you note any lineations not on the map that might be dikes with the N30E orientation?

By far the most frequently cited application of Landsat data to geological studies has been the recognition of lineaments, particularly those expressed as topographical features or discontinuities. These lineaments are usually joints, fracture zones, or fault breaks in the outer crust, often made visible at the surface through erosion, which carves out weaker materials. Their detection in Landsat imagery is due to several indicators. The most direct and obvious indicators are physiographical expressions such as elongated valleys, linear, commonly aligned stream channels, gaps, depressions, and abrupt discontinuities (from juxtaposition of rock units of differing degrees of resistance). Less direct, but often diagnostic, is the association of moisture and vegetation along the lineaments. Generally, the lineaments are revealed in images by distinct, sharp tonal boundaries consisting of a long, thick, dark line or a somewhat wider band abutting against lighter tones on one or both sides. This tonal pattern is caused by shadows along scarps or depression walls, by darkening moisture, or by a concentration of trees in a higher moisture zone.

The linear features, as seen at Landsat resolution, are normally at least 2 to 3 km (1.2-1.9 miles) in length. Many extend continuously, or more commonly in discontinuous sections, for distances up to several hundred miles. Most large linear features are associated with major faulting; these megalineaments frequently occur as single features, but in a structurally disturbed crust many individual fractures will be noted in a variety of orientations so that intersections are common. The lineaments may be straight or curvilinear (in segmented or concentric arcs). Those lineaments expressed as close-spaced, criss-crossing sets are more likely to be joints than faults. Metamorphic rocks commonly show a structural grain—expressed mainly as linear bands—which results from foliation or other factors that alter resistance to erosion. Such a pattern is especially conspicuous in the Appalachian Piedmont terrain we have just looked at.

To geologists, detection of lineaments assumes primary importance. Such natural linear features can disclose much about the structural or tectonic history of a region. Faults are the loci of earthquakes; thus, their detection may be of vital interest in protecting life and property. Engineering decisions as to locating large dams or power plants or to predicting landslides must take into account the presence of faults. Faults are often the critical factor in localizing petroleum, ground water, and many hydrothermal ore deposits, by guiding or trapping the fluids as they are emplaced. Intersections or curvilinear fracture zones are particularly favorable sites.

Obviously, some linear features are not geological in nature. Many linear patterns are associated with Man's activities.

#4-45: Name five such cultural patterns.

These are often confused with geological lineaments. However, linear features that are many kilometers in length, are somewhat irregular and discontinuous, and are found in wilderness terrain, away from cities, developed land, or other works of man, are most likely to be natural.

Probably no other observations from Landsat have caused as much confusion and controversy as those of lineaments. A typical case in point is for a full Landsat scene in which a total of three hundred lineaments are reported by four investigators, each analyzing the same scene independently. Perhaps only 20 of these lineaments were identified as the same by all four people, 50 by three, 100 by two, and the remainder are "one of a kind" observations. There are many explanations for this discrepancy, including operator bias, mistakes in identifying cultural features as natural ones, and inadequate criteria for recognition.

#4-46: Plots of the orientations of fractures and other lineaments (usually as "fan histograms" or "rose diagrams") detected in Landsat imagery show a tendency for an abnormally large number to trend in a northeast-southwest direction and a sparsity of those oriented to the northwest or southeast. Can you deduce a reason for this? (Hint: Think shadow.)

Despite the expansive cover of trees and grass in southeastern Pennsylvania, several investigators have located a fairly large number of linear features in the Harrisburg scene as part of a project to produce a lineaments map of the entire state based on Landsat observations. Before examining their results, you should try your hand at detecting these features.

#4-47: To run this analysis, place tracing paper over the bands 5 and 7 images (Figures 4-3 A and B) from the October 1975 Landsat overpass. (Back-illumination of a transparency on a light table is generally a superior way to highlight linear features.) Examine the images for a few minutes before drawing any lines. This should give you a feeling for the different characteristics of any lineaments that may appear to you. In fact, it is advantageous to decide on a set of criteria for recognizing linear features (and subdividing these into natural and cultural categories) and, as you carry out your delineations, to stick with these criteria unless some compelling evidence forces a modification. Mark any linear features longer than about 1 cm, making a red, dotted line along features evident only in the band 5 image, a red dashed line for any new features seen only in band 7, and a red solid line if the linear feature is visible in both bands. To help you learn to recognize these features, train on a conspicuous linear feature occurring below grid area B-20 (Overlay 1) in the October scene. Examine it and note its influence on local topography. The geological map (Figure 4-9B) reveals this feature to be an east-west trending fault offsetting Cambrian strata at South Mountain.

Do this now—you should need about 30 minutes to survey these two bands. Then put the scenes aside and take a coffee break. Return, and look again for a few minutes. Invariably, some new linear features will seem to materialize. Before leaving the scene, you may wish to look at the color composite (Figure 4-4). If any more linear features are spotted in that rendition, note them with a green dotted line.

Next, look at any of the summer images covering the Harrisburg frame you make the choice. On the same tracing paper, mark any new linear features with a blue pencil. Also, look to see if any of the geological lineaments picked from the October scene fail to show up. If so, place a blue line across the midpoint of each such feature.

#4-48: Now, place a new sheet of tracing paper over the December 1976 scene (Figure 4-9A) you examined earlier in this geology exercise. Draw brown lines over all the linear features visible in that band 7 image. Which date of coverage seems best suited to detection of the largest numbers of linear features? Why? (Hint: Compare Sun angles.) What do you think the effect of snow cover might be in emphasizing linear features? What else might make a winter scene more effective? (Hint: What is missing at that time of the year?)

You should now turn to the next two figures. Figure 4-14 is a reproduction of the lineaments map of Pennsylvania prepared from Landsat images by W. Kowalik[2] of ORSER (Office of Remote Sensing

[2]Kowalik, W.S., *Use of Landsat I Imagery in the Analysis of Lineaments in Pennsylvania*, M.S. Thesis, Pennsylvania State University, 1978.

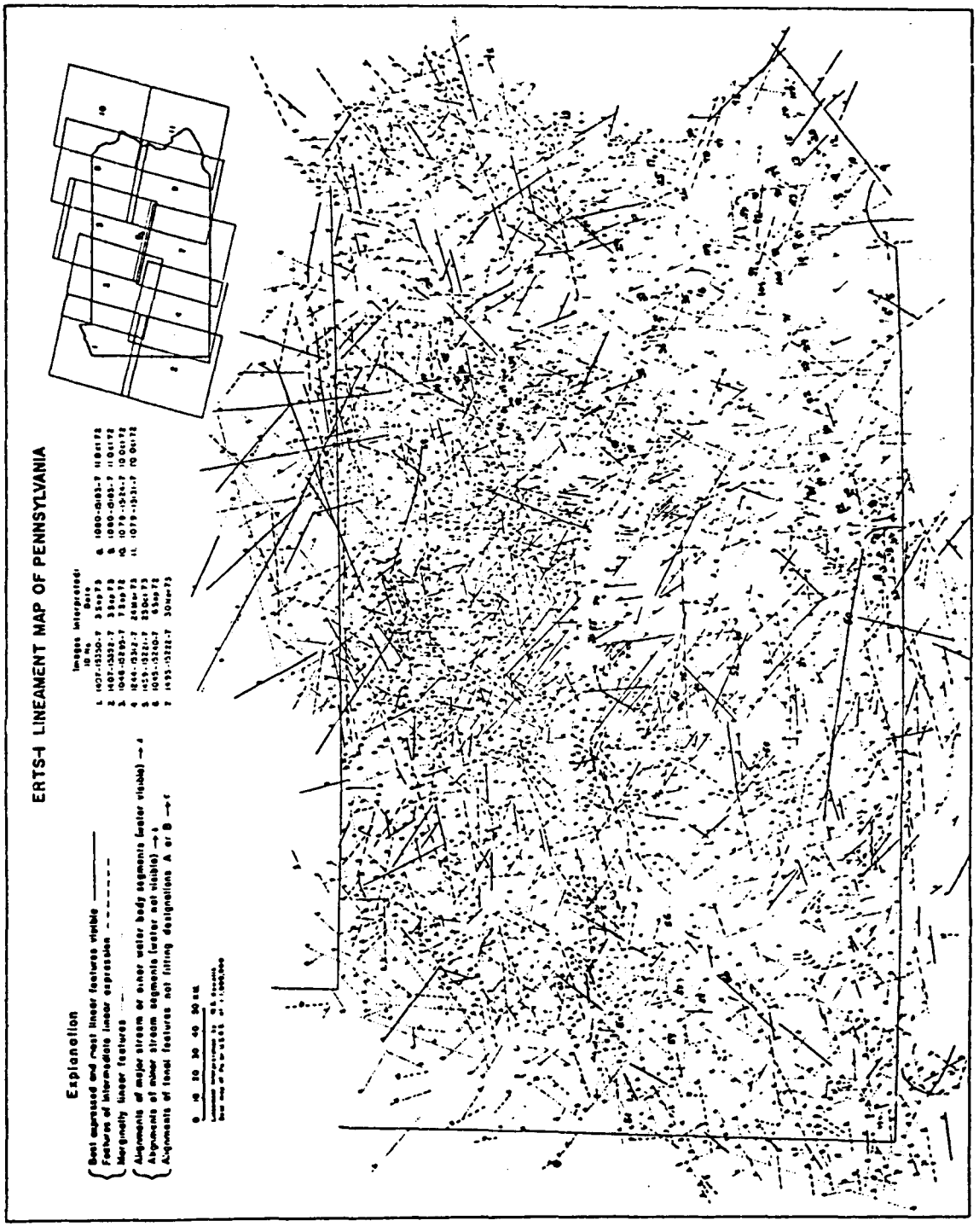

Figure 4-14. Lineaments map of Pennsylvania prepared from Landsat-1 data (after W. S. Kowalik).

of Earth Resources; Pennsylvania State University). Figure 4-15 is an enlargement of the part of that map that corresponds to the frame boundary of 1080-15185 (Figure 4-1). Line up your tracings on this figure to fit these boundaries.

#4-49: Roughly, what percentage of your linear features approximately coincide with those on the ORSER map? Did you pick more or fewer lineaments than shown on the map?

Go back to either the July 1973 (Figure 4-6) or December 1976 (Figure 4-9A) scenes (or both if you wish). On the enlarged map, pick about ten of the lineaments that you missed and, using some landmarks in the scene that you can approximately locate *in the map*, try to find some expression of, or evidence for, these in the scenes.

#4-50: Are you convinced or still skeptical about the value of using Landsat imagery to detect large linear features of geological origin?

You may wish to defer final judgment until you have worked with a computer-generated version of part of the Harrisburg scene (see page 159), in which processing specifically designed to enhance linear features was carried out.

Confidence in detection of linear features in Landsat images will necessarily remain low until some reasonable number of them are checked and verified in the field. This is usually a long, difficult, and costly process because of the large areas and often rugged and inaccessible terrains involved. For the ORSER study, a field check disclosed convincingly that most of the longer northwest-trending lineaments are probably real. The check consisted of a 60 km (40 mile) traverse on foot along the southwest trending Bald Eagle Mountain (west of Harrisburg) in which the geologist was given a list of confirmatory ground criteria. Of the 14 crossing lineaments, streng evidence for 12 of these was encountered during the traverse. Most of these lineaments were found to be fractured rock zones with widths up to 2 to 3 km. Their lengths were mostly greater than 80 km (50 miles); seismic data suggest that these zones extend to depths greater than 15 km (10 miles). These lineaments have been interpreted to be major zones of crustal fracturing (but not necessarily faulting, as offsets were seldom evident) that may continue through the crust even into the mantle.

Agricultural Features

So much for linear features—a controversial but challenging application of Landsat. Now, we shall consider some aspects of those agricultural practices that may be detected in the Harrisburg scenes. Although eastern Pennsylvania is not known as a major agricultural producing center on a par with the Great Plains, it does supply much of the populated region with important foodstuffs. Some of the advantages of repetitive (seasonal) coverage by Landsat will be evident from the next few questions, helping us to better appreciate why remote sensing from satellites promises to be a boon to the worldwide agricultural industry.

#4-51: Much of the land south and east of the folded Appalachians is used for dairy farming and for crops such as corn, oats, barley, wheat, alfalfa and hay, tobacco, and fruit trees. Using scenes (dates) of your choice, describe in terms of sizes and shapes the general farm layout pattern within the Piedmont belt of rolling hills southeast of York and Lancaster to the Susquehanna River mouth.

#4-52: Describe the main change between June and July of 1977 in the status of land cover in the rolling country around Lancaster, Pa. (arrow T in Figure 4-10A).

#4-53: From the observed patterns of surrounding agricultural lands, make a guess about one principal farming practice in this, the heartland of the Pennsylvania Dutch Country. (Hint: Keep in mind the nature of the topography; see also Figure 6-1E.)

Figure 4-15. Enlargement of part of Pennsylvania lineaments map (after W. S. Kowalik).

#4-54: What is the major difference in size and/or shape between farms in the southeastern Piedmont and those in the Coastal Plains further southeast (around the lower right corner of these Harrisburg scenes)?

#4-55: Compare the June 1977 and July 1977 Landsat scene renditions of the Coastal Plains farmlands south of the Chesapeake and Delaware (C & D) Canal (arrow U; Figure 4-10B) with respect to the stage of growth. Describe in general terms (percentage of plowed land, growing crops, etc.,) the major changes in the 36 day interval involved.

At this point, you can check your answers (which were based on Landsat observations) by referring to two black and white aerial photos (scale: 1:24,000) obtained during flights in 1978 by EPA over an area south of Lancaster (Figure 4-16A) and an area near the C & D canal in Delaware (Figure 4-16B). First try to locate these images within the October 1975 (computer enhanced) color composite (Figure 4-3C).

#4-56: Now, briefly describe the characteristics of the fields shown in each aerial photo, giving particular attention to relative sizes, shapes, and planting practices.

These areas will be examined again in the next activity as we learn how computers may be trained to recognize crop types and to estimate crop yields or production.

Water Features

Let us turn now to still another broad range of applications for which Landsat has demonstrated exceptional capabilities. As was first noted in Table 1-2, Landsat data are proving quite beneficial to the discipline of hydrology. Landsat is a very efficient detector of water bodies.

#4-57: How and why is Landsat an effective monitor of water bodies?

Observations from Landsat are, therefore, being applied to monitoring floods, inventorying lakes, making estimates of sediment pollution and water quality (e.g., eutrophication effects), and measuring areal distribution of snow to predict runoff and storage supplies as input to water budget calculations.

First, we shall consider large variations in available water supply resulting from rain-related floods or from rapid melting of extensive snow pack.

In terrain less hilly than central Pennsylvania, such as parts of the Midwest and Great Plains, flooding often produces significant lateral expansions of stream boundaries. Many cases of using Landsat to monitor floodplain inundations have been reported (see figure 22 and plate 42 in *Mission to Earth* for examples of the great 1973 floods along the Mississippi River). The extent of flooding under those circumstances can be accurately mapped for the dates in which imagery is acquired. Unfortunately, the number of cloud-free scenes obtained over a drainage basin in flood is usually quite limited by the current Landsat orbital frequency (one pass every 9 days when two Landsats operate on a ½ repeat cycle spacing, but usually only about 1 in 5 repeat overpasses by each satellite is likely to obtain adequate coverage). Since most floods dissipate in a few days to a week, the likelihood of acquiring imagery useful for monitoring flood damage during the height of inundation is low. For these reasons, no images of notable flooding within central Pennsylvania have been acquired by the Landsats. Also, many valleys have relatively narrow floodplains and effectively banked channels so that lateral spreading of flooded streams is reduced.

Prediction of runoff from snow melt is more readily accomplished through Landsat observations. This results from the persistence of snow over weeks or even months in the more Northern latitudes or at higher elevations in the mountains.

#4-58: To predict runoff, at least four variables associated with the snow cover must be known.

Figure 4-16A. Aerial photo (1:24,000) of area near Lancaster, Pa. (courtesy of EPA).
(Original photo is in color.)

Figure 4-168. Aerial photo (1:24 000) of area around C&D Canal, Delaware (courtesy of EPA).
(Original photo is in color.)

What are they? Which ones can Landsat measure? What can be done to obtain data on the variables not directly measurable with Landsat?

The best measurement results with Landsat have come from areas within the United States (e.g., Sierra Nevada Mountains) and worldwide (e.g., Himalayas) where large mountainous regions collect thick snow cover through the fall to spring seasons. However, good approximations can be made in areas of low to moderate relief. A typical winter snow condition for Pennsylvania is shown in Figure 4-17.

#4-59: Using Overlay 1, trace a line along the visible demarcation boundary between extensive snow cover and apparently snow-free land. Where does the snow appear thickest? Does it seem to be absent in places? Where? What accounts for the light tones within the Susquehanna River Valley south of Harrisburg?

#4-60: Specify three practical uses of runoff prediction from snow melt.

#4-61: Suggest a simple, practical way in which snow patches remaining at higher elevations in mountainous terrain during the warmer seasons may be distinguished from clouds. This can be a problem in some instances, especially since the two features may have very similar spectral signatures.

Subtle hydrological variations are evident from Landsat under favorable circumstances. Changes in lake and reservoir levels of just a few meters can sometimes bring about notable changes in total surface area. These result in shifts of shorelines that may exceed 100 m (330 ft) horizontally (thus, within Landsat detectability) if the water bodies are in generally flat terrain (unconfined by steep slopes). Where confined by damming of streams in hilly terrain, water level changes may still be detected even without much lateral shift because the shorelines tend to be barren and highly reflective; these form distinct narrow bands that stand out because of high (reflective) contrast between water, shore areas, and hillside vegetation. This latter configuration is not uncommon in the rolling hills and ridges of Pennsylvania.

In principle, the MSS, with its 70 X 56 m resolution (raw pixel size, before resampling), should be able to detect lakes as small as 0.44 hectares (about 4500 m^2 or 1.1 acres)—a single pixel in size—but in practice a lake must normally be at least 0.80 hectares (2 acres) to be consistently detectable.

#4-62: Can you explain why a lake must usually be larger than a single resolution element to be detected with consistency? (Hint: Ponder the effects on a single pixel brightness relative to its neighboring pixels if the image of a 0.44 hectare lake (a) falls entirely within the pixel, or (b) is outside the several pixels; consider probabilities.)

Changes in reservoir and lake levels (and hence storage volume) may sometimes be seen at individual water bodies within one or more Landsat scenes of the Harrisburg region. This has already been illustrated for the Deer Creek dam reservoir (p. 120). If, during a given year, average rainfall, evaporation and other conditions affecting water supply and storage are notably different from other years, it should be possible to detect and even measure this difference in Landsat imagery. Look at the color composites for the two October Landsat scenes (Figures 4-2 and 4-4). By visual inspection, compare the relative sizes of a number of the lakes in these scenes.

#4-63: Which year seems to have been wetter (i.e., produced conditions that increased water storage in October)? (The actual total rainfall between March 1 and October 30 each year for the Harrisburg area is recorded in footnote 3 on p. 138).

If differences in storage are substantial, it may be feasible to determine the relative amount of available water by measuring surface areas of large reservoirs. This is best accomplished through computer analysis by counting individual pixels assigned a water signature at each reservoir location. Where the unit of measure is 0.44 hectares (1.1 acres) in size (area of a Landsat pixel), this measure can often be fairly accurate for larger water bodies

Figure 4-17. Landsat-2 scene taken on January 23, 1979 showing the distribution of accumulated snow from winter storms.

with suitable basin configuration. Even visually, however, one can make a good estimate of water volume changes by noting comparative areas. As a check on this approximation, look at band 7 renditions of the two October scenes.

#4-64: Make a rough guess of the percentage change in surface areas of the three reservoirs listed below (and located by arrows V, W and X) by using 100 percent for each in the band 7 1972 scene (Figure 4-1B) as the baseline standard (for example, the area of reservoir (1) in 1975 might be 70 percent of the area noted in 1972). Follow the format below:

	1972	1975
1. Marburg Reservoir (arrow V)	*100%*	
2. DeHart Reservoir (arrow W)	*100%*	
3. Unnamed new lake in Middle Creek Wildlife Sanctuary (arrow X)	*100%*	

#4-65: Find the average of the three 1975 percentage values. How well does this average change agree with the percentage difference for rainfall change at Harrisburg for the 1972 (taken as 100 percent) and 1975 periods?

Several interesting changes within the Susquehanna River basin are noticeable in the Harrisburg scenes used in this workbook. Let us examine selected scenes for evident differences.

Begin with a direct comparison between bands 7 of the December 1976 (2688-14552; Figure 4-9A) and June 1977 (28680-14471; Figure 4-8) scenes. Choose any three equivalent locations—upstream, midstream, and downstream—along the Susquehanna in each scene.

#4-66: Summarize the major differences in discernible water levels. What is the most reasonable explanation for the differences?

#4-67: Several light-toned areas occur in the river in the winter scene, as at arrow Y. What are they? Why is one of these areas famous?

#4-68: What is a plausible explanation for the sudden change in stream width at arrow Z near Conowingo, Md., in Figure 4-8B (look for the same location in other images, particularly 1350-15190, Figure 4-6)?

#4-69: Now, examine the color composite of 2904-14452 (Figure 4-11). Note the bright blue pattern along the Susquehanna River around arrow AA on this figure. What do you think this is? Can you provide an explanation for this pattern that is related to its occurrence just below the confluence with the Juniata River (arrow BB)? Suggest a practical use for this type of observation.

#4-70: Next, examine the area in 2904-14452 where the Susquehanna River mouth meets the head of the Chesapeake Bay (Look at the equivalent area as shown in color composite and black and white images from the several other coverage dates, noting the gray level and color differences among these.) What accounts for the variations in bluish tones associated with the Bay in the 2904-14452 color composite? In what way(s) might such observations be useful to the fisheries industry?

#4-71: Finally, in this section on hydrology, inspect the October 1975 scene (Figure 4-4) once more. Describe the appearance of the water in the Susquehanna River as seen in the color composite. Note that this condition extends over the entire stretch of the river within the scene; however, the major tributaries to the west (e.g., the Juniata) show less of this effect. Assuming this to be a manifestation of turbidity due to an increased load of suspended sediments, devise a plausible scenario for the meteorological history of the several days preceding the October 23 overpass of Landsat. Then check your surmise with the review of the actual history in footnote 4 on page

#4-72: Why do some reservoirs (e.g., Marburg) appear blackish in the October 1975 color composite and others show bluish tones? (At least two different factors could be important.)

---

[3]Meteorological records for the Harrisburg Airport gauging station show a cumulative rainfall of 99.34 cm (39.11 in) in 1972 and 103.63 cm (40.80 in) in 1975 over the period of March 1 through October 31 each year. However, in 1975, 38.02 cm (14.97 in) were recorded in late September from Hurricane Eloise. It is therefore highly likely that the greater apparent volume of reservoir storage in October 1975 resulted from the hurricane contribution just a month earlier. Apparently, by October 1972 the effects from Hurricane Agnes had largely been accommodated through usage.

STILL OTHER APPLICATIONS

Coastal Zone Features

Before leaving this activity, we should look into several of the ways in which Landsat–designed mainly as a land surface observer–has demonstrated a surprising facility for gathering valuable information about coastal waters and even the open ocean. Landsat has been especially useful in (1) delineating the land/sea interface along coastlines; (2) providing details on the characteristics and distribution of wetlands; (3) indicating significant changes in offshore deposits, such as sand bars and islands, brought about by severe storms; (4) noting patterns of sediment movement, particularly off river mouths and deltas, as influenced by waves and currents; (5) defining bottom depths (to about 9 m or 30 ft) in clear shallow waters; this is of special concern to navigators; (6) locating shoals, especially near atolls; (7) monitoring sea ice in high latitude waters; (8) detecting direct and indirect evidence of nutrients (plant and animal organisms) in drifting or upwelling water; and (9) spotting pollution sources and effects, such as oil spills and waste dumped from ships. We shall examine the Atlantic Ocean along the New Jersey coast for examples of several of these observations.

Refer once more to the October 1972 (Figures 2-1 and 2-2) and April 1978 (Figures 2-10 and 2-13) scenes of New York City and adjoining New Jersey. You should concentrate first on the famous stretches of beach and backwater from just north of Atlantic City to the south end of Barnegat Bay. We shall return to this same coastal region in Activity 5 to learn about the effects of computer processing in classifying this type of environment.

#4-73: Which individual bands best delineate the boundary between wetlands (marshes) and open water in the broad baywaters west of the long, bright sand bars?

#4-74: Which bands emphasize the more turbid (silty) water?

#4-75: Describe the color tones of the subaerial marshlands in Figure 2-1.

#4-76: What could cause these wetlands to show up as darker gray or color tones in the images?

#4-77: On Overlay 1 (or on a sheet of tracing paper) trace the boundary of the coastal wetlands on the inland or continent side of the bays.

#4-78: Do there appear to be any discrepancies in the location of this inland boundary when the October 1972 and April 1978 images are compared? If so, why?

#4-79: Where do the wetlands extend inland from this generally straight western boundary?

#4-80: In either the black and white or color images, some of the pinewoods in the Barrens appear similar in tone to the wetlands. Describe any differences in any bands for either the October or April scenes that might help you to distinguish these two ground cover types.

Water Pollution

We shall now introduce a new scene specifically to look for one unusual feature. Look carefully at the vast expanse of ocean south of Long Island in the August 16, 1972, band 4 image (Figure 4-18). There are several light-toned patterns that must certainly be clouds. Search the image for another lighter toned pattern, which has a shape that eliminates clouds from consideration.

#4-81: Sketch this feature.

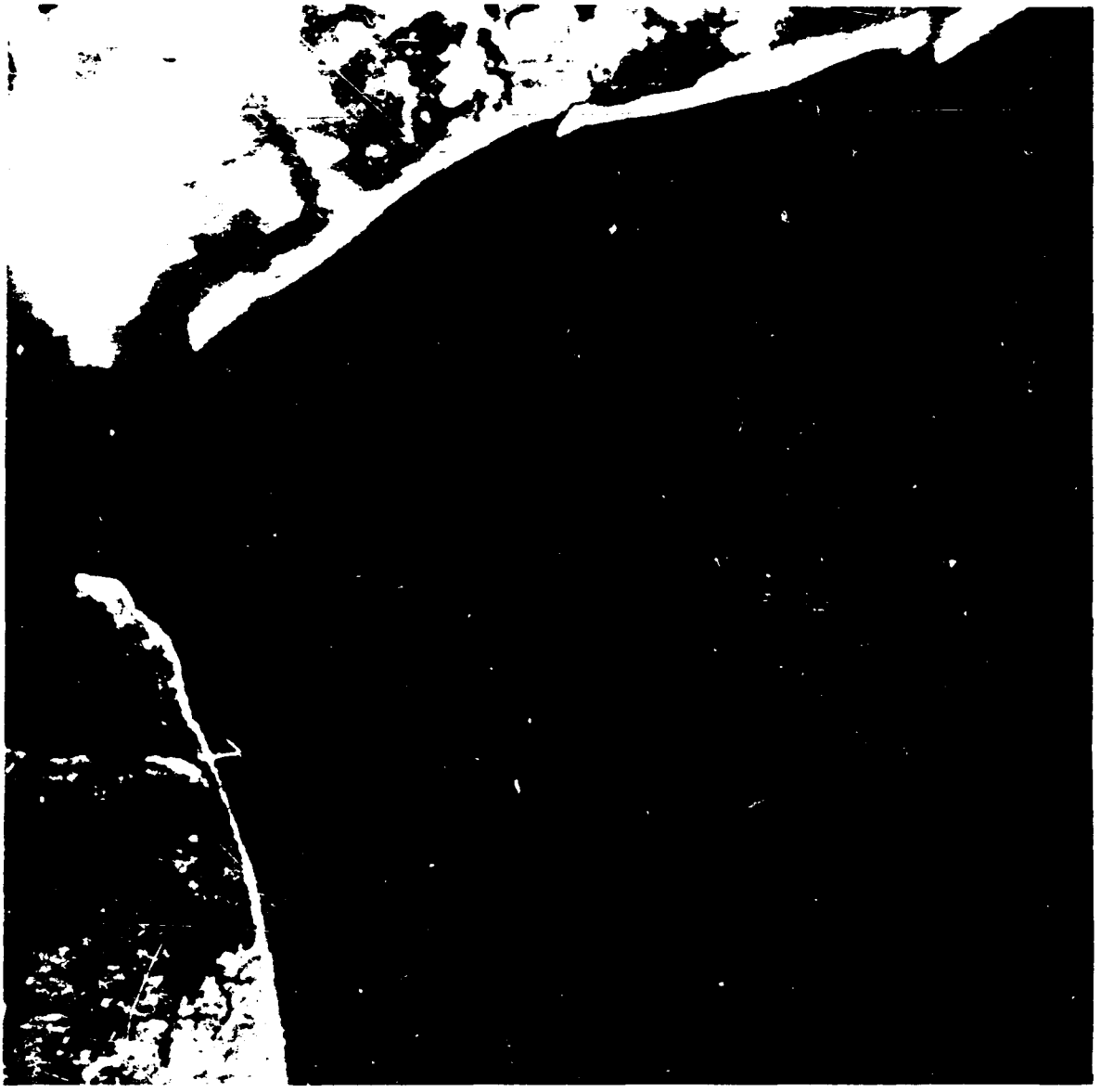

Figure 4-18. Enlarged subscene from Landsat 1024-15071, band 4, taken on August 16, 1972 over New York City; printed as a negative.

#4-82: Make a guess as to its identity. Do you have a second choice?

Perhaps a further clue is needed. The feature is persistent; it has been observed many times before and since 1972, in the same general location of the New York Bight. The pattern varies but nearly always consists of a contorted trail or streamer of milky material.

The feature was imaged by the Ocean Color Scanner (OCS), a prototype model of the Coastal Zone Color Scanner (CZCS; see page 338 for a description of this instrument) flown on the Nimbus-7 satellite launched in 1977. The OCS was operated from an aircraft to test performance and acquire data for developing analytical techniques. The OCS contains several channels in the blue and green, as well as red, selected to reproduce fairly accurately the color variations that characterize marine waters, their sediment load, and the presence of chlorophyll in plant nutrients. Figure 4-19 depicts this feature as imaged by OCS at a point about 24 km (15 miles) east of Sandy Hook, N.J. Also evident is a large plume of sediment mixed with a sludge being carried into the Atlantic from the Hudson River.

#4-83: Has the OCS image changed your mind; if so, what is your new opinion?

The identity of the feature is revealed at the top of page 142.

Figure 4-19. False color composite showing the New York Bight off Long Island made from Ocean Color Scanner data.

Siltation Patterns

In Figure 3-8, we saw the effects of producing a false color composite by projecting band 4 through a red filter, band 5 through green, and band 7 through blue. Sediment patterns are more sharply emphasized in this combination. These turbid water patterns may also be brought out by a photographic enhancement technique involving a shift in contrast and a lightening of the lighter gray levels. Figure 4-20 presents a superb example of this manipulation, performed on a band 5 image. This is the next scene south of the New York–New Jersey frame. Most of the Delmarva Peninsula (consisting of the state of Delaware, the Maryland eastern shore, and a small part of Virginia) is imaged. The Chesapeake Bay lies to the west and the Delaware Bay to the east.

#4-84: Locate three or four areas where the sediment load is apparently greatest (use an atlas to name some nearby reference locality).

[4] During the week before October 23, a storm dumped over 1 in of rain around Harrisburg, and similar or higher amounts fell in the mountains to the west. Rainy conditions persisted through the 21st, followed by rapid clearing.

#4-85: Where do you find patterns related to current circulation (stream flow, tidal movements)?

#4-86: What might you do to establish the persistence or variability of these currents?

Studies of sediment patterns in the Delaware Bay have been an integral part of a current Landsat investigation by Dr. V. Klemas and associates at the University of Delaware. Combined visual and computer analyses of these patterns for specific

Figure 4-20. Band 5 image of the Delmarva Peninsula, Delaware Bay, and southern New Jersey as scanned from Landsat-3 on June 11, 1978.

Landsat overpasses are coordinated with measurements of sediment load (expressed in milligrams per liter) through "water truth" sampling from boats and helicopters close to the times of overpass. From this a calibrated sediment distribution map (Figure 4-21) has been produced from data for several overpasses. The map correlates both water sample analyses and Secchi (Disc) depth data with radiances measured by the Landsat MSS.

#4-87: The Landsat image in Figure 4-20 was taken in mid-June 1978. However, in this rendition, most of the agricultural fields seem to have very high (bright) reflectances, as though only barren, light-colored soils were exposed, although many crops had been planted earlier and some were even approaching maturity. Offer an explanation for this apparent tonal anomaly. (Hint: Remember how the photo was processed.)

Inserted Discussion for Questions 4-81 through 4-83

The feature considered in questions #4-81 through 4-83 is produced by the dumping of acid wastes carried to sea in a barge. The material is a mixture of sludges and sulfuric acid, which accumulate as residues from operation of a refractory plant in New Jersey. The towed barge is emptied each morning at distances supposedly beyond a 48 km (30 mile) limit, off the continental shelf. A zigzag pattern of dumping is designed to improve rapid dispersion, but the reflective wastes remain coherent long enough to be detected by Landsat.

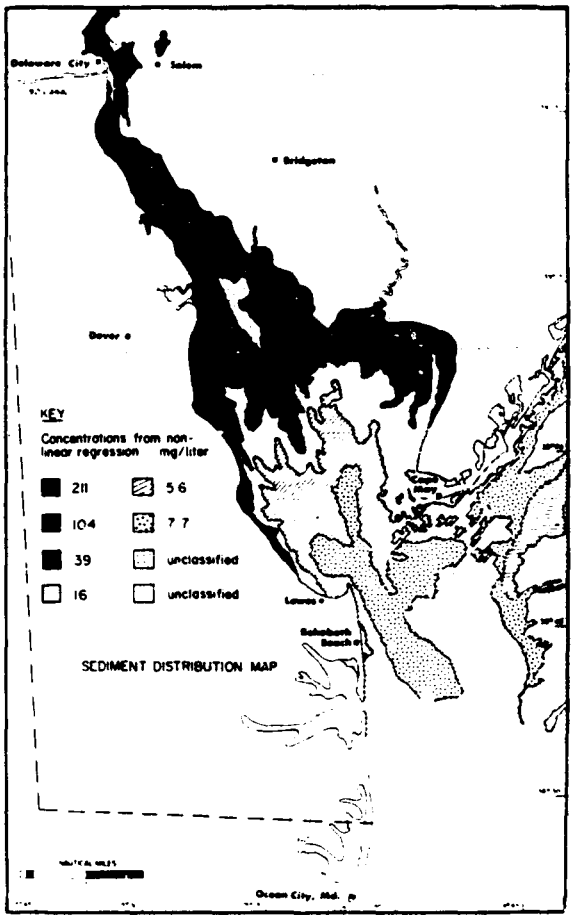

Figure 4-21. Sediment distribution in the Delaware Bay determined from Landsat and surface boat data sources (courtesy of J. Klemas, University of Delaware).

CONCLUDING REMARKS

Well, at last we have reached the end of this activity—the broadest and possibly the most challenging one in this workbook. By this time, you should have attained some really practical skills in analyzing and interpreting Landsat data. You will probably have formed some opinions—perhaps still tentative—on the merits and usefulness of Landsat as an information source to meet your needs. However, because of some obvious shortcomings in extracting this information by photointerpretation methods, you may not be ready to make a commitment to incorporate Landsat into your work activities (or those of your organization). Reserve judgment until after you complete Activities 5 and 7, which will introduce you to (almost certainly) the most powerful way to handle and interpret Landsat data: use of the computer to enhance your imagery, classify the scene, and coordinate Landsat-derived information with other data sets within a common geographical framework.

ACTIVITY 5

COMPUTER-PROCESSED LANDSAT DATA

LEARNING OBJECTIVES:

- *Establish or expand your background in the concepts, methods and terminology of computer processing of image producing data.*
- *Gain an insight into the advantages of computer-based image processing compared with the photo-interpretation approach for processing, classifying, interpreting, and applying remote sensing data.*
- *Acquire a broad perspective on the principal processing routines now developed to analyze Landsat data.*
- *Develop a solid working knowledge of the main techniques for image enhancement, pattern recognition, and thematic classification.*
- *Get a feel for the pros and cons of batch and interactive modes of image analysis.*
- *Examine and evaluate some specific computer-generated products for subscenes in Pennsylvania and New Jersey.*
- *Interrelate these particular examples of output with the more theoretical explanations of computer-processing strategies and procedures given in Appendix B.*

RATIONALE BEHIND COMPUTER PROCESSING

A great deal of useful information may be extracted directly from a Landsat image by the straightforward methods of photointerpretation studied in the previous activity. The *advantages* of this approach are clearcut:

- Familiarity with and use of aerial photographs (of which Landsat images are just a special case) are commonplace among resources specialists.
- The image scenes depict the real world in a visual sense in much the same manner that we might view the surface from space or, as most of us actually have done, from commercial jets.
- The spatial relations among surface features are displayed in the same context that we strive to represent on maps.
- The principles of aerial photointerpretation are easily extrapolated to Landsat scales, as long as resolution is sufficient to recognize the critical or diagnostic interrelations by which large features are identified.

For some applications, it is necessary only to examine Landsat data in the image format to carry out an effective analysis and obtain the desired outputs. There are also serious *limitations* to working primarily with Landsat photo products. Among these can be cited:

- The range of gray levels recorded on film or print is narrow; the number of color tones recognized by the human brain is greater but is still limited.
- The interpreter tends to be subjective in discerning subtle differences within the photo's range of gray levels or colors.
- It is often necessary to resort to less exact and reproducible measurement techniques (e.g., densitometry) to provide a quantitative basis for distinguishing features and associated spectral properties within an image.
- Copies (multigenerations) of photo images are frequently duplicated with low precision, that is, they experience degradation in visual quality.
- It may be necessary to reprocess images—using slower, but less costly methods—to enhance them by the customary photographic techniques, for instance, improving contrast by modifying the H-D curve (shifting gamma).
- Optical distortion within the image, which affects registration of multiband and multitemporal images, is normally a problem.

Since the early days of Landsat-1 there has been an ever-growing shift from the standard photointerpretive approach to a strong reliance on computers. Computers are now used routinely in various phases of data manipulation and analysis as well as in more sophisticated information extraction methods. They are also instrumental in integrating Landsat results with other data sources in models for status assessments and interpretations, decision making, and operational control. The ability of computer processing to overcome the limitations mentioned above is one reason for this. Another is just the fact that the sensor data are sent to receiving stations by telemetry in a format ready for reprocessing into computer-compatible tapes (CCT's).

Still other reasons are important: (1) Certainly an obvious one is related to the vast quantity of data. There are more than 7.5 million individual data points (the picture elements or pixels, as described more fully in Appendix B), each encoded to 6 bits, in each band of a Landsat scene. Thus, all four bands make up a total of *ca.* 30 million numbers, which must be kept track of and acted upon if the full data set is to be processed; (2) The Landsat data represent a series of related values derived from a number of variables, including the four channels themselves and temporal data from different passes. As such, the data are best organized and manipulated by methods developed for the *multivariate statistical* approach (see p. 421 ff.

of Appendix B for a review of certain concepts in statistics). (3) The computer manipulates data sets and subsets rapidly, efficiently, and systematically into improved working products by removing or reducing geometrical and radiometric errors internal to the sensor or introduced by perturbations in spacecraft motions and positions; (4) Corrections for radiance degradation or interference by the atmosphere, and for variations in radiance levels owing to seasonal changes in solar illumination, may be applied to any part of a scene because each discrete data point (pixel) within the CCT may be retrieved and modified by appropriate reprocessing; and (5) The full resolution (both spatial and spectral) of pixel signal levels can be maintained from step to step throughout the computer processing.

Perhaps the most compelling reasons for relying on computers to process Landsat data are evident from consideration of Tables 5-1 and 5-2. Table 5-1 consists of a simplified flow diagram that describes the sequence of steps (with several unspecified feedback loops) normally followed in acquiring, processing, interpreting, and using remote sensing data. Those steps in which computer processing can replace manual (photointerpretive) methods or otherwise play a key role are singled out by a double asterisk (**). It is obvious that nearly all steps are amenable to assistance from computer processing (also referred to as machine processing or automatic data processing [ADP]). A case can even be made for introducing the computer as an aid in the results/recommendations and evaluation/decision-making steps, although the human element usually dominates in these actions. Some of the major advantages of computer processing of Landsat data are summarized in Table 5-2, along with a list of some of the principal processing routines now in common usage with Landsat and other remote sensing data.

Table 5-1
Use Flow of Earth Resources Satellite Data

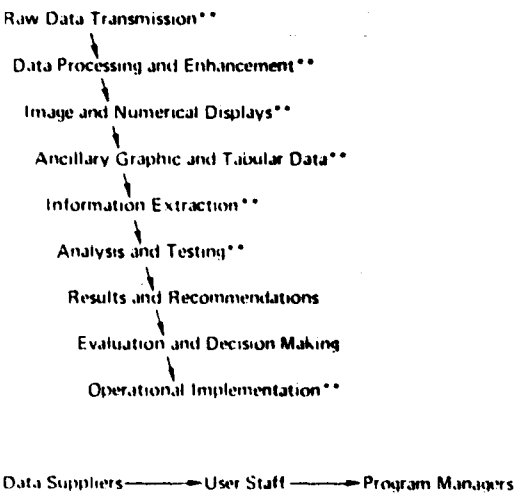

**Major Role for Computer Processing

Table 5-2
Some Uses of Computers in Satellite Remote Sensing

Advantages	Routines
Data Commonly Transmitted in, or Converted to, Digital Mode	Data Compression and Resampling
Analysis of Individual Data Points (pixels)	Geometrical Corrections
Handling of Large Data Volumes	Atmospheric and Illumination Corrections
Data Easily Manipulated by Mathematical and Statistical Analysis	Image Enhancement ("cosmetics")
Full Radiometric Utilization of Dynamic Range of the Sensors	Multivariate Analysis (using statistical techniques)
Correction of System Related Errors	Signature Extraction
Accuracy Assessment	Special Techniques (band rationing; canonical analysis)
Interactive Video (TV) Processing	Multiscene (temporal) Registration
Controlled Image Outputs	Training Site Selection
Rapid Hard Copy	Classification (theme mapping)
Data Base Correlation (map and graphic overlays, etc.)	Theme Area Measurement (acreage, etc.)
New or Revised Maps Generated by Printer Plotters	

Before proceeding, it is wise to review briefly several terms that were defined by a 1965 Committee on Processing of Remote Sensing Data. They recognized these following functions:

1. Signal Processing (usually, but not exclusively on the spacecraft)
   - *Detection *Amplification
   - *Digitization *Multiplexing
   - *Transmitting
2. Ground Processing
   - A. Data Preprocessing
     - *Receiving *Demultiplexing
     - *Digitization *Recording
     - *Reformatting *Re-Recording
   - B. Data Processing
     - *Corrections: Radiometric; Geometrical
     - *Products: Computer Compatible Tapes; Photos/Images
   - C. Data Analysis
     - *Classification
     - *Other types of Information Extraction

Despite this attempt to standardize the terminology, one still encounters discrepancies in the literature associating some particular step or routine with a stage of processing. Most specialists engaged in computer processing now consider radiometric and geometrical corrections to be a preprocessing function, although similar or more advanced corrections may be performed during processing to produce enhancements or classifications. (Some of the basic corrections applied to the "Raw" Landsat data at Goddard's IPF before any images are generated by the EROS Data Center or others are designated as Preprocessing.) Likewise, a user partial to digital data will probably treat classification as largely a processing stage function, whereas one who tends to "think analog" will perceive most classifying actions as analysis. The analytical approach will also include checking in the field and integrating classification maps and enhancements with kinds of data (these steps are referred to as "postprocessing" by some specialists).

HOW TO USE THIS ACTIVITY

In this activity, we shall be concerned primarily with examples of the most versatile computer-generated routines and output products. We shall use some of the same Landsat scenes and shall reexamine several of the same application topics that you worked on in the photointerpretation activity. Some new scenes and specialized applications will be introduced.

We recognize that many readers have only a casual and rudimentary knowledge of computer processing, especially in its application to remote sensing. If you fit into this category, you would be well advised to put aside this activity for the moment and carefully read through Appendix B, which provides a concise but nevertheless adequate summary of principles, concepts, and procedures being used in computer processing of remotely sensed data. You may even wish to consult one or more of the appropriate references cited in Appendix G to enlarge your understanding of computers as such.

However, you may decide to proceed through this activity without having diverted to Appendix B to build your foundation in computer processing. If so, you will be aided by brief explanations of some of the specific operations performed on Landsat data and the rationale for these routines. In this activity, we shall survey the types and uses of output from two of the three major groups of computer processing routines described in Appendix B: (1) preprocessing (information restoration), (2) enhancement (information enhancement), and (3) classification (information extraction). Examples of the first group, preprocessing, are not considered here (see pp. 428 to 432 for details), except for one indication of a resampling routine incorporated in the enhancement section.

IMAGE ENHANCEMENT

Sharpening a Landsat Image

Many novices are likely to express some surprise when they first see a computer-processed version of a full Landsat image, especially if they are familiar with the same scene only in its standard rendition produced from the electron beam recorder (EBR) or a similar photo-generating device. This is particularly true for the version seen by most users—the fourth or fifth generation of positives/negatives.

You may already have experienced this same reaction in the previous activity on photointerpretation. You have been given a strong hint of the improvement in image quality obtainable from computer processing when you compared Figures 2-1 and 2-6 in that section. Both false color images were constructed for the same scene from data acquired on October 10, 1972, at a time when clear fall air minimized atmospheric interference.

Figure 2-1 is a standard processing product made on the EBR at the Goddard Space Flight Center. As printed in this workbook, the figure has gone through six generations of positive-negative film (or print) steps, each of which imposes some further degradation in image quality. The original image was subjected to only the routine preprocessing (radiometric and geometrical corrections) applied to all Landsat data passing through the Goddard Image Processing Facility. The photoimage itself was initially one of many made in a mass production (batch) mode, with no tailored color or tone control. Figure 2-6 is a computer-enhanced version of this scene generated by IBM, using the processing steps listed below and then subjected to careful, customized color printing.

A major change in image quality of products delivered to the user community by the EROS Data Center (EDC) was introduced in 1979. At that time EDC began to produce computer-enhanced full scene images as standard output by using its EROS Digital Image Processing System (EDIPS). You have previously examined an excellent example of this enhanced product in Figures 4-3 and 4-4. The processing procedure is described in some detail on pp. 414 to 416 (Appendix A). The EDIPS standard processing "menu" follows these steps:

1. Radiometric correction of data to adjust for satellite and sensor anomalies;
2. Geometrical correction and resampling of data to the Hotine Oblique Mercator projection (see p. 430);
3. Compensation for atmospheric scatter (haze removal);
4. Display and analysis of the distribution of brightness values (DN's) leading to mapping of image gray levels to preassigned film density levels via logarithmic (nonlinear) tables.

In addition, the DN distribution may on special request be expanded to use the full dynamic range of film density (contrast stretch). Edge enhancement or high bandpass filtering routines are also done on special request. The images reproduced in Figure 4-3 are second-generation positive copies made from a first-generation negative film produced from data on an EDIPS High Density Tape (HDT) used to drive a laser beam recorder. The EDIPS data products are now being provided routinely by EDC in response to orders for scenes acquired after February 1, 1979.

Thus, when great care is taken in "cosmetically" treating images through computer processing, the results can be spectacular. The output products, be they the standard 1:1,000,000 scale or enlargements to 1:200,000 or better, are so superior that one might believe (or hope) that a new satellite, with a notably improved MSS, had been launched in secret. Judge for yourself by comparing a "before" and an "after" rendition of the famous Washington, D.C., image obtained on October 11, 1972 (Figures 5-1A and B). The "before" is another standard product generated first at Goddard and then reprinted by the General Electric Space Systems photographic laboratory to give a better than average version. The "after" is a spectacular version! Many consider it the best rendition yet made of any scene in the eastern United States. This was generated in 1976 by Ralph Bernstein and staff at International Business Machines (IBM) in Gaithersburg, Md. The principal processing steps were (1) reformatting CCT's to HDT's; (2) radiometric corrections (internal, to moderate varying detector response; external, to compensate for variable atmospheric alteration); (3) geometrical corrections (internal variations in mirror velocity and in detector sampling; external to correct for spacecraft attitude, panoramic distortion, scan skew, Earth rotation); (4) mapping or geographical fitting (UTM coordinate system; ground control points); (5) resampling (including filtering); (6) generation of black and white negatives and prints; and (7) production of color composites by registering black and white negatives for bands 4, 5, and 7 and exposing on cibrachrome color film.

Cross-examine these two images, particularly with respect to observable details. Use a magnifying glass where necessary. Using the GE version as a "before" base, and referring to an atlas or map as needed, appraise the IBM version by answering the following:

ORIGINAL PAGE
COLOR PHOTOGRAPH

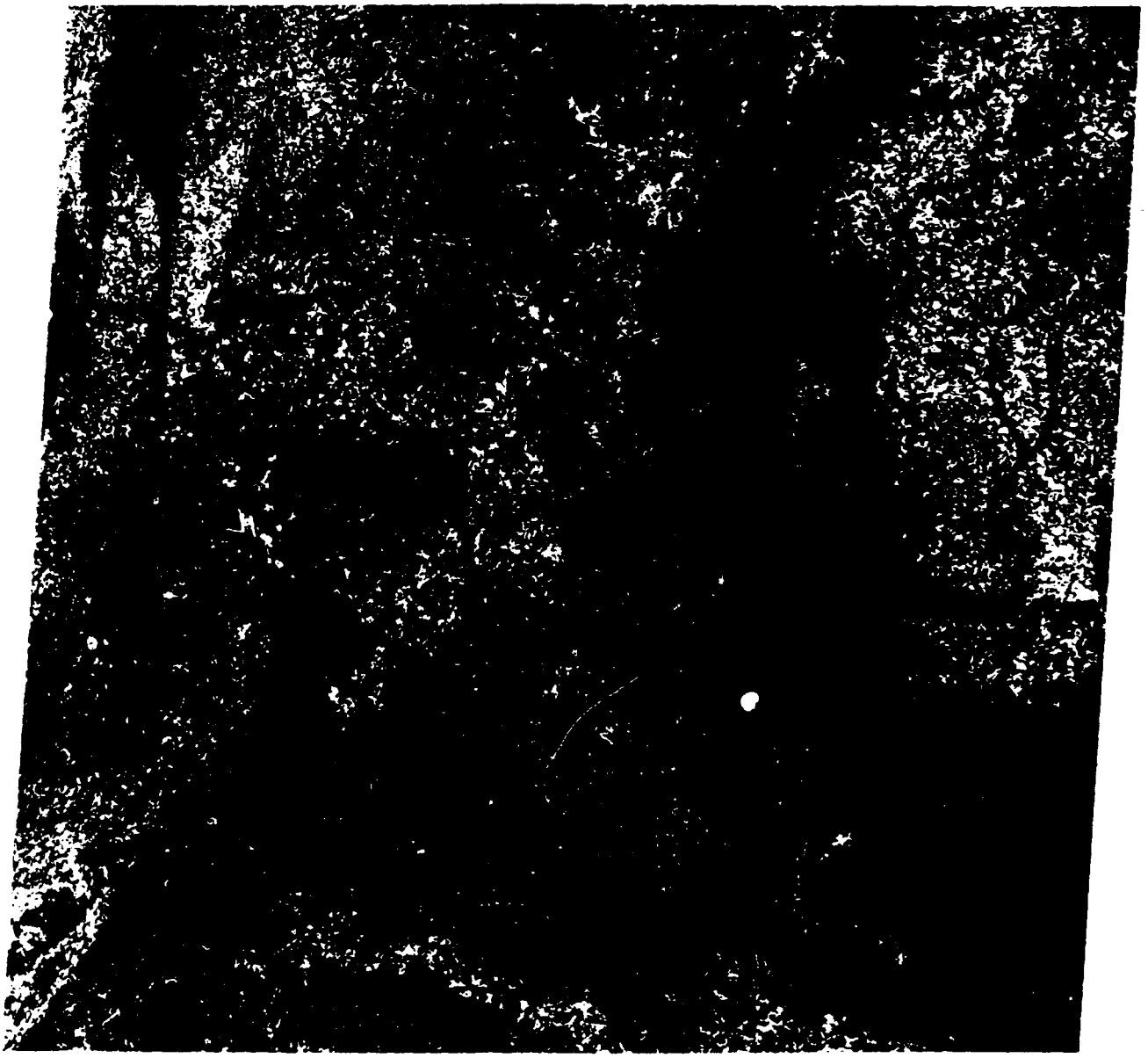

11OCT72 C N38-54/W076-48 N N38-52/W076-43 MSS D SUN EL38 AZ149 191-1114-N-1-N-D-2L NASA ERTS E-1080-15192-7 21

Figure 5-1A. The October 11, 1972 image of Washington, D.C., Baltimore, and the Chesapeake Bay.

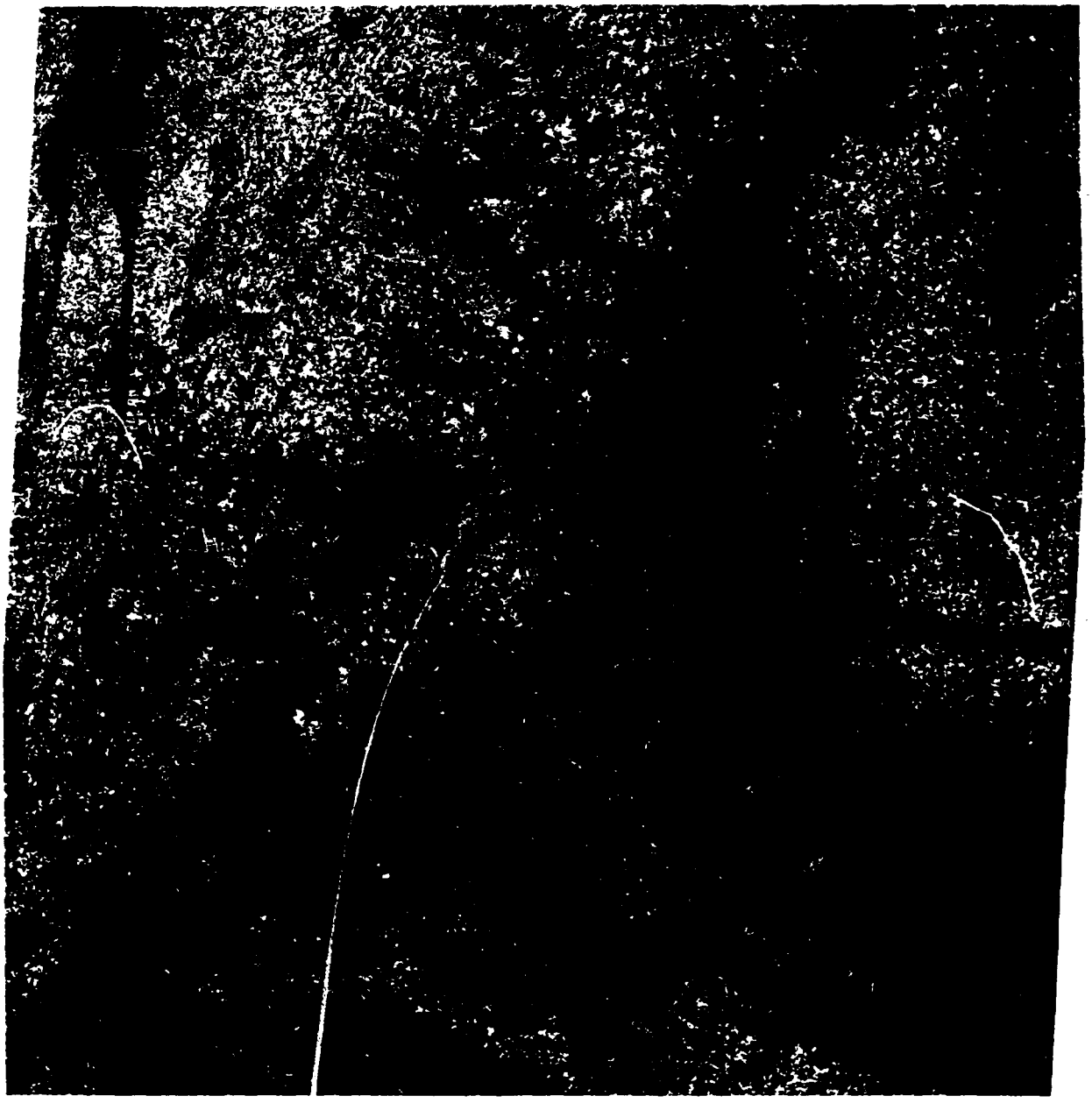

Figure 5-1B. The IBM computer-processed version of the Washington, D.C. scene.

#5-1: Describe the improvements in picking out details in the central area of metropolitan Washington, D.C.

#5-2: Why do the inner city and commercial regions (in blue) of Washington and Baltimore appear more widespread (larger area) in the IBM version?

#5-3: Locate additional major roads in the IBM version. Is there a significant increase in the number and/or length seen?

#5-4: Can you now find the Bay Bridge near Annapolis?

#5-5: What minute detail is evident in the runways of Dulles Airport, west of Washington? (Think of what an airplane does first after landing, as it taxis towards the unloading area.)

#5-6: Comment on the appearance of the agricultural lands, particularly in the Delmarva peninsula of the eastern shore of the Chesapeake Bay.

#5-7: Look at the forested countryside southwest of Washington. Many irregular dark, blackish patterns intersperse with the red tones in the IBM version but are obscure in the GE version. What might these patches be (remember a hallmark of southern woods)?

We shall turn next to several computer-generated enlargements of the Washington, D.C., area. Figures 5-2A and B are band 5 and 7 images of an April 1973 scene produced on the VICAR system at the Jet Propulsion Laboratory, Pasadena, Calif. In addition to the usual radiometric and geometrical corrections, the output data were contrast-stretched (by trimming low and high DN or brightness values in the pixel distribution histogram and expanding the remaining values to a fuller range).

#5-8: Can you begin to pick out any landmarks in downtown Washington? Name them.

#5-9: Some roads are better discerned in band 5; others in band 7. Why?

A further enlargement of part of the area is shown in Figure 5-3 as a color composite, made by using the VICAR program as adapted at Goddard. The processing steps included destriping, resampling, filtering, and contrast stretching.

#5-10: A blockiness is evident on close inspection of small sections of this image. It is especially noticeable at sharp tonal discontinuities, as along the river banks, at the airport, or along major road. What causes this?

#5-11: Some soils in the eastern half of the Washington area, especially those derived from marine sedimentary claystones, are reddish- to yellowish-brown in natural color. What color do they appear in this computer version? Why? (See category i, Table 3-3.)

Resampling

Still greater enlargements are shown in Figure 5-4. These renditions were subjected to several enhancement routines. After appropriate preprocessing, the image was resampled (see p. 431). Resampling is necessary whenever a geometrical operation such as rotation or enlargement is performed on a digital image. This is because the pixel brightness values (DN's) have to be estimated at locations where no measurements have been made. Such estimation is done by using available measurements in a neighborhood of the new pixel locations. Resampling is useful for correcting geometrical errors due to attitude variations and several other sensor effects. It is also useful in producing enlargements of images to a specific scale (e.g., 1:24000 to match the U.S. Geological Survey 7½ minute quadrangle maps). In general, resampling accomplishes two things: (1) It is necessary because many pixels in an array are not initially in the proper places owing to sensor and attitude errors during data acquisition; the pixels must be relocated to more accurate positions by using ground control points and other correction procedures; their new brightness values (DN's) must be calculated to

better approximate the actual values characteristic of these new locations. (2) Together with other routines, it can smooth out the blocky, mosaic-like pattern that results when individual pixels become visible. This appears to sharpen the scene and aids in approaching the best resolution limit obtainable from the observation conditions. In one special procedure, pixels smaller than those representing the inherent resolution of the sensor system (controlled by IFOV, sampling rates, optical fiber areas, etc.) are "created" by sub-dividing original pixels into smaller units and repeating the DN values of each original pixel within the derivative units.

The Nearest Neighbor resampling technique (p. 431) was used on the data set shown in the top view of Figure 5-4; although pixel locations are improved, the blocky effect from individual pixels remains. Application of the Cubic Convolution technique (p. 431), followed by high emphasis filtering and a contrast stretch, produced the sharper image in the bottom view.

#5-12: Look for the same buildings you sought in question #5-8. Are they now even more easily located? It is still difficult to identify these buildings unless one has prior knowledge of the region or good maps and other forms of ground truth. Comment on this statement.

#5-13: For some reason (which you may be able to deduce if you know the building), the White House does not stand out. However, the similar sized Jefferson Memorial and the Lee Mansion in Arlington National Cemetery are discernible as white dots. Explain the difference, if you can. (Hint: think roof.)

#5-14: Believe it or not, the shadow of the Washington Monument is visible in the large red area along the Mall. Find it!

#5-15: Do you feel that the levels of detail shown in the several enlargements and in the IBM version of a full scene would suffice as an adequate data source for updating a map of the major classes of features in an urban or metropolitan area (as, for example, commercial, industrial, residential, transportation routes, etc.)? Express your reasoning, and include shortcomings.

Keep this response in mind as you read through the description of a classification of Philadelphia on pp. 224 - 232.

Spatial Filtering

Most Landsat images contain some features with well-defined boundaries. Examples include roads, water/land interfaces, fence lines, field edges, and natural fractures (faults, joints). Contrast stretching will, to some extent, emphasize those boundaries characterized by large tonal differences on either side. Spatial filtering (p. 436) will produce sharper edges and better contrast. One special procedure in the filtering routines is called edge enhancement. This technique has been used to bring out linear patterns related to topography and fracturing. It works particularly well in arid, low vegetation terrains. A linear discontinuity is usually indicated by an abrupt step in reflectance (in imagery, a tonal difference) across the feature. Edge enhancement maximizes this effect by increasing the differences in brightness between the feature and its adjacent surfaces, in a sense, a localized contrast stretch. However, because the DN's values at the enhanced edge are modified to produce the visual effect, the radiometric fidelity in the immediate area is compromised.

The visual impact of a high bandpass filtered image also depends on the nature of the terrain itself. This is illustrated by Figure 5-5, a filtered image made from a subset of CCT data obtained during a Landsat overpass above Huntington, W.Va. (center), on October 17, 1979. The surrounding region is typical of the dissected Applachian Plateau several hundred kilometers west of Harrisburg. The combination of low Sun angle (24°) and edge enhancement strongly emphasizes numerous linear and curvilinear patterns, many structurally controlled, easily missed in standard scenes (especially those taken in summer). Compare the appearance of terrain in this version with that of the same area as constructed from merged radar-MSS data (Figure 9-24).

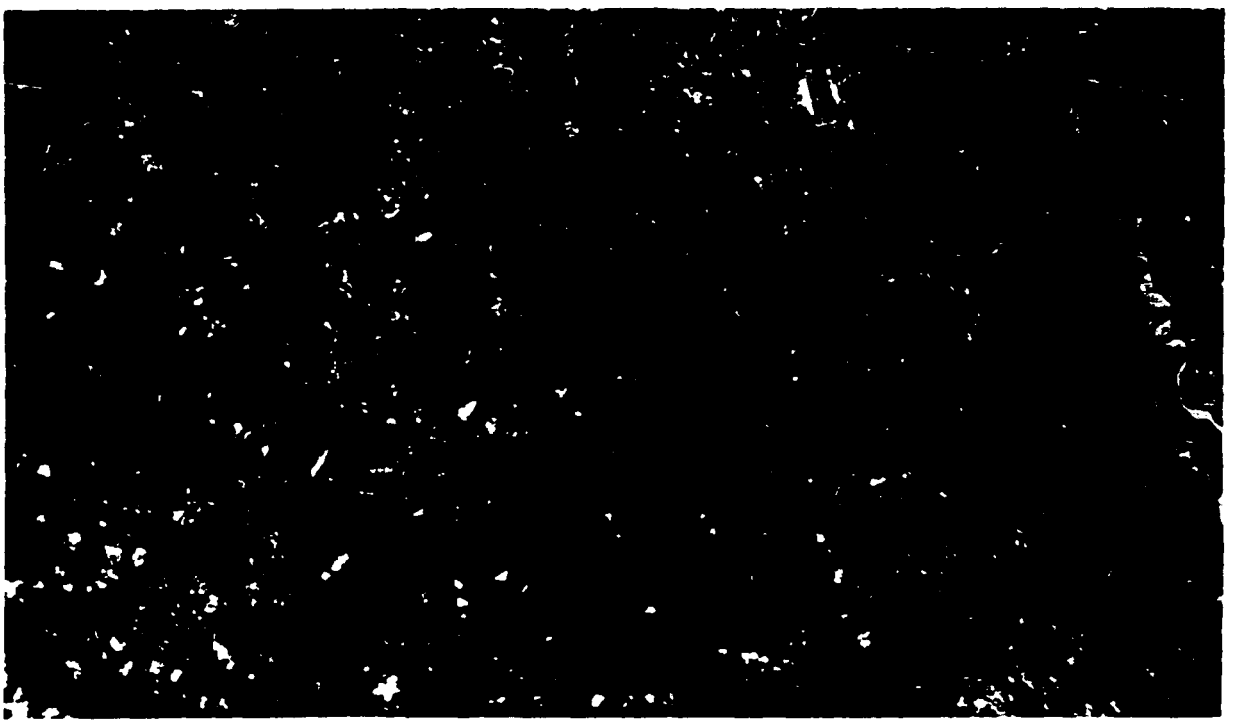

Figure 5-2A. A computer-enhanced enlargement of part of a Landsat-1 image obtained on April 3, 1973 showing the Washington, D.C. metropolitan area, band 5.

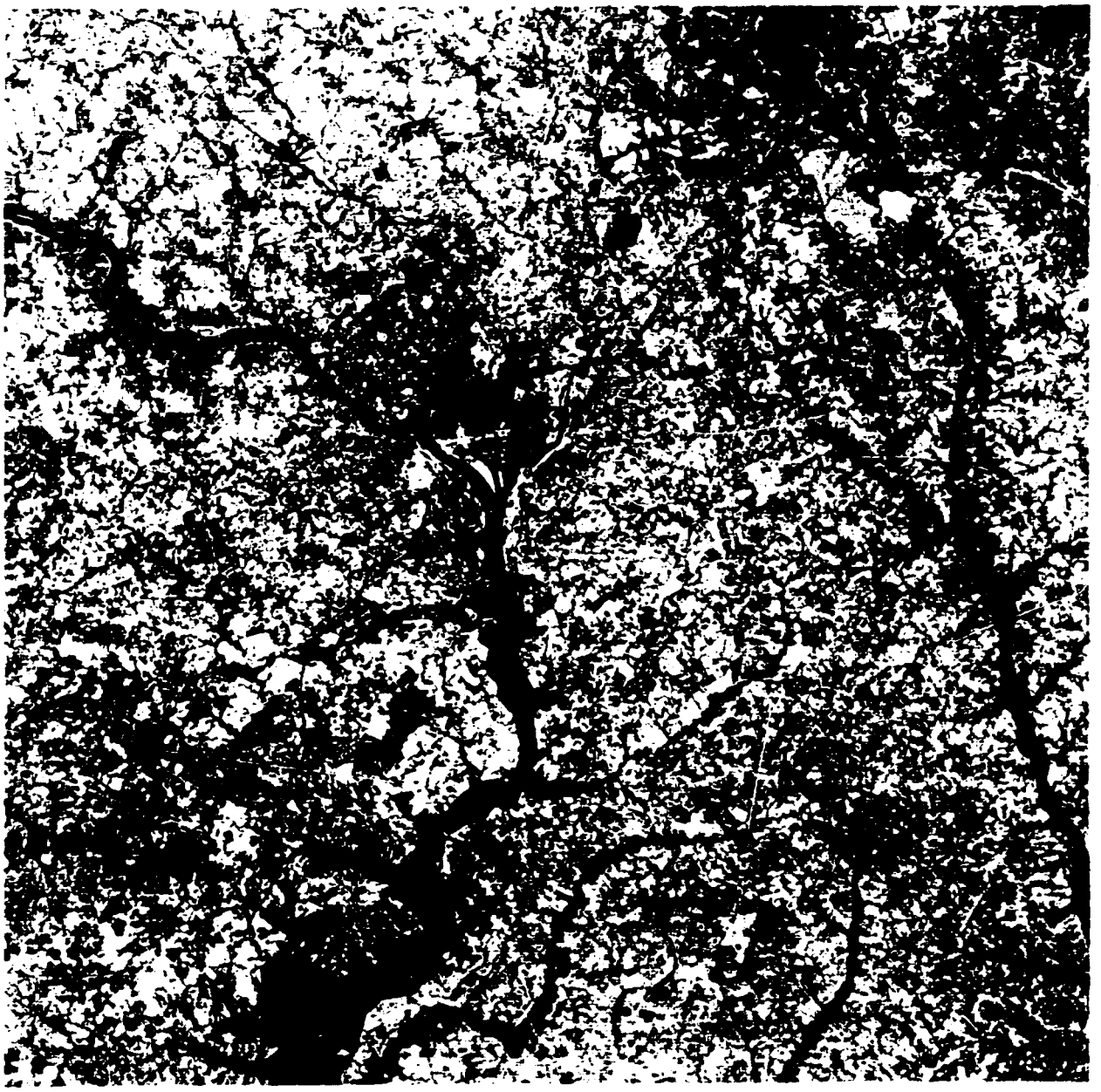

Figure 5-2B. Band 7 rendition of the April 3, 1973 scene.

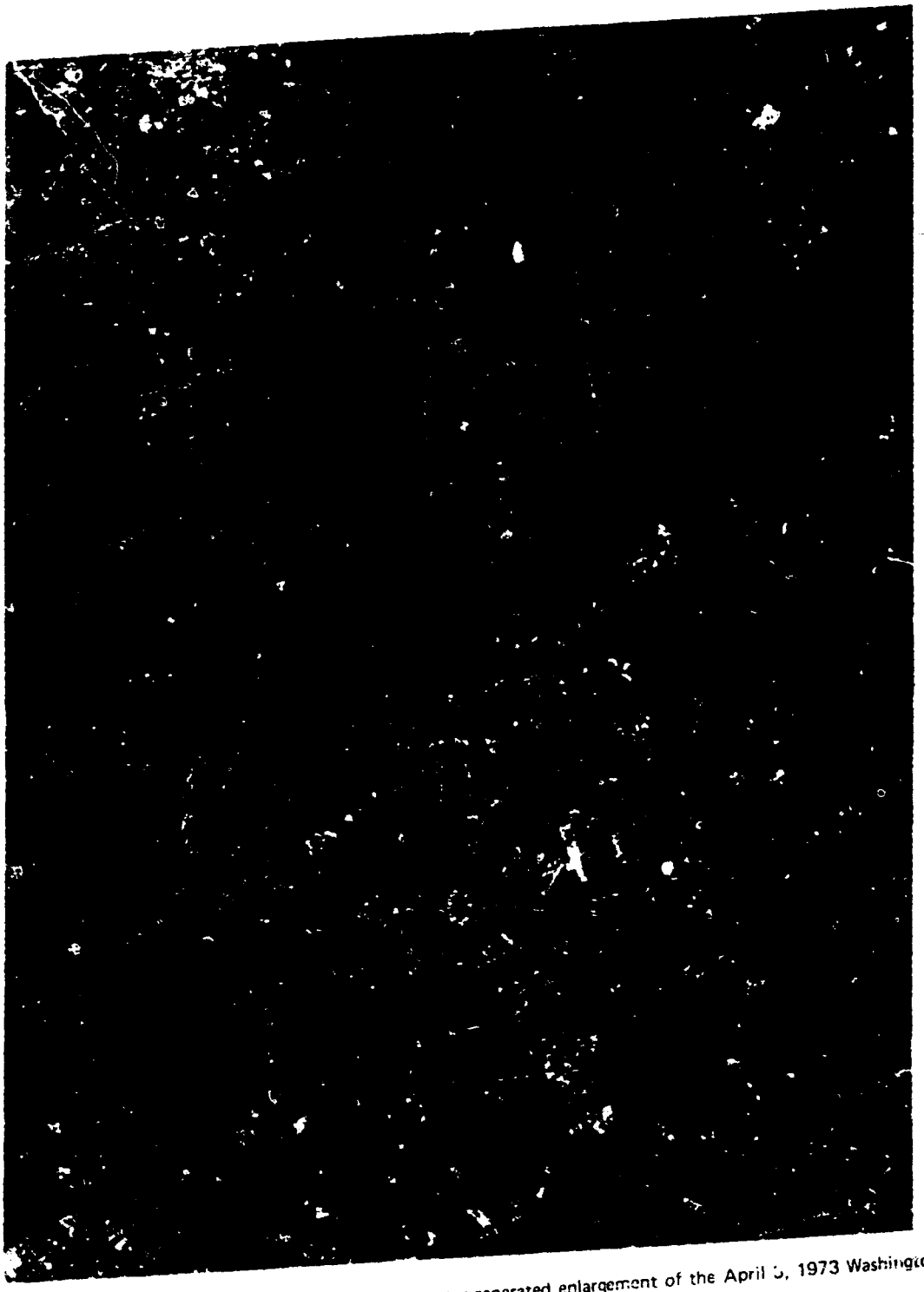

Figure 5-3. False color composite of the computer-generated enlargement of the April 5, 1973 Washington, D.C. scene.

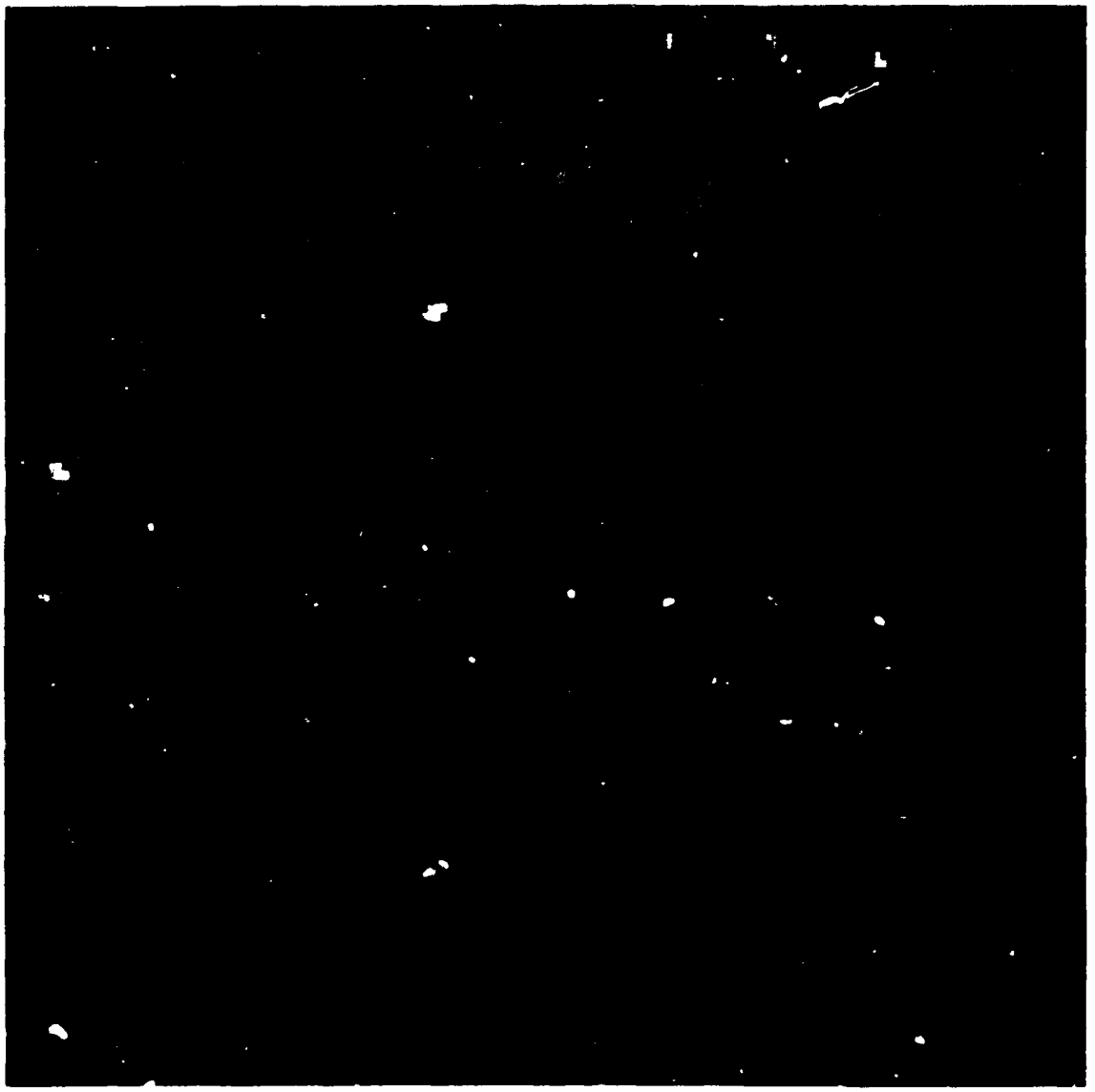

Figure 5-4. Further enlargement of the April 3, 1973 Washington, D.C. scene displaying the effects of resampling by the Nearest Neighbor (top) and Cubic Convolution (bottom) techniques.

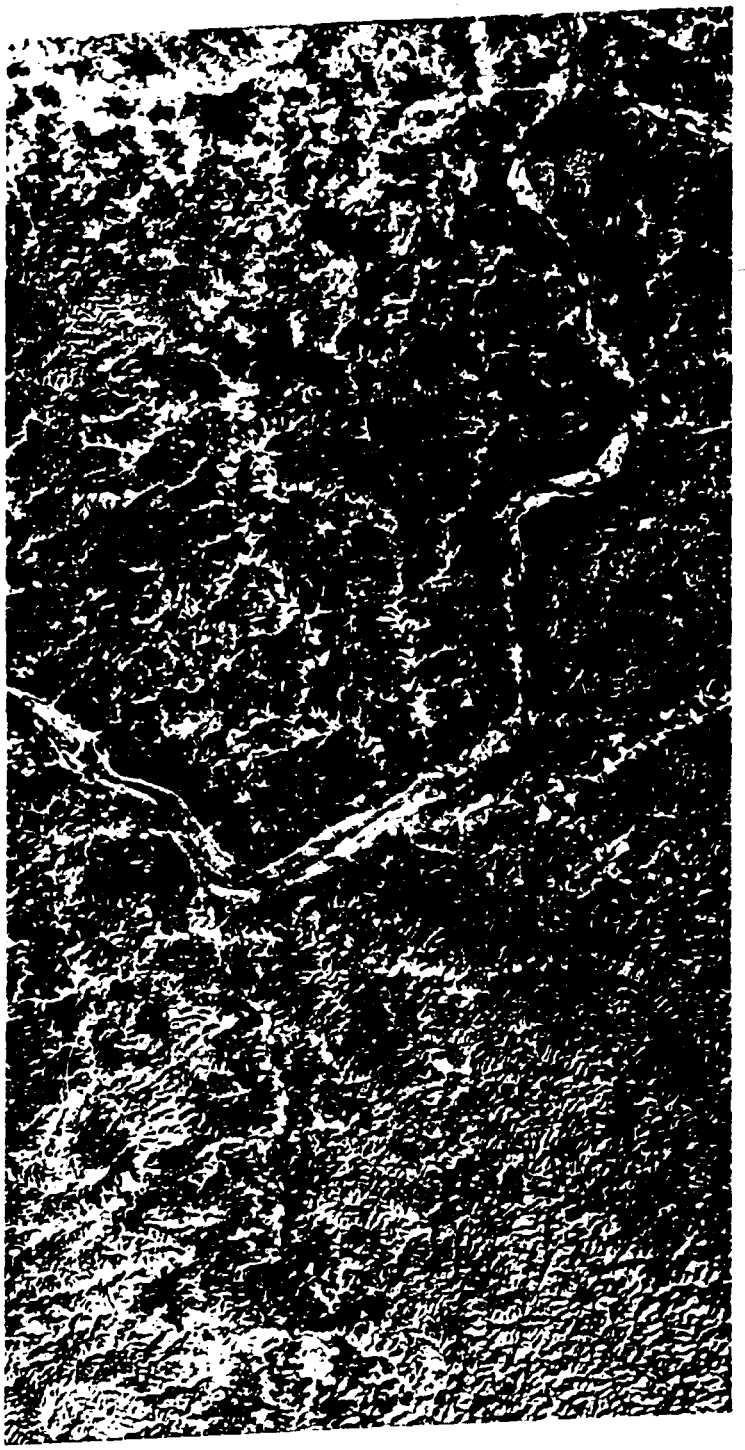

Figure 5-5. Highpass filtered Landsat subscene around Huntington, W. Va. (center) imaged on November 28, 1974.

Several computer enhancement routines were applied to a Landsat subset that covers a 30 km X 30 km section of the Piedmont in southern Pennsylvania-northern Maryland, south of Harrisburg. The resulting images are reproduced in Figures 5-6A to D. The town of Hanover, Pa., is evident near the left margin. The upper left view is a band 7 rendition of a June 1978 subscene in which a simple linear stretch was performed. The same subscene, now subjected to high bandpass filtering with a Fast Fourier Transform (see p. 438), is shown in Figure 5-6B. In 5-6C, the band 5 version of the area has been processed by Cubic Convolution resampling. The last subscene (lower right) is constructed from a February 1978 Landsat band 7 data set; the only manipulation was a linear stretch to increase the already sharp contrast imposed by a natural event, a thick blanket of snow.

#5-16: Using the same approach as you did with question #4-47, sketch all discernible linear features on a tracing paper overlay placed on the four subscenes in Figure 5-6. Select Figure 5-6A as a standard of reference. Which of the four seems best for picking out linear features? Do all such features appear to be natural? Compare the effectiveness of Fourier Transform and Cubic Convolution for enhancing linear features and sharpening details.

#5-17: Locate this subset within any of the images you used in answering #4-47. About how many more linear features do you find in the Figure 5-6 image than you noted within the same area in the full scene? Make a guess as to the identity (nature) of the irregular feature, marked by an arrow, that occurs in a wooded tract southeast of Hanover.

Multitemporal Comparisons

As we now examine several other enhancement methods, you should recall your experience during the photointerpretation activity in performing the change detection exercises applied to defoliation. To evaluate the utility of these enhancement methods, we shall once again focus on the gypsy moth defoliation in the vicinity of Harrisburg, Pa.

First, examine Figure 5-7 to place the change detection effects around Harrisburg in context with those noted earlier around Hazleton. This figure shows a computer-generated version of the same June 8, 1977 scene (Figure 4-8) used in our previous consideration of gypsy moth defoliation. However, this EROS Data Center enhancement was specially contrast stretched to cause the scene-wide areas of defoliation to appear as very dark (almost black) patches in the dark red foliage along the ridges. The resulting color composite therefore has an unusual set of color tones in which many farmland fields appear strongly bluish (barren) to faintly pink and red (in early crop growth stage).

As an optional exercise, outline the areas of strong defoliation throughout the computer enhancement (use Overlay 1). Compare your results with the outline of defoliation you may have elected to draw in following the #4-31 instruction.

#5-18: Do you note any discrepancies between the two versions? Does the computer version offer any significant improvement in the case of boundary delineation? Does it seem to be more accurate?

#5-19: For the computer version, carefully draw the defoliation boundaries along the Blue Mountain ridge in the area just west of Harrisburg on tracing paper. Now do the same for the color iR aerial photo (Figure 5-8) covering the same small area at a scale of 1:8,000. This photo was also acquired in June 1977. Comment on the relative efficiency of Landsat and large scale aerial photography in the overall detection of boundary limits and defoliation.

Gypsy moth defoliation may vary considerably from place to place during a single leafing season. A once defoliated stand of trees can even gain a second set of leaves in summer if the earlier destruction occurred in spring. This is documented by the series of six computer-enhanced enlargements (Figure 5-9) of the Williamsport area on the west branch of the Susquehanna River (located in the upper left corner of Figure 4-8), monitored by Landsat during 1977. Changes from year to year may be just as readily detected by the same visual inspection technique, as is evident from Figure 5-10 showing defoliation differences from 1976 to 1977 in the Blue Mountain ridges around Harrisburg.

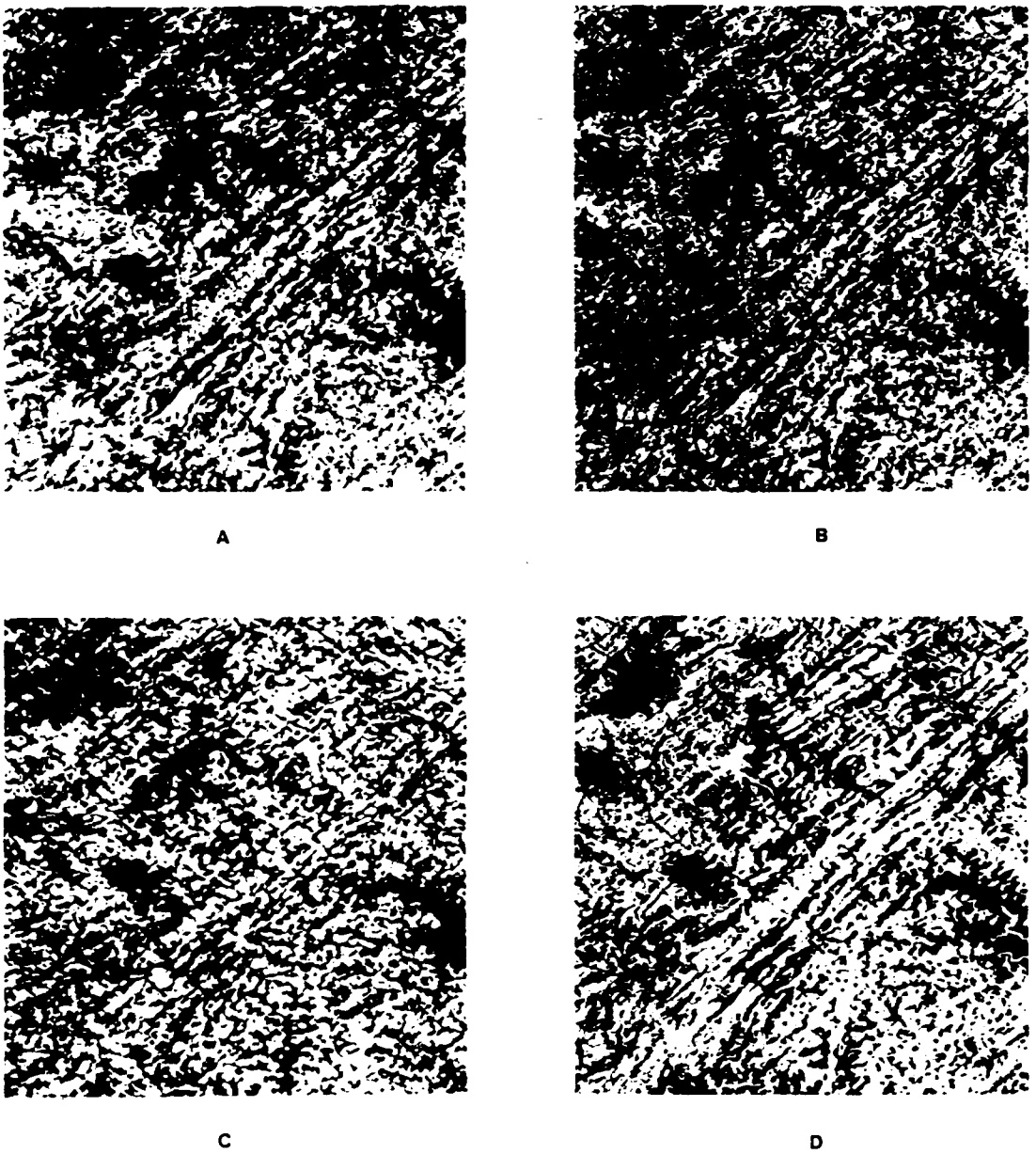

Figure 5-6A-D. Enhancements of Landsat subscenes around Hanover, Pa. using bandpass filters (see text).

ORIGINAL PAGE
COLOR PHOTOGRAPH

Figure 5-7. EROS Data Center computer enhancement of Landsat 2868-14471, June 8, 1977.

ORIGINAL PAGE
COLOR PHOTOGRAPH

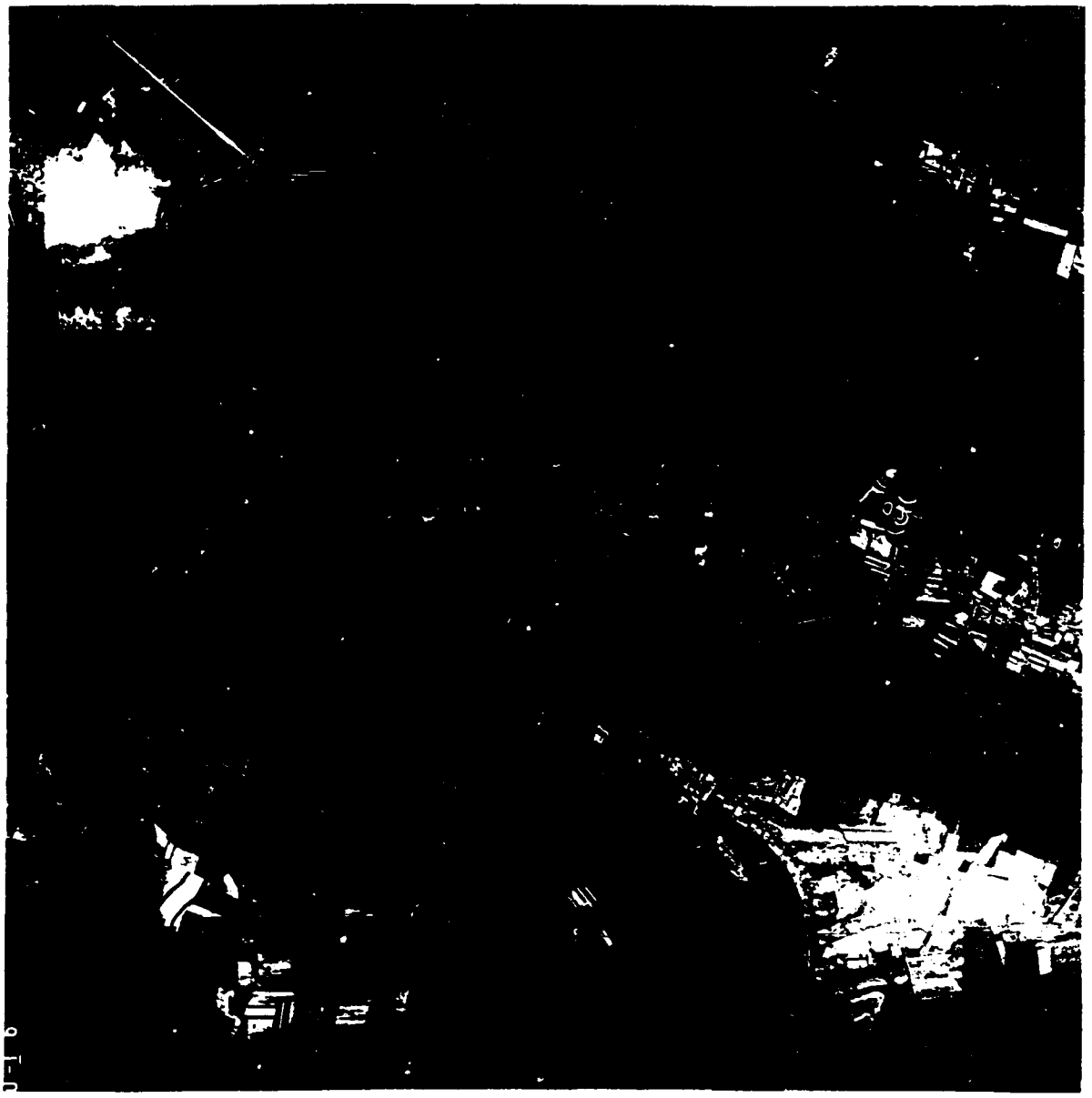

Figure 5-8. Color IR aerial photo (1:8,000) of defoliated Blue Mountain northwest of Harrisburg, Pa.

However, this approach is strictly qualitative, unless one estimates the defoliated areas manually by using a planimeter. More quantitative measures may be made from data used to produce enhanced images by a variety of specialized methods. Most of these operate on data from single dates. Enhancements from different dates are commonly compared visually to pick out obvious differences. One such method, ratioing, will be described in some detail. Another method, differencing, actually compares data from two different dates through a simple mathematical calculation.

Before illustrating these methods, we shall need to define a parameter called the Vegetation Index (VI). This index, normally applied to Landsat data from a single date, depends on mathematical manipulation of brightness values for bands 4 through 7 together or individual MSS bands 6 and 7 (sensitive to high infrared reflectances from vegetative matter) and 5 (sensitive to green foliation, which appears dark in this red band, and to soils, which are brighter in this band). Six specific VI's, each representing a particular combination of variables, may be calculated (see Williams et al., 1980[1] for details and the rationale for each VI). Thus:

$$\text{Ratio VI} = \text{MSS 7/MSS 5},$$

$$\text{Difference VI} = 2.40 \times (\text{MSS 7} - \text{MSS 5}),$$

$$\text{Transformed VI} = \sqrt{\frac{\text{MSS 7} - \text{MSS 5}}{\text{MSS 7} + \text{MSS 5}} + 0.5},$$

$$\text{Green VI} = -0.29\,(\text{MSS 4}) - 0.56\,(\text{MSS 5}) + 0.60\,(\text{MSS 6}) + 0.49\,(\text{MSS 7}),$$

$$\text{Perpendicular VI} = \sqrt{(\text{Soil 5} - \text{MSS 5})^2 + (\text{Soil 7} - \text{MSS 7})^2}$$

where Soil 5 = 0.85 (MSS 5) + 0.35 (MSS 7),
Soil 7 = 0.35 (MSS 5) + 0.15 (MSS 7).

$$\text{Linear VI} = -2.58\,(\text{MSS 4}) - 7.28\,(\text{MSS 5}) + 0.88\,(\text{MSS 6}) + 3.59\,(\text{MSS 7}).$$

[1] Williams, D.L., M.L. Stauffer, and K.C. Lewis, *A Forester's Look at the Application of Image Manipulation Techniques to Multitemporal Landsat Data*, 1979 Machine Processing of Remotely Sensed Data, IEEE, p. 368-76, 1979.

Ratio Techniques. In ratioing, the DN value of each pixel in one band is divided by the DN value of the same pixel in another band, pixel by pixel for the selected array (see p. 438 in Appendix B for details). To produce an image of the resulting quotients, the range of calculated ratios is stretched (expanded) through the full digital range available (for Landsat, $2^8 - 1$, or 0 to 255) with high values assigned light tones and low values dark tones in a photo product. An example is given in Figure 5-11. Thus, for an actual range of ratios between 0.19 and 3.20 fitted to 0-255, 0.36 would be given a DN value of 25, expressed in an image as a dark gray tone; a ratio of 2.15 is given a DN value of 148, which is shown as a medium gray-white tone. This scaling is performed conveniently by multiplying the lowest ratio value by zero and all higher values in the range by 68.7 (see the numbers below the image base). The distribution of DN's derived from pixel-by-pixel ratios of MSS bands 7/5 (Ratio VI) for the June 27, 1977 subscene in Figure 5-10 is shown graphically at the bottom of Figure 5-11. The corresponding black and white 7/5 image constructed from the expanded DN values appears at the top. This image as reproduced does not show a readily discernible pattern of gray levels because the human eye can typically discern only about fifteen to twenty distinct levels. If a broad range of more distinguishable colors is assigned (the human eye can discern hundreds of shades) to these few gray levels, the details of variation will be emphasized (Figure 5-12A). Note the color bar scale, with corresponding DN values, at the top of the figure. This procedure is equivalent to the density slicing techniques described in Appendix B (p. 433).

Figures 5-12B and 5-12C show rather similar color patterns for vegetation indices calculated first as a Difference VI and then as a Transformed VI. The resulting pixel-by-pixel values may be assigned gray levels or particular colors in the same manner as the ratio image.[2] These color images serve as an aid to the interpreter, who can now examine a color-coded rendition of the numerical data representing the spatial distribution of the different VI's.

[2] Different combinations of ratios, e.g., 4/6, 5/4, may be generated, as reviewed on p. 438, Appendix B. Each ratio image may then be considered as one input in producing a color composite (sometimes termed color band ratio composite), much like the formation of a standard false color composite (p. 94). An example from a different region of the United States is shown in Figure B-13.

A Landsat Illustration of the Temporal Dynamics of a Hardwood Forest Being Defoliated by Gypsy Moth Caterpillars

1977 Spring and Summer Landsat Imagery

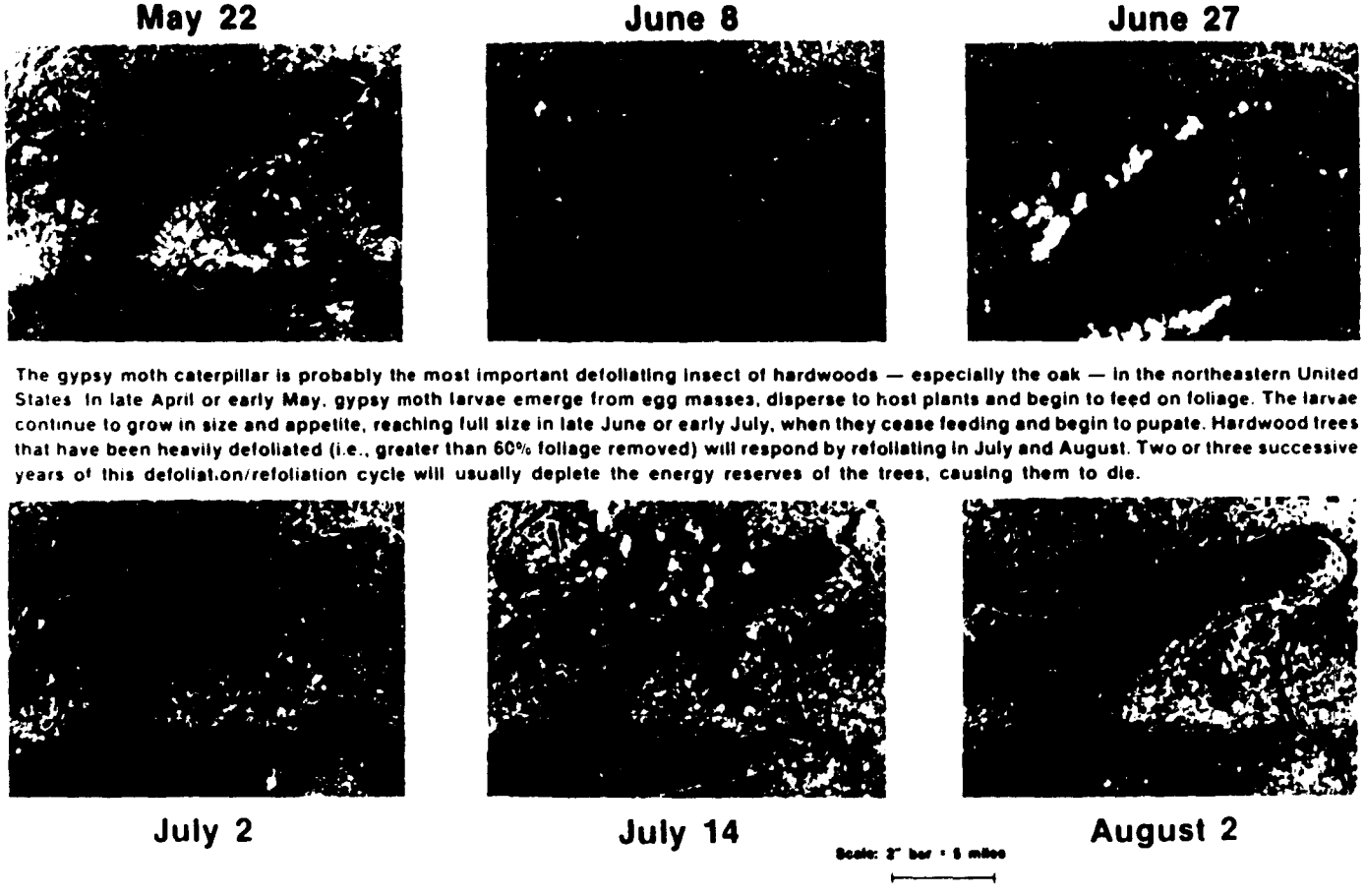

The gypsy moth caterpillar is probably the most important defoliating insect of hardwoods — especially the oak — in the northeastern United States. In late April or early May, gypsy moth larvae emerge from egg masses, disperse to host plants and begin to feed on foliage. The larvae continue to grow in size and appetite, reaching full size in late June or early July, when they cease feeding and begin to pupate. Hardwood trees that have been heavily defoliated (i.e., greater than 60% foliage removed) will respond by refoliating in July and August. Two or three successive years of this defoliation/refoliation cycle will usually deplete the energy reserves of the trees, causing them to die.

Figure 5-9. Seasonal changes in gypsy moth defoliation around Williamsport, Pa. as seen from Landsat.

LANDSAT SUB-IMAGES OF THE HARRISBURG, PA. AREA SHOWING AN INCREASE IN GYPSY MOTH DEFOLIATION BETWEEN 1976 AND 1977

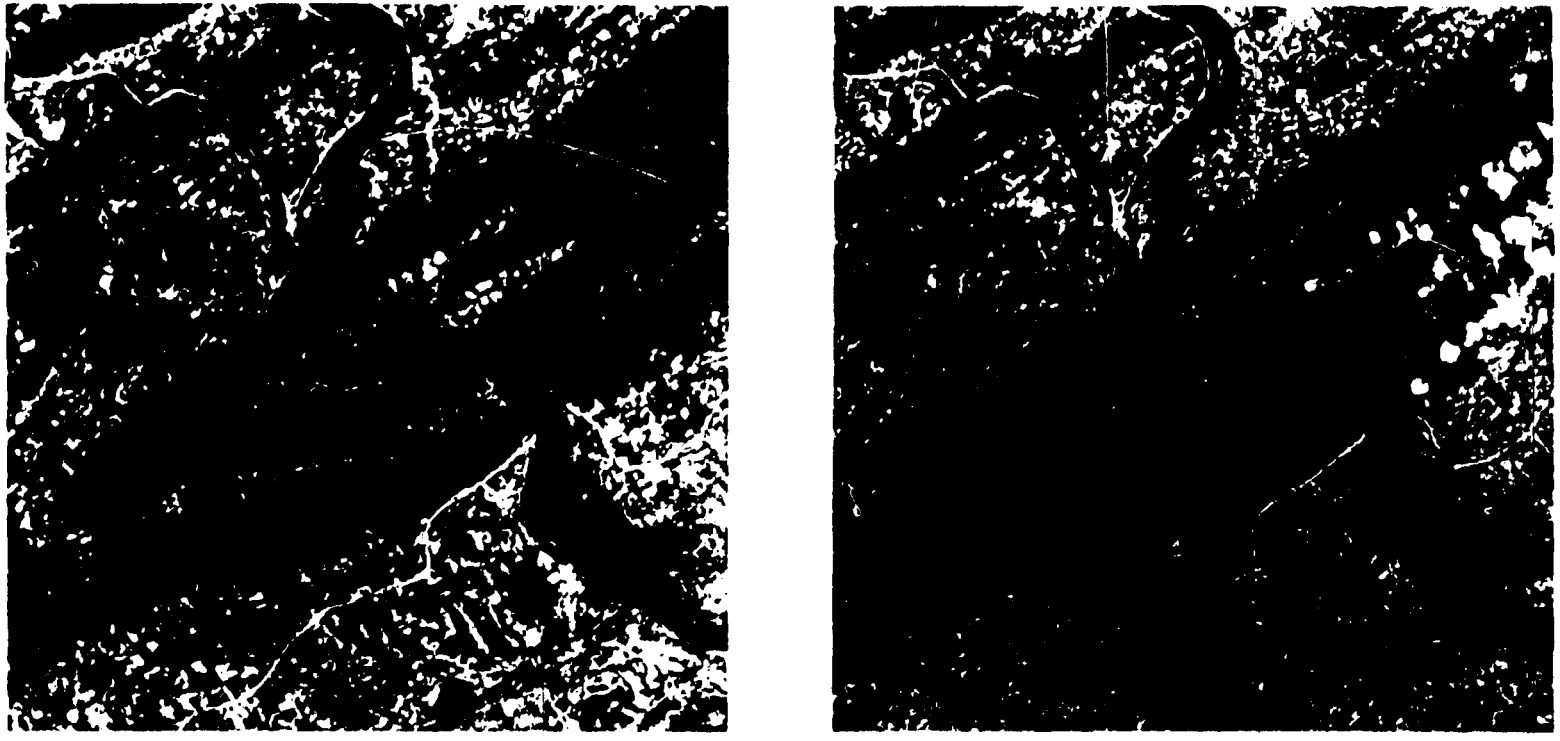

JULY 19, 1976

JUNE 27, 1977

10km/6.25 Mi.

NOTE: THESE IMAGES HAVE BEEN CONTRAST ENHANCED, GEOMETRICALLY CORRECTED AND REGISTERED TO ONE ANOTHER

Figure 5-10. Differences in extent of defoliation on Blue Mountain in 1976 and 1977.

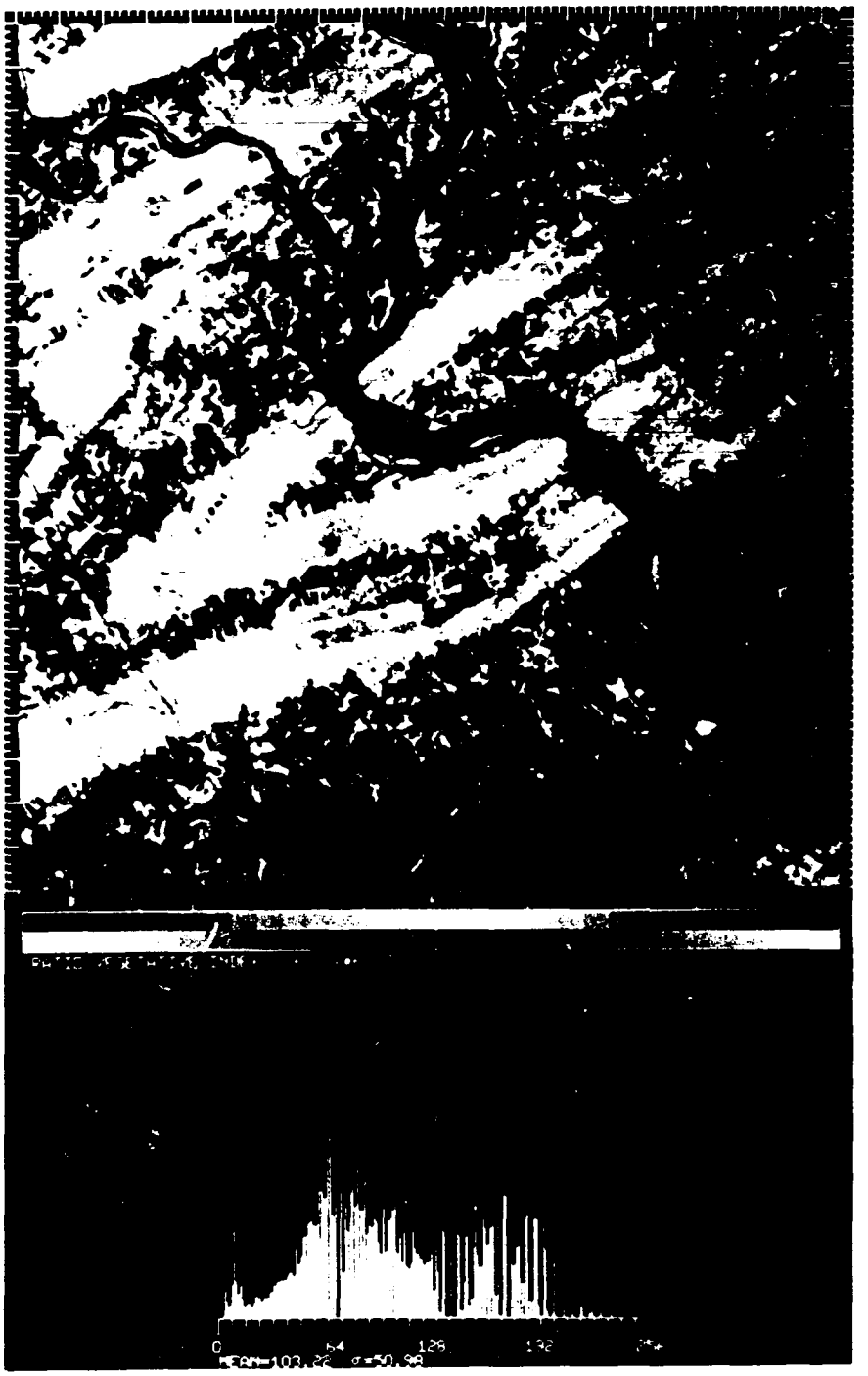

Figure 5-11. Ratio image (bands 7/5) of Blue Mountain area, June 27, 1977.

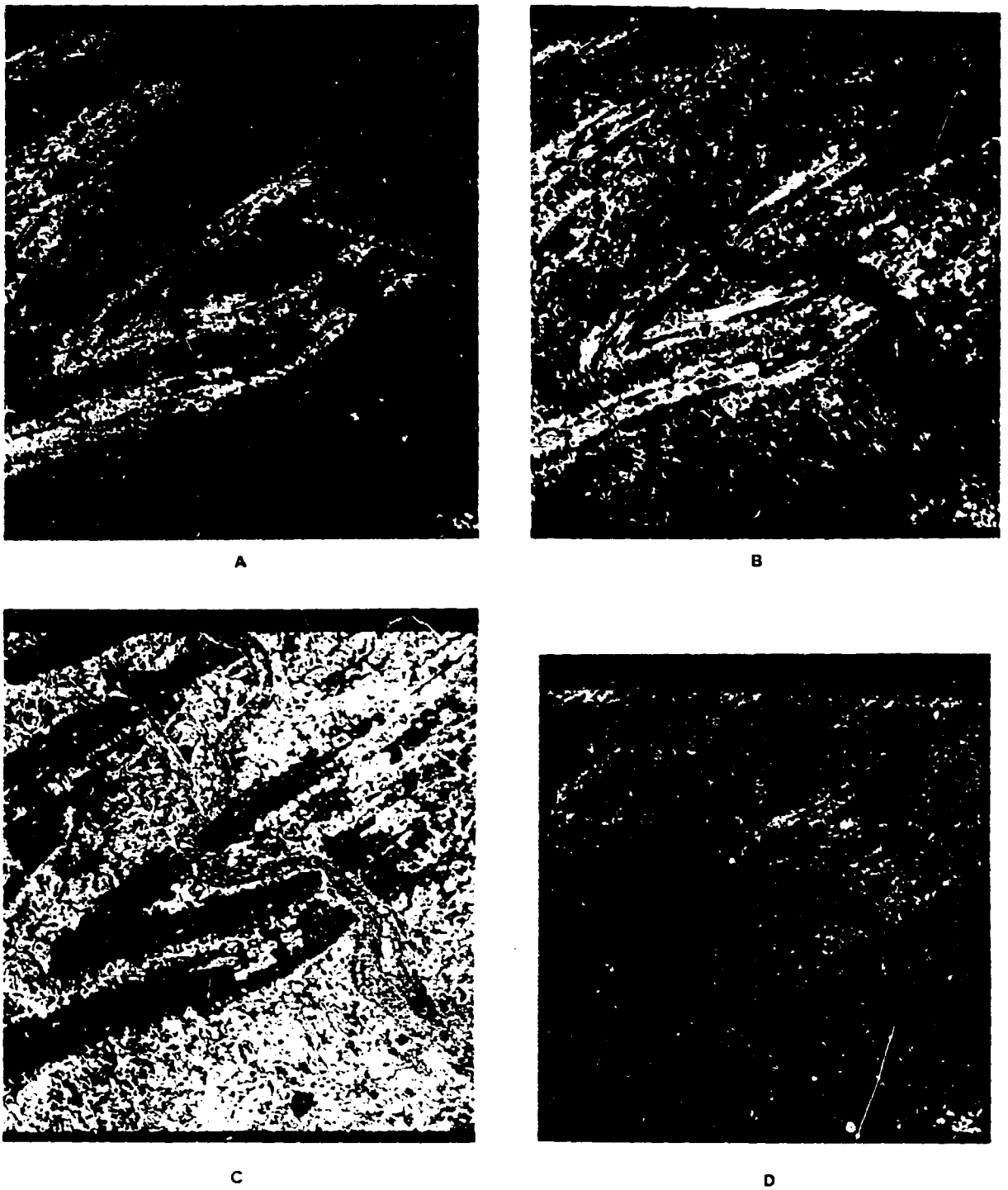

Figure 5-12A-D. Color-sliced renditions of four types of vegetation index images (see text) showing the June 27, 1977 Landsat subscene around Blue Mountain, Pa.

#5-20: Compare these three VI images with each other and with the 1977 side of Figure 5-10. Which ones best outline the defoliated zones?

#5-21: Is there a possibility of confusion between defoliated patterns and other ground features? Comment or explain.

#5-22: There are dark brown (Ratio VI and Difference VI) or gray (Transformed VI) patterns along the ridges. What is the cause of this?

#5-23: Why are the colors representing river water and central Harrisburg so similar (purplish) in the ratio VI image?

#5-24: Why do the highways (whitish lines in Figure 5-10) disappear in these VI renditions?

To show the flexibility and sensitivity of this type of enhancement in discriminating between variations in the same broad class, examine the special ratio product appearing in Figure 5-12D. In this version there is an attempt to eliminate all nonforest features and concentrate on the forests themselves. To accomplish this, the following steps were followed:

1. A general classification (see p. 182) of features in this scene was carried out by using training sites, from which two broad classes—forest and nonforest—were established.
2. In calculating ratios, all nonforest pixels were multiplied by 0 (thus eliminating them) and all forest pixels by 1 (keeping them).
3. From both classified data and ground truth it was determined that healthy vegetation had the larger ratio values and defoliated or stressed vegetation had lower values.
4. To make the image, all nonforest ratioed pixels were assigned a medium gray color. This blanking out of variable data not needed in the particular rendition is one form of a "masking" procedure. All forest ratios were assigned colors within the range 0 to 100 (see the color scale) in increments of 10, with high values (healthy) in the greens, medium values in purples, and low values (defoliated) in reds.

#5-25: Examine Figure 5-12D. Outline (in your mind or on tracing paper) the most extensively defoliated areas. Explain the light and dark shades of green.

#5-26: What can account for the purple and red patterns among the gray tones in the valley terrain?

A similar masking procedure coupled with color coding (density slicing) of the healthy to defoliated forest patterns may be carried out for the other specific vegetation index types. The resultant renditions are shown in Figure 5-13A. Each one shows certain subtle differences as well. The relative efficiency for each VI type in discriminating degrees of defoliation or healthy vegetation is shown graphically in Figure 5-13B.

#5-27: Remembering that defoliation subclasses and aspect (spatial orientation of slopes with respect to direction of illumination) subclasses were set up from field and map observations, comment on the ability to separate subclasses with this approach, namely calculation and display of vegetation indices. Look especially for ambiguity, that is to say, difficulty in effective separation of subclasses, and suggest a way to minimize this problem.

Ratio images of the same scene imaged on two different dates can, on quick glance, indicate significant changes of various classes or features. Changing factors such as shifting Sun angles or atmospheric conditions can lead to notable variations in gray levels or colors between images from two dates, such that one might think that real differences might exist for the same features at specific localities. However, the ratios of pixels representing those classes or features should remain similar if indeed no real changes have taken place.

The Differencing Technique. Enhancement by differencing is especially suited to analysis of change detection within multitemporal data sets. Thus, the data for the two dates, July 1976 and June 1977, displayed in Figure 5-10, may be compared by the differencing method to highlight significant changes in reflectance. The procedure is as follows: (1) The approximately equivalent ground areas from the two dates are geometrically corrected, scaled, and registered pixel by pixel; (2)

The DN values for each band in one data (and date) set are subtracted pixel by pixel from their registered counterparts in the other set; (3) Small differences (similar DN values) from the two dates are assigned medium gray tones in a resulting image; larger differences are expressed in progressively lighter or darker tones depending on which date is subtracted from the other as reference; and (4) Color composite images can be made from difference images for any three of the four bands. The individual band difference images for the two dates are shown on the right-hand side of Figure 5-14. In this case, the subtraction was carried out as:

$$DN_{1977} - DN_{1976} + 128 = \text{Difference Value.}$$

The largest negative values are displayed in the darkest tones and the largest positive values in the lightest tones. The color composite on the left side of Figure 5-14 is constructed from difference band 5 = blue; difference band 6 = green; and difference band 7 = red.

#5-28: Explain how the yellow color represents small differences between the dates. (Hint: recall which two primary additive colors produce yellow when superimposed.)

#5-29: Why do large differences representing defoliation along the ridges show up as blue?

#5-30: Some, but not all, of the fields are also defined by this blue color. Why?

The differencing technique just described can be applied to ratios as well as single band DN's.

Principal Components and Canonical Analysis

For many applications, Principal Component Analysis (PCA) and Canonical Analysis (CA) have proved to be among the most powerful techniques in image processing of remote sensing data. PCA and CA are particularly effective in pinpointing subtle variations in composition of soil and rock materials, for instance, differences in rock type and in chemical alteration associated with ore bodies. Less definitive results have been developed for vegetation. However, we can judge this for ourselves by applying PCA to the defoliated area around Harrisburg.

Before proceeding, it would be wise for you to master or review the brief summary of the principles underlying PCA and CA in Appendix B (p. 440). Both techniques are based on mathematical concepts and operations, such as covariance matrices and eigenvectors. The following synopsis[3] of PCA may provide you with a sufficient overview to proceed directly through this section without referring to the appendix.

The principal components method makes use of the fact that for a single Landsat scene there is a great deal of redundancy (for example, between MSS bands 6 and 7); in addition, there may be redundancy between the same bands on different dates. Because redundant data do not carry any added information for classification, one objective of PCA is to eliminate this redundancy. The method defines a rotation of the p-dimensional coordinate system such that the data are arranged along axes (consisting of linear combinations of the original data axes) of decreasing variance. The linear combination of the radiances from the various bands is selected such that the variance of the transformed data is a maximum along the first principal axis. The next axis is selected in the same way from the remaining dimensions. This procedure is continued until all axes, i.e., the entire p-dimensional space of the data, have been rotated to a set of axes of decreasing variance. The last several dimensions can then generally be rejected with no loss of significant information.

Both the PCA and CA methods combine the data from the Landsat measurement bands and produce new bands called components. PCA produces components that each provide "information independent of the others." CA produces components that "optimally separate" a given set of land cover categories. The maximum number of rotated components thus produced will be equal to the number of measurement bands (sensor channels), or one less than the number of categories, whichever is less. Each component may contain input from all the channels.

[3] From Cornillon, P., *Land Cover Classification in Southern Rhode Island using Multidate Landsat MSS Data*, in Proceedings of the First Eastern Regional Remote Sensing Applications Conference (N. M. Short, edit.), 1981.

VEGETATIVE INDEXES WITH FOREST/NONFOREST MASK

(OUTPUT SCALED 0-100 BASED ON TRAINING SITE MINIMUM, MAXIMUM VALUES)

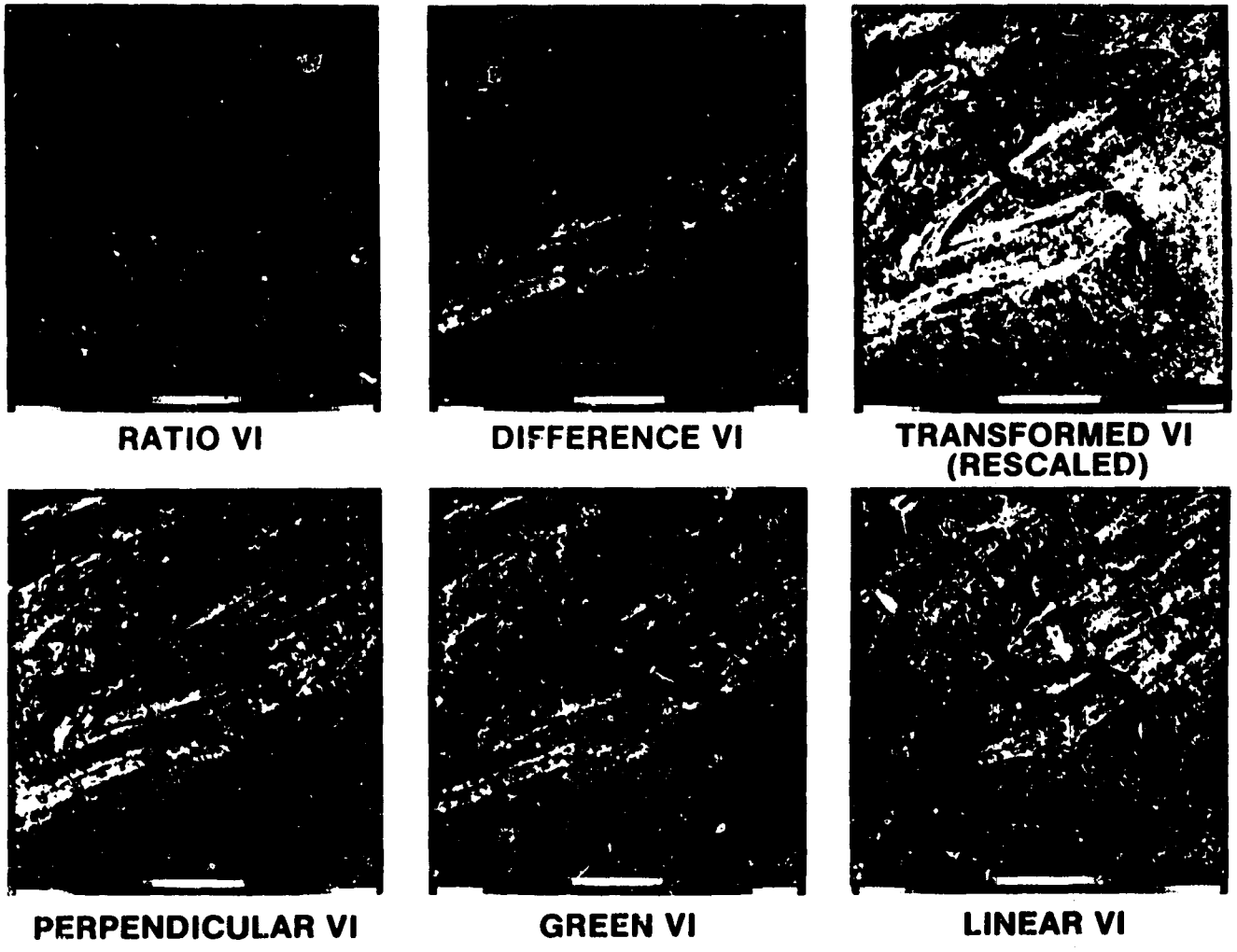

Figure 5-13A. Various VI types, with nonforested areas masked out.

RESULTS OF APPLYING VEGETATIVE INDEXES TO TRAINING SITE DATA

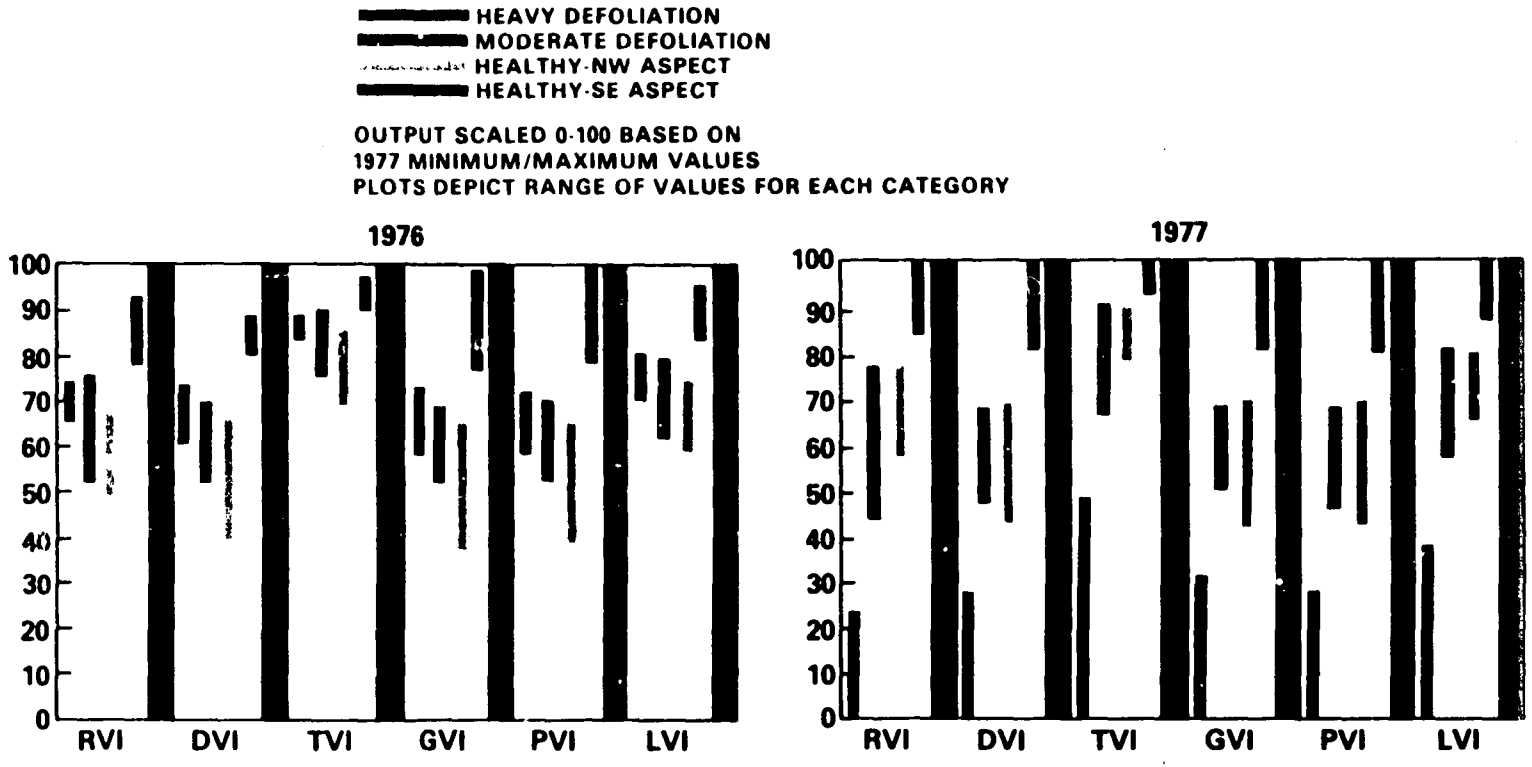

Figure 5-13B. Graphical plots of types of VI, with values scaled to 0 to 100, for forested sections of the Blue Mountain area in 1976 and 1977.

Figure 5-14. Difference images (1977-1976) for Blue Mountain area subscenes.

The results of PCA of the June 27, 1977 subscene are shown in Figure 5-15A-D and Table 5-3. The four black and white images in Figure 5-15 are the visual depiction of the transformed data points representing the first, second, third, and fourth principal components. Figure 5-16 is a color composite made from printing the first, second, and third components through red, green, and blue filters respectively. Although this color rendition is appealing, and can be revealing, the black and white images are generally more informative.

#5-31: Describe your impressions of each of the four individual component images, touching upon the distinct differences between pairs, the kinds of detail revealed, and the relative amounts of information present in each.

Now consider Table 5-3, reconstructed from a printout sheet containing various statistical parameters obtained during the computer run in which the PCA was carried out. The data in step 2 of the table are used to calculate a variance-covariance matrix (step 3); note that the sample variance for each band (channel) is s^2 and is recorded in the main diagonal positions. The covariances occupy the off-diagonal positions. Both i and j represent the same channels in this and the subsequent correlation matrix. Thus, the covariance between channels 3 and 1, or $s_{ij} = s_{31}$, is found by moving to the third number (i = 3) in column 1 (j = 1). Numbers are not recorded above the main diagonal because the matrix is symmetrical and thus the number array is simply a repeat of those in the array below the diagonal in corresponding symmetrical positions.

The correlation matrix r in step 4 is derived from data in step 3 according to the relation:

$$r_{ij} = \frac{s_{ij}}{(s_{ii}^2)^{1/2} \cdot (s_{jj}^2)^{1/2}}$$

where s_{ii}^2 and s_{jj}^2 are channel variances.

As an example, note the correlation between channel 3 (MSS band 6) and channel 1 (MSS 4). For the calculation, $s_{31} = 15.941$, $s_{11}^2 = 38.552$, and $s_{33}^2 = 130.156$. Entering the values into the above equation, and solving, yields $r_{31} = 0.225$. This value indicates a low correlation between channels 3 and 1, that is, little redundancy, and hence both MSS bands 6 and 4 tend to provide useful, essentially uncorrelated, independent measurements. A high value for r, such as 0.945 for channels 4 and 3, suggests strong redundancy, that is, MSS bands 7 and 6 tend to provide similar values for certain classes that together offer little discrimination (separability).

The calculations in step 5 follow the procedures described on p 442 of Appendix B. Note here that the i rows refer to channel related values and the j columns to component data.

Of special significance are the calculation of the total variance-component relation and correlation of channel (band) contribution with components shown at the bottom of this table. Channels 1, 2, 3, and 4 in the table are equivalent to MSS bands 7 through 4 respectively. In step 6 the percentage of total variance explained by each channel is obtained by first summing the channel (i) variances (the variance is the square of the standard deviation) shown in the diagonal set of numbers at the top of the covariance matrix, dividing the eigenvalues by that sum, and multiplying by 100.

#5-32: Calculate the percentages of total variance for the second and third Principal Components (see Table 5-3).

These percentages are interpreted to mean that most of the useful data from the four channels (Landsat MSS bands) are contributing to the first component, somewhat less to the second component, and least to the third and fourth components.

The correlation between principal components and individual channels is calculated from the relation

$$\text{Degree of correlation, } R_{ij} = \frac{a_{ij} \cdot (\lambda_j)^{1/2}}{s_{ii}},$$

where i = channel; j = component; and a_{ij} = Eigenvector, for i^{th} row, j^{th} column; λ_j = Eigenvalue for j^{th} component; s_{ii} = standard deviation for i^{th} channel.

#5-33: Calculate R for channel 2, component 2, and for channel 1, component 4 (see Table 5-3).

Table 5-3
Principal Components Analysis Data Sheet

Subscene from 2887-14527 (June 27, 1977)

(1) Data set consisting of n = 242, 491 pixels; each pixel contains a measurement on p = 4 channels.

(2)

Channel	1	2	3	4
Mean	20.34	19.95	51.93	26.29
St. Dev (s_i)	6.21	8.42	11.41	7.49

(3) Variance (s_{ii}^2) — Covariance (s_{ij}) Matrix (S)

i \ j				
	38.55			
	50.42	70.92		
	15.94	15.47	130.16	
	-2.25	-8.16	-15.47	56.12

(4) Correlation Matrix (r)

i \ j				
	1.000			
	0.964	1.000		
	0.225	0.151	1.000	
	-0.048	-0.129	0.945	1.000

(5) Eigenvectors Computed for Covariance Matrix

Eigenvalues (λ_i)	184.755	108.267	1.863	0.857

Eigenvectors (a_{ij})

i \ j				
	0.130	0.563	0.767	-0.279
	0.134	0.787	-0.458	0.391
	0.837	-0.063	-0.247	-0.473
	0.515	-0.245	0.361	0.738

i = channels (row data)
j = components (column data)

(6) Percentage of Total Variance in the Data (All Channels) Explained by Each Component:

$$\text{Percentage } i = \frac{\text{Eigenvalue } i \times 100}{\sum_1^p \text{Eigenvalues } i} = \frac{\lambda_i \times 100}{\sum_1^p \lambda_i}$$

(for p = 4)

(Note: Σ Eigenvalues for all channels (1, 2, 3, 4) = Σ Covariance values along diagonal of Covariance Matrix [Step 3]). The eigenvalues are radiances. Since rotating the axes does not change the total variance, it remains the same and thus the equality of the sums of the diagonal elements.

Sample Calculation:

i = index of variable

$\Sigma_{i=1}^{p} \lambda_{ii} = 184.76 + 108.27 + 1.86 + 0.86 = 295.75$

$\Sigma_{i=1}^{p} s_{ii}^2 = 38.55 + 70.92 + 130.16 + 56.12 - 295.75$

Percentage variation in the first PC = $\frac{184.76}{295.75} \times 100 = 62.5\%$

Percentage Assigned To Each Channel:	1	2	3	4
	62.5%	—	—	0.3%

(7) Degree of Correlation R of Each Channel i with Principal Component j:

$R_{ij} = \frac{a_{ij} \cdot (\lambda_{jj})^{1/2}}{s_{ii}}$, where a_{ij} = Value in Row i and column j; a_{ij} is any element ij in the A matrix

Sample Calculation for $R_{11} = \frac{0.130 \times (184.76)^{1/2}}{(38.55)^{1/2}} = \frac{1.76}{6.21} = 0.284$

$R_{42} = \frac{-0.245 \times (108.27)^{1/2}}{(56.12)^{1/2}} = \frac{-2.55}{7.49} = -0.342$

(i = Channels 1 and 4; j = Components 1 and 2)

R_{ij} Table

i \ j	1	2	3	4
1	0.284	0.947	0.167	—
2	0.216	—	-0.074	-0.043
3	0.997	-0.058	-0.029	-0.083
4	0.935	-0.342	0.075	0.091

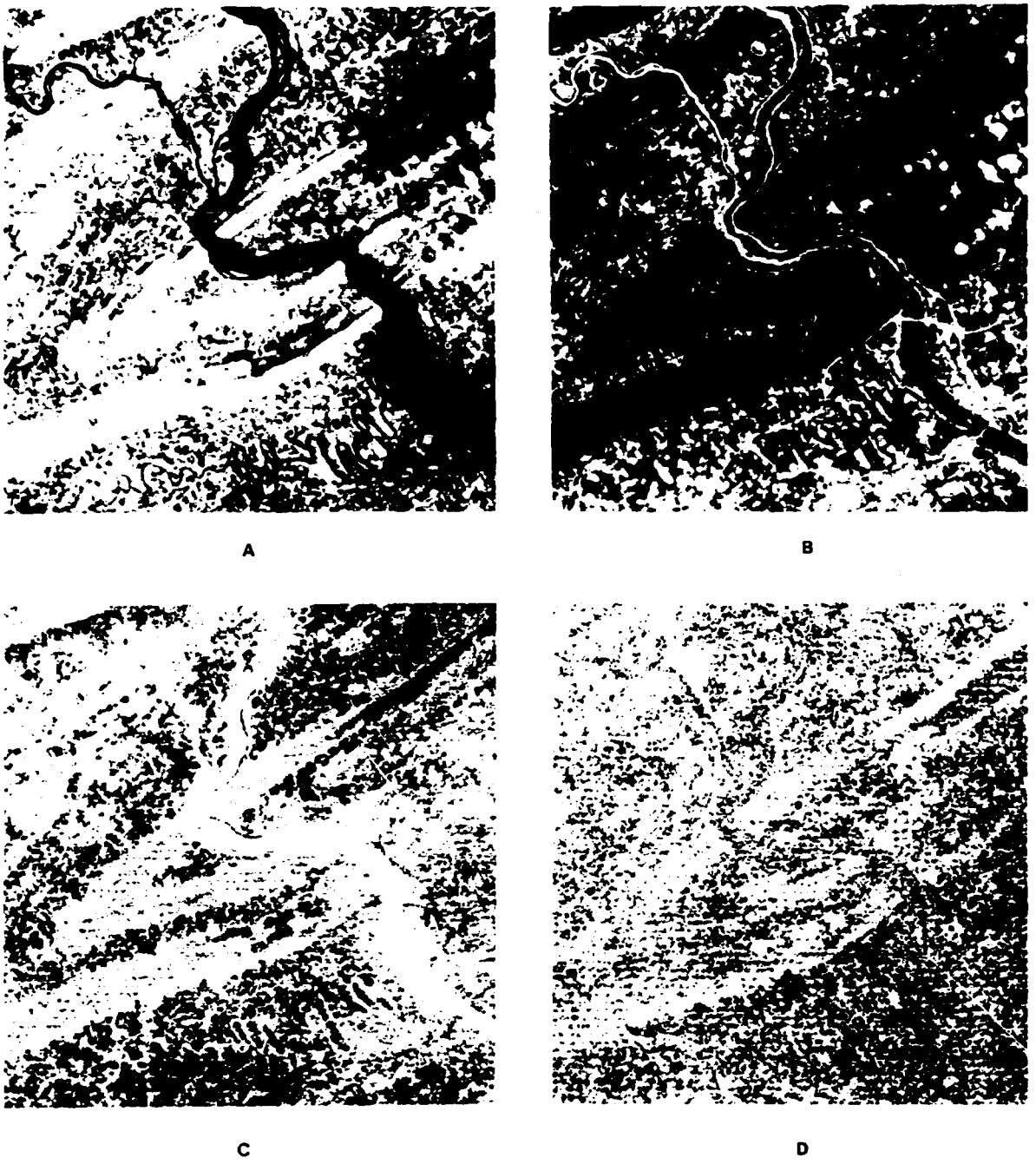

Figure 5-15. First, second, third, and fourth principal components images made from June 27, 1977 Landsat subscene.

Figure 5-13. Color composite made from PCA 1 = red, 2 = green, and 3 = blue, using subscenes shown in Figure 5-15.

The other values of R are recorded in the table. The higher values indicate the specific channels that contribute most to the information contained in each component.

Look again at the four black and white images. The first component image, for this type of heavily vegetated terrain, provides a vegetation-sensitive indicator. The image in this case resembles MSS band 6 and 7 images. It also displays the greatest detail. In some respects it also bears similarities to the black and white version of the vegetation index ratio (Figure 5-11). The second component image is especially sensitive to urban areas, roads, bare soils, and silt variations in water. It renders vegetation in dark tones and thus resembles MSS band 5 images. The third component image contains little definitive information, but gross terrain features are still evident and some sensitivity to water remains. The fourth component image appears degraded as most of the patterns are obscured and seem overprinted with noise.

#5-34: Compare the color versions of the composite PCA image (Figure 5-16) and the density sliced vegetation index ratio image (Figure 5-12D), especially with reference to defoliation and to details in the valley west of Harrisburg.

Merging of MSS and RBV Images

As evident from many examples in this workbook, Landsat MSS data are especially useful in studying large areas. However, for many applications, the coarse (80 m) resolution of the MSS is not sufficient to identify ground features that may be of interest. For example, in parts of the world like China and India where farming is done in very small fields, Landsat cannot resolve individual fields. When field identification is difficult, crop type classification and yield estimation are next to impossible. An obvious solution to this problem is to use aerial photography. Even if it is affordable in developing countries, such photography is often unavailable for many areas of the globe—at least at the frequency of coverage provided by the Landsats.

Recently, work has started on devising programs to merge digital Landsat-3 MSS data with digital Landsat-3 Return Beam Vidicon (RBV) data. You may remember from p. 57 that there are two RBV cameras on Landsat-3, mounted side by side perpendicular to the flight path of the satellite. The cameras are similar to a TV camera because they store radiation from the scene viewed onto a photosensitive plate in the camera itself, which acts like an electronic film. Each camera instantaneously "sees" a square area on the ground covering 98 km × 98 km, about half as long and wide as an MSS scene. Unlike the MSS, the RBV is panchromatic, being sensitive to light from 0.505 to 0.750 μm (blue to near IR). Once every 12.5 s the RBV cameras snap a picture of the Earth beneath them, covering an area equivalent to the top half of the corresponding MSS scene. For every two pairs of snapshots, the same ground area in a full MSS scene is imaged by four RBV scenes, one located in each quadrant of the MSS scene.

Let us now look at how the RBV digital data are created. Recall from p. 82 that MSS pixels are generated as the electronic signal across a scan line is sampled at discrete intervals, integrated, and then converted to a digital value. The sampling interval along a scan line results in a pixel 56 m wide on the ground, while the movement of the satellite in space coupled with the sweep rate of the scan mirror produces a pixel 79 m long. For a full scene, the scanning process takes 25 s and hence yields a geometrically distorted picture as the Earth rotates beneath.

The RBV system works somewhat differently. Because each image is frozen instantaneously on the vidicon plate during shuttering, it captures a planar or undistorted view of the Earth's surface (except for distortion caused by the Earth's spherical shape). As in an ordinary TV camera, the image is converted into a video signal. This signal is beamed to a receiving station if in line of sight or is recorded on board for later transmission. At this stage, the video signal represents a ground resolution of 24 m and can be processed directly to produce imagery. In order to merge the RBV and MSS data, the video tape must be converted to digital format during ground processing. After removing any geometrical errors, the video data are assigned appropriate digital numbers (DN's). These DN pixels are each resampled to create a pixel equivalent to 19 m × 19 m on the ground. In this new format, the

data are ready to be enhanced to make high quality black and white images or to be merged with MSS data to make high resolution (from the RBV) color (from the MSS) images.

The characteristics of merged imagery, and the steps involved in matching the RBV with the MSS subscenes, will be illustrated in Figure 5-17A-B. Figure 5-17A shows a computer-enhanced black and white RBV image of the Washington, D.C. metropolitan area, enlarged from a single RBV frame acquired on June 30, 1978. The geographic control points—mainly road intersections—are also superimposed on this image. The merge of RBV and MSS images from these data appears in Figure 5-17B. A further enlargement of the downtown Washington subscene is inset in the lower right.

The procedure for merging digital MSS and RBV data is straightforward but requires a good deal of human analyst time and a powerful image processing computer system. The first step is to locate ground control points (GCP's) on both the MSS and RBV images. These points will be used later to fit the MSS to the RBV image. More than forty GCP's were identified on each image. The location of each point is recorded by line and sample number and stored in a computer file.

The next step is to apply a least squares fit to produce a transformation equation, a mathematical expression that describes the rubber sheet stretch required to match the MSS and RBV GCP's. The entire MSS data set is passed through the transformation equation one pixel at a time. The 56 m X 79 m pixels are preserved and still retain a blocky appearance.

In order to make the MSS data more closely resemble the RBV data, the computer must create the same number of pixels in the MSS set as in the RBV. To make the MSS pixels represent the same area as the 19 m X 19 m RBV pixels, each MSS pixel is subdivided into six parts. The computer then examines its location and also the eight nearest pixels to it. If the new pixels are in a homogeneous area, they keep the value of the pixel from which they are created. However, if the initial pixel's neighbors are different—as when they occur at an edge of some sort, for example, at the shoreline of a lake—the values assigned to the new pixels are adjusted. This resampling smooths out the blocky nature of the MSS data giving rise to a more photolike image in quality. The two digital images now have the same number of pixels, cover the same area, and both represent a flat plane projection of the Earth's surface. The data sets are now ready to be merged.

At 19 m X 19 m resolution, the RBV data contain a great deal of spatial information. This high resolution information is particularly important for delineating boundaries and showing texture within relatively homogeneous areas. Any merging technique should preserve this unique high resolution quality. The resampled MSS data, now represented by 19 m^2 pixels, produce an image that appears to have much higher resolution than in the original form, but this is illusory since only the raw data were used in the smoothing. However, these multispectral data contain considerable "color" information, albeit at a coarser resolution, which should be retained for purposes of distinguishing different land cover types.

To merge the RBV and MSS data while preserving the high resolution boundary information and textures of the RBV and the "color" from the MSS images, the DN values for each MSS band used in compositing a color image must be normalized as follows:

$$\frac{\text{MSS 4}}{\text{MSS 4} + \text{MSS 5} + \text{MSS 6} + \text{MSS 7}} = \text{NORM 4},$$

$$\frac{\text{MSS 5}}{\text{MSS 4} + \text{MSS 5} + \text{MSS 6} + \text{MSS 7}} = \text{NORM 5},$$

$$\frac{\text{MSS 7}}{\text{MSS 4} + \text{MSS 5} + \text{MSS 6} + \text{MSS 7}} = \text{NORM 7}.$$

To factor in the scene brightness of the image from the RBV, each of the normalized MSS bands must be multiplied by the RBV value, one pixel at a time. The resulting band images are then combined into a false color composite by using color filters (for a photo-image) or the TV color guns (in an interactive computer display) in this way:

NORM 4 X RBV = Blue,
NORM 5 X RBV = Green,
NORM 7 X RBV = Red.

The final merged image is seen in Figure 5-17B. Compare the merged image with the high resolution raw RBV image. Note the differences made by color in the ability to discriminate land cover types.

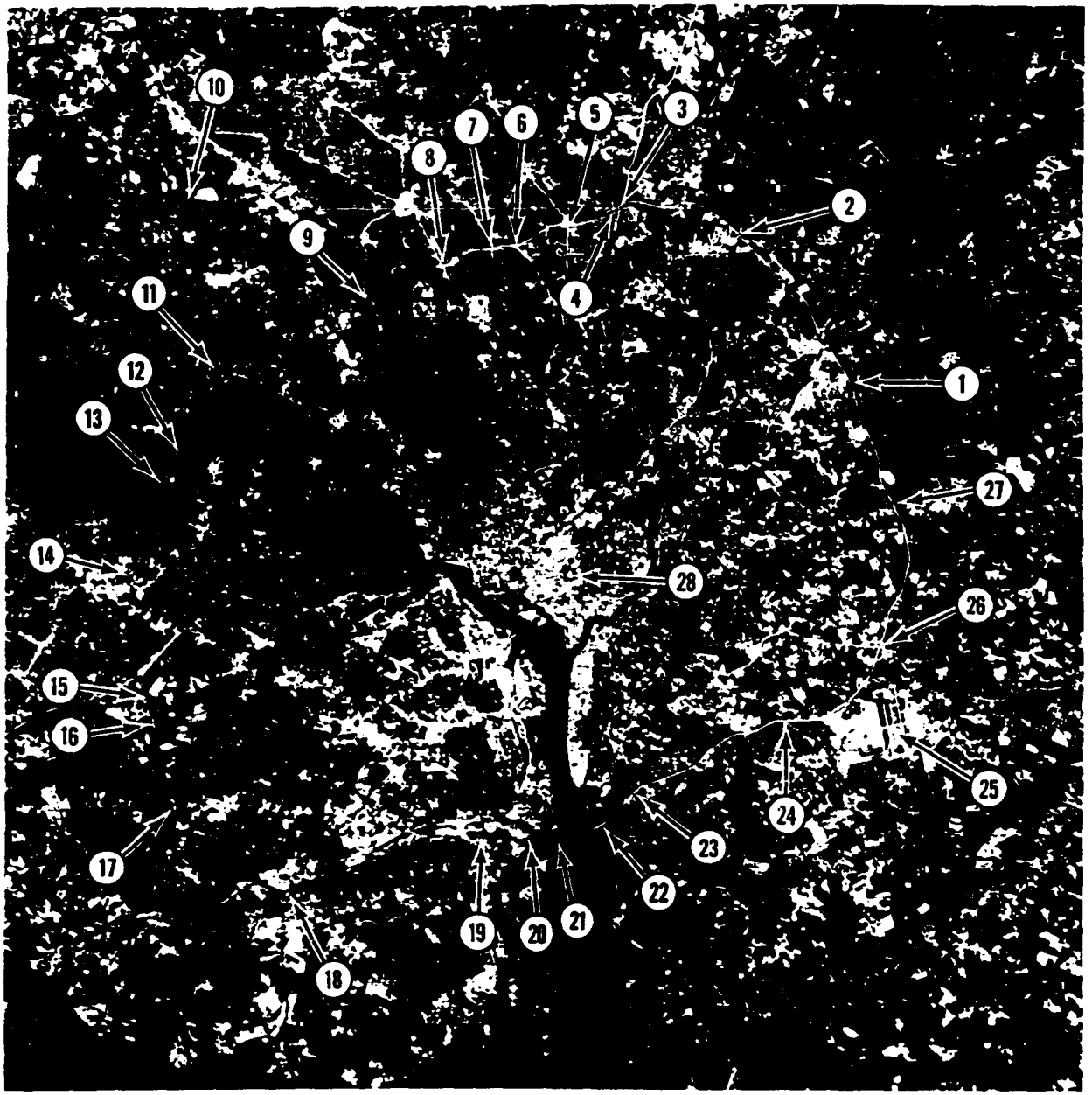

Figure 5-17A. Enlargement, produced on IDIMS, of part of RBV image 30117-15075, obtained on June 30, 1978, showing the Washington, D.C. metropolitan area. Various ground control points (GCP's) used to merge RBV and MSS data sets are located along the Capitol Beltway (I-495).

Figure 5-17B. The final merged image made from the RBV and MSS data. View of downtown Washington, D.C. enlarged by computer from the RBV/MSS merged data is shown as an inset.

We now know that merging of MSS with RBV data can provide useful images for visual interpretation because of the higher resolution beyond the standard MSS product. The next task for future research is to determine how merged data might be used in computer-aided classification to determine if the improved resolution makes significant gains in classification accuracy of small land cover areas and of similar crops.

CLASSIFICATION

The most frequent use of computers to process Landsat data lies in the production of classification maps showing the identities of major cover and use types on the Earth's land surface. If you have not yet read the review of principles of classification in Appendix B on pages 445 to 451, do so now. Two key points alluded to in Appendix B are stated here to emphasize their importance: (1) The classifications are carried out by setting up separable *spectral classes*. A spectral class consists of a set of multispectral properties (for example, values of DN's for different bands representing radiant intensities integrated through selected wavelength intervals) whose means and variances fall within a characteristic range that allows that class to be discriminated from most others. To be meaningful, a spectral class should correlate with a particular information class, such as some land cover type: (2) Identification of the information or land cover classes may be *a priori* (supervised) or *a posteriori* (unsupervised). In a supervised classification, training sites corresponding to the different classes sought are located within the scene of interest. The computer is "taught" to recognize both these sites and unknowns most like them by comparing spectral classes of unknowns with the spectral classes determined as standards for the training sites. In an unsupervised classification, the output is simply those spectral classes that are separable one from another. The analyst must then independently identify these classes with corresponding information classes through field work, matching with map categories, etc.

Types and Levels of Classification

The classifications described in this workbook follow the two-level system developed by the U.S. Geological Survey for applications of remote sensing data to land cover mapping and other geographic uses.[4] The categories that constitute this system are listed in Table 5-4. A two-level land use map of Harrisburg, made by the U.S. Geological Survey using conventional ground surveys combined with aerial photointerpretation, is copied in Figure 5-18 from part of USGS Open File Map 77-109-1 (Land Use Series). The numbers within the map units correspond to cover type numbers given in Table 5-4. The section of this map shown in Figure 5-18 was subsequently colored at Goddard.

Remote Terminal Systems: ORSER

We shall start our study of classification methods by following the production of a set of intermediate and final classification printouts obtained with procedures from the ORSER software package developed at Pennsylvania State University (see pp. 449 through 451 of Appendix B for a brief review of the major steps in producing classifications with the ORSER system). The area selected for study is centered along the Susquehanna River northwest of downtown Harrisburg, roughly equivalent to the area extracted from the 1974 7½-minute topographic sheet published by the U.S. Geological Survey (Figure 5-19). The subscene we shall classify is 95 pixels (N-S) by 140 pixels (E-W) in size.

=5-35. Keeping in mind that the pixels have not been squared by resampling and therefore retain their original dimensions of 79 m across (N-S) and 56 m along (E-W) a scan line, calculate the dimensions of the classified Harrisburg area in (a) square kilometers, (b) square miles.

The initial scale of the printout maps is approximately 1:32,000, but the versions in Figures 5-20A-E are reproduced at a reduced size. The subscene will be classifed first by an unsupervised

[4] Anderson, J.R., E.E. Hardy, J.T. Roach, and R.E. Witmer, *A Land Use and Land Cover Classification System for Use with Remote Sensor Data*, U.S. Geological Survey Prof. Paper 964, 1976.

Table 5-4
Land Use and Land Cover Classification System For Use with Remote Sensor Data

Level I	Level II
1 Urban or built-up land	11 Residential 12 Commercial and services 13 Industrial 14 Transportation, communications, and utilities 15 Industrial and commercial complexes 16 Mixed urban or built-up land 17 Other urban or built-up land
2 Agricultural land	21 Cropland and pasture 22 Orchards, groves, vineyards, nurseries, and ornamental horticultural areas 23 Confined feeding operations 24 Other agricultural land
3 Rangeland	31 Herbaceous rangeland 32 Shrub and brush rangeland 33 Mixed rangeland
4 Forest land	41 Deciduous forest land 42 Evergreen forest land 43 Mixed forest land
5 Water	51 Streams and canals 52 Lakes 53 Reservoirs 54 Bays and estuaries
6 Wetland	61 Forest wetland 62 Nonforested wetland
7 Barren land	71 Dry salt flats 72 Beaches 73 Sandy areas other than beaches 74 Bare exposed rock 75 Strip mines, quarries, and gravel pits 76 Transitional areas 77 Mixed barren land
8 Tundra	81 Shrub and brush tundra 82 Herbaceous tundra 83 Bare ground tundra 84 Wet tundra 85 Mixed tundra
9 Perennial snow or ice	91 Perennial snowfields 92 Glaciers

HARRISBURG, PENNSYLVANIA
LAND USE AND LAND COVER, 1972

URBAN OR BUILT-UP LAND
- 11 RESIDENTIAL
- 12 COMMERCIAL AND SERVICES
- 13 INDUSTRIAL
- 14 TRANSPORTATION, COMMUNICATION AND UTILITIES
- 15 INDUSTRIAL AND COMMERCIAL COMPLEXES
- 16 MIXED URBAN OR BUILT UP LAND
- 17 OTHER URBAN OR BUILT UP LAND

AGRICULTURAL LAND
- 21 CROPLAND AND PASTURE
- 22 ORCHARDS, GROVES, VINEYARDS, NURSERIES, AND ORNAMENTAL

FOREST LAND
- 41 DECIDUOUS FOREST LAND
- 42 EVERGREEN FOREST LAND
- 43 MIXED FOREST LAND

WATER
- 51 STREAMS AND CANALS
- 52 LAKES
- 53 RESERVOIRS

WETLAND
- 62 NONFORESTED WETLAND

BARREN LAND
- 75 STRIP MINES, QUARRIES, AND GRAVEL PITS
- 76 TRANSITIONAL AREAS

Figure 5-18. Colored version of two level land use map of Harrisburg, Pa. region, prepared by the U.S. Geological Survey (see Table 5-4).

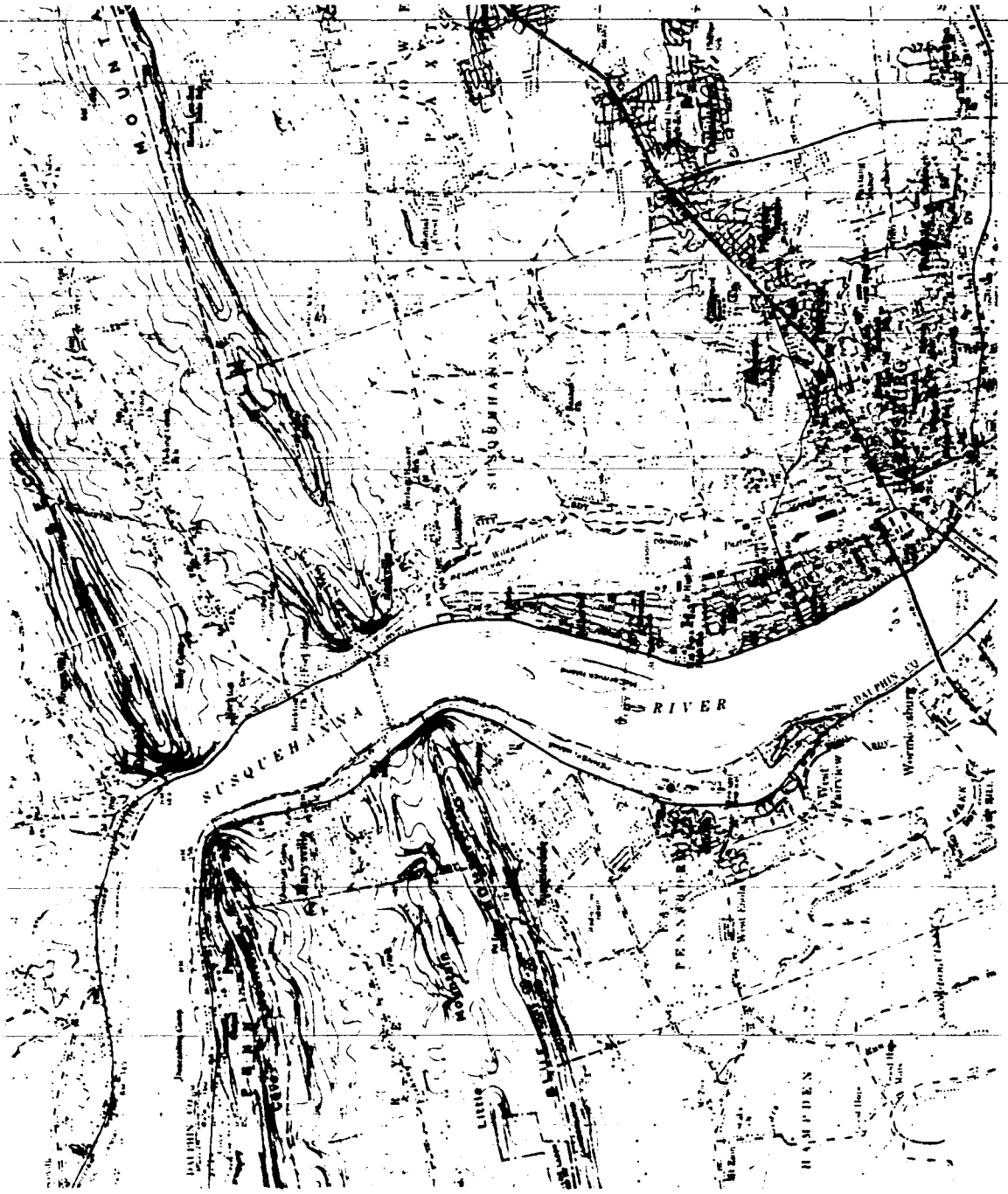

Figure 5-19. Part of the 7½' topographic sheet (USGS, 1974) covering the Harrisburg, Pa. area.

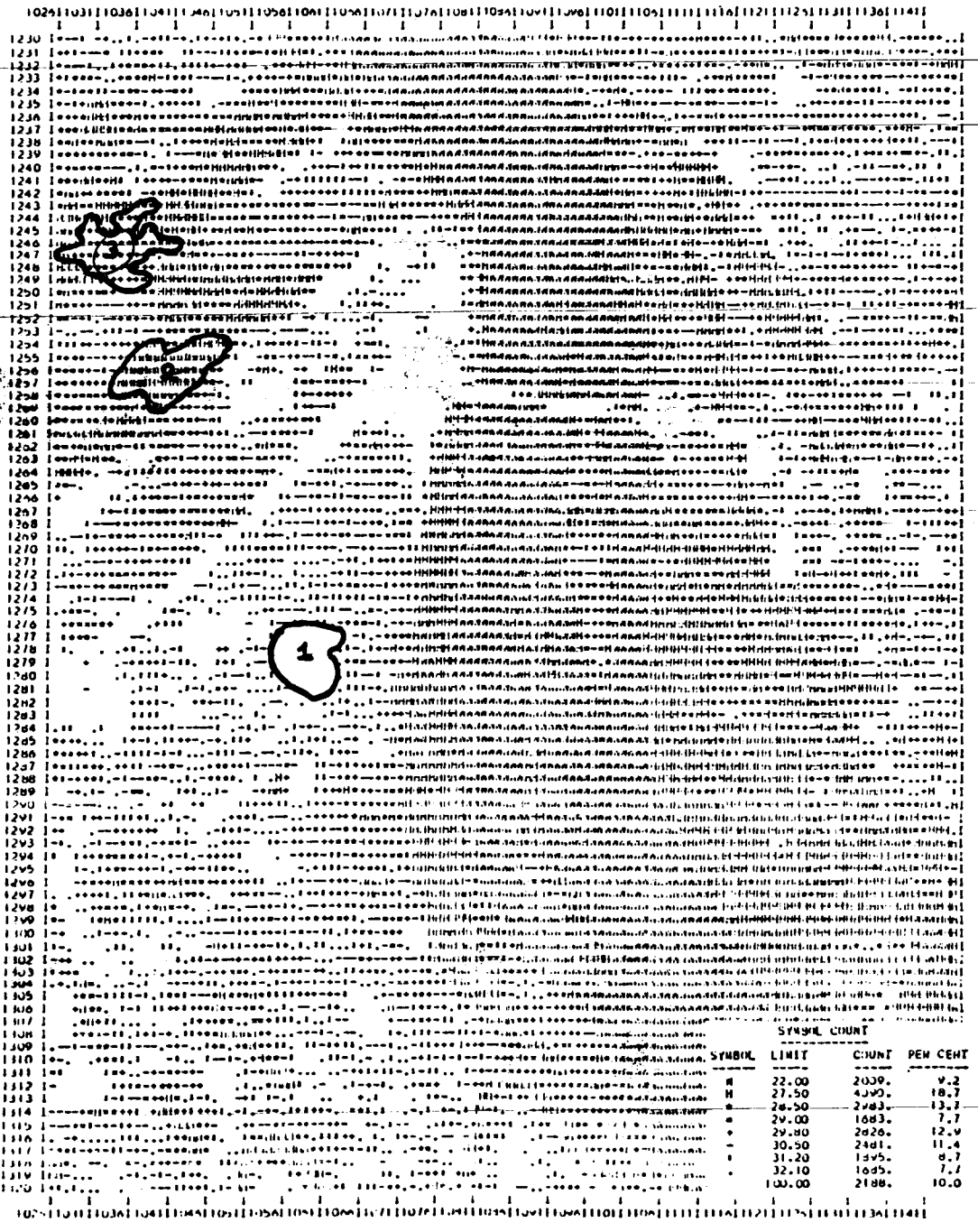

Figure 5-20A. ORSER produced NMAP of part of 1973 Harrisburg scene.

Figure 5-20B. NMAP for 1977 Harrisburg scene.

Figure 5-20C. Unsupervised ORSER classification map for 1977 Harrisburg scene.

Figure 5-20D. ORSER UMAP, 1977 scene.

Figure 5-20E. Supervised ORSER classification map made for 1977 Harrisburg scene.

procedure and then by a supervised approach. For both, the first step is to generate an NMAP. Figures 5-20A and B contain a pair of NMAP printouts generated from the July 8, 1973 (1350-15190), and July 14, 1977 (2904-14452) scenes. NMAP is essentially an alphanumeric-coded plot of brightness levels that serves to help the user locate the main features in a small subscene of a Landsat image. In the plots shown, the brightness level data are calculated as the norm for all four channels.[5] NMAP's of individual band data of any other number of bands can also be made. The legend (lower right corner of each NMAP) is a symbol count that gives the symbol character, the upper threshold, the counted number of pixels associated with each character, and the percentage of pixels in each brightness class. The symbols and their statistical data are arranged with the class of lowest brightness at the top. Thus W represents the darkest reflectance values and " ", a blank, refers to all brightness values above the 32.10 limit (upper threshold).

#5-36: In the 1973 NMAP printout, outline on Overlay 1 or tracing paper the approximate boundaries of the Susquehanna River. (Hint: water usually shows the lowest reflectances.)

#5-37: Now, within these boundaries, draw other boundary lines around contiguous groups of five or more of the same brightness symbols. Some of these may represent patches of greater reflectance from the water; others do not. Suggest an identity for such patterns. (Hint: look at the band 7 photo image, Figure 4-6B.)

#5-38: What brightness level (limit) would you expect from concrete roadways? Outline the location of Interstate 83 and its interchanges, which have concrete surfaces.

#5-39: The ridge top on Blue Mountain, just to the north of the interstate, consists of a light colored sandstone unit. Outline this feature.

#5-40: What might explain the pattern of H's along the west bank of the Susquehanna? (Hint: engage your train of thought.)

#5-41: Turn now to the 1977 printout. Examine the bright (blank) strip along the west side of the Susquehanna. What might cause this? (Hint: refer to the color composite, Figure 4-11.)

#5-42: Three patterns (numbered 1, 2, 3) in the 1973 printout have been isolated by linear boundaries drawn in Figure 5-20A. These features appear again in the 1977 image but may show somewhat different reflectance ranges. In the 1977 plot, draw boundary lines roughly equivalent to these 1973 features and list corresponding reflectances by symbol.

As you can see, it may be necessary to consider more than one symbol when trying to establish patterns. In general, it is wise to sketch boundaries around the larger, more homogeneous patterns in an NMAP. This is tedious work but is often necessary to organize the patterns in order to define areas that can be related to photo images or to maps used in picking training sites or identifying classes. If you are ambitious, try that task here.

#5-43: Otherwise, from inspection of the printout, comment on the overall homogeneity of normalized reflectance patterns in this scene. (Here we shall define homogeneity as a cluster of ten or more of the same symbols.) Account for the variability you detect.

#5-44: What is the range of limits (normalized brightness values) for the 1973 NMAP symbols W through : ; for the 1977 symbols W through • ? (Note also the increments between W and H and between = and +.)

These limit values are roughly equivalent to percentage reflectance. Usually but not always, the reflectance range is somewhat larger for individual bands. The number and values of the limits are selected empirically from the statistical data obtained during processing to produce the final NMAP. You should conclude from these numbers that the differences in reflectance from one pixel to the next can be small, particularly if most of

[5] The norm in this case is the grouped brightness value representing a multispectral pixel that results from combining the brightness values for each spectral band. It is calculated as a resultant vector in four-dimensional space.

the scene is composed of features with similar reflectances in at least some bands.

Indeed, the differences observed in this Harrisburg data set correspond to a narrow range of reflectances (12-32 for 1973). Extremely bright objects (for example, clouds, ice, sand) are not present in the subscene, and water generally shows norm reflectance limits between 12 and 22. Thus, the frequency distribution of reflectances is biased towards lower values owing to the absence of clouds or other bright objects. The heterogeneity of symbols over much of the NMAP is a function of the natural variability of features in the subscene (including resolution and mixed pixel effects) as well as the choice of limits based on the statistical data.

#5-45: Locate the area covered in the NMAP's in the band 5 images for 1350-15190 and 2904-14452 (Figure 4-6A and 4-10A). Match any of the norm reflectance patterns you discern in the NMAP to their expressions in the band 5 images. Which has more apparent variability and appears to recognize smaller local differences in reflectance, the band 5 image or NMAP?

After the NMAP has been used to verify that the area to be classified has been correctly selected, several options exist for subsequent processing. Normally, the data are classified into land cover types by using either unsupervised or supervised procedures. The data may also receive special processing on ORSER to produce enhanced output (band ratio, canonical analysis, etc.) as character or gray line maps or as color images (on RAMTEK or DICOMED systems).

The unsupervised classification procedure is used when detailed ground truth is not available. Although this is not the case for the Harrisburg subscene, we shall move through this procedure to exemplify the characteristics, accuracy, and interpretability of this output type.

The analyst enters the subscene data set into the ORSER program called CLUS. He also provides certain parameter values such as total sample size, maximum number (up to 60, but usually much lower) of desired clusters (sets of spectral signatures developed by cluster analysis; see p. 446), and limits of Euclidian distances as criteria for separability. The computer program then selects trial clustering centroids from the first scan line in the data block. An initial pass through the data establishes these cluster centroids. The pixel brightness values are compared with each of the cluster centroids during a second pass. Each pixel is thus assigned to the cluster with the nearest centroid. Then, in the printout, each pixel is recorded by the alphanumeric symbol that designates the cluster to which it belongs. If the user is not satisfied with the first results, he may rerun the program with changes in the parameter values until an acceptable classification map is obtained. *Acceptability is somewhat subjective during the processing and may depend on the analyst's judgement that the results "look right" based on his familiarity with the scene or direct comparison with aerial photos and other ancillary data.* Usually a trip to the field or a search through maps is the final recourse in deciding upon validity.[6]

An unsupervised classification map for the Harrisburg subscene within 2904-14452 is shown in Figure 5-20C. Sixteen clusters were set up for the run. Only 54 percent of the pixels in this scene could be matched to a cluster. A seventeenth category (blank symbol) represents all remaining unclassified data. This results from (1) scene heterogeneity (diverse ground features), which introduces so much variability that there are not enough pixels to establish a cluster, and (2) the mixed pixel effect (p. 83).

#5-46: Color part of this map from line 1120 to 1160 (top to bottom). For elements (horizontal) 961 to 1021, mark each pixel with the color you choose to assign to the symbols. For elements 1022 to 1076, ignore "strays," i.e., one or sometimes two pixels of a different character located in a larger array of the same characters.

#5-47: Using any source of information available to you, try to guess the identity of the classes present.

[6] This was aptly demonstrated to the author after he produced his first unsupervised classification with the LARSYS system developed at Purdue University. Six classified maps were made for an area on the western flank of the Wind River Mountains in Wyoming. These subdivided the terrain into five to ten classes. None of these made any interpretable sense until the author looked out over the scene from a ridge and visually selected the most meaningful map. The importance of field verification is treated in Activity 6.

The supervised procedure is used when the analyst already has detailed ground truth (usually in the form of maps and aerial photos but also as "windshield" surveys, personal knowledge, etc.). The spectral signatures of homogeneous training sites established from the ground truth become the reflectance standards to which all unknown pixels are referred in generating the final classification.

The first step is production of a spectral uniformity map (Figure 5-20D). The UMAP program examines the reflectance values for each pixel and compares these with the values for three nearest neighbors. If the pixels are very different, or far apart in vector space,[7] the index pixel is considered to have very low uniformity (high diversity with respect to its surroundings). This would occur, for example, where a concrete bridge crosses water and one pixel corresponds only to the bridge and the others only to water. However, if the pixel and its three neighbors to the east, southeast and south are very close spectrally, the index pixel is considered uniform; this happens where all four pixels represent water. Every pixel in the data set is tested in turn in this way and the conclusion displayed as a character map. For the 1977 Harrisburg scene, the symbols indicate

U = greatest uniformity,
- = moderately high uniformity,
= moderately low uniformity,
* = very low uniformity.

*#5-48: On tracing paper, draw boundaries around at least ten groups containing ten or more U's. Also, draw boundaries around five groups of *'s. Note the wide variety of shapes these groupings can take.*

These U groups now become favored "training areas," which would serve as the best data values to establish training signatures for the land cover types of interest. The UMAP only singles out the areas of spectral homogeneity; the NMAP and available ground truth data must be used as guides to determine what the land cover actually is within each U group.

[7] In mathematics as applied to image processing, this term refers to a point in multidimensional space, as defined by a vector from the origin of the coordinate system, which specifies the intensity value for the combined individual variables (bands or channels) in an N-space multivariate system.

*#5-49: For each of the ten U groups you picked, place the symbol of the dominant norm reflectance found on the NMAP to lie within that group. Inspect the * groups to ascertain that each one indeed contains a wider variety of NMAP symbols.*

By using this approach and by drawing upon information from the USGS topographical and land cover maps and aerial photographs, a total of sixteen spectral signature clusters representing different named categories were selected and statistical parameters acquired to confirm separability calculated for each. After carrying out several intermediate steps (omitted here), a final supervised classification map (Figure 5-20E), at the same scale as NMAP and UMAP, was printed. In this map, the legend in the lower right gives the category (class) names, symbols, and pixel count (frequency of occurrence), which may also be calculated as a percentage of the total area occupied by each symbol (category). As would be expected in the real world, some categories extend over broad uniform areas much larger than their training areas, yet other categories are isolated or interspersed.

#5-50: Color as much of the CLAS map as your time permits. Use the same colors, and sequence, as you chose for the CLUS map. In general, ignore "strays" in a larger, more homogeneous symbol group by assuming that the strays belong to that group (this "smoothing" process may be unwise as it rejects truly different features, but it is commonly done to provide a simplified end product.)

#5-51: Compare the corresponding colored sections of the CLAS and CLUS maps. Which has a more realistic look?

#5-52: Some categories have the same general cover type name. Can there be real differences between these categories? Comment on this and explain how you might improve the categorization of the classes.

#5-53: What possible real features might be represented by the blank symbol?

#5-54: Why were several diverse features lumped into this "other" category?

#5-55: What would you have done to minimize the occurrence of the "other" category and come up with some new identities (categories)?

The classifications we have just surveyed are invaluable for three reasons: (1) They can be made fairly rapidly. ACLUS or a CLAS map can usually be generated in less than an hour, using only a few minutes of computer time; (2) They tend to show intimate details. Each pixel, or aggregate of pixels, is displayed by a symbol that can be *found* in the printout and considered as an individual parcel of data; and (3) They are inexpensive to produce. Costs in computer time and terminal rental required for the production of a CLAS map of the size in Figure 5-20E amount to only a few dollars.

Interactive Systems: IDIMS

Despite the advantages of time, detail, and costs, many users find the alphanumeric maps rather sterile, hard to read, and a nuisance when they must be hand-colored. There is a growing shift towards use of interactive computer systems, even though these can range in cost from several thousand to half a million dollars, since experience with their extreme versatility and quality of output endows them with an "aura of popularity."

To appreciate more fully the typical procedures for constructing a classification from training data by using an interactive computer/display, we shall next simulate the activities that might be carried out if you were the analyst at the console of the image analysis system at ERRSAC. Once again, we shall classify a subscene that includes Harrisburg, Pa. The photographs shown later in Figures 5-27 and 5-29 through 5-32 were actually taken (with a camera) from the TV monitor display coupled to this system.

This system, called the Interactive Digital Image Manipulation System (IDIMS), designed and marketed by Electromagnetic Systems Laboratory (ESL) Inc., of Sunnyvale, Calif., is a complete self-contained image processing system capable of extracting information from imagery of all types including multispectral data from Landsat. Its capabilities result from an effective combination of a minicomputer and a floating point array processor. This hardware configuration provides both the processing speed and memory capacity necessary to handle the large quantities of digital data returned from the Landsat MSS. Figure 5-21 is a simplified block diagram describing the IDIMS configuration at Goddard's Eastern Regional Remote Sensing Applications Center. The minicomputer is a Hewlett-Packard HP 3000 Series II unit with 512 kilobytes of core (CPU) memory. Programs and raw data are read into and stored on discs whose capacity is expandable to 1200 megabytes. CCT-recorded data are read into disc from low (1600 bpi) or high (6250 bpi) density tape drives. Use of an array processor permits fast computations for classification or other processing by using the four MSS band data sets. The Advanced Scientific Array Processor (ASAP), built by ESL, performs computations on a matrix of numbers in parallel (in an array) instead of serially as do standard computers.

The Comtal monitor displays 512 raster lines on its screen; each line can accommodate up to 512 pixels. Typically, the size of a Landsat subscene is matched one-to-one to the monitor resolution capability, that is to say, is constructed from a 512 X 512 pixel set (equivalent to an area about 40 km [25 miles] on a side), assuming that the pixels are squared to 80 m X 80 m equivalent dimensions. Larger areas can be displayed full screen by using only every nth pixel and dropping those between (thus, in displaying a 2048 X 2048 image, every fourth pixel is entered in both horizontal and vertical directions, and the three intermediate ones are not used; this obviously reduces image resolution). Smaller areas (enlargements) are displayed by repeating the same pixel n times along each line (a 128 by 128 pixel display repeats the same pixel four times). The ASAP can process as many as fifty different classes from a 512 X 512 data set in less than five minutes. The operator typically requires about two hours to carry out all phases of a classification in a Landsat scene or subscene by interacting directly with the computer from a command console or terminal keyboard. Either a CRT screen or a line printer serves to display the

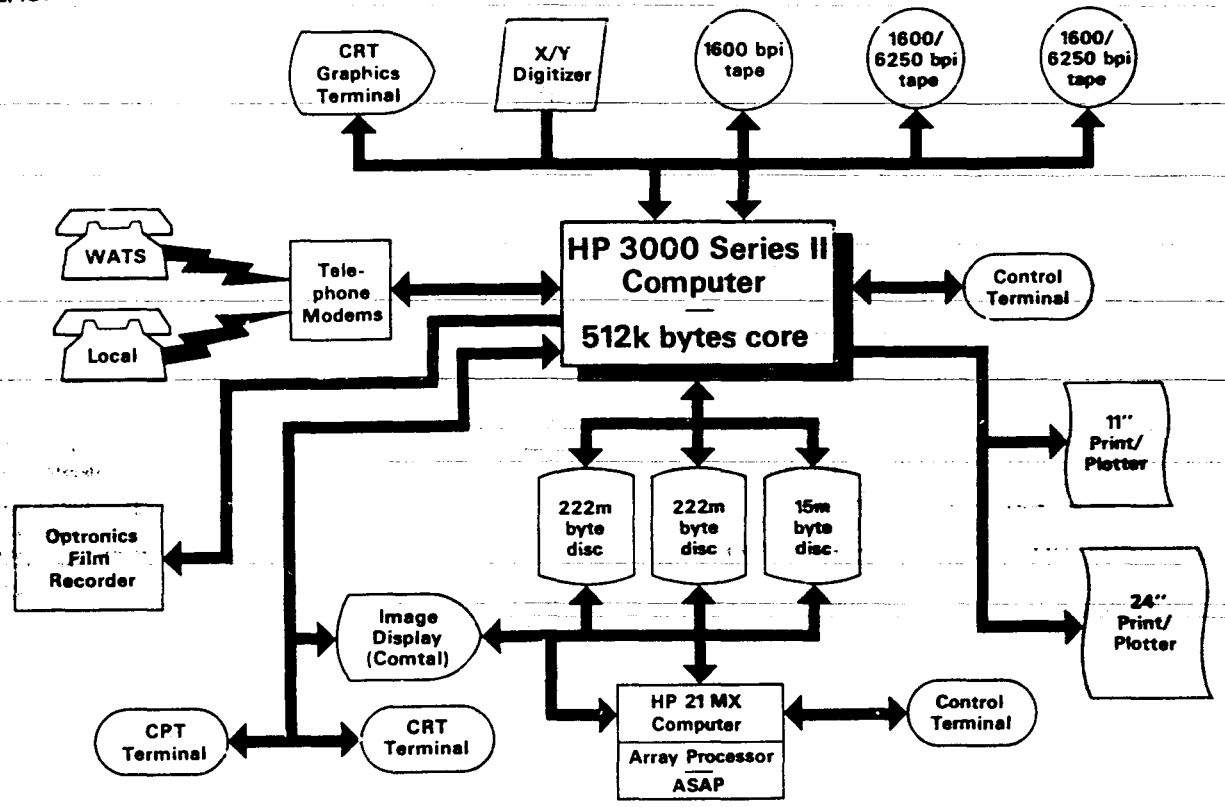

Figure 5-21. The IDIMS configuration at ERRSAC.

Figure 5-22. Operator (W. Campbell) at keyboard and display console of IDIMS at ERRSAC.

commands input by the user or analyst and the prompts, messages, and numerical data returned from the system. The operator may also access the computer from terminals or display tied to the system via a telephone linkage, called a modem.[8] Figure 5-22 shows an operator at the keyboard and display console of the IDIMS facility at the Goddard Space Flight Center.

The software consist of programs drawn from an expandable library currently containing more than 250 processing functions. The analyst may also consult a menu to choose processing and display functions; those lists are usually displayed directly on the screen. The most frequently applied functions consist of classification algorithms using maximum likelihood or minimum distance classifiers (see p. 447) and analysis algorithms providing class summaries and statistical evaluations. Other useful functions perform image or data manipulations such as geometrical transformations, intensity transformations (including contrast stretch), spatial filtering, Fourier transformations, mensuration, grid and graphics overlays, and specialized enhancement techniques (see Appendix B for more detailed explanations).

In addition, IDIMS may be integrated with software packages for processing other types or sources of data. ERIS (Earth Resources Inventory System) is a set of digital files containing ancillary data of many kinds (for example, ground truth measurements, field surveys, census statistics, aircraft flight observations), which can be merged or correlated with Landsat data and analysis output. The GES (Geographic Entry System) allows data from thematic maps (e.g., topographical, land use, political boundaries) to be entered in line, point, or polygon formats by using an X, Y digitizer and, if desired, registered to Landsat data. Input/output from IDIMS-ERIS-GES may also be integrated with a Geographic Information System (GIS), which organizes and compares diverse kinds of information (for example, topography, climate, soils, land ownership, population density) referenced to a common data base (usually geographical coordinates).

We shall now proceed to run through a classification of a 512 X 512 pixel data set covering Harrisburg, Pa., and its environs. Landsat data from both October 11, 1972 (see Figure 4-2) and July 14, 1977 (Figure 4-11) will be used interchangeably.[9] This classification results from a supervised procedure that depends on correlating spectral classes with known categories of ground features.

Training sample sites around Harrisburg may readily be set up by reference to several sources of ground truth. The U.S. Geological Survey land cover (Figure 5-18) and topographical (Figure 5-19) maps employed in the ORSER classification (p. 182) may again be consulted. However, the primary source, used most frequently during the actual classification, is shown in Figure 5-23. This is a color IR photo (scale 1:117,400) taken on February 5, 1974 from a high altitude (18 km) RB-57 aircraft. It should be of interest to compare this photo (ground resolution of about 5 m) with an enhanced (stretched and filtered) subscene (resolution 79m) from the October 11, 1972 Landsat overpass that covers almost the same area (about 24 km [15 miles] on a side). The color in this summer subscene, shown in Figure 5-24, was adjusted to look roughly like that of a winter aerial photo by subduing red and increasing blue.

#5-56: Locate the subscene in the fall 1972 (1080-15185; Figures 4-1 and 4-2) frame.

#5-57: First, calculate the ratio of the altitudes of the Landsat spacecraft and the RB57. Then, compare the aerial photo and Landsat subscene, making allowances for differences in resolution and in time of year. Give your appraisal of the degree to which this Landsat image can substitute for or "compete" with small-scale aerial photography in terms of ability to recognize level I land cover categories (see Table 5-4).

#5-58: List at least four level II categories identifiable in the aerial photo. Put a checkmark next to any of these that you believe to be also identifiable in the Landsat subscene.

[8] Modem = Modulator-Demodulator.

[9] Most of the classification steps are demonstrated on the July 1977 scene (easily identified by the completed section of Interstate 81). Owing to problems in recovering camera-quality imagery, the final classification and several intermediate images were necessarily selected from the earlier 1972 scene. However, a classification of the 1977 scene, with somewhat different classes, is depicted in Figure 7-13B.

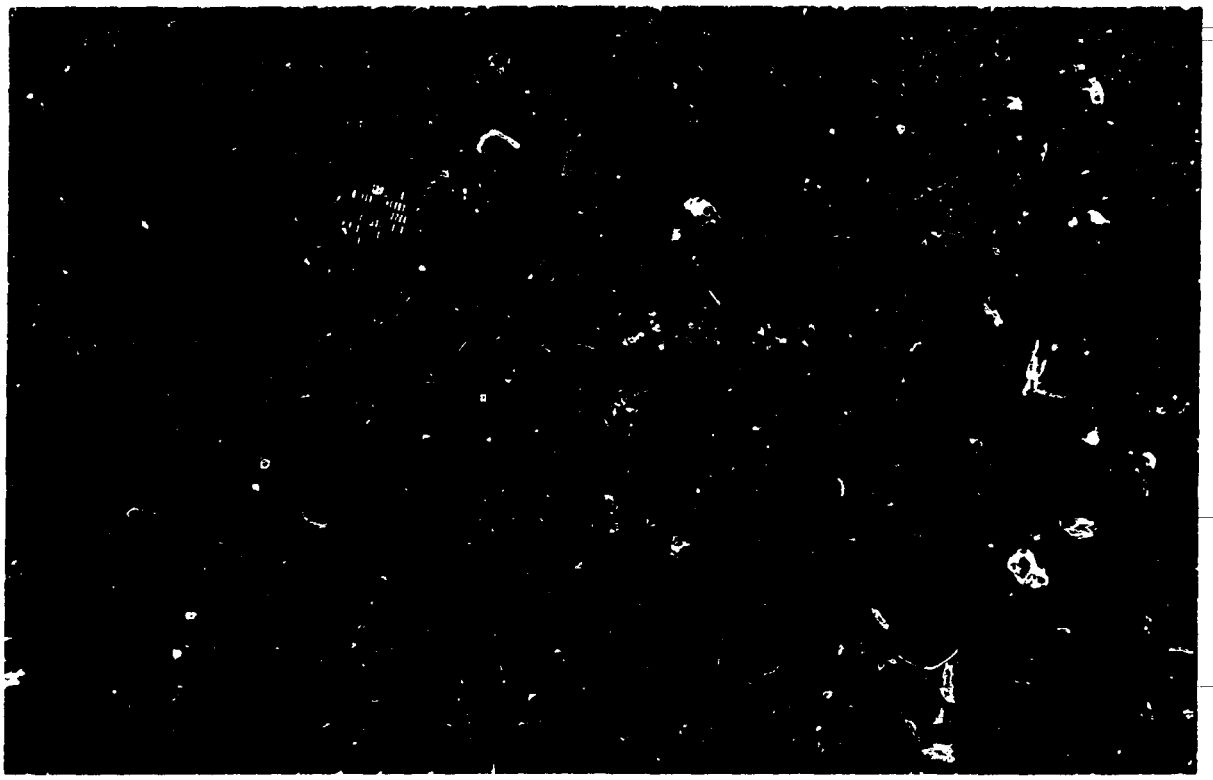

ORIGINAL PAGE
COLOR PHOTOGRAPH

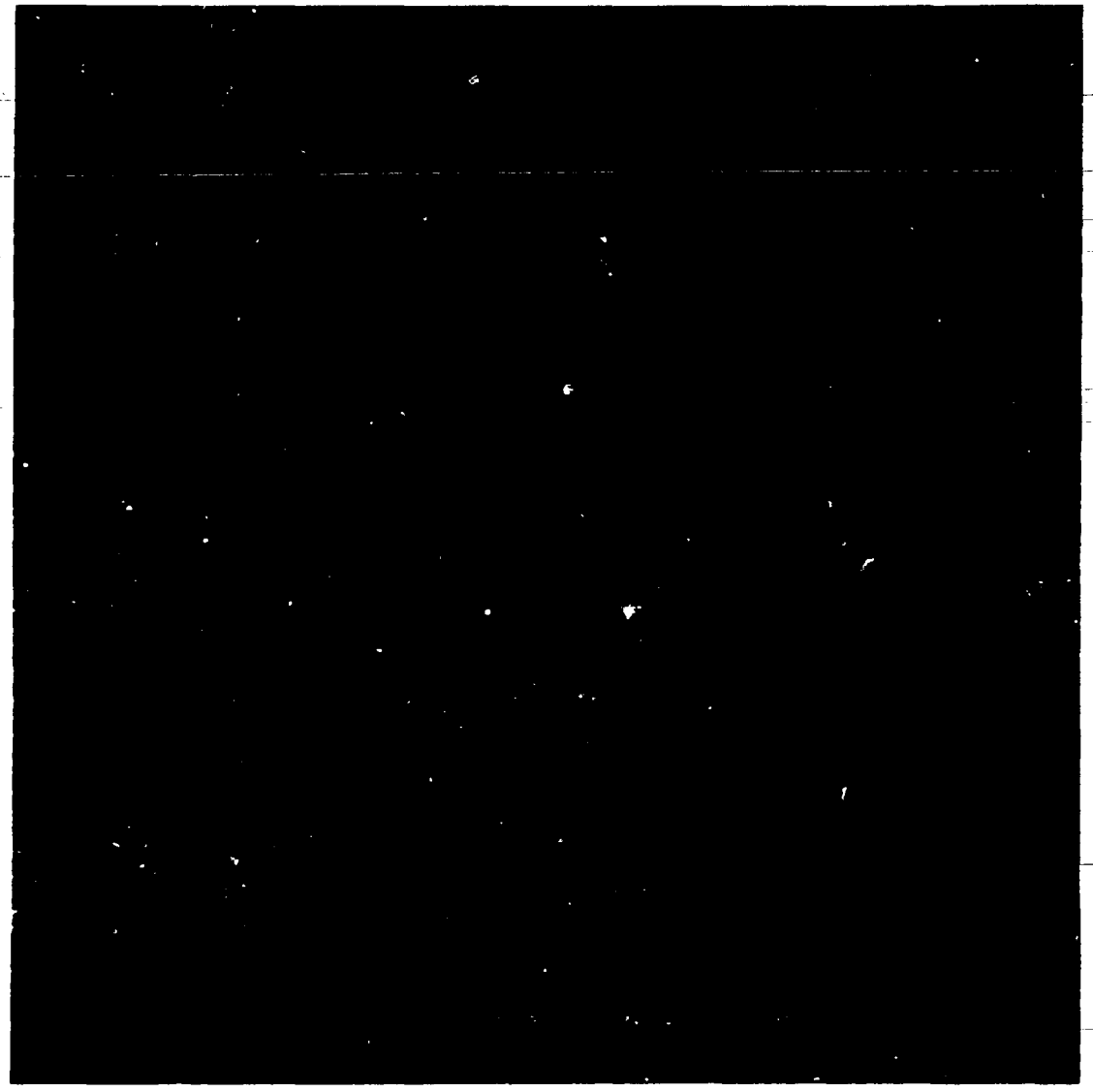

Figure 5-24. Computer-enhanced enlargement of Harrisburg region made on IDIMS from Landsat overpass on October 11, 1972.

#5-59: Place a piece of tracing paper over Figure 5-23. Outline various small area (typically, 0.04 to 0.16 sq. km or approximately 10 to 40 acres) samples of as many different and separable land cover categories as you can recognize. Make a list of these categories. Then, try to find their discernible counterparts on the 1972 Landsat subscene in Figure 5-24.

Figure 5-25 is a generalized flow chart outlining the procedural sequence analysis of Landsat images on IDIMS. Figure 5-26 is a sample of part of the line-by-line session history of image analysis as displayed in real time on the terminal screen and, in this case, copied as output on a line printer. Some of the lines were typed in by the operator or analyst as commands, decisions, or comments. The computer responds with appropriate information or instructions, either instantly if the response is an automatic, or default, statement, or after some delay if calculations are performed. In this example a routine was created for point operations on a single band of Landsat data; this is then "saved" in a command file for retrieval and use on subsequent data sets.

In carrying out that classification, the usual first step is to display the area of interest within a Landsat scene on the IDIMS monitor screen. In one routine, each quarter strip of a full scene can be displayed by itself, or in succession until the entire frame has been assembled. The geometrically uncorrected quarter strip containing the Harrisburg subscene (see arrow) is shown in Figure 5-27A.

#5-60: Locate this strip in the full Landsat scene (Figure 4-11). Is the direction of distortion or foreshortening in the quarter strip horizontal, or vertical?

From inspection of the full image, any desired subset is blocked out by using a trackball-driven moving cursor to position arrows at subset corners (see arrow in Figure 5-27A). The coordinates of these corner points, given as line and sample numbers, are read from the screen.[10] These coordinates are entered through the keyboard to display each band of the subset image; band 5 (red) is shown in Figure 5-27B. A separate reference map of this subscene may also be printed out on a printer/plotter at up to 32 gray levels (Figure 5-28). Because a pixel has the same coordinates in each of the bands, any three bands, usually MSS 4, 5, and 7, are easily registered and each assigned a color from the monitor color guns to produce a false color composite (Figure 5-27C).

Some geometrical corrections are generally applied at this point. The most important of these is an *aspect* correction made to eliminate the foreshortening effect. The diagram and discussion below explain the rationale for this.

Suppose the objective is to display a 512 X 512 Landsat pixel subset in its correct geometrical state, that is geographically valid and with no distortion, on a monitor consisting of 512 raster lines, with each line subdivided into 512 pixels (similar to the standard home TV screens). Each Landsat pixel, however, represents a ground dimension of 79 m X 56 m (see page 83) and is therefore rectangular (*a*). Each TV pixel is square in shape (*b*). In reading Landsat pixel data from a

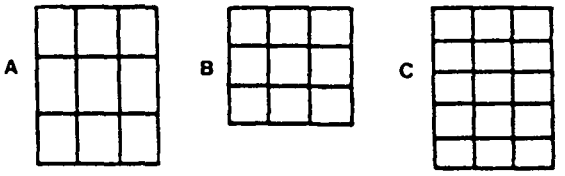

CCT onto a TV display, each of the 512 Landsat pixels for a scan line will produce a TV pixel. Thus, a rectangular Landsat pixel is represented as a square TV pixel. As displayed on the screen, the array of Landsat pixels will experience an aspect foreshortening of about 29 percent vertically (calculated as 100 - [100 X 56/79] = 29). Because of the square TV pixel constraint, the aspect correction must be made by adding some number of new lines to the original 512 MSS lines to produce a new array (*c*). This number is (79/56 X 512) - 512 = 722 - 512 = 210 new lines. In effect, this requires

[10] Information on this and other characteristics of the image is presented as display annotation for the scene as shown in the left corner of Figure 5-27C. The point at the head of the cursor arrow (left of center) is referenced as follows: (1) The number pair under AB refers to screen coordinates (in the Y, X direction); thus Y = 227 and X = 171 for a 512 X 512 raster-pixel screen; (2) the pair under PR gives line l and sample s number for the image data set; thus l = 220 and s = 172; (3) the three numbers under IV correspond to the reflectance values of the pixel at the arrow top; thus channel 4 (= band 7) is 22, channel 2 (5) is 25, and channel 1 (band 4) is 20.

IDIMS APPROACH FOR IMAGE ANALYSIS

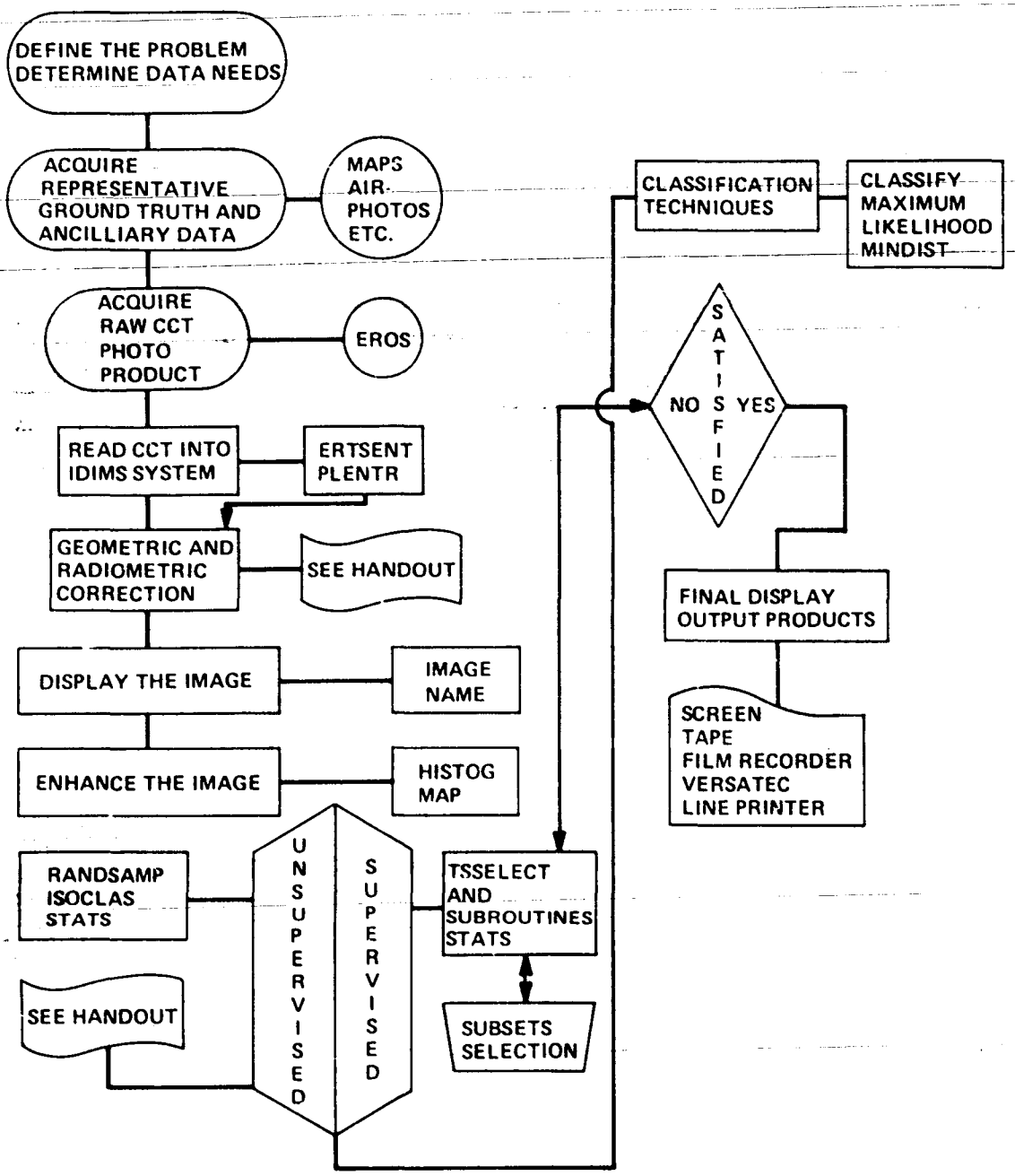

Figure 5-25. Flow chart showing procedures using IDIMS for image analysis.

```
 1    TITLE: BAND BY BAND DISPLAYS AND SINGLE BAND
 2    TITLE: MAPPING (POINT OPERATIONS)
 3    IM2: MAG.HBG.SS
 4    COMMENT: 57METERS X 57 METERS PIXELS)
 5    COMMENT: BAND BY BAND IMAGE DISPLAY NEXT.
 6    C512>
 7    IM2>
 8    COMMENT: THIS IS BAND BY BAND IMAGE DISPLAY
 9    COMMENT: THIS IMAGE AHS BEEN ASPECT-RATIO-CORRECTED USING
10    COMMENT: MAGNIFY. (VERTICAL MAGNIFICATION=3240/2340)
11    COMMENT: INFRARED BAND DISPLAY AND HISTOGRAMMING OF IT FOLLOW.
12    >PAUSE
13    SE 0
14    HISTOG
15    >PAUSE
16    MAP 0 127 TO 0 255
17    HISTOGV
18    COMMENT: HIT Z TO GET DFM OF MAPPING DONE JUST NOW
19    >PAUSE
20    DFM
21    >PAUSE
22    MAP 26 82 TO 0 255
23    HISTOGV
24    COMMENT: THIS IS A LINEAR MAPPING WITH SATURATION.
25    COMMENT: HIT Z TO GET DFM.
26    >PAUSE
27    COMMENT: HIT Z TO GET NONLINEAR MAPPING.
28    >PAUSE
29    MAP 0 26 27 82 83 127 TO 0 26 27 240 241 255
30    HISTOGV
31    COMMENT: THIS IS A NONLINEAR (PIECEWISE LINEAR) MAPPING.
32    COMMENT: HIT Z TO GET DFM.
33    DFM
34    COMMENT: DENSITY SLICING NEXT.
35    COMMENT: HIT Z TO CONTINUE.
36    >PAUSE
37    FR:0 8 9 22 23 52 53 64 65 255
38    TOM: 0 0 80 80 100 100 180 180 255 255
39    MAP FR TO TOM
40    COMMENT: THIS IS DENSITY SLICING.
41    COMMENT: HIT Z TO CONTINUE.
42    >PAUSE
43    DFM
44    COMMENT: PSEUDOCOLOR MAPPING NEXT.
45    COMMENT: HIT Z TO CONTINUE
46    >PAUSE
47    TCC OLD DKBLUE 0
48    TCC OLD LTBLUE 80
49    TCC OLD GREEN 100
50    TCC OLD DKGREEN 180
51    TCC OLD RED 255
52    COMMENT: END OF POINT OPERATIONS ON SINGLE BAND.
53    COMMENT: TYPE TCH3 TO START ON MULTIBAND OPERATIONS.
54    IM2:
```

Figure 5-26. Typical "menu" (line by line IDIMS session history) seen on console monitor (here, a line printer product).

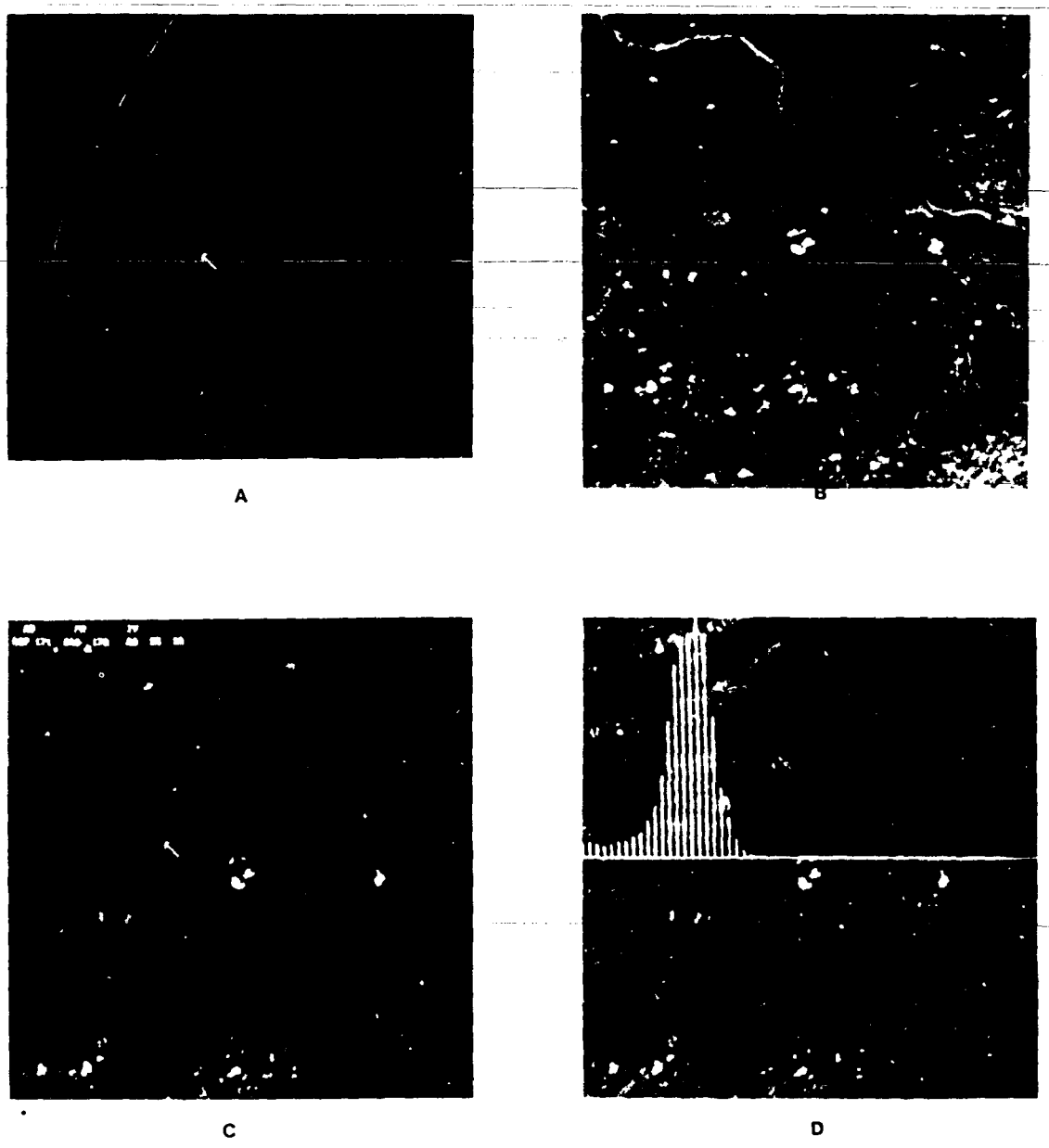

Figure 5-27A-D. Monitor display of steps in IDIMS processing (see text) of Landsat Harrisburg subscene.

Figure 5-28. Printer/plotter map of density levels in IDIMS display of Landsat band 5, Harrisburg subscene.

new pixels to be "created" to insert 210 "dummy" lines. The DN values assigned to the full array of pixels (722 lines X 512 pixels/line) are determined by resampling procedures, such as the Nearest Neighbor resampling described on page 153.

The new array with these added lines may be used to make a photographic product on a film recorder. This image is expanded in the vertical (normal to raster lines) and is thus a geometrically correct rectangle. However, to fit this new array, with its extra lines, onto a square screen, some subsampling procedure must be adopted. One procedure is to display a 512 X 512 subset of the 722 X 512 image by omitting part of the top and/or bottom of the image. Another is to hold the number of MSS scan lines in the original subset to 56·79 X 512 = 362; the necessary new lines when added make up a total of 512. A third procedure is to reduce the total of 722 to approximately 512 by dropping every nth line from the array (for example, if n = 3, then dropping 722/3 = 241 leaves 481 lines).

The next step is to improve image quality as an aid to recognition of favorable and identifiable training sample sites by activating some enhancement procedures. Destriping is commonly required, followed by some type of contrast stretch. To stretch each band the computer calculates the distribution of DN's or brightness levels, that is, the total number of pixels of each DN value in the subscene, and then displays this as a histogram. This has been done for band 7, in Figure 5-27D, with the initial distribution histogram appearing in yellow in the upper left. The horizontal baseline for that histogram spreads across the full screen; this allows full use of the 512 monitor pixels to hold the 256 DN values. This histogram occupies the upper half of the screen, or 256 raster lines, within which are plotted the frequencies of each DN value (number of pixels of each DN value divided by the total number of pixels in the subset). The initial histogram contains very few pixels with values exceeding about DN = 100, that is, there are few bright objects in the scene (with the exception of the clouds), so that the corresponding image tends to be dark and of subdued contrast. By simple "trial and error," new upper and low DN values are picked, the stretch is carried out, and the new image appraised for a pleasing and informative appearance. The lower yellow histogram has been expanded by a straight linear stretch to limits of DN = 0 to DN = 210 (Figure 5-29A). The displayed image resulting from this stretch is shown in the background.

Sometimes the full dynamic range (0-255) available for stretching is selected. The histograms may be displayed graphically without the image background (Figure 5-29B). In this stretch the few end pixels (low DN's = very dark tones shadows, water; high DN's = very light tones clouds, snow, sand) have been trimmed (removed) from the distribution, after which the remaining DN's have been expanded to the full 255 range. This stretch is plotted as the red histogram in the lower half of Figure 5-29C (the spacing of the lines is now one every nine units in the 512 scale; this corresponds to an increment of eight DN units between successive lines). The stretched image is displayed in the background.

#5-61: State one way in which to further increase the contrast resulting from this last stretch.

#5-62: What is the effect of not trimming any pixels from the low DN end while removing even more of the high DN distribution?

#5-63: A stretched version of the band 5 image shown first in Figure 5-27B is reproduced in Figure 5-29D. Describe the most obvious visual changes in the stretched image.

The TV display of one combination of enhanced bands 4, 5, and 7 in the normal false color rendition of the July 1977 subscene appears in Figure 5-30 as photographed from the screen. You have already seen a similar combination (Figure 5-24), having more subdued color hues and high bandpass filter effects, for the October 1972 subscene; the hard copy print in that example was produced by an Optronics film recorder.

It is sometimes helpful to execute a crude but quick separation of tonal patterns in a single band by means of density slicing. In this procedure, continuous intervals of DN's are grouped into discrete single gray levels and a color is assigned to each composite level. This leads to distinct color patterns that *tend* to differentiate broad classes of surface features. The stretched band 5

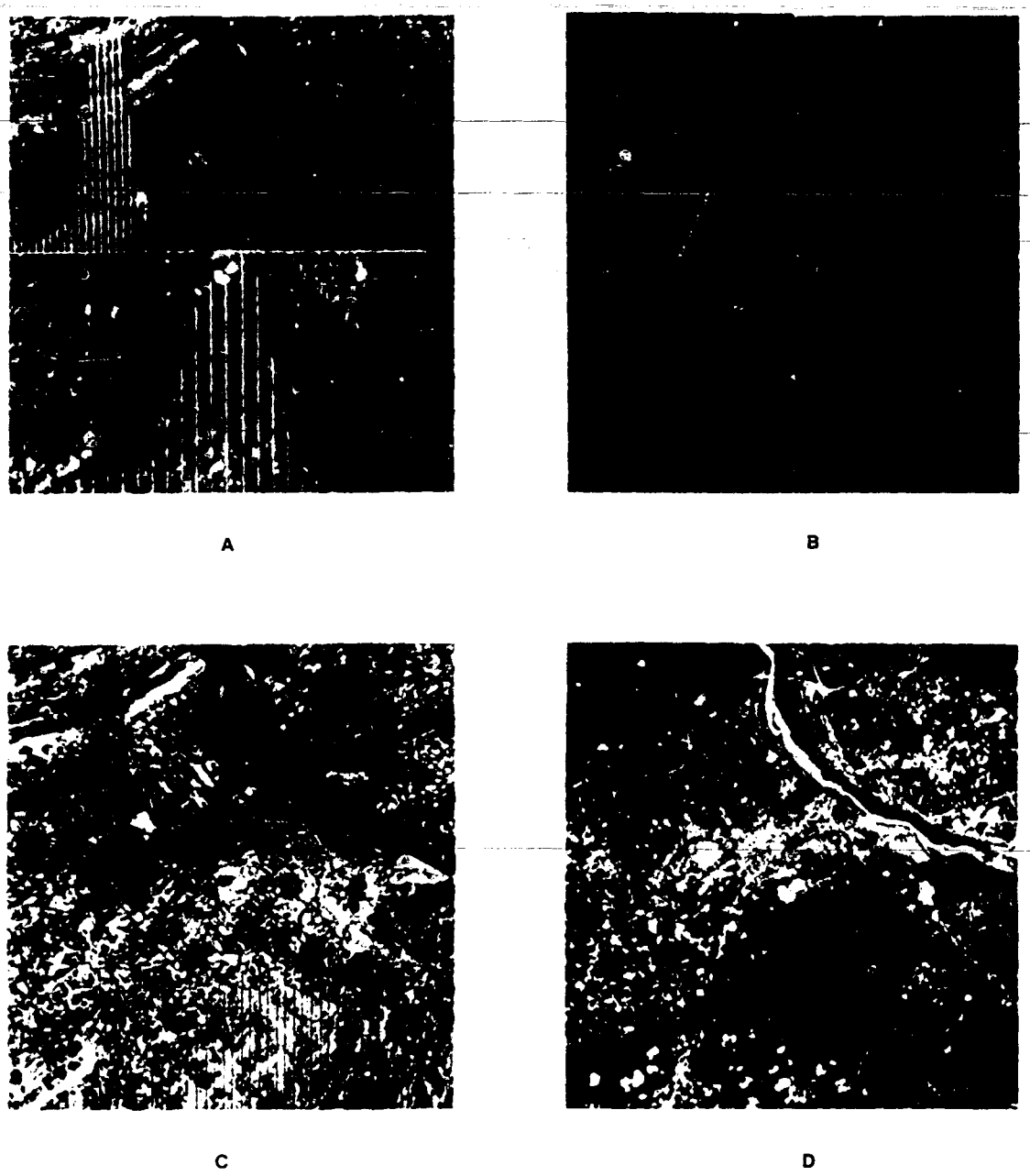

Figure 5-29A-D. Monitor display of IDIMS processing steps (continued, see text) of Landsat Harrisburg subscene.

ORIGINAL PAGE
COLOR PHOTOGRAPH

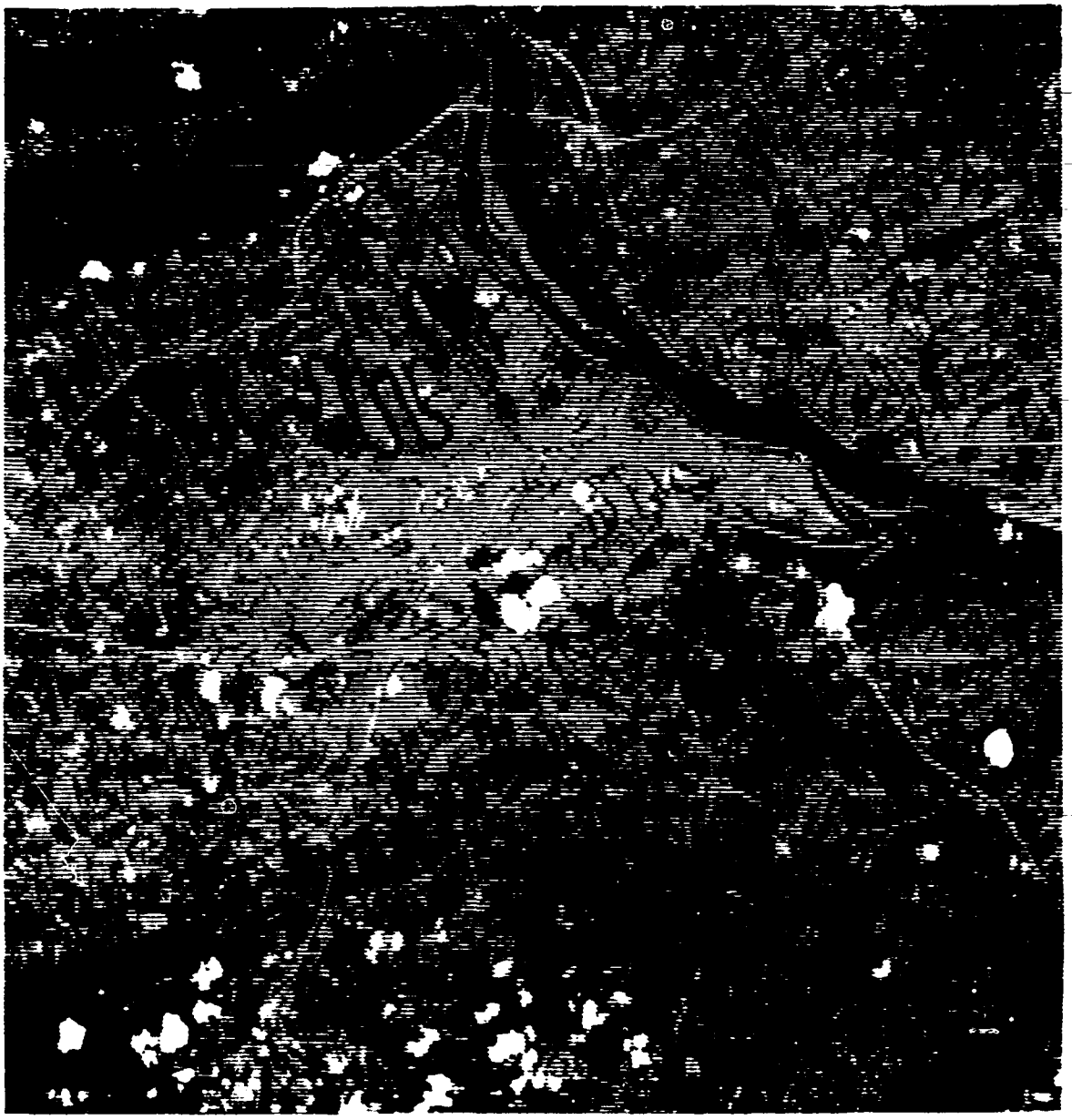

Figure 5-30. Computer-enhanced Harrisburg subscene, July 1977.

image was density sliced into five levels, colored in two shades of blue, two of green, and one red (Figure 5-31A).

#5-64: Several truly different classes may be depicted in the same color because their reflectances are similar in a given band. By comparing Figures 5-30 and 5-31A, try to identify classes that might be confused. The blue associated with river water is also assigned to what different feature? Red is most commonly associated with what feature in the density-sliced image? With what else might it be confused? The light greens correlate in part with cultural features (mainly buildings and streets) but have also been assigned to what?

In general, density slicing has limited value in pattern recognition, and an accurate classification must rely on multivariate statistical analysis.

We are now ready to perform a classification of the Harrisburg 1972 subscene by using the maximum likelihood classifier (p. 447). The first step is to select training sites. By analysis of statistics, together with inspection of the monitor display, aerial photos, maps, and field experience or familiarity with the area, some number of classes is decided upon and each assigned a class name. It is often convenient to enlarge a part of each subscene even further to accurately circumscribe boundaries about specific training sample sites for the several classes. Visually, we try to enclose representative areas within each training site by seeking out groupings of more or less homogeneous (similar pixel colors) areas. These areas are blocked out by a moving cursor (electronically generated on the screen; in other systems a light pen may be used) that produces line segments bounding pixels to be included in statistical tests for separability (Figures 5-31B and C). For the entire Harrisburg subscene, the locations of training areas for water, forest, and urban classes have been outlined in Figure 5-31D.

#5-65: The bounded area marked by the arrow in Figure 5-31C is an example of a poorly chosen training site. Why?

After data from the training site pixels are stored and statistical tests performed, a "first cut" classification is carried out. Once determined, each class may be displayed on the screen in its proper spatial distribution by using an assigned color. In Figure 5-32A, a class named *urban: industrial/commercial* has been depicted in yellow. Two classes, vegetated cropland/pastureland (in brown), and barren/open land (purple) are shown in Figure 5-32B. In this example, it may be seen that a large part of the total scene area—perhaps too much when compared with aerial photos and other ground truth—is taken up by these two classes. Mensuration of the percentage area occupied by each class is merely a pixel-counting procedure within the computer program.

When a scene is fully classified at the levels chosen, all classes are displayed together in a multicolored thematic map (Figure 5-32C). Eight classes were arbitrarily specified for the 1972 Harrisburg subscene. Colors assigned to and areas calculated for each class are as follows:

	Color	Area (%)
Urban: industrial/commercial	Yellow	5.8
Urban: residential/mixed	Red	8.1
Vegetated cropland/pastureland	Brown	36.5
Barren/open land	Purple	14.2
Deciduous forestland (sunny)	Medium Green	16.1
Deciduous forestland (shaded slopes)	Olive	15.0
Water (streams and lakes)	Blue	2.8
Unclassified (final iteration)	Black	1.9

This classification map has been enlarged to a full-sized illustration in Figure 5-33, which also contains a color-coded legend.

#5-66: Some of these classes may be somewhat artificial or not "pure" (that is, they are mixed, containing several unrelated ground features). Some features appear to be misclassified, especially where the class assigned at some specific place seems at odds with what you might have chosen by photointerpretation of Figures 5-23 and 5-24. Still other features evident in those figures were not classified in Figure 5-33. Look closely at all three figures. Evaluate (critique) this computer classification and suggest at least three other classes you might have established.

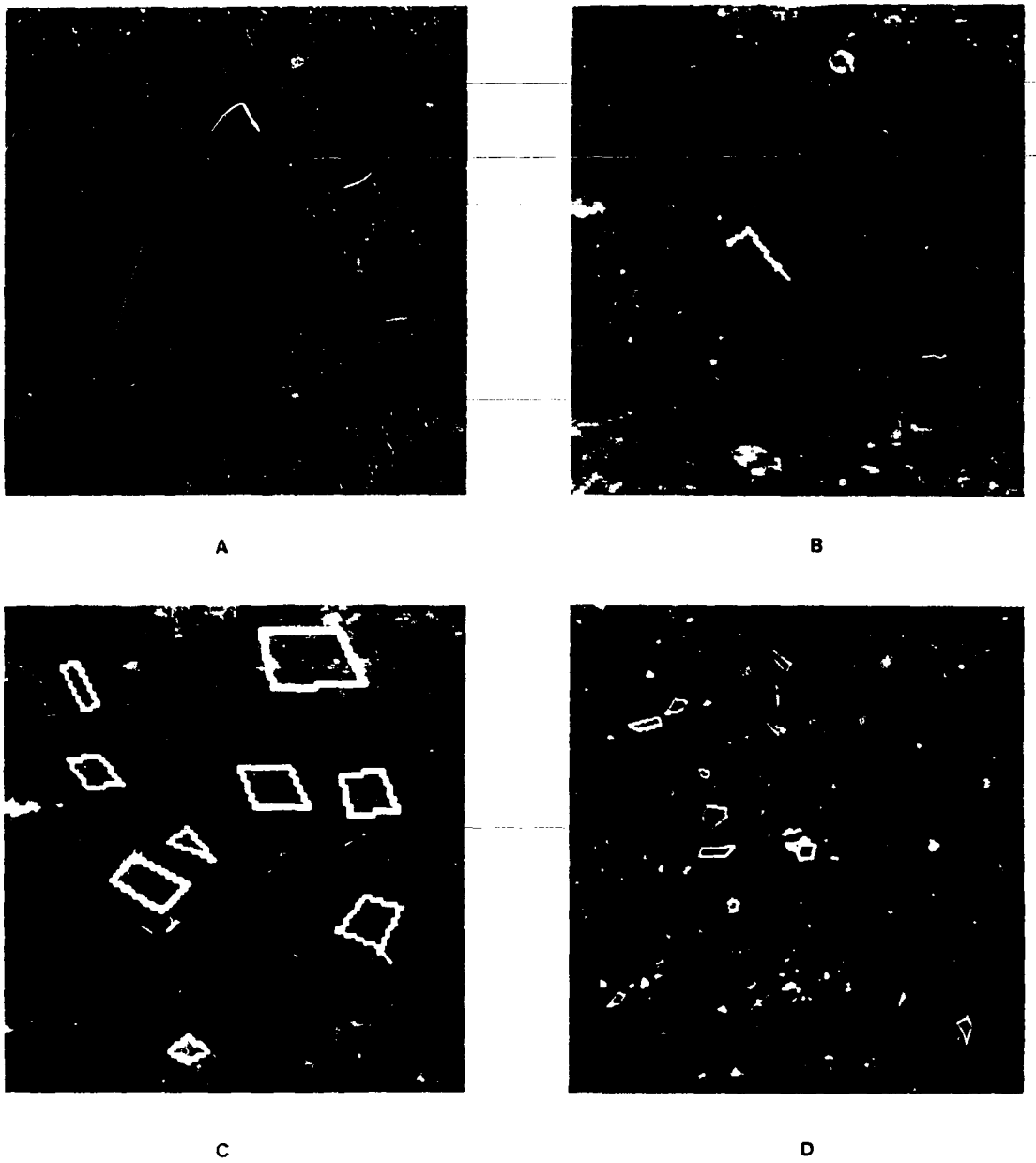

Figure 5-31A-D. Monitor display of IDIMS processing steps (continued, see text), Harrisburg subscene.

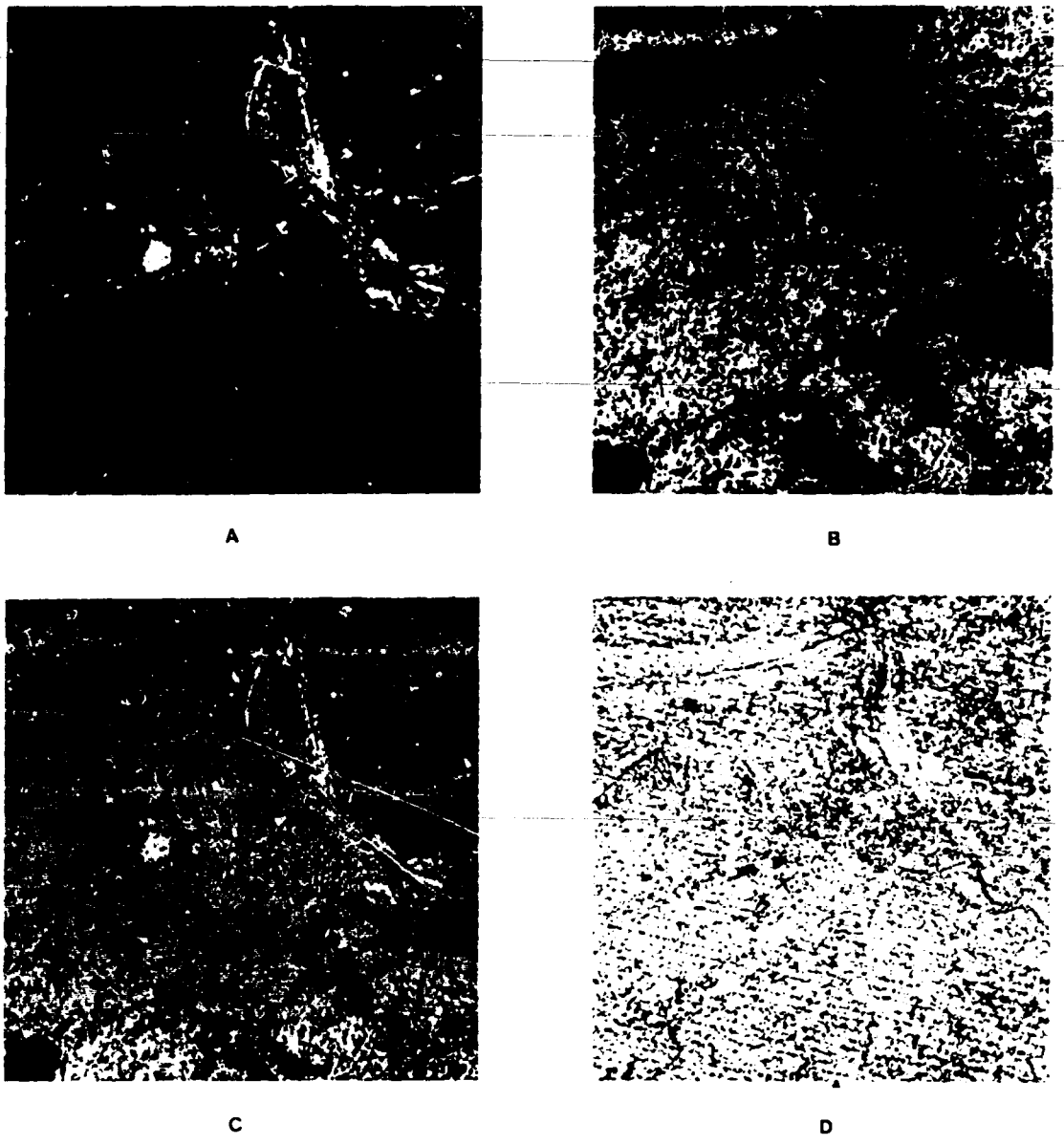

Figure 5-32A-D. Monitor display of additional IDIMS processing steps.

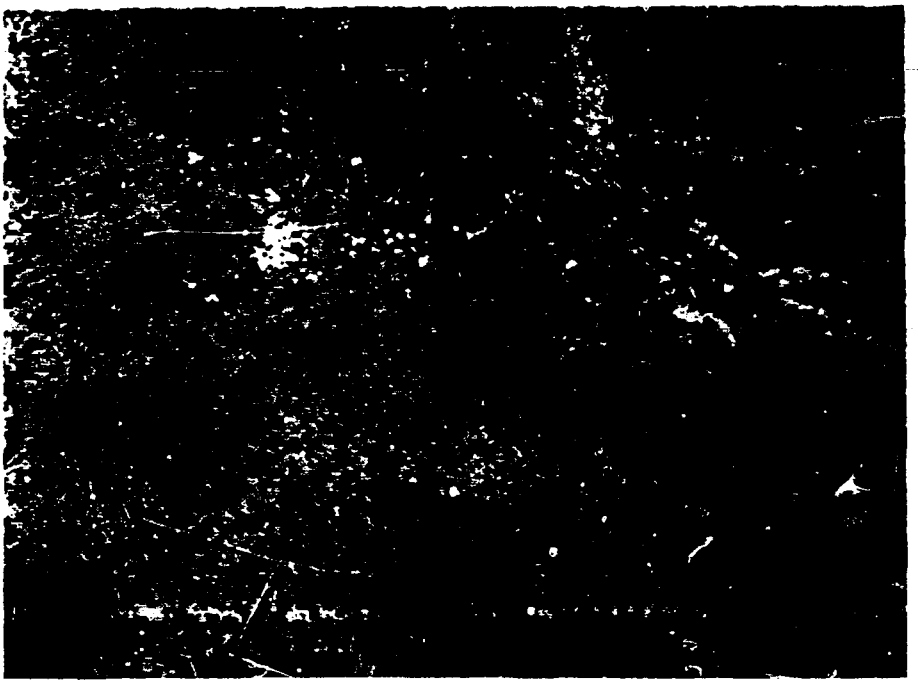

	AREA [%]
URBAN: INDUSTRIAL/COMMERCIAL	5.8
URBAN: RESIDENTIAL/MIXED	8.1
VEGETATED CROPLAND/PASTURELAND	36.5
BARREN/OPEN LAND	14.2
DECIDUOUS FORESTLAND (SUNNY)	16.1
DECIDUOUS FORESTLAND (SHADED SLOPES)	15.0
WATER (STREAMS AND LAKES)	2.8
UNCLASSIFIED (FINAL ITERATION)	1.9

Figure 5-33. Final IDIMS-generated classification of 1972 Harrisburg subscene.

An assessment of accuracy should be made after each trial classification. One way to do this is to subject the data to the Chi-square test. This test is described in most textbooks on elementary statistics. The extent of misclassification thus calculated may be displayed on the screen, as illustrated in Figure 5-32D. Pixels whose classification is uncertain (statistically) are rendered dark; those of high reliability are presented in light tones.

The *urban: industrial/commercial* class shown in yellow in Figure 5-32A illustrates one type of misclassification, that of errors of commission. Certain major roads, the concrete-lined banks of the Susquehanna, and the meandering tributary Conodoguinet Creek, are all "alarmed," i.e., respond positively, as part of the yellow pattern when the color display appears. Reasons for this misclassification are not clear. The Conodoguinet Creek should properly fall into the class *water*, but the contaminating presence of buildings (mostly waterfront homes) and the subpixel width of the stream may have caused the confusion. Had the creek been considered as a distinct class, and therefore sampled during the training step, it might have been correctly classified.

Poor classification may usually be reduced by adjustments such as modifying statistical parameters, eliminating ill-defined classes, establishing new classes, and/or selecting new or additional training sites. Several iterations may be required to achieve a specified level of accuracy. For the Harrisburg classification, the initial level consisted of less than 5 percent unidentified classes and 95 percent confidence of proper identification of the named classes.[11]

#5-67: The Interstate 81 roadway passing near Blue Mountain was only partially completed in 1972. One segment of the west side shows up as a black (linear) pattern in Figure 5-32D. Why is this feature likely to have been misclassified?

For the case we are considering, a final 2 percent error was accepted, after which no subsequent classifications of the 1972 subscene were conducted. This error is not, however, a direct measure of the classification accuracy that would result from a field check or comparison with maps and other independent sources of ground truth (see p. 256). A classification of the July 1977 Landsat pass over the same area is presented later in Activity 7 (Figure 7-13B).

#5-68: Compare the 1972 and 1977 classification maps. List five differences or changes evident in the 1977 scene. Give three factors responsible in part for these dissimilarities.

By participating in an unsupervised and a supervised classification, you should now have developed some understanding of what happens in a computer-assisted classification of Landsat data.

#5-69: Summarize in a key-word outline the principal steps followed in performing a supervised classification.

Microprocessor Systems: APPLE.[12] There is another end to this range of image processing systems. We have discussed the expensive and highly interactive approach exemplified by the IDIMS system. We have also looked at the less expensive but more awkward batch-oriented approach illustrated by the ORSER system. The other end of the spectrum, the inexpensive yet highly interactive approach, has always been an intriguing concept. Today the revolution in microprocessor-based personal computers is indeed making low-cost digital image processing systems a reality. Instead of high priced minicomputers and their elaborate peripheral equipment, or a large computer software system operating on still larger "mainframes," we have been introduced to the striking potential of the other end of the scale.

There are any number of personal microcomputers commercially available on the market today. You may have seen advertisements for such microcomputers as the Tandy Radio Shack TRS-80, the

[11] *Proper* in the sense that the classes selected have been correctly mapped. However, as will be seen in Activity 6, these classes are only as good as the training sites on which they are based—themselves often selected from maps containing inaccuracies. If these sites have been inadequately defined, and do not properly represent the real world, the validity and accuracy of the classification will be diminished.

[12] APPLE is the registered trademark for a series of microcomputers produced by APPLE Computer, Inc.

Commodore PET, and the APPLE. These and other microcomputers should not be seen as toys but as indispensable instruments for our serious scientific and educational endeavors. A number of commercial organizations have taken steps in this direction, and there are digital image processing systems already on the market.

One example of a microcomputer system is the APPLEPIPS (an acronym for APPLE-II Personal Image Processing System), which is scheduled to be marketed early in 1981. Like the IDIMS system, APPLEPIPS is a complete, self-contained image processing system capable of extracting information from imagery of all types, including multispectral data from Landsat.

APPLEPIPS is built around a standard APPLE-II microcomputer with 48 kilobytes of core memory, and APPLE's DISK-II, a microfloppy (5.25 in) disk drive. A standard color television set serves as the system's monitor, completing the system's minimum configuration at a cost of about $2000.

The APPLEPIPS system makes three levels of detail available to the analyst. The full 230 km^2 scene (LORES) fills two microfloppy diskettes and can be displayed quickly. The monitor displays 192 lines each containing 280 pixels, equivalent to a ground scene of roughly 230 square kilometers (90 sq. miles) or 60,000 acres. Each quadrant of that scene–approximately 59 km^2 (23 sq. miles) (MIDRES)–may be selected for more detailed analysis and display. The most detailed view (HIRES) is a 40 by 40 pixel display (5 km^2 or 2 sq. miles), where the emphasis is on spectral rather than spatial resolution.

The APPLEPIPS system has been designed to move and display image data as quickly as possible. For example, the MIDRES scene (96 by 140 pixels) can be loaded in four seconds, and a density slice takes only six seconds to appear on the TV screen. Thus, unlike other computer environments, the system does not put off the investigation. An investigator's time is most fruitfully spent in formulating the questions, not in waiting for the answer.

Two examples of stages in the analysis process with a microcomputer system are shown in Figure 5-34. A six-interval density slice has been performed on band 6 digital data for 2904-14552 (July 14, 1977) to produce a LORES display (192 by 280 pixels) (Figure 5-34A). This view assists the investigator in choosing a MIDRES quadrant (Figure 5-34B) in which to search for adequate training sites. At this stage a roaming frame is employed to delineate the HIRES (40 by 40 pixels) band 7 data set for this scene (Figure 5-34C). Most of the statistical analysis proceeds at this detailed level.

The colors assigned to the density levels (expressed as intensities) for each display level are:

Color	Intensity	Color	Intensity
LORES			
Black	0-22		
Brown	23-42	HIRES	
Lavender	43-48	Dark blue	0-7
Green	49-52	Light blue	8-10
Blue	53-56	Medium green	11-13
Gray-Blue	57+	Dark green	14-16
MIDRES		Brown	17-19
Black	0-19	Beige	20-22
Blue	20-34	Olive	23-25
Pink	35-44	Gray	26-28
White	45-5-	Slate blue	29-31
Orange	55-69	Light blue-gray	32+
Green	70+		

#5-70: Locate the LORES scene within the larger data set (more pixels) that was density-sliced into five intervals on IDIMS (Figure 5-31A). Match and compare any pattern similarities in equivalent areas at the two scales (but remember that the data sets were acquired on two different dates). Describe what you have noted. Also examine the NMAP's in Figures 5-20A&B. These are at a scale more similar to the HIRES rendition in Figure 5-34C. Try to colocate equivalent areas within the HIRES data set and the NMAP pixel distribution generated on the ORSER system (Figure 5-20B) for that date. Review also the IDIMS-produced classification map for the Harrisburg area (Figure 5-33) as well as the USGS Land Use Map (Figure 5-18) for that area and the high altitude aerial photo (Figure 5-23) and low altitude aerial photo (Figure 7-14). How well did you succeed in locating the HIRES image within the NMAP print? Can you make any sense of the density-sliced patterns in this image in terms of possible classes or features represented by the patterns?

At the HIRES stage of analysis, the researcher might create new pseudo-channels: the results of mapping the norm, creating a uniformity map, ratioing bands, or convoluting the image. The analyst then chooses two from among the original or pseudo-bands for color mapping. The first channel is mapped on the primary graphics image dis-

ORIGINAL PAGE
COLOR PHOTOGRAPH

Figure 5-34. Color-coded density sliced images produced by APPLE-PIPS program, Harrisburg subscenes: A. LORES; B. MIDRES; C. HIRES.

puters are especially suited to training a beginner in the basics of computer science and now are providing some experience in the fundamentals of remote sensing-related image processing. At present, of course, microprocessors cannot compete in data volume capacity or in versatility with larger systems. However, especially in today's real world of limited budgets, costs and capabilities must both be weighed. Microcomputers are well within the budgets of individual university departments; "micros" are already being used in local high schools as an introductory hands-on training tool! State and local governments can test the validity and value of an ongoing remote sensing program without extraordinary "up-front" expenses.

An inexpensive microcomputer image processing system, selling for thousands rather than tens or hundreds of thousands of dollars, can open up practical hands-on remote sensing experience to new students, to new disciplines, and to new directions. The affordable image processing system could well be the vehicle to break through the technology transfer barrier.

Another Approach to Classification

The methods described in the preceding sections have evolved into the conventional ways in which satellite remote sensing data are normally classified. However, some analytical alternatives have been devised to circumvent the use of either training sites or preliminary (candidate) feature delineation as part of the class identification and change detection procedures. For example, the LAND ANALYSIS procedure developed in Canada from the earlier ERTS ANALYSIS procedure (both by J.S. Schubert) provides geometric, radiometric, and signal rectification before any classification is done. Then, by acting on rectified, normalized data (including atmospheric absorption corrections), LAND ANALYSIS goes through a dichotomous key to separate land and water, then bare and vegetated surface, etc., continuing through the key to classify vegetation types, soil features, surface water quality, etc. In conjunction with a crop calendar, crop identification can also be done. The approach underlying this method is summarized in Table 5-5.

Such a system is based on the laboratory and field spectra of many classes of surface objects and features, checked against actual Landsat observations and field surveys in various parts of the world. This approach has recently been shown to be faster, and thus cheaper, than more standard procedures.

Perhaps the most fundamental difference is that concerning the use of statistics. Standard methods calculate statistics by which to separate the data classes. The data class bounds are adjusted by the analyst to fit his observations about the number of classes and their distribution. The data classes are thus related to the actual surface features through the analyst's experience. But, the classes are originally derived solely through statistical rules. The only constraints on the classification are the use of training sites and the analyst's empirical assessment of "goodness of fit."

In the LAND ANALYSIS procedure classes are not derived but are defined *a priori* from radiometric measurements. Class boundaries are determined by physical observations of the classes themselves as they appear to sensors in the field and in the laboratory. While statistics are calculated for some of the rectification parameters, a direct comparison of DN ranges of observations and those defined in the dichotomous keys (classes) leads to feature identification on a pixel by pixel basis. The procedure is therefore much faster on the computer and may be more accurate than the standard way. The apparent reason for this increased accuracy is that much of the scene variances are removed by rectification prior to classification; the feature or class variances are accommodated by appropriate range settings for each of the classes in each of the MSS bands. Also, running through the dichotomous key prevents class variances from confounding class identities. For example, removing all water pixels from classification of land features removes or partitions the water pixel variance from the total scene variance; eliminating bare surface from consideration of vegetation features further "purifies" variance, etc. In standard procedures class variance is not partitioned from the total or pooled scene variance. The range of DN's (or confidence limits) required for feature separation is thus larger.

The procedure especially designed for vegeta-

Table 5-5

DECISION FLOW

LANDSAT-CCT DATA TESTED	ANALYSIS	DECISION FLOW	PRINT MAP SYMBOL	DEFINITION
MSS7	WATER DISCRIMINATION	WATER? YES →	•	WATER
		NO ↓		
MSS5 & RATIO (MSS7/MSS5)	BACKGROUND DISCRIMINATION	VEGETATION PRESENT/ NO →	BLANK	BACKGROUND (SEE BELOW)
MSS7	BACKGROUND ANALYSIS	NO → BACKGROUND LOOK-UP TABLE/ → YES	/	WATER BORDER
			-	
		YES ↓	=	BRIGHT SAND
MSS5	IBP LEVEL 1 ANALYSIS (VEGETATION STRUCTURE)	IBP1 VEGETATION CLOSED? NO → IBP2 VEGETATION OPEN? NO → IBP3 VEGETATION SPARSE? LOOK-UP TABLE 3 →	:	SPARSE SCRUB
			;	SPARSE GRASSES
		YES ↓ YES		
MSS7	IBP LEVEL 2 ANALYSIS (VEGETATION STRUCTURE)	CLOSED VEGETATION LOOK-UP TABLE 1 / OPEN VEGETATION LOOK-UP TABLE 2 →	W	OPEN FOREST
			+	STEPPE
			x	GRASS LAND (OPEN)
RATIO (MSS7 & MSS5)	IBP LEVEL 4 (ENVIRONMENT)	(SPECIAL LOOK-UP TABLE) →	D	TREES DOMINANT
			(S)	SWAMP
			B	SHRUBS DOMINANT
			G	GRASS DOMINANT
			(M)	MARSH
2 DATE COMPUTER OVERLAY RATIO	IBP LEVEL 3 (PERSISTENCE)	VEGETATION PRESENT? (GROWING SEASON) NO →	BLANK	BACKGROUND (SEE BELOW)

VEGETATION CLASSES (GENERAL)

CLASS	SYMBOL	DN VALUE RANGE† MSS 7	DN VALUE RANGE† MSS 5
1. SHORT GRASS/MARSH	M	7–10	<15
2. SPARSE SCRUB, SPARSE GRASSES	: ;	11–21 11–21	15–34 34–50
3. STEPPE	+	22–36	15–34
4. SEASONAL GRASSES	G	22–26	<15
5. DECIDUOUS FOREST	D	27–36	<15
6. EVERGREEN FOREST	E	11–14	<15

†ALL VALUES RADIOMETRICALLY NORMALIZED TO A STANDARD SCENE

BACKGROUND CLASSES (NO VEGETATION)

CLASS	SYMBOL	DN VALUE RANGE† MSS 7	DN VALUE RANGE† MSS 5	RATIO RANGE* MSS 7 x 10 / MSS 5
1. WATER	.	0-6	–	–
2. WATER BORDER (UNVEGETATED)	-	6-11	14	–
3. WATER BORDER (VEGETATED OR ORGANIC)	/	6-8	<15	–
4. EXPOSED SOIL, SOME ROCK	--	11-27	>55	OR <5
5. DRY SOIL, SAND, CONCRETE	=	27	>55	OR <5

*ADAPTED FROM SCHUBERT, J. S. AND N. H. MACLEOD, VEGETATION ANALYSIS WITH ERTS DIGITAL DATA: A NEW APPROACH, UNPUBLISHED

tion analysis attempts to classify Landsat spectral data successively into the hierarchical levels of the International Biological Programme (IBP) system of classes. Decision tests which closely parallel the IBP decision categories have been established. The digital values used in the decision processes are from ground spectral measurements for vegetation classified by the IBP system, or when field data were not available, from a sample of MSS radiometrically normalized digital values for classified test sites. This supervised classification does not require current ground-truth data to perform vegetation analysis within the regions for which IBP categories have been defined. For these regions and for regions with similar vegetation, results obtained from the LAND ANALYSIS system classification of different dates compare with ground survey results very successfully. However, classification for regions in which IBP categories have not been determined are only successful at the higher hierarchical levels.

The IBP hierarchical levels are : (1) density of vegetation, (2) lifeform or structure of vegetation, (3) seasonal persistence, (4) functional or environmental relationship, and (5) species associations. The first two hierarchical levels in the system, density and lifeform, are related to the optical character of the plant communities observed. The third level of information, seasonal persistence, is measured by changes in optical parameters with time, just those parameters observed in repetitive coverage by the ERTS MSS system. The combination of MSS data and IBP classification is, therefore, an optimum one.

The radiances of some features interact in a manner which makes the sensor "see" an impure signal. This was discussed earlier in regard to boundaries but not in relation to compound features. A leaf observed against a black background will appear to have a lower reflectance than when observed against a white background. About nine average leaves piled one on the other are needed to overcome the background difference. This number of leaves is equivalent to a Leaf Area Index (LAI) of 9. In nature one rarely finds an LAI greater than 6. Thus, the background against which vegetation is observed from space affects the radiometric measurement of the vegetation. (It is interesting to note that one can predict that algae [phytoplankton] are not observable in waters whose bottom is dark, as in bogs, swamps, and deep ocean water, unless the cell population is very high, equivalent to an LAI of about 2. Observation bears out this prediction.)

The background influence is mentioned here as a factor which is explicitly taken into consideration in the LAND ANALYSIS design. However, the nonuniformities of soils at test sites (and all other places), in terms of both color and degree of hydration (wet soils are dark in bands 6 and 7), are included in the feature variances used in maximum likelihood and other such standard analytical procedures. This may lead to errors of commission and omission in feature classification.

Additional Examples of Classified Scenes

There is as much variety in classification maps as there are varied terrains on the face of the Earth. We shall close this activity by briefly looking over five more classified subscenes, all east of Harrisburg, that depict some of this terrain diversity. The main classification theme sought in each subscene is, in order, (1) defoliation, (2) coal wastes, (3) crop types, (4) coastal lands, and (5) urban development.

Defoliation. The first of these maps was produced on a General Electric Image 100 (I-100) interactive system located at Goddard. This computer system uses the parallelepiped classifier routine to establish themes (classes). The subscene (512 × 512 pixels) shown in Figure 5-35 covers about three quarters of the same July 8, 1973 Landsat subscene (Figure 4-6) around Hazleton, Pa., examined in Activity 4 as part of a photointerpretation mapping exercise (see Figure 4-12 and pp. 123 to 126). An unsupervised approach to classification was followed such that the themes in the legend of Figure 5-35 were initially displayed without knowledge of identity and then labeled by comparison with the mapped categories deduced from Figure 4-12.

#5-71: Locate the area in Figure 5-35 within the subscene in Figure 4-12. Which version, the I-100 computer display or the EROS Data Center photo product, seems superior? Try to reason as to why.

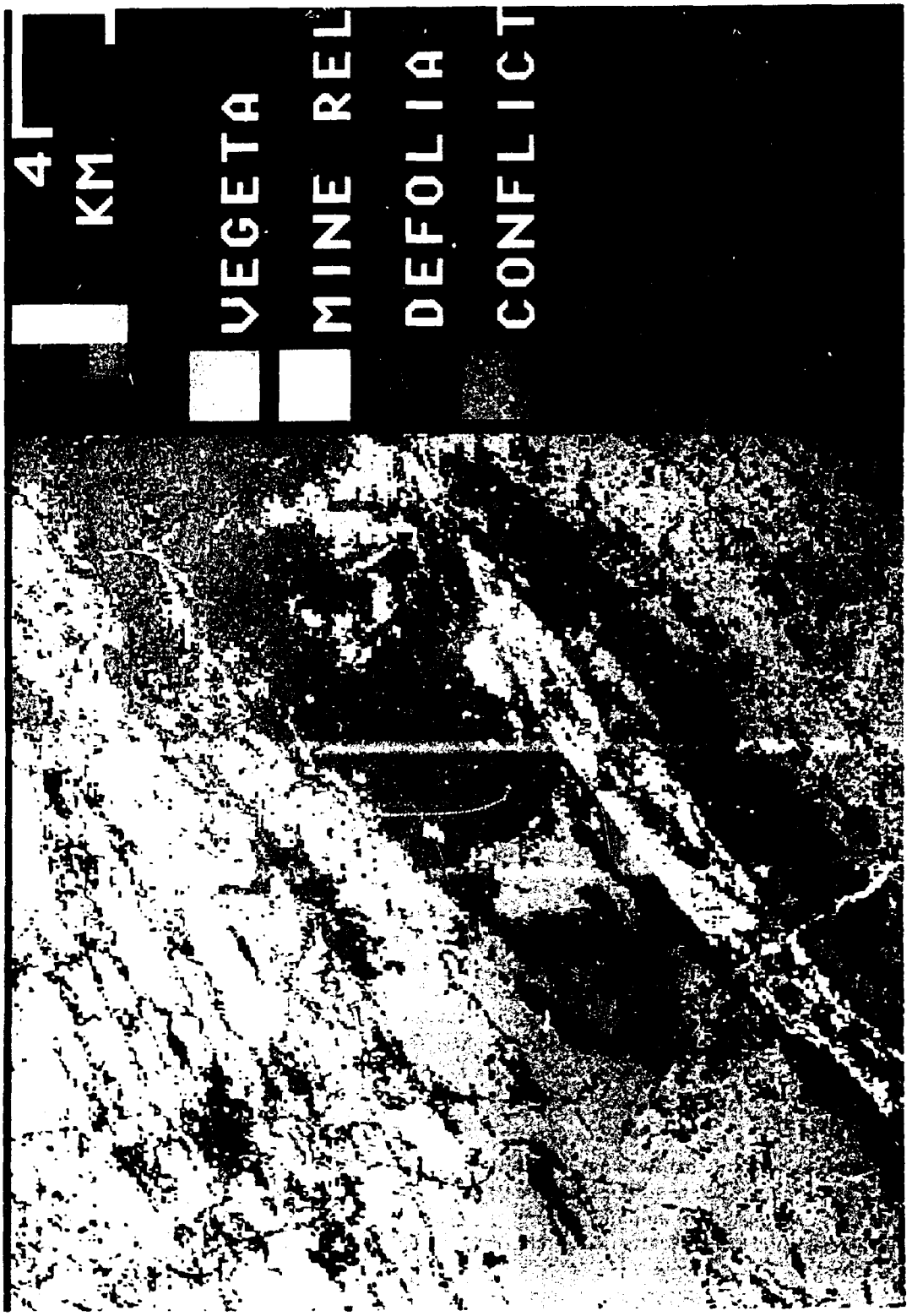

Figure 5-35. Classification of 4 cover types around Hazleton, Pa., made on Image-100 system.

#5-72: You have already been asked to pass judgment (p. 126) on the relative merits of your photo interpretation map versus the computer classification. Are there areas in the computer version that might be grossly misclassified or otherwise incorrect? Specify.

#5-73: The maroon themes are labeled "conflict" (syn., confused, misclassified, unidentified). By inspecting Figure 4-12 (see also Figure 4-13), and from general experience, can you name several land cover categories that appear to be represented by some of the pixels in this theme?

Coal Wastes. A supervised classification on the ORSER system, based on map data and field inspection of a smaller subset within this scene, was acquired during an independent study of coal wastes conducted by Pennsylvania State University staff. A portion of the printout map from the study is reproduced in Figure 5-36.

#5-74: Locate the area of this map in the 1-100 version (Figure 5-35). Then reexamine Figure 4-12 to see if there are patterns that might correspond to the categories listed in the legend of Figure 5-36. What discrepancies or uncertainties did you discover?

#5-75: Explain the large all-white background for the legend categories. What does it represent, and why was this done?

In their report on this project, the Penn State staff point to difficulties in separating the category *refuse* from *silt*. In the field, several different types of coal material could be recognized; coal piles waiting for shipment, wastes from crushing and other processing, exposures on strip mined surfaces, and coal sludge in washing basins.

#5-76: Account for these difficulties.

#5-77: How might reclaimed land be distinguished from other coal-related surfaces?

Crop Types. A supervised classification of an agricultural terrain, characterized by two dominant field crops, fallow land, forest cover, water, and several small towns, was conducted on IDIMS. The area considered, shown in a false color enlargement in Figure 5-37A, taken from the July 1977 Landsat overpass (2904-14452, Figure 4-11), is located around the Chesapeake and Delaware Canal in the northern Delmarva peninsula (see Figure 4-16B). Ground truth (mainly crop identification of some twenty fields) was supplied for the July 1977 Landsat scene by the New Castle County agent for the Soil Conversation Service and by staff of the Agricultural Stabilization and Conservation Service (ASCS) office in that area (see pp. 244 to 245). The resulting classification map and legend are reproduced here as Figure 5-37B. Although a field check on accuracy has not been made, it is believed that in this case at least 90 percent of the pixels are correctly identified with the classes established. However, when this classification technique was applied to the Lancaster, Pa. farm country studied earlier (see Figure 4-16A), the resulting map did not appear realistic or valid, and a much lower accuracy may be assumed because of the notably smaller sizes and more irregular shapes of the crop fields there.

#5-78: If you consult a map of this local area, you will conclude that most of the larger lavender patterns are indeed associated with towns and villages. However, there are numerous smaller clusters of lavender pixel patterns that are suspect. If some are real, what might they be? If some are "false alarms," can you devise an explanation for this?

#5-79: Can you give a reason why many of the regular shapes (mostly rectangles) of the corn and soybean fields so evident from Figure 4-16B do not show up as regular in this classification?

This classification of agricultural lands should give you some insight into a major practical use of Landsat in monitoring and forecasting production (area X yield) of several of the main crop types that serve as worldwide food staples. The most ambitious project in the 1970's for testing the value of remote sensing in predicting global food supplies has been the LACIE (Large Area Crop Inventory Experiment) program, conducted jointly by NASA, the U.S. Department of Agriculture, and the U.S. Weather Bureau (NOAA).[13] In this

[13] See Review by McDonald, R.B. and F.G. Hall, *Global Crop Forecasting* Science, vol. 208, pp. 670-679, May 16, 1980.

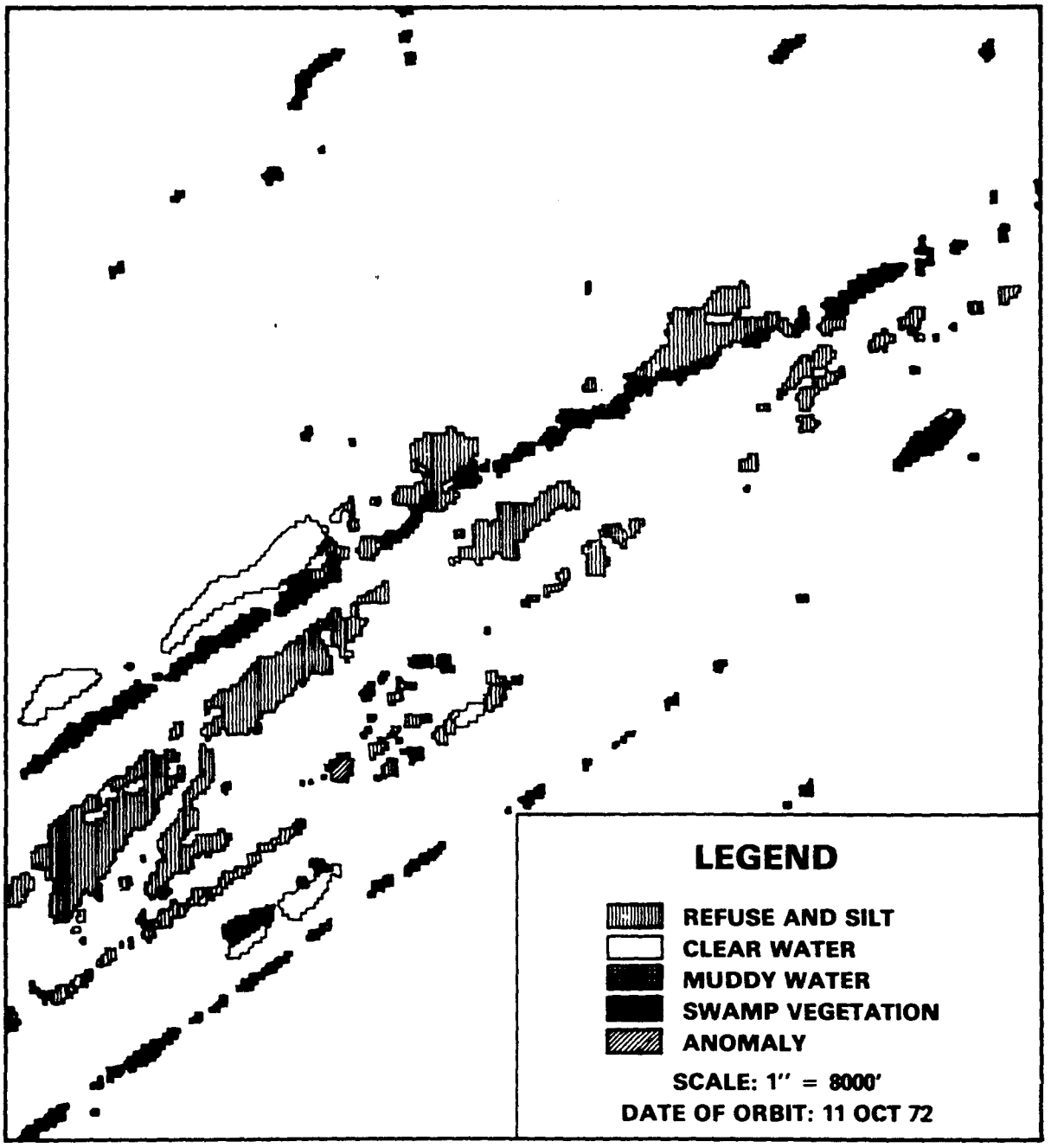

Figure 5-36. Classification of coal waste area southeast of Hazleton, Pa., made on ORSER system.

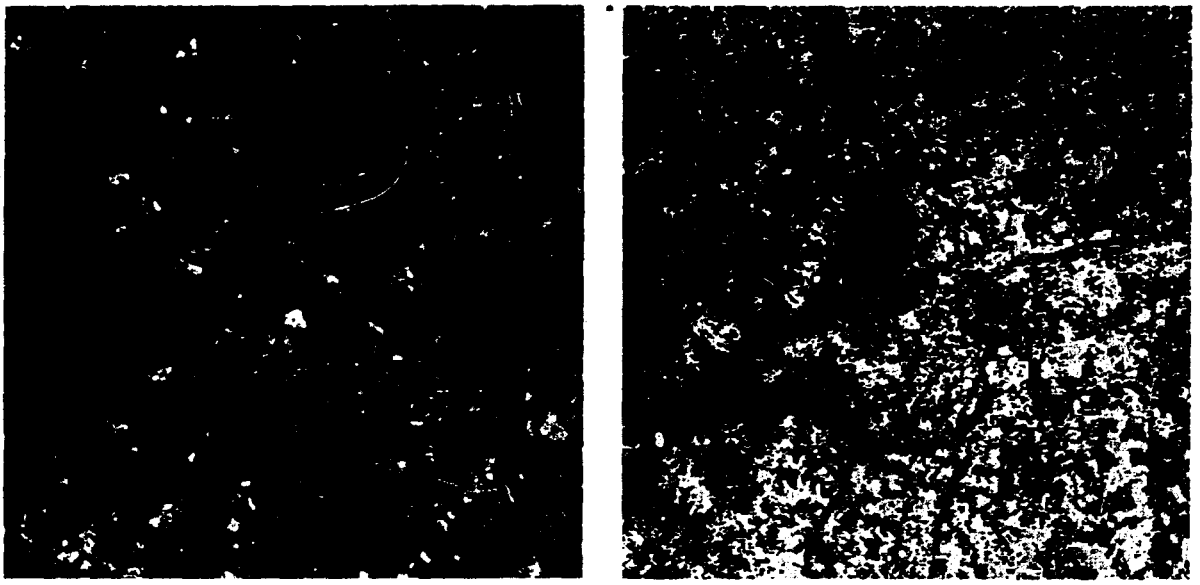

Figure 5-37. Middletown, Delaware - Elkton, Maryland Landsat subscene. Left: Computer-enhanced false color composite. Right: Classification of subscene.

program, data from Landsat, meteorological satellites, aircraft, and conventional ground sources have been used to estimate the annual yield (productivity) of winter wheat in the principal producing countries (including the United States, Canada, Russia, India, Australia).

Landsat observes which fields are planted in wheat, so that acreage can be determined, and also provides information on stages of growth. Independent estimates of yield per acre are derived from rainfall and other weather-related data obtained by NOAA satellites as correlated with surface stations. Because of the vast areas involved, a sampling strategy has been devised to reduce the total area to selected regions and to rely on representative training sites. The key to a successful estimate lies in making observations at several times during the growing season, in other words, to correlate spectral signatures with the crop calendar (see p. 275). A goal in this first experimental large-scale coordinated effort among nations to monitor the annual output of a basic staple is to achieve a 90 percent accuracy level for winter wheat acreage 90 percent of the time in the foreign countries.

#5-80: Suppose you are appointed to design the experiment to determine the feasibility of large area crop inventories from Earth-observing satellites. Make a list of the important variables to consider and the measurements required. Try your hand at laying out a flow diagram showing experimental design in a logical sequence.

Coastal Areas. In Activity 4, we made an attempt to recognize one or more wetlands classes in the Barnegat Bay area along the Atlantic coast of New Jersey. It was evident from the photo images that the land/water interfaces in the brackish lagoons and bays could be fairly well detected in the infrared bands (MSS 6 and 7) and in the false color composite. Silt in the estuaries and offshore in the Atlantic is most easily seen in MSS bands 4 and 5. However, some of the classes of interest on the land proved difficult to recognize. Figure 5-38 includes a supervised IDIMS classification of the coastal region of New Jersey from Atlantic City to Barnegat Bay. The color key in this figure designates thirty-eight subclasses, some of which are gradations within a single class. However, the eye cannot distinguish many of these subclasses in the scaled-down map as reproduced in the figure. This is a common problem in color-coded maps and can be alleviated by making enlargements and using "zip tone" patterns within different colors.

#5-81: Return to the New York/New Jersey scene in Figure 2-1. With the aid of the IDIMS classification, center your attention in the Landsat images on the Barnegat Bay area. How many of the computer-mapped classes can you now recognize in the image?

#5-82: Which classes might you have misidentified or failed to separate in the photo images?

In the lagoonal wetlands behind the offshore bars and islands on which Atlantic City is built, the terrain consists of open water, mudflats, and brackish marshes laced with drainage channels. Several plant types are characteristic of this ecosystem along the mid-Atlantic coast: chiefly *Spartina alterniflora* and *Phragmites* in the salt marshes; eel grass, widgeon grass, and sea lettuce in submerged saline aquatic environments. Different wetlands vegetation, mainly a preponderance of fresh-water species (spatterdock, wild rice), occurs along the flood plains of rivers such as the Mullica. Ground- and air-surveyed wetlands maps usually show a meaningful subdivision of the principal vegetation communities. Under favorable conditions, it is possible to recognize and delineate some of these classes in wetlands classifications made from satellite observations. An example of this more refined classification will be considered in Activity 8. (p. 321).

Computer processing has proved successful, under favorable circumstances, in delineating water quality levels in lakes, rivers, estuaries, and marine environments observed by Landsat. The water quality conditions that can be sensed are suspended solids, turbidity, algal blooms, some types of nutrients, plankton, and chlorophyll (its presence, and sometimes its concentrations under certain conditions in regions of high biological activity). Trophic states (degree of eutrophication) in lakes, which depend on interactions of several of these and other parameters, can also be assessed. Generally, water quality effects related to particulate matter will show up best in MSS bands 4 and 5 (Figure

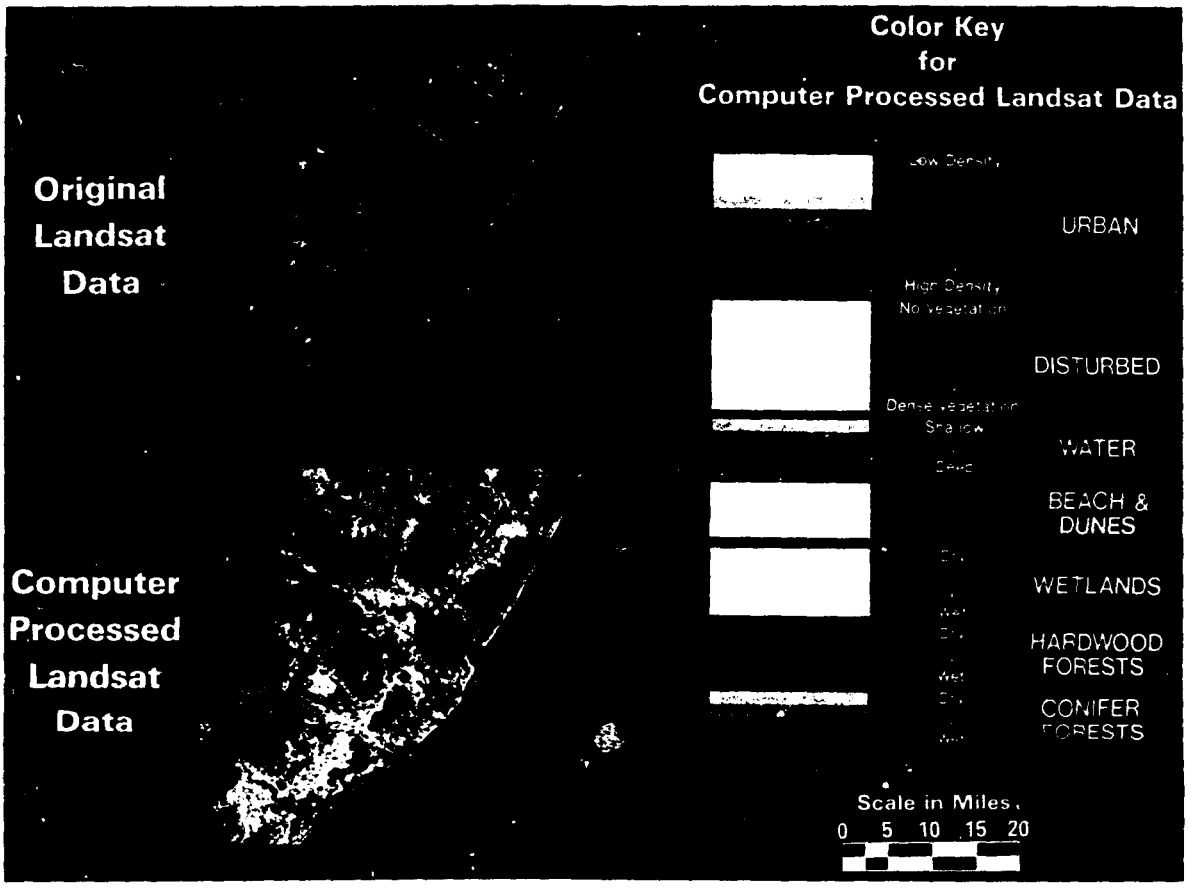

Figure 5-38. Computer-enhanced subscene (top) of New Jersey coastal and inland areas, and computer-processed classification (bottom) of these areas. The color key defines 38 classes.

4-20), but chlorophyll determinations in suspended organic matter make use of band 6 as well (calculations based on some regression models may include band 7). To derive quantitative results for mapping water quality parameters over wide areas, a comprehensive on-site sampling program is required; field measurements and collection of samples for laboratory analysis close to the time of a Landsat overpass usually lead to the best estimates.

A part of the Chesapeake Bay at its head in northern Maryland was classified on IDIMS in terms of several categories of water. The data were acquired on May 28, 1978. Seven water classes are depicted in Figure 5-39. Note that five refer directly to broad limits of turbidity in waters from training sites in the Bay or along the Bush River. The class *river water* was established by training on the Romney Creek embayment; estuarine waters in other rivers are similarly classified, but the bay water west of Spesutie Island appears to be misclassified. In this rendition, land categories other than wetlands are masked out (not identified) and assigned a dark blue-black color in the relevant areas.

As Landsat and similar systems become operational, the computer will play an increasing role in conducting a variety of analyses for applications to water resources. The diagram in Figure 5-40 shows implicitly that digital data processing must be incorporated into the analysis procedure in two prominent ways, first, to classify the types, location, and extent of water bodies and related land surfaces, and, second, to integrate these derivative information categories into dynamic models that provide up-to-date estimates for various parameters relevant to making timely management decisions. Although analysis can proceed along two separate pathways, namely by following movement of water in rivers through watersheds and by observing the status of water collected in discrete bodies (lakes, coastal waters, open oceans), the end parameters may be interrelated so that, by comparison, each set of model outputs supply new knowledge pertinent to the other.

Urban Growth. As a final example of a Landsat-derived classification, we shall consider the delineation of land cover themes within a major metropolitan region. We shall then demonstrate how this information may serve as updated input for defining areas of rapid growth along the urban fringe zone. Satellite observations of this type are even now being evaluated as a supplemented data source for charting changes or expansion of population densities during intervals shorter than the decennial census. Such demographic knowledge may also be put to effective uses by regional planners.

The subscene selected for classification is centered around Philadelphia, Pa., as scanned by Landsat-3 on June 11, 1976 (30098-15013). Training sites for a classification were picked from aerial photos (Figures 2-7A and 2-7B), several pertinent thematic maps, and the familiarity of the analyst (W. Campbell, a native Philadelphian) with much of the region. The classes to be mapped were chosen from earlier experience gained at Goddard in classifying Detroit, Mich., Washington, D.C., and Austin, Tex., as part of a pilot project carried on jointly with the U.S. Bureau of the Census.

In this previous work, the major urban classes most readily identified in Landsat imagery were industrial, commercial, and up to three levels of residential, each of which is characterized by some typical range of population density. In general, these classes also separate along lines of building density, best expressed as relative proportions of rooftops, streets, lawns and trees, and other internal features. At Landsat resolution, such features are spatially unresolved and are thus subject to the complexities introduced by mixed pixels (pages 82 to 88). Generally, however, the classes themselves (and, indirectly, the population densities therein) in a large metropolitan region in the eastern United States may be determined from the relative contributions of the inorganic building materials (concrete, asphalt, roofing, metal, etc.) and vegetation (trees, lawns, parks) components characteristic of the urban environment. In a processed Landsat color composite, an industrial area consisting of flatroofed factories, storage yards, rail lines, roads and the like will appear as dark bluish-gray owing to higher reflectances in bands 4 (and 5) and almost no vegetation-related reflectances in bands 6 and 7. Conversely, an affluent residential neighborhood is structured along very different lines, namely widely spaced, sloping-roofed homes surrounded by lawns and/or trees, and narrow access streets, and shows up in various reddish tones. The proportion of the surface covered by buildings, parking lots, etc. decreases

ORIGINAL PAGE
COLOR PHOTOGRAPH

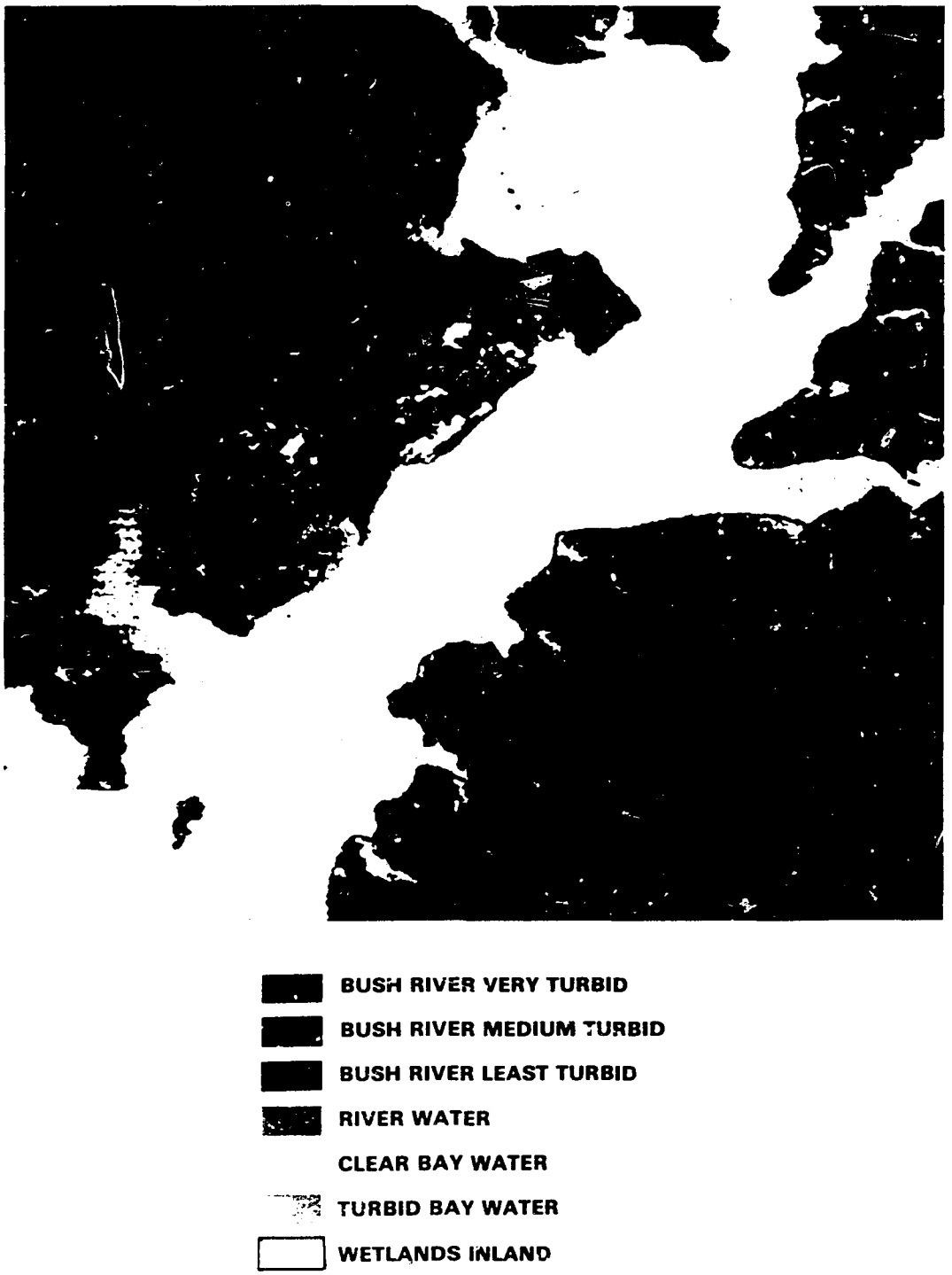

Figure 5-39. Classification of headwaters of the Chesapeake Bay, showing various water quality categories.

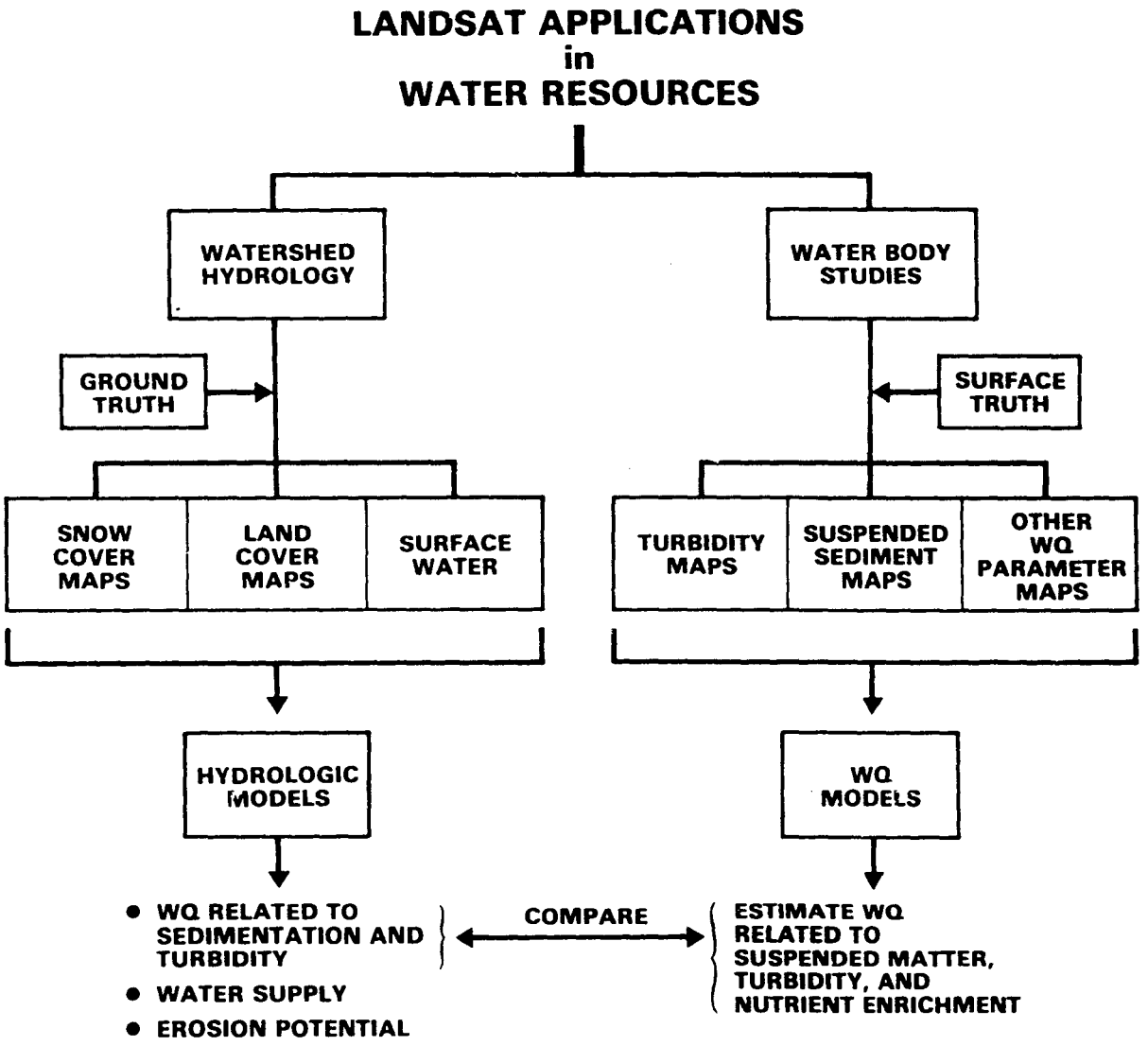

Figure 5-40. Flow diagram showing analysis sequence for deriving hydrologic and water quality models using Landsat data.

and the proportion of trees, shrubbery, grass, etc. increases in the general sequence: Industrial→commercial→high residential→medium residential→low residential→rural. In early fall, for example, a Landsat false color composite image of a city such as Philadelphia (Figure 2-1) would show distinctive color patterns. In broad terms, these range from dark bluish-gray in the inner city and along major transportation arteries, to lighter bluish-gray tones in commercial districts (office buildings, shopping strips and centers), to slightly pinkish-blue through progressively more reddish tints as high to moderate density city residential neighborhoods are gradually replaced by more sprawling and scattered suburban communities in the outlying districts.

The Level I classification of Philadelphia presented in Figure 5-41A is in one sense a color-coded thematic expression of the kinds of classes listed in Table 3-3. An attempt was made to identify them by their characteristic blue and red tints in a false color composite. The following classes were set up:

Class	Color Code
Industrial (and some commercial)	Red
High Density Urban (mainly commercial and row house/apartment residential)	Yellow
Medium Density Urban (commercial apartment; single dwelling residential)	Purple
Low Density Urban (houses; scattered commercial)	Orange
Open Land (bare field; dumps; sand pits, excavations; miscellaneous)	Gray
Water	Blue
Forests; heavily wooded residential	Dark Green
Grass; low-density trees; parks; cemeteries; farmland	Light Green

Inspection of this classification map suggests that it is a generally realistic portrayal of the overall distribution of building (population) densities around Philadelphia. However, several glaring misclassifications cast some doubts on its accuracy. For example, the ability to separate the Schuylkill River course from its surroundings seems to diminish rapidly upstream. Where this river narrows as it swings to the northwest, its theme color changes from blue (for water) to yellow (high density urban). While this does not seem to fit the expected situation in a meaningful way, the incorrect classification results in part from the presence of waterfront factories, mudflats and cleared, barren flood plain, and riprap (rock boulders used to stabilize river banks) in some upstream segments.

A section of the classification that depicts part of inner Philadelphia along the Delaware River and the industrial and residential areas on the New Jersey side is enlarged in Figure 5-41B. Some classes in this rendition may be compared directly with easily recognized urban units in the high resolution aerial photo (Figure 2-7B) examined in Activity 2 (review question #2-28).

#5-83: Locate and give the class name in Figure 5-41B that corresponds to: (a) Factories/warehouses and docking wharves along Delaware River; (b) Nearby U.S. Navy Airfield; (c) Franklin D. Roosevelt Park; (d) JFK Stadium; (e) Railroad yards; (f) Interstate 95 as it turns north; (g) Row houses in downtown residential section; (h) Petroleum Tank Farm.

#5-84: By selecting a number of individual pixels (or a continuous group of pixels assigned the same class name) that you can associate with recognizable features in Figure 2-7B, comment on the general degree of correlation between the classes established from the Landsat data and their specific representation in the real world. In particular, do you think that the quality of classification and the degree of accuracy estimated by comparing pixels with aerial photo classes is of sufficient merit to have practical utility? Be specific.

Your response to the last two questions has, most probably, convinced you that there are obvious limitations to a Landsat classification, especially if details (small individual surface features) are germane to interpretation and application. One intuitively feels uneasy when various different constituents are "lumped" together in

ORIGINAL PAGE
COLOR PHOTOGRAPH

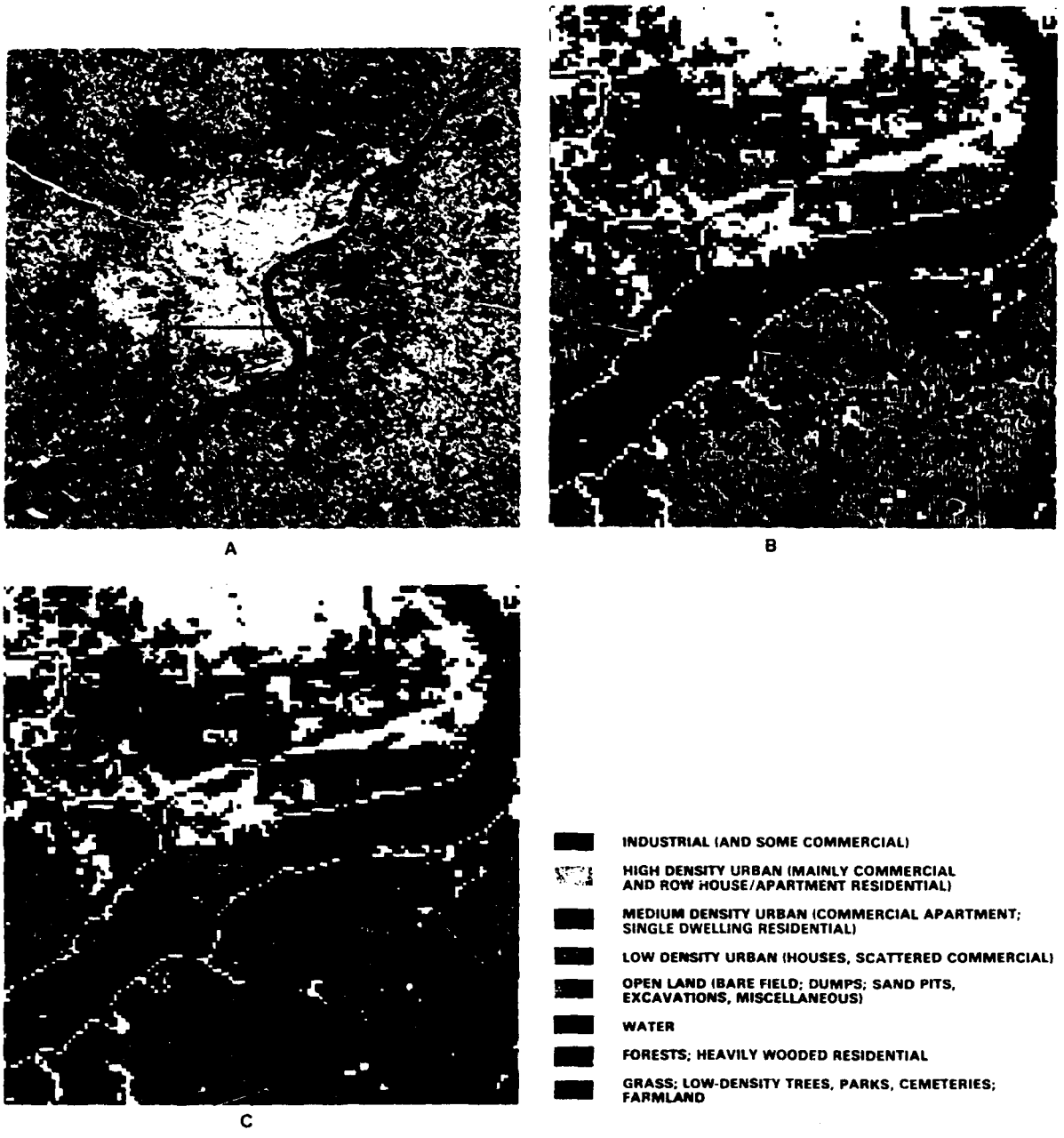

Figure 5-41A-C. Classification showing urban categories around Philadelphia, Pa.

some single, generalized category or class. An obvious solution would be to reclassify the scene after expanding or subdividing the number of classes, in effect, "cleansing" certain classes of spectrally similar but often unrelated features.

This purification of one class was attempted on the same data set shown in Figure 5-41B. Examination of Figure 2-7B indicates that, visually at least, the railroad yards constitute a distinct feature having a more or less homogeneous spatial character. Several training samples were specified from the sets of railroad tracks below Franklin Field. A new map containing the additional class – rail yards, in white – is shown in Figure 5-41C.

The results are clearly disappointing. Although the railroad yards from which training sites were selected are now singled out, similar yards west of Roosevelt Park are not assigned to the new theme. However, this white-shaded theme now appears fairly consistently along the river shorelines and within much of the downtown sections occupied by row houses.

#5-85: Try to explain this unanticipated result. What might be done to reduce the confusion?

Assuming you answered, or at least thought about, this last question, let's delve deeper into the implications of the misclassifications that led to the confusion. An attempt to improve the classification was made by a more judicious selection of training sites, relying even more on low altitude aerial photos, followed by a data point transformation through Canonical Analysis. The results continued to be disappointing. Although several newly established classes were correctly mapped, some of the previously classified areas were erroneously reassigned to the new classes. For example, the railroad yards were better defined just north of the river and were eliminated from the class of row houses (FTR, or Flat Top Roof class), but still were not picked out west of Roosevelt Park. Also, a new class called Tank Farms (oil storage) was properly identified at three locations but the interstate freeway passing through the subscene was then mislabeled as tank farms.

The causes of misclassification can often be deduced from the statistical output obtained during classification. Figure 5-42 contains excerpts of the actual numerical and graphical data printed out during the Maximum Likelihood classifying procedure on IDIMS. It will be instructive to examine some of these data as quantitative indicators of the efficiency of classification. The relative homogeneity of the classes Flat Top Roof (FTR), Railroad (RR), Residential (RES), and Industrial (IND) are depicted by histograms of the frequency distribution of pixel reflectances scale from 0 to 100 percent truncated to fit the diagram (plotted on the abscissa; ordinate scale refers to [variable] number of pixels in the sample). Compare the histograms for FTR and RR (A and B). Both show very similar shapes and spread of values. This is confirmed by the means and standard deviations for each of the four MSS band reflectances (remember: Channel 4 = MSS 7; 3 = 6; 2 = 5; 1 = 4). The standard deviations, in particular, are relatively small, also suggesting little variation in the defined class. Some information about variability is provided by the Variance-Covariance Matrix. This matrix specifies the concentration of data points about the mean vector in the multivariate space in the same manner that the variance alone specifies the concentration of data points about the mean in univariate space (p. 422). Recall from p. 173 that the diagonal records the variance of each band by itself and the values off-diagonal refer to covariances (bands 1 to 2, 2 to 4, and so forth). Large values imply strong positive or negative interband correlation. However, more readily interpreted information is contained in the Correlation Matrix, in which variance-covariance values are scaled (normalized) so that each variance becomes unity and covariances range from 0 to 1.00. Numbers approaching 1.00 or -1.00 indicate strong cross-correlation and also may express the influence of higher standard deviations. Strong cross-correlation reveals band redundancy, which means that both bands are measuring similar variation and either band would have sufficed to obtain representative reflectances. In general, the best training sites for any given class are those with small standard deviations (or variances) and low values in the off-diagonal positions of the Variance-Covariance and Correlation Matrices.

The data for classes FTR and RR are so alike that separation by spectral characteristics will be difficult from values supplied by the MSS on Landsat. Better spectral resolution should help but, more probably, improved spatial resolution that picks up distinctive patterns (rectangles/squares for row houses and lines for railroad tracks) would be

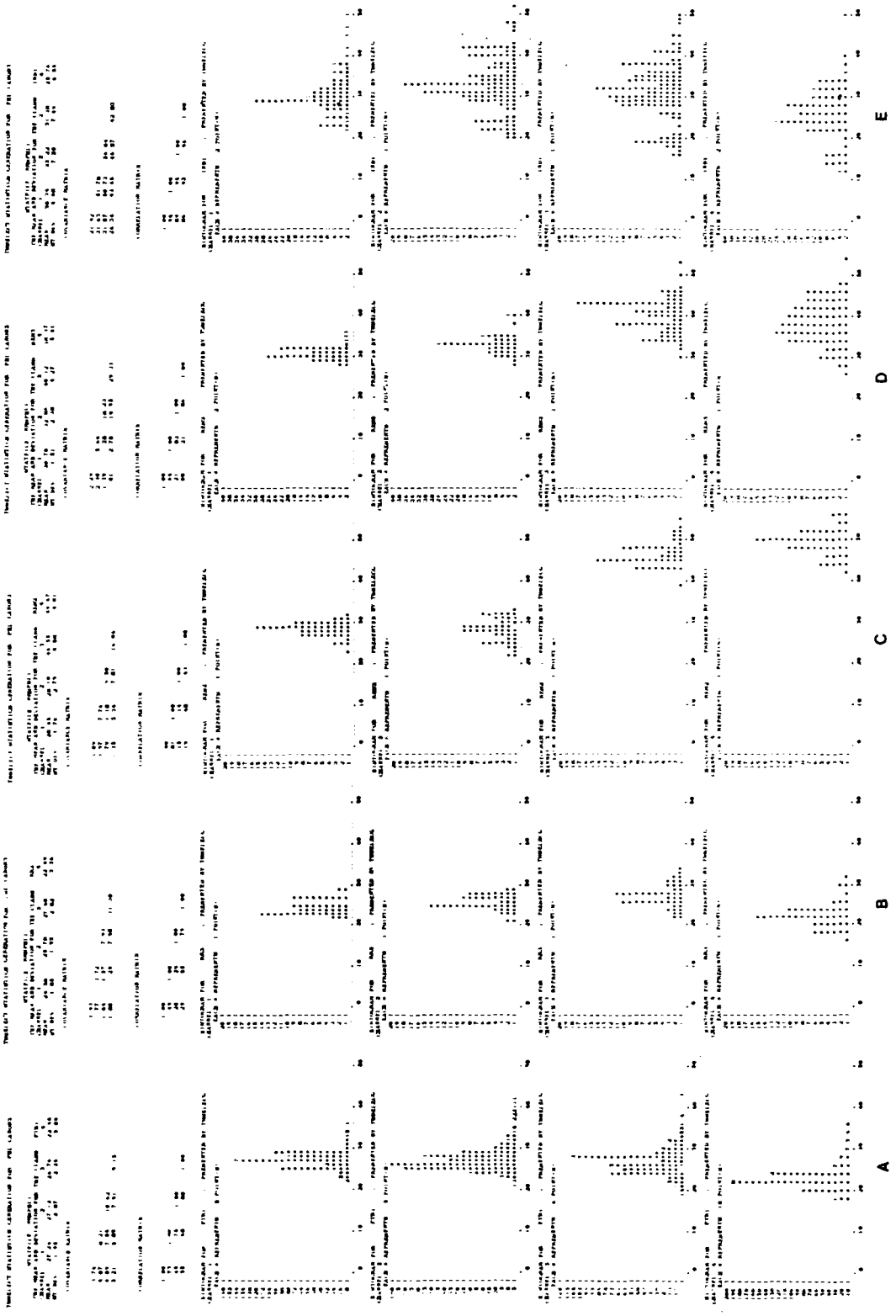

Figure 5-42. Statistical data for Philadelphia classification.

required to distinguish between the two classes.

A different situation exists with the two training sites chosen to represent the class RES (C and D). At first glance, the numerical data seem to mark each site as statistically acceptable and indeed they are valid from that standpoint. Both sites show nearly identical means and standard deviations for channels 1 and 2 (bands 4 and 5) but the means are distinctly different for channels 3 and 4 and the standard deviations are higher. Moreover, similar variations are noted between these first two sites and two other RES sites. When data for all four training sites were lumped together to comprise the defining statistics for the single class RES, the final classification map contained large areas correctly identified as residential. But, sporadically distributed smaller areas were mixed with other classes (e.g., commercial) such that comparison with the aerial photos indicated evident misclassifications. The problem here was that the more or less homogeneous individual training site samples were representative of a much more variable general class. The variation was induced mainly by the variable amount of vegetation (mostly trees and some grass). Some areas of the scene in downtown Philadelphia consisted of stores and other commercial buildings intermixed with enough vegetation to begin to look like residential areas. To get a better classification of RES, it might have been further subdivided into Urban Residential - Low V (low vegetation) and Urban Residential - High V (abundant vegetation), with more stringent limits on the allowed percentages of vegetation. That class probably overlaps into the general class of Medium Density Residential in the original classification, which usually implies suburban residential in part, except for its location in the inner city. In places, also, Urban Residential Low V would probably grade into the class Commercial (not specified uniquely in the original classification), especially in sections of the city that have been landscaped by the city, merchants, etc.

The class designated IND(E) illustrates further difficulties. Inspection of the histograms shows a high variability (large standard deviation) with a pronounced bimodal and trimodal distribution of pixel reflectances. The values for the Covariance and Correlation Matrices are also high. The standard deviation exceeds 5.00 for three of the four channels. As a rule of thumb, a standard deviation greater than 5.00 is cause to suspect the quality of a training sample as representative of a *desirable* class. However, this conclusion should be tempered by one's understanding of the nature of a defined class. In the real world, extensive variability would be expected for a class such as IND. Industrial facilities are characterized by buildings of many sizes, with varied roofing, by parking lots and diverse outdoor features (storage bins, piled-up materials, etc.), and by considerable variation in vegetation cover. Without a high spatial resolution, it is extremely difficult to compensate for the broad range of spectral variation expected from this diversity of industrial facilities within what is conveniently grouped into a single class name. The likelihood is high that many building complexes and other assemblages of ground features not used for industrial purposes could fall within the spectral limits of the training sites chosen for IND.

The bottom line to the arguments and conclusions just drawn is that the Landsat MSS, with its current spatial and spectral resolution, is generally an inefficient tool for classification of areas consisting of many different and variable individual ground features. An urban/suburban metropolitan area is a prime example of this statement. Improved resolution available now from the Landsat RBV and anticipated for the new Thematic Mapper (TM) on Landsat-D (see p. 378) will certainly help to alleviate this shortcoming. But, for some purposes, resolutions characteristic of aerial photos may be mandatory. However, as will be espoused in the next 3 paragraphs, certain other classification tasks for metropolitan areas can already be performed by the MSS.

Despite the serious shortcomings suggested by this Philadelphia example, the pilot studies on urban area classification reported to date indicate that valuable information may be gathered from Landsat data. In support of this contention, an overall accuracy of 73 percent was achieved in defining residential areas within the urban fringe zone to the south and east of Washington, D.C.[14] The classification derived from an April 1973 Landsat scene was compared, point by point, with a map sheet for the area from the latest Metropolitan Map Series (MMS) prepared by the U.S.

[14] Christenson, J.W., J. B. Davis, V. J. Gregg, H. M. Lachowski, and R. L. McKinney, *Landsat Urban Area Delineation*, Intralab Project 75-3, GSFC, 1977.

Bureau of the Census. Some 180 residential subdivisions were identified. Changes in the nearly three years since the 1970 census were readily detected. Most of these relate to new housing developments at which natural vegetation has been removed and new plantings have not yet grown to the extensive tree cover characteristic of older neighborhoods.

This conversion of land use to some recognizable residential category is of vital interest to both the Census Bureau and the citizens of a region. Federal and state funds for a variety of projects are commonly allotted on some population density-distribution formula. A base unit within small geographical areas called Enumeration Districts (ED) (themselves key components in the Standard Metropolitan Statistical Area [SMSA] set up for each of nearly 200 cities in the United States), is specified in terms of population density. In the simplest case, the base units in a fringe zone are arbitrarily divided into urban area (UA) and rural area (RA). Portions of an ED containing 1000 or more persons per square mile are designated UA's. Before 1980, the UA's had been reviewed for boundary changes, or RA's reclassed to UA's, only during decennial census years, i.e., once every ten years. Congress has now mandated intercensal UA updates, at least every few years, in fast growing SMSA's.

Current conventional methods prove too costly and inefficient. The Bureau of the Census has therefore turned to a combination of satellite and aircraft remote sensing techniques together with appropriate statistical sampling procedures on the ground to estimate changes in status within the urban fringe zone. The stated goal is a 50 percent reduction in the size of the fringe zone and in the number of ED's that must be field checked. Success would lead to significant savings in time and money.

#5-86: Explain how a classification at the levels attained in the Philadelphia example might meet the goal set by the Census Bureau. (Hint: define the training sites in some suitable, quantitative way.)

CONCLUDING REMARKS

We have at last reached a stopping point in this rather long activity. Hopefully, you are now a "convert" to computer processing as an elegant and efficient means for displaying Landsat images and extracting information from the data. If not, you should reserve final judgment until you look through *Earthwatch*, a striking new book, containing more than 80 computer-enhanced images and a text dealing with sophisticated processing techniques published just as this workbook goes to press. *Earthwatch*, written by Charles Sheffield, is published by Sedgwick and Jackson, London, 1981, and will be distributed in the U.S. by Macmillan and Co., New York. Your convictions should be strengthened even further as you complete the next four activities, each of which touches upon still more examples of the role of computers in data processing. First, you will shift your perspective from space to such aspects of ground truth as training site selection, accuracy assessment, and field measurements. Then, you will learn how to interrelate Landsat classifications with other kinds of data as key steps in evaluating information needed in the decision making process. Next, you will work through a case study that demonstrates the impact of Landsat on the day-to-day operation of natural resources agencies within one state. Finally, you will learn about other satellite systems that provide additional remote sensing data.

ACTIVITY 6
NEAR SURFACE OBSERVATIONS[1]

LEARNING OBJECTIVES:

- *Develop an understanding of the implications of the term "near surface observations."*
- *Associate the appearance of large ground features as seen in satellite imagery with their appearance as seen from the ground.*
- *Learn criteria and procedures for selecting training sites on the ground for use in supervised classification.*
- *"Run through" an example of training site selection.*
- *Be familiar with several methods for accuracy assessment.*
- *Become aware of the approach and value of making supporting measurements of spectral and other physical properties of materials on the ground and from aircraft.*
- *Take note of the different types of instruments used in making specific ground measurements.*
- *Appreciate the rationale underlying laboratory and field studies on or near the Earth's surface for the purpose of developing new sensor systems.*

[1] The term "near surface observations" is used here to mean acquisition of information about the Earth's surface both from the ground and from aircraft. Another term, "ground truth," is now regarded as a colloquial or slang expression for any reference data on ancillary information obtained from a variety of sources (maps, field work, laboratory tests, published accounts, historical records), including measurements specifically in support of remote sensing observations. Implied in the concept of ground truth is the assumption that such data can serve as standards for correct interpretation of accuracy assessment of remote sensing results.

TYPES OF OBSERVATIONS

Until now, the emphasis in the workbook has been on the appearance of the Earth's surface from *on high*, that is, looking more or less straight down (at or near nadir) from spacecraft or aircraft platforms. In this mode, objects and groups of related features are displayed in outline or plan form much as they would be depicted on maps. Those who frequently use maps and/or are skilled in photointerpretation are already familiar with the characteristic shapes and patterns associated with these objects so that their identification is often easy. However, most novices in remote sensing tend to rely, at first, on their experience as ground dwellers in that they think of these objects as they would view them from horizontal or low-angle panoramic vantages. This is a customary frame of reference and is an appropriate attitude to maintain as one masters the principles of remote sensing. In fact, the remote sensing specialist should retain a surface-based perspective of the Earth during all phases of data gathering, analysis, and application, since most interpretations and decisions dealing with natural resources will be implemented at the ground level.

The above conclusions are deceptively simple. The subject of near surface observations is more varied and complex than evident from a first consideration.

#6-1: To appreciate this statement, consider for a few minutes the various kinds and aspects of near surface observations that come to your mind: list them.

Compare your selection with the entries in Table 6-1, which together constitute a representative, although not complete, outline of the types of tasks and operations associated with the analysis of ground and aircraft data obtained to support remote sensing applications.

In the remainder of this activity, we shall consider five topics culled from Table 6-1, which together make up the operations most frequently performed during near surface observations.

1. Correlation of familiar surface features and localities with their expression in satellite imagery
2. Selection and identification of training site samples for supervised classification
3. Verification of classification accuracies
4. Field measurements to support data analysis
5. Measurements pertinent to sensor development

We shall also touch upon several subsidiary topics where appropriate.

The "Multi" Approach

The essence of the ideas listed in Table 6-1 is that the key to effective use of remotely sensed data lies in obtaining appropriate information about the real world and then relating this knowledge to the data. A strategy to do this is embodied in the "multi-" concept. Thus, data should be acquired whenever possible from different platforms (*multistage*), at various distances from the Earth's surface (*multilevel*). This gives rise to *multiscaled* images or classification maps. Different sensor systems (*multisensor*) should be employed simultaneously. These sensors provide data over various regions of the electromagnetic spectrum (*multispectral*). The data must often be obtained at different times (*multitemporal*), whenever seasonal effects or illumination differences are factors or change detection is the objective. Supporting ground observations must come from many relevant, but not necessarily interrelated sources (*multisource*). Some types of surface data may be correlated with one another and with remote sensing data (*multiphase*).

FAMILIARIZATION WITH GROUND APPEARANCE OF IMAGE FEATURES

The first operation, which seeks an on-the-spot perspective, is among the easiest and usually most enjoyable actions you can undertake in analyzing a Landsat image. When in the field you need

Table 6-1
Role of Ground and Aircraft Observations in Utilizing Satellite Remote Sensing Systems for Earth Resources Applications*

Orient and familiarize the user with information contained in Landsat images, i.e., correlate the small-scale vertical view with the user's surface experiences as an aid to recognizing major land cover categories
Provide input and control during the first stages of planning for analysis, interpretation, and application of remote sensing data (landmark identification, logistics of access, etc.)
Reduce data requirements (e.g., areas of needed coverage) for exploration, monitoring, or inventory activities
Assist in mapping from space imagery by photointerpretive methods
Select test areas for aircraft or other multistage/multisource data support missions (e.g., simultaneous underflights)
Specify sampling strategies
Select training sites for supervised classification
Identify classes defined from unsupervised classification
Obtain quantitative estimates (e.g., field size, forest acreage) relevant to class distributions
Verify accuracy of classification (error types and rates) by using quantitative statistical techniques
Collect physical samples for 'laboratory' analysis of phenomena (e.g., water quality, insect induced disease, rock type) detected from remote sensing data
Acquire supplementary (ancillary) nonremote sensing data (e.g., from Data Collection Platforms, or "Windshield" Surveys) for interpretive model analysis or for integration into Geographical Information System operations
Develop standard sets of spectral signatures for analysis of data already acquired, by using ground-based instruments
Measure spectral and other physical properties for specifying characteristics and parameters needed to design new sensor systems

*Major ground-oriented data sources: field observations; on-site measurements; maps; descriptive reports; inventory tallies; aerial reconnaissance; large-scale aerial photos.

only to locate your ground position within the image, look around, equate and compare the surface features you note with those evident in the image. The key to a successful correlation is often just to be able to see a large surrounding area and note distinctive features or locations whose different patterns (defined by shape and spectral variations expressed as ranges of gray or color tone levels) can be matched in the same image. To do this on the ground, you may need to "filter out" details (usually a multitude of small features, below image resolution) and see only the gross features that show up as fairly uniform patterns. The vantage points of a hillside, a tall building, or, best of all, an aircraft, serve as close-up platforms for this large area or *synoptic* overview.

In early October of 1978, the author conducted a ground reconnaissance of much of the terrain and many localities that we have been studying in the New Jersey and Harrisburg scenes. This trip of about 700 km (450 miles) required two days. Ground photographs taken at twelve selected localities are reproduced in Figures 6-1 and 6-2. The number-letter pair (e.g., 1F) assigned to each locality indexes its approximate location (at arrows) in the June 8, 1977 Landsat scene (Figure 6-3). These localities are identified as follows (consult a map for additional information):

Figure 6-1:

A. Orchards and fields within the Pennsylvania piedmont, near New Freedom, Pa., south of York looking northwest
B. Valley from side of Blue Mountain and northeast of Carlisle, looking south from Highway 34 toward South Mountain in the distance
C. Juniata River at Port Royal, looking east toward a ridge
D. Harrisburg, Pa., bridge crossing the Susquehanna River, looking northeast
E. Blue Mountain, with patches of gypsy moth defoliation, northeast of Harrisburg, looking east
F. Multiple small crop fields in the Pennsylvania Dutch Country, near Strasburg, looking west

Figure 6-2:

A. Town of Mahoney City, Pa., looking south from hill
B. Coal refuse pile near Shenandoah, Pa., looking east
C. Nesquehoning Reservoir west of Nesquehoning (Town), looking north toward Broad Mountain
D. Green Lane Reservoir, south of Pennsburg, looking southwest
E. Chesapeake and Delaware Canal, with railroad bridge and pipeline visible from Route 301 bridge, looking east
F. Soybean and corn fields in farmlands northwest of Middletown, Del.

Some of these photos lend themselves readily to certain questions that will help you to orient yourself and to better interpret the scene. Use Figures 2-1, 4-2 and 4-4 in your cross-correlations between images and photos.

#6-2: Imagine yourself at the roadside along State Highway 34 looking across the panorama shown in Figure 6-1B. Are any features visible in this photo also recognizable in the October 1972 Landsat image? Note the low forested hills in the mid-ground of the photo. Can you find their possible equivalent in the image? There are several curvilinear rows of trees among the fields. To what might they correspond? Note the hills near the horizon. Can you find them in the image? Name the physiographical unit (mountain) they represent. About how far across the lowlands are you looking?

#6-3: In Figure 6-1D, you are standing at the west end of the bridge that carries Interstate 83 across the Susquehanna River. From landmarks in the photo (such as the railroad bridge and downtown Harrisburg), try to locate yourself in a full Landsat scene. (Hint: Use Figures 5-23 and 5-24 as a guide.)

#6-4: Examine the field patterns in Figure 6-1F. Estimate their dimensions. What is one characteristic field shape? How well can you see fields of these sizes and shapes in the full Landsat scenes (Figure 4-2 or 4-4)? Now look at Figure

6-4, a computer-produced Landsat enlargement of the area south of Lancaster, Pa., in which the ground scene is embedded. The approximate location of this site in the Figure 6-1F photo is marked by an arrow in Figure 6-3. Are the field patterns you deduced from the photo readily or poorly discerned in the computer version? Explain your conclusion.

#6-5: Figure 6-2A is a view of the town of Mahoney City, photographed from a wooded hill (with homes) on its north side. There is no arrow in Figure 6-3 to locate this town for you. Mahoney City is typical of a small mining town in the anthracite coal belt of Eastern Pennsylvania. The combination of businesses, along a single east-west main street, and frame houses encompasses at least forty pixels in area. Much of the nearby terrain is covered by coal waste (spoil banks) now partly vegetated. From what you perceive in the photo, would you expect to see the town in a Landsat image? What factors (spectral characteristics, etc.) might render it visible? Now try to find the town ('ain't easy!) in any version of this Landsat scene in this workbook. As an aid, use the section of the 1:250000 National Topographic Map Series NK 18-10 (Harrisburg) reproduced as Figure 6-5. Hint: locate Frackville and a small lake to the east in the imagery—they usually show up well—as reference points also evident in the map. Try the triangulation method to approximate where Mahoney City should be. Did you succeed or fail in your search? If you failed, try to explain why.

#6-6: It is possible to locate yourself fairly precisely along the elongate Nesquehoning Reservoir within the Landsat images. Look at Figure 6-2C. There are at least two features in this ground view that appear in many of the images of this scene (color composites may be best). What are they? Where is the point on the ground from which the photo was taken (west, east, or middle of the lakes edge)?

#6-7: Note the surface "scum" in the water near shore in Figure 6-2D. This is caused by floating fresh water algae, often mixed with other vegetative matter. Fairly high surface concentrations of these organisms tend to develop by late summer and spread over much of the top surface of (usually shallow) lakes. This, then, is a seasonal condition that can indicate increasing lake eutrophication, usually caused by nitrogen and phosphorus pollutants. Suggest how this bloom effect might appear in Landsat imagery (both color and individual bands) and therefore be monitored.

TRAINING SITES

Probably the most common reasons for conducting field activities lie either in the necessity of selecting training sites prior to supervised classification, or identification of key classes after unsupervised classification. The best way to do this, if feasible, is simply to spend a few days or more actually examining the terrain for which a classification is to be prepared. Obviously, the scale of the effort will depend on the area(s) to be classified: one or more full Landsat scenes will require considerable travel and field time (perhaps weeks), while examination of a typical subscene (such as a 512 X 512 pixel image) may often be accomplished in a day or two. If field observations are limited by logistics (for example, in an inaccessible foreign area or during an off-season such as winter), then one must rely instead on aerial photography, maps, interviews with residents, etc. In practice, the specification of training sites will normally involve integration of these several sources of information—direct observation from ground and/or air photos, a variety of maps, personal familiarity, etc.

We shall concentrate here on rules and procedures for selecting training sites to be used in preparing a supervised classification. Much of this material is taken from the review by Joyce (1978) published as a NASA document describing such procedures.[2]

[2] Joyce, A.T., *Procedures for Gathering Ground Truth Information for a Supervised Approach to a Computer-implemented Land Cover Classification of Landsat-acquired Multispectral Scanner Data*, NASA Reference Publ. 1015, 1978.

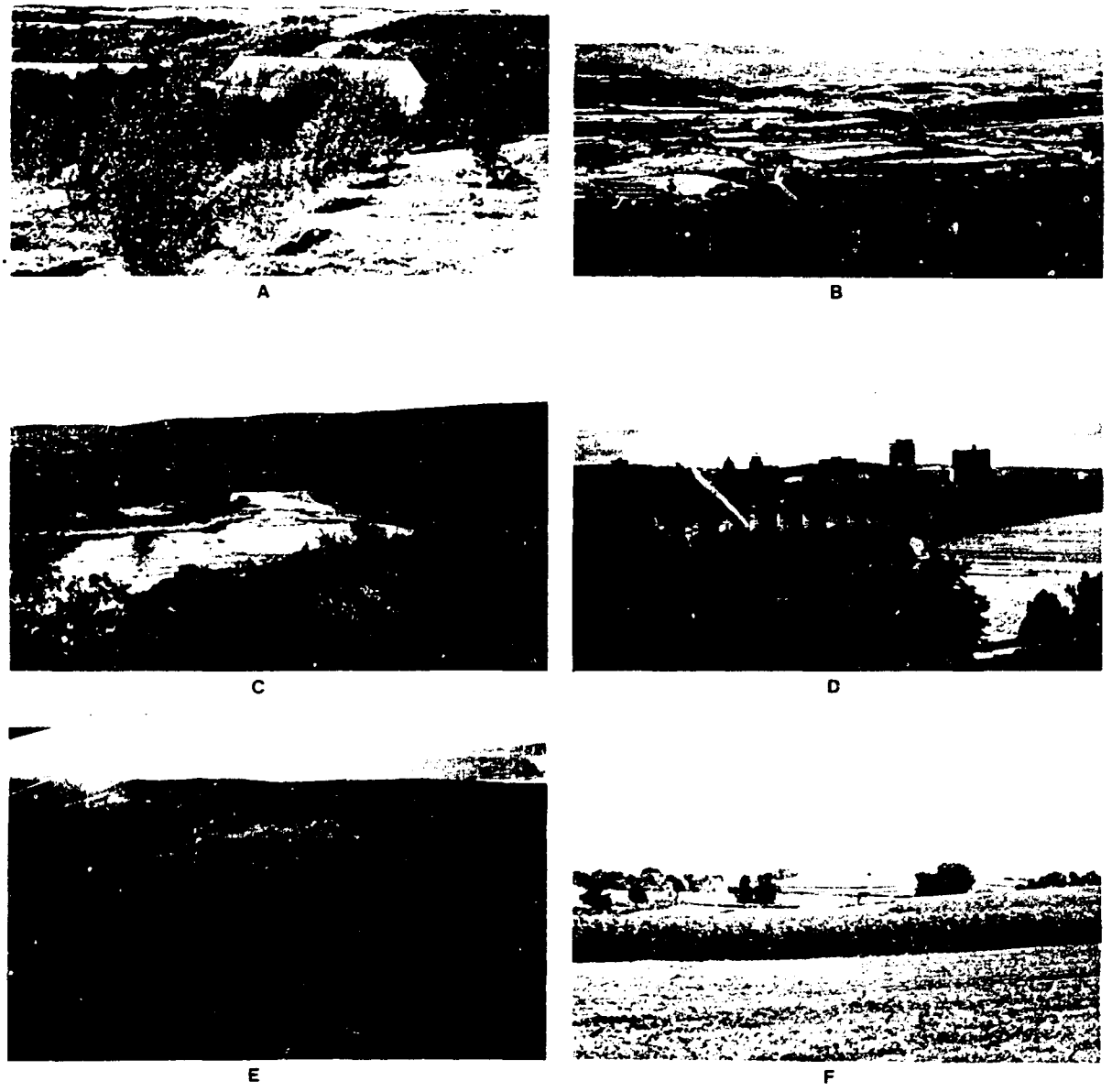

Figure 6-1A-F. Ground views of areas (located in Figure 6-3) within Landsat Harrisburg scene (mid-September 1978) (see text).

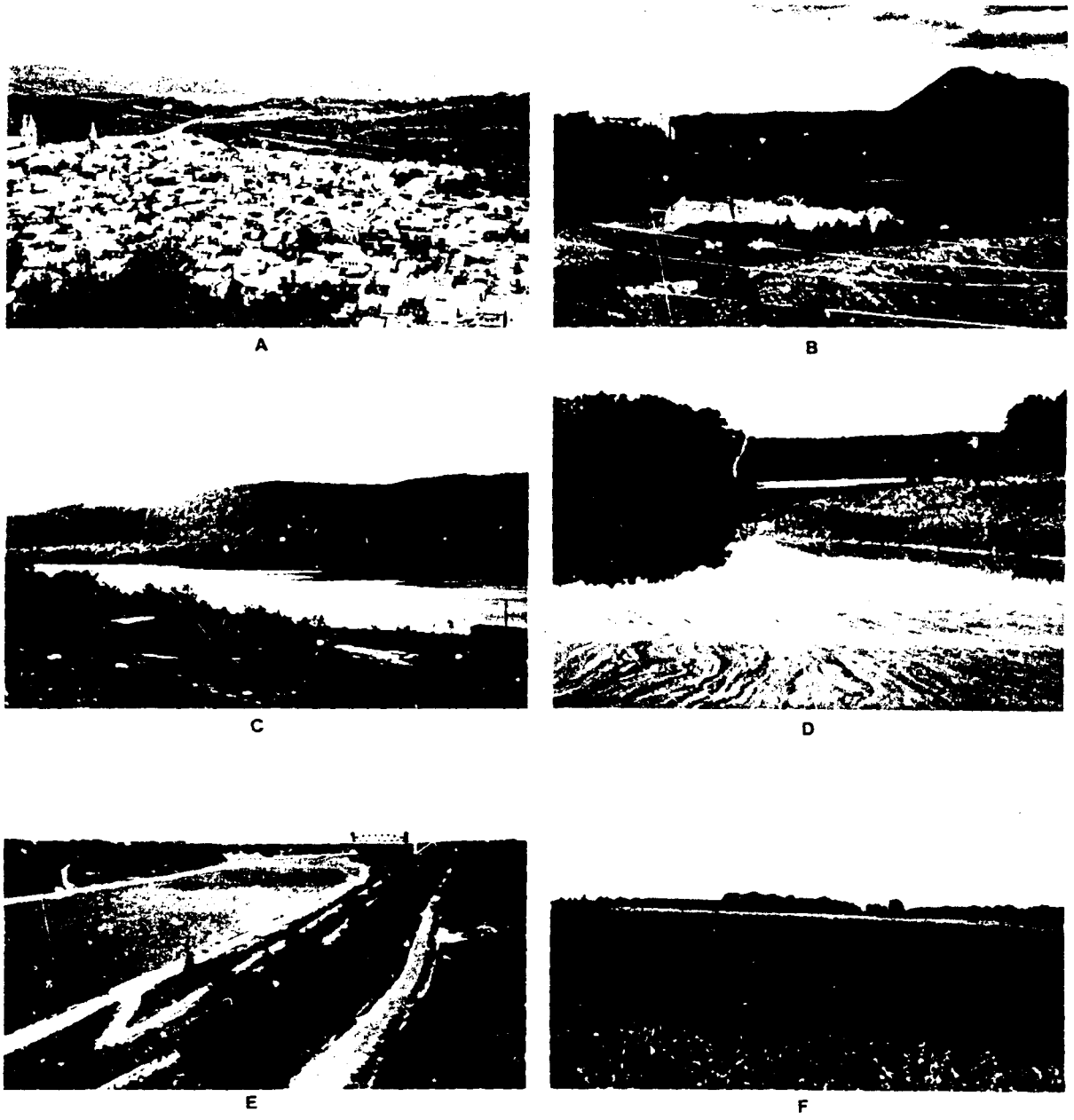

Figure 6-2A-F. Ground views (continued).

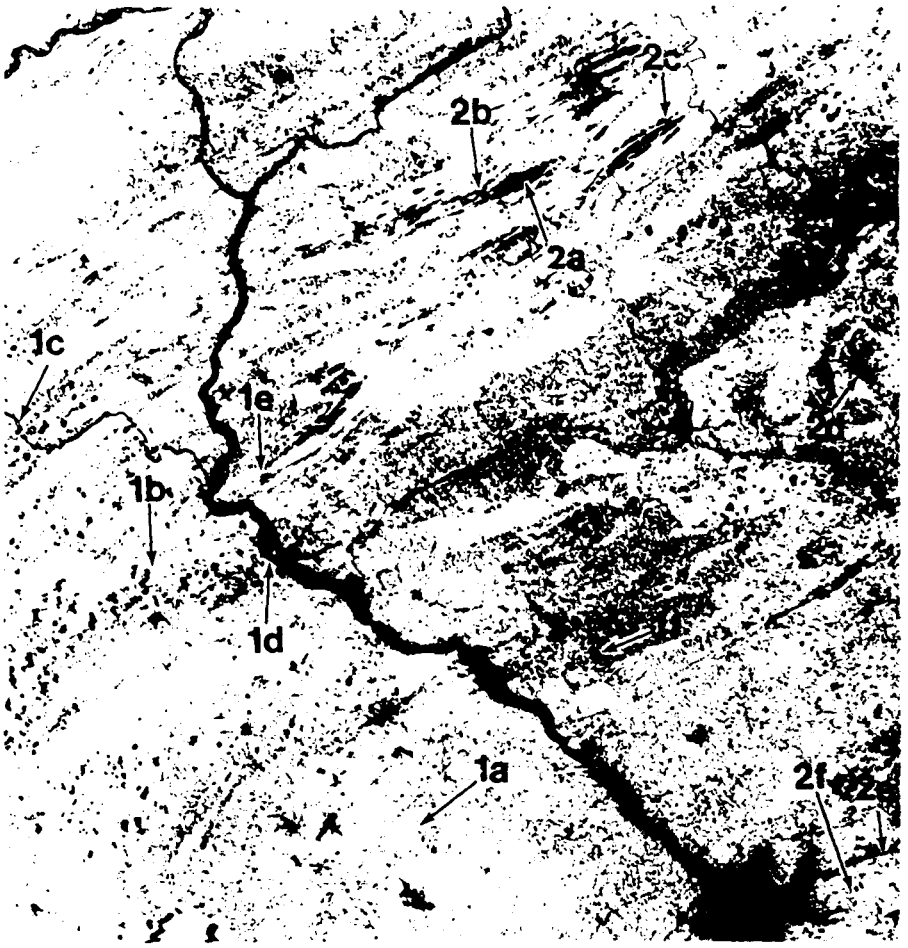

Figure 6-3. Location of ground views; Landsat band 7 scene acquired in June 1977.

The primary reason for establishing training sites is to determine and define Land Cover (and/or Use) categories to be mapped (classified) from Landsat data, assisted by other sources of information. It follows that the sites to be visited or otherwise identified must be carefully chosen in sufficient number, variety, and distribution to maximize the accuracy of classification of large homogeneous areas in the imagery. Five factors listed by Joyce control this choice:

1. General categorization of cover use classes
2. Size and shape of training sites
3. Number and distribution of sites
4. Homogeneity and uniformity of cover types
5. Distribution of sites throughout the scene

Categorization

A land surface may be treated in terms of three broad characteristics: (1) vegetated cover (vegetation constitutes more than 40 percent of surface); (2) nonvegetated cover; and (3) topographical variations. When considering the attributes of vegetation, these are the principal influences:

Plant species: Usually the cover may be classed under a single species name if it constitutes 75 percent or more of the types present (examples: corn field, pine forest).

Plant association: The cover consists of two or more species or types, making up more than 25

Figure 6-4. Enlargement (512 X 512 pixels) of Landsat Subscene (band 5) of Lancaster, Pa. and farmlands to the southeast.

percent (examples: oak-hickory association; brushland, composed of sage and grasses).

Plant age: Stage of growth or maturity.

Plant vigor: Health, as affected by insect infestation, disease, moisture and nutrient deficiencies.

Plant density: Soil/plant classes with densities of less than 40 percent, 40 to 60 percent, 60 to 80 percent, more than 80 percent.

Understory vegetation: Two or more communities whose tops lie at different heights above surface; influenced by percentage crown cover.

Seasonal state: Extent of leafing, color, etc.

Nonvegetated land cover is composed of water bodies, soil alluvium, exposed rock, extractive areas (e.g., gravel pits), mud flats, beaches, and works of man (roofs, pavement, etc.).

Topographical variables include slope (slopes less than 30 percent [15°] may usually be ignored) and aspect (i.e., compass orientation, influenced by direction of slope with respect to Sun elevations and azimuth angles).

Size and Shape

The shape (outline) of a distinct feature is often not crucial but its size may well be. A natural feature given a specific class name should be more than 40 acres (*ca.* 35 Landsat pixels) in area to provide an adequate population of sample points (pixels) for statistical significance testing. However, sites larger than about 160 acres (*ca.* 140 pixels) tend to be nonhomogeneous. Exceptionally, sites as small as 10 acres may be used if the feature is naturally in that dimensional range, but this may yield poor statistics in classification.

Figure 6-5. Part of 1:250,000 AMS map of area around Frackville, Pa.

Number and Distribution of Sites

The total number of necessary training sites will depend on the number of classes set up as well as the size (area) of the subscene. This is usually a minimum of about three sites per category, and may be as high as ten if a class has considerable natural variability. These sites make up only a small fraction of the total area involved. Even for a full Landsat scene classified into 10 to 15 categories, the 90 to 150 training sites that might be required (for a scene with diversified land forms, cover types, and uses) will generally occupy less than about 1/100th of the total area within this scene.

Homogeneity and Uniformity

This factor is governed by the need to have an established class defined by some spectral property (such as spectroradiance, expressed as a digital number for each band) whose variability approximately follows a normal (Gaussian) distribution. A key rule-of-thumb is to find a training site on the ground whose principal feature (or dominant characteristic) is spatially spread out in a more or less uniform distribution.

If two or more surface cover types are in-

volved (as in a multispecies forest association), each type should be randomly spaced rather than grouped sporadically in small clusters within the site. This point becomes important when the individual members of a class are small compared with pixel dimensions. A poor distribution could result, in which a few pixels in a training site would contain twice as many (or more) individuals as neighboring pixels, or one of several cover types making up some composite class would fall selectively within only a few of the pixels in an array. Implicitly, this is one effect of the mixed pixel problem discussed on pages 83 through 89. A training site of 40 typical pixels for each class will normally suffice to separate two different class signatures. The optimum number depends on whether all pixels contain a uniform random distribution of individual ground features, or some of those pixels contain more of one cover type or erratically varying concentrations of several types.

Location of Sites

When a Landsat subscene is to be classified, the location of sites will depend primarily on their overall degree of homogeneity with respect to number, variability, and geographical distribution of classes as well as other factors such as climatic differences. A typical Landsat scene in the eastern United States is fairly uniform in this respect. Thus, such a scene is frequently dominated by vegetation (a summertime color composite appears red all over). For such conditions, all training sites could be located in a smaller section of the scene; this simplifies the logistics of field visits and hence reduces costs. In a western United States scene it is common to find considerably more variation, and so wider-ranging and more costly excursions into the field will be required. For instance, a scene in the southwest is characterized by diverse physiographical and ecological units: low barren mountains in one part, high forested mountains in another part, desert valleys elsewhere, unusual localized geological features (for example, a basalt flow), and cultivated land (field crops) confined to a few river courses (see Figure C-1, Appendix C for an example). For all terrains the problems of scene variability generally diminish when small subscenes are classified, since both geological and geographical diversity tend to increase over larger regional areas. In most instances, the location of sites depends mainly on convenience of access and ability to be picked out in the imagery. Sites that can be associated with features that are linear (roads), or possess recognizable interfaces with other features (fields), are usually best.

Signature Extension

In light of the five factors discussed previously, it is appropriate here to make some brief comments about the concept of *signature extension*. This term refers to the assumption that a single, more or less constant, spectral signature may be defined as characteristic of any class, and that this signature has broad (universal) applicability to any scene in a region, or even worldwide. As a specific example, the signature for winter wheat at its maturation should be essentially the same for fields in the United States Great Plains, Argentina, Soviet Russia, and Australia provided that such variables as differing air masses, Sun position, soil types, etc., are compensated for. If that proves true, then an unknown feature or class in some given scene would be identified and classified by comparing its spectral properties (for a Landsat pixel, its four representative DN values) to a "data bank" containing standard values for each of many classes. The closest fit of the unknown's DN values to those of some one class in the bank is assumed to identify it.

This approach will probably work well (i.e., will achieve an acceptable accuracy) for a few common features such as deep, clear water bodies, clouds, snow, desert sand, perhaps central urban areas or certain forest types, and winter wheat. However, in most cases, signature extension does not work well for a variety of reasons, including (1) the natural variability of most classes; (2) the

"mix problem" of undetermined proportions of several features within a class; (3) the often artificial or arbitrary way in which some spectral class is defined (rocks are classified [named] by mineral content and texture in hand specimens, which often bear no simple relationship to gross spectral properties observable from space); (4) the influence of (usually undetermined) differences in atmospheric conditions (weather and climate effects) from place to place and on different dates; and (5) the seasonal variability of vegetation. From experience with Landsat data, the use of the signature extension approach has been demonstrated as inaccurate and ineffective. The now prevalent approach is to pick out training sites from within the scene to be classified and proceed through the specified steps in supervised classification by using the statistics for these sites from the equivalent pixels within that scene. This is roughly analogous to the practice developed by analytical spectroscopists of using "internal standards," which in some methods are selected from one or more of the same chemical elements being sought in the analyzed unknowns.

Strategies for Site Selection

To apply some of the ideas developed in this section, we shall now reconstruct the sequence of actions taken prior to actual computer processing, to set up suitable training sites for the Delaware agricultural district whose classification has been described on page 219. Before pursing this, you should try to design your own program for site selection.

#6-8: Do this by outlining, from start to finish, a set of reasonable steps that you might follow, before and during field visits, in establishing adequate training sites.

In actual fact, the selection of training sites for the Delaware classification followed several of the customary steps but also deviated from the normal approach. Whenever practical, ground observations should be made close to the date of the classified Landsat scene. The classification of the July 14, 1977 Landsat overpass (2904-14452) was performed on IDIMS in the fall of 1978, but Landsat CCT's for the 1978 growing season were not available at that time. This necessitated the use of historical rather than current records of crop plantings and, further, meant that a detailed field check in 1978 would be of limited applicability.

The first step was to build a photo base on which to plot the field data for crop identifications. A NASA U-2 flight over the agricultural district of Delaware had taken place in the summer of 1974. The frame (Figure 6-6) including Middletown, Delaware and the farmlands to the north was selected for use as ground control. Next, the 1977 subscene (512 X 512 pixels) to be classified was processed on the IDIMS system, which yielded a geometrically corrected band 5 rendition as hard copy from the Optronics recorder (Figure 6-7). A further enlargement (Figure 6-8) of the area selected for obtaining field truth was photographed directly from the IDIMS monitor screen; this version was not corrected for aspect, and hence the ground patterns are distorted ("squashed") in the north-south (vertical in Figure 6-8) direction. The areas in the enlargement were then collocated within the U-2 photo.

The problem at this stage was to determine where these areas were on the ground and what had grown there in 1977. This was best accomplished by a visit to Delaware to gain some familiarity with the setting and to talk with local farmers and other informants about crop history. The visit took place on October 8 and 9, 1978. Obviously, many fields in the 1978 growing season were dedicated to crops different from the previous year, and by fall harvest even the 1978 crops could not be adequately identified at many sites. Inspection on site therefore proved helpful mainly to locate road intersections, forest copses and other distinctive landmarks of nonagricultural nature.

Fortunately, the New Castle County office of the U.S. Agricultural Stabilization and Conservation Service (ASCS) had adequate records of 1977 crops for about 60 percent (higher than normal) of the farm fields. These records were obtained by direct questioning and from reports filed by local farmers. Also, intermediate altitude aerial photography had been flown by the ASCS over the area of interest in mid-May 1977. The aerial photo

(scale 1:40000) shown in Figure 6-9 was taken just two months before the Landsat overpass, so that the field patterns closely correspond, although many of the crops approaching maturity by mid-July had not significantly developed in May. The ASCS had also recorded some of their 1977 crop reports on photos acquired in previous years. Figure 6-10 is an actual example of one such large scale photo sent to a local farmer who then returned it with annotated crop and yield data

Using all of the aerial photos and the Landsat maps, the director of the local ASCS Office, the New Castle County agricultural agent, and the author succeeded in associating crop types in thirty-two fields with their corresponding patterns in the Landsat imagery. This effort was hampered by uncertainties in correlating specific fields between photo and Landsat image and more importantly, in knowing exactly which reported crop went with which field once located. The most common crop in 1977 was corn, followed by soybeans. Barley, alfalfa, wheat and hay together constituted less than 10 percent of the crops growing in July. A serious problem in specifying soybean sites resulted from the practice of planting two soybean crops in one year. Some soybeans were planted early and harvested by July; a second planting in June or later was harvested in the fall. This was not always recorded as such, thus leading to confusion as to the soybean distribution and stage of crop maturity in July. Some of the barren fields seen in the July Landsat image may have supported soybeans earlier or, in a few instances, later. Generally, data for these barren (fallow) fields were ignored.

The final agricultural classification presented in Figure 5-37 simply combines these various crop and field conditions into three general classes: Corn, soybeans, and fallow. Training site data were insufficient to subdivide the field crops further, i.e., to set up classes for barley, alfalfa, pasture, etc. This introduces an error in classification that could be reduced only by considerably more field surveys or other sources of accurate identification. Classification accuracy would also have improved if scenes from several dates had been employed: the multitemporal or crop calendar approach, which relies on stages of maturation for each crop during the growing cycle.

#6-9: To appreciate the problem of locating training sites within Landsat imagery, you should now attempt to locate the feature at the arrow tips, marked 1 through 8 in Figure 6-8, as these might appear in (1) the U-2 photo, and (2) the ASCS photo. Keep in mind the different dates of coverage that give rise to different land patterns. Suggest at least three reasons (or factors responsible) for these differences.

#6-10: Then, try to locate in these aircraft images the scene represented in the color photo (Figure 6-11) obtained during an October 1978 low altitude mission flown by the Environmental Protection Agency (EPA) for chemical pollution studies.

#6-11: Can you recognize either of the two oval rings (racing tracks used on horse farms) in the Landsat rendition?

ACCURACY

Importance in Classification

Most interpretation-oriented analyses of Landsat data have as their goal the *identification* of specific individual ground features (e.g., lakes, fractures and faults, airports) and/or *classification* of land cover types. These identified or classified categories are usually expressed on maps that show the geographical location (distribution) of each category at any point on the Earth's surface and its boundaries with respect to adjacent categories. Two fundamental questions can be posed: Is each category in a classification really present at the points specified on the map? Are the boundaries separating categories or classes valid as located? Both of these are questions of accuracy. Accuracy

Figure 6-6. NASA U-2 high altitude red band photo (August 1974) of C&D Canal area in Delaware-Maryland.

may be defined, in its simplest sense, as the degree (often, as a percentage) of correspondence between *observation* and *reality*.

In general, the greater the accuracy of classification, the more effectively are Landsat observations applied. Three examples will make this obvious:

1. In the LACIE program (p. 219), estimates of crop production depend in part on the correct determination of the area (number and sizes of fields) given to each crop. If corn is incorrectly overestimated by 20 percent and soybeans underestimated by 30 percent, the value to the market place of this assessment from Landsat data may be severely compromised. Errors of incorrect identification and inexact boundary locations made when using Landsat, and/or imprecise yield (and hence improper areal

Figure 6-7. Enlargement (512 X 512 pixels) of Landsat subscene (July 1977) around C&D Canal.

and biomass) measurements made by independent means, seriously compromise estimates of food supplies as well as of dollar losses. These errors weaken decisions to harvest, ship, store, or sell these crops—decisions that were made in good faith from unverified acceptance of Landsat results.

2. Fractures identified in Landsat imagery may be considered serious hazards to nuclear power plant sites, dams, roads, or other engineering projects as well as to people in population centers. Many linear features in Landsat scenes are assumed to be natural when, in reality, some may be cultural or even processing artifacts. Unless these fractures are properly checked out in the field, and their existence confirmed, some very real danger may be missed or decisions to avoid the problem may have been unfounded.
3. Public Law 208, as enforced by the Environmental Protection Agency, requires a statement to be filed regarding the effects of land development (for example, building a "new town") on nonpoint sources of water pollution. Assessment of potential pollution involves, among other things, knowledge of watershed runoff conditions. In an urban area, the nature of land cover plays an

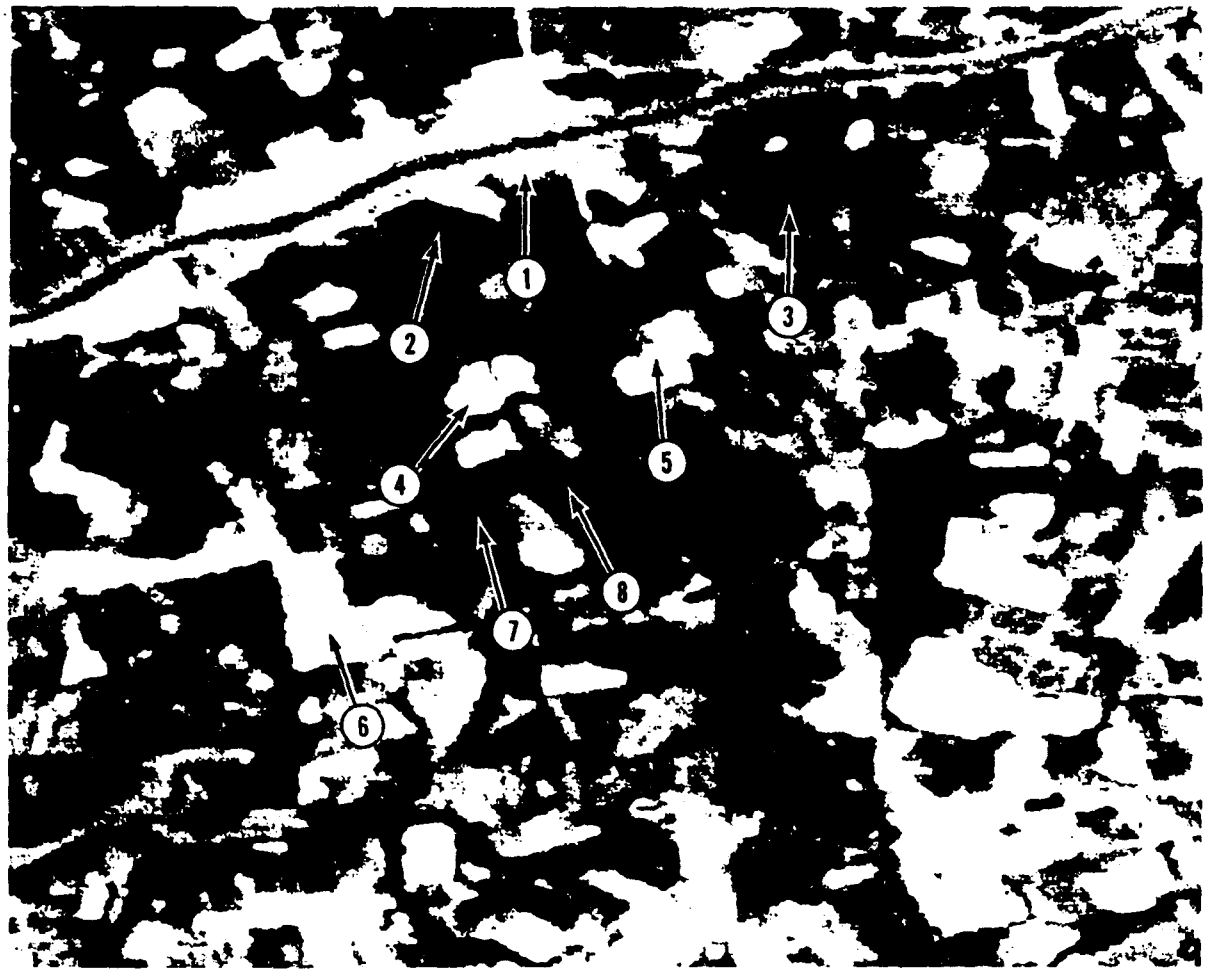

Figure 6-8. Further enlargement of Figure 6-7. Individual or grouped fields indicated by arrow.

important part in predicting this runoff. Land cover maps may be produced rapidly from Landsat data, and the percentage of each cover type used in models relating cover to runoff may be determined from these maps. Errors in categorization and in mensuration will lead to poor model predictions, which, in turn, may discredit the 208 statement, thus causing delays and added costs to the project.

Types of Errors

In remote sensing procedures, most errors are generally made either in measurement or in sampling. There are many sources of error of each type involved in a Landsat classification. These may be further categorized into three groups: (1) Data acquisition errors, (2) Data

processing errors, and (3) Scene-dependent errors.

The first group includes errors associated with the configuration of the Earth's surface, the conditions of viewing, the stability of the platform, and sensor performance. Some errors may be reduced or compensated by making systematic corrections (such as by calibrating detector response with on-board light sources generating known radiances). Others require mathematical analysis to determine the causes and extent of variability.

#6-12: It would be instructive at this point to list as many sources of error in this group as might occur to you. Consider all aspects of the data gathering process, giving special attention to

Figure 6-9. Medium altitude aerial photo of C&D Canal area, flown in May 1977 by ASCS.

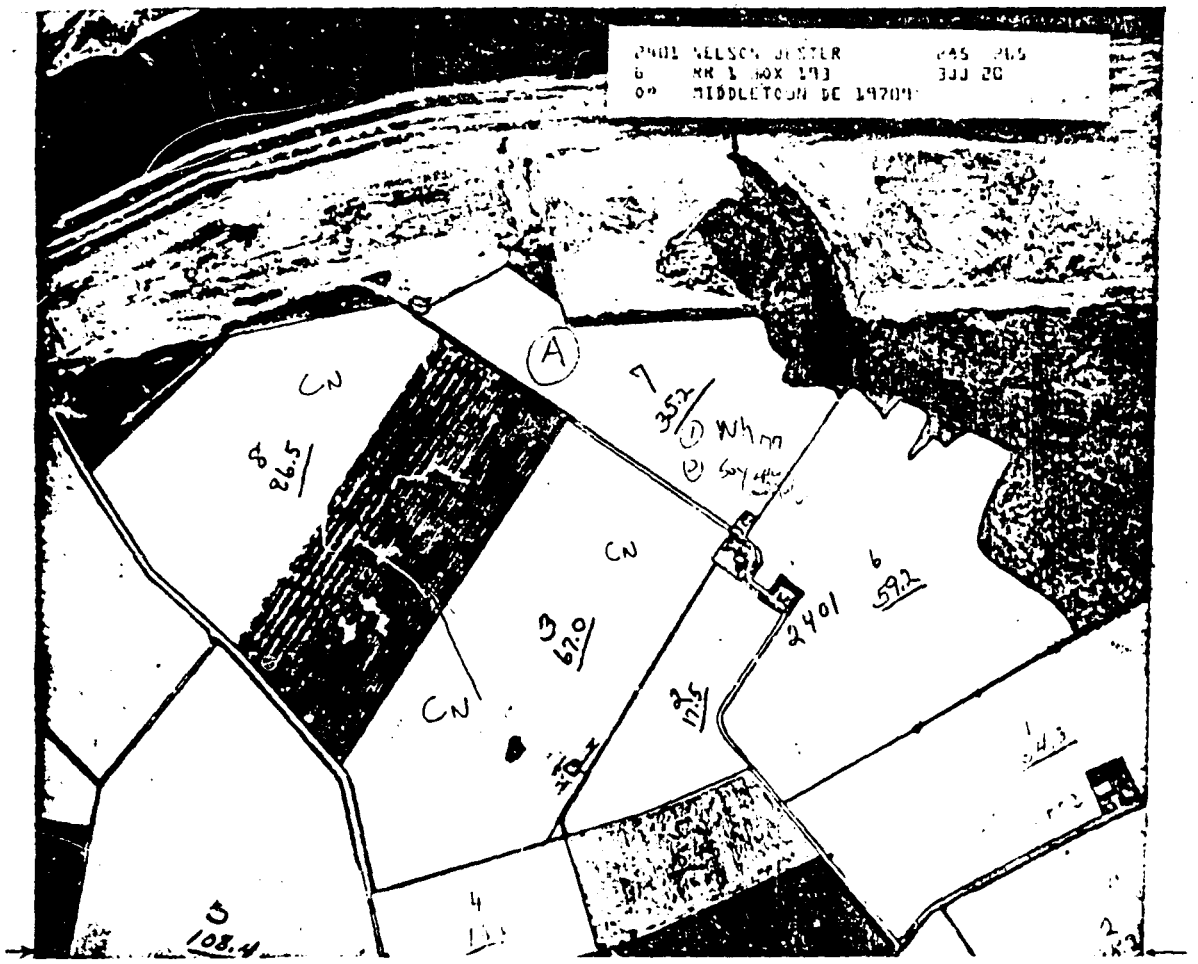

Figure 6-10. Paper print of actual aerial photo (low altitude) used in cooperative ERRSAC-ASCS selection of field training sites.

errors of a geometrical or a radiometric nature. Then compare your list with the extensive, but by no means complete, list in the answers section.

Many of these errors are routinely corrected during the initial processing of the raw Landsat data by NASA, subsequent processing at the EROS Data Center, or later processing by the user.

The second group of errors results from the methods applied in converting the raw data into some output format. Problems are frequently encountered during batch production of photo images (such as some of these in this workbook in which the initial negative is made on an electron beam recorder and the final image is reproduced by conventional photo techniques after passing through several generations of negatives and positives). An example of this type of error would be improper quality control of conditions in the developing or printing stages; this could lead to a nonlinear range of film densities or gray levels. Another type of error may occur if the product is an enhanced image, a classification map, or an alphanumeric array, generated by manipulating the data through series of computer-controlled processing steps. An example of this type of digital processing error is found in the resampling procedures in which new pixels are

Figure 6-11. Low altitude aerial photo, flown in EPA mission, showing Middletown, Del. and environs.

"created" from data contributed by surrounding pixels; the resulting new pixels may be different in size and shape and will differ in their characteristic digital numbers (DN's).

Still another processing error may develop from gross misregistration of equivalent pixels from the different bands. When a registration procedure is applied to the raw data during geometrical correction at Goddard's IPF, the goal is to hold the mismatch of the same pixel in all bands to a displacement of no more than one pixel. Because most ground features of interest in a scene of Landsat scale consist of several or many pixels of similar spectroradiances, this mismatch introduces only small errors except at boundaries with other features (Figure 6-12). Under ideal conditions and with as many as 25 ground control points (GCP's) spread more or less uniformly throughout a full scene, this goal can be realized. However, more commonly the number of identifiable GCP's will be variably less (ten or fifteen if, for instance, the scene is partly cloud-covered), resulting in registration mismatches of several pixels or more (for example, pixel A of one band might be displaced three pixel positions from the equivalent pixel in the second band when both are superposed). In this case, the potential accuracy can be significantly compromised.

The subject of processing errors is broad and will not be further treated here. You are invited to ferret out other such errors on your own, particularly after you have absorbed the review of computer processing in Appendix B.

The third group, related to the scene itself, is probably not so much a set of errors as a measure of inherent differences between the real world, our concept of it, and the representation of that world in imagery or maps. Part of the problem is semantic. For convenience, classes of features may be assigned names with some intended meaning that commonly depends on the purpose or objective in classification. Thus, we can establish a class called "Orchard," which connotes a land cover type that implicitly also specifies land use. This, however, is a subjective definition designed to convey a concept, that is, a picture of fruit-bearing trees that supply a foodstuff to people. Now, if the lower resolution Landsat multispectral scanner records light from a small section of the Earth (say, 0.4 hectares of 1.1 acres) containing apple trees, that sampled area would be represented on multiband photo-images by a set of regular-edged pixels with differing shades of gray that indicate the brightness levels in several wavelength intervals. A coincident high resolution photograph of the same surface (here of dimensions 79 m X 79 m to approximate the size of one Landsat pixel) might reveal this orchard to consist of apple and pear trees, some scattered oaks, a few bushy plants, spotty grass, soil, a small shed, and a roadway. Each individual object within a 79 m^2 (pixel-equivalent) surface—be it a clod of soil, a blade of grass, an apple, a full tree or a road—will make a finite contribution to the spectroradiant energy sensed by the scanner. The total intensity of reflected radiation at any wavelength is the sum of the varying intensities characteristic of each different object in proportion to its aggregate percentage within the surface. This composite radiation is further integrated into a single (averaged) value over the wavelength interval sampled by each MSS band. This is a manifestation of the mixed pixel problem discussed on page 83.

However, in a Landsat classification or on a smaller-scale map, this complex surface would be simplified by combining all components therein into the precise class name "Orchard."[3] If the orchard is large (encompassed by an array of neighboring pixels), each set of pixel DN's (for the four bands) will probably differ somewhat from other sets in the pixel array. This comes from the natural variability of components within the class "Orchard." The numbers, kinds, and spacing of trees will vary within the scene, as will roads, buildings, ground cover, etc. This variation will be somewhat irregular so that, for each pixel, its ground equivalent surface will contain differing proportions of the features present. Some pixels may have a set of DN's that depart sufficiently from those typical of the class "Orchard" to be identified with sets characteristic of other, often unrelated, classes.

Another aspect of this disparity between a class as defined and the real world is illustrated by two geological examples. In the first, suppose that

[3] This class illustrates the distinction between the concepts of land cover and land use. A phrase such as "terrain partly covered by regularly spaced trees" would describe a land cover type. The term "orchard" specifies a particular land use involving these trees.

Figure 6-12. This difference image compares registration done with 65 accurately located GCP's with a registration done using the 14 worst of the original GCP's. Pixels assigned correctly to the classification *urban* in both data sets are shown in black, *non-urban* in gray, and pixels assigned incorrectly to one or the other class in the two data sets in white because of misregistration. As expected, the differences occur primarily along boundaries between two classes due to shifting of one data set with respect to the other. The gray swaths passing subhorizontally through the upper half of the image correspond to forested mountains on which little or no land urban land uses, and hence few boundaries, occur. Numerous towns and developments lie along the Susquehanna River, giving rise to the large amount of light-toned border that indicates urban and non-urban misclassification. The image was generated as part of a study to determine the impact of errors in Landsat data sets on the feasibility of using Landsat data sets as inputs to Geographic Information Systems.

the Landsat MSS operates on a thick sequence of interbedded sedimentary layers consisting of quartz sandstones and carbonates (limestones and dolomites). Over the wavelength range of the four MSS channels, the carbonates and sandstones (if they are light colored and low in iron) may, in fact, have similar spectral responses. At Landsat resolution, these spectrally similar but geologically distinct rocks would show up in an image (or a classification map) as a single unit. However, a map made on the ground by a geologist using conventional methods would portray this sequence as several distinguishable units defined on the basis of different stratigraphic ages (geological formations), perhaps determined from characteristic fossil content. This is a property that does not lend itself to multispectral sensing, yet is one that properly separates truly different units.

Now, let the sensor scan another area containing scattered outcrops of sedimentary arkose (a sandstone composed of reddish feldspar and quartz as free grains held together by cement) and nearby exposures of igneous granite (commonly composed of the same two minerals as interlocking crystals). Observations in the field of the geological setting of each rock type (e.g., bedding in the arkose; massive structure of the granites), hand specimen examination, or microscope analysis, can usually separate these two significantly distinct rock types. It is on such criteria that these rocks are classified as genetically and historically different, even though they appear quite similar in color, composition, and texture. Indeed, on the basis of these physical and mineralogical properties, the arkose as sensed from space may be indistinguishable from a red granite.

Still other factors must be considered. The MSS, as with most sensors, records radiation emanating from only the outermost thin (essentially, micrometers in thickness) surface layer of the ground or objects thereon. Geological units, and soils as well, are best treated as three-dimensional bodies. Soils, in particular, are defined and identified by their subsurface profiles. Rock bodies exposed at the Earth's surface are subject to considerable physical and chemical alteration such that the materials examined by the scanner may be quite different from the fresh rock underneath. Geologists gain critical information on rock type by breaking off surficial layers to get at characteristic bedrock; pedologists likewise penetrate through the soil with augers or trenching tools to see the field profile. Only then can a geologist or soil scientist be sure of the validity of the field classification.

The point in the above two geological examples is this: geologists in direct contact (i.e., on the ground) with rock materials will probably correctly classify these materials according to criteria explicitly established to permit recognition of each class (geological formation; rock types) only when the materials can be examined *closeup* (sampled on-site). These materials may be identified and separated by different criteria when remotely sensed. The distinguishing spectral properties do not necessarily coincide with the natural differences in the materials by which they are mapped in the field. Thus, in many instances it is difficult—at times even impossible—to classify and hence to map these materials from remote sensing data alone. Maps of rock units made from field studies will not generally coincide with those produced from classification of remotely sensed data. The field maps will be the *standard of reference* as far as they are based on observations and decisions about field or specimen characteristics that meet conventional criteria and are of practical use. Disparities between field and remote sensing maps will usually be reconciled by adjusting the latter to the "ground truth." However, rock and soil surfaces examined by remote sensing devices are often revealed to have anomalies and other interesting features undetected in field mapping. These may be incorporated in the field maps if relevant.

The above discussions should lead you to pose a key question: Accuracy with respect to what? It is almost absurd to suggest that every individual distinct object or entity on a surface be identified and mapped. The maps we use are abstractions, or more rightly, extrapolations. We seek to record the presence and locations of some particular feature distributed on a surface among other features of different nature. The feature sought is the signal. The others are, in a sense, noise. Thus when a geological map is produced, the interpreter considers only the rocks and largely ignores vegetation and soil, which often cover more than 90 percent of the surface. The interpreter imagines what rock unit would be present at any given point by applying geological reasoning to predict (extrapolate) what is actually there underneath soil, vegetation or other cover types.

Intrinsic Accuracy

There is another often overlooked point about maps as reference standards that concerns their intrinsic or absolute accuracy. Just as a remote sensing classification map must be checked by reference to another map as the valid representation of the surface, so also does that map itself require a separate frame of reference to establish its own validity. For decades -perhaps even centuries -maps have been constructed without regard to assessment of their inherent accuracy, although in recent years some responsible mapping organizations have published maps accompanied by some quantitative expression of level of confidence or accuracy. The U.S. Geological Survey has reported results of an accuracy assessment of land use and land cover maps compiled at 1:250,000 or 1:100,000 scales using aerial photos to recognize Level I classes.[4] This study finds that predominant categories can be mapped to meet or exceed the 85-percent accuracy criterion at the 95-percent confidence level.

Thus, one should always keep in mind when defining accuracy for a computer-assisted classification that the standard of comparison, be it a map, an interpreted aerial photo, or "eyeball" field observations, is itself subject to variable, frequently undetermined (and possibly indeterminate) inaccuracies. As a general rule of thumb, the level of accuracy obtainable in a remote sensing classification depends on such diverse factors as the suitability of training sites, the size, shape, distribution, and frequency of occurrence of the individual areas assigned to each class, the sensor performance, and especially resolution, and the methods involved in classifying (photointerpretation versus computer; statistical classifier, etc.), as well as on others already discussed in the workbook.

Influence of Spatial Resolution. The effect of improving spatial resolution of a sensor system can bring about a surprising result. Intuition and experience together would lead one to predict higher accuracies of classification as the resolution becomes higher. This is not necessarily the case (J.R.G. Townshend, personal communication). Studies by several groups show that the classification error may decrease or increase with smaller IFOV (increasing resolution), and may pass through an optimum value (lowest percentage error), as evident in Figure 6-13A. In part, the specific behavior of the curve of error versus resolution is scene-dependent, in other words, is strongly influenced by terrain or land cover types. Two opposing trends operate to determine the curve: (1) statistical variance (s^2) of the spectral response values decreases with coarsening (lower) resolution: classification accuracy improves, and (2) the proportion of mixed pixels (and degree of mixing) increases with coarsening resolution: classification accuracy worsens.

In effect, a lower (poorer) resolution may actually increase the classification accuracy by smoothing or averaging out internal heterogeneities within ground classes because this tends to lower the variance. Again, the result depends on how a class has been defined. If the objective is to classify the broader class *orchards*, a coarser resolution may suffice, but if the purpose is to identify individual trees or other scene components as classes, high resolution is required for high accuracy. Another significant factor is the area and shape of land cover units and their relation to spatial frequency and configuration of boundaries. If the unit or class is so small at some location that a large fraction of the pixels used to define it straddle the actual boundary, then the mixed pixel effect becomes important. In other words, the class at that spot is rendered more "impure" by inclusion of pixels containing contributions from surrounding or adjacent classes. As a rule of thumb, the extent of a localized class should be at least three or four times the linear dimensions of a pixel if the boundary effect is to be reduced. Thus, the argument for decreasing pixel size to improve accuracy given on p. 86 and in Figure 3-1 is a cogent one.

One would also expect accuracy to increase by sampling different parts of the spectrum, that is, by using more spectral bands located in different wavelength regions. However, both field experience and laboratory tests have demonstrated that

[4] Fitzpatrick Lins, K., *The Accuracy of Selected Land Use and Land Cover Maps at Scales of 1:250,000 and 1:100,000*, U.S. Geol. Surv., Circ. 829, 1980, 24 pp.

three to six bands in a limited spectral region (e.g., the 0.5 to 2.5 μm interval) are sufficient to reach a certain level of accuracy. Examine Figure 6-13B. The sets of curves were established with an aircraft-mounted multichannel scanner during aerial flights over several terrain types. Two bands are adequate for recognizing various Level II land use classes, and four bands are enough to pin down agricultural classes. However, even more channels are needed to improve progressively accuracy in classifying geological units. Overall, accuracy may be improved somewhat by operating several sensors over a broader range of the spectrum, as in the VIS-NIR, TIR, and microwave regions (see Activity 9) or by using narrower band widths. However, the substantially increased costs of building and flying these extra channels can outweigh the (often modest) gains in accuracy.

The reason for the gradual to abrupt flattening of the accuracy curves lies in the nature of the spectral response curves (Figures 1-4, 3-5, 6-18, 6-19B and 6-20B). As we learned in questions #1-13 to #1-21, and #3-11, the reflectance values for certain diverse classes (e.g., vegetation versus soil) may be quite different at some wavelengths and similar at others. Also, spectral curves for similar subclasses (wheat versus alfalfa) may be very much alike in shape and even in magnitude. If fundamental differences exist, usually only a few wavelengths need be sampled for intensity to separate classes and, in many instances, subclasses. Commonly, the variations in one wavelength region for various classes are matched by similar variations in another (but not every other) region. Two bands with similar spectral response patterns are said to covary. The bands are therefore redundant, a.k.a. measurements made in one are cross-correlated with the other. There may be only a few narrow wavelength regions in which significant differences occur. However, since those specific regions may be at different wavelengths for different classes, more than four or six bands can sometimes produce better separated classes and hence higher accuracy.

Accuracy Tests

We normally try to test remote sensing classification accuracy against an existing map as the frame of reference. However, if that map is constructed to show only a single theme (forests, or soils, or rock types), which is often the case, we are comparing a simplified, homogenized idealization against the complicated, heterogeneous reality of the actual surface. The specific accuracy (or more to the point, inaccuracy) owes much to this difference between a single component (theme) map and the real world. A correspondence between map and reality may be improved, but seldom ever fully realized, by comparing a satellite sensor-derived classification with a high-resolution aerial photo. Only in this way can many of the individual features making up a multicomponent (mixed) surface be discerned and usually identified.

In practice, accuracy of classification from Landsat data may be tested in four ways (all require, or benefit from, surface observations acceptable as ground truth): (1) Field checks at selected points (usually nonrigorous), (2) Estimate of agreement between Landsat and reference maps or photos (usually visual, nonrigorous), (3) Statistical analysis (rigorous), and (4) Confusion matrix calculations (rigorous).

The first method is almost self-evident. The observer goes to a few accessible localities and looks at the scene, compares it with the classification, and judges whether the Landsat rendition is a valid representation. This is subjective in that it assumes that the observer makes correct judgments. However, in a multitheme map (many classes) it may be necessary to carry out a point-by-point accuracy check, for example, by visiting a large number of field stations laid out in some sampling grid, especially if reference maps and other ancillary data are suspect. The total number of ground checks depends in part on the number of classes but ideally, to achieve a quantitative status, should be a minimum of twenty per class for a full Landsat scene.

The second method is commonly performed by overlaying correctly registered Landsat and reference maps. The degree of correspondence between similar themes, features, classes, and class boundaries is estimated or calculated by an appropriate statistical measure.

The third method works on numerical values

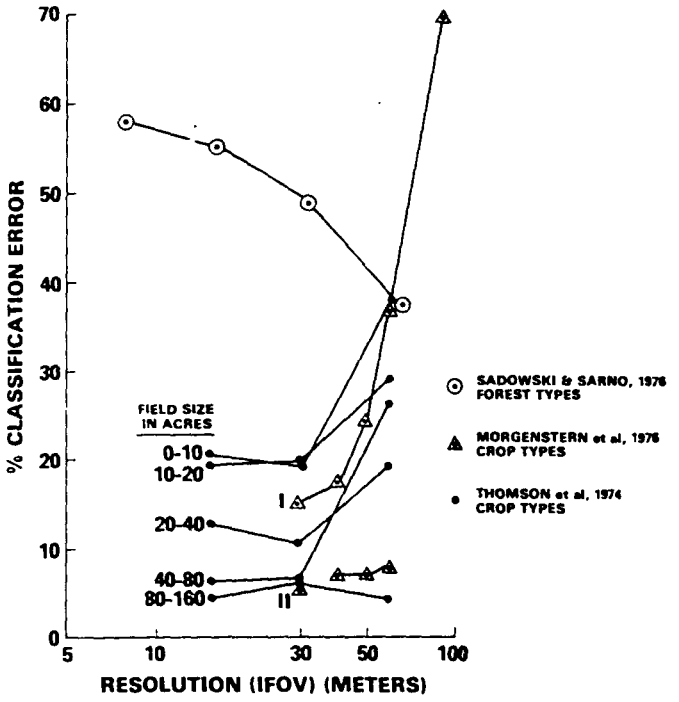

Figure 6-13A. Effect of a changing IFOV on classification error.

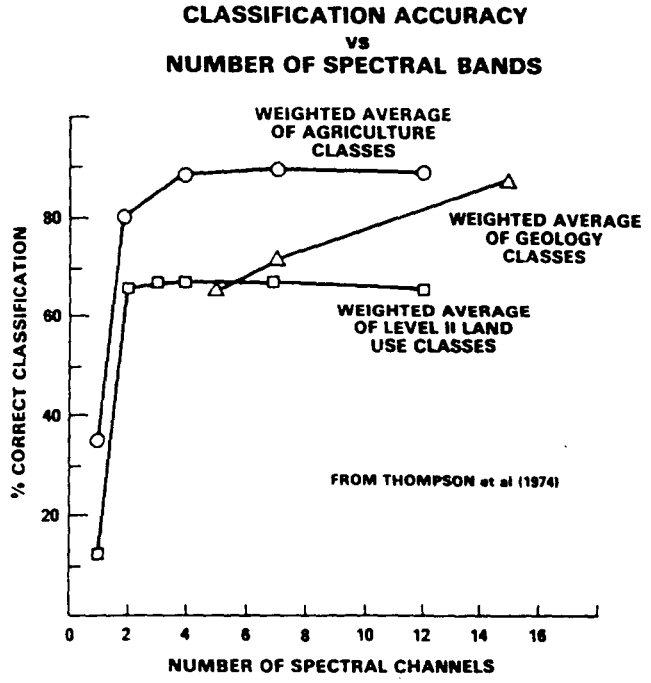

Figure 6-13B. Classification accuracy as a function of number of spectral bands.

developed in measuring, sampling, or processing data. Various statistical devices or tests applied to accuracy assessment may be applied to the basic data and/or the end results. Among these tests are root mean square, standard error, analysis of variance, correlation coefficients, linear or multiple regression analysis, and the Chi-square test (see any standard text on statistics for explanation of these tests). Of special concern are tests to determine the error in geographical (spatial) location of any pixel (usually, in a geometrically corrected, resampled image).

The fourth method is best explained by an example. Consider the case discussed on pp. 219 and 221, in which corn and soybeans near Middletown, Del. were classified. The Landsat-derived classification maps of these two crops, as well as a third category of other crops (barley, wheat, etc.), were rectified and scaled to fit over an aerial photo on which a number of fields other than those used as training sites had been identified from photointerpretation and ASCS records. The map, as a transparency, is overlaid on the aerial photo and pixel-by-pixel comparisons of class identities are made.[5]

After taking a random sample of the classified pixels, and with the photo classification as the standard, the number of pixels correctly assigned to each class and those assigned to the other classes are arranged in a confusion matrix. The table derived from the matrix is a summary of omissions, commissions, and overall classification accuracies. Mapping accuracy for each class is stated as the number of correctly classified pixels (equal to the total in the correctly classified area) in terms of all pixels affected by its classification (equal to this total in the displayed area as well as the pixels involved in errors of commission and omission). For the example shown, of the possible 43 pixels classed as corn from photointerpretation and ground data, 25 were similarly classified by Landsat. Of the 63 pixels classed as soybeans in the aerial photo, 50 were classed as such by Landsat. Of the 72 forests pixels, Landsat correctly recognized 60. Look now at Table 6-2.

#6-13: Why are the mapping accuracies for individual classes lower than that of the overall classification?

#6-14: Deduce and explain what is meant by errors of commission and omission for corn.

#6-15: List three scene-dependent sources of errors for this case.

Recognition of these errors can be instrumental in aiding the analyst to improve classification mapping. An error of omission in a gross sense occurs whenever a class or category actually present is not identified and is therefore left out of the classification. More commonly, the error relates to individual pixels that should have been identified as that class but were not. An error of commission results when a class is incorrectly identified as other classes. A variant in commission error results from improper separation of some single class into two or more classes. Once these errors are recognized by reference to "ground truth," they may be reduced by selection of new training sites, renaming of classes, combination of categories, creation of new classes, or other corrective measures. With each set of changes, the classification procedure is repeated (iterated) until a final level of acceptable accuracy is reached.

Comments

To sum up this section on accuracies: A clear goal in any identification or mapping endeavor is to achieve the highest accuracy attainable. There is often some minimum acceptable accuracy, which depends on the uses to which the remotely sensed classified data are put. Thus the agronomist will opt for accuracies exceeding 90 percent (currently achievable) for classifying major crop types whose seasonal yields are needed in world productivity models. The geologist, however, would not accept accuracies of 50 percent (typical values) for recognition of rock units because such expensive decisions as "where to drill" require more definite

[5] This is a hypothetical example; the actual check was not done in this case.

Table 6-2
Landsat Accuracy Assessment

Photo/Ground Classes	Landsat Classes				Total Possible	Omissions	Commissions	Mapping Accuracy*
	Corn	Soybeans	Forest	Other				
Corn	25	5	10	3	43	$\frac{18}{43} = 42\%$	$\frac{7}{43} = 16\%$	$\frac{25}{25 + 18 + 7} = 50\%$
Soybeans	2	50	6	5	63	$\frac{13}{63} = 21\%$	$\frac{11}{63} = 17\%$	$\frac{50}{50 + 13 + 11} = 68\%$
Forest	3	4	60	5	72	$\frac{12}{72} = 17\%$	$\frac{18}{72} = 25\%$	$\frac{60}{60 + 12 + 18} = 67\%$
Other	2	2	2	100	106	$\frac{6}{106} = 6\%$	$\frac{13}{106} = 12\%$	$\frac{100}{100 + 6 + 13} = 84\%$
Total	32	61	78	113	284			

$$\text{Overall Landsat Classification Accuracy} = \frac{25 + 50 + 60 + 100}{284} = 83\%$$

*Mapping Accuracy (MA) for any Class X:

COMMISSIONS ↓ / OMISSIONS →

$$MA = \frac{\text{Pixels of } X_{correct}}{\text{Pixels of } X_{correct} + \text{Pixels of } X_{omission} + \text{Pixels of } X_{commission}}$$

Pixels of $X_{omission}$ = All other classes in X Row

Pixels of $X_{commission}$ = All other pixels in X Column

identification and location. There is also a cost-dependent constraint related to optimum accuracies. If the cost of attaining a high accuracy by any available mapping method is itself prohibitively high, then a compromise value that may not satisfy all needs might be tolerated. Many Landsat classifications achieve less than optimum accuracies, but there is often no practical alternative way to obtain the desired results. The classifications then become acceptable as a "first approximation" until better ones are produced. This is particularly true for large area (regional) repetitive classifications which are otherwise quite expensive by conventional ground/air techniques. And, finally, current classifications from Landsat data may actually exceed the specific requirements for detail in some types of maps. If, for example, the output sought is the percentage of dense forest cover rather than the distribution of tree species over a large region, Landsat may well serve as an adequate data source for that level of classification, whereas costly aerial photography would be "overkill."

SUPPORTING STUDIES

There are various kinds of ancillary data that prove helpful in interpreting Landsat data. Some of these data types will be considered in the discussion of Geographic Information Systems (Activity 7). Other types include data from diverse remote sensing systems, ranging from ground stations through aircraft to geostationary satellites (Activity 9). Some data were acquired before analysis of individual Landsat scenes and are documented or archived in many places. Much of the data must be collected by the user at later dates, or, if feasible, during actual Landsat overpasses. In most instances, the best ancillary data are those obtained as close to the overpass dates as practical.

Aircraft Missions

Often the most valuable data are obtained from sensors mounted on aircraft that fly over the areas under study. In the NASA aircraft support program in remote sensing, test sites are specified by NASA staff or outside investigators for data acquisition missions along predetermined flight lines. Airborne platforms (Figure 6-14A) assigned to this program currently include (1) an NC130B aircraft operating at altitudes up to 9200 m (30,000 ft) and two RB57F planes operating to 18,500 m (60,000 ft), (Figure 6-14B) based at Johnson Space Center near Houston, Tex., (2) the NP-3A aircraft operating up to 7600 m (25,000 ft.), now based at Wallops Station, Va., and (3) two U-2 aircraft, operating at 19,000 m, based at the Ames Research Center near San Francisco. There are a variety of versatile sensors in the payloads on these aircraft. These include: (1) several film camera systems (metric, high resolution, multiband) that produce small- and large-format photographs by using color infrared, color, panchromatic black and white, and black-and-white infrared film; (2) multispectral scanners, such as the M^2S system (eleven channels covering 0.33 to 13.5 μm) and the Thematic Mapper Simulator (nine channels covering 0.45 to 12.5 μm); (3) microwave sensors, both passive (such as radiometers and scatterometers) and active radar (X, K, L bands); (4) special request equipment not routinely flown (such as a Radiation Thermometer PRT-5); and (5) systems under development (such as the Linear Array Pushbroom Radiometer [LAPR], which uses a pushbroom-type detector). Electronic sensor data are recorded on multitrack tape recorders. These data may be played back to produce images or may be reformatted to a computer compatible digital mode.

Ground Measurements

Many investigations require ground data obtained by field parties assembled to occupy observation stations as the Landsat or aircraft overpass occurs or, alternatively, a few days later. (In some applications, certain field studies may be undertaken much later if the season and the atmospheric conditions are similar.) Among the kinds of field observations that might be incorporated in the analysis are those that tend to be transient or dynamic:

1. Meteorological conditions (air temperature, wind velocity, humidity, etc.)
2. Insolation (solar irradiance)
3. On-site measurements of reflectance
   a. Calibration targets
   b. Natural objects
4. Soil moisture
5. Water levels (stream gauge data)
6. Snow thickness
7. Siltation in lakes and rivers
8. Surface temperatures

#6-16: State three other types of field observations.

ORIGINAL PAGE
BLACK AND WHITE PHOTOGRAPH

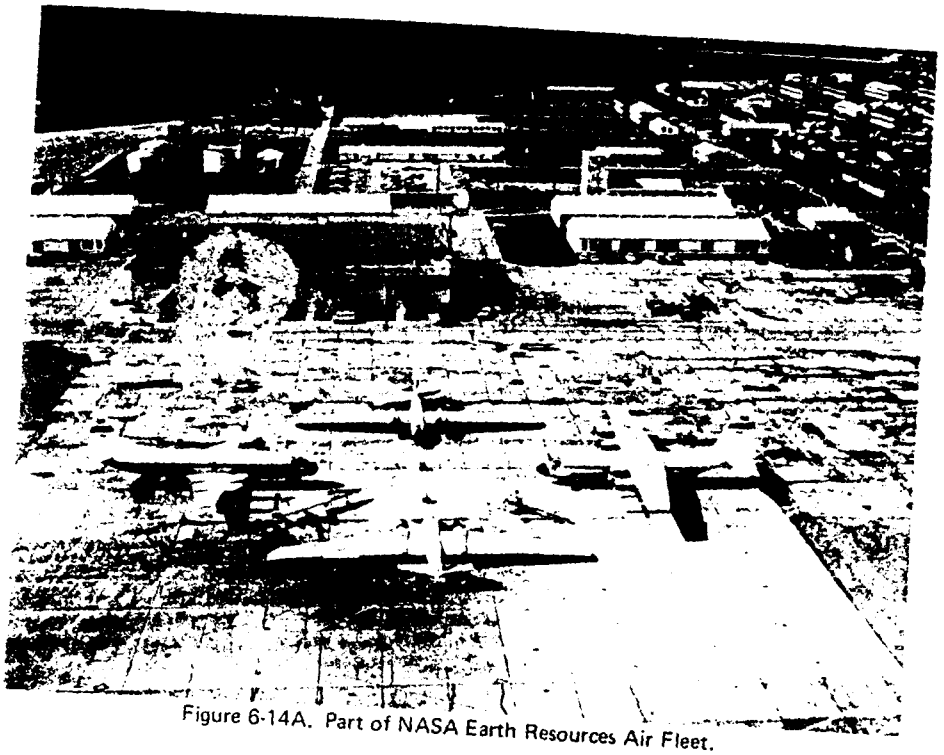

Figure 6-14A. Part of NASA Earth Resources Air Fleet.

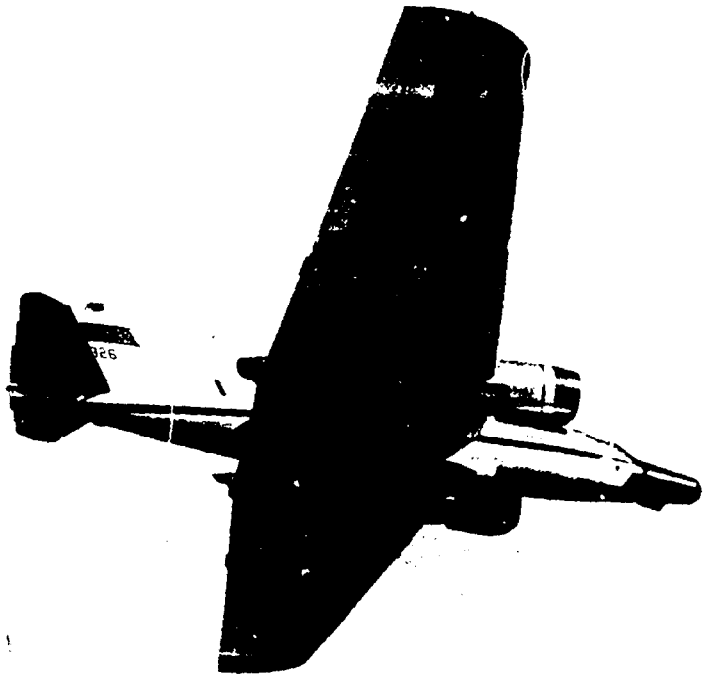

Figure 6-14B. The RB57 airplane in flight.

Most of the observations must be quantitative and require specialized instruments to make the necessary measurements. One category of equipment consists of instruments used to measure radiation emanating from the ground. These include the following:

1. Reflectance spectrometers and spectroradiometers, which measure spectral signatures as a continuous response or as a series of incremental narrow spectral intervals, typically in the 0.38 to 2.5 μm wavelength region;
2. Emittance spectrometers and spectroradiometers operating in the 8 to 14 μm region;
3. Radiometers and radiance flux meters that collect integrated energy or power in discrete spectral intervals within the 0.3 to 15.0 μm region;
4. Radiation thermometers (Barnes PRT-5), used to sense emitted radiation in the 8 to 14 μm region over a temperature range of −20°C to +75°C. A second related category consists of instruments designed to measure direct, diffuse, and total solar irradiance; these include:
   a. Pyranometers and Pyrheliometers (0.3 to 3.0 μm region)
   b. Universal Sunshine Recorders

Some instruments in the foregoing categories may be used for both ground radiance and solar irradiance determinations. Radiance properties of the atmosphere are determined directly or through special procedures; these measurements are applicable to certain atmospheric corrections made on Landsat or aircraft data. Most measurements are calibrated with internal references (for example, a lamp emitting at a fixed output) or with targets placed on the ground. Several of these ground instruments (e.g., PRT-5) can operate effectively on aircraft. Other observations or measurements may be less time-dependent, for example, (1) location of field boundaries, (2) establishment of ground control points (for geometrical corrections), (3) estimates of percentage cover (class densities), (4) determination of harvest yields, and (5) description of extractive sites.

#6-17: Suggest two more field observations that may be made at any convenient time.

An example of a data sheet used to record field observations is the Ground Truth Form for Urban Areas, reproduced as Figure 6-15, taken from the previously cited publication by Joyce (1978).

Remote Field Transmitters (DCP's)

Obviously, it is difficult and costly to send field parties into many different parts of even a single Landsat scene. Generally, only a few proximate sampling sites can be visited. It is to be hoped that they are representative of the full scene or are pertinent to subscenes. Sometimes, however, there is need to collect data from a broad area or inaccessible sites, or over extended time periods. With such requirements, it may be most expedient to set up automated remote sampling sites at which measurements are continuously acquired or obtained at fixed intervals.

To accomplish this in the Landsat program, a series of Data Collection Platforms (DCP's) has been deployed by some users to transmit radio signals from the collection sites through the Landsat spacecraft as a relay station. The Data Collection System (DCS) is described in Appendix A. In essence, signals from some sensors capable of making nearby measurements are encoded at the platform, sent on to Landsat (or another relay satellite in the system) when it passes within "line of sight," and then beamed to an appropriate ground receiving station for processing. Data are usually relayed continuously but the signals are monitored only when an appropriate satellite receiver is within range.

The following are typical examples of the kinds of measurements carried out in the DCS program: (1) air and ground temperature; wind motions, (2) stream heights and velocities, (3) soil moisture, (4) snow pack densities, (5) seismic disturbances, and (6) surface tilting (on volcano slopes).

GROUND TRUTH DATA FORM FOR URBAN AREAS[1]

Training Sample ID No._____
Collected by:_____ Date:_____

High Density Urban ( )[2]
Low Density Urban ( )[3]

If High Density Urban - Predominantly Concrete ( )
Predominantly Asphalt ( )
Predominantly Other ( )
Inert Material Complex ( )_____ e.g., metal roof

Comments:[4]_____

If Low Density Urban
Main type of inert Material - Roof tops ( )
Concrete ( )
Asphalt ( )
Other ( )_____

Main type of vegetation - Grass (Lawns) ( )
Pine trees ( )
Hardwood trees ( )
Mixed pine/hardwood ( )
Mixed grass/trees ( )

Comments:[4]_____

1 An urban area training sample should be 310 m X 310 m (1000 ft X1000 ft) or larger; however, if homogeneous areas of such dimensions cannot be located, areas of 150 m X 150 m (500 X 500 ft) or larger (approx. a city block) are acceptable.

2 High Density Urban is defined as an area essentially devoid of vegetation but with up to 10 percent covered with vegetation in small scattered parcels whose largest dimension is generally less than 31 m (100 ft).

3 Low Density Urban is defined as an area within which inert materials (roof tops, concrete, asphalt) are predominant; but with up to 45 percent of the surface covered with vegetation, including overtopping trees, occurring in small, scattered parcels with the maximum dimensions of each parcel no greater than 62 m (200 ft).

4 Appropriate comments include identification of scenario, e.g., airport runway, industrial complex, downtown commercial area, etc.; height of buildings, e.g., one or two story, three to five story, six or more stories; pitch of roofs, e.g., flat, moderate angle, steep angle; or any other information pertinent to measurements made with overhead remote sensors.

Figure 6-15. Standard ground truth form for urban areas, developed by ERL.

Figure 6-16A shows an example of a DCP station at which hydrographical measurements are being made within a river in the eastern United States. A set of data on stream gauge heights and snow-water content, sampled at one or more discrete times each day from the continuous reading recorders, is reproduced in Figure 6-16B, representing records for a similar DCP elsewhere in the United States.

#6-18: Can you suggest still other candidates for continuous on-site DCP measurements that might prove useful in evaluating Landsat data and in supporting applications? Try for at least four. Think especially in terms of the New York and Harrisburg scenes with which we have been working.

SENSOR DEVELOPMENT

Sensor Limitations

Laboratory and field studies in remote sensing are frequently directed with an eye to the future as well as the present. Invariably, existing satellites in operation send back data that may have serious shortcomings. Most commonly, these problems originate in the sensor system. Consider these points:

1. The spectral intervals or bands may not have been chosen at the best wavelengths for certain types of observations;
2. The bands might be too broad and thus incapable of discretely sensing some diagnostic structure (such as an absorption band) in the spectral response curve;
3. On the other hand, certain bands may be highly redundant or cross-correlated in relation to other bands at least for identification of some classes; that is, variation in spectral response of a material may be so close in two bands that measurements in one band would have been sufficient;
4. The inability to distinguish between faint signals and electronic noise (i.e., instrument sensitivity, measured by S/N ratio) may impair detection of slight but significant differences in target materials of related nature (for instance, different soil types);
5. Spatial resolution may be too low (poor) to recognize individual features whose occurrence could prove essential to the mission and its applications.

Other variables independent of the scanner may greatly influence the measured values of radiance. Such diverse variables as moisture content, physical and chemical states of the surface (for example, roughness, degree of alteration, or intermixing of unusual or extraneous components), characteristics of the atmosphere, and variations in direction (azimuth and zenith angles) of illumination and viewing, all contribute to the spectral responses measured from any platform. The effects of these and other variables must be understood and corrected if reference spectral signatures are to be derived.

"Breadboard" Systems

In order to design new instruments and test improved sensors (as well as to better analyze and interpret data acquired by currently operating sensors) for future space and aircraft remote sensing systems, various research and development programs have been sponsored by NASA and other organizations to build and evaluate these sensors as prototype ("breadboard") models. A sensor is regularly checked by engineering tests as it is fabricated. Further tests in the field, both on the ground and from aircraft, may also be conducted. An excellent example of this procedure is illustrated in Figure 6-14B, which shows the open instrument bay in the underside of the RB-57 in flight. After

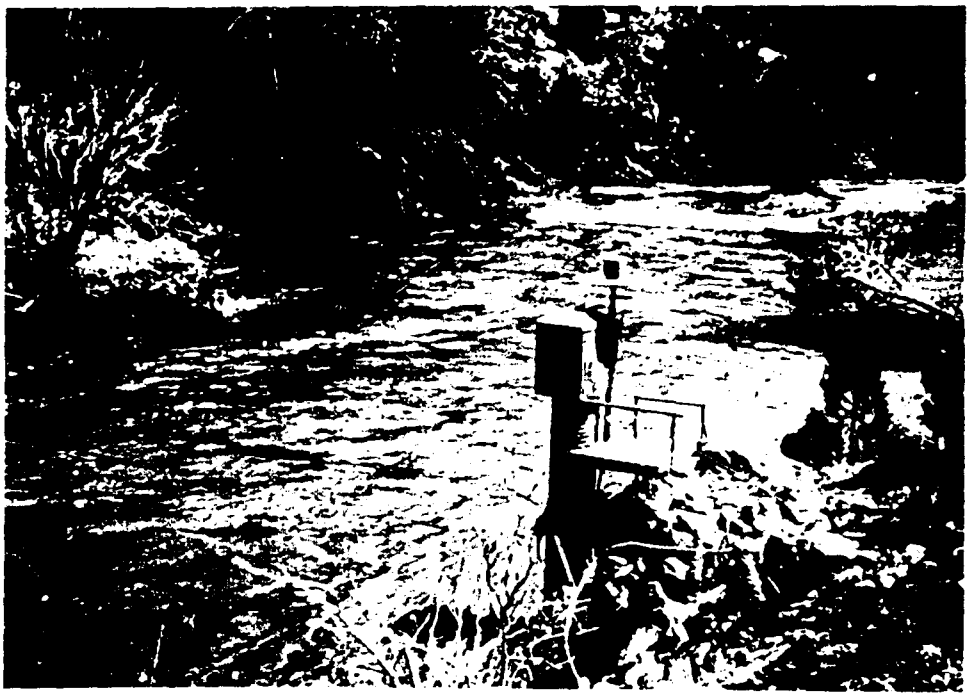

A

Figure 6-16A. Stream gauge and DCP (note antenna) measuring water height along a river in eastern U.S.

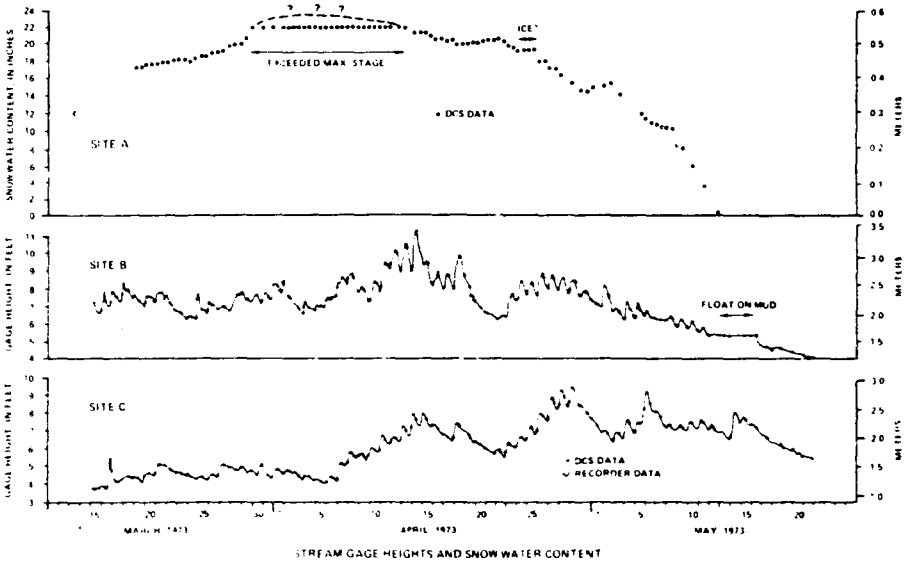

B

Figure 6-16B. Measurement records from DCP in western U.S.

numerous tests in the laboratory, a prototype scanner configured to match the Multispectral Scanner (MSS) on Landsat was flown in a series of aircraft missions. This provided not only a test of the functional capabilities of the scanner in one operating mode, but also furnished some data that closely simulated the expected output from the MSS on Landsat itself. The upper photo in Figure 6-17A shows the images for the four simulated Landsat channels made from data obtained by the prototype during an NP3A flight on October 21, 1971, at an altitude of 2460 m (8,000 ft) above the Delmarva Peninsula. Resolution in this strip (approximately 8 km X 19 km [5 miles X 12 miles]) is about 10 m (33 ft). The photo densities of patterns corresponding to various ground features were measured with a reflecting micro-densitometer. These tonal densities, adjusted to a range of 0 to 2.0 for black and for white calibration surfaces respectively, may be plotted as histograms for each identified ground target (Figure 6-17B). Although not quantitative, these plots constitute a crude spectral signature for each feature; the histograms are broadly comparable to similar plots made from actual Landsat data (Figure 3-4).

#6-19: Many of the fields have an irregular, distorted shape or pattern. This is typical of scanner data from aircraft flights. Can you account for this?

#6-20: The histogram bar heights for hardwoods and old hay are characteristic of vegetation with higher reflectances in the infrared than the visible. This pattern is reversed for fields labeled corn, soybeans, and small grains. Explain.

Laboratory Measurements

From the standpoint of interpretation, analysis of aircraft and spacecraft multispectral data is made easier by referring to standard spectral response (signature) curves for the surface materials and feature classes of interest. Curves obtained in the laboratory generally apply to some more or less homogeneous materials, i.e., the spectral data are from a single "pure component." Those obtained on the ground may represent single components, as sensed in situ, but for larger fields of view (typically 10 m^2, or 1000 sq ft) this target is usually a mixture of two or more similar (rock + alteration) or dissimilar (soil + vegetation) materials. Laboratory measurements serve as a practical starting point in building a reference library of spectral signatures. A series of such measurements on various sedimentary rock units from Wyoming (identified by the stratigraphic formations from which they were sampled) is plotted in Figure 6-18. These are actual tracings of spectral curves produced on an *X–Y* recorder coupled with a Cary 90 Dual Beam Spectrometer. Samples are irradiated with diffused light (from a rhodium-plated hemisphere that integrates over π steradians). A small beam of light reflected from a sample surface is collimated through a hole in the hemisphere, passed through a chopper, and then through a double monochromator (prism and grating) that measures variable intensities over a continuum of spectral wavelengths, and finally on to an immersed thermopile detector. The chopper also sends alternating light beams from a reference light source of constant intensity into the monochromator. The resulting signals are amplified and then transmitted to the *X-Y* recorder. The signals consist of the ratio of sample reflectance to the light source output, from which one may derive the total reflectance (consisting of both specular and diffuse components) in relative intensity units as a function of wavelength for each rock type. Examine these curves and refer also to Figure 1-2.

#6-21: What is the major difference among the various rock units in the visible region?

#6-22: Which rock unit shows a distinct green color? How did you tell?

#6-23: What color is most likely for the Chugwater Formation? For the Thermopolis Shale?

#6-24: Explain the absorption bands at 1.5 μm; at 1.9 μm; at 2.3 μm. Are these most likely caused by the atmosphere or do they indicate some intrinsic characteristic of the specimens? Give your reasoning.

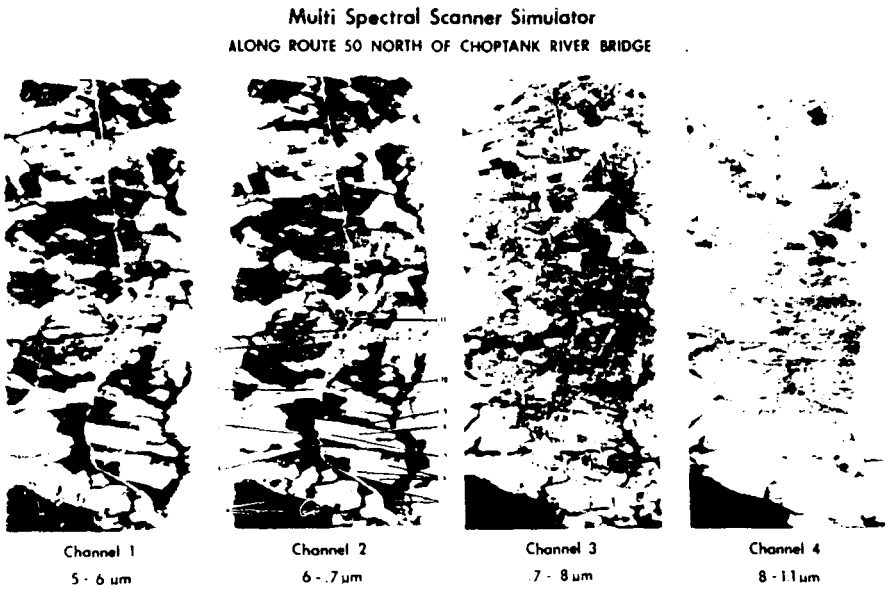

Figure 6-17A. Images of Choptank River farmland acquired by the MSS Simulator on October 21, 1971.

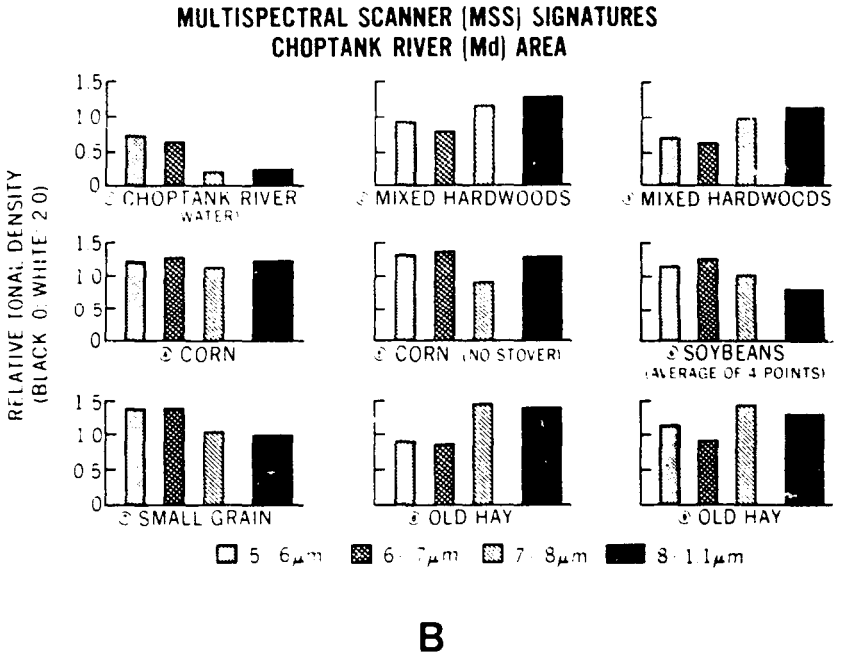

B

Figure 6-17B. Relative densities of ground class signatures of the 9 cover types shown in A.

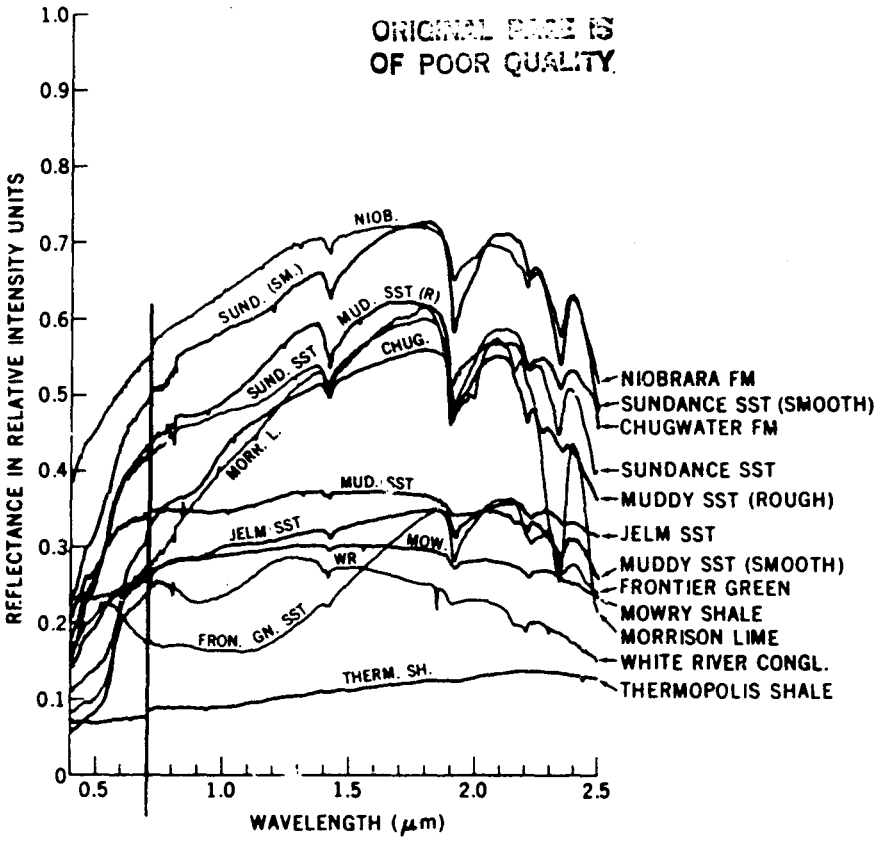

Figure 6-18. Reflectance spectra of Wyoming rock-stratigraphic units.

#6-25: Describe the main differences in the spectral curves for Muddy Sandstone (SST) Rough (natural weathered specimen surface) and Muddy Sandstone Smooth (flat sawed fresh surface). Can you account for the differences?

Field Measurements

The effective size of the sample surface irradiated in the Cary 90 Spectrometer is about 9.7 cm^2. More meaningful spectra may be acquired from natural rock surfaces in the field. These surfaces are more representative of those sensed from the air or outer space, in that they display the variability of composition, texture, alteration, and vegetative cover (such as lichens or algae) encountered in the natural environment. The acquisition of spectral signatures in the field involves some difficulties, the main one being the design of a lightweight transportable system with an adequate power source. Also, data reduction requires several specific corrections to remove the effects of varying (1) solar angle, (2) surface slopes, and, (3) atmospheric conditions.

The Jet Propulsion Laboratory (JPL) at Pasadena, Calif., operates a portable field reflectance spectrometer (PFRS) that resolves these difficulties. The PFRS (Figure 6-19A) consists of (1) an optical head into which light from the target passes through a circular variable filter wheel (0.45–2.5 μm) onto cooled PbS detectors, (2) an electronics pack containing a power source, amplifiers and recorder assembly, (3) a backpack frame, and (4) a tripod. The optical head mounted on its tripod is placed 1.3 m (4.3 ft) from the target. A 30 s scan is made of the target field of view (200 cm^2) and a second scan is made of a standard surface consisting of Fiberfax (a ceramic wool matte with flat, well defined spectral response). Analog signals are converted to a digital data stream. Field

data are reduced after each day. The data are normalized to the Fiberfax reference by dividing sample radiance by reference radiance, point by point, at each recorded wavelength. Variations related to atmospheric conditions, solar illumination, and slope effects are eliminated in this way.

#6-26: Suggest three advantages in acquiring spectral data in the field.

#6-27: How does normalization remove Sun, air, and aspect effects?

Some spectral response curves obtained for various rocks and soils by JPL scientists at a geological site in the western United States are reproduced in Figure 6-19B.

#6-28: These spectral curves show much less structure (peaks and troughs) and less amplitude (intensity) variation than the laboratory-produced curves for the Wyoming rocks. Explain this difference.

Most spectrometer systems are too large and heavy to be carried manually in the field. A common approach is to operate such systems in a truck in which the sensor head is mounted on a moveable lift platform, or "cherry picker," and the power source, electronics, and recording systems are located elsewhere. One such configuration (Figure 6-20A) is used by the Earth Resources Branch at Goddard Space Flight Center to measure spectral reflectances of agricultural and geological features in support of a research program to establish specifications for new sensor systems. The Goddard sensor system consists of (1) a Spectroradiometer Sensing Head, which is a telescope with a selection of narrow to wide fields of view, manual filter wheels with ten narrow or broad band filters per wheel, a chopper to partition light alternately from target and reference cards with fixed reflectivities, and cooled PbS detectors, and (2) a Programmable Control Unit containing associated electronics and a computer microprocessor with software programs that control system functions and reduce and display the data.

Data obtained by this instrument for crops and soil at an agricultural test site are plotted in Figure 6-20B. Also shown are a series of "Critical Bands," which were arbitrarily selected to be investigated in more detail to ascertain which wavelengths afford maximum separability among the classes of interest. After the data were analyzed, it became evident that some of these narrow bands were not optimal or even useful, whereas other new ones (not shown) were better choices.

#6-29: If you were designing a two-band radiometer to detect vegetation and vegetation changes, which bands would you select? Why?

#6-30: Which band might be best for monitoring soil moisture?

#6-31: Specify two bands you might reject. Why?

#6-32: From the plot alone select six bands from the total of fifteen that are well suited to distinguishing between vegetation and soil (also rocks, many of which have similar spectral response curves).

After doing this, compare your results with the bands selected for the Thematic Mapper (TM), a sophisticated scanner destined to be the main sensor on Landsat-D scheduled for launch in 1982. These bands are plotted in Figure 6-21 (see also Figure 9-27) in relation to a set of spectral response curves for vegetation experiencing several levels of moisture stress.

#6-33: Why are the troughs (downward peaks) at 1.4 μm and 1.9 μm not considered for the TM?

#6-34: The four sycamore leaf samples in Figure 6-21 differ in moisture content. Which TM band is most sensitive to these variations?

Data such as these from numerous field studies of a variety of natural materials were intensively analyzed by statistical and other mathematical methods (for example, regression analysis) to obtain quantitative estimates of detectability and separability. As an example, the curves in Figure 6-22 represent the difference in reflectance (spectral contrast) between a soil and a vegetation type for varying conditions of leaf and soil moisture.

A

Figure 6-19A. The JPL portable field reflectance spectrometer in the California desert.

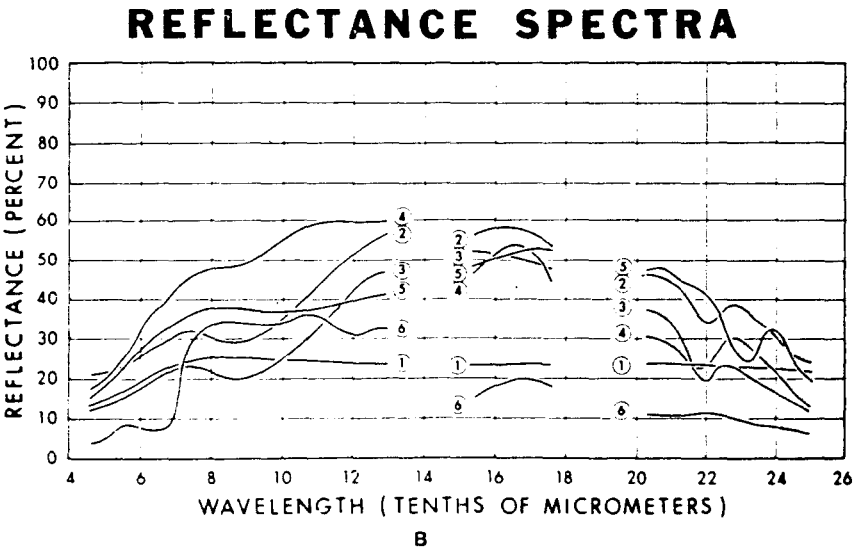

B

Figure 6-19B. Reflectance spectra of surficial materials taken *in situ* by JPL PFRS. Materials: (1) Gray-brown tuff fragments with soil; (2) Argillized andesite fragments; (3) Silicified dacite; (4) Opaline tuff; (5) Tan dolomite fragments; (6) Ponderosa pine.

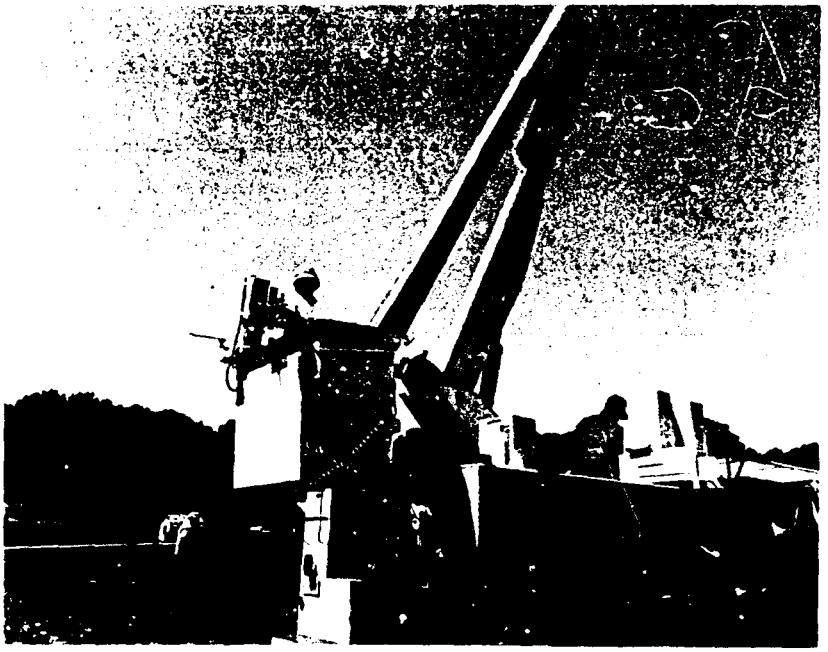

A

Figure 6-20A. The Barnes Spectrometer operating from a truck-mounted "cherry picker."

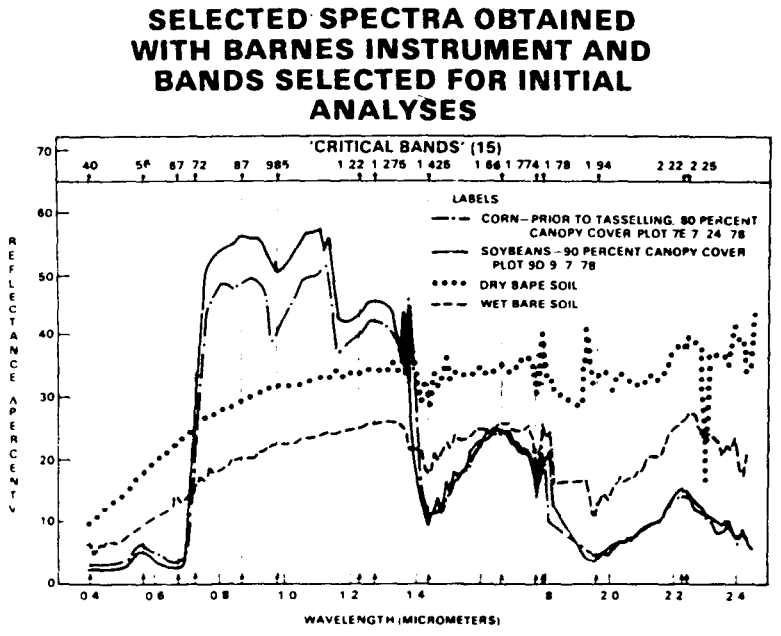

B

Figure 6-20B. Field spectra obtained by Barnes instrument.

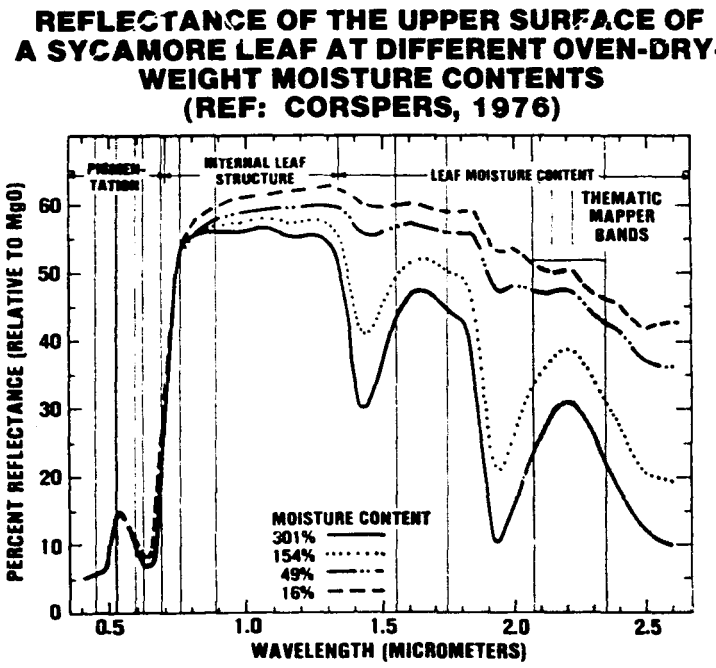

Figure 6-21. Progressive changes in spectral response curves for a sycamore leaf with varying moisture content.

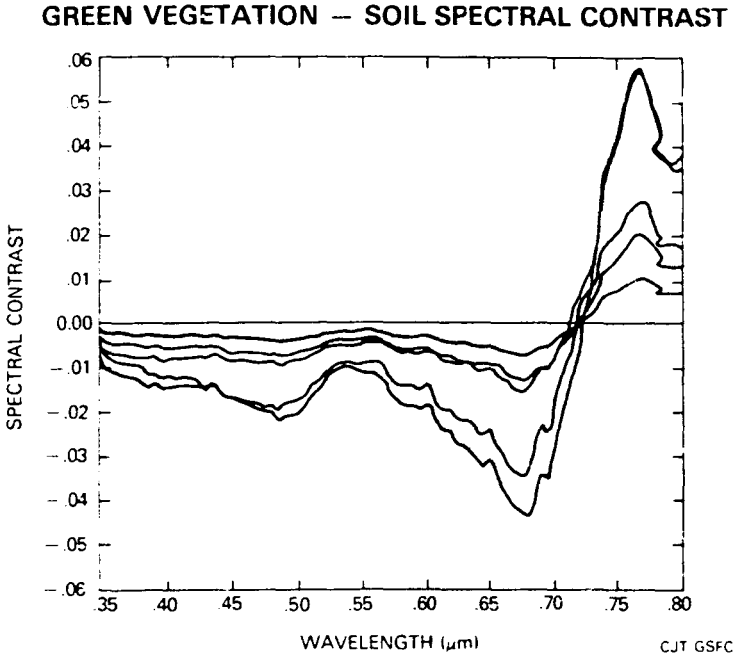

Figure 6-22. Spectral contrast between vegetation and soil.

#6-35. Which two wavelengths appear to define maximum separability?

#6-36: TM band 2 might seem to be a better choice than 3 but is not. Why not? (See Figure 6-21.)

Results such as this account for the selection of TM bands 3 and 4. These two bands lie on either side of the abrupt rise (steep slope) in reflectance (related to chlorophyll absorption around 0.65 μm and high cell structure reflectance at longer wavelengths). Spectral reflectance contrast is greatest in this wavelength region.

Spectral reflectance characteristics of a class will change for other reasons as well. Consider a crop in a field. As the crop grows, both its total biomass within the field and the percent canopy cover will change in a systematic way. Examine Figure 6-23 which contains spectral response curves for alfalfa measured over the same field as this crop proceeds through its growth cycle. A bare field signature is represented by the zero biomass line. Note that several distinct absorption bands and reflectance peaks, at 1.4, 1.7, 2.2, and 2.35 μm, persist as characteristic of the soil regardless of the amount of biomass present. As the canopy broadens and thickens, the response curves show increasing contributions from the vegetation. The progressive increases in reflectances in the 0.7 to 1.3 μm intervals relate to increasing green biomass and canopy thickness. The percent canopy cover and the biomass can, in principle, be determined from these reflectance values and, in particular, from ratios of TM band 4 to either TM 5 or 6, as well as TM 1, 2, or 3.

#6-37: Calculate the approximate ratio of TM band 4 to 5 and TM 4 to 1 for (a) zero cover (and biomass), (b) 50 percent cover, and (c) maximum cover (and biomass).

A Two-band Radiometer. The above results also led to the development of an easy-to-use hand-held radiometer that measures reflectances in two narrow bands closely matched to the optimal pair (TM 3 and 4) just listed. This portable instrument permits frequent measurements in the field over extended (trans-seasonal) periods. Results of such a measurement of a single winter wheat stand over a one-hundred-day interval that includes most of the growing season (from March to July; Julian [calendar] dates 80 to 180) are shown in Figure 6-24. Data obtained from this include (1) red radiance (curve A), (2) photo-infrared radiance (B), (3) IR/red radiance ratio (C), and (4) normalized difference (D), defined as ND = (IR-Red)/(IR+Red), all as functions of Julian date, ND as a function of crop calendar (growing degree days) (E), and ND as a function of grain yield (F).

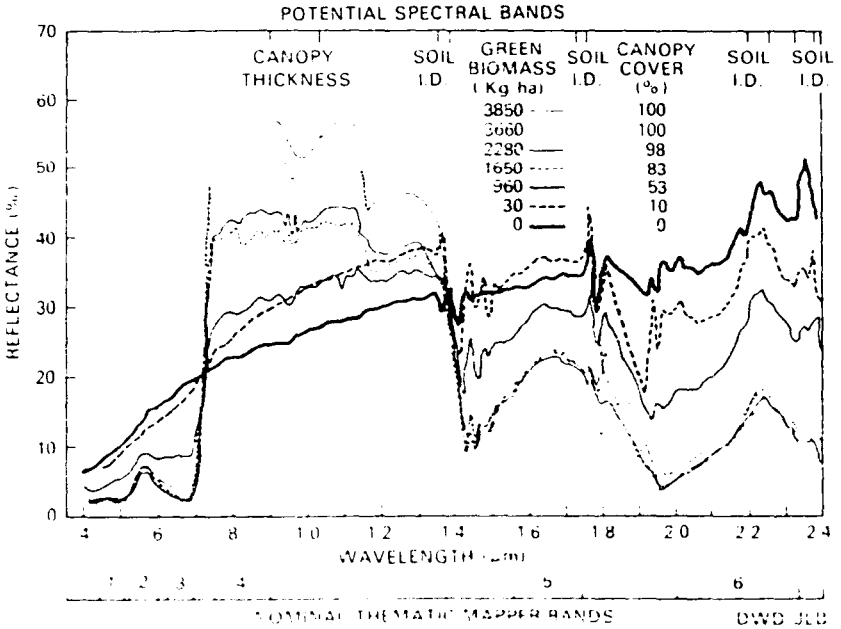

Figure 6-23. Variations in spectral reflectance as functions of amounts of green biomass and percent canopy cover.

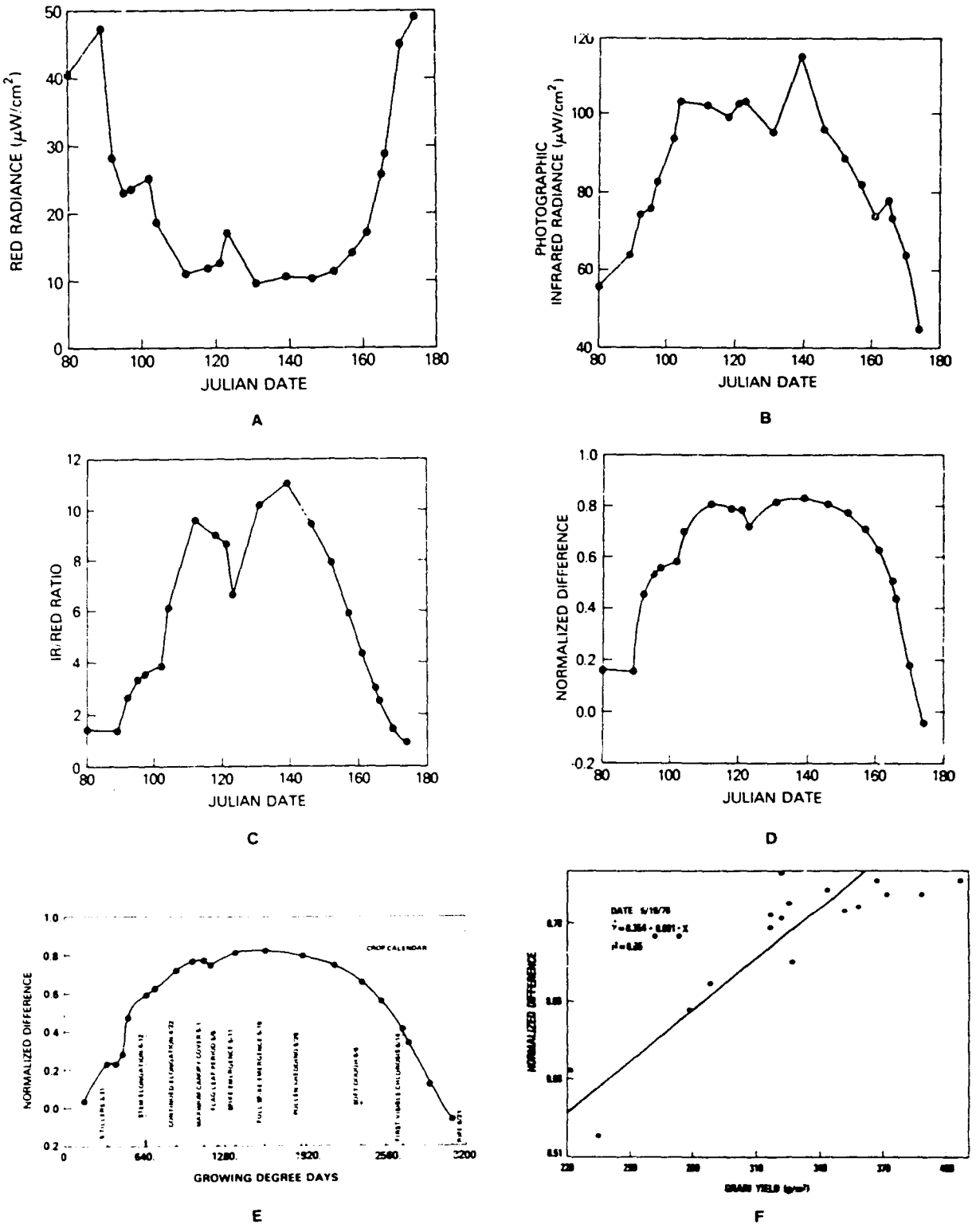

Figure 6-24. Variations in red and IR band radiances as a function of temporal growth history (crop calendar).

#6-38: Suggest a way in which observations over time in these two wavelength regions may be used to establish (1) the stage of growth, (2) the crop yield, and (3) the wheat water stress.

There are, of course, inevitable problems in relating the spectral measurements to yield. The absolute value of the IR/red ratio with respect to a third variable, yield, can be confused by several factors, such as:

1. Any *additive* (rather than multiplicative) variable not removed by ratioing (the atmosphere is one such variable) will bias the values, often nonsystematically.
2. Different varieties of a single crop can, and in fact usually do, have different planting dates. This results in different canopy densities, and thus different IR/red ratio values, for different varieties which can have identical yield values.
3. The different canopy densities of the (2) scenario cannot be differentiated from a healthy versus stressed situation within a single variety except by continuous monitoring and observing the unexpected change in the stressed crop.

Regardless of these complications, this use of spectrally measured temporal change can take advantage of the natural crop calendar (E). The wheat, for example, displays a rapid rise in both IR/red ratio (C) and ND (D) soon after the plants (tillers) first appear. A maximum is reached around Julian date 139, near the time of full spike emergence. This is an estimate of the stage in growth when the largest IR reflectance from the wheat canopy correlates with the greatest green leaf biomass. A yield function for this stage is calculated by comparing maxima for different training sample sites with their respective yields. This may be quantified through use of regression plots (F). The curves in Figure 6-24 decrease as the wheat enters senescence prior to harvest; this relates to chlorosis (decrease in chlorophyll) as the wheat ripens to a golden brown. The peaks, or troughs, around date 123 in the four curves (A-D) represent the effects on red and IR radiances from moisture loss during a mild drought which ended with week-long rains between dates 124 and 130.

Field studies with this radiometer were also undertaken to assess the influence of changing the direction (aspect) of view and view angle at a near constant Sun position. Typical results are plotted in Figure 6-25. Such a plot establishes a set of criteria from which corrections for varying aspect and angle can be applied. This kind of information is helpful in determining orbital parameters (such as altitude, eccentricity, and time of day, which affect image characteristics, the size of field of view, illumination angle, and resolution) for new spacecraft missions. At least one NASA mission (proposed for the future) would carry a pointable sensor that can look off nadir to provide data for features beyond the normal ground track ("footprint").

#6-39: What variation or distortion, for which suitable corrections must be made, would such a pointable imager encounter?

CLOSING REMARKS

We shall finish this extended treatment of the concepts of near-surface observations by re-emphasizing the dual nature of the remote sensing approach. On the one hand, remote sensing is an efficient way to gather large quantities of information from vast areas without actually having to be on the observed surface. On the other hand, this information will seldom be effectively applied unless the interpreter has first-hand familiarity with the surface of interest, or at least with models of such a surface. This knowledge is acquired in several ways—from single field observations, from judicious investigations at training sites, from sophisticated measurements of spectral properties of materials in the laboratory, on the ground, or from the air, and ultimately, from a rigorous mathematical analysis of the data to test for validity and correlation. Having thus constructed a foundation in the interrelation between surface materials and data describing them as sensed from

a distance, we shall proceed in the next activity to discover a powerful and flexible way to organize, retrieve, and interpret data of many kinds and sources through integration into a geographic information system.

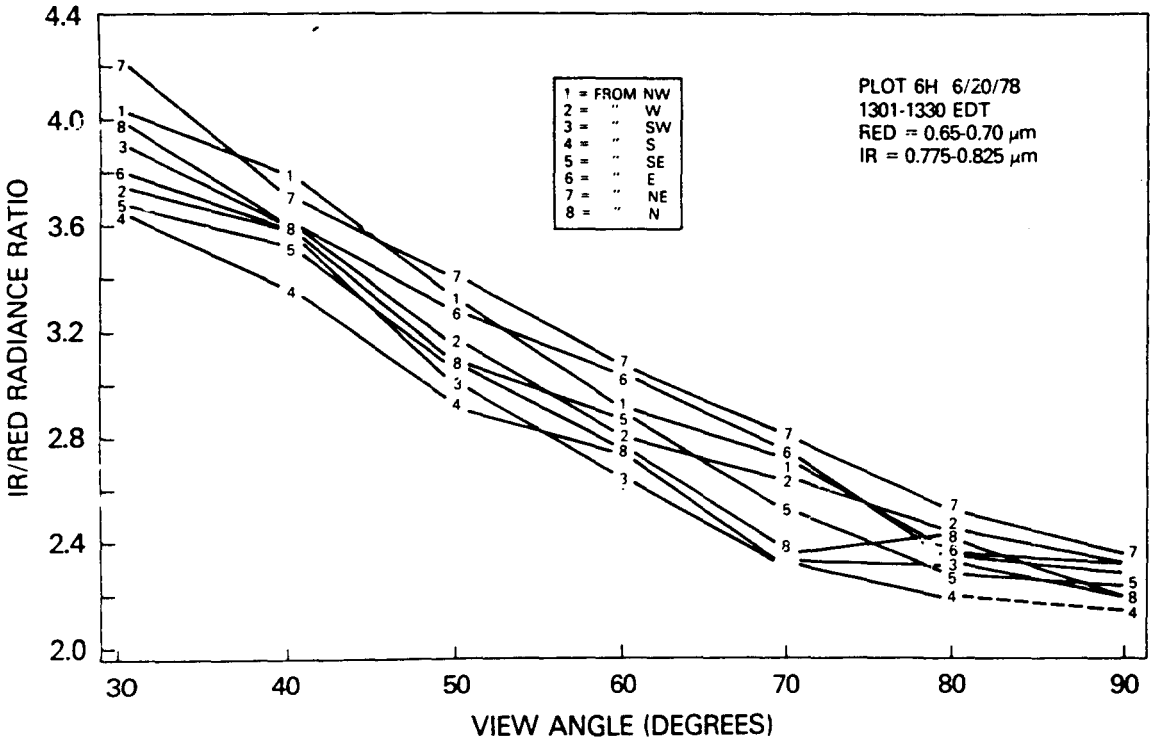

Figure 6-25. Variation of IR/red radiance as function of view angle and azimuth angle.

N83
10465

UNCLAS

ACTIVITY 7

GEOGRAPHIC INFORMATION SYSTEMS[1]

LEARNING OBJECTIVES:

- *Be able to distinguish between a Geographic Information System and a Data Management system.*
- *Have an understanding of spatial data handling by conventional methods versus the automated approach.*
- *Be aware of GIS design and capabilities*
- *Understand the concepts and problems of data base development and management.*
- *Recognize how a computerized GIS can model conditions in the present "real world" to project conditions in the future.*
- *Recognize the utility of integrating Landsat and other remotely sensed data into the GIS.*

[1] This activity was prepared by Mr. William J. Campbell of ERRSAC.

YOUR DATA REQUIREMENTS

Even though you may be moving relentlessly through this workbook, we ask you to slow your pace of learning just long enough to ponder the following seven questions before starting this important activity:

1. What kinds of data have I (the reader) been relying on up to now in accomplishing my tasks as a discipline specialist (or manager, planner, entrepreneur, information processor, or whatever)?
2. Do I appreciate the self-evident or deducible interrelations or correlations among the data types?
3. How can I best organize or reference the different data types to preserve and test their relations?
4. What methods do I use to translate diverse data into the coherent information necessary to understand my problems, make decisions, and manage my operations?
5. Is there a better way (than I am now using) to organize, store, retrieve, rescale, analyze, interpret, model, inventory, update, and display the data that serve as inputs to my information requirements?
6. How can Landsat fit into this scheme or system?
7. Would any such new system really help me do my job better, or at least, to influence others in arriving at a consensus on decisions?

We shall attempt to reach answers to these provocative questions as we look carefully into the concepts embodied in the term Geographic Information System, hereafter referred to as GIS.[2] Before we go into details, let us look at some of the general characteristics and the rationale for a GIS.

LANDSAT - SUPPLIED INFORMATION

As we have seen repeatedly in the preceding activities, Landsat data can provide some very specific kinds of information. These include:

- location and identification of major crops
- distribution and identification of forests
- location and status of lakes (greater than 2 acres)
- major categories of land use
- broad patterns of urban development
- characteristics and interrelations of major landforms
- extent of snow cover
- indications of offshore sediment concentrations

There are obviously many others.

#7-1: Think of at least four more kinds of information obtainable from Landsat.

The most common form of representing Landsat data as processed output or information is in some type of thematic map. This map is derived mainly by a classification procedure tied either to appropriate computer methodology or to manual photointerpretation. For many uses, particularly those of a problem-solving nature, such a map may be all that is required. However, more generally, a Landsat thematic map will be just one of a series of data sources that must be integrated, compared, considered jointly, and then synergistically manipulated to arrive at some kind of end result that points to decisions or other actions. Let us illustrate this with a realistic example.

[2] Also known as Geobased Information System or Natural Resources Information System.

TYPICAL GIS TASKS

Suppose we are faced with the task of selecting a site for a large steel plant in some section of central Pennsylvania near (but not within) Harrisburg. What do we need to know? Certainly many things, some not obvious or seemingly related. Let us just brainstorm a few, without regard to any logical order:

1. land ownership
2. topographical relief
3. proximity to railroads
4. direction of prevailing winds
5. slope stability (if mountainous)
6. extent of forest cover
7. access to power lines
8. bearing strength of soil
9. existing buildings
10. proximity to housing
11. EPA requirements
12. cost of living.

This is by no means an exhaustive list. These factors or information categories constitute what is known in GIS terminology as data elements.

#7-2: Try to think of five more data elements that are pertinent.

#7-3: Underline any of the first twelve entries that are likely to be handled or assisted by Landsat observations.

Implicit in this sort of problem is a variety of data types that fall into different categories of concern: land cover assessment, regional planning, engineering studies, site safety, political considerations, energy needs, environmental regulations, socioeconomic conditions, and numerous others. Clearly, the sources of data must be varied and often independent.

We can examine another somewhat different application or activity that will expand on the ideas we are exploring. This time, the task is to design, develop, and operate an efficient agricultural complex dedicated to growing sugar beets in the Swatara Creek Valley west of Lebanon, Pa. In this instance, a new dimension has entered the picture, namely time, as expressed in the dynamic nature of the processes involved in the cultivation of a crop. Important changes take place with the seasons—some fixed and dependable, others random and erratic. Again, let us list a few new factors to consider, in addition to some, such as land ownership, forest cover, railroads, etc. that were mentioned in setting up a steel mill site but that also apply to this crop siting case:

1. soil types
2. seasonal rainfall
3. history of crop productivity
4. soil moisture
5. distribution of existing farms
6. flooding potential/frequency
7. market conditions
8. cost of fertilizer
9. number of sunny days
10. frost dates
11. sources of water
12. insect infestation.

#7-4: Can you think of any more? Underline those factors that are probably dynamic or transient.

In this example, something more is needed. To operate an enterprise prone to the vicissitudes of climate, economics and public tastes it is necessary to have some understanding of how the factors, as variables, interact in the continuing process of production. Thus, what changes in fertilizing are demanded when a farm has been dedicated to the same crop over a long period (nutrient depletion)? How much water must be diverted during a drought? Should some farms be reallocated to another crop type in response to long-term market fluctuations? Are regulations imposed by federal, state, or local governments being met or violated?

The interactions among variables can be incredibly complex. To control the production process, it is necessary to formulate a *model* for crop growth that takes into account the dynamic interrelations and cause-effect responses of the appropriate factors. A model in this context establishes the functions, sequences, and feedback effects of the determining variables in the dynamic operation of a system.

GEOGRAPHICAL ACCURACY OF CLASSES

While you may not have noticed it, there has been a common denominator in the two examples just considered, which is inherent to most (but not all) of the data types. We have been dealing with activities of man at the *surface* of the Earth he inhabits. One prominent attribute of things *surficial* is that they have *location*, that is, they can be referenced to some geographical locator system, as for example longitude-latitude, township-range, distance from x, y, z, etc.

Another characteristic attribute is simply that features, objects, or materials at the Earth's surface may be conveniently grouped into distinct classes, categories, units, or themes. These entities are made discrete by placing boundaries around each class, wherever it occurs, to separate it from neighboring classes, and by surveying in the locations of each class on the surface by using some locator system. When the distribution of classes is rescaled and depicted in a two-dimensional plot, the result is a map—a collection of located and identified categories or classes distributed throughout a surface continuum. Normally, no given class contains ; describes all meaningful objects within any (bounded) parcel of surface assigned to that class. Typically, a class may be subdivided (e.g., water with or without sediment; field crops into corn, alfalfa, hay, etc.). Different classes may be set up for different combinations of objects or for different themes. Thus, different kinds of maps (land use vs. land cover classes; geological vs. rock units; geographical vs. cultural features, etc.) may be specified.

In general, similar or related classes occur discontinuously throughout a map, in patches or other patterns, with the boundaries of any one patch usually irregular or polygonal. Unrelated classes (from different hierarchies) on separate maps may (but rarely do) coincide with the identical surface area when overlaid. More commonly, when several maps, each with its particular assemblage of classes, are overlaid (imagine each as a transparency and all placed on a light table), the superposed polygonal patterns of the several classes will overlap (cross-cut) in such a way that some may fit one another to some degree but others show almost no geometrical correlation (i.e., are randomly distributed). A close fit usually, but not necessarily, describes some spatial correlation which may be accidental or may indicate some genuine relation.

INTEGRATION OF DIVERSE DATA SOURCES

The method described in the preceding paragraph is one way in which discipline specialists have utilized and interpreted maps of various kinds taken together as inputs in analyzing a problem, arriving at a decision, or running an operation based on a model. Sometimes, maps are actually overlaid, or several map types are combined in a single sheet (e.g., a topographical and a geological map), or, more often, the user simply glances back and forth among several maps and mentally establishes connections and relations.

However, most problems or applications dealing with the surface require consideration of many sources of data input. The eye becomes confused and the mind tends to "boggle" when more than two or three maps are visually compared simultaneously. Although land planners and managers rely mainly on graphic data displays—maps and drawings—they must also incorporate data from other formats, such as general descriptions, tables, statistical plots, etc. In the demanding technologies of today, the sheer volumes of data, with the corresponding need to keep track of and continuously interrelate and update both the data and their information outputs, soon become unmanageable.

Is there a solution to this surfeit? Fortunately yes, as a consequence of the advent and general adoption of the computer in modern technology. Almost any kind of data may be organized into digital format. An image or picture, as we noted in Activity 5, is an orderly array in x-y space of points that each constitute the locus of a variable. If that variable is an intensity function, such as a radiance

value or percentage reflectance, it can be assigned a number expressing that intensity (or a correlative density). Systematic sampling of the variable in x-y space permits a data stream in sequence to be easily recorded on a computer tape or a card series. A map or a graphical plot may likewise be readily digitized by assigning a unique x, y value to each selected point along lines. Even tabular data, if applicable to specific localities, may be recast in spatial terms.

Thus, these varied data are all suitable as components or inputs to an information system. When they possess spatial singularities, they may be referenced to a geographical base common to all as part of a Geographic Information System. The usual practice with geobased data is to reduce or enlarge and rectify the spatial entities to one scale and projection. The geographical coordinate system selected for the base is easily specified in x-y coordinates. The classes or other spatial information are entered into the data base by sampling each input map along this uniform-scale coordinate system. In the digitization process, the natural, usually polygonal, boundaries of a class at any one location are outlined by a finite number of x-y points, and relevant information about the class is specified (encoded) by keyword descriptor terms or phrases. Alternatively, the x-y grid (at a spacing representative of a scaled distance) will form cells (usually, but not necessarily square), which are superimposed over the classes. Decision rules permit assignment of the relevant information from one or more classes that happen to fall within each cell. Once all the map, graphic, tabular, statistical, and descriptive data have been encoded and their relative positions indexed by a polygon or grid locator system, it now becomes an almost straightforward routine for the computer to compare data sets, produce new overlay combinations, assess the influence or interaction of different variables, and provide input to models. This is the "heart" or essence of the GIS approach to data management (Figure 7-1).

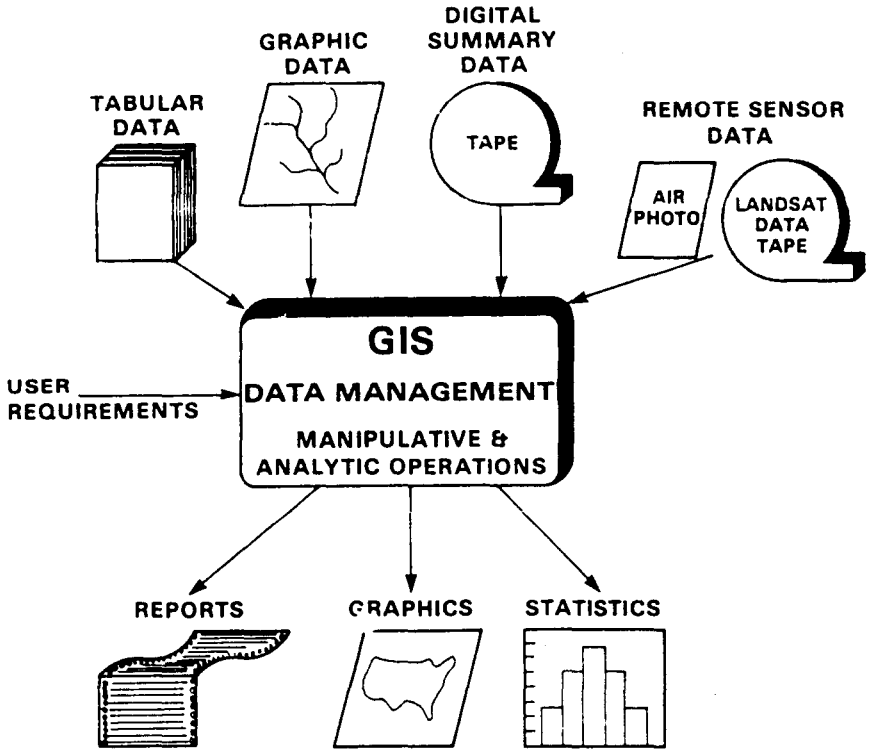

Figure 7-1. Schematic showing a generalized Geographic Information System (GIS) for data management.

Who Is Using GIS?

Many state and local governments, federal agencies, and private industry are now on the GIS "bandwagon."[3] Organization of data previously acquired and continuing to inflow into a GIS promises to revolutionize worldwide the way in which we store and retrieve data and convert the data into new information, analyze dynamic systems, and present the results for decision making. Land planning and management seems to be the principal driver behind the adoption of a computerized GIS as the preferred, most viable information handling technique. The primary importance of Landsat, and other remote sensing systems, to GIS is that they provide frequent quantitative updates for certain input variables connected with those surface features or classes important as components to a GIS.

One such GIS has been much publicized in recent years. This is the *Decision Information Display System* (DIDS) developed at Goddard Space Flight Center for the United States Congress, the Executive Branch (White House), and the Department of Commerce (Bureau of the Census). Information may be displayed on a TV screen or as hard copy pictures at scales ranging from the entire United States down to county levels or Standard Metropolitan Statistical Areas (SMSA) (see p.232). Twenty-five major categories include: population, labor force, income, housing units, presidential vote, retail trade, agriculture; each category is further subdivided into as many as twenty-five subcategories. Examples of several output displays are given in Figure 7-2. At present, DIDS does not use remote sensing data, but Landsat classifications could be accepted.

You should by now have an idea of what GIS is and what it can do. In the remainder of this activity we shall go into some detail about the system and shall explore through examples the role of Landsat as a major component in a GIS.

DISTINCTION BETWEEN GIS AND A DATA MANAGEMENT SYSTEM

A Data Management System is a set of programs used for the manipulation and retrieval of logically related files containing data and structural information. It allows analysis to be used in some decision-making process. A GIS is a georeferenced system for the specification, acquisition, storage, retrieval, and manipulation of data. These data may be related to a place; that is, the data elements link the data to a location identifier, whereas a Data Management System does not require the location distinction.

 # 7-5 Mention one data element related to water consumption lying in each dimension (spatial, temporal, thematic) that is appropriate for a GIS. Give an example of a GIS that contains data elements in all dimensions (spatial, temporal, thematic). Differentiate it from a comparable data base (show how this same information could be organized in a data base that was not a GIS).

[3] A broad non technical review of GIS is presented by P. A. Tessar and L.M. Carton, *A Legislator's Guide to Natural Resources Information Systems*, available from National Conference of State Legislatures, 1125 Seventeenth Street, Suite 1500, Denver, Colo. 80202.

ORIGINAL PAGE
COLOR PHOTOGRAPH

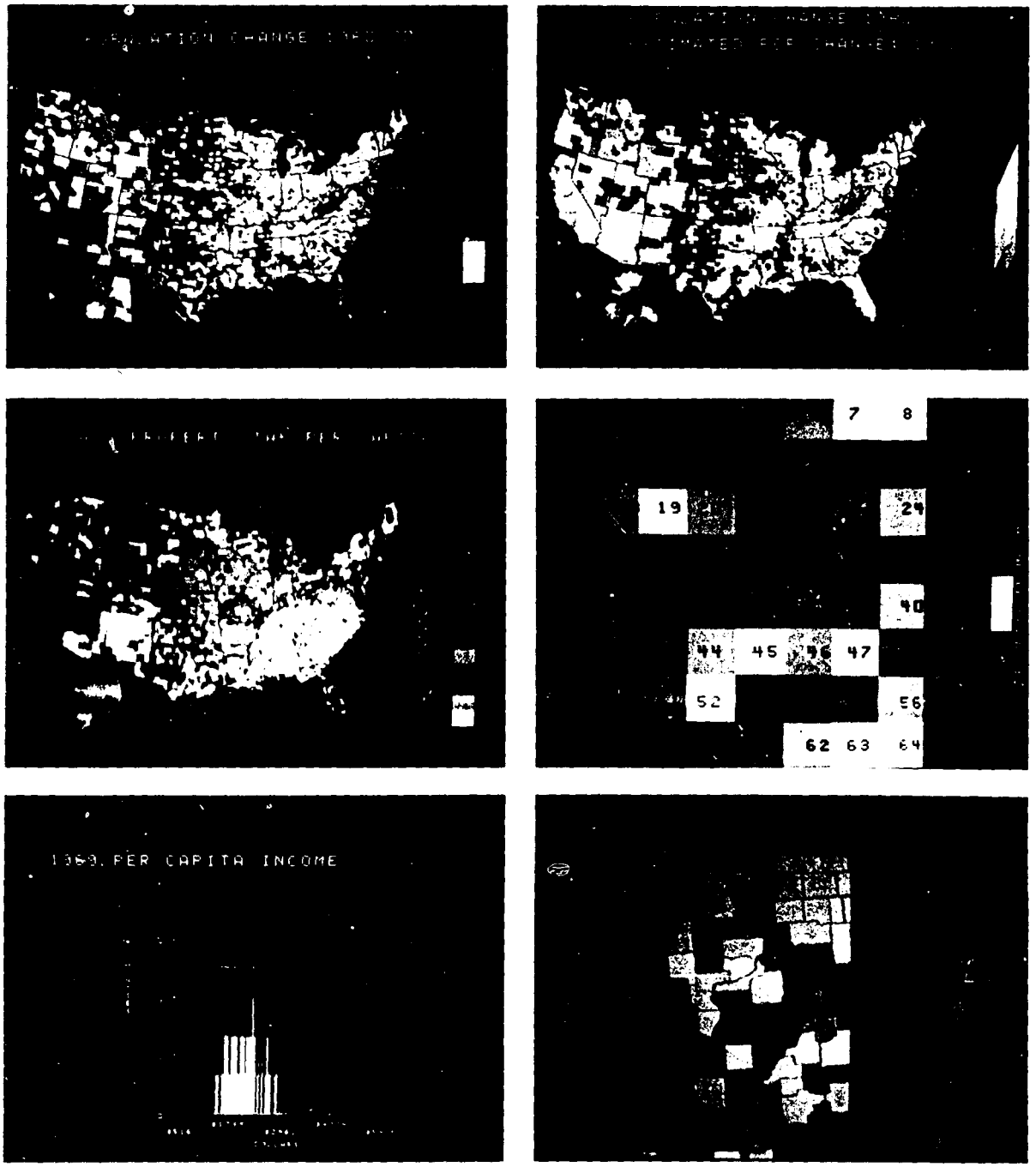

Figure 7-2. Some typical graphic displays on the screen of the Decision Information Display System.

System Design and Capabilities

The system design and flexibility are directly linked to cost. The higher the degree of flexibility and independence, and the greater the size of the data base, the more it will cost. The system design should address geocoding, input processing, data management, manipulative and analytical operations and statistical and graphic output (Figure 7-3).

Hardware

Because we are considering a computer-aided GIS, we should mention some of the special hardware needed for input, display and output of graphic data. An interactive display is certainly a requirement for the 1980's. The CRT is usually accompanied by a keyboard terminal that will interact with a "host" computer or have its own "local" intelligence. Display and hardcopy output may take a variety of forms, some of which are:

1. plotters or drafting table -this will draw maps, charts, graphs, etc
2. line printer -this can draw maps or displays and is available in alphanumeric or electrostatic format; overprint or dot matrix capability is also available
3. raster scanning device
4. ink jet plotter
5. color film recorder–some of these products will be illustrated later
6. CRT -this has already been discussed above.

These devices have a wide range of cost and sophistication. The optimal combination of equipment should be carefully reviewed. The description of other hardware components, such as array processors, central processing units, disk drives or tape drives, is beyond the scope of this activity.

Geocoding—Developing the Data Base

It is not our purpose in this activity to discuss all the particulars of data base development but rather to present a summary of the available techniques. For a detailed description see, for example, Tomlinson and Calkins (1977).[4]

Two main points should be considered: first, the background of the data to be encoded (such as cartographic) and second, any statistical or other attributes attached to the data, such as stream flow, area measurements, or soil erodibility index. Encoding of geo-referenced data may be accomplished manually, for example by photointerpretation of aerial photographs, or automatically from computer classification of Landsat data.

The Grid Format. The first choice the user must make is the format of each spatial layer: grid format, polygon or both. A uniform grid system is a relatively simple way to organize data in relation to computerized data input. Once the data are collected they may be overlaid on a specific grid size and the collected data coded into each grid cell. The information is coded numerically, row by row, and digitized onto computer cards (batch processing), alternately may be entered and displayed on a cathode ray tube (CRT, interactive processing), or can be input through an optical scanning device or by using a digitizing table.

With the grid system an important decision must be reached: What will the resolution size be? In other words, what will be the size of each unit in which the spatial data will be housed? (For example: one grid cell = 12 acres.) A disadvantage of the grid is that if any smaller grid size is required after the data have been collected for a grid of a particular size, the data must usually be recollected; however, it is relatively easy to aggregate cells to a larger grid cell size.

A second consideration with the grid system is grid coding types. This encoding can become

[4] Tomlinson, R.F. and H.W. Calkins, *Geographic Information Systems, Methods, and Equipment for Land Use Planning*, 1977.

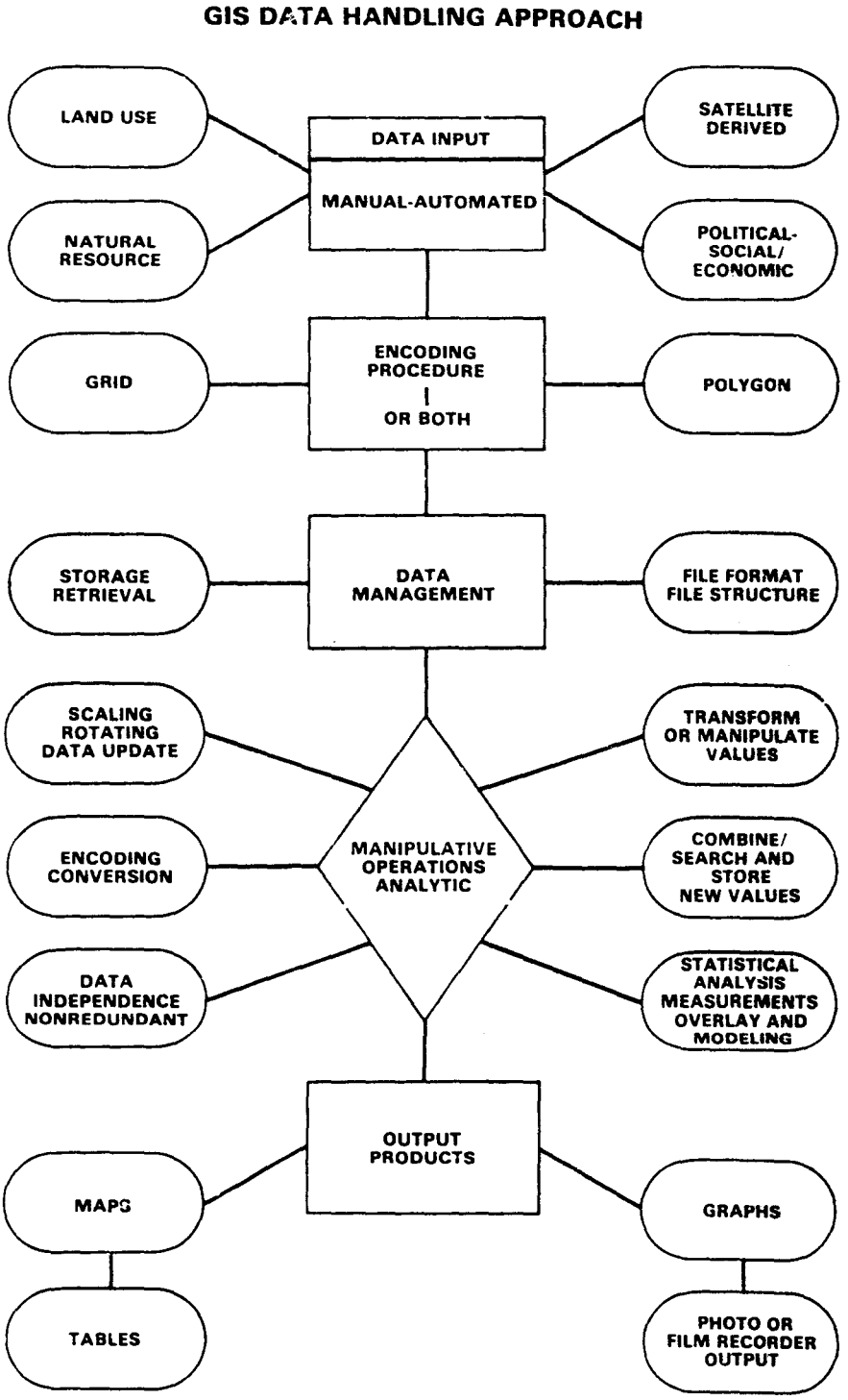

Figure 7-3. Flow diagram of steps in a typical GIS data handling routine.

quite complex. The simplest method can be a nominal code, either numerical or alphabetic. This permits retrieval of that file, but does not give exact locations of data within the cell, and therefore some geographical accuracy is lost. Obviously, according to our definition of a GIS, it is preferable to have more detail and accuracy.

Inherent in grid systems is the lack of precise conformity to political or natural boundaries. Because of these inherent imprecisions a grid system cannot exactly duplicate the relations of political or natural boundaries. However, a smaller grid size (e.g., 10 m) would minimize this problem.

#7-6: Identify the major political and natural boundaries important in a GIS. How would you encode them into a grid system? Can you think of more than one way? How many mutually exclusive layers must be developed in your data base?

To generalize, the problem can be stated in terms of location and composition. For example, New York State's grid system, LUNR, an acronym for Land Use and Natural Resource Information System, is based on the location generalization. Each grid cell size is 1 km^2. Let us examine an agricultural coding example. It could be stated that a given cell contains both corn and soybeans, corn occupying 35 percent of that cell and soybeans occupying the remaining 65 percent. Therefore, the cell will be coded by percentage of cell occurrence. However, the location distributions within that cell cannot be recorded, thus resulting in a loss of geographical accuracy. If an area is homogeneous (for example, a forest), a degree of generalization is acceptable. If, however, an urban area, which has a diversified landscape is considered then generalization can greatly reduce the system's utility.

The grid cell configuration also loses a certain degree of accuracy by generalizing the composition of certain types of data. This may be illustrated, for example, when encoding a soils map. Under natural conditions, soil types can change dramatically in a very short distance. If three or more soils are found in, for example, the LUNR square kilometer grid cell, definition of the composition becomes difficult. When problems of this nature arise, options such as in the following examples of encoding methods are available:

1. The dominant soil type within the grid cell can be encoded; i.e., the encoded soil type occupies the largest amount of land in that cell.
2. The percentage of each soil type within the grid cell can be encoded. A high degree of detail can be achieved with this method, but at an increase in cost.
3. The presence or absence of each soil within the cell can be encoded.
4. The soil type found at the centroid of the cell can be encoded to represent the value for the entire cell.

#7-7: There are at least four other methods that can be used to encode grid data; can you describe them?

Points, Lines, and Polygons. A second approach to geocoding is point or line configuration, which represents spatial data such as an intersection of two highways or the confluence of two rivers. A polygon may be considered as an extension or variation of a line. Polygons are used to describe the boundary of an area, and also enable one to enter, store and retrieve real field shapes and geographical political boundaries. Entities in the real world are thus more accurately represented with a polygon than with a grid. However, with polygon data, organization, encoding, storage, manipulation and retrieval become more time-consuming, complex and expensive than with grid data. The optimal system would be one that could display both polygon and grid, and convert from one to another.

To summarize, points, lines and grids are fairly simple to encode and manipulate, but geographical accuracy is reduced. Polygons minimize information loss but require more time, money, and system management.

#7-8: Suppose that the Office of Taxation has asked you to develop a GIS showing property ownership, assessed value, zoning, land use (current and previous four years), and receipt of taxes (current year, plus past due, if any). Would you choose a grid format, polygon format or mixed? Why?

Input Processing

We have discussed a variety of encoding methods, but not how the information is transformed into a digital format; this is called digitization. The actual digitization is accomplished by using a digitizing tablet or table (Figure 7-4). Most tables have electrical wires beneath an opaque glass surface upon which data (such as a map) are placed. An arm or cursor is used to reference the data to the computer.

The operator or analyst locates the specific point, line or polygon and presses a numerical key (system dependent) to record that segment of data into the computer. Depending on the system software, the following are usually required: a particular identification for each data element (points, lines, etc.), the geographical data associated with the system (census tracts, watershed, etc.), and any analyst input specifications such as map size, projection, symbols used or other data that are necessary for map output display.

Data may also be entered by raster scanning or photo cell head methods that trace lines and reference the data automatically. It should be emphasized that the data input process is crucial to output accuracy.

Figure 7-4. Use of X-Y digitizer to select data points from a topographic map.

Data Base Management

Now that we have the data in an acceptable format and have input these data into the computer, what happens now? If you think about it, some questions would be: how do we locate a specific piece of information, store this information, reroute or build work files, convert formats (if needed), or actually specify how much information the system can hold?

Data base management should address the interrelation between data sets, minimize data redundancy, and allow for easy, rapid data retrieval. Management of the data base should be given as much consideration as any of the other elements already mentioned. The proper organization of the file structures allows for ease of data access and updating, which obviously makes the entire use of the GIS more efficient.

Software Data Manipulation/Analytical Operation

The GIS software is the heart of the system. The appropriate software should be considered before any special hardware is purchased. It is the software that determines the activity and utility of a system within the constraints of the hardware system. However, a well-designed hard-wired system will be faster and more efficient than a programmable processor using software. In our brief discussion of the difference between a data management system and GIS, we said that beyond input and output, we need spatial answers to resource management questions. There are a wide variety of data manipulation capabilities on the market, and the list is growing every day. However, in general there are a few computer-aided operations that will be addressed:

1. scaling or rotation of reference coordinates for "best fit" projection overlays and changes
2. conversion from polygon to grid—already mentioned
3. rapid update—ability to change or add data values with relative ease
4. projection accuracy assessment
5. multiple user environment
6. multiple interactions between compatible data bases
7. data independence and nonredundancy.

Now for the analytical operations. In order to have a GIS accommodate multiple users, the system design should be flexible enough to accept a variety of types that can be analyzed with one common operating procedure. Optimally the system should:

1. retrieve one or more data elements from a data file;
2. transform and manipulate the values in the data element retrieved;
3. transform, manipulate, or combine all data elements retrieved;
4. store the new data elements created by an analysis in the data file;
5. search, identify and route a variety of different data items and score these values with assigned weighted values (for example, search for optimal highway routing)—this capability is highly desirable and complex;
6. perform statistical analysis, such as multivariate regression, correlations, etc.;
7. measure area, distance, and compare these data;
8. overlay one file variable onto another, for example, census tract data over a land use map;
9. be capable of modeling and simulation. i.e., developing scenerios (generally in map form) to predict a future event; this is perhaps the forte of a GIS. These scenarios should be developed with direct interaction from the user group. This interaction provides for greater acceptance by the overall community affected by these decisions. The Delphi technique is one such approach.

In summary, development of a GIS is a costly, complex, somewhat frustrating experience for the newly arrived. Perhaps it should be stressed that data base design and encoding are major tasks that require time, skilled personnel and available funds. However, once developed, the information possibilities are exciting, and the marginal costs of handling all the various data are low.

#7-9: How would you design a study to determine what capabilities your organization needs in a GIS and what types of information should be included in it? What factors would you suggest they consider? (Reread the last section).

LANDSAT DATA AND GIS

It has become obvious to many researchers, planners, and others, that the incorporation of Landsat digital data into a digital spatial information data base could be a fairly straightforward operation (assuming a prior knowledge of Landsat data processing). Data from Landsat and other sources can be combined to produce data elements, which are further convolved to produce interpretation maps that then become a viable part of environmental resource planning and modeling (Figure 7-5). Operational use of a Landsat/GIS interface incorporates machine data processing, modeling and natural resource assessment. (So that there is no confusion, we are referring to Landsat computer compatible tapes that have undergone some preprocessing.)

#7-10: What preprocessing has been performed on the Landsat tapes? Why is that important?

For this activity we shall assume that federal, state or private concerns intend to use Landsat digital data in an operational resource system. (The cost of developing the appropriate algorithms to input Landsat data would not be justified for a "one shot" experiment.) A second option is to time-share a system on a remote access computer. In this instance you only pay for what you use and have no control or responsibility for algorithm development. A third option is to load, compile, and store programs in executable form, paying a fee for maintenance of the program library and data files.

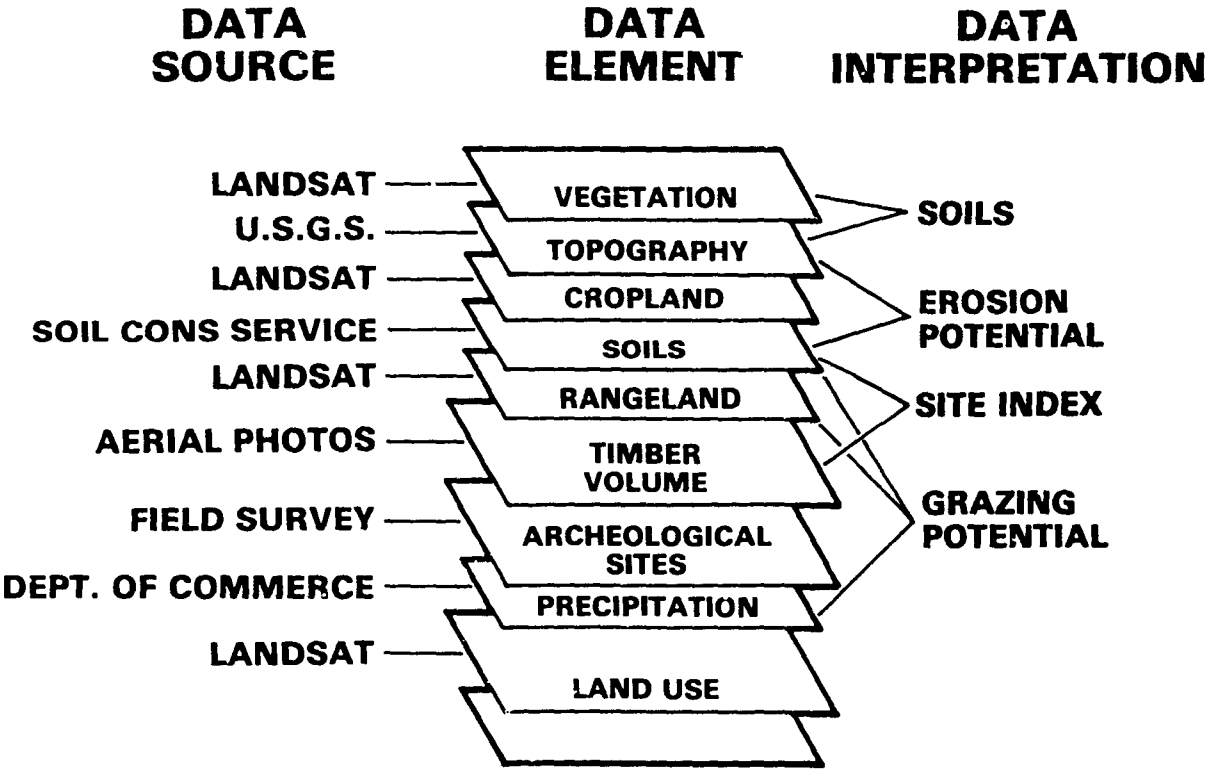

Figure 7-5. Integration of Landsat data with other sources to derive data elements input to a GIS interpretation model.

Once the Landsat digital data have been geo-corrected or reformatted, they must be registered to the other files to ensure that one geo-referenced file matches or overlays another file. One last technical problem is to aggregate (if necessary) the 0.44 hectare (1.1 acre) Landsat (nonresampled) pixel size to the spatial resolution size of the other files. For example, let us assume that our data base is composed of 8 hectare (20 acre) grid cells. Aggregation would require approximately 18 Landsat pixels to "best fit" the other data. It must be realized that some geographical accuracy with regard to Landsat data would be lost.

Once the data have been placed into the GIS, the other coded files form thematic files in the data base; these may be analyzed in conjunction with Landsat data to perform spatial and statistical modeling and analysis. With proper registration and aggregation, annual or monthly updating with new data would be feasible. The Universal Transverse Mercator mapping system can be planned to minimize cost and geometric losses as well.

The ERRSAC-ESRI Geographic Information System

The ERRSAC mission is to transfer to the public the capability of using remotely sensed data, specifically Landsat data. ERRSAC recognized the need to demonstrate, train and perform pilot projects with a GIS as a "driver" for the technology transfer mission. Such a system can aid in Landsat classification, assess the potential and accuracy of Landsat data analysis, and complete the overall data requirements for successful resource management decisions. A survey of available geographic information systems was conducted, and from this survey the Environmental Systems Research Institute (ESRI) software was chosen. It is discussed here as an example of how a GIS can provide the analytical tools needed for resource management. The software contains three major subsystems: PIOS, AUTOMAP/GRIPS, and GRID. These subsystems are designed to work independently or in combination. The following summaries of the subsystem programs are taken from the ESRI literature.

Polygon Information Overlay System (PIOS)

Briefly, this software subsystem was designed to deal with polygon data, that is, to encode, correct, analyze and receive input referenced to x, y coordinates. There are twenty-one basic PIOS programs that utilize the system capabilities. Some of these program capabilities convert digitized data to the appropriate PIOS format to merge files, edit coordinates, and manipulate coordinates for polygons that completely surround other polygons. The PIOS subsystem can also calculate area, centroid, or minimum and maximum coordinates for any given polygon overlay. The polygon modeling subsystem allows geographical variables (soils, land cover, etc.) to be compared with other polygons containing the same information. File element ranking, such as additive or multiplicative weighting, can be applied to allow for complex and unique spatial analysis. For example, let us assume that a county planner needs to locate a solid waste disposal site within the data base area. The composite weighted polygon, when properly "massaged," can provide the optimum site. The software can also perform route evaluation by locating the optimal route as it crosses various data files (water, forest, urban, etc.) and chart the least impact or the most desirable route. Power utilities require this type of analysis.

#7-11: What other factors should the planner consider? How should they be weighted?

AUTOMAP/GRIPS

The GRIPS software is designed to convert polygon data into a format that can be used in the GRID software system. The AUTOMAP program is used to scale map range, map size and map symbols. This program produces three types of maps. The first, *chloropleth*, generates color-coded displays of quantitative or qualitative geographical data in the polygon mode (population district, tax zones, etc.). *Contour mapping* uses a two-dimensional drawing symbolizing a three-dimensional surface such as topographical elevations. The third type of map is built from *proximal* or *discontinuous* data by using a single point to represent an areal unit. Basically, the computer searches an area around a given grid on a printer map until it finds the closest coordinate and assumes the grid value to be associated with the closest coordinate. The method provides a general pattern of data but does not contain the accuracy properties of the other map displays.

GRID

The GRID subsystem consists of nineteen programs for the input, storage, manipulation, analysis and output of spatial data in a grid format. The programs can be executed separately or in combination by persons with little programming experience. The data can be retained as a single file or can form a multivariable file. The data input is in sequence along a grid "row," which is created in equally spaced cells that contain a predominant data variable such as forest or water. A simple procedure for identifying several variables is to create a composite, such as soils, slope, or land-cover, and store this information in a multivariable data file (Figure 7-6). A variation may thus be stored for further manipulation, recall or map output. Statistical summaries, value ranges, legend materials and map classes may be output with this software. A variety of manipulations may be performed on the data (once encoded); some are:

1. Isolate a user-defined variable such as tree species within the entire data set and display only that variable;
2. Search program, which allows three basic capabilities: (a) A minimum distance routine that analyzes an area surrounding a cell. It can then identify the shortest distance from that cell to a predetermined cell value. The radius of the search is specified by the user. The calculations can be actual counted cells or linear values such as miles, meters, etc. An example of this

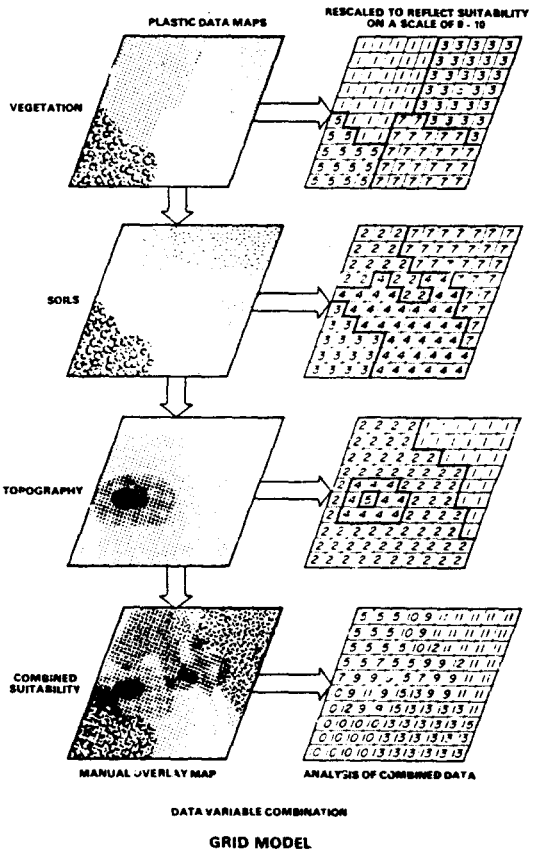

Figure 7-6. Digitization of data elements using a GRID model.

search would be to find the cell at a minimum distance from water, and containing a specific soil type. (b) A variety of spatial analyses requires knowledge of the number of times a "match value" occurs within the user-specified distance search. For example, let us assume that we are attempting to locate a new shopping mall within a given radius, and a given cell is available for development. Another cell area outside the radius is not of interest for our objectives and therefore need not be searched. (c) Contrary to our above example, there will be certain spatial analyses that require a search outside a given study area. For example, suppose irrigation is needed for a newly planted agricultural field. An adequate supply of water is not available within the study area, and therefore, a search with weights assigned outside the study area must be performed. A coefficient is produced that approximates the number of possible occurrences. Any combination of search routines may be applied for a given resource problem.

Topographical Analysis

An additional subsystem integrated into ESRI is designed to carry out certain specific manipulations of a topological nature.

Slope Analysis. This program is used primarily for a land use planner's need for accessibility, pattern, etc. for location potential. The slope is calculated by steepest drop, steepest rise and drop, mean of absolute slopes, and a variety of vector summations. Slope analysis may be performed rapidly and consistently within the grid program.

Aspect Analysis. Aspect (a condensed way of saying directional orientation) is of significant value to other related parameters, such as temperature, humidity, wind, etc. Consider aspect's importance to the location of solar energy technology.

Exposure. Exposure, also known as viewshed analysis or land form exposure, is a grid-oriented program that determines user-defined observation points in a study area from which any other specified point or area in a scene is open to view (Figure 7-7). The user has a variety of options for specifying the observation point(s). The user must choose the direction of orientation (north, southeast, etc.) and the elevation associated with the point or area to be observed. The exposure program can also calculate all other areas visible from any observation point. As an example of a program objective, one might wish to locate an industrial complex without interrupting the scenic qualities of a given area.

Views. The views program differs from the exposure program in that it produces three-dimensional line drawing displays from topographical surface data (Figure 7-7). The views program decides which parts on the surface are hidden and which parts are viewable. The program can also produce a cross section or vertical slice through a topographical surface, provided that subsurface information is available. The surface being viewed can shift in attitude and/or azimuth to present a different perspective or visual feeling for the area under study. The views program is effectively used for location analysis with respect to topographical relief, direction and elevation. As an example, consider its utility in locating hiking trails that are both physically demanding and aesthetically pleasing.

Topographical Transformations. The Defense Mapping Agency (DMA) has digitized the 1:250,000 National Topographic Map Series for the entire United States. Elevation data are stored in a 64 m^2 (208 X 208 feet) grid cell array. Topographic data for this series may be obtained from the National Cartographic Information Center (in Reston, Va.) in a digitized format convertible (with appropriate software programs) to an image format for display and analysis. Using this data base, computer processing can produce a stereo pair for a full Landsat scene or any subset thereof. One procedure involves these steps: (1) Resampling of Landsat pixels to the 64 m^2 cell size. (2) Registration of Landsat and digital terrain data. (3) Transfer of terrain elevation data to equivalent Landsat pixel locations. (4) Calculation of parallax shifts between pixels as a function of elevation (5) Displacement

xels in X and Y directions as a function of lax shift, and (6) Production of a Landsat containing shifted pixels. An example of a uter-generated stereo pair (one image normal; ther with shifted pixels) for a band 5 Landsat (October 13, 1977) covering Harrisburg, Pa. surroundings, using Map NK 18-10 data, was ced by Geospectra, Inc., Ann Arbor, Mich. pair is located in the back pocket of this book. Examine it under a stereoscope.

The DMA data may be used in other ways to show combinations of topographical elements. Figure 7-8 is a three-band image made from the digital terrain data showing slope, aspect, and elevations in color-coded patterns of a mountainous region similar to the Harrisburg, Pa., area. In addition to this use, digital terrain data can aid in classifying Landsat data by stratifying the elevation data into areas where certain types of vegetation will or will not grow, thereby dramatically improving the Landsat classification accuracy.

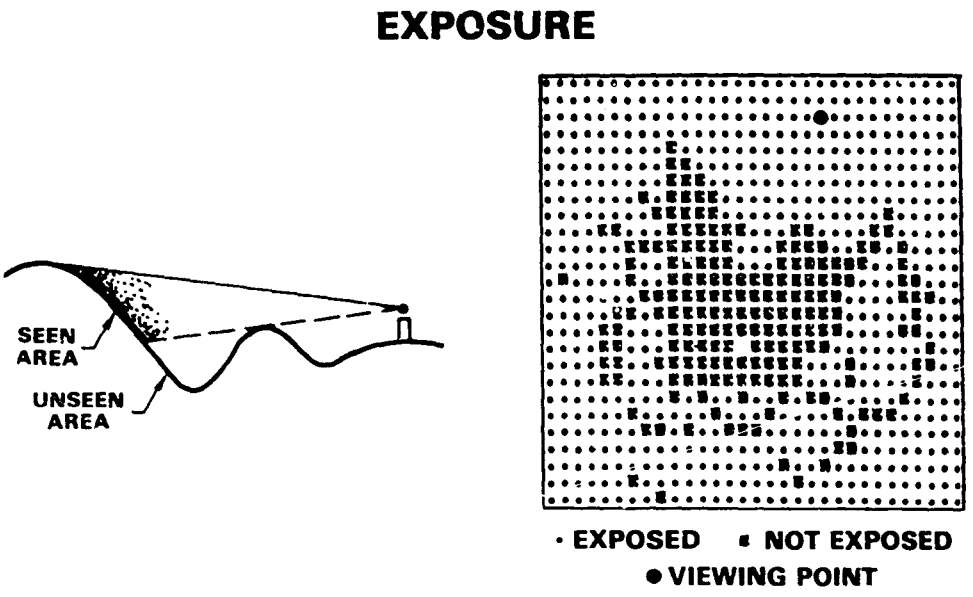

Figure 7-7. Schematics showing concepts of Views and Exposure routines for topographic analysis.

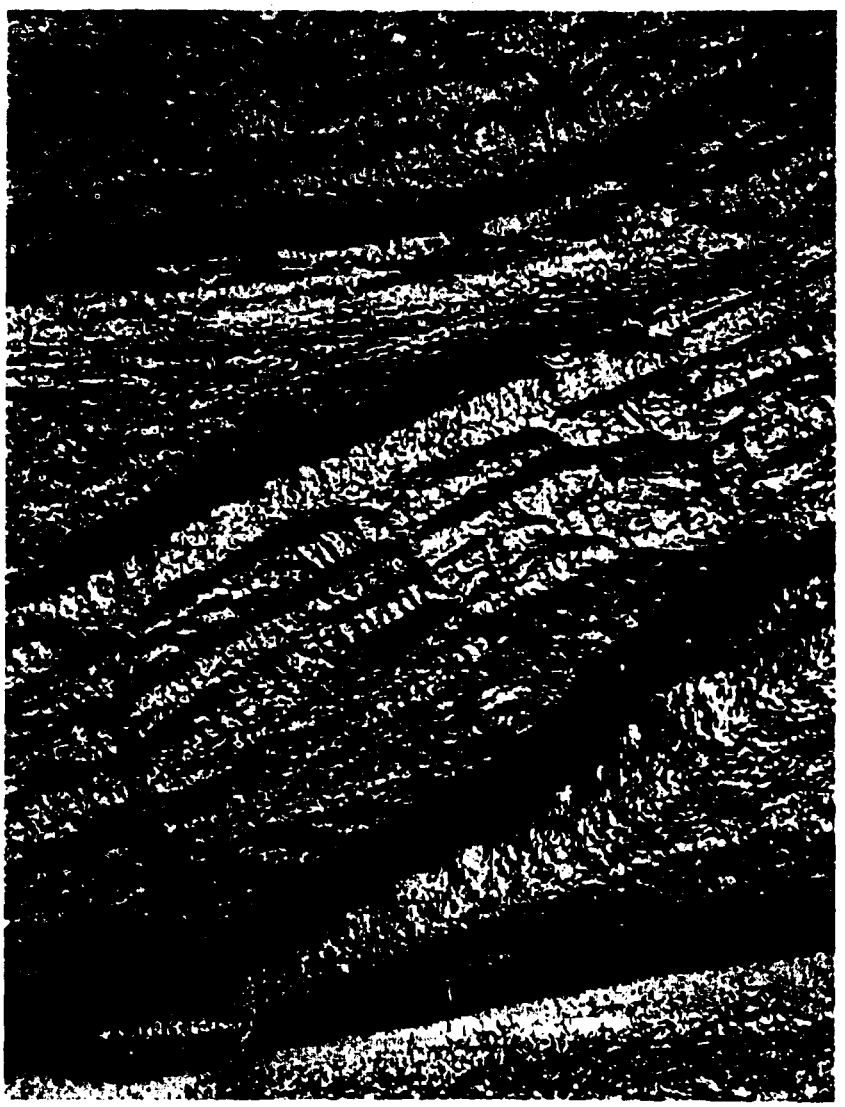

Figure 7-8. Computer-generated relief diagram made from a Defense Mapping Agency digital terrain tape.

GIS AS A POWERFUL MODELING TOOL

In the previous discussions we have described an example of the total spatial analysis package that is interactive, provides area summaries, converts from grid to polygon format, and provides tabular and map form output. A software interface between ERRSAC's GIS and the computer image analysis system is used to convert the geo-referenced files into images. This next section of Activity 7 deals with modeling and includes a Landsat/GIS output example.

Developing a Model

A model is an attempt to duplicate nature. In the computer environment, it is a manipulative process to quantify a specific set of variables as defined by the model analyst. To be successful in the model building process, the analyst must have a full understanding of the data variables and their interrelations. This requires identification of the variables that will give the desired results when properly manipulated. A computerized model has an advantage in speed and accuracy (given proper instruction).

The purpose of a model is to predict and to provide new information about the situation being analyzed. A model generally involves four steps:

1. problem formulation,
2. data manipulation,
3. interpretation and analysis,
4. display of results.

By imposing constraints, the analyst can test the consequences of alternative strategies specified as plans, programs, policies, new legislation or any combination of these, given the proper data in a compatible sequence. Any combination may be examined (within the constraints of the system) and various scenarios developed.

Examples of Models

We shall now consider three models that typify the model development process. As described here, each model "stands alone" in its functions but can easily be interfaced with, and improved by, Landsat data. We have chosen examples that are of practical value to state, regional or local environmental or other planning agencies. The three examples deal with environmental conservation, erosion potential and industrial siting. Briefly, the data elements relevant in these models are:

1. vegetation,
2. geology,
3. ground water,
4. soils,
5. land use,
6. watersheds,
7. topography,
8. political boundaries,
9. population projections,
10. resources.

#7-12: Suppose some farmers adopt new agricultural practices such as no fall tilling. How might you include this information in the model.' What are the advantages and disadvantages of each approach.' How would you collect the data.' How would you determine its effect on soil erosion.' If it proves beneficial, how might you encourage more farmers to use it.' How could the model or GIS help you in these efforts.'

Environmental Conservation Model. The purpose of this model is to determine the effect of diverse state and local priorities on areas of critical environmental concern. A GIS may be used to predict effects of different land use plans on landscapes of a study area that affect the conservation of a given area within the data base.

The conservation model requires the analyst to identify and rank those areas that, in his opinion, would protect the greatest number of resources. Among the data elements to be considered are:

1. soils, by type, location and amount,
2. water quality and quantity,
3. wetlands,
4. forested areas,
5. natural wildlife sanctuaries,
6. those elements that would present a potential infringement on areas that are to be preserved (such as urban boundaries).

The GIS programs require location and measurement of those areas that include the highest or most sensitive combinations. If we continue in this manner, the most important areas are identified by their extent, location and, especially, their spatial relation to those elements of the environment that may present a threat (through encroachment) to those areas we wish to preserve. Legislators and planners can, on the basis of this information, introduce the appropriate institutional measures to ensure preservation.

It should be noted that this model may be subdivided into a variety of future scenarios from which to base future policies on growth. For example, an attractiveness model based on visual quality identifies visibility patterns from any origin or combination of origins in the study area. Quality of views (as influenced by the diversity and distance of a given visible land use) and landscape types may also be incorporated into the model.

Some questions that might be addressed are:

1. What are prime sites for urban development?
2. Where is the visual corridor of a specific element?
3. Which land use patterns will preserve most of the prime wildlife habitats?
4. What are the tax impacts that would constrain or promote growth?
5. What will be the effect on people living on a river floodplain if the headwaters of the stream are developed?
6. How does land use affect water quality? In what portions of the watershed is land use significantly important?

Erosion Potential Model. To determine agricultural pollution due to erosion we must first consider what is being polluted. Agricultural activities are considered nonpoint sources that contribute to the degradation of water quality. Therefore, water quality managers need a methodology to implement "best management practices." To establish erosion potential, we must determine the proximity to surface water of total acreages involved by erosion and total acreage along water courses within the data base.

The objective of the model is to assign a numerical value that is a measure of the agricultural land lost to erosion near surface waters from a given precipitation event. To accomplish this, we must make certain assumptions:

1. We can identify as an input into a cell any Landsat classified data that identify land in agricultural use; this measure is encoded by cell percentage.
2. To obtain a relative measure of the erosion potential of soil in a given cell, a nominal weight may be assigned, and this relative measure is a function of soil type and slope of the land.
3. Since we are concerned with soil that reaches water courses, the closer a cell is to water the more severe erosion becomes because of the accumulation of precipitation runoff.
4. Depending on the topography of the study area, there is a maximum distance from surface waters beyond which soil cannot be transported (unless the icecaps melt!).
5. Depending on cell size and encoding methods, a cell may contain both surface water and agriculture.
6. It is possible to describe the potential amount of erosion due to a precipitation event without describing the amount of precipitation (this is the case as long as the model seeks to describe relative measure of erosion severity).

So, what variables do we need to address for our modeling objectives? First, we must create a soils file that can define soil erosion potential by combining erosion type with slope category. Let us code this combined file *slight*, *moderate* and *severe* erosion potential.

Next, the water file as identified by Landsat is coded as present or absent in a given cell. The agricultural file (kept current by Landsat) may be separated into species of agriculture such as corn, soybeans, etc., or combined to form one file. By using an appropriate search routine for the water file, and by assigning weights to the agricultural and soils files, we should find a multiplicative combination of these files that reveals the model objective, namely to locate those cells containing:

1. weighted value of soil (ai)
2. weighted value of agriculture (bi)
3. weighted proximity to water (ci).

Therefore, the higher the cumulative numerical cell value, the greater the potential for erosion, in other words ai X bi X ci is equal to the maximum likelihood for agricultural nonpoint source or water pollution due to sheet erosion. The model serves as an indicator of priority areas to address and implement "best management practices" based upon the previously defined parameters.

The computer erosion modeling techniques could be modified, expanded, or connected to other models, and this would greatly enhance their utility to a regional or local government or planning agency (Campbell, 1979).[5] The erosion model

[5]Campbell, W.J., *An Application of Landsat and Computer Technology to Potential Water Pollution from Soil Erosion*, Proceedings Fifth Wm. T. Pecora Symposium, Sioux Falls, S. Dak., 1979.

enables the planner to predict agricultural source load generation based on watershed parameters such as soil, slope, vegetation cover, and spatial relations. To improve the utility of the model, the following recommendations are:

1. The model could be upgraded by incorporating a submodel that calculates the amount of soil passing from one cell (assuming a grid format) to a neighboring cell as a result of a given precipitation event. This information would show the spatial influences of the numerous factors that control the hydrological responses of a watershed.
2. Coefficients could be incorporated into the system to predict urban land use effects on a watershed or a region. When a data file change is from one land use to another, the coefficients are used to determine the amount of change.
3. The existing model, along with the suggested recommendations, could be connected to other models already in use, such as the STORET model developed by the federal EPA. Connecting to other models will, of course, greatly increase the predictive capabilities of any given user; however, time and cost constraints would have to be a consideration.

Industrial Siting Model. The final example, into which we shall delve in some detail, is a rather simplified approach for manipulating a few variables to locate the optimal site for construction of a heavy industrial complex within the data base area. In this instance, we shall use an actual data base now being applied by a major electrical utility.

The Pennsylvania Power and Light Company (PP&L) serves 30,000 sq. kilometers (11,600 sq. miles) in central Pennsylvania. PP&L has a computerized GIS covering the company's service area. The system is primarily used for environmental impact analysis, land use analysis, energy facility siting and other technical assistance. There are ten general data categories, as listed in Table 7-1. Each general category will contain some number of data elements totaling forty-three elements for the ten categories (Table 7-1). The standard grid cell size of the PP&L data base is 9.2 hectares (22.9 acres).

Using the digital data stored in the GIS files, any of these PP&L elements can be displayed on a TV monitor, as color-coded maps, or as printer/plotter output. Figure 7-9 A-F illustrates six typical elements on which some analytical operations have been performed. The distribution of each element is depicted as a map covering part of PP&L's Harrisburg Service Area. Each map shows the thematic content or ordinal ranking assigned to each grid cell. These are color-coded as follows:

A. Landforms

Urban:	Red
Water:	Dark Blue
Plateau	Brown
Mountain Top	Purple
Steep Slope	Dark Green
Valley Bottom	Light Green
Depression	White
Floodplain	Aqua

B. Slope

0 – 3%	White
3 – 8%	Light Green
8 – 15%	Dark Green
15 – 25%	Purple
25%	Yellow
Urban	Red
Water	Dark Blue

C. Stream Order

1st Order	Dark Blue
2nd Order	Orange
3rd Order	Aqua
4th Order	Light Blue
5th Order	Yellow
6th Order	White
7th Order	Purple
8th Order	Red

* D. Soil Permeability

Excellent	Red
Good	Yellow
Moderate	Orange
Poor	White
Excessive	Dark Green

Table 7-1
PP&L Multivariable File of Data Elements

Data Category	Layer	Element Variable
	1	Row
Location	2	Column
	3	Map Module
Service Areas	4	Service Areas
PP&L Facilities	5	PP&L Facilities - Point Data
	6	Highways
	7	Railroads
Linear Features	8	Transmission Lines
(Infrastructure)	9	General (Pipelines, Vortac Stations, etc.)
	10	Scenic Roads/Canals/Trails
	11	Historic Sites/Natural Areas (WPC) County Prefix
Public Lands	12	Historic Sites
(Point Data)	13	Natural Areas (WPC)
	14	Other
Public Lands (Polygon Data)	15	Public Lands (Polygon Data)
Course Lines	16	Course Lines
Future Land Use Trends	17	Future Land Use Trends
	18	Land Use and Land Cover
	19	Political Units
LUDA	20	Hydrological Units
	21	Census County Subdivisions
	22	Federal Land Ownership (to be added)
	23	State Land Ownership (to be added)
	24	Terrain Unit Polygon Number
	25	Vegetation/Land Cover
	26	Landform
	27	Slope
	28	Soils
	29	Agricultural Potential
	30	Soil Depth
	31	Soil Permeability
	32	Seasonally High Water Table
Terrain Unit	33	Geological Code Number
	34	Rock Type
	35	Bedding
	36	Surface Drainage (Stream Order)
	37	Groundwater
	38	Porosity
	39	Ease of Excavation
	40	Cut Slope Stability
	41	Foundation Stability
	42	Mineral Resources
	43	Flood Prone

ORIGINAL PAGE
COLOR PHOTOGRAPH

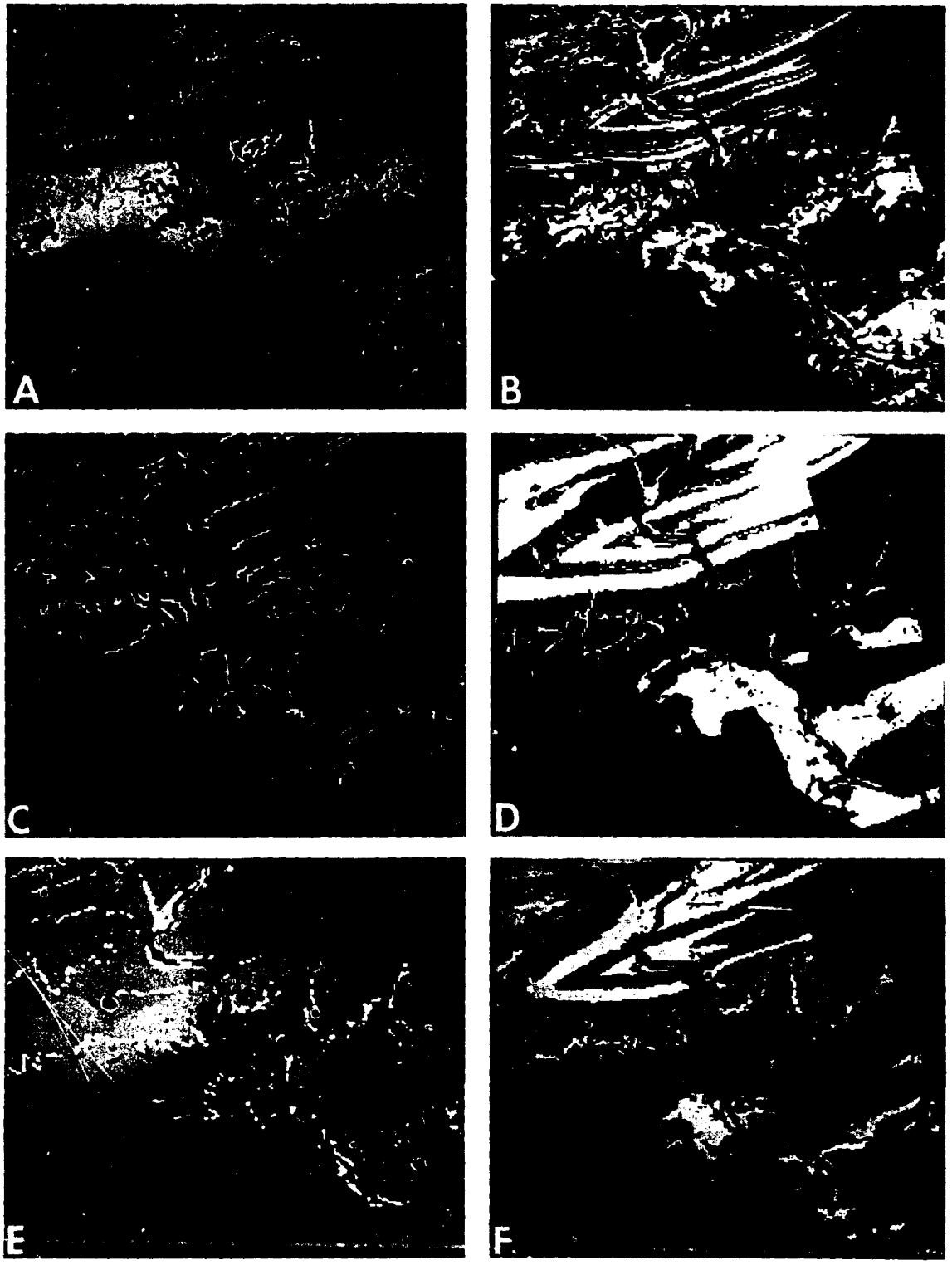

Figure 7-9. Color-coded displays of six data elements from the PP&L GIS data base.

* E. Flood Prone Areas

Urban	Red
Water	Dark Blue
Flood Prone	Yellow
Not Flood Prone	Orange

* F. Agricultural Potential

No Limit	Dark Green
Few Limits	Light Green
Moderate Limits	Yellow
Severe Limits	Brown
Extreme Limits	Purple

For the three elements preceded by *, several steps are involved in producing the final map. For instance, the Soil Permeability map is created from the soils file. The Flood Prone Areas map is derived from 7.5′ U.S.G.S. Quadrangle Sheets. For Map F, the soils file is first coded by productivity, and then the slope file is coded by percentages and overlaid with the soils productivity file to generate the Agricultural Potential File.

Figure 7-10 shows the landforms element, as rendered in black and white characters on a Versatec Electrostatic Plotter.

In defining our hypothetical heavy industrial siting example, the institutional or socioeconomic problems associated with locating the optimal site for the complex will not be addressed. In real life, however, data such as population, tax base or other thorny issues could be incorporated into the model.

#7-13: Do you think PP&L needs to protect the confidentiality of their data? Why or why not? How do you think they might do it?

#7-14: Look at the PP&L data categories. How accurately is each one located if the grid cell size is 9.2 hectares? Which categories will be most seriously affected?

The data were formatted and interleaved by pixel, meaning that for pixel 1,1 (first x and first y pixel), as many as forty-three values were assigned. The next decision was which elements should be incorporated into the model. The following six elemeats and their thematic content were applied to the model:

1. Landform: The landform elements file contains nine terrain types, of which three are considered amenable to development:
   a. valley bottom of shallow slope,
   b. plateau (slopes less than 15 percent),
   c. Piedmont Plateau.
2. Groundwater: The computer file for groundwater is essential for input to a manufacturing process and is coded as potential well yield. The following three parameters are considered as acceptable:
   a. 0.19–0.75 m^3/min (50–199 gal/min),
   b. 0.75–2.6 m^3/min (200–699 gal/min),
   c. 2.6 m^3/min (700 gal/min) or greater.
3. Porosity: The ground soil porosity rate is also essential for the manufacturing process; the acceptable files are:
   a. medium magnitude,
   b. high magnitude.
4. Ease of Excavation: The most commonly encountered geological unit is coded low, medium or high resistance. The parameters considered are:
   a. low resistance: may be excavated with light construction equipment,
   b. medium resistance: may be excavated with heavy construction equipment,
   c. high resistance: requires blasting and is considered too costly a process.
5. Foundation Stability: This file is coded on the basis of excavation to solid rock for each geological unit. The coding was poor to excellent. The files used were:
   a. good,
   b. excellent,
   c. generally good to excellent, but may contain solution cavities.
6. Distance to Surface Water: This file is not part of the PP&L data set, and had to be developed. The "distance to water" file was considered of primary importance to the decision-making process. In our hypothetical example, tertiary sewage treatment was performed on waste water potentially generated by the complex. Therefore, discharge into an acceptable water body was imperative. The "search

PP&L LANDFORM LAYERS

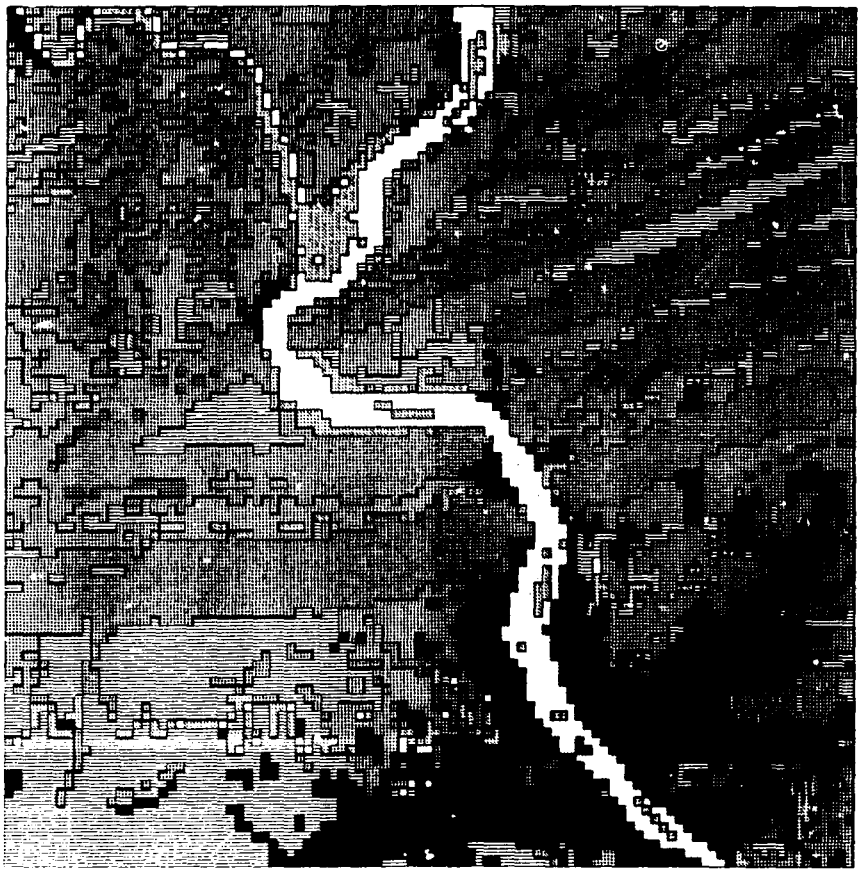

LEGEND

- WATERBODY
- DEPRESSION (NOT IN SCENE)
- FLOOD PLAN
- VALLEY BOTTOM
- STEEP SLOPE
- PLATEAU
- RIDGE
- URBAN LAND
- PIEDMONT PLATEAU (NOT IN SCENE)

Figure 7-10. Types of land forms around Harrisburg, Pa., generated from PP&L data base using Versatec Plotter.

from water" routine was generated by considering those cells that bordered water out to a maximum linear distance of fifteen cells (15 X 9.2 hectares = 138 hectares = 343 acres) away from water. Fifteen cells were considered the maximum distance that construction cost of sewer lines would allow.

These resulting elements are the variables that would constrain development. Each element was examined for the values or factors that would contribute to or determine development of the site. For example, from the ground water file, a certain rate of water uptake was required for a specific manufacturing process. Any rate less than the minimum standard was considered unacceptable. Continuing in this manner, all the variables were chosen.

The final step was to display those areas that met the acceptable tolerances. Figure 7-11 shows the fifteen-cell search from surface water bodies as well as the spatial relation of the variables chosen. Figure 7-11A meets all the conditions in the data set. Figure 7-11B meets all the conditions but groundwater, Figure 7-11C all but porosity rate, Figure 7-11D all but foundation stability, Figure 7-11E all but landform and Figure 7-11F all but ease of excavation as previously defined.

Owing to the complexity of data manipulation by conventional map overlay techniques, this is as far as most planning operations proceed. By using a GIS within a digital computer environment, we can examine the interaction between various suitability maps. In the previous example, suitability maps were digitally generated by creating a binary mask (0's and 1's for reject or accept) for each data plane and then adding all the data planes together to form a composite image. The results of that process are shown in Figure 7-12. The color coding scheme is the same as in Figure 7-11.

Let us not stop here but take the process one step further. From our visual inspection it is obvious that, within the optimal site area, those areas corresponding to the surface water boundaries bring us closer to locating the precise x acres site. The insert in Figure 7-12 is an enlargement of the area finally selected. The red line that borders the Susquehanna River is the optimal site to include the waste water discharge requirements. This may now be compared with land ownership, tax base, population predictions or other appropriate files to finalize the selection or identify the problem.

Landsat Integration With PP&L Data

Any combination of the forty-three elements in a GIS data base may be displayed in a color-coded map similar to Landsat classification maps. Figure 7-13A is a computer-generated image constructed from selected sublayers in PP&L's Land Use file (layer 25). The data cell size is once again 92,500 m^2 (22.9 acres). This file is referenced to six 7.5' U.S.G.S. topographical quadrangle maps. The irregular boundary of the map is defined by PP&L's service area. The classes selected from elements in the data file are as follows:

Urban	Red
Agriculture	Light Green
Mixed Forest	Medium Green
Broad Leaf Forest	Dark Green
Tree Plantations	White
Forested Wetland	Violet
Unforested Wetland	Yellow
Scrubland	Peach
Meadow	Aqua
Barren	Tan
Water Bodies	Dark Blue
Areas outside PP&L Service District	Black

This map may be considered a user-oriented GIS display for a particular region. The categories chosen here are mostly those identifiable in a Landsat image. Landsat's principal use is to update and refine these categories.

Given the appropriate software, integrating Landsat digital data into a GIS is a rather straightforward procedure. To illustrate, a July 14, 1977, Landsat scene of Harrisburg, Pa., was selected for comparison with the PP&L data set. The Landsat data were configured to the same PP&L service area shown in Figure 7-13A by the binary mask procedure. These data were then classified by using a supervised maximum likelihood algorithm.

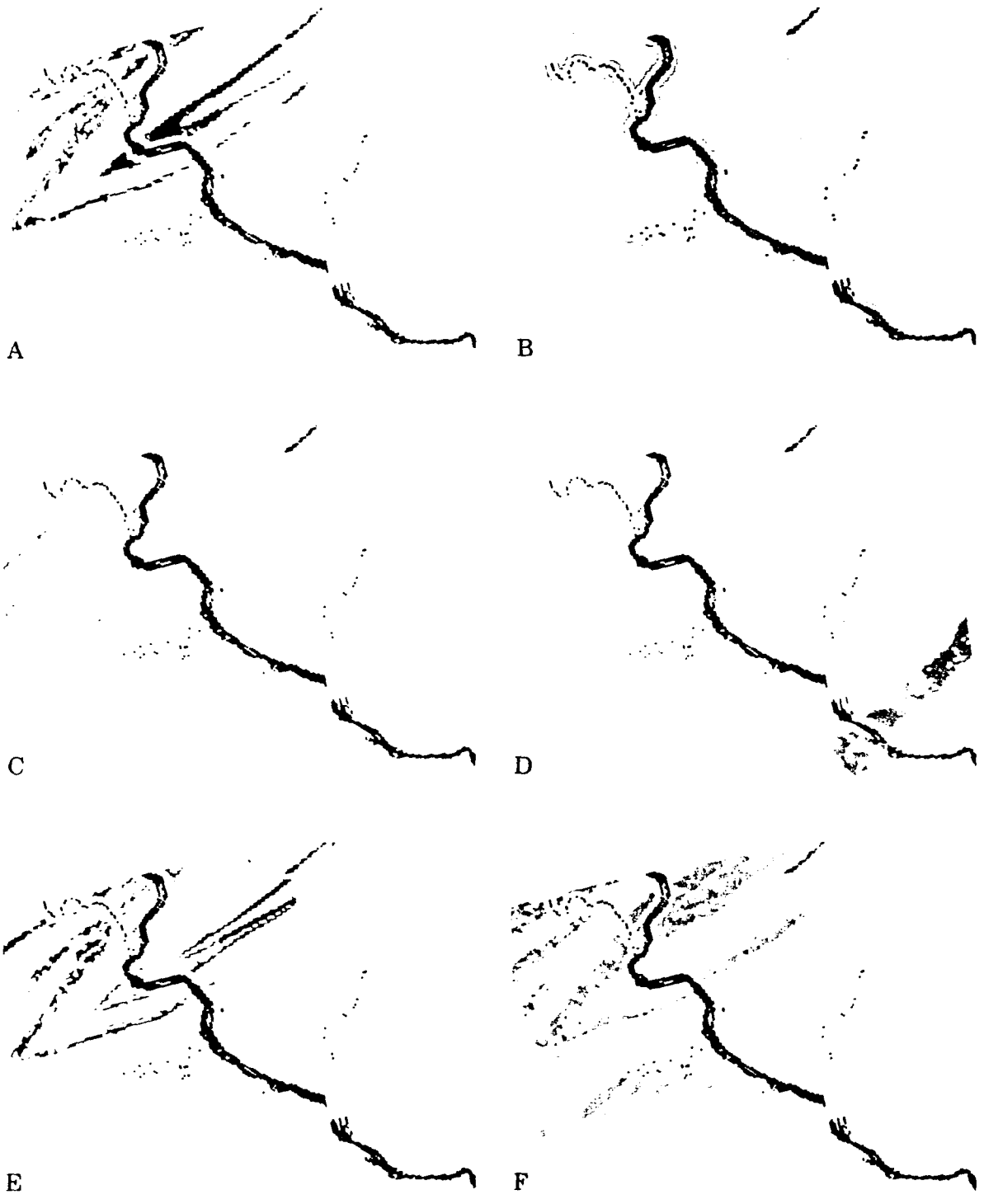

Figure 7-11A-F. Elements displaying acceptable (color) or unacceptable (gray) conditions for selection of a suitable industrial site based on a water (blue) proximity model (see text).

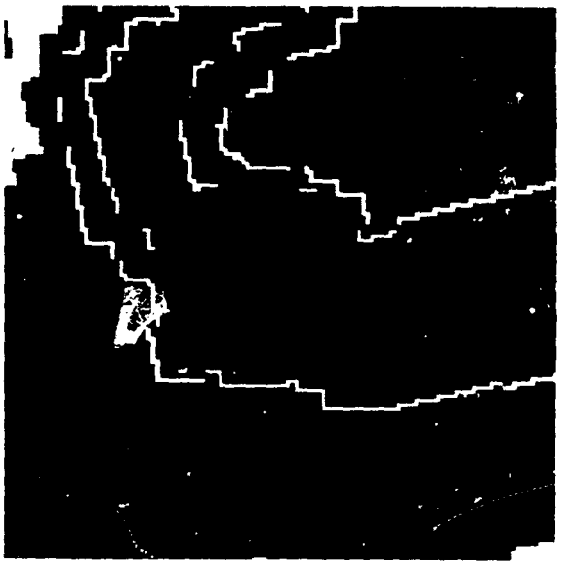

Figure 7-12. Final version of a suitability map for location of an industrial site north of Harrisburg (key area shown in enlargement). Developed from PP&L data base (see text).

Figure 7-13A. A 12 class map of the Harrisburg service area, made from PP&L digital land use data file.

ORIGINAL PAGE
COLOR PHOTOGRAPH

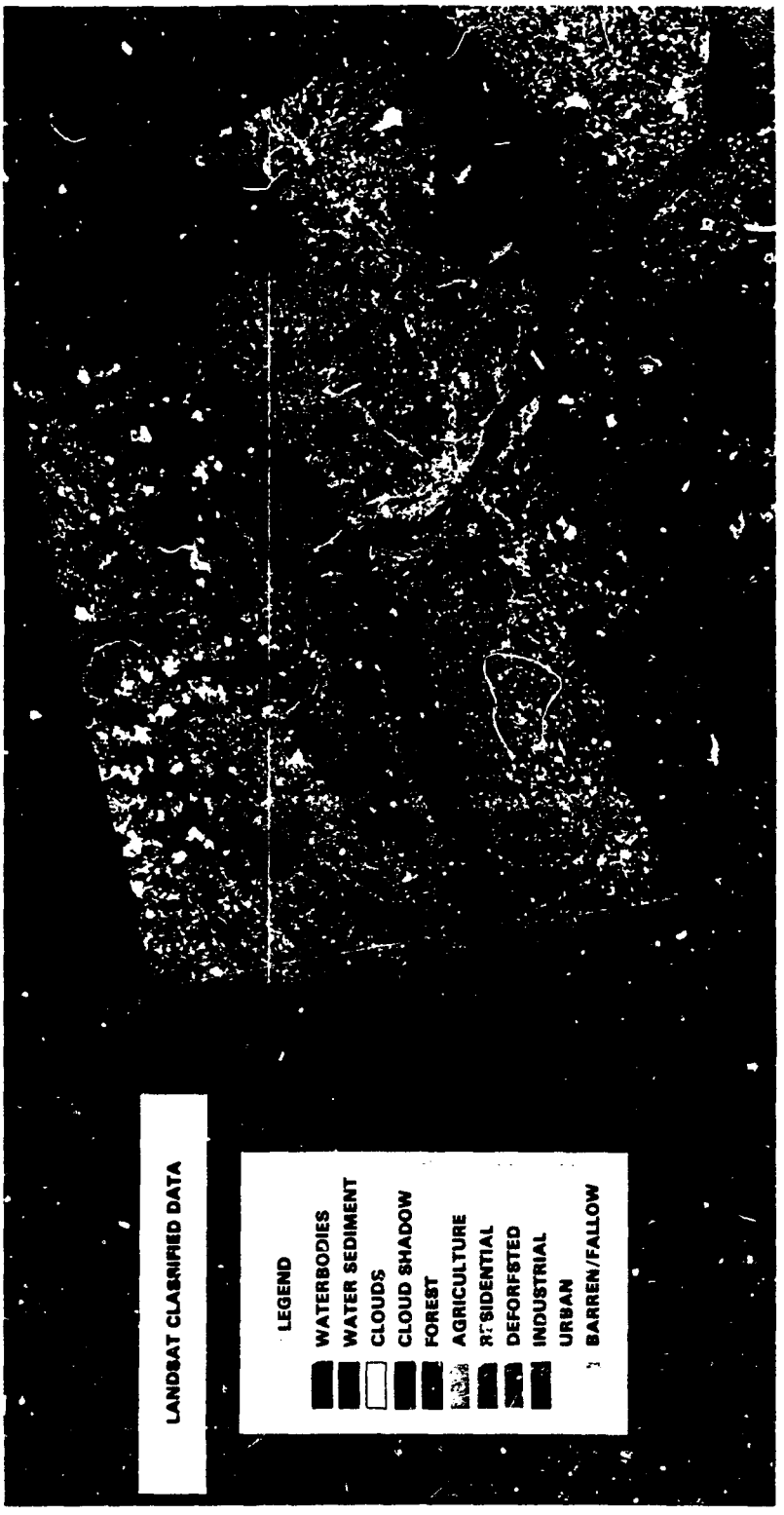

Figure 7-13B. An 11 class map of the Harrisburg service area developed by classifying Landsat data.

In this instance, ground truth for training sites came primarily from interpretation of representative high resolution air photos (Figure 7-14). An initial twenty-two classes were re-combined into eleven classes (Figure 7-13B), some of which were chosen to match those of the PP&L map. The following is the classification scheme selected:

Industrial	Red
High Density Urban	Yellow
Medium Density Urban	Violet
Agriculture	Light Green
Mixed Forest	Dark Green
Gypsy Moth Defoliated Forest	Brown
Fallow or Bare Land	Dark Gray
Water Bodies	Dark Blue
Water with Sediment	Light Blue
Clouds	White
Shadow; Also Area Beyond PP&L Service District	Black

#7-15: Compare the two map images shown in Figure 7-13. What are the main similarities? The main differences? What factor(s) are largely responsible for the differences?

#7-16: Using the aerial photo (Figure 7-14) as a guide, examine the metropolitan area in Figure 7-13B. How well do the classified medium density urban (violet), high density urban (yellow), and industrial (red) areas appear to correspond to their counterparts in the photo? Point out several areas where updating or refinements must be made in the PP&L map by using the Landsat classification input.

#7-17: Overall, which map in Figure 7-13 seems to better depict the actual distribution of classes in and around Harrisburg? Can you think of reason(s) why the PP&L GIS classification might be used instead of the Landsat one for certain purposes or applications?

SUMMARY

This activity illustrates the significant resource and environmental information that may be gained from a computerized geographical information system. The activity also shows how Landsat data may be incorporated into a GIS and extended to many different uses by environmental and resource managers and workers.

Future Earth resource satellites will provide greater resolution that could be used to differentiate and perhaps identify rock and soil types, water quality parameters, vegetation stress and other data that influence environmental and resource planning. The essential focus of this activity was to demonstrate the utility of Landsat and GIS technology as tools for providing relevant, timely and cost-efficient information to potential users in a manner that is easily understood and reproduced. Further, it illustrated that large-scale gathering of information, the manipulation of such information, and the filtering and/or display of such information on maps may be accomplished with accuracy and speed.

Activity 8 is a real life application of how a state government agency used Landsat data for its resource and environmental management issues. The role of a GIS approach is further developed in this activity.

Figure 7-14. Medium scale aerial photo of Harrisburg, Pa. and environs.

ACTIVITY 8

A CASE STUDY IN THE PRACTICAL USE OF LANDSAT DATA[1]

LEARNING OBJECTIVES:

- *Become familiar with the ways in which Landsat has been beneficial to a state natural resource management program.*
- *Learn how a research and development system is becoming an "operational" remote sensing system to help decision makers.*
- *Be aware of nontechnical issues that can assist or hinder an agency in adopting a new technology.*
- *Chart the progress of Landsat use by state government from the earliest stage of curiosity through to incorporation in actual state planning methods.*
- *Develop an understanding of the many potential applications of Landsat data to real information needs and solutions to problems.*
- *Be aware of the problems and mistakes that have occurred in using Landsat data in the past and how these problems have been overcome.*
- *Spur your imagination into thinking of how you would use Landsat data if you were a state planner or environmental engineer.*

[1] Prepared by Scott Cox, ERRSAC, Goddard Space Flight Center.

Relax a bit. You should look upon Activity 8 as an interesting diversion from the preceding, more demanding activities, which deal with introducing you to Landsat and what it does. In fact, by a discussion of an actual case study we shall now help you to synthesize much of the previous material into a cohesive picture of practical applications. This activity is a story of how one state, New Jersey, has developed a successful Landsat program to help manage a rapidly changing landscape. We shall begin by seeing how one agency took a need for easily accessible, recent information, a curiosity in Landsat, and a little bit of salesmanship and turned them into a successful experiment in the use of satellite data for an actual planning program.

IMPACT OF EPA 208 ON NEW JERSEY

Let us begin this activity by examining some pertinent background information. The United States Environmental Protection Agency (EPA), under the mandate of Section 208 of the Federal Clean Water Act, disburses funding to state governments to produce water quality management programs aimed at controlling both point and nonpoint source pollution in our nation's rivers, streams, and lakes. In many states, areas had been designated by EPA for which water quality plans had to be developed immediately. New Jersey, for example, was mandated to produce plans for state watersheds covering 69 percent of the state. Using federal funds, plans for these designated areas were to be produced by state or regional planning agencies. By funding this ambitious program, the federal government placed de facto responsibility on the state for the water quality planning in these "designated" watersheds.

#8-1: What impact do you think this federally mandated program had on the state agencies responsible for water quality planning?

#8-2: What were the legal implications for the water quality planning in the remaining 31 percent of the state, the so-called "nondesignated" areas?

The answer to the last question was finally settled by the U.S. Supreme Court which ruled that the State of New Jersey was responsible for 208 planning in the "nondesignated" areas. However, most of the funding from 208 had been spent on planning for the designated areas, while, at the same time, many state programs were being severely cut to halt ever expanding state budgets and accompanying taxes. As a result, the state had to search for cost saving methods to complete its newly assigned task. Increasing public demand for competent environmental planning made the situation even more pressing.

Water quality planning in response to Section 208 requires that a great deal of environmental data must be gathered and analyzed. For example, point source pollution monitoring includes historical research to find the locations of discharge pipes into lakes and streams. It involves environmental detective work (such as ground surveys) to measure stream flow rates, determine where pollution has been abated and locate new sites for future monitoring. Some of this can be done with high resolution aerial photography.

Nonpoint source pollution is that which cannot be pinpointed to a discharge from a pipe, a leaking settling pond, etc. Much of the nonpoint pollution of a watershed is not toxic waste, but dissolved nitrogen and phosphorus. These two chemical elements encourage the growth of algae and other microorganisms, which in turn reduce the amount of dissolved oxygen in the water, which in many cases kills fish, and so on. Fertilizers used in farming are the major sources of nitrogen and phosphorus. Another example of nonpoint pollution is silting of streams from runoff, which is primarily caused by poor farming practices and large-scale construction. In summary, much of the nonpoint pollution that takes place within a watershed comes from two sources, urbanized land and agricultural land.

#8-3: List four sources of nonpoint water pollution, and from what you have learned about Landsat discuss whether or not this pollution can be "seen" directly, indirectly, or not at all by Landsat.

#8-4: Do you think it is possible to predict the amount of dissolved nitrogen and/or phosphorus in a stream by knowing the makeup of the surrounding land cover? How would you go about doing it? (Hint: What variables would you look at in a mathematical model?)

EVOLUTION OF THE NEW JERSEY 208 EXPERIMENT WITH LANDSAT

The U.S. Environmental Protection Agency has determined that a rather straightforward means exists to relate dissolved nitrogen and phosphorus to land use. Research presented in an EPA document, *The Influence of Land Use on Stream Nutrient Levels* (January 1976), was the basis for the New Jersey 208 approach. A simple linear regression model was shown to predict the amounts of these dissolved elements, based only on the amount of urban land and the amount of agricultural land in a watershed. Conventionally, this information may be easily interpreted from aerial photography. Even though New Jersey is a "small" state compared with Alaska or Texas, or even Arizona and Colorado, aerial photography for up to 31 percent of its area would be extremely expensive. Furthermore, photointerpretation of the photographs and calculation of the areas is time-consuming, and therefore expensive. Could it be that Landsat might be a viable alternative to aerial photography? One state agency in New Jersey thought so.

SOLUTION OF THE 208 DILEMMA

The New Jersey Department of Community Affairs (DCA), in the Division of State and Regional Planning, had, for several years before the 208 mandate, been experimenting with computer aided classification of Landsat data and merging it with other types of geobased information. DCA proposed to the New Jersey Department of Environmental Protection, Division of the Water Quality (DWQ), that as the agency responsible for the state 208 work they would provide DWQ with land cover maps and area statistics that were derived from computer aided classifications of Landsat data. To keep within their planning budget, DWQ decided that the DCA proposal was a reasonable alternative, and would be used for the nondesignated areas. DCA saw the opportunity to extend their "experimental" system into a real planning environment to prove the utility of Landsat as an operational data gathering tool. Figure 8-1 shows the cover page of the "Maps from Orbit" brochure that was produced by DCA to introduce the idea of how land cover maps can be produced from Landsat data.

#8-5: From what you have learned about Landsat's resolution and about computer classification, is the determination of the amount of land in urban and agricultural uses a good application of the technology? Why or why not?

#8-6: What geographical data could be combined with the Landsat data to give the information needed to more accurately calculate dissolved nitrogen and phosphorus in a river or stream?

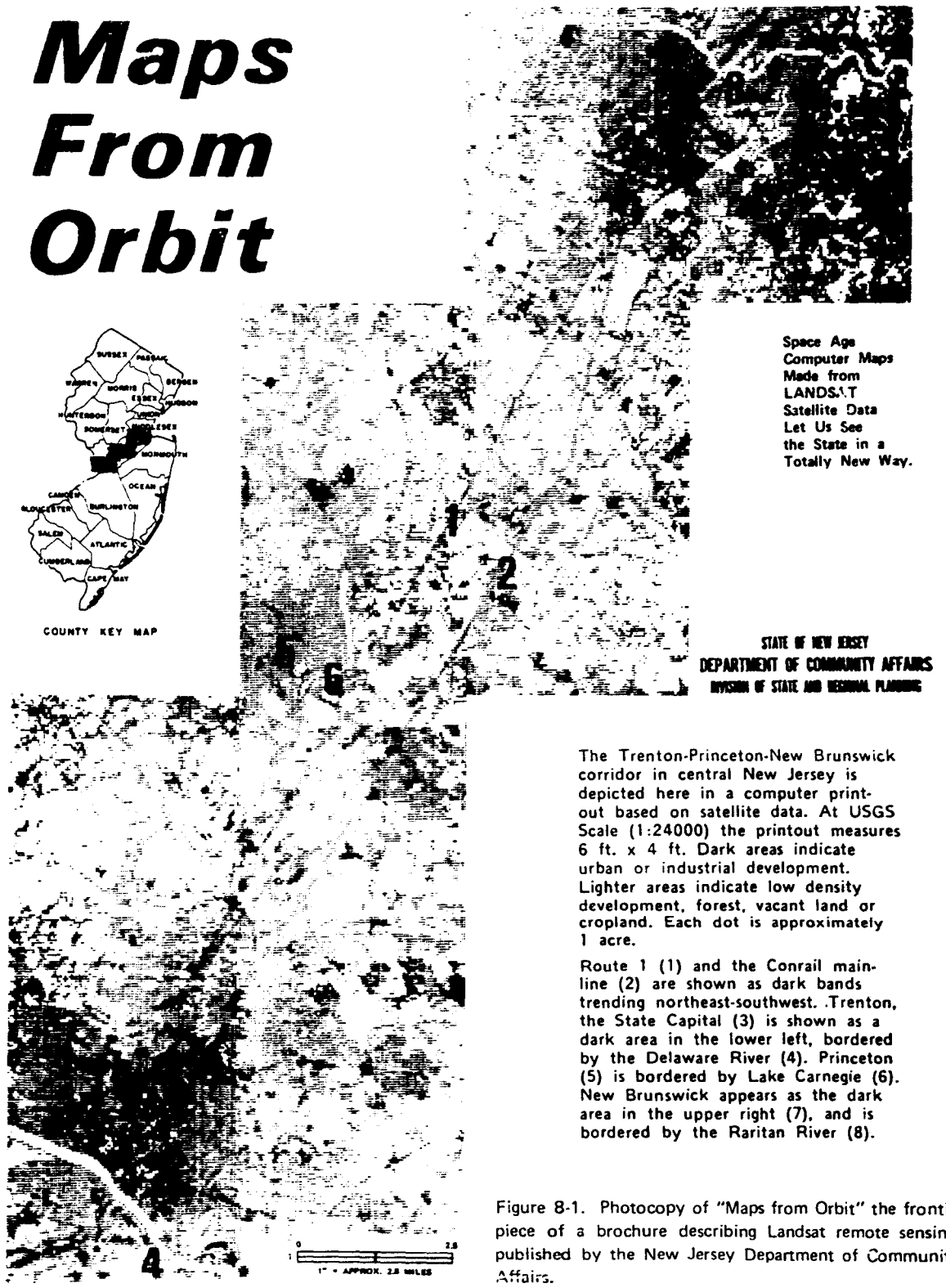

The Trenton-Princeton-New Brunswick corridor in central New Jersey is depicted here in a computer printout based on satellite data. At USGS Scale (1:24000) the printout measures 6 ft. x 4 ft. Dark areas indicate urban or industrial development. Lighter areas indicate low density development, forest, vacant land or cropland. Each dot is approximately 1 acre.

Route 1 (1) and the Conrail mainline (2) are shown as dark bands trending northeast-southwest. Trenton, the State Capital (3) is shown as a dark area in the lower left, bordered by the Delaware River (4). Princeton (5) is bordered by Lake Carnegie (6). New Brunswick appears as the dark area in the upper right (7), and is bordered by the Raritan River (8).

Figure 8-1. Photocopy of "Maps from Orbit" the frontispiece of a brochure describing Landsat remote sensing, published by the New Jersey Department of Community Affairs.

THE 208 PROJECT PLAN

In reality, classifying the Landsat data was the least of the technical issues that had to be addressed in order to make the data usable by the people who would be doing the 208 work for the state. DCA wisely decided to produce the "Maps from Orbit," the classified Landsat data, in a form that would not require extensive training of the end users in order for them to be able to understand the results, and therefore to use them effectively. DCA committed its resources to a six-step project that was described by Robert Mills, the project manager, as follows:

1. Achieve a geocodable base of Landsat data, covering the state, which could be used directly by planners and be flexible enough to be used in other applications;
2. Incorporate a statewide geographical data base showing the outlines of New Jersey's 567 municipalities and 21 counties;
3. Digitize the statewide map of watersheds (primary, secondary, and tertiary basins);
4. Merge the data sets–Landsat, municipal and county boundaries, and watershed boundaries–by relating them to the state plane coordinate system;
5. Develop interactive computer software for using the data bases;
6. Use this software to map almost one-third of the state within the optimistic time of one year from the start of the project.

CARRYING OUT THE COOPERATIVE 208 PROJECT

In order to develop an understanding of the technical issues involved in the use of Landsat data for a statewide application, it will be instructive to highlight each step in the process. In the next few paragraphs we shall outline the steps taken by DCA to fulfill their contract with DWQ. The questions will draw on what you have learned about Landsat and challenge you to speculate on why things were done as they were.

Selection of Landsat Scenes

Actual work on the project itself began in October 1976 with a visit by the DCA project staff to Goddard Space Flight Center's Landsat Browse Facility to inspect Landsat imagery. The date chosen as being the best representation of the land cover conditions over the entire state was July 18, 1976. As a base map to guide the project, the DCA used the controlled satellite image mosaic (1:500,000 scale) constructed from three October 10, 1972, Landsat scenes of New Jersey, as published by the U.S. Geological Survey.

#8-7: Refer to the Landsat Path and Row Chart in Figure 2-2. Why is New Jersey an ideal state for constructing a full-state Landsat mosaic? (Hint: About how many seconds does it take to scan the entire state of New Jersey from top to bottom?)

#8-8: Why would you use a single summer date for this project? List some reasons why certain land cover classes are easy to discriminate in the summer.

#8-9: List some land cover classes that might be confused by using summer data, why the confusion exists, and why in this case study it may not matter.

Geometrical Correction

An early decision made by DCA was to geometrically correct the raw Landsat data. The Landsat data were fitted to the state plane coordinate system by choosing matching points in the Landsat data and their corresponding locations in the state plane coordinate system. This was done to develop a transformation equation between the two coordinate systems (line and sample locations on Landsat data versus Northings and Eastings in feet for the state plane system). When the transformation is run in the computer, the Landsat data are shifted and resampled if necessary to fit the new coordinate system. The result can be a map of Landsat data that will precisely fit a map that has been drawn by using a state plane projection.

#8-10: DCA might have chosen to geocorrect classified Landsat data, rather than geocorrect the raw data first and then classify. Can you suggest strengths and weaknesses of either choice?

The state plane projection was chosen rather than UTM because the geographical files containing municipal boundaries and digitized watershed boundaries were originally drawn from a state plane projection. Maps of either raw or classified Landsat geocorrected data were produced on a line printer at a scale of 1:24000. This format was used for all further DCA work.

#8-11: Look at the letter print used in this workbook. Can you see that each character will fit inside a small rectangle? A standard line printer will print ten characters to an inch horizontally and eight characters to an inch vertically. Why is a scale of 1:24000 good to use when making Landsat maps with an output device like a line printer described above?

#8-12: What is another reason for wanting to produce Landsat maps at a 1:24000 scale?

Classification

Once the Landsat data were in usable format, i.e., geocorrected and registered to the municipal and watershed outlines, the next step was to classify the data. DCA planners used a supervised classification procedure to produce the land cover maps to be delivered to DWQ. Training site selection was based on the use of aerial photographs, maps, and ground surveys to determine sites of known homogeneous ground cover.

The classifications were made on a remote terminal tied to a central computer that used the ARGOS software programs developed by New Jersey's Department of Environmental Protection. Tapes containing the classified data were sent to ERRSAC so that color-coded maps could be generated on the Optronics Color Film Recorder.

DCA elected to by-pass the standard square, rectangular, or parallelogram map formats; instead they produced maps shaped to the irregular boundaries of the study areas. One such map, of the Navesink Watershed in northeastern New Jersey, is shown in Figure 8-2. In making the color maps, and also the line printer maps, the data are passed through a routine known colloquially as a "Cookie Cutter." All data within the boundary of a specified polygon are preserved in their original form; anything outside the boundary is given a value of zero. On the film recorder output, this value is expressed as black; on a line printer, it would be a blank. A similar procedure was used to produce the PP&L maps of the Harrisburg Service Area discussed in Activity 7.

EVALUATION BY USERS

DCA did an admirable job in providing DWQ with up-to-date information on the land cover of the "nondesignated areas," and within the time specified. Despite the success of the DCA effort, some problems existed that prevented DWQ and various citizens advisory groups from using the data to its fullest potential. Despite a concerted effort to educate the end users, resistance prevailed. Many peo-

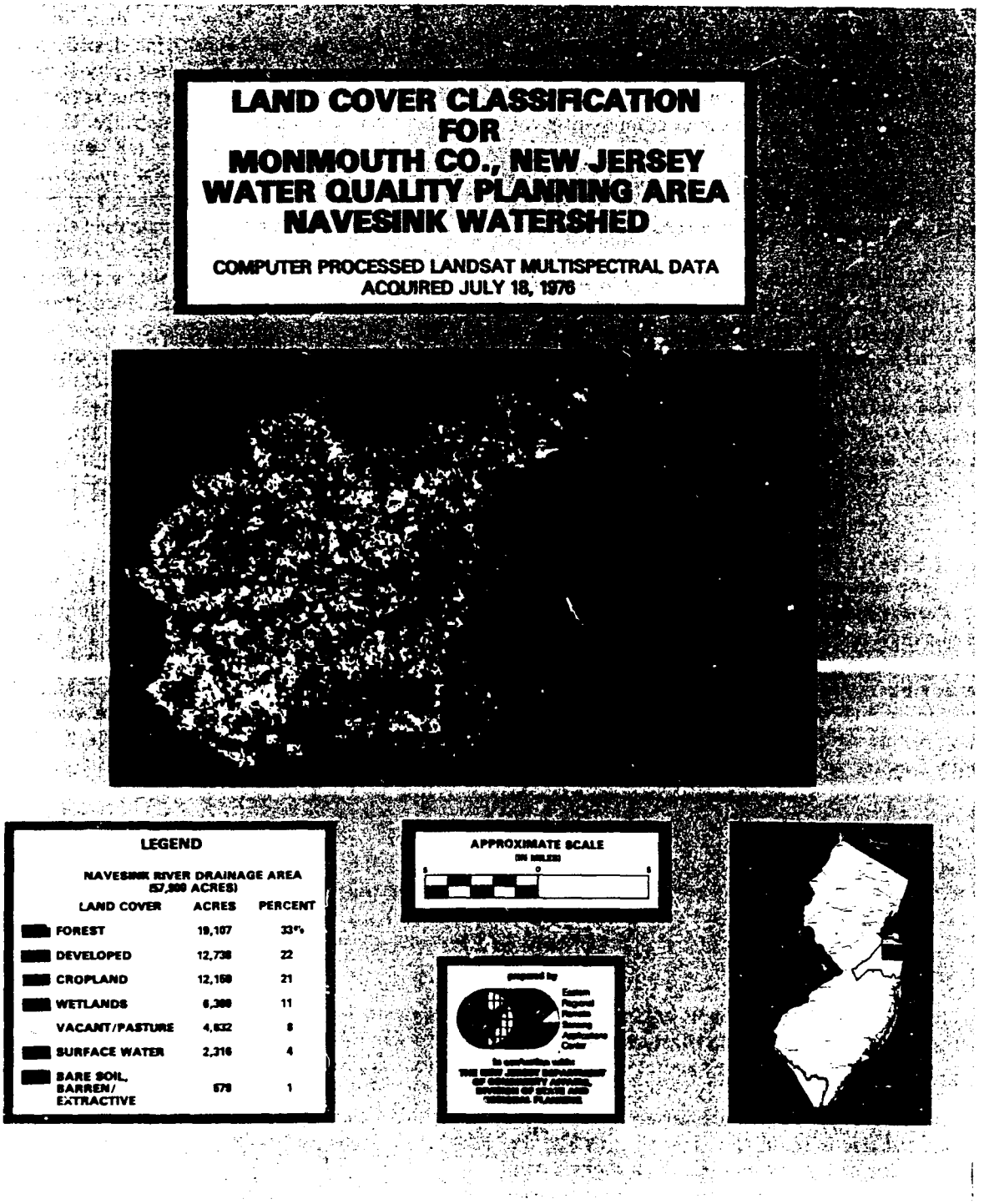

Figure 8-2. Classification map (produced on IDIMS) of the Navesink Watershed, New Jersey.

ple found the gray-scale line printer maps difficult to use even though they were at a suitable scale (1:24000) and had been cookie-cut to a recognizable shape. Another problem was conceptual. DCA emphasized that the maps represented current *land cover* and not *land use*. In many cases, areas with similar land cover may be under entirely different land uses.

#8-13: Can you think of three examples of this confusion between land cover and land use?

Another problem that soon became apparent was that the particular Landsat imagery chosen, a July scene, may not have been the optimum choice for performing a Level I classification. For example, bare soil caused by summer replanting or harvesting subtracted from the total agriculture acreage. And of course there existed a problem frequently encountered by users of Landsat data, namely that the data may be too accurate. In a sense, one reason for using Landsat data is that they are up to date. Many of the data from maps and old surveys used to check the classification accuracy are out of date. If photography is used for verification, it is often from another season or another year, and land cover does change. Then again, what do you say when planners tell you that your Landsat estimate for agricultural land is only 50 percent of what their figures claim? You later find out that the conventional estimate used the known acreage of the county and subtracted from that the acreage of the urbanized area within it, and everything else was called agriculture. In another situation, it is not always easy to convince someone that your estimate of surface water is correct, even though no one mentioned that the reference data used for comparison neglected to include impoundments, rivers, streams, but did include salt water shoreline, and was probably 10 years out of date.

EXPANSION OF THE NEW JERSEY PROGRAM

The challenge to transfer Landsat technology to those agencies and users who can truly benefit is not easy, nor can it be done by one agency alone. In many ways, satellite remote sensing represents such a big technological jump, and a somewhat uncertain one at that, which many potential users have neither the time nor the money to experiment with Landsat applications to find out what works for them. What was needed was a coordinated effort and a reserve of expertise to test at the state level some promising or trustworthy applications that could be undertaken with low risk to capital and manpower.

As indicated earlier in this activity, the state of New Jersey had a fairly good start on its own in processing Landsat data. How could NASA's Regional Applications Program[2] assist DCA to increase its capability in using Landsat data, and, at the same time, foster development of a statewide operational Landsat analysis capability? The answer to this question is fourfold and corresponds to the four activities of the Eastern Regional Remote Sensing Applications Center (ERRSAC) at Goddard. ERRSAC commits its resources to (1) user awareness, (2) training, (3) cooperative demonstration projects, and (4) technical consultation.

User Awareness

ERRSAC's user awareness activity begins by identifying people and state organizations expressing an interest in applying Landsat data, perhaps because of some previous experience of its use. These state organizations are usually departments of natural resources. In New Jersey, as well as the Department of Community Affairs and other state agencies, nongovernmental organizations have also played an important role. Rutgers University, for example, helped ERRSAC and DCA conduct a statewide Landsat symposium to introduce Landsat users to potential clients. By showing results of actual applications and answering questions from potential users, we began to formulate a statewide program that would be multiagency in scope and multidisciplinary in the applications eventually

[2] A description of this program is given in Appendix F.

chosen. Following the Rutgers symposium, several return trips to Trenton led to further discussions with prospective users to define reasonable projects with reasonable expectations and to get commitments of staff time and effort for any demonstration projects. When the dust had settled, three state agencies, all from the New Jersey Department of Environmental Protection (NJDEP), were chosen to codevelop Landsat demonstration projects with ERRSAC. The final step was to staff each project and train those people who would be working on them.

Training

Throughout the brief history of ERRSAC our philosophy has been that a prospective Landsat data user can be trained in a relatively short time to process the data and become virtually self-sufficient in that regard. Thus, within the short span of one week at Goddard we teach enough about satellite remote sensing and computer data processing to state foresters, wildlife biologists, planners, geographers, etc., so that they can begin a demonstration project with NASA when they return to their offices. In April 1979, ten representatives of the New Jersey Department of Environmental Protection arrived at Goddard Space Flight Center for one week of intensive training as the initial step in a 1-year cooperative demonstration project in the use of Landsat data.

As you recall, ERRSAC's goal was not to turn people from state organizations into remote sensing experts during their week at Goddard. What we did accomplish with the New Jersey training course, and many times thereafter, was to give people the tools they needed to begin a cooperative demonstration project. The topics covered in the course are listed in Table 8-1. Any problems, technical or otherwise, could be worked out later between the ERRSAC State Program Manager and the participants.

Table 8-1
ERRSAC 5-Day Training Course

Day 1			
a.m.	Principles of remote sensing–overview Landsat system and products Landsat image interpretation Image approach versus numerical approach	p.m.	Principles of digital image processing IDIMS demonstration and analysis OCCULT terminal familiarity
Day 2			
a.m.	Steps in a Landsat project Spectral reflectance characteristics of vegetation Technical library and browse facility Statistics for Landsat data analysis	p.m.	Self-teaching aids Introduction to OCCULT Hands-on OCCULT–NMAP
Day 3			
a.m.	Ground truth and training site selection Review hands-on Hands on OCCULT–UMAP GSFC visitors center	p.m.	Spectral characteristics of Earth surface features Applications lecture Review of Hands-on Hands-on OCCULT:UMAP and STATS
Day 4			
a.m.	Hands-on OCCULT–STATS and CLASS Geographic entry system:geographic information systems	p.m.	Applications lecture Accuracy assessment Review hands-on Hands-on OCCULT–CLASS and CANAL
Day 5			
a.m.	Other image processing systems Field trip: gathering ground truth	p.m.	Review of course Optional time Hands-on OCCULT–CLASS and DISPGM Conferences with ERRSAC staff

Demonstration Projects

Before the training course, we at ERRSAC had already been negotiating with DEP personnel to design effective demonstration projects. Two central points of contact were established: a state program manager at ERRSAC, and a Landsat program coordinator with the Bureau of Planning and Automated Systems of the NJDEP. Three agencies from NJDEP took part in the New Jersey State Landsat Technology Transfer program, as it became known. The Division of Forestry (DOF) was interested in developing a forest inventory for northern New Jersey. The Division of Parks and Green Acres (DPGA) needed up-to-date land cover information for an area within the pine barrens of central New Jersey. Finally, the Office of Coastal Zone Management (OCZM) was developing a land cover inventory to serve as a benchmark for future urban growth monitoring in Cape May County. Figure 8-3 shows the three project areas.

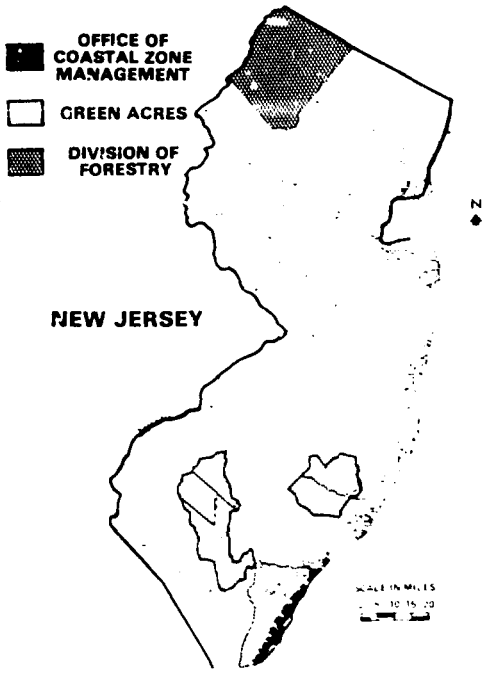

Figure 8-3. Map showing location of New Jersey state projects.

ERRSAC has learned, mostly through trial and error, that a demonstration project must be visible to state decision makers, must supply data to an ongoing state-defined program and must be proved cost effective. If Landsat allows the state to do something previously considered impossible within state capabilities, then the problem is unique and cannot be judged cost effective. A successful state demonstration meets the above criteria and has the power to convince state decision makers that Landsat is a viable tool, ready for use now.

Forestry Project. The Division of Forestry was warranted by the State Development Plan to produce forest cover maps for each of New Jersey's 21 counties by the early 1980's. These maps are to be updated periodically to reflect trends in the loss of forest lands caused by fires, development, and logging. This information will be used by state regulatory agencies as an aid to planning, and should reduce negative aspects of the environmental impact of future land use changes. The proposed Landsat demonstration was simply to produce a forest cover map for a single county by using computer processed data, and compare it with conventionally gathered information. One approach to this would be a procedure such as that shown in Figure 8-4 which shows how state agency personnel, working closely with ERRSAC project people, follow a series of analysis steps carried out on several computer systems. The key question was: Could Landsat provide information about forest locations and tree species within a county, equal to or better than conventional techniques in accuracy and at a cost saving to the state over those conventional techniques both in time and dollars?

#8-14: As you have probably noticed, different tree species in forests are intermixed with the exception of commercial tree plantations or orchards. What is a reasonable alternative to the almost impossible task of trying to identify individual tree species in space acquired imagery? (Hint:

Keep in mind the resolution of Landsat and try to develop forest "classes" that you might identify from imagery.)

The study area chosen by the Division of Forestry was Sussex County, in the northernmost part of New Jersey. Sussex County represents four separate ecological regions: (1) the upper Delaware Ridge and Terrace, rolling terrain characterized by a mix of forests and agriculture; (2) Kittatinny Mountain, just east of the Delaware River Terrace, a steep series of ridges whose land cover is predominately forested; (3) Kittatinny Valley, rolling terrain surrounded by forested ridges, with much of the land cleared for agriculture; (4) The New Jersey Highlands, an area of rugged partially forested land with numerous deep lakes. Look elsewhere in the workbook at some of the imagery that shows northern New Jersey, particularly Figure 2-1, and see if you can identify these distinct zones.

Sussex County was chosen primarily because it is heavily forested, but also because it is an area under heavy development pressure as a resort area near New York City, and is similar to the Catskills and Poconos in recreational opportunities. In this era of energy shortages, such an accessible area becomes one of critical interest to DEP. Also, even if its recreational development is slowed, the attractive market for firewood in New York City has accelerated logging in the area.

At the time of writing, about nine months into a one year project, the foresters in DEP have produced the forest cover classification shown in Figure 8-5 using a combination of Landsat and ground data. A special effort was made to pick out and classify the dominant tree species or associations in Sussex County. Preliminary checks on the gross accuracy of the map have been made in the field. The results are an encouraging 90 percent overall classification accuracy. The final accuracy assessment of the individual species type associations must await the production of precise geometrically corrected overlays of classified Landsat data at a scale of 1:24000. Ground survey teams will be sent out to determine the accuracy of classifications of individual pixels. By using Landsat data, the Division of Forestry has shown that they can almost match the accuracy of air photos in forest location. Landsat makes it possible to determine species associations that would otherwise be impossible to derive, given the cost and time constraints of a project such as this.

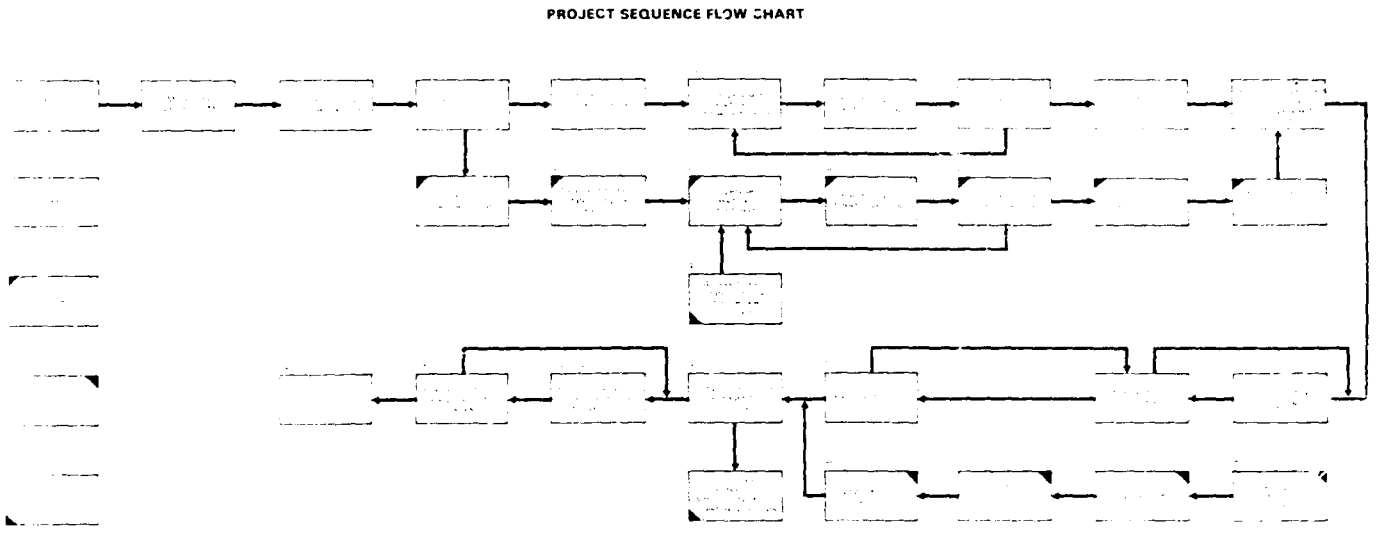

Figure 8-4. Flow chart showing sequence of data processing and analysis done comparatively between ERRSAC and the Virginia State Division of Forestry.

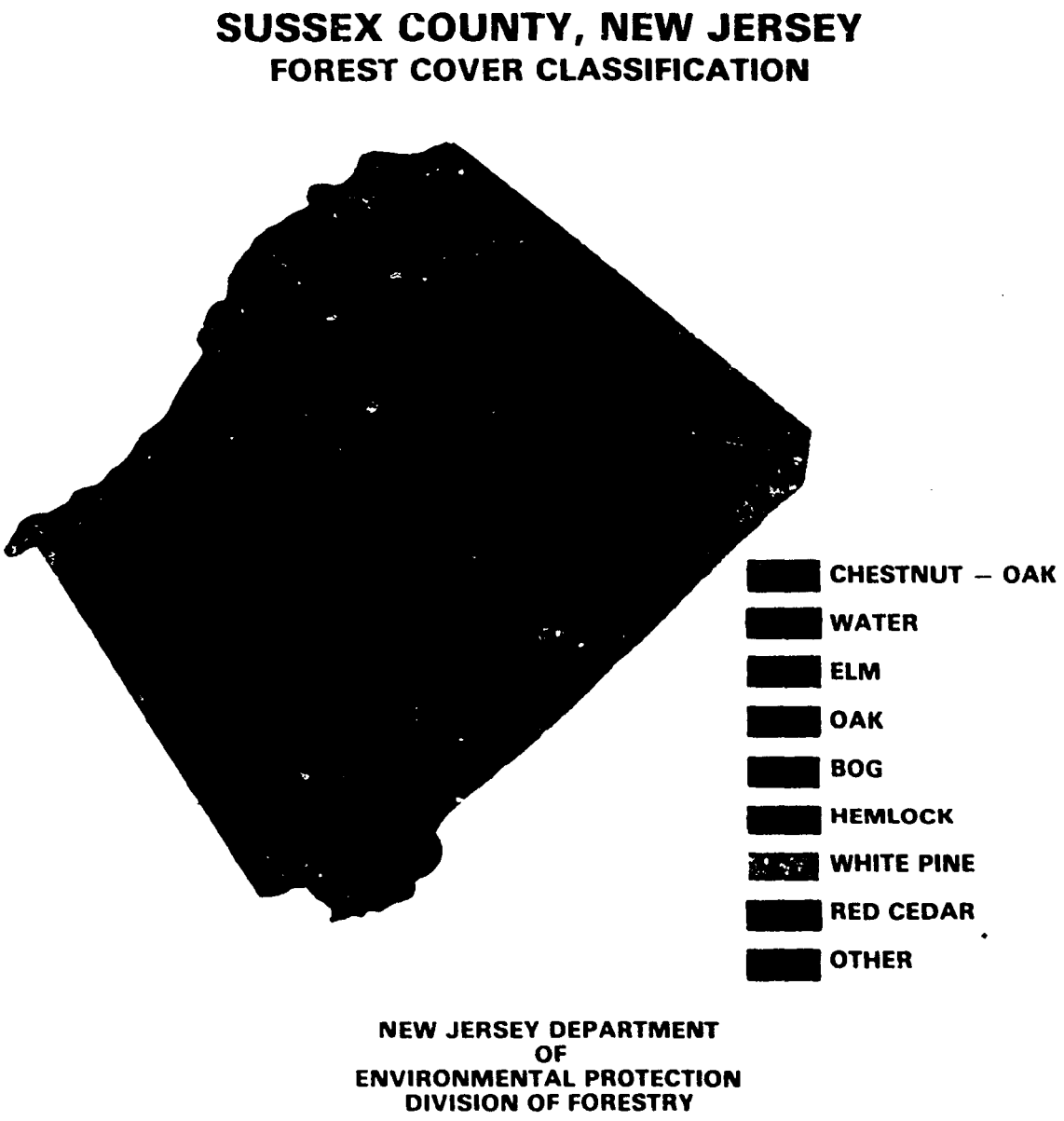

Figure 8-5. Forest cover map of Sussex County, New Jersey showing IDIMS classification of Landsat data.

Green Acres Project. The Division of Parks and Green Acres, or Green Acres, as it is usually called, is a unique state agency created to manage New Jersey's environmentally sensitive areas. Rather than receiving funds through state appropriations, Green Acres is supported by the sale of public bonds. These sales enable Green Acres to purchase environmentally sensitive areas to be placed under state protection, with some monies used to manage state-owned parks. In addition, Green Acres is responsible for carrying out the mandates of some important federal legislation such as the Wild and Scenic Rivers Act and the Endangered Species Act. For the types of activities in which Green Acres is involved, current land cover information is a prerequisite for many programs.

Landsat was seen by Green Acres staff as capable of providing the types of land cover information judged useful in defining the environmentally sensitive areas. The focus of the Landsat demonstration project is to define those areas that contain unique flora and fauna communities under threat by developmental pressures. Looking at the map of project areas (Figure 8-3), it is evident that such pressures from New Jersey's coastal resort areas, particularly Atlantic City, are and will continue to be a very real threat to wild plant and animal communities in the nearby Green Acres study area.

This particular demonstration project makes use of multitemporal Landsat imagery to provide greater discrimination of and much higher classification accuracies for land cover types (particularly forest species). The classified Landsat data are interfaced with the Green Acres Endangered Species data base to determine whether land covers of particular floral species are, in any way, predictive of the wildlife in those habitats. If a predictive capability can be devised, then the task of Green Acres to identify and procure sensitive lands is made much easier. As of early 1981, much of the Green Acres project remains to be done. However, from work completed, the project team has learned that, when using single date Landsat data only, many of the plant communities can be identified with accuracies no better than 50 percent. However, when multiple date Landsat data are applied, land covers can be identified with sufficient accuracy to begin the study of habitat associations and prediction.

Urban Growth Project. The third project follows a similar scenario for meeting state or federal data mandates and determining the benefits, if any, of Landsat data. The Office of Coastal Zone Management became interested in Landsat data as a consequence of the EPA 208 study. Figure 8-6 shows a classification of Cape May County made by DCA during the 208 project. This project is interesting from an institutional standpoint, as well as in its technical application. Cape May County has a progressive planning board, which has frequently collaborated with OCZM in designing the specifications for a geobased information system that follows the coastal land acceptability method. Here again is an area under intense development pressure as a resort area. The explosive growth of Atlantic City to the north already has overspill effects on Cape May County. The liaison between OCZM and the Cape May Planning Board allowed us to directly involve county planners in Landsat data analysis. One planner attended the ERRSAC training course and has made regular visits to Trenton and Goddard to process data and evaluate results.

The goal of the Cape May County Urban Growth Project was two-fold. First, OCZM wanted to produce an accurate land cover classification and define specific land covers to provide a benchmark to compare previous or future Landsat scenes. The objective was to monitor trends in land cover change. Second, OCZM wanted to develop the expertise in processing Landsat data for interfacing with a geographic information system.

One area of particular interest to OCZM is the salt water wetlands that predominate the county.

#8-15: How would you use Landsat data to map the different types of Salt Marsh vegetation? What types of ancillary data would you need prior to selection of Landsat imagery for such a task?

After three visits to ERRSAC to work on in-house computers, as well as much work in state offices to choose training sites and evaluate preliminary results, the OCZM project is now completed. A section of the final Cape May land cover classification is included in the map of the southern New Jersey coast reproduced in Figure 5-38. What began as a highly optimistic plan to classify Cape

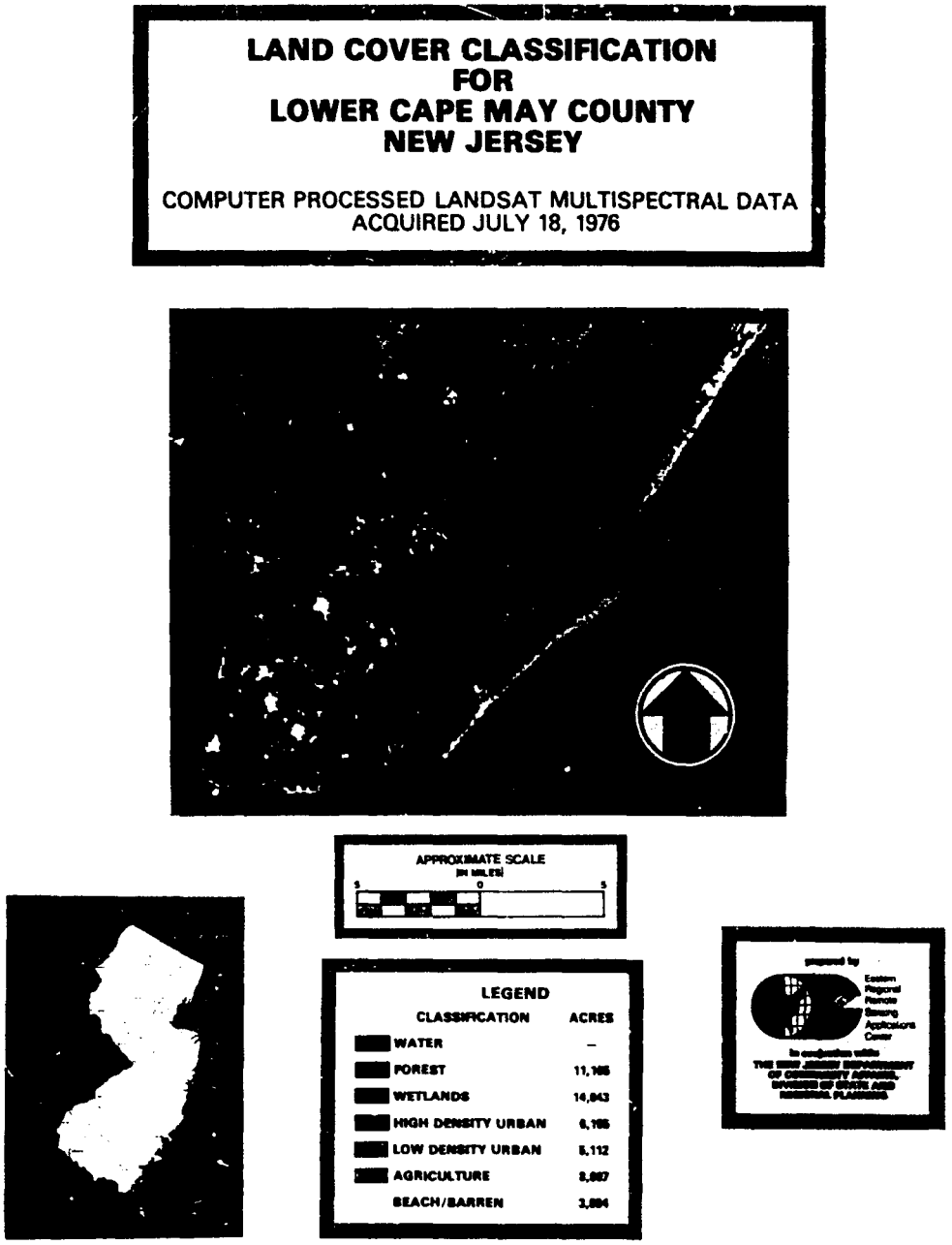

Figure 8-6. Classification of land cover in lower Cape May County, New Jersey.

May County cover types to Level III, seems, in some cases, to have been surprisingly successful. The classification map shows 35 different types of ground cover, including 9 different urban density classes. The classification of the salt water marshes astounded even those people who had been working with the data for the past year. Compare the earlier Cape May classification, performed during the 208 study (Figure 8-6), with the 38 classes map (Figure 5-38) that was made for this project.

Planners for the Cape May County Planning Board are now attempting, in their offices, to verify the accuracy of the Landsat map by comparing the results with recent air photos and field surveys. As evidence that Landsat has caught on in Cape May, the local coast guard air station has offered limited helicopter time to assist in checking the coastal wetlands.

A word of caution should be inserted here. The final classification appears to be highly accurate. High accuracy coupled with the detail of the classification has only been achieved by very hard work and painstaking analysis. It may be that the time invested to make this a successful project is not practical for an operational use of Landsat data. Until New Jersey and other states are truly operational, this question cannot be answered.

The classification produced in this demonstration project, if of acceptable accuracy, will be used by OCZM and Cape May County as a benchmark for the land cover of the county as it existed in 1978. Subsequent Landsat land cover classifications can be compared with the benchmark to look at changes in the land cover over time. By building up a series of maps, year by year, planners can develop trend analyses to show where more changes are most likely to occur. While this is a significant step, it is only the tip of the iceberg. The real power of digital remotely sensed information emerges when it is combined with other geobased information such as the one being developed by OCZM, the Coastal Land Acceptability Method, or CLAM. CLAM is a technique developed for assessing the acceptability of certain types of development in the coastal zone. It is used to determine not only whether development is acceptable, but also the degree to which environmental, socioeconomic, and development potential points of view are in conflict. This is done by producing a detailed rationale for ranking the acceptability of land, on the basis of proposed needs for (1) socioeconomic welfare, (2) development site criteria, and (3) environmental conservation. The final product is a set of three maps, one for each of these three needs; each map shows those areas that are of special interest. For example, environmental conservation is concerned with those areas that are sensitive to human encroachment. Therefore, the final map is a composite of several maps designed to show overall environmental sensitivity. Figure 8-7, depicting two categories of farmland conservation areas based on soil classes, is typical of a Landsat-aided classification map that was used as input to the composite acceptability map for environmental conservation.

In an operational situation, local planners use the three maps in combination to resolve conflicts and determine the trade-offs that exist and their associated costs. Socioeconomically, a housing development may be ideal for a particular area, but the area may have high potential erosion. If the costs of rectifying this erosion are passed on to the developer, the cost benefit of the project could be evaluated reasonably.

SUMMARY

As remote sensing gains wider acceptance, each state will tend to approach its utilization of Landsat observations in ways sometimes uniquely designed to handle the state's special capabilities and particular needs especially as that information source is integrated into a GIS. Different states will therefore develop different analytical procedures. Consider how a state such as New Jersey might decide to upgrade or expand its program in water resources management to take advantage of the increased sophistication in data processing being reported by the user community. The precise approach depends on the desired end product. For example, Vermont is concerned with measuring individual lake parameters, such as water clarity, phosphorus concentration, and chlorophyll content at specific times (Figure 8-8A). To do this, each parameter can be measured by using surface water quality data acquired from surface sampling on dates close to a particular Landsat overpass.

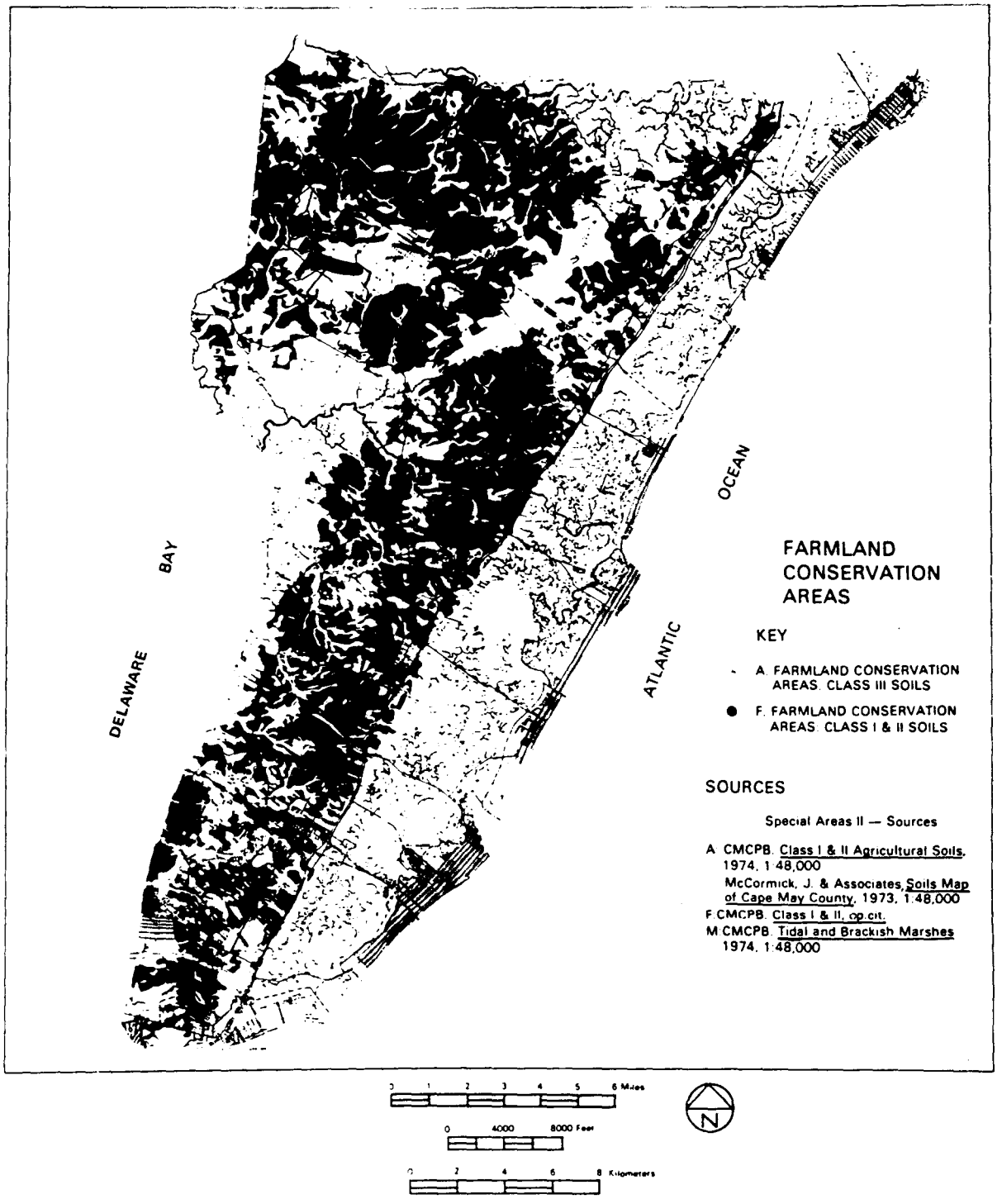

Figure 8-7. Map of farmland conservation areas in Cape May County, generated by the Coastal Land Acceptability Method (CLAM).

The extraction of quantitative values from the combined surface truth–Landsat inputs depends strongly on the decisions made as the analyst interacts with intermediate results during processing. On the other hand, Wisconsin's environmental agencies have elected to measure an average condition, the lake's trophic state, which includes contributions from a number of variables (Figure 8-8B). They find that data obtained on three dates, in spring, summer, and fall, best describe the average trophic state for a given year. Their analysis relies mainly on an automated classification procedure that receives previously collected input stored in a GIS, so that surface truth is needed only as a check on the validity of the results.

Both kinds of end use are pertinent to the requirements that New Jersey must satisfy to comply with Section 208 (nonpoint sources) and its companion Section 314 (lakes) of the EPA Clean Water Act of 1972. However, the program likely to be chosen by New Jersey to monitor its lakes, as well as its streams and coastal waters, will be influenced by another set of conditions. These consist of a mix of factors that include those relevant to Vermont and Wisconsin needs as well as those peculiar to this Atlantic Coast state; for example, the number and size distribution of the lakes over most of New Jersey are dissimilar to that of the two inland states. In order to draw up an operational monitoring system to meet 208 and 314 statutes, New Jersey would have to examine the characteristics of its water bodies, determine its past, current, and prospective sources of ancillary data, and decide which monitoring tasks can be accomplished by Landsat. To aid in this endeavor, the state could consult a checklist of capabilities and strategies such as shown in Table 8-2. Ultimately, however, New Jersey, or any state or user group, must tailor its operational monitoring and analytic systems to fit the data base it establishes to accommodate the demands and goals of the regulatory and planning agencies within the state.

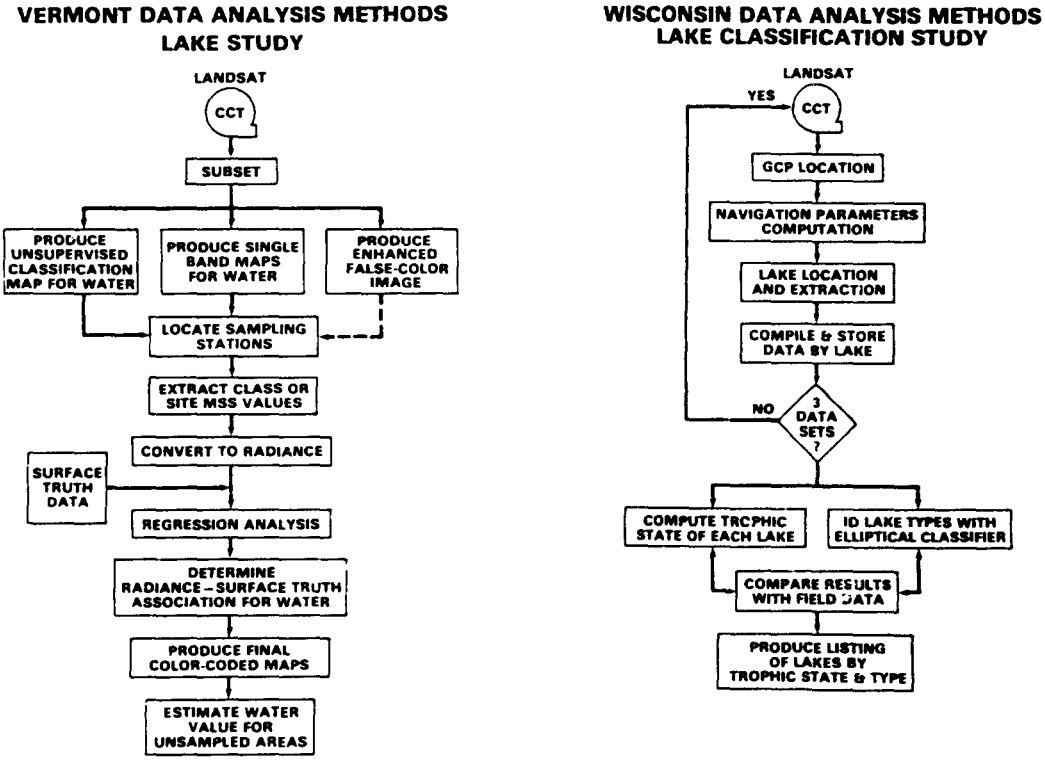

Figure 8-8. Processing sequence for lake water quality analysis as carried out by (A) Vermont, (B) Wisconsin.

The most difficult, time consuming, and costly feature of any geobased information system is that of keeping the information current. The real power in using Landsat will come as users update their land cover classifications. Until now, thematic maps have been revised by hand, using aerial photos, windshield surveys, etc. In the future, application of Landsat digital classification to update maps may become a largely automated process. The day is close at hand when local planners can design economic development models, assess development potential and environmental risk factors, and analyze trade-offs and cost-to-benefit ratios. Remote sensing will play an important role in future land use planning. Landsat is putting modern technology to work today by providing up-to-date information and by introducing many people to computer-aided analysis through Geographic Information Systems.

Table 8-2

CLEAN WATER ACT, SECTION 314

INFORMATION REQUIRED	REQUIREMENT FOR		POTENTIAL DATA ACQUISITION				
	LAKE CLASS	PHASE I OR II	L	L + MAP	L + FIELD	L + OTHER	NO L
WATER BODY – GENERAL							
LOCATION; SURFACE AREA	●	●	●				
ALTERNATE SITES		●	●				
HYDROLOGIC RELATIONSHIPS		●	NPt	●			
POLLUTION	●	●	●			● Pt	
TROPHIC CLASSIFICATION	●	●	● T		●		
ECOLOGY; PUBLIC ACCESS; RESIDING POPULATION		●				●	
WATER BODY – SPECIFIC							
SECCHI DEPTH; SUSPENDED SOLIDS; NUTRIENTS; CHLOROPHYLL A	●	●			●		
ALGAL BLOOMS; MACROPHYTES		●			●		
WATERSHED							
AREA; TOPOGRAPHY		●		●			
GEOLOGY	●	●				● S	
LAND USE		●				●	
FOLLOW-ON MONITORING		●			●	●	
OTHER SOILS; SPECIFIC GEOLOGY, BIOLOGY & CHEMISTRY; WATER USES, etc.							●

ACTIVITY 9

OTHER REMOTE SENSING SYSTEMS: RETROSPECT AND OUTLOOK

LEARNING OBJECTIVES:

- *Review the history of remote sensing.*
- *Become aware of the scope and versatility of the several satellite remote sensing systems already in orbit, especially those with sensors operating in other EM spectral regions.*
- *Appreciate the multisensor approach by interrelating Landsat observations with data from other satellite systems.*
- *Understand the basic principles and practices underlying the use of thermal infrared and radar sensors.*
- *Develop familiarity with the types of observations and interpretations emanating from the Nimbus, Heat Capacity Mapping Mission, and Seasat programs.*
- *Preview several approved or proposed Earth resources-oriented missions in the 1980's.*

LANDSAT: YOUR PERSONAL OPINION

Let us begin this activity by asking you to be introspective for a moment while you indulge in a bit of whimsy. If you have progressed this far through the workbook, you have most certainly formed some rather firm ideas about Landsat and its usefulness to your program or professional duties. One quick way to sense how you really feel about Landsat is to give it a "nickname" or describe it by some phrase that seems to express your appraisal—good or bad—of this "bird," as we in the trade refer to our satellites. I, as the author, am biased heavily in favor of this (to me) marvelous information system.[1] But perhaps you are not impressed. Nevertheless, Landsat is worthy of some appellation or slogan. Three occur to me: "Supersat"; "A Satellite for all Seasons"; and "The Miracle Worker." Challenge your wit to come up with your own nickname or phrase.

The point behind this bit of levity is, first, to force you to take a stand on Landsat—is it a remarkable technological advance, or not? But second, and more subtle, as you sought a nickname you might just have glimpsed some fleeting thoughts that are logical lead-ins to the principal subject of this activity. Such thoughts are:

- Does Landsat do all the things for me that I want?
- Are there other ways to gain useful information from space?
- What about other regions of the spectrum? Can some problems be solved, or applications developed by, say, looking at the Earth with a microwave or a thermal sensor?
- What is "up there" now, or in the past, or, we hope, in the foreseeable future, that can supplement or even supersede Landsat as a source of timely data for Earth resources applications?
- Is Landsat the only "Supersat" among the space "birds"?[2]

These provocative questions deserve suitable answers. This activity is designed to do just that: in effect, to expand your vistas, as far as remote sensing is concerned, to new horizons beyond those we have been exploring with Landsat and supporting aircraft programs. We shall accomplish this by first looking at the history of remote sensing. Then we shall review past satellite programs that provided useful information about the Earth's surface. Next, we shall survey several recent missions that specifically addressed research into the value of other parts of the spectrum for a variety of terrestrial and marine applications. Last, we shall peek into the still uncertain future of remote sensing by examining anticipated results from several new approved or proposed satellite missions.

THE ORIGINS AND DEVELOPMENT OF REMOTE SENSING

To set the stage, we have tried to organize the main highlights in the history of remote sensing into a summary outline, as presented in Table 9-1.[3] Many of the events listed appear in retrospect to be relevant to Landsat and other NASA programs that apply space technology to Earth resources monitoring and management. The table is so arranged as to present the view that aerial photography, traceable to the mid-1800's, has been the precursor to modern remote sensing.

[1] A Personal Note: The author, on record as a skeptic up to the moment of launch of ERTS-1 in mid-1972, was privileged to be among the more than 100 scientists, engineers, and managers gathered two days later in the NASA Goddard Operational Control Center as the sensors began to send back data and was the first to see a processed Landsat image on a viewing screen. My transformation to a dedicated "booster" was almost instantaneous. Within minutes, the central idea for *Mission to Earth* was conceived and the commitment to produce it was made.

[2] This last question should prompt you to an obvious play on a famous saying if you had trouble with the nickname challenge, namely, "Look, up in the sky; it's a 'bird,' it's a plane, it's SUPERSAT!"

[3] This table has been adapted from chapter 2, "History of Remote Sensing," vol. I of the *Manual of Remote Sensing*, 1975.

Table 9-1
Highlights in the History of Remote Sensing*

I. Photographic Methods

1759:	First statements by Lambert (France) of principles underlying photogrammetry.
1839:	First ever photographs by Daguerre and Nepce, in France.
1840:	French used photos in making topographic maps.
1850's:	Photographs important in documenting exploration of the U.S. West (through 1870's).
1855:	Maxwell proposed proof of trichromatic color vision by photographic experiments (1861; Sutton).
1858:	Pictures of Paris from cameras mounted in free and captive balloons.
1862:	Du Hauron analyzed multispectral imagery with single-lens beam splitter technique.
1860's:	Claims of photos for military observations from balloons during American Civil War; none survive.
1870's:	Simple additive color projection and viewing developed.
1880's:	Cameras airborne on kites in England, France, Russia.
1895:	First color separations produced.
1895:	Photos used by Seville in topographical surveys in Canada.
1900:	Ives invented three-lens multispectral camera.
1903:	Cameras attached to carrier pigeons (see Figure S-6).
1909:	Wilbur Wright took first photos (movies) from an airplane.
1909:	Berthon's lenticular color film process for additive system.
1910:	Orel-Zeiss Stereoautograph: precursor to aerial stereo-photos.
1915:	Aerial photos used by British R.A.F. for reconnaissance, changing tactics of work in W.W.I.
1917:	United States Signal Corps used aerial photos in Mexican border war.
1920:	Aerial photos used by petroleum geologists for exploration.
1923:	Zeiss Stereoplanegraph.
1924:	Multilayered color film developed.
1930:	First aerial spectrophotography of the Earth by Krinov and colleagues (Russia).
1930's:	Extensive use of aerial photos in Earth sciences and agriculture.
1931:	Testing of aerial IR sensitive film from stratospheric balloon.
1935:	Kodachrome appeared on market.
1937:	Color film used in aerial surveys.
1938:	Bausch and Lomb multiplex photogrammetric plotter.
1940:	Kelsh plotters came into wide use.
1940 to 1943:	Rapid advances in development of black-and-white and color IR (CIR) film for camouflage detection and haze penetration.
1941:	Eardley's *Aerial Photos: Their Use and Interpretation* published.
1940 to 1945:	Tremendous strides in aerial photography and photogrammetry resulting from W.W.II military needs.

*The term "remote sensing" is itself a relatively new edition to the technical lexicon. It was coined by Ms. Evelyn Pruitt in the 1950's when she was with the U.S. Office of Naval Research. The term generally implies that the sensor is placed at some considerable distance from the sensed target, in contrast to close-in measurements made by "proximate sensing."

Table 9-1 (continued)

1944: First edition of ASP's *Manual of Photogrammetry.*
1944: Military studies of water-depth penetration by two-band aerial photography.
1947: Publication of Krinov's *Spectral Reflectance Properties of Natural Materials.*
1950's: Orthophoto mapping became popular.
1952: Color aerial photos used in geological mapping.
1953: Colwell (U.S.) demonstrated detection of disease and stress in vegetation (published 1956).
1956: Soviets published on spectro-zonal photography for mapping soils.
1960's: Color film entered into common use in aerial photography.
1960: Colwell's *Manual of Photointerpretation* and Ray's *Aerial Photographs in Geologic Interpretation and Mapping* published.
1960's: Considerable activity in multispectral photography applications.
1960: Wheeler's colorvision additive multispectral system.
1962: United States and Russian nine-lens multispectral cameras; Itek camera (ten lens) in 1963.
1963: USAF built Additive Color Viewer-Printer.
1964: NASA inaugurated programs in testing usefulness of multiband photography for Earth resources.
1965: Multispectral additive color system developed by Yost and Wenderoth.
1967: First practical uses of UV photography.
1967: Two-volume *Earth Resources Surveys from Space* prepared by U.S. Army Corps of Engineers.
1968: ASP's *Manual of Color Aerial Photography*.
1968: S065 multispectral photography experiment on Apollo-9.
1975: Publication of ASP's *Manual of Remote Sensing*.

II. Non-Photographic Sensor Systems

1800: Discovery of the IR spectral region by Sir William Herschel.
1879: Use of the bolometer by Langley to make temperature measurements of electrical objects.
1889: Hertz demonstrated reflection of radio waves from solid objects.
1916: Aircraft tracked in flight by Hoffman using thermopiles to detect heat effects.
1930: Both British and Germans work on systems to locate airplanes from their thermal patterns at night.
1940: Development of tracking incoherent radar systems by British and United States to detect aircraft and ships during W.W.II.
1950's: Extensive studies of IR systems at University of Michigan and elsewhere.
1951: First concepts of a moving coherent radar system.
1953: Flight of an X-band coherent radar.
1954: Formulation of synthetic aperture concept (SAR) in radar.
1950's: Research development of SLAR and SAR systems by Motorola, Philco, Goodyear, Raytheon, Philco and others.
1956: Kozyrev originated Frauenhofer Line Discrimination concept.
1960's: Development of various detectors which allowed building of imaging and non-imaging radiometers, scanners, spectrometers and polarimeters.
1968: Description of a UV nitrogen gas laser system to simulate luminescence.

Table 9-1 (continued)

III. Space Imaging Systems

1891:	First proposal (Rahrmann) for using a rocket as a photo platform.
1908:	Maul (Germany) developed gyro-stabilized camera mounted on rocket (launched by 1912).
1946:	Space pictures obtained from V-2 rockets launched at White Sands Proving Ground (New Mexico).
1957:	Launch of Sputnik I by USSR.
1960:	Images obtained from U.S. meteorological satellite TIROS-I.
1961:	Orbital photographs from unmanned Mercury spacecraft MA-4, followed by astronaut photographs from MA-8 and MA-9.
1964:	Nimbus research meteorological satellite program begins; TV and other sensors.
1965:	First manned Gemini flight (GT-3), with some color photos.
1965:	Gemini GT-4 space photography experiments.
1965:	Recommendation of ERTS (Landsat) program by U.S. Department of Interior to NASA.
1966:	Launch of ATS series of geosynchronous satellites, with imaging sensors, followed by SMS (GOES) series beginning in 1974.
1967:	Apollo mission Earth-orbital flights (Apollo-6, -7) culminating in S065 multispectral photography experiment on Apollo-9 (1968).
1972:	Launch of ERTS-1 (Landsat); Landsat-2 (1975); Landsat-3 (1978).
1972-3:	Skylab launch; series of experiments by astronauts with EREP (Earth Resources Experiment Package).
1975:	Apollo-Soyuz flight; some photography.
1978:	Seasat-1 launched in June (failed after 99 days).
1978:	Heat Capacity Mapping Mission (HCMM), first AEM.
1979:	Nimbus-7 launched.

One attribute of aerial photos that makes them particularly attractive for a host of applications is their inherently high resolution. Optical cameras are capable of discerning—and usually also identifying—objects on the ground as small as a few centimeters. This is especially true of large-scale photos taken during low altitude aerial flights. However, one occasionally sees claims in the public press of incredible resolution capabilities—such as spotting a golf ball on a fairway or reading a license plate—from cameras on military "spy" satellites that orbit more than 160 km (100 miles) above the Earth's surface. In any event, most photo-camera systems routinely provide coverage of small segments of the ground (per photo) at resolutions that range from less than 1 m to 5 m or greater, depending on altitude and optics.

However, there are both "pluses and minuses," or tradeoffs, in shifting a camera from air to space platforms. Individual pictures or frames acquired by aircraft seldom cover an area more than 250 km^2, and more typically enclose only a few tens of square kilometers at the scales most frequently used. To image large areas, therefore, numerous individual pictures must be obtained and then mosaicked. Many problems are encountered in producing mosaics.

#9-1: List three such problems.

Recognition of the intrinsic benefits from imaging large areas at one time and at some reasonable frequency (repeat time) lies at the heart of the concept of synoptic viewing from space satellites.

#9-2: Mention at least four practical uses or advantages of viewing the Earth from space (refer to question 2-52 to recall your response to a similar inquiry).

Experience very early in the space program confirmed the usefulness of and need for synoptic imaging. It also verified a limitation that many felt intuitively would compromise the value of the observations for many applications.

#9-3: Identify that limitation if you can. (Hint: it begins with an "r.")

The "name of the game" in those early days was to define the types of observations that would best be achieved from space and would be meaningful at small scales and lower resolutions.

#9-4: Can you think of two promising categories of Earth observations from space that merit development of sensor and satellite systems optimized for such observations?

Examples of several types of observations made both from unmanned satellites and from manned missions are portrayed in Figure 9-1.

Full Earth Views From Space

The full-disc (actually, almost a hemisphere) seen in Figure 9-1A is one of many fabled color views of Earth as a planetary body; these views are obtained in one of two ways. Straightforward "out-of-the-porthole" photographs of Earth were taken by the astronauts en route to or from, or circling, the Moon during each of the seven Apollo lunar missions. However, images may be collected on a daily basis from satellites "parked" in geosynchronous orbits, i.e., orbiting the globe at the same angular velocity as the equatorial rotational velocity of the Earth itself. To accomplish this, a geosynchronous satellite is normally positioned in an orbit approximately 36,000 km above the surface. In this configuration the satellite can continuously view the same face of the Earth both day and night. In geosynchronous satellites dedicated to meteorological observations, a variety of sensors usually operate through an optical system to obtain time-lapse imagery in the visible or thermal infrared. The communcations satellites, another group, function as relay stations capable of line-of-sight transmission over most of the hemisphere.

The scene in Figure 9-1A was obtained by ATS-3 (launched in November 1967 and still operating as of early 1981), one of the six Application Technology Satellites flown by NASA. This series was designed primarily for communications experiments such as setting up links between widely separated countries or parts of a given country (e.g., India) to operate educational (workshops in the "boondocks") and medical ("doctors call") teleconferences. Meteorological experiments were also conducted from those platforms. The view shown here, covering all of South America, much of North America and a vast expanse in the Pacific, was constructed from a multicolor spin-scan camera used to monitor cloud cover and track weather fronts and other patterns of atmospheric circulation. The ATS series has given way to the SMS or Synchronous Meteorological Satellite program conducted cooperatively between NASA and NOAA. NASA's SMS will support NOAA's GOES, or Global Operational Environmental Satellite, program as part of the international effort to mount a World Weather Watch.

This type of satellite provides an exceptional opportunity for still another mode of operation of an Earth resources observation system. Through the use of a pointable telescope with a long focal length (e.g., 3 m) and zoom capability, small areas of the hemisphere may be examined at will in real time by using multispectral sensors with sufficient resolution (100 m or better) to perform many of the same kinds of observations now done from Landsat. Recommendations to orbit up to six SEOS or Synchronous Earth Observations Satellites, providing almost total global coverage, have been made, but no program to implement this has yet been authorized.

#9-5: Suggest at least four practical uses for a SEOS capable of observing selected areas on the Earth's surface on command, or at least daily, which cannot currently be accomplished with the Landsats.

Astronaut Photography

The scene depicted in Figure 9-1B consists of blique natural color photo looking from space km (400 miles) northward across North lina and Virginia toward the Delmarva nsula, eastern New Jersey, and Long Island in distance. This is one of many such photos n by the astronaut crew of Apollo-9 in March 9. The SO65 experiment during that mission lved multispectral photography from four mm Hasselblad cameras fixed in a frame nted against the spacecraft porthole window. cameras used panchromatic film with red and n filters, and a third used black and white IR with an appropriate infrared filter. Together, e produce rough equivalents to the black and te Landsat-1 images made with the RBV eras. These Hasselblad photos have been com- d by additive techniques similar to those de- ed on page 94 to produce false color composites. The resulting products compared favorably with—in fact were superior to—the color IR film photos obtained with the fourth Hasselblad. Most of the four-camera array series from Apollo-9 were essentially "straight down" pictures taken close to the vertical. The orbits followed by Apollo went only as far north as 34°, well below the latitudes of the New Jersey and Harrisburg scenes now so familiar to us. However, glimpses of more northerly areas were provided by pointing a handheld Hasselblad, usually containing a magazine of color film, obliquely out of the window.

#9-6: Remember that the photo shown in Figure 9-1B is in natural color. Note, however, the numerous pinkish-brown areas on the ground (mainly in the lower left). This resembles the false color signature of vegetation, but isn't! What are you really looking at?

Meteorological Satellites

The lower pair of images in Figure 9-1 are tal products obtained during two Nimbus sions. Nimbus refers to a family of "Metsats" gned and managed at Goddard Space Flight ter as a mainstay in the experimental program eloped within NASA for meteorological re- ch. This program was initiated in 1958, shortly r the birth of America's space program an nt generally tied to its successful launch of plorer-1. The first Nimbus was launched in 1964 n Vandenberg Air Force Base in California. The bus vehicle is essentially the same spacecraft d in the Landsat program except for the latter's propriate modification to accommodate the MSS RBV payloads. Since 1964, seven Nimbus llites have been successfully placed in orbit.

Unlike their predecessors, the TIROS levision-Infrared Observation Satellite) series, Nimbus satellites have an advanced stabilization tem that keeps their sensors locked or aligned within 1° of nadir. Like Landsat, a Nimbus is into a nearly circular and polar Sun synchro- us orbit. The orbital altitude, close to 1110 km (600 nautical miles),[4] favors a local noon time pass during the northbound segment of the orbit. A considerable variety of sensors operate on the different missions. These sensors include cameras (e.g., IDCS or Image Dissector Camera System), radiometers (e.g., HRIR or High Resolution Infrared Radiometer; THIR, or Temperature-Humidity Infrared Radiometer), and Atmospheric Sounders (e.g., IRIS or Infrared Interferometer Spectrometer; BUV, or Backscatter Ultraviolet Spectrometer).

The sensors were selected to facilitate observations and measurements over large areas within the atmosphere. Depending on the specific sensor and mission, picture dimensions from imaging cameras are typically of the order of 2100 km × 2100 km or 2700 km × 2700 km (some cover smaller areas), and swath widths ("footprints") of some radiometers range up to 7100 km. Obviously, the resolution at the subsatellite point is compara-

[4] Nimbus-1 failed to achieve this orbit and passed to within 422 km (228 n mi) during its perigee.

tively low for these sensors. Imaging systems produced resolutions from 330 m (Nimbus-1 at perigee) to 3.3 km for vidicon cameras to 3.3 to 7.7 km for HRIR and 74 to 150 km for IRIS. Thus, typical scenes cover large areas within continents or open ocean, in which the details of surface features are lost at the expense of encompassing first-order features of regional scale. One can see mountain ranges (and sometimes major valleys within them), large lakes, broad deserts, and agricultural activities along rivers, but little else of interest to the Earth resources specialist. Nevertheless, some valuable observations were recorded and served to support arguments favoring the use of higher resolution satellites to monitor regional features. Several large geological faults were discovered, phenological (seasonal) changes in vegetation growth (the "green wave") were documented, snow cover extent was mapped, ice shelves and sea ice were monitored, and sediment and current movements in large lakes and the oceans were followed.

#9-7: Can you think of three other types of surface features likely to be observable from a Nimbus satellite?

The color-enhanced (density-sliced) map of the Arctic region shown in Figure 9-1C is a splendid example of the kind of sophisticated data returned from a specialized sensor on Nimbus-5. The ESMR (for Electrically Scanned Microwave Radiometer) on that satellite sensed radio brightness temperatures to an accuracy of ±3°K. This temperature is a radiant quantity proportional to the surface (kinetic) temperature and the emissivity of the material(s) making up the surface. The data cells (squares representing 30-km resolution elements) in this map record average brightness temperatures that extend through a range from less than 182°K to more than 282°K. The microwave (1.55 cm) data were averaged over a period of three days. In general, continental surfaces show the highest brightness temperatures owing to higher emissivities for soil and vegetation. Gross variations in soil moisture (producing lower temperatures) may be detected. ESMR has been especially effective in recording conditions in the polar region. Open ocean may be readily distinguished from sea ice; first year sea ice is often separable from older ice, and the development of leads (breaks) in the ice is discernible.

#9-8: Despite the time of year (late August), ice persists in the regions around the North Pole. What is the temperature range associated with this ice? Parts of the open ocean are marked by brightness temperatures as low as 135 to 155°K. This is notably colder than the sea ice further north. Yet ice, from one's experience, is colder than water. Account for this paradox.

In Figure 9-1D, a large deep blue patch correlates with a huge oil slick detailed by the Coastal Zone Color Scanner on Nimbus-7 (see p. 338). This is direct evidence of the massive spill from Ixtoc 1, an offshore well in the Mexican field in the Bay of Campeche northeast of Cuidad del Carmen and Tampico. That spill, which followed a blow-out on June 3, 1979, persisted well into 1980 as the largest ever to contaminate the open seas. The spill has also been detected in Landsat imagery, but only after careful reprocessing of digital data. The fine globules of oil cause a rise in reflectance of just 1 to 2 DN units relative to uncontaminated ocean water. A drastic contrast stretch was needed to highlight the spill from the surrounding waters.

#9-9: How might such observations of spills be used in a practical way (from both environmental and legal standpoints)?

Figure 9-2A shows a large section of the eastern half of the United States as imaged by the Direct Reading Infrared Radiometer (DRIR; a real-time [not tape recorded] readout version of HRIR) on Nimbus-3. The resolution is 8.9 km (5.6 miles) and the swath width is 7900 km (4937 miles). This daytime view shows a flat response (little contrast) in the 3.4 to 4.2 μm interval (in the transitional region between reflected and emitted radiation) sensed by this instrument. Note that this thermal image shows clouds (normally cooler) printed in light gray tones, and land surface and water (warmer) in dark tones—a convention adopted by meteorologists to display clouds as white, as commonly seen in visible light imagery. Other satellites, such as NOAA-6 (TIROS series), send back multichannel data at high enough resolution to be utilized in some specialized Earth Resources Applications (Figure 9-2B).

#9-10: When compared with standard map projections, the outlines of the continent and many

ORIGINAL PAGE
COLOR PHOTOGRAPH

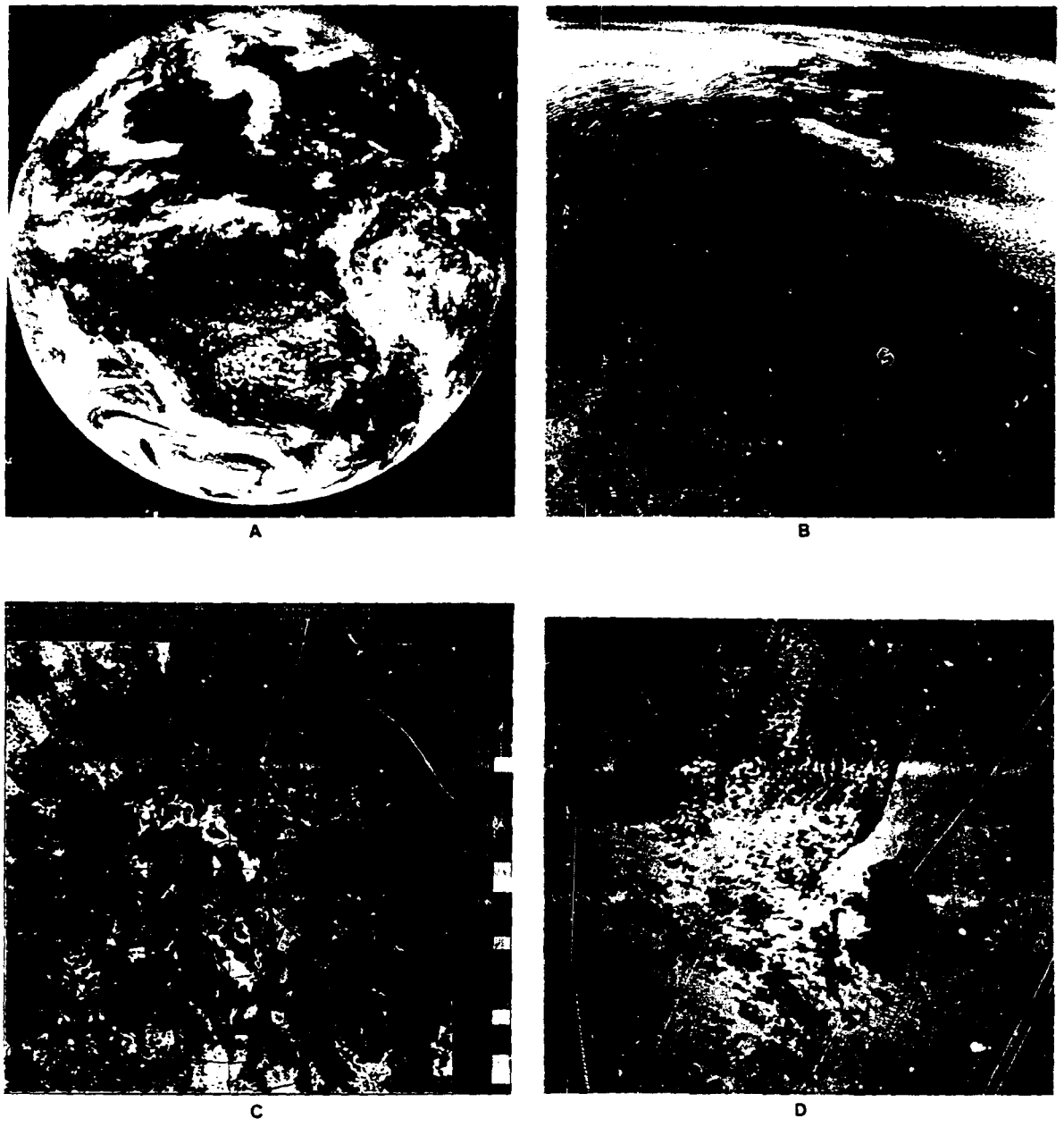

Figure 9-1A. ATS-3 image of full Earth disc; B. Apollo-9 oblique photo of eastern U.S. coastal region; C. Nimbus-5 ESMR color-coded display of north polar region brightness temperatures; D. Nimbus-7 CZCS image of Mexican oil spill (see text).

Figure 9.2A. Eastern U.S. and Canada imaged by the DRIR on Nimbus-3.

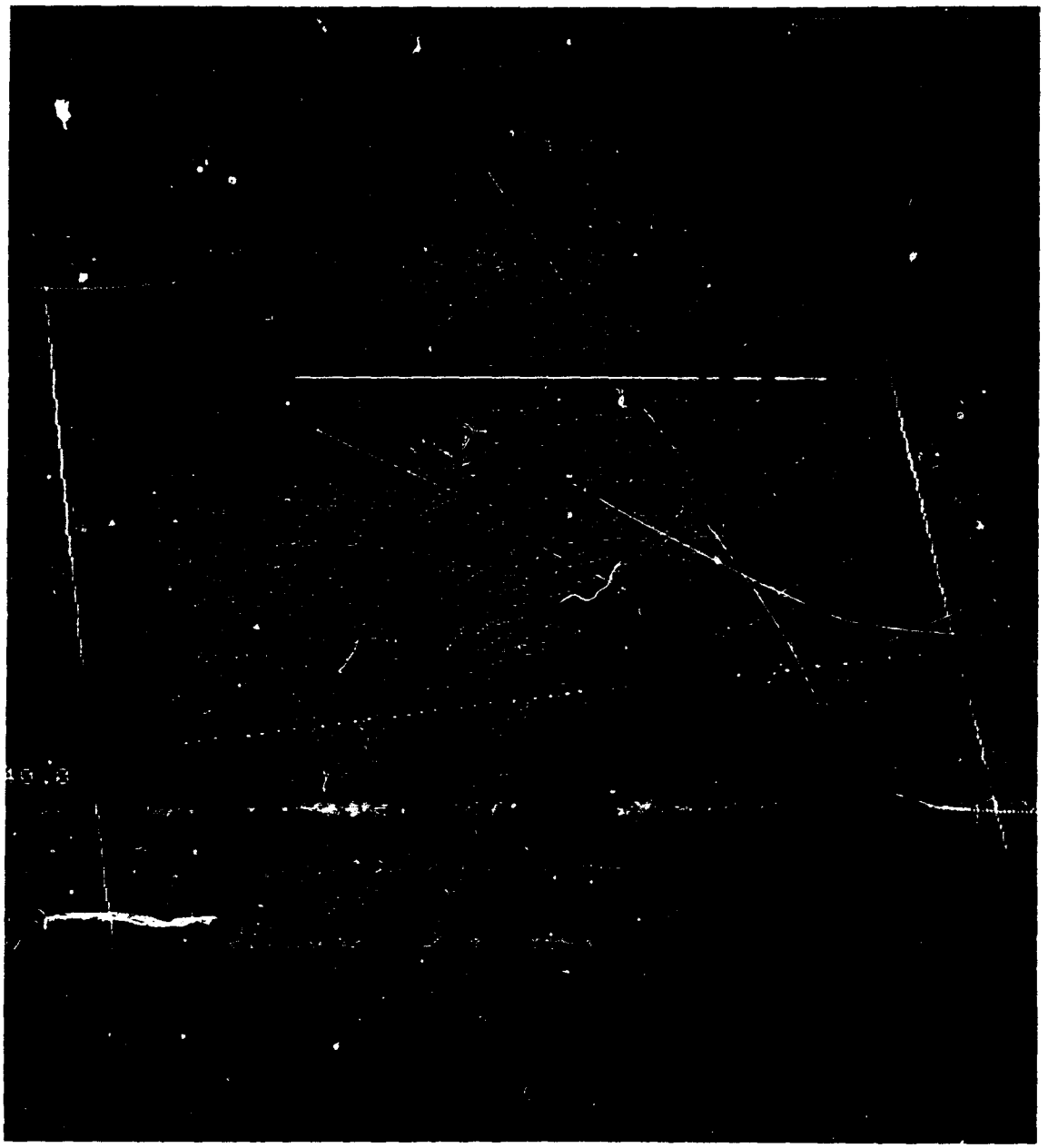

Figure 9-28. A color coded Vegetation Index (VI) map derived from data obtained by the NOAA-6 AVHRR sensor on June 21, 1980 (orbit 5115). The area covered extends from Lakes Erie and Ontario to New Jersey, including most of study areas considered in this workbook. The four AVHRR channels (Ch) operate in wavebands (1) 0.55 - 0.68 μm, (2) 0.72 - 1.1 μm, (3) 3.3 - 3.6 μm, and (4) 10.4 - 11.5 μm; spatial resolution is 1.1 km. The VI data are calculated as the ratio: Ch 2 — Ch 1/Ch 2 + Ch 1. The reds and oranges in this map correlate well with extensive and continuous forest (canopy) cover whereas the green and medium blue correspond to areas of moderate to light vegetation including croplands and meadows. Dark blue depicts both water and cloud cover (upper right corner). White latitude and longitude lines are located on the image relative to the projection used. Courtesy J. Tucker, NASA GSFC.

recognizable features in the interior (such as the Great Lakes) show very evident distortions. Why is this so? (Hint: Keep the scale and the geometry of the surface in mind.)

The Reststrahlen Principle (SCMR). An experiment was approved for flight on Nimbus-5 that takes advantage of the "reststrahlen" effect to make qualitative estimates of the silica composition of soils and rocks. The concept of reststrahlen or "residual rays," refers to reduction of thermal radiation (decreased emission) in the 8 to 14 μm region of the IR. In this interval, emitted energy from silica (SiO_2) and silicates is variably influenced by resonance vibrations associated with silica tetrahedra (specifically, with silicon-oxygen bonds). Spectral signatures of silicate minerals and silicate rocks in the 8 to 14 μm range reveal at least one prominent drop in emissivity at some characteristic wavelength. This emissivity "trough" shifts towards lower wavelengths as the silica content of the mineral or rock increases. Other factors enter in to make the determination of silica far more complex than implied in the previous statement, but the ability to separate ultrabasic (SiO_2 < 40 percent) from basic (silica content > 40 percent < 55 percent), and these from silicic (SiO_2 > 65 percent) rocks,[5] has been demonstrated from measurements made by a two-band radiometer flown on a low-altitude airplane. Each band provides a measure of radiant temperatures from the same target. These temperatures will differ, depending on the emissivity sensed in each interval, which in turn may be moderated by the reststrahlen effect. Thus, a silicic rock has reduced emittance (excitance) in the 8 to 9.5 μm range, whereas a basic rock will show lower emittance in the 10 to 12 μm range. Ratios of emittances measured in these two intervals are therefore sensitive to compositional differences.

A two-band (8.4 to 9.5 μm and 10.2 to 11.4 μm) radiometer, called SCMR (for Surface Composition Mapping Radiometer), was included in the Nimbus-5 payload. Unfortunately, this instrument (with cooled detectors) failed within a month after launch. Useful data were returned and, despite limited analysis, tend to confirm the capability of sensing compositional variations from space. Figure 9-3A reproduces the SCMR image of part of the Caribbean, taken with the 8.4 to 9.5 (8.8) μm channel during the night. The parameter shown is radiant temperature rather than emissivity. The temperature range extending from 265 to 305°K may be displayed in a color-coded map (Figure 9-3B).

#9-11: What are the blue and green patterns over open waters northeast and southwest of Florida? Which is cooler at this time of orbital overpass, the land or the oceans?

#9-12: Comment on the thermal patterns evident in marine waters off Florida, the Bahamas and Cuba.

The CZCS (Nimbus-7). The latest in the series, Nimbus-7, launched in October 1978, carries nine sensors capable of monitoring several vital aspects of the Earth environment. In keeping with its meteorological role, eight of the sensors were designed to make important measurements within the atmosphere. These sensors are:

- Earth Radiation Budget (ERB),
- Limb Infrared Monitoring of the Stratosphere (LIMS),
- Stratospheric and Mesospheric Sounder (SAMS),
- Stratospheric Aerosol Measurement Radiometer (SAM II),
- Scanning Multichannel Microwave Radiometer (SMMR),
- Solar and Backscatter Ultraviolet Spectrometer (SBUV),
- Total Ozone Mapping System (TOMS),
- Temperature Humidity Infrared Radiometer (THIR).

Some of these sensors provide new categories of information never before acquired from space platforms.

[5] Rocks of intermediate silica content (between 55 percent and 65 percent) give ambiguous results; this is caused by partial loss of signal in the 9.3 to 10.4 μm interval owing to absorption by ozone.

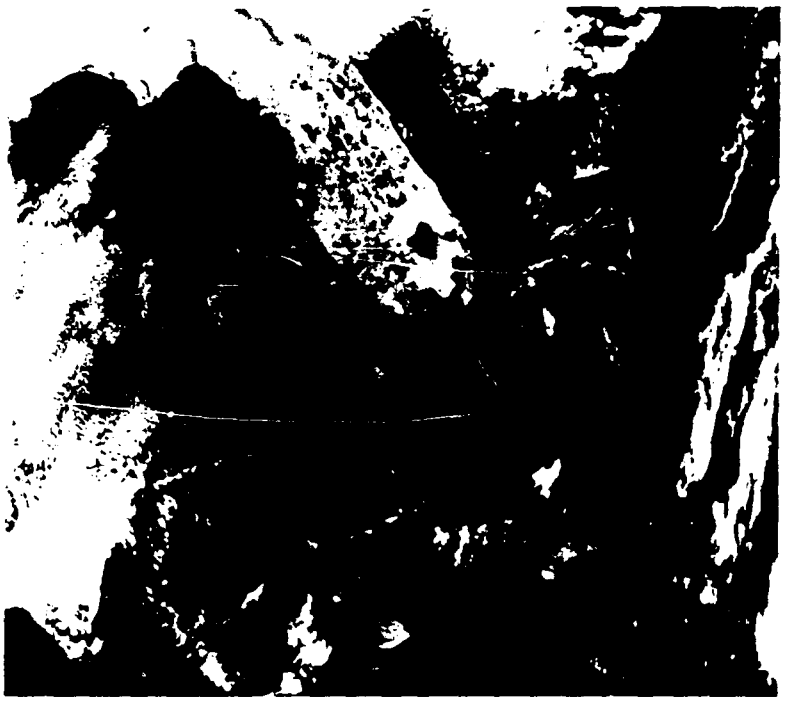

Figure 9-3A. Nimbus-5 SCMR nighttime IR image of Florida, the Bahamas, and Cuba, recorded on December 24, 1972 (orbit 173).

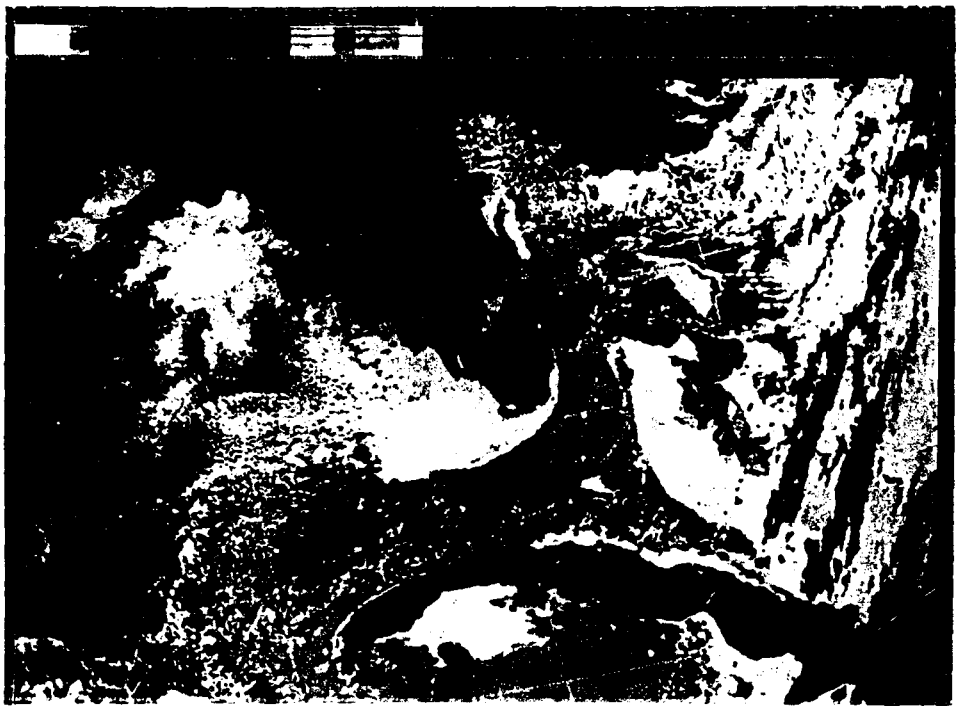

Figure 9-3B. Color-coded temperature map of land, water, and cloud features in above scene (corrected geometrically).

The ninth sensor, the Coastal Zone Color Scanner (CZCS), is of particular interest to Earth resources specialists in that it sends back valuable data on living nutrients in coastal and deeper marine waters. The principal food supply for higher life forms in the oceans consists of phytoplankton—microscopic plants that photosynthesize chemicals in sea water. This process depends on the plankton's content of chlorophyll *a*, a pigment that strongly absorbs blue and red light. As plankton concentrations increase there will be a corresponding rise in the spectral radiance peaked in the green. Upwelling masses of water (usually associated with thermal convection) containing phytoplankton will take on green hues, in contrast to the deep blues of ocean water with few nutrients or other particulates.

The CZCS contains five channels chosen to center on spectral bands sensitive to chlrophyll *a* effects and other diagnostic color phenomena. Two bands are located at 443 and 670 nm,[6] in regions of high chlorophyll *a* absorption. Two other narrow (20-nm width) bands are centered at 520 and 570 nm, in regions where variations in radiance resulting from changing chlorophyll concentrations are minimal. A fifth broader (100 nm) band is centered at 750 nm (just in the infrared). A sixth band in the 10.5 to 12 μm region measures surface temperatures as indicators of upwelling. The four shorter wavelength bands have high radiometric sensitivities (CZCS band 4 [670 nm] is 60 times more sensitive to small variations in radiance than Landsat MSS band 5).

Examples of images produced from individual bands on CZCS are given in the next three figures. In a full scene, the swath width is about 1600 km (1000 miles); maximum resolution at nadir is *ca.* 825 m (2720 ft).

Figures 9-4A through C show the Atlantic Ocean around Georges Bank off the New England shoreline as imaged from bands at 443, 520, and 670 nm (3, 2, and 1 in the annotation). Two color composites (with colors indicated in the legend) were made on the IDIMS interactive computer (Figures 9-4D and E). The colors in Figure 9-4E resemble the natural color of the ocean; note that the land has been made to appear black (by thresholding out its range of brightnesses) while the clouds (toward bottom) retain their white tones. Figure 9-4D is a false color rendition that seems to better define variations (in red hues) of particulates in the famous fishing grounds of Georges Bank.

After proper processing and correlation with field data (ocean truth), CZCS data have proved remarkably effective in estimating the distribution of and changes in chlorophyll *a* content, and hence variations in phytoplankton content, within marine waters. Consider Figure 9-5. This scene covers much of the Gulf of Mexico and surrounding land masses as imaged by CZCS on November 2, 1978.[7] An algorithm was applied to computer-processed data to remove the backscatter contribution from aerosols in the atmosphere to the measured radiances. A second algorithm computes chlorophyll *a* concentration by ratioing CZCS bands 1 (443 nm) to 3 (570 nm). To make a color composite for the ocean, band 1 is assigned a blue color, band 2 (520 nm) a green color, and band 4 (670 nm) a red color. The colors associated with the land and the clouds were made by combining bands 1, 2 and 3 data in blue, green, and red colors respectively for those pixels identified with these two classes; pixels for open water areas are omitted from this step by a threshold algorithm, which uses band 5 (near zero reflectances from water in the IR) to mask them out.

The concentrations of chlorophyll *a* from 0.05 to 1.00 mg/m^3 are shown in the color-coded scale at the base of Figure 9-5. Concentrations above 1.0 mg/m^3 were not determined with acceptable accuracy and are rendered in red-brown. However, in a computer analysis of CZCS data acquired later in November, 1978, more accurate results for the area off the West Coast of Florida were obtained by using additional algorithms. To check these results, a set of concentration changes were measured along a sampling track of a boat that sailed almost immediately after the Nimbus overpass. These measurements were found to correspond quite well to the later estimates (made from the CZCS data) of concentration along that track.

[6] Another convenient unit for wavelength is the nanometer (nm), or 10^{-3} μm. Thus, 600 nm is equivalent to 0.6 μm.

[7] This figure and related data taken from Gordon, H.A., D.K. Clark, J.L. Mueller, and W.A. Hovis, "Phytoplankton Pigments Derived from the Nimbus-7 CZCS: Initial Comparisons with Surface Measurements," *Science*, V. 210, pp. 63-66, Oct. 3, 1980.

ORIGINAL PAGE
COLOR PHOTOGRAPH

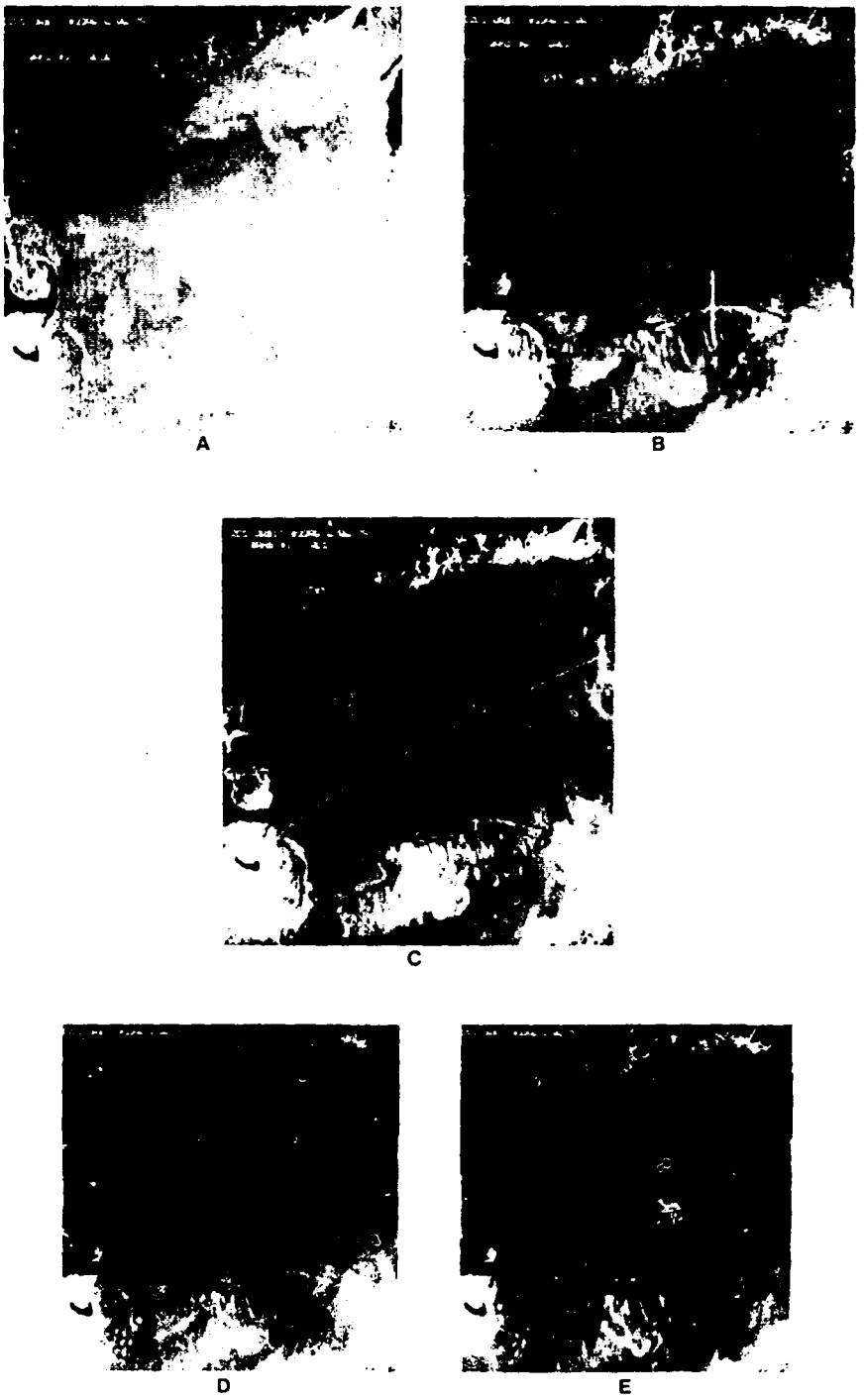

Figure 9-4. Images of Georges Bank open ocean area, made from data acquired by CZCS on Nimbus-7, June 6, 1979. A. Red band; B. Green band; C. Blue band; D and E. False color.

ORIGINAL PAGE
COLOR PHOTOGRAPH

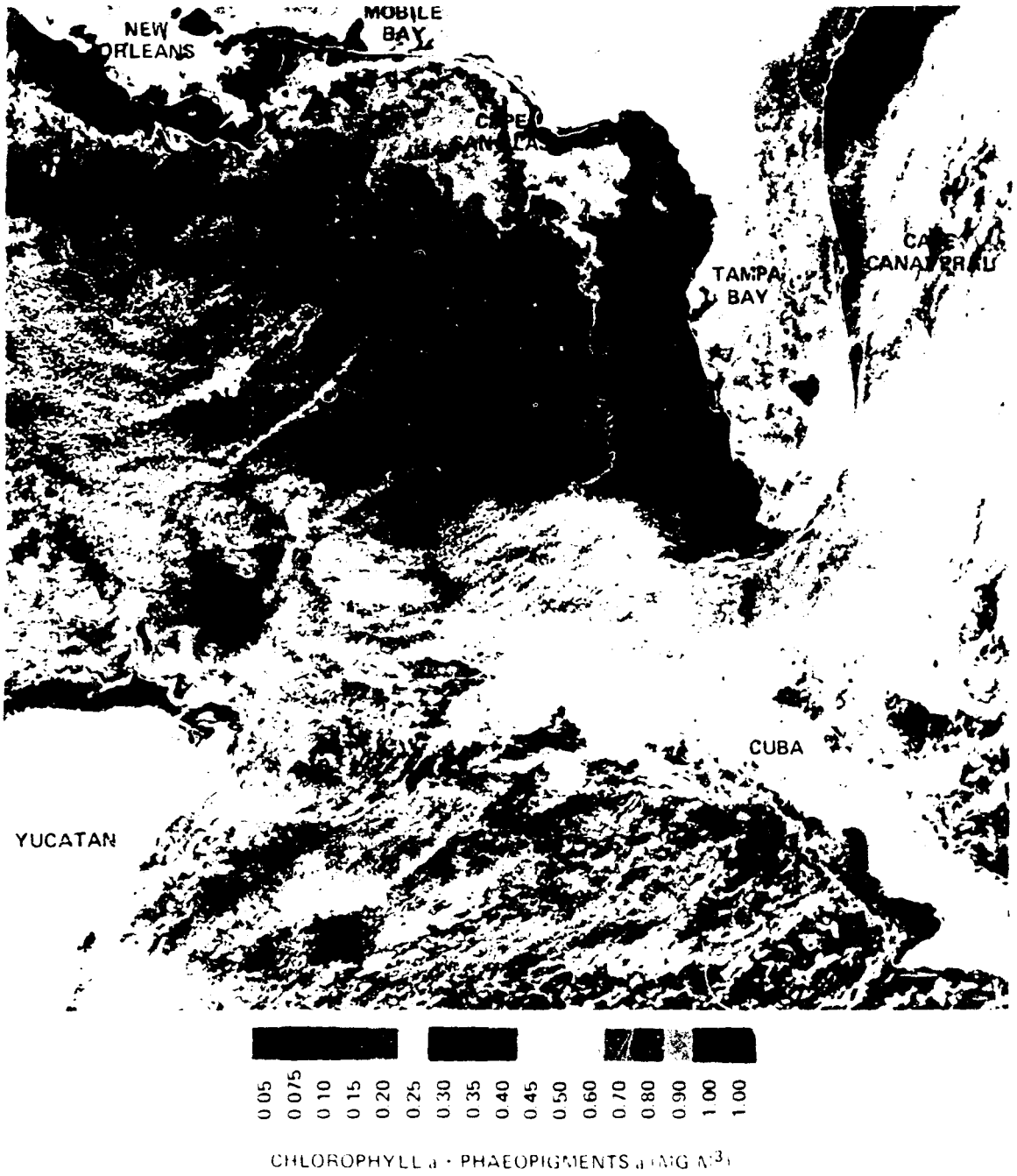

Figure 9.5. Estimate of Chlorophyll *a* and Phacopigments *a* concentrations in Gulf of Mexico waters, made from CZCS data obtained on November 6, 1978.

#9-13: Where would you send the fishing boats in the scene depicted in Figure 9-5, assuming that you processed the CZCS data in near-real time?

Computer manipulation of gray levels in the individual band images may improve the contrasts within CZCS images. The spectacular view of the eastern United States and southern Canada shown in Figure 9-6 was produced from band 1 (443 nm) expanded by a factor of 2 and projected through blue, band 2 (520 nm) projected through green, and band 5 (750 nm) expanded by a factor of 3 and projected through red. A small part of the eastern Pennsylvania area we have been studying appears at the bottom.

THERMAL IR SYSTEMS

So far in this activity, we have looked at low resolution images produced from sensors that operate over several regions of the spectrum, from the near UV-visible boundary to the microwave. We shall next focus our attention on higher resolution data for the thermal IR region.

Review of Concepts

The thermal emission region between 8 and 14 μm can reveal much about various types of materials, as we have already seen from our consideration of brightness temperatures measured by a variety of Nimbus sensors. Before working through the next few paragraphs, reread the discussion on thermal principles presented on pp. 27 to 28. Some of the concepts treated there will be reviewed in more depth now, while others remain implicit but important.

Temperature is a measure of the concentration of heat. Heat is an indication of the kinetic energy within a collection of atoms and molecules making up a material body (such as a solid with finite boundaries, but also liquids and gases without definite shapes or dimensions). This energy stems from the random motions of oscillating or otherwise moving atomic particles. Collisions among these particles lead to changes in energy, which may be emitted as radiation. The radiant temperature T_R is related to the kinetic temperature T_K by the relation $T_R = \epsilon^{1/4} T_K$, where ϵ is the emissivity. Emissivity is a dimensionless number between 0 and 1 calculated as the ratio of F_R/F_B, where F_R is the radiant flux of a real body and F_B is the flux of an ideal blackbody (perfect emitter). A high value of ϵ (0.80 to 1.00) describes a high efficiency of a substance in its ability to absorb and emit radiant energy. Thus, the radiant temperature is significantly higher for a blackened surface (high ϵ) than for a shiny surface (low ϵ), even if the underlying materials are at the same kinetic temperature; for real materials ($\epsilon < 1$), the radiant temperature measured at the surface is always less than the kinetic temperature of the body.

Heat may be transferred from surficial layers of the Earth (which are heated internally, as from the geothermal heat of the Earth, and/or externally, as from the Sun or a fire) by conduction, convection, and radiation. A thermal sensor picks up radiant emitted energy from a surface target that has been heated through radiation (solar insolation), convection (atmosphere), and conduction (ground). For a body at a given kinetic temperature, there is some wavelength, corresponding to a maximum radiant temperature, which marks the peak output of radiant power. This wavelength is determined by Wien's Displacement Law (p.28). for the Sun (photosphere radiant temperature of *ca* 6000°K), the peak is in the visible (*ca* 0.55 μm); for the Earth as a radiator, this peak is within the 8 to 14 μm interval; and, for a burning forest the peak is around 5.0 μm.

Temperature Measurements. The branch of remote sensing in which measurements of temperatures of surface features are considered is called *thermography*. Fortunately for remote sensing, the

thermal waveband regions of practical interest correspond to windows of reduced atmospheric absorption and also lie within the response range of several types of detectors. For scanners designed to sense in the 8 to 14 μm interval, the detector is usually a mercury-cadmium-telluride (HgCdTe) alloy that acts as a photoconductor in response to incoming photons with a range of energies in this thermal region. Efficient operation requires cooling of the detector to temperatures less than 100°K. This is done either with cooling agents, such as liquid nitrogen or helium in appropriate containers, or, for spacecraft, with radiant cooling systems that take advantage of the cold vacuum of outer space. The cooling is necessary to improve the signal-to-noise ratio (S/N) of the detector to a level at which it has a usable signal response. Signal modulations, representing changes in the magnitude of the radiant energy along each scan sweep, are reproduced as amplified electrical signals to be transmitted or stored and subsequently converted into a suitable data medium (e.g., film or magnetic tape). If the ultimate medium is black and white film, the convention is to use light tones or gray levels on a film positive to indicate warmer temperatures and dark tones for cooler temperatures.

To obtain a quantitative expression of radiant temperatures, the detector output must be calibrated. A thermistor or some other controlled temperature output device is located in the scanner and is sampled intermittently at some portion of the scanning cycle when active measurements are not being made. Calibration sources at different temperatures near the extreme expected from the

Figure 9-6. A quasi-natural color rendition of portions of the eastern U.S. and Canada imaged by the CZCS (bands used described in text).

ground are used to provide a correction function. The radiant temperatures reported for a surface are not normally converted to kinetic temperatures because emissivities of the diverse surface materials are not sufficiently well known to permit this determination.

Interpretation of Thermal Images

Other factors must be considered in interpreting thermal imagery. Topography, particularly shape, slope angle and orientation (aspect), is one example. Near surface atmospheric conditions can make a significant contribution to the thermal signatures as measured. Thus, effects of winds, humidity, and other meteorological influences should be removed if more accurate temperatures are required, but this is seldom attempted unless data from ground stations are acquired simultaneously. Electronic noise in the sensor may add significant perturbations to the signal; they are commonly expressed as regular patterns superimposed on the image product. Attitude changes (roll, pitch, yaw) of the air or space platform during flight often lead to pronounced geometrical distortions in the thermal imagery. These are minimized by using attitude control systems (e.g., a gyroscope) to maintain stability by detecting and correcting for variations within the control limits. Systematic distortions, such as tangential or lateral scale changes in directions normal or at angles to the flight line (which compress and curve regular geometrical features), may be removed by methods common to photogrammetry or by computer processing.

The most critical factor in analyzing thermal data is that of knowing the physical and temporal conditions under which the surface is heated. Heat from the Earth's interior tends to flow through the surface at a nearly constant rate, and makes only a small contribution compared with thermal effects from the Sun and sky. Materials at and just below the surface are largely heated during the day by incoming solar radiation and heat transfer from the air; temperatures drop at night primarily by radiative cooling. During a single diurnal (daily) cycle, the near surface layers (usually of unconsolidated soils) experience alternate heating and cooling to depths typically between 50 and 100 cm. Over the annual seasons, small changes in temperature occur to depths of 10 to 20 m in such materials. The daily mean surface temperature is commonly near the mean air temperature. Observed temperature changes are induced mainly by changes in the diurnal solar heating cycle, but seasonal average temperatures and local meteorological conditions also influence the cycle from day to day. The curves shown in Figure 9-7 depict the qualitative changes in radiant temperature during a twenty-four hour cycle, beginning and ending at local midnight, for five generalized classes of materials found at the surface. This temperature range is mainly a function of the thermal history and the physical properties of the materials absorbing and re-emitting the solar radiation. From these curves, one may deduce the expected relative gray levels representing different surface materials classes displayed in thermal images acquired at different times in the diurnal cycle.

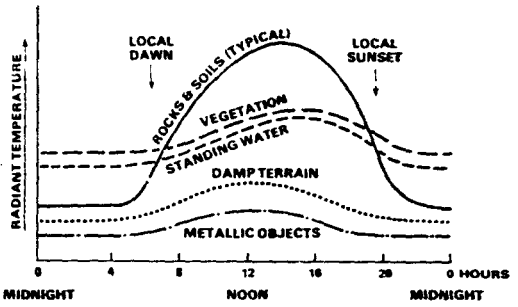

Figure 9-7. Changes in radiant temperatures of 5 surface cover types during a 24-hour thermal cycle. From *Remote Sensing: Principles and Interpretation* by F. F. Sabins, Jr., W. H. Freeman and Company, Copyright © 1978.

#9-14: Keep in mind that, when sensed by a detector, higher radiant temperatures generate larger signals. When transduced to an optical output recorded on film positive, the range of signal magnitudes is expressed by light gray levels (darkest densities on a film negative) for highest temperatures to dark gray for lowest temperatures. However, the gray levels at any one time are relative to the temperature range in the scene at that time of

day. A dark gray at 1300 hours and another at 2100 hours do not necessarily represent the same temperature. Referring to Figure 9-7, predict the relative gray level, in steps of (1) light gray, (2) medium gray, (3) dark gray, (4) blackish, on a positive print for the three classes stated below at the indicated times, using this format:

	Time			
	04:00	10:00	13:00	21:00
Class				
Rock/Sand				
Vegetation				
Water				

#9-15: What time(s) of day is there a maximum thermal contrast (difference in radiant temperatures)? Suggest two convenient times to fly a day-night aircraft mission. What time(s) should be avoided? These are termed thermal crossover times. Why?

Analysis of Aerial Thermal Imagery. You should now know enough to look at a series of thermal images taken at different times by an aircraft-mounted sensor. Examine Figure 9-8. The site shown is a power plant complex on the east bank of the Delaware River south of Philadelphia (you can quite easily locate the small jutty of land containing the site within Figure 2-4B). The images were collected on December 28 and 29, 1979, under clear skies, from an altitude of about 1800 m (5500 ft). Data were collected by Daedalus Enterprises, Inc., of Ann Arbor, Michigan, on their DS-1230 system by using a 1.7 mrad HgCdTe detector with an 8.5 to 11.0 μm response. The tidal conditions at acquisition were:

Top:	Flood tide	08:00 hrs.	Air temp - 9°C
2nd:	Low Tide	05:59 hrs	Air temp - 9°C
3rd:	Ebb Tide	14:20 hrs.	Air temp - 2°C
Bottom:	High Tide	10:59 hrs.	Air temp - 4°C

Each image was processed to emphasize thermal differences in the water; this tends to darken and diminish details on that surface.

#9-16: Which time(s) show the best apparent thermal contrast in the river water? On the land? At what time is the interior land drainage best defined?

#9-17: From Figure 9-7 it is evident that maximum thermal contrast should occur shortly after noon. Compare the ebb and high tide image in Figure 9-8. Which shows greatest contrast? Explain the apparent contradiction.

#9-18: Circle the "hot" area(s) on the power plant site. Which part of the plant would account for this?

#9-19: Can you explain the light colored plume in the river just off the power plant site, which was the main target of the aircraft mission?

#9-20: Speculate on why the plume moves upstream in the top two figures, and more or less downstream in the bottom two (Warning: the low tide case is tricky).

#9-21: Why are air temperatures recorded during the flight?

Another set of thermal images is reproduced in Figure 9-9. All were acquired by the Reconofax IV thermal infrared scanner (9-15 μm range), operated from the NASA NC-130 aircraft. The sites, more specifically identified below, are all in the vicinity of Harrisburg around the Susquehanna River. Relevant conditions for each image are shown in Table 9-2.

Table 9-2

	Date	Time of Day	A/C Altitude (ft)	A/C Speed (mph)	PRT-5 Temperature (°C)
A. Harrisburg, E-W	2/13/74	15:28	15000	340	15
B. Harrisburg, N-S	4/29/74	16:30	12500	240	27.5
C. East of Harrisburg (E-W)	4/29/74	16.50	12900	260	27
D. North of Harrisburg (NE-SW)	2/13/74	17:00	5900	221	14

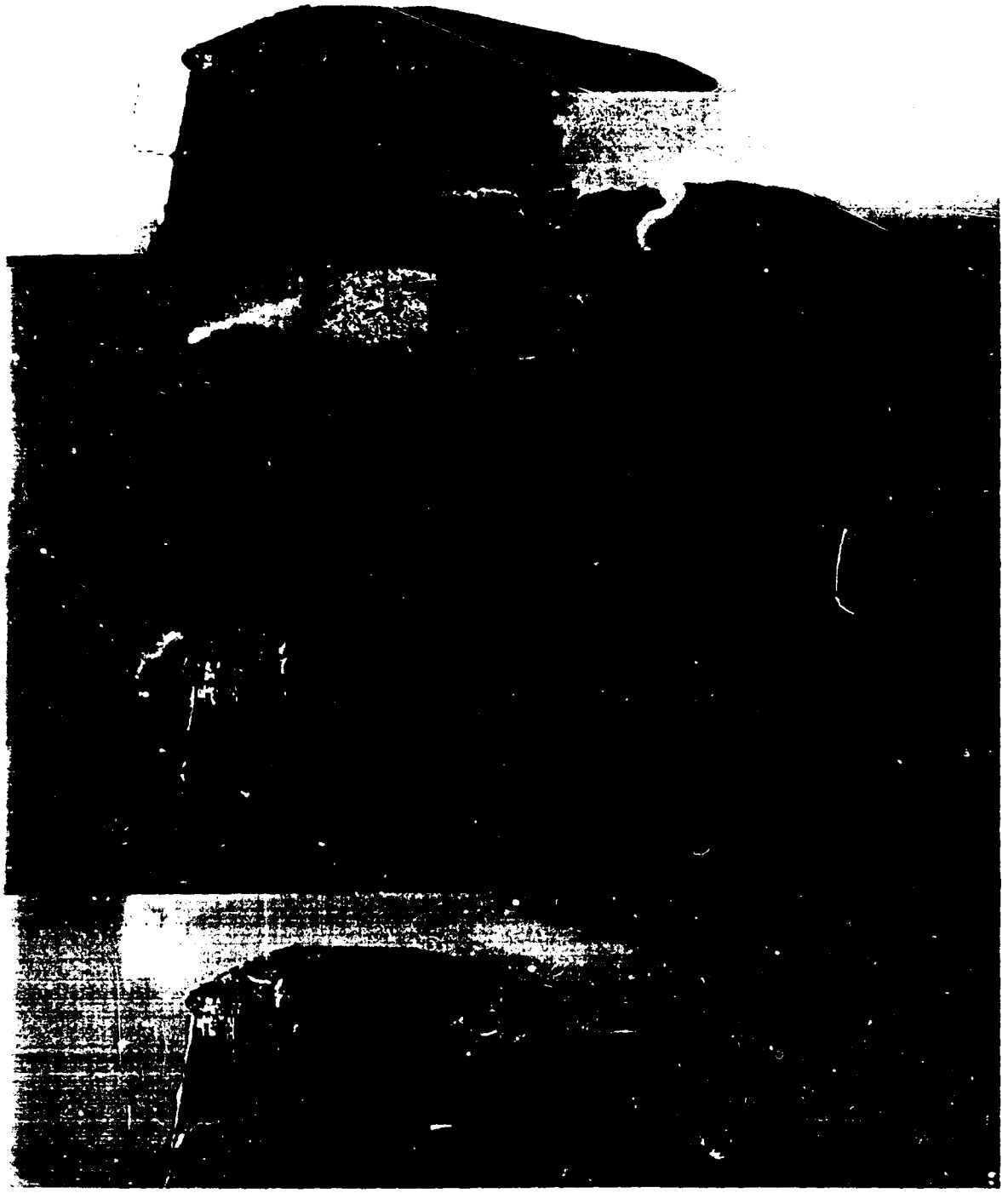

ure 9-8. Power plant on east bank of Delaware River imaged at (top to bottom): 08:00, 05:59, 14:00, and 10:59 hours by the airborne Daedalus DS-1230 thermal IR scanner.

Figure 9-9. Strip images of 4 areas in central Pennsylvania, made from Reconofax IV thermal IR scanner data.

#9-22: Which image(s) seems to be most affected by aircraft distortions?

#9-23: Which image shows the warmest areas overall? Why?

#9-24: On which side of image D is the Sun? How did you reach this conclusion?

#9-25: In B, how do you distinguish barren fields from those with some crop growth?

#9-26: In B and C why do roads have lighter tones than adjacent countryside?

#9-27: In C, some of the stream valleys are marked by darker shades, wider than the channels through which they flow, although such small drainage is dry much of the time. What might cause this effect?

At this point, you should now have enough familiarity with thermal image interpretation to tackle some space imagery. Turn back to the section from pp. 71 through 76 which dealt with the thermal band 8 on Landsat-3. Look again at Figure 2-19A. You will recall that we commented then on the relatively flat appearance of the scene. Now we would say that it lacks thermal contrast. Reread the text for that section, and consider Figure 9-7 once more. Before starting the next paragraph, try to answer #9-28.

#9-28: There are several reasons why the thermal image in Figure 2-19A is so flat. Can you suggest any?

This is a difficult question, which may have stretched you beyond the limits of your experience. There are at least four answers to #9-28, all of which are contributing factors:

1. The scene was imaged at about 09:45h local time. Inspection of Figure 9-7 indicates this time to be close to a crossover time. Radiant temperatures for most ground materials are still similar at this stage in the diurnal cycle and so thermal contrast is low.

2. The NEΔT (p. 37) for the thermal channel is no better than 1.5°K. Surface temperatures at this time of year are low, and the range of radiant temperatures is probably not great (*ca.* 10°K).

3. The number of gray steps available to express these temperature differences is also limited (for digital data, the DN range of 2⁸ [64 levels] is assigned to a temperature range of 80°K).

4. The data have not been converted to a CCT mode and so computer reprocessing has not been performed. Contrast stretching, for example, would no doubt improve image quality (see Figure 2-19B).

Intrinsic Thermal Properties

By now, you must be aware that interpretation of thermal imagery is not a simple matter. In many instances, one's efforts may be confined to looking for patterns of relative temperature differences rather than absolute values, owing to the complex factors that make quantitative determinations difficult. At the risk of adding still more complexities, the following discussion should clarify some aspects of the problems already alluded to.

The temperatures measured by the sensor are indirectly inferred from radiation emanating from the target. This thermal emission is usually only affected by that thickness of the target (e.g., the Earth's surficial layer) located within centimeters to a meter or so from the surface/air interface. The surface ambient environment itself influences the sensed temperature values. A primary objective of the temperature measurements is to infer something about the nature of the target's composition and other physical properties. For a given material, certain characteristic internal properties will play important roles in controlling the temperature of a body at equilibrium with its surroundings. These properties include:

1. Heat Capacity (C): the measure of the increase in energy content (Q) per degree of temperature rise. It is given in units of $cal^{-1}\ cm^{-3}\ °C^{-1}$ and expresses the capability of a material to store heat, measured as the energy, in calories, required to raise a given volume of material by 1°C (at 15°C). A related quantity, specific heat (c), is defined as $c = \frac{C}{\rho}$ where ρ is density (Units: $cal\ g^{-1}\ °C^{-1}$); it is the ratio of heat added in raising the temperature of 1 g of material by 1°C (at 15°C).

2. Thermal conductivity (K): the rate at which heat will pass through a finite thickness of a substance, measured as the calories delivered in 1 s across a 1 cm^2 area through a thickness of 1 cm at a temperature gradient of 1° C (Units: $cal\ cm^{-1}\ s^{-1}\ °C^{-1}$).

3. Thermal Diffusivity (κ): the rate at which the temperature changes between the surface and the interior, or the reverse—a measure of internal heat transfer given by $\kappa = K/c\rho$ (ρ = material density) (Units: $cm^2\ s^{-1}$).

4. Thermal Inertia (P): the resistance of a material to temperature change, indicated by the response during a heating cycle, and defined as $P = (Kc\rho)^{1/2} = \rho c\sqrt{\kappa}$ (Units: $cal\ cm^{-2}\ °C^{-1}\ s^{-1/2}$). P is a measure of heat transfer rate across a boundary between two materials. Materials with high values of P possess a strong resistance to temperature perturbations at a surface boundary and thus show less temperature variation per cycle than those with lower thermal inertia.

#9-29: Calculate the value of thermal inertia P of the following materials, given the associated parametric values K, c, and ρ.

	Stainless Steel	Basalt	Sandy Soil	Water (20°C)*
K	0.030	0.0050	0.0014	0.0014
c	0.120	0.20	0.24	1.0
ρ	7.80	2.8	1.8	1.0
P	———	———	———	———

*Data taken from Chapter 4, p. 83, of volume 1 of *the Manual of Remote Sensing* (1975); see References.

Which of the materials (steel, basalt, soil, or water) will show the largest ΔT or diurnal temperature change?

The interplay among these varying properties combines to affect the rate of heating, total heat exchanged, and temperature profile within the outermost surface layers. In general, a 1-meter layer shows an increase in ground temperature with depth prior to dawn. In the early morning sunlight, the uppermost 10-20 cm of a typical layered material (e.g., a soil) will begin to heat rapidly but the lower profile remains the same. By shortly after high noon the surface reaches its maximum temperature and the lower layers also have experienced warming that decreases with depth. Following sunset, the gradient starts to reverse so that temperatures are lowered at the surface but remain progressively warmer down to some intermediate depth. Regardless of time of day, the temperature profiles converge on a nearly constant value at some depth below 50-100 cm.

The actual surface temperature maximum and minimum depend largely on the extent of buildup of the heat reservoir or storage capacity within the affected layers. For a given material (constant density and albedo), the difference in predawn (low values) and midday (high values) temperatures at each depth horizon down to the stable (convergent) value will increase with increasing conductivity and decreasing specific heat. If the behavior of the surface layers is described by observed thermal inertia changes, these changes can be predicted by varying one thermal property while holding others constant. For the case in which density only is varied (albedo, specific heat, and conductivity remain constant), the effect of increasing the material density (and thereby P, or thermal inertia, as well according to the relation $P = (\rho K c)^{1/2}$) is to require more and more heat to be used in raising the temperature in a given volume of increasingly dense materials. As a result, less heat is transferred (is available) to the lower layers. With increasing density, the total added heat is confined to layers closer to the surface, the maximum temperature reached at midday in the cycle becomes progressively less, and the minimum at night is greater than for less dense materials. Thus, the spread of daily temperature extremes (ΔT) is reduced as density increases and the size (thickness) of the Sun-influenced heat reservoir decreases. The concomitant rise in thermal inertia simply expresses the increased resistance to temperature change. However, if thermal conductivity is increased (albedo, specific heat, and density kept constant), more heat is transferred to greater depth. Less heat is concentrated at the surface and the temperature extremes diminish (lower daytime and higher predawn values). Again, this decrease in ΔT with increasing conductivity is consistent with the corresponding increase in thermal inertia.

Thus, one or more of the intrinsic thermal properties enters into the physical factors that influence diurnal surface temperature variations in the materials in response to solar heating. Consider the four curves plotted in Figure 9-10.[8] The upper left curves in A show temperature variations resulting solely from differences in thermal inertias of materials, with other factors held constant. Note the distinct crossover points. Values of P much higher than 0.05 (as for metals) produce diurnal curves that approach a straight line passing through the crossover points; this is consistent with the statement that materials with high thermal inertias undergo smaller radiant temperature changes during a full heating/cooling cycle. Curves in B show the effects of different reflectances (as albedos); both the maximum and minimum daily temperatures and their differences (ΔT) increase with decreasing albedos that lead to more and more incident solar radiation being absorbed. In C, the curves represent changes resulting from different emissivities; most natural materials have values ranging between 0.8 and 1.0. The curves in D indicate the temperature effect introduced by sky (atmospheric) radiance, a parameter that may be calculated from other data (e.g., PRT-5 temperature measurements) during a thermal scan. It should be obvious from these sets of curves that natural surface materials will show considerable variability in radiant temperature owing to intrinsic differences in total reflectance (albedo), emissivity, and thermal inertia, as well as external meteorological conditions at the time(s) of observation.

[8] Curves published in Pohn, H.A., T.W. Offield, and K. Watson, *Thermal Inertia Mapping from Satellite – Discrimination of Geologic Units in Oman*, J. Research, U.S. Geol. Survey, vol. 2, no. 2, Mar-Apr 1974, p. 148.

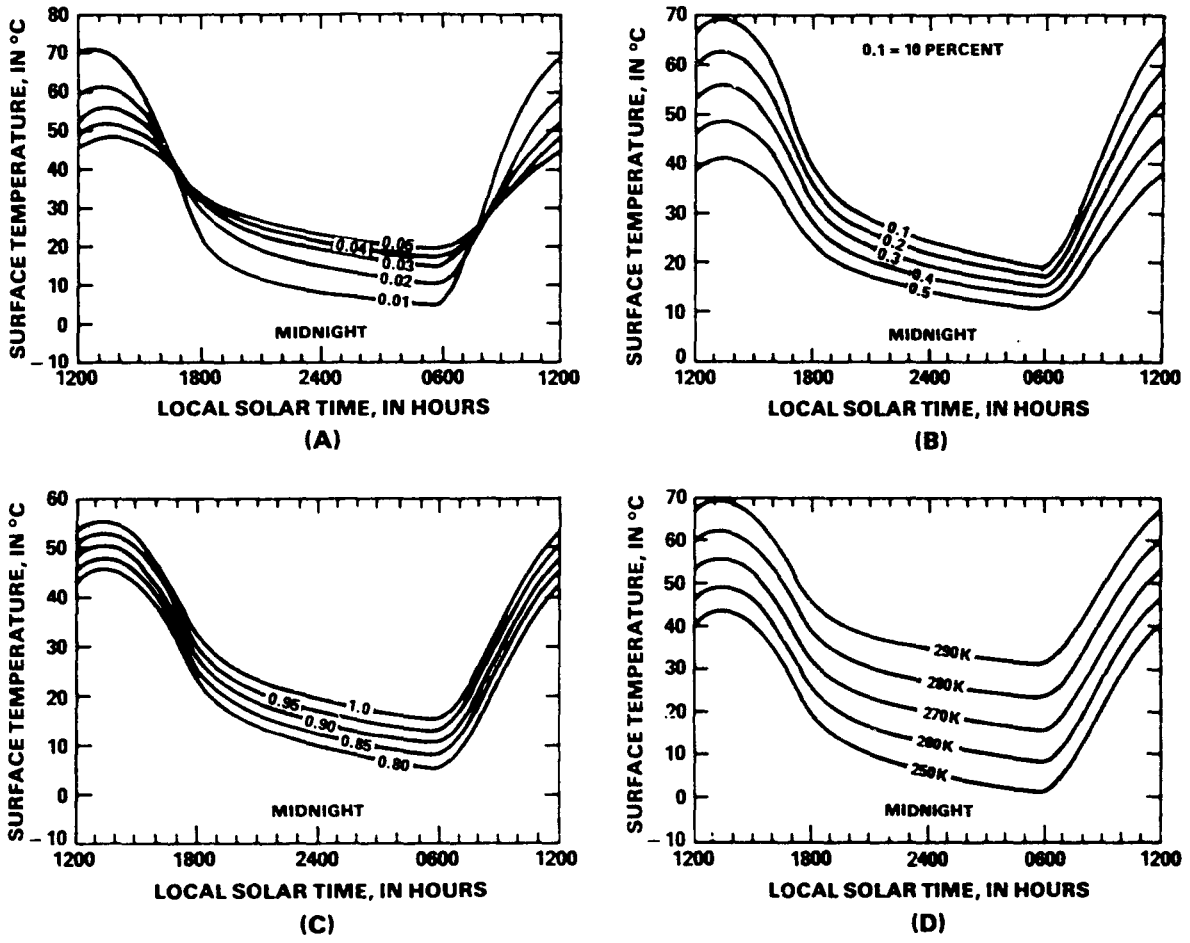

Figure 9-10. Variations of surface temperatures during a 24-hour cycle relative to different: A. Thermal inertias; B. Albedos; C. Emissivities, and D. Sky radiance temperatures.

#9-30: In comparison to a terrain dominated by sandy soil, how will a basalt surface appear (in gray tones) in a positive thermal image acquired during (a) midday? (b) midnight? (Refer to curve A, Figure 9-10; see also #9-29.)

When the same reasoning used in #9-30 is applied to predict gray levels for water and soil, results may be unexpected unless certain factors are considered. P values of 0.038 for water and 0.024 for soil would lead one to expect a smaller temperature range (ΔT) for water, with somewhat warmer temperatures at night and cooler temperatures in the day for water relative to soil (and much of the natural land surface). This is indeed the case, but examination of day and night thermal IR images (see Figures 9-12 and 9-14) shows water to have very dark tones in the day and light tones at night. Water in natural conditions (lakes, rivers, oceans), being nonsolid, tends to experience considerable mixing and thermal "smoothing" by convection and turbulence so that its temperatures do not vary much (in a sense, these water bodies are thermally buffered). Thus, at night, water remains warmer than the land, which cools rapidly by radiative transfer, and during the day water heats up much less than the land and so appears noticeably cooler. (Keep in mind too that the gray tones are usually adjusted or expanded to emphasize land patterns; this tends

to increase contrast in both day and night images.) From a practical standpoint, natural water acts as though it has higher thermal inertia than the 0.038 obtained for "laboratory" water.

Thermal inertia can be a diagnostic property for natural materials, leading under favorable circumstances to their identification. Values of thermal inertia for rocks and soils range between 0.009 for loose porous materials to 0.075 - 0.085 for dense materials. In theory, thermal inertial values can best be estimated by remote sensors if early morning and early afternoon temperatures (maximum thermal contrast) are determined, and the rate of solar irradiation absorbed by a material at the surface is also measured. Absorption rate (as power) may be approximated by the expression S (1 - a), where S is the solar flux incident at a point on the Earth's surface and a is the apparent albedo at that point. (Both S and a will vary with latitude, solar declination, and other factors).[9]

The Heat Capacity Mapping Mission

NASA has designed and launched a sensor system capable of measuring temperatures from which the apparent thermal inertia (ATI) of materials at different points on the global surface may be calculated. The term "apparent" is a qualifier to indicate that true values are not obtainable unless the influence of atmospheric processes and other factors are taken into account in the calculations.

The sensor, a modified version of the SCMR on Nimbus-5, has been named the Heat Capacity Mapping Radiometer (HCMR). It was the only sensor in the payload of the Heat Capacity Mapping Mission (HCMM)[10] satellite, launched on April 26, 1978, as the first of a low cost series of Applications Explorer Missions (AEM). During daylight operations, one of the two channels of the HCMR measures visible-reflected IR radiation (0.5 to 1.1 μm), while the other measures thermal IR radiation (10.5 to 12.5 μm). This thermal channel is used again to measure nighttime temperatures over approximately the same areas. From a near-polar Sun synchronous retrograde orbit at *ca.* 620 km (385 miles), the satellite passes over the Equator in its ascending node at *ca.* 2:00 p.m. (local time). In the mid-latitude regions (where most HCMM investigations are located), the day-night crossing times cluster around 1:30 p.m. and 2:30 a.m.[11] Opposing day-night orbital tracks are symmetrically inclined relative to longitudinal lines by 11.5° at the Equator; day-night pairs of scenes cover the same ground areas at an interval of twelve hours for latitudes from 0 to 20° and 35 and 78°, and thirty-six hours for latitudes between 20 and 35°. This orbital configuration permits acquisition of thermal data during half of a single diurnal heating cycle (twelve hours) for some regions and one and a half cycles (thirty-six hours) for others. Over most of the United States, successive day-night passes separated by approximately 12 hours produce diamond-shaped track patterns (Figure 9-11). A given orbital track is repeated in a sixteen-day cycle, but adjacent coverage occurs on a five-day cycle.

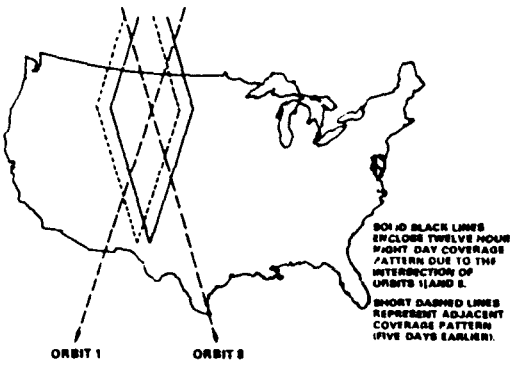

Figure 9-11. Coverage pattern of HCMM orbits over U.S. for the indicated intervals.

Under these orbital conditions, the swath width is 715 km (445 miles). Spatial resolution for the thermal channel is nominally 600 m (1950 ft) at nadir, about one-third as good as that prescribed

[9] The incoming solar flux at the outer limit of the atmosphere, termed the solar constant, is approximately 2.0 cal cm^{-2} min^{-1}.

[10] The term "heat capacity" in the satellite's official designation is a misnomer, in that this property is not directly measured (although it is related to the variable c in the function that defines true thermal inertia, P).

[11] Owing to small inclination errors, the local time of crossing drifts by about forty-five minutes earlier per year. The HCMM orbit was lowered in February 1980 to reverse this drift.

for band 8 of Landsat-3. However, the maximum thermal sensitivity (NEΔT) for the HCMR is about 0.3°C at 280°K, or approximately five times better than for the Landsat-3 thermal band.

Thus, the HCMR provides data on reflected radiances, from which apparent albedos may be calculated, and on day and night radiant (equivalent blackbody) temperatures, from which a temperature difference ΔT is obtained. These data are inputs in determining the apparent thermal inertia, according to the function $ATI = NC(1-a)/(T_{Day} - T_{Night})$, where N is a scaling factor (set at 1000) that brings ATI into the range 0 to 255 (8 bits), a is the apparent albedo, and C is a constant related to the solar flux. C itself varies with latitude, θ, (0 to 90° N and S) and solar declination, ϕ, (from -23.5° to +23.5°), and thus compensates for seasonal variations in solar insolation.[12] Images can be made, pixel by pixel, from any of the direct (day reflected and thermal or night thermal radiances) or derived (ΔT; ATI) measurements.

#9-31: Calculate ATI for the following parameters:

$N = 1000$,
$C = 1.5165$ (for $\theta = 45°$, $\phi = +20°$),
$a = 0.20$,
$T_{Day} = 310°K$,
$T_{Night} = 280°K$.

The ATI of a pixel representing the Earth's surface has a different numerical value from that of the true thermal inertia, P, of a material. The quantitative relation between ATI and P has not yet been established by HCMM investigation teams. Generally, the ATI of a pixel-sized surface area will be a weighted average (mix) of ATI's of each of several component materials within the area.

HCMM data sets used to construct the Day-VIS, Day-IR, and Night-IR images must be correlated geometrically and adjusted for other errors or variations. To obtain ΔT values, the day and night thermal data are carefully registered, pixel by pixel, through an overlay procedure. Pixels from two separate passes covering the same surface area must be carefully registered. The pixel shapes themselves do not coincide even when properly superimposed, because of the different day and night directions of passage due to the offset from true polar inclination: the day pass moves southeast to northwest, whereas the night pass (twelve or thirty-six hours later - not the night segment of the same orbit) goes from northeast to southwest.

#9-32: Assuming square pixels, make a simple sketch that shows the misfit of a pair of day and night pixels covering the same immediate area in the two successive (twelve hours) ground tracks, which are each inclined at 11.5° from a longitudinal line. (Hint: Draw a single vertical line in the sketch to plot the center point of each pixel at the same spot on the line. For convenience, mark the top side of the day pixel and the bottom of the night pixel with a heavier pencil line.)

The complex geometrical nature of the digital data necessitates approximate registration (by a technician using control points) prior to computer processing; this is the best way to effect precise registration of the day and night data. The computer is also essential in applying a thermal model to these data, point by point, to calculate the apparent thermal inertia from the temperature difference and albedo values.

The temperatures measured by the sensor depend on the relative contributions of both surface and air temperatures. Temperature changes are brought about primarily by solar heating and cooling. Other factors that influence the sensor measurements, and hence the values of the parameters in the ATI equation, are:

1. Emissivities of the surface materials,
2. Bidirectional reflectances of these materials,
3. Geothermal (internal) heat flow,
4. Topographic irregularities,
5. Evaporative cooling at the surface (water; vegetation) and/or heat released by dew formation (latent heat changes),
6. Heat transfer effects from convection and conduction in the surficial layers and the atmosphere (sensible heat changes),
7. Absorption and re-emission of thermal energy by aerosols and water vapor,
8. Cloud cover history (during heating cycle),

[12] For details, see the *Heat Capacity Mapping Mission Data Users Handbook*, November 1979, available from the Mission Utilization Office (Code 902), Goddard Space Flight Center.

9. Temperature profile of the atmosphere,
10. Surface wind effects.

Some of these factors have fixed or constant effects on the temperatures; others vary with each pass. It may be possible to correct for the influence of some of the variable factors but this is not done routinely. Measurements are made usually at isolated individual points in a scene and extrapolation to the general scene has limited value.

The HCMM program is a research effort oriented towards "proof of concept." The main objectives are to develop a systematic methodology for producing regional (small-scale) thermal inertia maps of the Earth's surface and to verify that such information may be put to practical uses. Proposed applications include (1) discriminating rock types; (2) mapping gross variations in soil moisture; (3) measuring plant canopy temperatures related to evapotranspiration and stress effects; (4) noting temperature changes in snow fields to predict runoff; (5) detecting natural and man-made thermal effluents; and (6) monitoring effects and changes of urban heat islands.

Much of the eastern United States from North Carolina to upper New York State was imaged from the HCMM satellite, under conditions of sparse cloud cover, on May 11, 1978. The midday thermal IR image is shown in Figure 9-12. This depicts not only land and cloud patterns, but also some of the thermal differences related in part to the Gulf Stream, in the open Atlantic Ocean. The temperature differences may be accentuated by producing a color-coded density-sliced map, as presented in Figure 9-13 for the May 11, 1978 day IR image. Although the map is not calibrated for actual temperatures, the relative temperature increases from cooler to warmer proceed from black, purple, and blue, through green, brown, orange, red and white.

#9-33: Where are the clouds? What colors are used to depict them?

#9-34: What color denotes the Gulf Stream? Is it warmer or colder than its surrounding waters? Why?

#9-35. Note the string of light-toned (whitish) spots trending to the southeast near the lower left corner of Figure 9-12. What do these spots represent?

#9-36: Locate the position of Baltimore, Philadelphia and New York in both figures. What color and gray tone characterize these? Why are they warmer than adjacent rural areas?

A thermal image of the same general area obtained during a nighttime pass on June 11, 1978 is shown in Figure 9-14.

#9-37: Locate the New York–New Jersey and the Harrisburg scenes within this pair of images. Describe the gray tones or levels in the day and night images for the following features: (1) Atlantic Ocean; (2) Susquehanna River; (3) Baltimore and Philadelphia; (4) Pine Barrens (N.J.); (5) Blue Mountain and other ridges; (6) Valleys between ridges; (7) Agricultural land in Delmarva Peninsula.

#9-38: What large (transient) feature present in the May 11 daytime thermal IR image is absent in the June 11 nighttime image?

#9-39: What thermal characteristics of lakes enable them to be recognized in the two scenes?

#9-40: How do large metropolitan areas differ from lakes in their response to the thermal heating cycle?

#9-41: What gray (tone) levels characterize the area of Pennsylvania occupied by the anthracite coal belt and associated surface wastes in the daytime thermal? Nighttime thermal?

#9-42: Can you explain the apparent high temperatures of this coal belt in the day imagery? (Hint: think blackbody.) Considering also the nighttime response of this belt, make a qualitative judgment about the thermal inertia of coal (relatively high or low for rock materials).

#9-43: Note a very bright area in the day image (but noticeably dark in the night image) south of the Albemarle Sound in North Carolina (near bottom center). This used to be a rather heavily forested and cultivated region, but field

information shows several large sections of recently cleared land (also evident in Landsat imagery), exposing dark soils. Explain the thermal behavior of this area in the light of this information.

#9-44: Parts of the Valley and Ridge (folded Appalachians) are marked or outlined by dark fringes in the day thermal IR image. The areas that appear to correspond to these are lighter (brighter or warmer) in the night IR image. Speculate on the explanation of this observation (Hint: consider both topography and surface cover.)

#9-45: The valleys between ridges seem brighter in the day and darker at night over most of the folded Appalachians from the Piedmont to the Allegheny Front. Again, speculate on the reason.

#9-46: Note the tone patterns along the south end of Lake Erie (upper left corner) in the nighttime image. What is the cause of this?

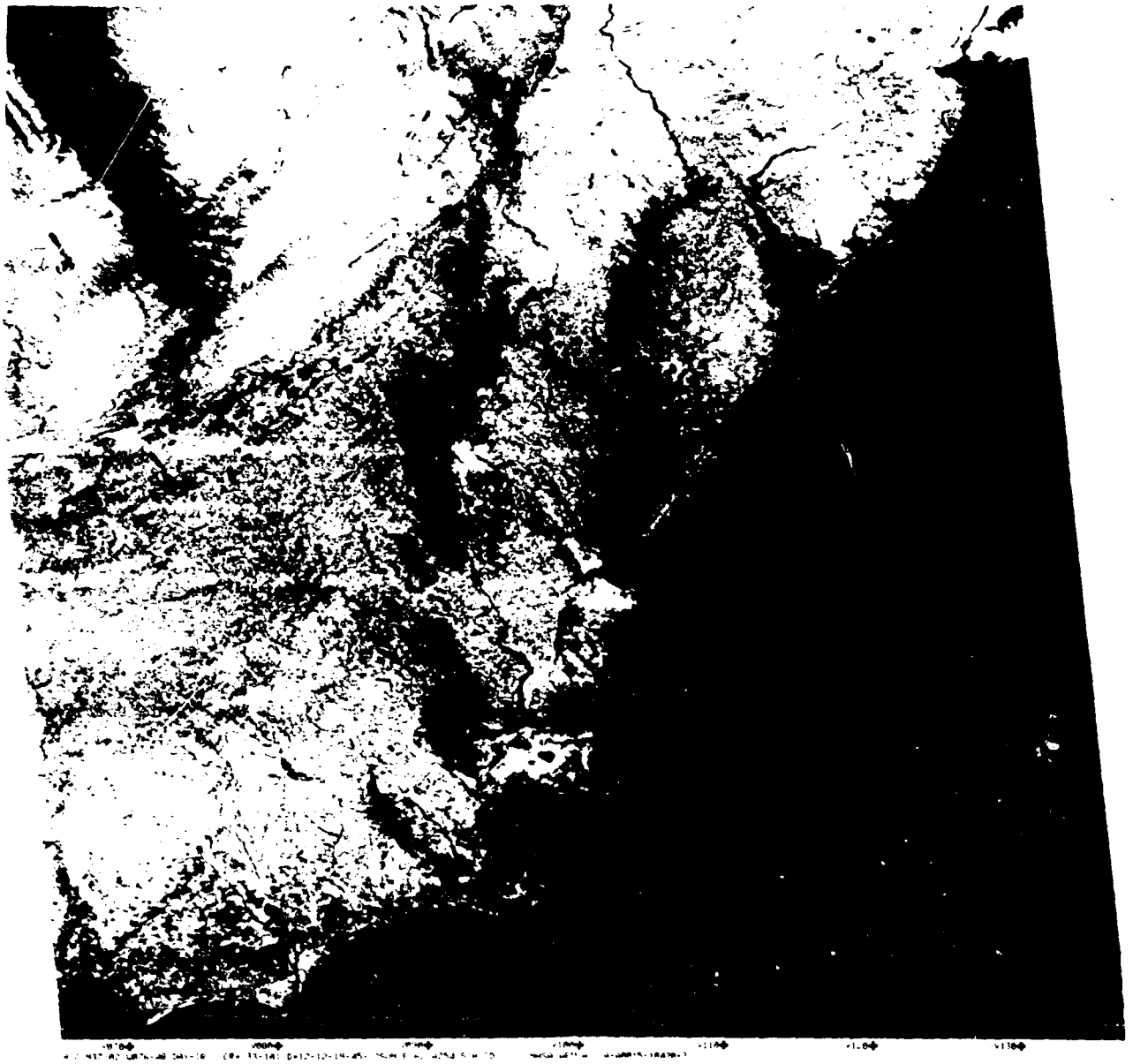

Figure 9-12. Day IR image of part of eastern U. S. taken by HCMM on May 11, 1978.

Figure 9-13. The scene in Figure 9-12, extended to the Great Lakes, in which gray levels representing temperatures have been color-coded from black (coolest) to white (warmest) (see text).

Figure 9-14. Night IR image obtained by HCMM on June 11, 1978 over much of the same region of the eastern U.S. as shown in Figure 9-13.

Ideally, the apparent thermal inertia values for an HCMM scene should be calculated from day and night temperature readings taken as close together in time (12 to 36 hours apart) as practical. This was not accomplished during the HCMM mission for the scene with which we have been working. In the spring of 1978, the first usable night thermal IR image after May 11 was obtained one month later (Figure 9-14). The extent of diurnal heating had changed significantly by then as early summer neared. Nevertheless, the ΔT image (Figure 9-15) obtained by subtracting the June 11 night thermal IR pixel values from the May 11 day thermal values provides a good approximation of the diurnal temperature history that would have transpired on either date.

#9-47: Move back and forth to Figures 9-12 and 9-14, and also to Figure 9-15. How is the cloud bank in the day IR image (slanting southeast from the upper left corner of Figure 9-12) displayed (as a gray level) in the ΔT image? How do the clouds in the night IR image (very dark areas along the lower left margin of Figure 9-14) show up in the ΔT image? How do the bright fringing areas along the ridges, as seen in the night IR image (see #9-44), appear in the ΔT image? How does the water in the Atlantic Ocean and adjacent bays appear in the ΔT image? Explain why the ΔT values for these large bodies of water should be so low, and hence are expressed in black tones (Hint: Review, p. 351). Formulate a simple chart for predicting the gray levels in a ΔT image, based on day and night thermal IR patterns.

The apparent thermal inertia (ATI) image derived from the Day-VIS and Day-IR data from May 11 and Night-IR data from June 11, 1978 passes is shown in Figure 9-16. This and the ΔT images were generated at NASA Goddard's IPF using special processing algorithms based on JPL's VICAR program. The day and night images are registered in steps involving rotation, tie-point correlation, and "rubber sheet" stretching. In the resulting ATI image, most land features appear in dark to medium gray tones corresponding to low to moderate ATI values. Since water has a low albedo (somewhat higher if silty), the $(1 - a)$ term approaches 1.0, giving rise, along with the small ΔT in the denominator of the ATI equation, to apparent thermal inertias likely to be much higher than most land materials. Scattered clouds in the Day-IR image are unlikely to show up in the same places as in the Night-IR image and hence ΔT's for the areas subtended by clouds do not represent a valid diurnal thermal history of the surface. In an ATI image, daytime clouds appear in whitish tones and nighttime in dark tones. Because the temperatures of clouds during the day are lower than the temperatures of underlying cloud-free surfaces at night, the $T_{Day} - T_{Night}$ or ΔT term will be negative. In the calculations, a negative denominator is treated as zero, producing an infinitely large ATI that is assigned a white tone. Conversely, at night the cloud temperatures are considerably lower than corresponding cloud-free surfaces during the day. This yields a large ΔT term that in turn leads to small ATI values shown as dark gray levels. In the case of both day and night clouds superimposed on the same area, ΔT is again small but positive and ATI tones are light. Note that the $1 - a$ term (a is large for clouds) is not critical to the results but does affect the actual ATI values.

Several HCMM scenes acquired in November 1978 over the eastern United States display exceptional image quality owing to a favorable conjunction of viewing conditions and subsequent data reprocessing. Consider the day visible and day thermal IR images taken on November 17, 1979 (Figures 9-17A and B).

#9-48: Compare the day visible (Day-VIS) scene with the December 10, 1976 Landsat band 7 scene (Figure 4-9A). Allowing for some distortion in the HCMM image, comment on the ability of the HCMM scene relative to Landsat in picking out: (a) Harrisburg and Lancaster; (b) The structural grain in the Piedmont; (c) The fold patterns in the Valley and Ridge Province; (d) Tributaries to the Susquehanna River.

#9-49: There are several very dark areas in the center and top of the day IR image. Look at the equivalent areas in the Day-VIS scene. What might cause this dark area pattern? Note also that the general tone of the land surface is distinctly darker in the northwest region beyond the general southern boundary of the folded Appalacians (Blue Mountain). Offer a plausible explanation for this.

Figure 9-15. Day/night temperature difference (ΔT) image made from May and June 1978 HCMM data. Larger ΔT's are shown in lighter shades of gray.

ORIGINAL PAGE
BLACK AND WHITE PHOTOGRAPH

Figure 9-16. An experimental version of an Apparent Thermal Inertia (ATI) image developed from May and June 1978 HCMM data. A high value for ATI is depicted in light tones, low values in dark tones.

#9-50: Locate Pittsburgh in the day thermal IR image. What reveals its presence? Identify the broad lighter gray-toned patch lying along a diagonal about 2.5 cm in from the upper left-hand corner of the scene. Compare the pattern of "hot spots" (light gray) in the Baltimore area as seen in the HCMM image and the computer-enhanced subscene made from the Landsat-3 thermal channel, band 8 (Figure 2-20A). Next, examine the night thermal IR HCMM image obtained on November 2, 1978 (Figure 9-18).

#9-51: Is there any evidence of a counterpart to the very dark areas observed in the November 17, 1978 day thermal IR scene? There are several broad, blackish patches in areas southwest of Pittsburgh and, again, southwest of Scranton, Pa. What might these be? Describe the difference in appear-

Figure 9-17A. A day-VIS (visible) HCMM image over a section of the eastern U.S. November 17, 1979.

ance between Piedmont and Coastal Plains terrain.

#9-52: HCMM is being used to search for large fault zones, especially where these are more permeable and concentrate groundwater. Describe the appearance of possible faults or linear features in the dissected Appalachian Plateau in northern Pennsylvania and southern New York from the Buffalo area eastward through the Catskill Mountains region.

Because HCMM data are digitized, enhancements comparable to those performed on Landsat scenes will give rise to notable improvements in image quality. Examples of this treatment for the regions from Harrisburg and Philadelphia northward to the Great Lakes are shown in Figures 9-19A and B. The scene was acquired September 26,

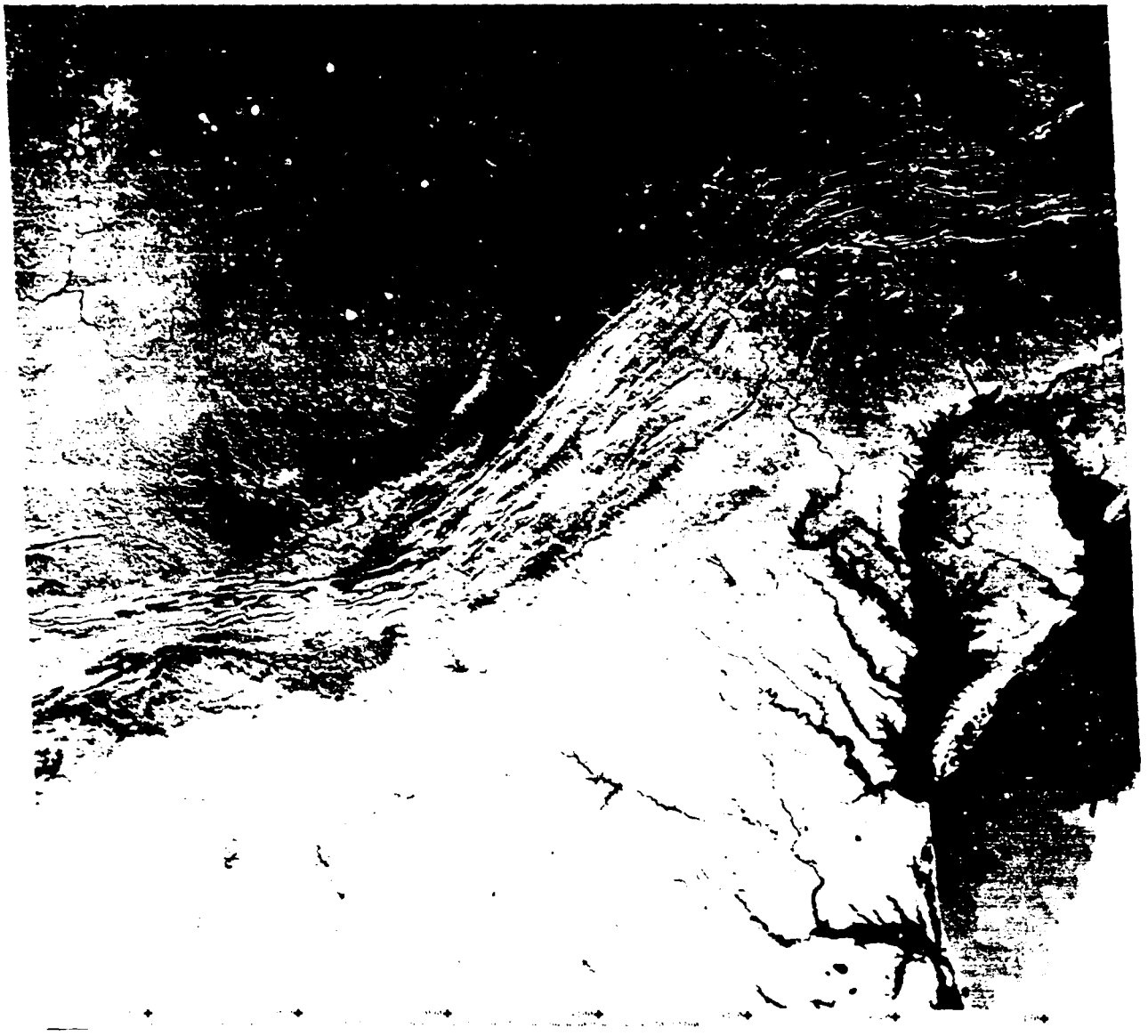

Figure 9-17B. The day IR HCMM image for the November 17, 1979 eastern U.S. scene.

Figure 9-18. A night IR image acquired by HCMM on November 2, 1978 over a part of the western U.S.

1978. In A, a Day-VIS enhancement, the topographic "grain" from the Coastal Plains through the Appalachian Mountains and Allegheny Plateau to the glaciated surfaces in New York and Pennsylvania is strongly expressed despite the small scale of the print. In the Day IR image, the very dark tones associated with the ridges in the fold belt have been interpreted by H. A. Pohn and others of the U.S. Geological Survey as related to the influence of sandstone units (such as the Tuscarora Formation) and other rock types; the thinner soils overlying these types, together with much denser stands of forests, probably combine to bring about a reduction in radiant temperatures. To the north a large, more or less continuous, pattern of dark tones correlates in part with the distribution of rocks, soils, and trees within topographic highs underlain by synclinal folds.

#9-53: Account for certain of the very light-toned patterns in the Day-IR image.

A digital tape containing night thermal data for the HCMM scene from the June 11, 1978 pass was processed on IDIMS, primarily to improve the contrast between cooler (darker-toned) and warmer (lighter-toned) areas. An enlargement of the area around Harrisburg and another in the anthracite coal belt are shown in Figures 9-19C and D.

#9-54: Does the metropolitan area of Harrisburg stand out in the night IR image (Figure 9-19C) (compare with the classification in Figure 5-33)? Comment on your observation.

#9-55: With what is the bright area near the lower left edge of Figure 9-19C associated?

#9-56: Looking next at Figure 9-19D, where are the most likely areas of coal waste dumping? (Indicate by gray level).

From such observations of HCMM imagery, a set of criteria relating gray levels to emittances from surface materials and classes can be extracted and organized into a table similar to that devised for identification of classes by their relative reflectances in different bands (see Table 3-3). Table 9-3 has been prepared from correlation of gray levels in HCMM images with corresponding ground features, coupled with predicted relative levels at 0200 and 1400 hours for pairs of the classes plotted in Figure 9-7. Assignment of broad gray level ranges in this table follows a rather subjective procedure to which only qualitative significance should be attached. Most of the variables listed on page have not been compensated for, or even considered, and the images used tend to vary somewhat in photo density of equivalent steps in the gray scale. Still, this chart provides a practical guide to a rough-cut identification of many common surface classes present in HCMM images.

Computer processing is now being used in novel and eye-catching ways to display thermal data from HCMM. For this purpose, Rupert Haydn, an HCMM Principal Investigator from West Germany, has modified the technique described on p. 292 that draws upon digitized topographical data to produce a Landsat stereo pair. In this modification either Day-IR or Night-IR temperature values can, in effect, be considered as analogs to topographical elevation data in the sense that they could, if desired, be contoured to generate a map of temperature variations as distributed on a spatial or geographical framework such as a Landsat scene. The end product is a temperature-based stereo pair made by merging a single Landsat image with HCMM data. Under a stereoscope, the pairing gives rise to a 3-D stereo effect much like that evident in the Harrisburg Landsat image pair found in the back pocket of this workbook. (See p. 292 for a general description of how that pair was created; a similar technique is used to generate the HCMM stereo effect by registering subdivided HCMM pixels to aggregated Landsat pixels and shifting the HCMM pixels in a pseudo-parallax manner in proportion to differences in temperature [or equivalent DN values].) Haydn has generously produced a stereo pair from the July 14, 1977 Landsat scene (Figure 4-11) registered to the June 11, 1978 HCMM Night-IR data (Figure 9-14) for inclusion (also in the back pocket) in the workbook. Examine this stereoscopically and compare the variations in apparent relief with the relief expressed in the Landsat topographical stereo pair. You will note at once that, although there appears to be some visual correlation between the undulating temperature surface that you see and the topography (as viewed under the stereoscope or as deduced from landforms patterns) along the moun-

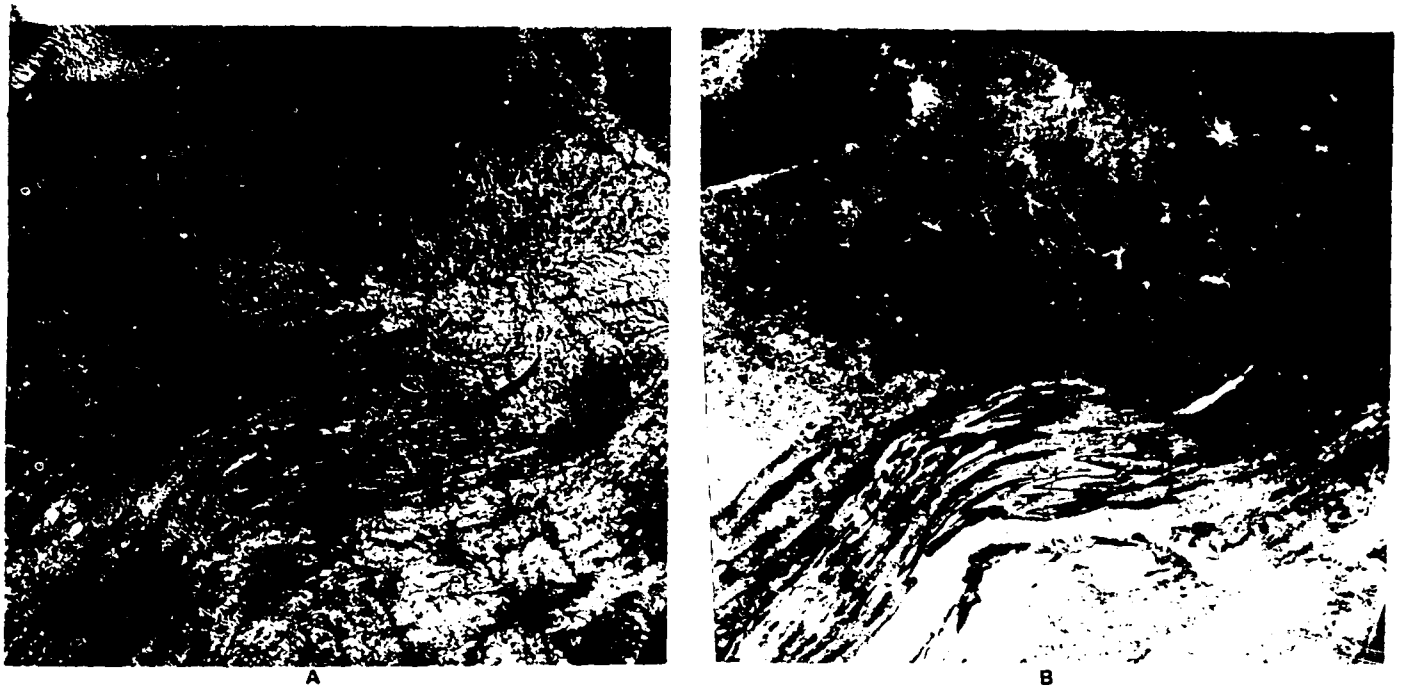

A B

Figure 9-19A&B. Computer-enhanced HCMM images obtained September 26, 1978 over the eastern U.S. from Philadelphia to Lake Ontario. Processing was done by the U.S. Geological Survey, Denver. A. Day-VIS; B. Day-IR.

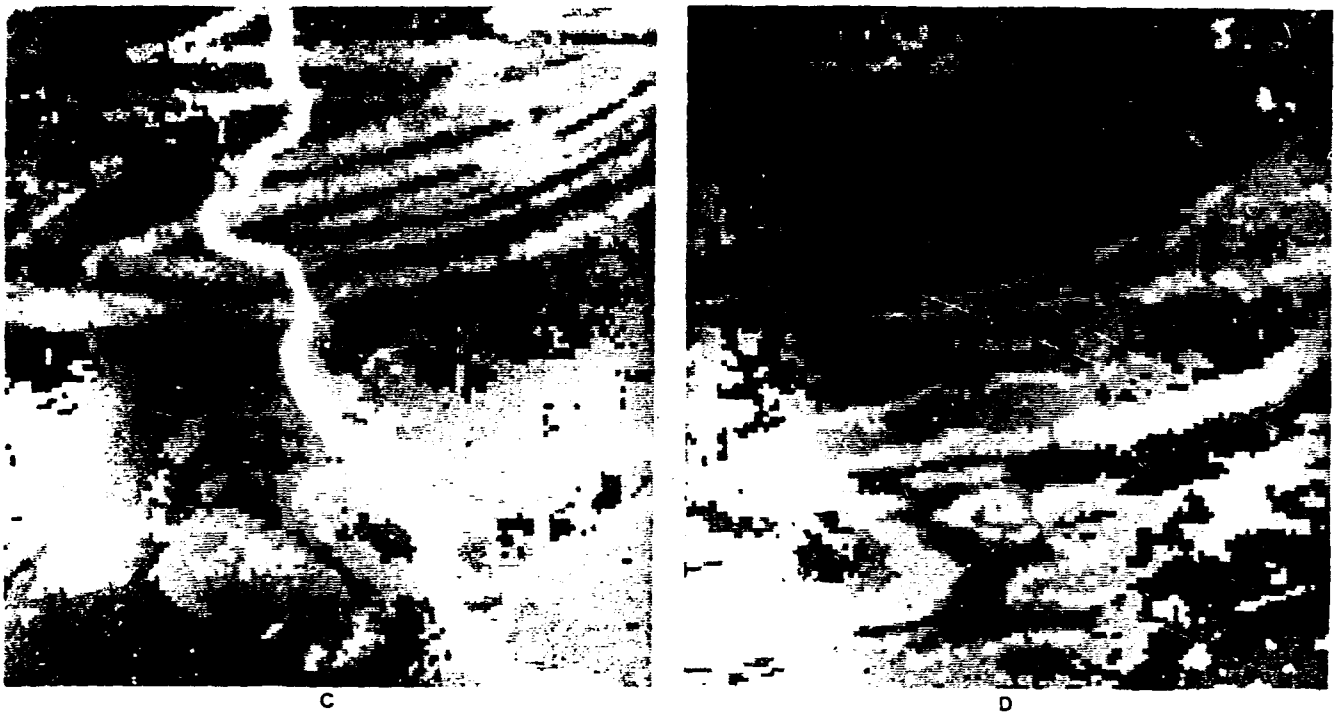

C D

Figure 9-19C&D. Computer-produced enlargements of the June 11, 1978 HCMM night IR scene around C. Harrisburg, and D. Anthracite belt to the east.

Table 9-3
Classification Based on Gray Levels in HCMM Images

Class/Feature	Day-VIS	Day-IR	Night-IR	ΔT	ATI
Rock:					
Basalt	VD	L	M-L	MD	L-VL
Granite	M-L	M	L-M	MD-M	M-L
Soil/Alluvium	M-L	L-VL	MD-M	L-VL	MD-M
Desert Sand	L-VL	L	MD-L	ML-L	M-MD
Vegetated Surfaces[1]	MD-M	MD-L	M-L	MD-L	L-MD
Field Crops	MD-D	MD-VL	MD-M	M-L	MD
Pure Standing Water	D	D-MD	VL	D	VL
Silty Water[2]	MD-L	MD-M	M-L	MD	L
Damp Soil	MD-M	M-L	MD	M-L	MD-D
Cities	D-M	M-VL	MD-L	MD-M	L-M
Metallic Objects	L-VL	D	D	D	VL
Snow	VL	D	D	D	VL
Clouds	VL	D	D	D (day) VL (night)	VL D
Lineaments	D	MD	D	MD	L
Nonvegetated Sheltered Valleys	MD-M	M-L	L	M	M
Vegetated Slopes					
Sun-facing	M	L-VL	M-L	M	M
Shaded	MD	MD	MD	MD	L

KEY:[3]

Gray Level	Symbol
Very Light	VL
Light	L
Medium	M
Medium Dark	MD
Dark	D
Very Dark	VD

T°, ΔT, ATI ↑

[1] Evergreen trees tend to have less temperature variation than deciduous trees.

[2] Gray level variations may result from differences in silt content and/or differences in ΔT of unmixed water bodies (e.g., warmer river water emptying into cooler marine water).

[3] These qualitative gray level values are relative such that dissimilar levels can correspond to similar temperatures, e.g., the levels of D and VL for water express the condition (small absolute ΔT) in which the day and night IR water signatures show up as relatively cooler and warmer with respect to land temperatures.

tain ridges and elsewhere, more commonly there are strong disparities between what you expect and what actually appears. Thus, in some places the Susquehanna and other rivers tend to run "up and down hill" with reference to the HCMM stereo surface but in general tend to tower over their surroundings (as do lakes) (why?), as dramatically exemplified around Harrisburg. This type of "quasi-stereo" image, using some varying surficial parameter other than elevations, is being developed from other isopleth maps, such as contoured gravity or magnetic data plots, and can be integrated with Landsat imagery to provide startling but frequently useful visual displays (see p.400). Little experience in interpreting such data merges has yet been reported but mineral and petroleum exploration companies, in particular, are showing considerable interest in learning how to apply these unusual products.

RADAR SYSTEMS

We shall switch our attention now to the one *active* remote sensor to be treated in some detail in this workbook. *Radar* is an acronym for Radio Detection and Ranging. Radar, then, operates in the microwave region of the EM spectrum, specifically in the frequency interval from 40,000 to 300 MHz, which extends just into the higher frequency end of the radio (broadcast) region. Commonly used frequencies in megahertz (MHz) and their corresponding wavelengths in centimeters are specified by a band nomenclature, as follows: Ka Band: 40,000-26,500 MHz (0.8 to 1.1 cm); K band: 26,500-18,000 (1.1 to 1.7 cm); X band: 12,500-8000 (2.4 to 3.8 cm); and L band: 2000-1000 (15.0 to 30.0 cm).

Principles Underlying Radar

Unlike the other sensors which passively sense radiation from targets illuminated by the Sun or thermal sources, radar provides its own illumination (hence, active) as bursts or pulses of energy that are directed to the target and then sensed upon return. Thus a radar system is a ranging device that measures round trip travel times and signal modification of a directed beam of pulses over specific distances. In this way, the directional location and separation distances from radar to reflecting target, as well as information about target shape and certain diagnostic physical properties, may be determined by the system. By supplying its own illumination, radar can function during both day and night and, for some wavelengths, without significant interference from adverse atmospheric conditions. These characteristics prompted development of radar in World War II as a dynamic range finder for tracking aircraft and ships; both ground (fixed) and airborne (mobile) radar systems are extensively used today for navigation and air traffic control.

A radar system consists of (1) a pulse generator that presents time pulses of microwave/radio energy to (2) a transmitter, then through (3) a duplexer, to (4) an antenna that shapes and focuses the pulse stream as transmitted and then picks up returned pulses, sent to (5) a receiver, capable of amplifying the weakened signals, which are then carried to (6) a real-time display device (typically a cathode-ray tube or CRT) and/or recorded on tape or film. The duplexer serves to separate the outgoing and returned pulses (eliminate their mutual interferences) by functioning as an on-off switch to block out reception during transmission, and vice versa. The antenna on a ground system is generally a parabolic "dish." Antennae for radars flown on aircraft for survey (remote sensing) purposes are normally mounted on the underside and direct their beams to the side of the plane, that is, normal to the flight path, during operation. This mode of operation is implied by the acronym SLAR, for Side Looking Airborne Radar. A real aperture SLAR system is characterized by a long (5-6 m) antenna

usually shaped as a section of a cylinder wall. This type generates a narrow, focused beam of noncoherent pulses and utilizes its length to obtain the desired resolution (related to angular beamwidth) in the azimuthal (flight line) direction. A second type of system, synthetic aperture radar (SAR), uses an antenna of much smaller physical dimensions, which sends out a relatively broad beam. This system depends on the Doppler effect[13] to determine azimuth resolution. As the coherent pulses transmitted from the radar unit reflect from the ground to the advancing aircraft, the target experiences an apparent (relative) motion. This motion results in changing frequencies, which give rise to variations in phase and amplitude in the returned pulses. These data are recorded for later processing (by optical or digital methods), in which the moderated pulses are analyzed and recombined to synthesize the signals obtained from a narrow beam (real aperture) system. The SAR beam, however, retains a constant width (resolution) in the azimuth direction, in contrast to the real aperture system, which experiences decreasing resolution with distance outward.

Consider now the information presented in Figure 9-20. The upper half (A) depicts a strip of surface being scanned by the radar beam. The aircraft moves at some altitude above the terrain in an *azimuth direction* while the pulses spread outward in the *range (look) direction*. Any given line-of-sight from radar to a ground point within the terrain strip defines the *slant range* to that point. The point closest to the aircraft flight trace establishes the *near range;* the pulsed point at the greatest distance normal to the flight path fixes the *far range*. The distance between the aircraft nadir point and any ground (target) point is referred to as the *ground range* to that point. The angle between a horizontal plane and the slant range direction defines the *depression angle* for any target point within the surface strip. The depression angle decreases outward from the near range to the far range limit. Pulse travel times increase outward between these limits. The duration of a single pulse (in microseconds), as produced by the generator, establishes the resolution along the range or look direction. Range resolution (the minimum distance between two reflecting points along the range direction at which these points may be sensed as separate and distinct) increases outward for a given pulse duration since it varies inversely with depression angle.

The variations in pulse intensities of signals returned from the target features within the beam-swept strip are plotted in the lower half (B) of Figure 9-20. Note first the intensity peak associated with the steep slope of the mountain facing the passing aircraft. A significant part of the transmitted pulse is reflected directly back to the receiver. However, as the depression angle decreases, the beam fails to reach the opposing slopes, leading to no return from the shadow area. The vegetation, encountered next, consists of a rough irregular surface with some individual leaves oriented toward the radar. This feature acts as a diffuse surface, scattering the beam, but with variable return of intermediate intensity. The metal bridge, with its planar surfaces, is a strong reflector. The lake, with its smooth surface, acts as a specular reflector to divert most of the signal away from the receiver in this far range position. Smooth surfaces at near range locations will return much more of the signal.

The signal trace shown in the figure represents a single scan line. The succession of scan lines produces an image by varying either the light intensities on a display or the density levels in a film in proportion to the signal intensities. On film, strong intensity peaks are assigned light tones and weak returned signals are rendered dark. A radar film image shows certain similarities to both a panchromatic or near-IR film positive and a thermal IR image. Water is generally dark, roads and streets are light (bright). Moist and bare fields tend to be dark, whereas croplands show somewhat lighter tones. Rugged terrain (high topographical relief) resembles an aerial photo in which hill shadows are prominent, as at lower Sun angles. However, the radar-blocked shadows increase in length as the far ranges are approached. Hill or ridge slopes facing the radar system are subject to a distorting effect called "foreshortening"—expressed as a compression of slopes on the facing (bright-toned) side and an elongation on the side likely to be shadowed (darker-toned). Visually, these slopes take on an

[13] The Doppler effect describes the changing frequencies of signal waves owing to relative motions between the signal source and the receiver; frequency increases (audible pitch rises) as the source approaches the receiver (listener) and decreases (pitch falls) as the source moves away.

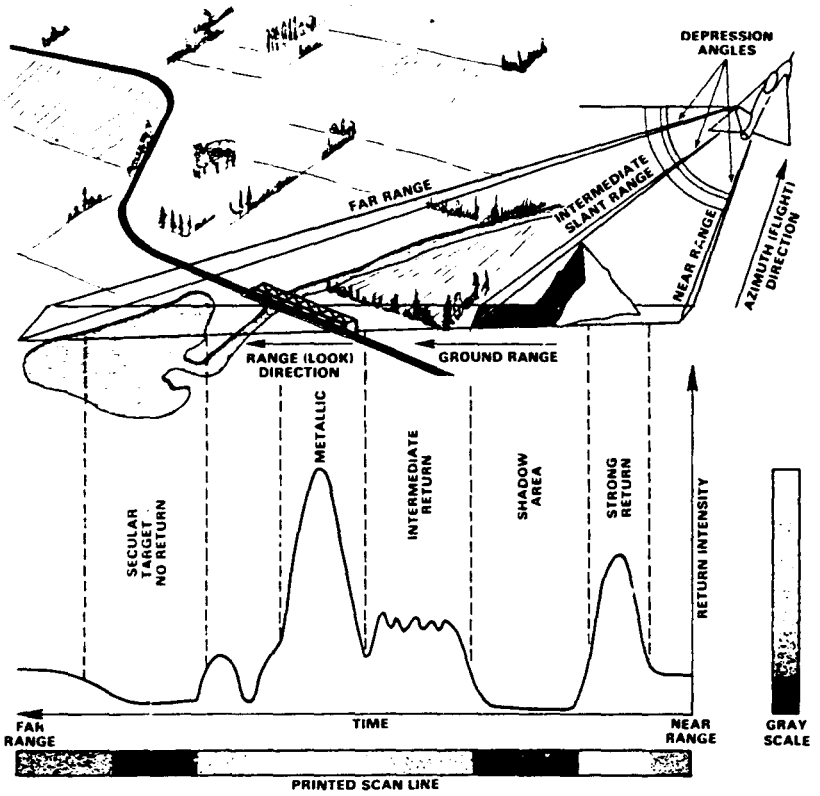

Figure 9-20. Schematic diagram showing radar beam terminology and characteristics of returned signals from different ground features (modified from Sabins, 1973).

asymmetrical form, with the facing slopes appearing to lean toward the aircraft as though steeper. In the extreme, "layover"—in which such slopes are inverted and laid over—occurs when the look angle is less than the foreslope angle. The effect is most pronounced in the near range side of an image and becomes less distracting as the depression angle decreases (far range). Shadowing develops when the sum of the look angle and the backslope (slope inclined away from the radar) angle exceeds 90°. Slant range images also show a geometrical compression, accompanied by distortion of regularly shaped features (square fields may have rhomb-like outlines), which is maximum on the near range side. Still other distortions may be caused by erratic motions on the aircraft during flight. Linear features in rolling or mountainous terrain (such as long, straight valleys) may be emphasized by a combination bright slope-shadow effect, with maximum enhancement achieved for features parallel to the flight line.

Radar image tones may also vary in a systematic and controlled way. When a pulse of energy is sent from the radar transmitter, its electrical field vector is vibrating in either a horizontal (H) or a vertical (V) direction. The design of the system determines whether polarization is H or V. Most of the reflected pulses are parallel-polarized, i.e., return with the same direction of electric field vibration as the transmitted pulse. Thus, either HH or VV polarization pairing of the transmitted and returned signals will ensue. However, upon striking the target, the pulses can undergo depolarization to some extent so that reflections with different directions of vibration may be returned. A second antenna will pick up cross-polarization orthogonal to the transmitted direction, so that either a VH or HV mode is possible. Many ground features appear about the same in either parallel or cross-polarized images. Vegetation, however, tends to show different degrees of brightness in HV or VH images, owing to depolarization by multiple reflecting branches and leaves.

Other factors contribute to the brightness or intensity of pulses from a reflector. Two properties of a surface material afford clues about its com-

position and state by the manner in which they affect the intensity. One, the dielectric constant, provides a measure of the degree of polarizability of a material subjected to an applied electric field. Radar waves penetrate deeper into materials with low dielectric constants and reflect more efficiently from those with high constants. Values for the dielectric constant range from 3 to 16 electrostatic units (esu) for most dry rocks and soils to 80 for water. Moist soils have intermediate values, typically in the range of 30 to 60 esu. Thus, variation in intensities of reflected pulses may, other factors being equal, indicate differences in soil moisture. The variation among rocks is generally too small to allow identification of most different types by this property.

Various kinds of surface materials differ from one another in their natural or cultivated state of roughness. Roughness, in this sense, refers to small irregularities or textural differences on a surface, as might be represented by pitted materials, granular soils, grass blades, gravel and other covering objects whose dimensional variability is of the order of millimeters or centimeters. The height of an irregularity, together with radar wavelength and grazing angle at the point of contact, determines the behavior of the surface as smooth, intermediate, or rough. A smooth surface acts as a specular reflector to minimize pulse return to the radar. A rough surface acts as a Lambertian or diffuse reflector to backscatter enough energy to be detected as a strong signal. As wavelength increases, a surface with an irregularity height of 0.5 cm will respond to Ka band (λ = 0.86 cm), X band (λ = 3 cm), and L band (λ = 25 cm) radar waves in the reflection sequence of smooth, intermediate, and rough respectively. Other average heights produce different sequences, from combinations of "all smooth" to "all rough" for the three bands used. This gives rise to the possibility of using several bands simultaneously (multiple radars on a single platform) in a quasi-multispectral mode. Thus, patterns of relative intensity (or gray level density in an image) for images made from different bands will appear as diagnostic tonal signatures for several kinds of materials whose surfaces show characteristically different roughness.

The particular radar wavelength also influences penetrability below target surfaces. Depth of penetration increases with wavelength: L band radar will penetrate deeper than K or X bands. Radar, however, does not truly penetrate a forest canopy, since most leaf sizes are of the same order of magnitude as the radar wavelength and are thus fairly efficient backscatter points. At typical radar resolution (10-20 m) individual trees are not resolved, but where dense canopy tends to be uniform in height above the ground, the tree-top "surface" will closely follow the ground contours and create the impression of a topographical surface below. Signals for all common radar bands pass through the fine droplets of moisture making up clouds, so that these clouds become transparent or invisible. However, large ice crystals or raindrops do backscatter K band radiation but produce no returns from L band radar.

Aircraft Radar Images

You should now know enough about radar to appreciate and interpret images made from both air and space platforms. Figure 9-21 shows a familiar scene along the Susquehanna River. This pair of images was made from a SLAR flight over Harrisburg on July 22, 1966. The radar system is a Ka band (0.86 cm) instrument developed and operated by Westinghouse. The sharper strip (left) is a parallel-polarized (HH) image; the other (right) is a cross-polarized (HV) image. Compare these SLAR images with aerial photos and Landsat subscenes to orient yourself and to appraise differences in the information each conveys.

#9-57: Why is the HH image sharper?

#9-58: Estimate the resolution.

#9-59: Can you deduce the look direction? How did you tell?

#9-60: Are layover and shadowing pronounced? Explain.

#9-61: What types of distortion are evident?

#9-62: Describe the pattern of returned

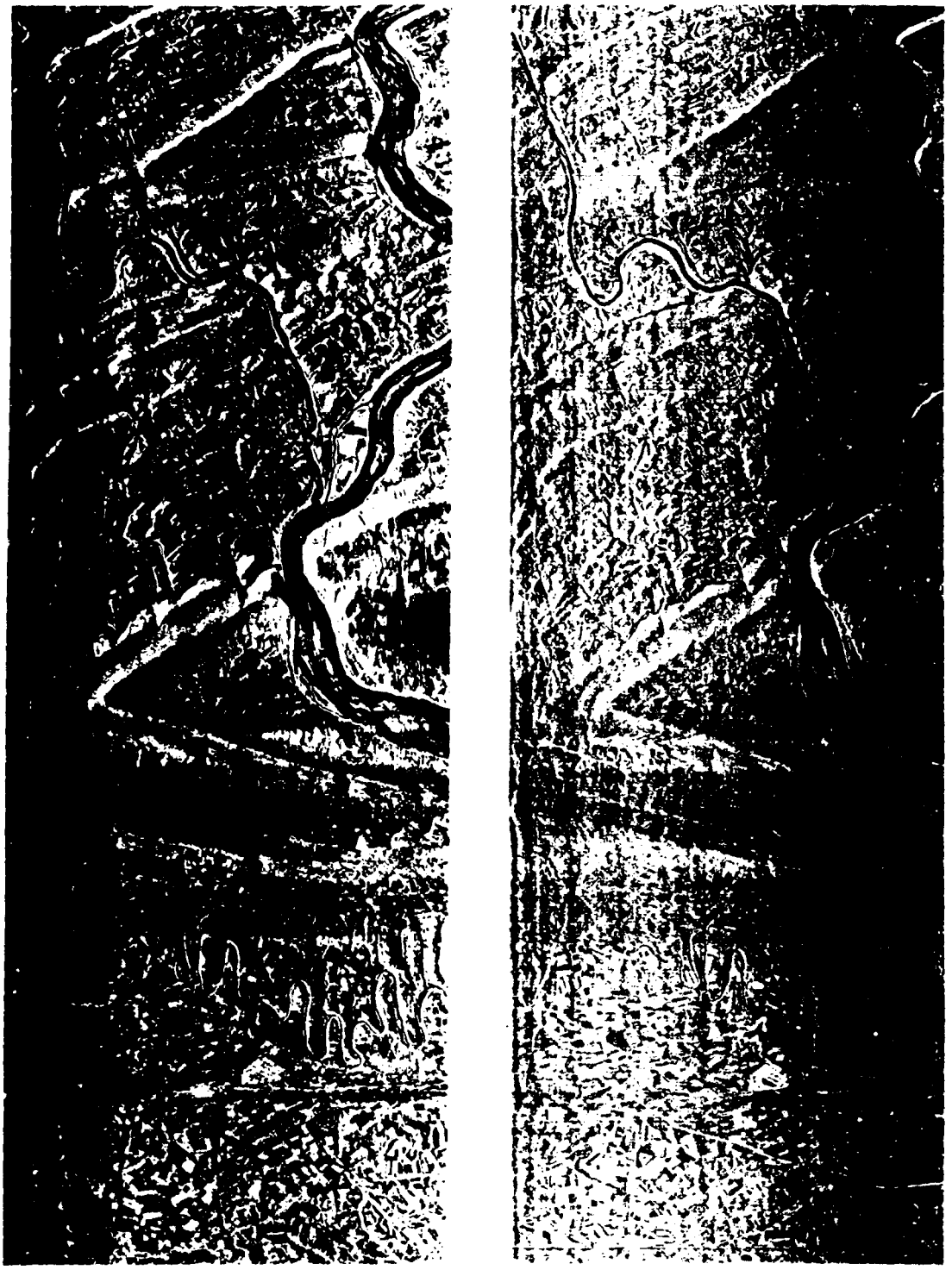

Figure 9-21. SLAR images of central Pennsylvania obtained on July 22, 1966 with an airborne Westinghouse K-band radar system. Left: HH; Right: HV images.

signals from the forested slopes of Blue Mountain. What causes this?

#9-63: What is/are the principal difference(s) in the tonal patterns in the HH and HV images?

#9-64: Name any feature(s) that show up better in the HV image.

Seasat Radar

The first civilian imaging radar system in an unmanned satellite was part of the package carried by Seasat. Seasat-1 was launched on June 26, 1978, into a slightly elliptical (nominally *ca.* 790 km [perigee as low as 761 km; apogee up to 803 km]) near-polar orbit. The orbital configuration allows day/night full coverage on a 36 hour repeat cycle for sensors with a 1000 km cross track swath width. The main goal of the Seasat mission was to provide timely data for oceanographic research and applications. Approximately 95 percent of the global oceans is scanned during the twenty-one orbits in the 1.5-day cycle. Seasat was designed to function for at least a year, but after 99 days it experienced a circuit failure that ended its useful life. The sensors carried by Seasat, a satellite system managed by the Jet Propulsion Laboratory, were:

1. Visual and Infrared Radiometer: this provides images at low resolution (3 km - visible; 5 km - thermal IR) to aid in feature recognition and to measure sea surface temperatures;
2. Scanning Multifrequency Microwave Radiometer: this produces data at frequency-dependent resolutions (16 km X 25 km for 37.0 GHz channel, 87 km X 144 km for 6.6 GHz band) to determine sea surface temperatures and wind speeds;
3. Wind Field Scatterometer: this is a radar system (21 cm wavelength) with low resolution (50 km) designed to measure surface wind speeds (from 4 to 20 m/s) and direction;
4. Synthetic Aperture Imaging Radar: this was primarily developed to measure direction and wavelength of ocean waves exceeding 50 m fetch (wavelength) (Figure 9-22A) of imaging sea ice and land features;
5. Short Pulse Radar Altimeter: this is a K-band (13.5 GHz; 2.2 cm) system that senses a spot size of 1.6 to 12.0 km; it is used to determine satellite altitude relative to ocean surface to a precision of ±10 cm and wave heights in the 1 to 20 m range to an accuracy of ±0.5 m.

We shall confine our attention to the imaging SAR on Seasat.[14] The radar operates in the L-band region (1.275 GHz; 23.5 cm), delivering 1463 to 1640 pulses/s through a 10.7 m X 2.2 m baseline antenna (peak power at 1000 W) that focuses a 1° X 6° HH polarized beam pointed starboard at 20° off nadir. The swath width of the image strip, located between 24 and 240 km from the orbital ground track, is 100 km (62 miles) and the maximum track length is 4000 km (2480 miles). The SAR repeat cycle over the same ground tracks is 24 days. The high depression angles (67° - 73°) reduce shadow effects when the SAR is operating over rugged land terrain. The resolutions achievable by the system depend on the method by which the synthetic aperture data are processed. With an optical correlator, image resolutions are of the order of 70 to 80 m. Processing by a digital correlator has produced images with resolutions up to 20 m; so far, only a selected number of scenes have been run through this more complex procedure.

The Seasat SAR was turned on at various times during passes over the eastern United States. Part of a scene obtained during orbit 1296 on September 25, 1978 is shown in Figure 9-22B. The full swath extended from the Atlantic Ocean off southern Virginia northwestward into northern Pennsylvania. The four individual processing strips appearing in this figure have been mosaicked. This image was generated by the digital correlator and therefore has a resolution of *ca.* 25 m.

[14] Many of the best SAR images obtained by Seasat, together with a description of their information content, have been collected in an atlas published by NASA's Jet Propulsion Laboratory. See J.P. Ford et al., *Seasat Views North America, the Caribbean, and Western Europe With Imaging Radar*, JPL Publ. 80-67, 1980.

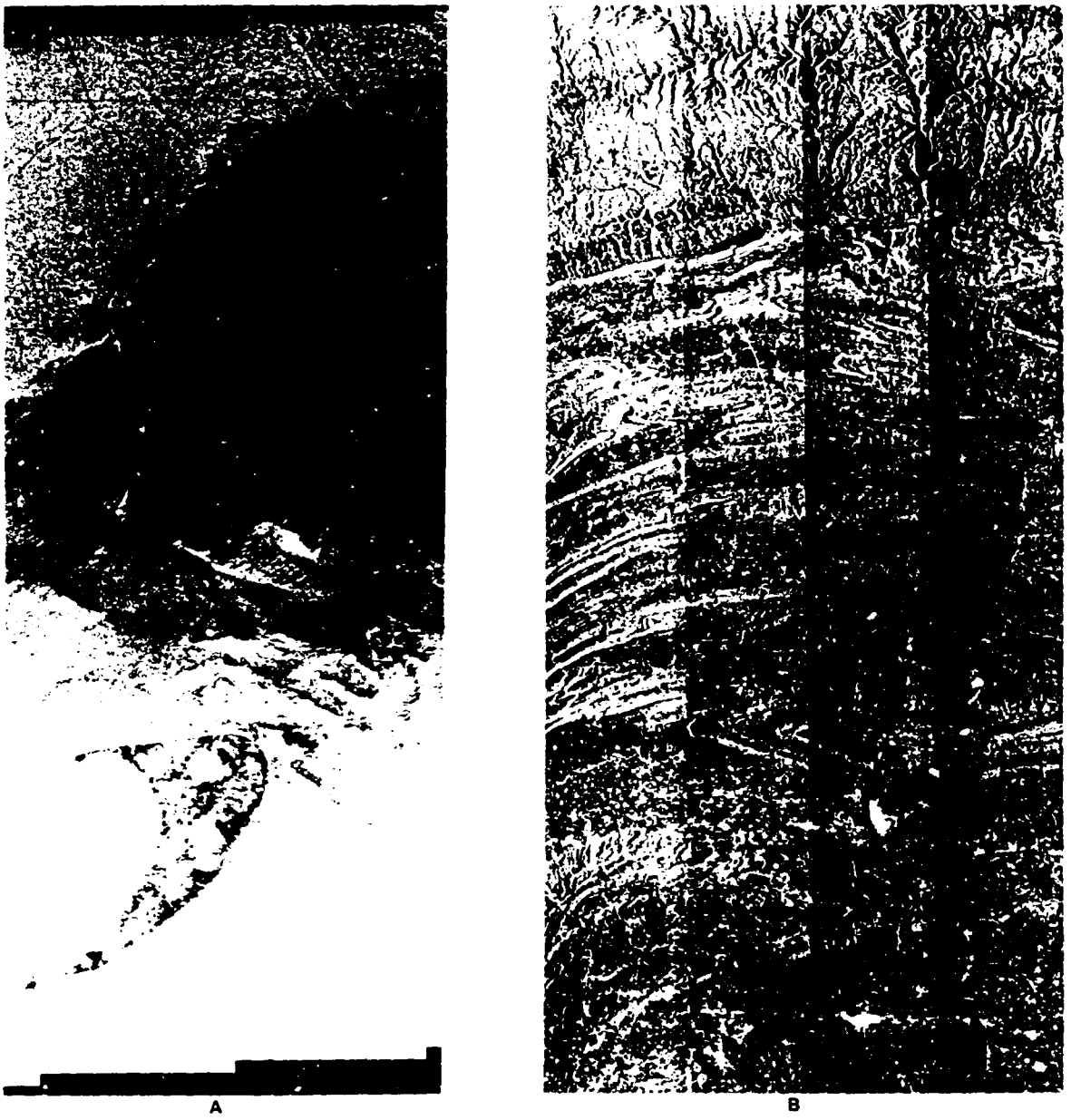

Figure 9-22. A. Computer-enhance Seasat SAR image (25 m resolution) showing sea state in vicinity of Nantucket Island, off Rhode Island. Varying degrees of surface roughness and the effects of shoaling are evident. (Orbit 880; August 27, 1978). B. SAR image of central Pennsylvania, acquired by Seasat during an ascending orbit (1260) on September 28, 1978, and processed on the digital correlator system at JPL. The SAR will produce an image with opposing look direction during a descending orbit. Since radar provides its own illumination, it can scan a surface at any time day or night. L-band radar is generally able to "see through" clouds and has a high penetrability through vegetation foilage.

#9-65: Can you determine the look direction in this image? Is it east or west?

#9-66: Why do the folded ridges (for example, Blue Mountain) look "flat," i.e., without much relief?

#9-67: Near the top, the dissected Appalachian Plateau seems to have some evident relief. What is causing this effect? Why is there a preferred N-S orientation of ridge crests?

#9-68: What minor topographical feature within the folded ridges shows up better in the SAR image than in Landsat images?

#9-69: Comment on the degree of distortion (feature displacement) evident in a strip. What aspects of the data acquisition system favor this condition?

#9-70: Locate Harrisburg. Why does it show up as a very bright (whitish tone) feature (without much internal structure)?

Digital tapes containing SAR data may be processed on various computer systems capable of reading the tapes and applying suitable routines. By using a CCT containing orbit 1296 SAR data, two enlargements of the Harrisburg area were imaged on the IDIMS system (Figures 9-23A and B). Except for contrast stretching, the raw data were not reprocessed and the resolution does not approach the optimum. Nevertheless, individual buildings in the suburban areas serve as reflectors whose outlines can be roughly discerned.

#9-71: Note the sharp tonal discontinuity (a boundary between whitish on the south side to speckled gray on the north side) in Harrisburg near the top of Figure 9-23B. Inspection of aerial photos (cf. Figure 7-14) indicates that this abrupt change is not related to a large decrease in building density. One geometric pattern evident in the photos does change. What is it? Can you suggest how this might affect the radar signal returns?

#9-72: Note the bridges across the Susquehanna into Harrisburg (arrow). They seem to be subdivided into segments by dark lines. What might explain this? (Hint: See Figure 6-1D.)

We have already demonstrated with several examples in this workbook (see pp. 178-182) how different data sets may be merged. After appropriate scale changes and other rectification, Seasat SAR or other radar system scenes may be combined with corresponding Landsat images. This superposition leads to integration of the multispectral character of Landsat data with the topographical expression of the same area as displayed in the Seasat image. The net effect is to provide a scene with some of the visual impact that is evident in a stereo image (although no genuine stereo effect is produced) while retaining the color or black-and-white patterns in a multispectral image. This is a further aid to classification; the classification itself could be merged with the radar image as another type of display.

Figure 9-24 consists of the image subset constructed by merging (on the IDIMS computer) the Seasat SAR data set obtained on June 16, 1979 over the Huntington, W. Va., area with a Landsat false color composite of the same area made from data acquired on July 18, 1977. The resulting merge is displayed over most of Figure 9-24, but the lower right corner shows only the Landsat subscene so that the effect of adding the radar imagery is evident from comparison.

FUTURE REMOTE SENSING SYSTEMS

Now, let us "switch gears" from past to future. What you have learned about narrow band visible, thermal IR, and radar images should have generated some enthusiasm and support for proposals to launch more advanced, diverse, and sophisticated multisensor systems into space. NASA's Earth Resources programs are in a constant state of evolution. Both agency (scientific/engineering/manager) personnel and members of the general user community outside NASA are charged with suggesting improvements in existing or new hardware (sensors), mission constraints, and

A B

Figure 9-23A&B. Progressive enlargements of scene shown in Figure 9-22, photographed from the IDIMS TV monitor.

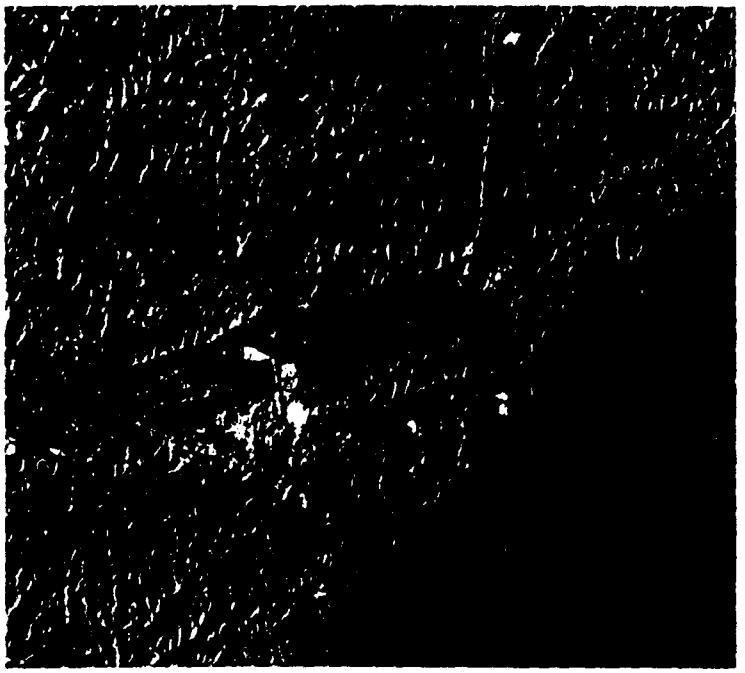

Figure 9-24. Computer-produced merge of MSS subset covering Huntington, W. Va. with corresponding area as imaged from Seasat data. MSS image alone shown in lower right.

program goals. Those deemed feasible and attractive are often evaluated for several years before being proposed to Congress and the administration as a "new start." Table 9-4 summarizes the status of approved and suggested systems in Earth observations, using both EM remote sensing and potential field measurement techniques, that are currently being considered by NASA. Several such systems, both approved and pending, will be considered here, along with reference to Earth-observation satellite systems under development by other nations.

The NOAA Role

Undoubtedly, the most significant event for the 1980's in the growth of the United States Earth Resources program will be the gradual evolution of an operational remote sensing satellite sys-

Table 9-4

CURRENT STATUS OF MEASUREMENT TECHNIQUES

	ELECTROMAGNETIC REMOTE SENSING			POTENTIAL FIELD MEASUREMENT	
	VISIBLE / NEAR IR	THERMAL IR	MICROWAVE	MAGNETIC FIELD	GRAVITY FIELD
IN ROUTINE USE	GEMINI/APOLLO, SKYLAB PHOTOGRAPHY LANDSAT (MSS, RBV) AIRCRAFT SCANNERS	HEAT CAPACITY MAPPING MISSION (HCMM) AIRCRAFT SCANNERS	SEASAT SAR AIRCRAFT SAR SYSTEMS (X, C, L BAND)	POLAR ORBITING GEOPHYSICAL OBSERVATORY (POGO 2, 4, 6) MAGSAT	SATELLITE TRACKING GEOS-3 SEASAT ALTIMETER
IN DEVELOPMENT	LANDSAT (THEMATIC MAPPER) SHUTTLE MULTISPECTRAL INFRARED RADIOMETER (SMIRR) LARGE FORMAT CAMERA (LFC) MULTISPECTRAL LINEAR ARRAY SCANNERS	8-CHANNEL AIRCRAFT SCANNER	SHUTTLE IMAGING RADAR A (SIR A)		
UNDER STUDY	SHUTTLE STEREO IMAGER PASSIVE FLUORIMETRY	SHUTTLE MULTIBAND THERMAL IMAGER MULTISPECTRAL LINEAR ARRAY SCANNERS	SIREX • VARIABLE ANTENNA • DEPRESSION ANGLE • MULTIFREQUENCY • MULTIPOLARIZATION	TETHERED MAGNETOMETER MAGSAT B	GRAVSAT GRAVITY GRADIOMETER TOPEX

tem. Following issuance of Presidential Directive 54 in late 1979, the National Earth Satellite Service (NESS) of the U.S. National Oceanic and Atmospheric Administration (NOAA) has developed a planning document[15] for transfer to its responsibilities of many of NASA's functions in operating the Landsat program. Both NOAA and the civilian sector are expected to assume major roles in providing Earth resources data to both the national and international user communities. The highlights of this plan are as follows:

1. Continuity of the Landsat Program through the transitional period in the 1980's will be assured, although it is possible that there may be gaps in data coverage at any one period, especially if a satellite should fail prematurely.
2. A Fully Operational System, under private sector ownership and operation, could be on-line by 1990.
3. An Initial Operational System, under NOAA management, will be implemented during most of the 1980's. This will consist primarily of a series of Landsat-D's (see below). These will include the MSS and the Thematic Mapper (TM), an advanced sensor (unless the TM is not ready for the first launch in mid-1982).
4. Sometime in 1983 NOAA will begin taking over NASA's responsibility for controlling the Initial System, after launch of Landsat-D and checkout of the TDRS data relay and ground data processing systems.
5. Requirements for future satellite design and systems operation will be sought from major sections of the worldwide user community (primarily, those concerned with agricultural, mineral extraction, and land use/cover applications) in developing the Fully Operational System.
6. The private sector will be encouraged to seek eventual ownership and management of the operational system before the end of the decade. As a possible scenario, one or more profit-making organizations could be chartered by federal legislation to invest in the system, thus assuming a significant fraction of the financial risk. The resulting institution must agree to abide by certain regulations (e.g., comply with the Outer Space Treaty provisions; foster nondiscriminatory dissemination of data to all public users; protect possible classified information) specified by the federal government. Any eventual private sector operator will manage the Operational System under federal regulation.
7. NOAA will retain or expand current policies favoring international participation in the U.S remote sensing program. This will include satisfactory scheduling of satellite operation over areas specified by user nations and continued transmission of data to foreign Ground Receiving Stations.
8. The United States, through its State Department and other agencies, will work cooperatively with foreign organizations or countries that elect to compete in an open international market by building and operating civilian remote sensing satellites to provide Earth resources data. A principle of complimentarity is proposed to encourage the United States and foreign satellites to have complementary coverage patterns and orbital repeat cycles and to adopt compatible data handling systems.
9. Pricing of data products and other output will be set at a high enough level to assure acceptable recovery of systems costs in accord with public needs. Some federal underwriting of costs will likely be needed prior to self-financing by the private sector in order to maintain affordability.
10. As the transition to NOAA operation progresses, the primary NASA role will shift to emphasize various R&D functions, including development of new sensor and platform systems and specialized processing and applications activities.

[15] Satellite Task Force Report, *Planning for a Civil Operational Land Remote Sensing System: A Discussion of Issues and Options*, United States Department of Commerce, National Oceanographic and Atmospheric Administration, June 20, 1980.

Landsat-D

The next firm step into space for NASA's Earth Resources program will be Landsat-D, now scheduled for launch in 1982. Consideration of a new generation of observing systems, with significant improvements over the current Landsats, has been underway since 1970, culminating with an intensive study of sensor, mission, and user requirements in the Landsat Follow-on program. Overall, the system is being designed to provide better spatial and spectral resolution and improvements in processing and delivery of data for the user community.

Landsat-D, which will be launched by an augmented Delta rocket, uses a new platform the Multimission Modular Spacecraft (MMS). The spacecraft will orbit at an altitude of 705 km; retrieval by the Space Shuttle is possible from this altitude. That orbit provides a repeat time of sixteen days and, if the launch of Landsat-D' is authorized, the cycle between observations of a scene can be reduced to eight days. For a single satellite in orbit, adjacent swaths will be covered in 7 to 9 day intervals. When two spacecraft operate in the eight day mode, adjacent swaths may be sampled on consecutive days in a westerly direction, and any given scene will be imaged every eight days. A swath width of 185 km will be maintained, with a daylight equatorial crossing time of around 9:30 a.m. local time.

A recent version of the flight segment for the Landsat-D mission is shown in Figure 9-25. Several supporting satellites in the data acquisition and transmission system are to be placed in geostationary (synchronous) orbits. A series of NAVSTAR Global Positioning System (GPS) satellites will be used to improve the accuracy of ephemeris (location in orbit) data for Landsat. One of two Tracking and Data Relay Satellites (TDRS) serves to receive signals from Landsat-D as it transmits from lower orbit anywhere within the line-of-sight to that TDRS that is covering most of a hemisphere. Two TDRS's (at 41° W and 171° W longitudes) will provide reception and transmission capability for most of the globe. One TDRS will communicate directly with a station at White Sands, N. Mex., to service most of the Western Hemisphere, while the second satellite, positioned to monitor Europe and Africa, can communicate with the first TDRS. This configuration eliminates the need for reliance on tape recorders to acquire data away from ground stations. Those foreign stations now operating or planned will continue to receive raw data directly as desired. Data at the White Sands facility will be compacted for retransmission via Domsat (Domestic Communications Satellite) to Goddard Space Flight Center for initial processing. After processing at GSFC, the data will be relayed again by Domsat to the EROS Data Center (EDC) near Sioux Falls, S. Dak., for further preparation into images and CCT's. The relay satellites, together with high data rates in transmission and processing, permit rapid handling of much larger volumes of data than previously possible with Landsats-1, -2 and -3. This entire processing procedure is being configured to provide a "turn-around" time of forty-eight to seventy-two hours between transmission from Landsat to reception at EDC, where final processing times of a week or less are anticipated. An indication of the complexity of data management for just one ground segment of this relay link is evident from the flow diagram in Figure 9-26, which shows the sequence involved in processing at Goddard.

In order to preserve continuity with the MSS data obtained by the first three Landsats, an identical instrument (except for the thermal band) will be on board Landsat-D. However, Landsat-D will carry a new sensor with significantly improved spatial, spectral, and radiometric characteristics. The Thematic Mapper (TM), even though officially an experimental or R&D (Research and Development) instrument, is eagerly awaited by the user community because of its notably improved performance specifications. There will be seven channels on TM, selected to optimize detection of vegetation (Figure 6-21); their characteristics are summarized in Table 9-5.

The placement of these bands within the EM spectrum may be readily visualized from Figure 9-27. Note that TM 1 lies in the blue, thus allowing production of natural color images.

#9-73: Which three TM bands are needed to produce a natural color image?

The quantization level for TM is a factor of 4 (256 versus 64) better than on MSS. This means that smaller differences in reflectance can be measured, so that discrimination among objects or features with close spectral similarities should be somewhat better. Thus, variations within plant communities, which might consist of different crops, deciduous tree species, or evergreen types, may be more closely defined on a quantitative basis. Although the choice of wavebands was governed largely by requirements from the agricultural community, other disciplines will find that several bands are particularly suited to their needs as well. Both SWIR bands, TM 5 and 6, will prove useful in identifying inorganic as well as organic materials. TM band 6, for example, is sensitive to water content in certain mineral constituents (such as the clay minerals) in rocks and soils. Experiments with imagery and numerical data acquired by a TM simulator flown on an aircraft have convinced exploration geologists of the efficacy of the three new bands (TM 1, 5 and 6) outside the MSS spectral range, along with greater radiometric sensitivity and higher resolution, as a powerful new tool to search for surface alteration products as guides to ore and petroleum deposits.

A striking example (Figure 9-28) shows the effect of using TM bands 1, 5 and 6 added to bands now on the MSS in discriminating rock types and alteration zones at the White Mountain area of southwestern Utah (see also p.443 and Figure B-16). The data, acquired with a Bendix 24-channel

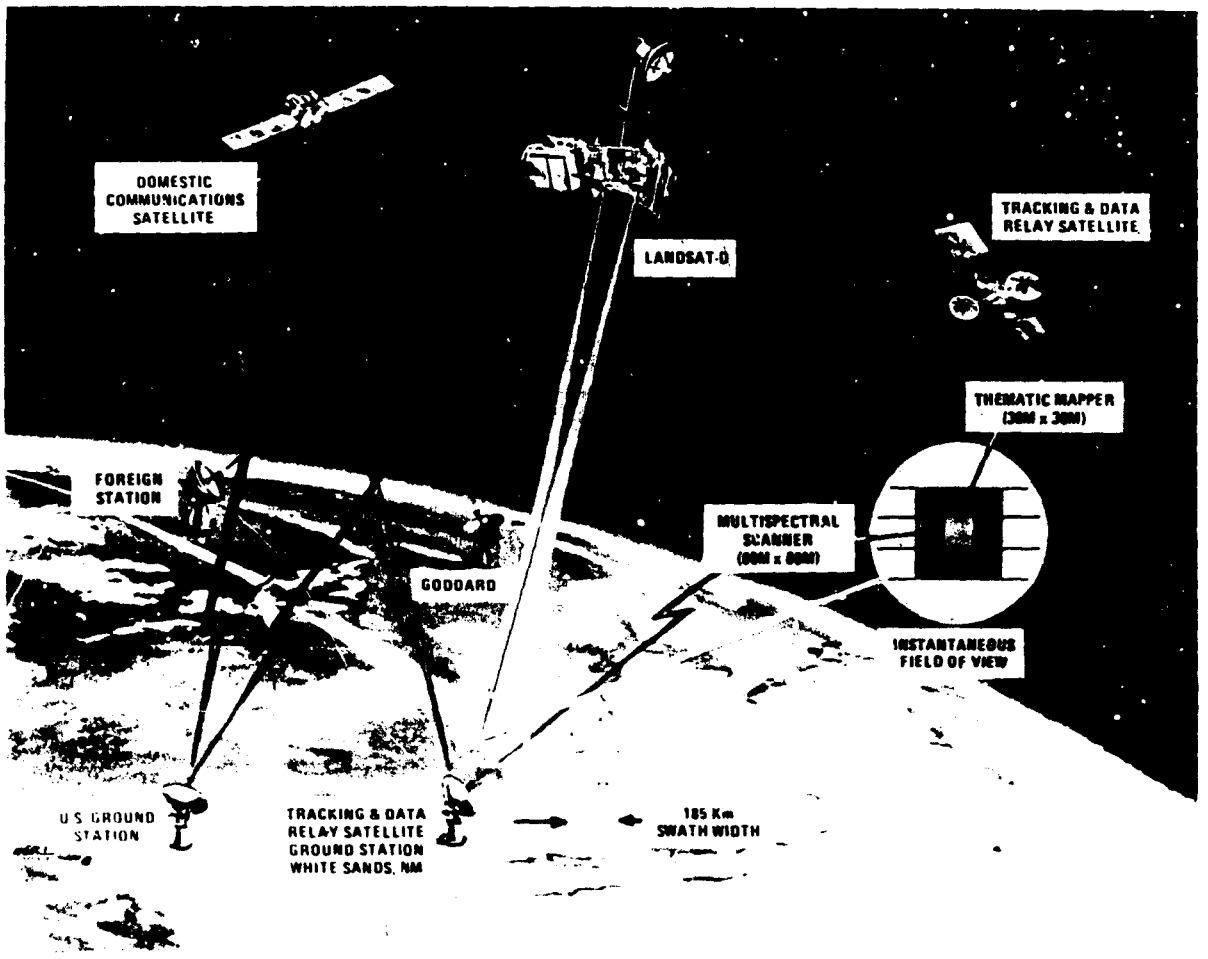

Figure 9-25. The Landsat-D data acquisition and transmission (relay) system.

scanner, have been subjected to Principal Components Analysis (see p. 440); original 3 m pixels were reformatted to a pixel size of 30 m. The rock units are remarkably defined in this representation. Clay-rich alteration (alunite-kaolinite) zones, often previously misclassified from MSS data alone, stand out (pink tones) as easily separated from hematitic alteration (lime green). The limestone is uniquely identified (red). Basalt (purple-pink) is generally distinguishable from andesite (deep blues and greens). Deviations of rock class patterns from mapped boundaries (see map in Figure 9-28) are largely explained by variations in vegetation cover and effects of slope wash (which extend beyond mapped contacts).

The increased resolution is achieved in part through larger optics that better the signal to noise ratio. Improvement is also realized by using sixteen smaller detectors per band (compared with 6 for each MSS band), arranged in an array that receives radiation during a scan timed to cover a ground strip of 185 km by 0.48 km (480 m). The resolution of 30 m (480/16) is equivalent to an IFOV of 42.5 μrad. The number of pixels per scan line is initially 185000/30 = 6167, but this is adjusted to 6320 by adding repeat pixels. Unlike the Landsat-1 scanner, in which radiation is admitted to the detector only during the counter-clockwise (west to east) oscillation of the scan mirror, the mirror on TM will obtain data in both directions of a scan as it oscillates back and forth. This allows for more dwell time on the smaller IFOV targets.

#9-74: The IFOV of Landsat-1 is 79 m by 79 m. What decimal fraction of this is the IFOV for TM? The ground resolution of a Landsat-1 pixel is sometimes quoted as 1.1 acres. What is the size of the IFOV (ground resolution element) of TM in acres?

#9-75: Assuming that a training field requires a minimum of 25 pixels for statistical validity in signature extraction (by clustering), what is the approximate size in hectares (2.47 acres, or 10000 sq. m) of such a sampling site when scanned by TM? (Note: For the MSS, the corresponding size of a training field is 16 hectares.)

The increase in spatial resolution from MSS to TM, that is, from 79 m to 30 m, will produce

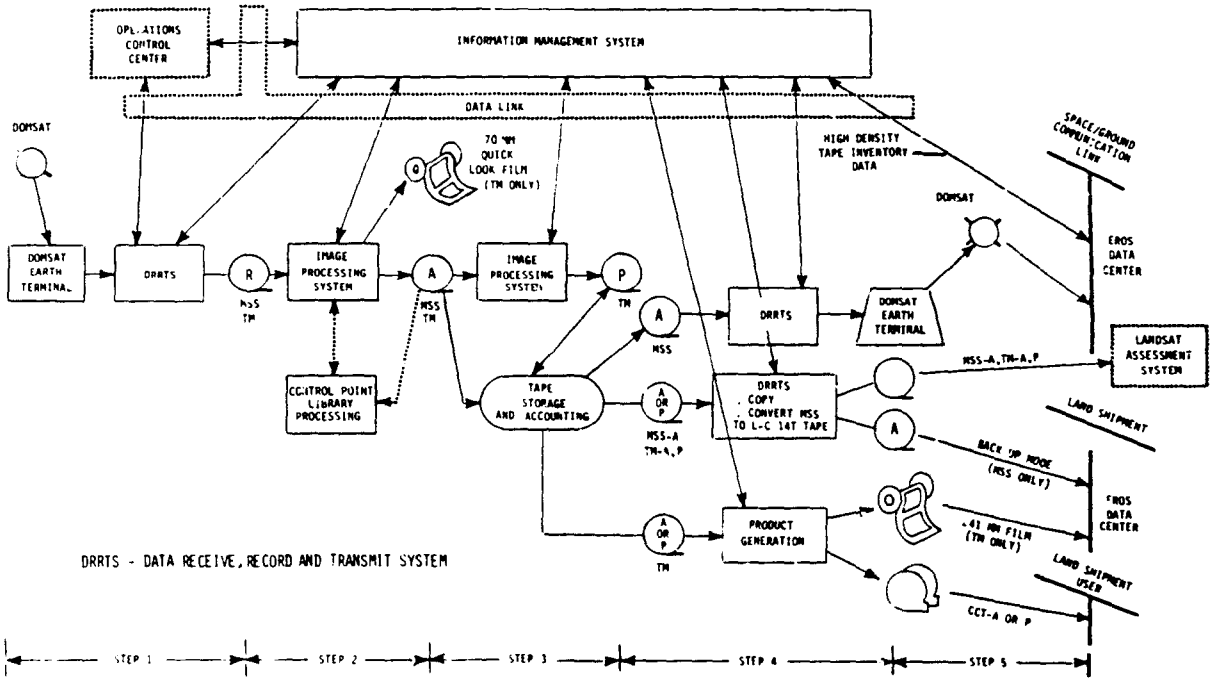

Figure 9-26 Data flow within the Landsat-D data management system.

Table 9-5

BAND	Spectral Width (μm)	Radiometric Sensitivity (NE $\Delta \rho$)	Primary Use for Vegetation Detection
TM 1	0.45-0.52	0.8%	Chlorophyll and carotinoid variations
TM 2	0.52 0.60	0.5%	Mainly green color response
TM 3	0.63-0.69	0.5%	Sensitive to chlorophyll concentration
TM 4	0.76-0.90	0.5%	Vegetation density (biomass)
TM 5	1.55-1.75	1.0%	Water in plant leaves
TM 6	2.08-2.35	2.4%	Water in plant leaves
TM 7	10.4-12.5	0.5°K (NE Δ T)	Thermal properties

Resolution: Band 1-6 = 30 m
Band 7 = 120 m

Quantization Levels: 256 (2^8) bits
Data Rate: 85 megabits/s (compared with 15 megabits/s for Landsat-1)

images comparable with the RBV cameras on Landsat-3. To get a feel for improved image quality due primarily to spatial resolution, examine the photo and images in Figure 9-29 (see also Figure 5-17). The ground scene, mainly fields in the North Carolina coastal plains, was photographed on color IR film at high altitude from a U-2 and then imaged somewhat later by a TM Simulator and a Landsat MSS mounted in aircraft flying at altitudes chosen to provide the appropriate resolutions.[16] Essentially the same spectral intervals contribute to each false color rendition.

The advent of the TM and its supportive systems promises much for the user community. Applications of many kinds, and particularly to most Earth resources disciplines, will probably be much more feasible, efficient, and effective because of the development of this new instrument. However, these high expectations must be tempered by one constraint that will challenge the user's processing capabilities.

#9-76: *What is this constraint? (Hint: think quantity.)*

#9-77: *Throughout this workbook as you examined numerous applications, you no doubt felt frustrated by the lack of spatial resolution or the limitations in radiometric sensitivity or absence of natural color imagery. List at least five applications of interest to you that should become more workable and beneficial because of the characteristics of the TM.*

[16] The author has noted certain dangers in this type of comparative simulation. Although calculations from flight and sensor parameters lead to some stated value for resolution, other factors (such as photographic reproduction) may distort the relative differences in apparent resolution among images. Thus, the 2 m U-2 photo resolution does *not* look dramatically better than the 30 m TM resolution.

LANDSAT-D

Thematic Mapper Spectral and Radiometric Characteristics

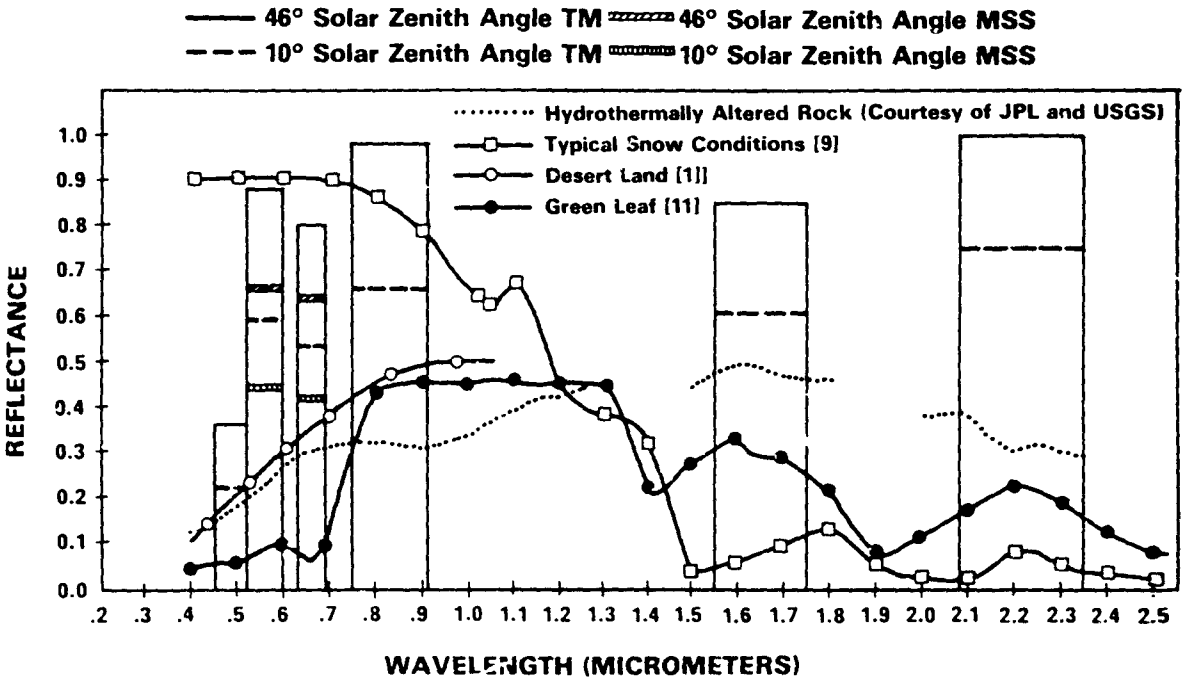

Band	Wavelength (μm)	NE$\Delta\rho$	Basic Primary Rationale for Vegetation
TM 1	0.45-0.52	0.008	Sensitivity to chlorophyll, and carotinoid concentrations
TM 2	0.52-0.60	0.005	Slight sensitivity to chlorophyll plus green region characteristics
TM 3	0.62-0.69	0.005	Sensitivity to chlorophyll
TM 4	0.76-0.90	0.005	Sensitivity to vegetational density or biomass
TM 5	1.55-1.75	0.01	Sensitivity to water in plant leaves
TM 6	2.08-2.35	0.024	Sensitivity to water in plant leaves
TM 7	10.4-12.5	0.5 K	Thermal properties

Figure 9-27. Spectral and radiometric characteristics of the Thematic Mapper on Landsat-D.

Figure 9-28A. PCA image of White Mountain, Utah altered rock units, produced by computer from the aircraft-mounted Bendix 24-channel scanner; pixels resampled to 30 meter squares.

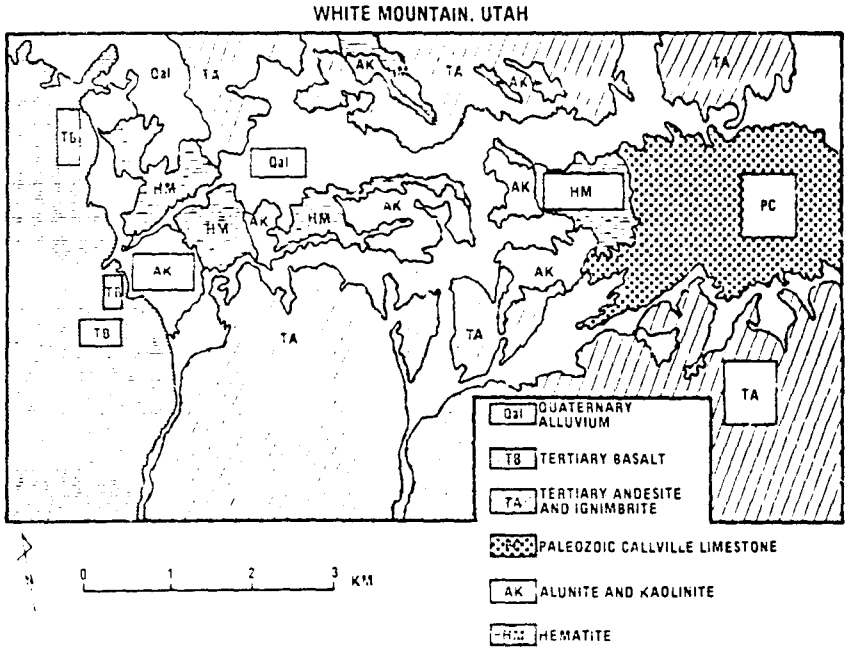

Figure 9-28B. Geological map of area showing main alteration zones.

ORIGINAL PAGE
COLOR PHOTOGRAPH

Other Systems

Beyond Landsat-D, the plans for specific new satellites, sensors, ground systems and missions are still tenuous, but, on the basis of programs now being considered, the outlook is promising. Under consideration by NASA is a sensor that utilizes a different type of detector. Closely spaced, micro-sized (*ca.* 10 μm) radiation-sensitive elements—termed charge-coupled devices (CCD's)—are positioned in a linear array arranged normal to the direction for forward motion. Several thousand elements in this row (the number affects both the IFOV resolution and swath width) are sampled at a very rapid rate to produce a current stream that varies with radiation-induced charges on the array elements. The elements are discharged in time to receive radiation from the next sampled ground line as the spacecraft moves on. This use of fixed solid state detectors for scanning obviates the need for a moving mirror, which largely eliminates the distortions and displacements of pixels that hinder the geometrical accuracy (and necessitate resampling) of MSS data. The process is known as "push-broom" scanning by analogy to the motion of that janitorial tool (Figure 9-30). A prototype sensor, called the Linear Array Pushbroom Radiometer (LAPR), has been developed at Goddard. A sample

COMPARISON OF U-2 AERIAL PHOTOGRAPHY WITH TM SIMULATOR AND LANDSAT-2 MSS COMPOSITE IMAGES

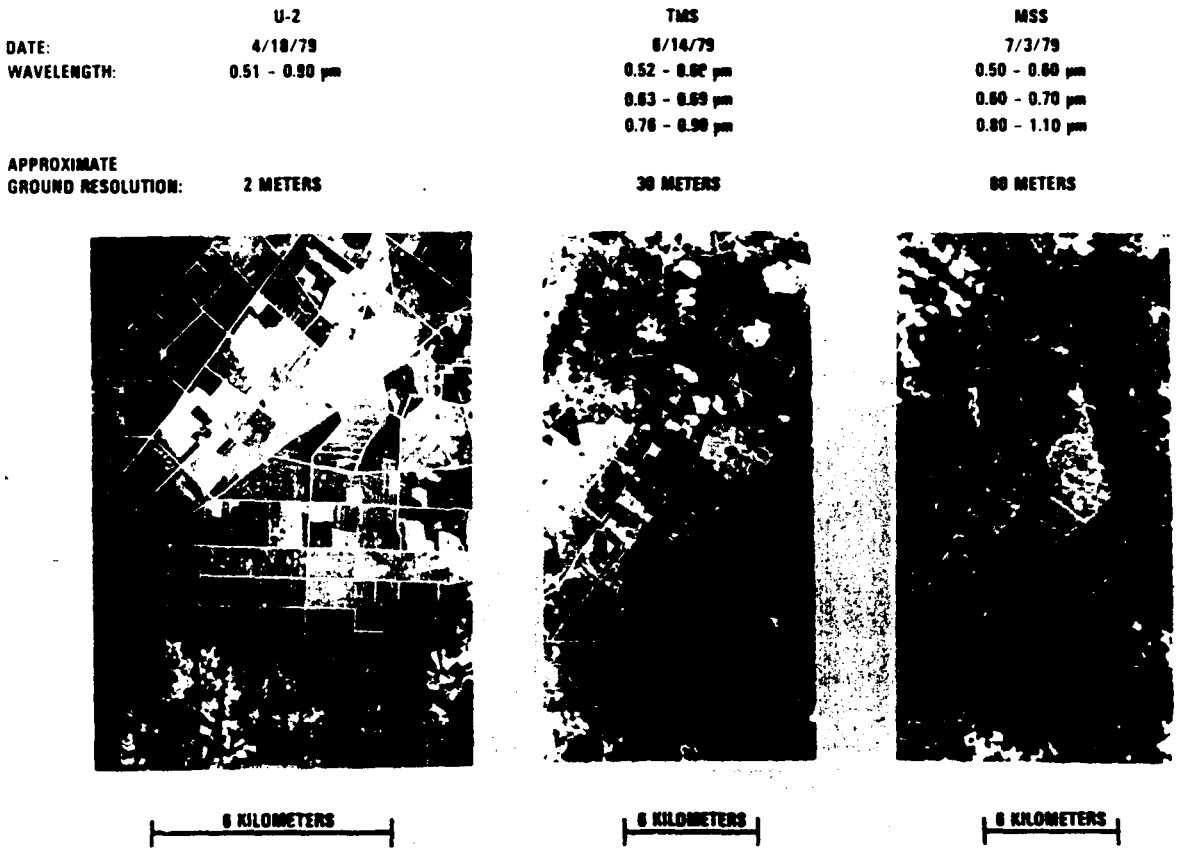

Figure 9-29. Comparison of North Carolina farmland imaged at 3 different spatial resolutions.

Table 9-6

SPOT

(Système Probatoire d'Observation de la Terre)

ORBIT	Sun Synchronous, Circular
Altitude	822 km
Inclination	98.7°
Equator Crossing	10:30 AM
Coverage Cycle	26 Days, Pointing capability across track allows several looks at adjacent areas.
SENSORS	
Multilinear Array	2 Pointable
Pointing Direction	Across Track to 26°
Spectral Bands	.50-.59 =m (20 M)
(3-Dichroic Prisms)	.61-.69 =m (20 M)
or	.79-.90 =m (20 M)
Panchromatic (IFOV)	.5-.9 (10 M)
SWATH WIDTH	60 to 200 km (Max)
LAUNCH	Early 1984 (Ariane Rocket)

of imagery produced by this LAPR is shown as a false color composite (made from LAPR bands: (1) 485 nm (blue filter); (2) 600 nm (green); (3) 825 nm (red); each with 45 nm bandwidth), in Figure 9-31.

NASA is also pursuing development of a spaceborne linear array system. Several designs for an MLA (for Multispectral Linear Array) sensor are being considered as the prime instrument to be chosen for OLOS, an acronym for an Operational Landsat Observing System to be developed by the late 1980's. According to present plans, the operational satellites to be launched then (from the Space Shuttle) will be designated the Landsat-E series.

This new sensor technology is likely to be space-tested first by the French. A satellite, SPOT-1, is scheduled to be designed and built in France and launched from a United States facility sometime in the mid-1980's (Table 9-6). As now planned, the pushbroom device on SPOT-1 will have both panchromatic and multispectral capabilities, will achieve resolutions to 10 m, and will view both downward and to the sides by using a "pointable" optical system.

Many Landsat users have commented on the value of stereoscopic viewing, especially for cartographic and geological studies in rough terrain. The geological community, in particular, has proposed a Stereosat system (see p. 79) as defined by JPL, or a Mapsat as specified by the United States Geological Survey. One configuration would mount two high resolution panchromatic sensors at an angle (26° off nadir) between them. This allows viewing up and down track (fore and aft) with sufficient separation between principal points in overlapping image pairs to achieve an effective differential parallax. A higher range of base to height ratios than the 0.07 to 0.174 (latitude dependent) obtainable from Landsat-1 will be sought, to in-

crease the vertical exaggeration in stereo viewing so as to improve photogrammetric accuracy. One way to raise the ratio is simply to lower orbital altitudes, but this decreases swath widths.

Probably the key element in future Earth resources programs is the advent of the Space Transportation System, better known as the Space Shuttle. The Shuttle can be used in a variety of ways to assist and expand observations by remote sensors. The manned mode permits resumption and extension of experiments in sensor testing and in visual documentation of both preselected surface features and "targets of opportunity"; this constituted a major part of the Skylab mission. Among new equipment for Earth observations is the Large Format Camera (LFC), capable of photographing scenes at a scale of 1:1,000,000 with a resolution of 15 m or better. Other sensors will be mounted on pallets that can be dedicated to specific missions and applications and then later re-outfitted with different instruments. NASA has already accepted the European Space Agency's proposal to fly its own space laboratory, the Spacelab, which will include remote sensing devices among its equipment. Different payloads will be launched on Multimission Modular Spacecraft (MMS) from the Shuttle and then serviced periodically in space by subsequent missions or retrieved for repair back on

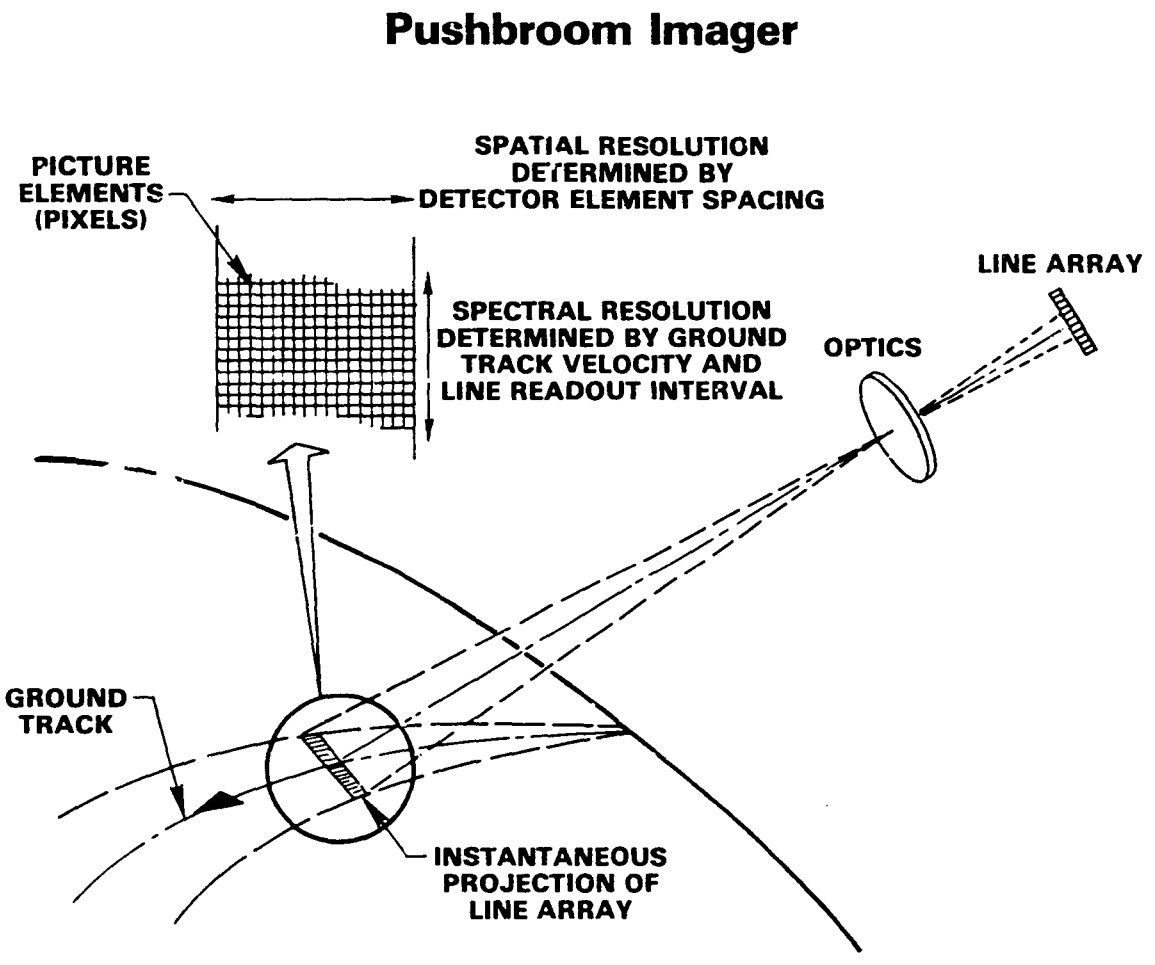

Figure 9-30. Schematic showing the general characteristics of a pushbroom imaging sensor.

Earth and relaunched if warranted. Truly, the options open to the Earth resources user community as Shuttle flights become routine should broaden our horizons into uncharted domains in the ever-expanding realm of applications of remote sensors.

A SUMMATION

SOME CLOSING THOUGHTS: PRACTICAL PAYOFFS FROM SATELLITE SYSTEMS

What is there left to say about Landsat and remote sensing? Not much more, really – at least not in this workbook. The best summary at this point in our survey should now be solidly embedded in your mind. Still, we shall ask you at the end of this section to transfer some of these mental treasures to paper, by writing in your own words a brief précis and an appraisal of your perception of remote sensing as a practical tool in the applied side of your professional life.

Before then, however, we shall delve into two new topics in some detail. One concerns the economic payoff or benefits-to-cost ratio of satellite remote sensing, both as a substitute for conventional methods of monitoring and assessing resources and as a supplement to these methods. The other topic is concerned with how Landsat and related satellites fit into more comprehensive models for resources management. This recognizes that remote sensing should only be, and indeed is, but one essential component in a complex system that aggregates technical, socioeconomic, political, cultural, and other factors in the human decision process of "running the world."

ECONOMIC BENEFITS

Some Previous Studies

Perhaps no other facet of remote sensing technology is in as much need of a well-defined set of principles, a lucid exposition of underlying concepts, and an objective evaluation of conflicting and often confusing factors, as that of the benefits-to-cost values resulting from commitment to a satellite-based Earth observations system. Stated more simply, the subject of the dollars-and-cents value of Landsat to both the United States and the worldwide user community is a very touchy topic and triggers outspoken differences of opinion and severe criticism on any attempt to be quantitative and specific. As in so many other types of economic estimates, there are ill-defined variables, unreliable inputs, subjective assumptions and incomplete or even omitted quantities that together enter into a "best guess" calculation of the expected returns from investments in a government-sponsored remote sensing program. Yet in the Landsat program, the U.S. Congress, the Office of Management and Budget (OMB), federal agencies, private industry, and other segments of the user community have all demanded an accounting of the monies spent on Landsat, balanced against the demonstrated and projected benefits in terms of dollars, before Landsat-D was approved. Early estimates, mainly

using reports from the more than three hundred Principal Investigators in the Landsat-1 and -2 research studies, were nebulous, since most participants were researchers without operational responsibilities who lacked the expertise to make valid assessments. Several subsequent studies made under contract to NASA were carried out by experienced economists working together with systems and discipline specialists. The results were credible in a general sense but suffered from the uncertainties introduced by the same generality and imprecision that characterized Investigator Reports and other sources. In other words, the methods applied to the studies were sound, but the data on which benefits were determined remained inadequate.

As the Landsat program matured through experience, it became more fashionable as well as more practical to include statements about benefits-to-cost in published reports, papers given at meetings, and reviews, testimony, or proposals presented to various government or industrial organizations. In fact, the growing importance of the subject has actually led to three Conferences on the Economics of Remote Sensing, held in California in 1976, 1978, and 1980. However, many of the papers in the Proceedings of these Conferences, as well as other sources of commentary on benefits-to-cost, continue to concentrate on generalities and difficulties rather than meeting the topic head-on by providing specific values for different applications.

Cost-benefit studies are particularly relevant to the international community, especially the developing nations in need of assistance from the United Nations through such sponsored agencies as UNESCO, the World Bank and the Food and Agricultural Organization (FAO), as well as from such American groups as the Agency for International Development (AID). Many countries have no affordable means to conduct inventories of their natural resources or to map their lands and population distribution. This translates not only into a lack of funds but also, more importantly, into a scarcity of trained personnel able to execute the surveys. In this context, a summary of cost-benefits, with special reference to underdeveloped nations, appearing in a 1977 National Academy of Sciences Report[1] is relevant to the points already raised in preceding paragraphs. The following sections extracted from that report apply in general to the entire problem of developing meaningful benefits-to-cost analyses:

> " . . . A decision to commit resources should be based, at least in part, on a careful weighing of costs and benefits. The complex and mutable character of space remote sensing, however, makes benefit-cost analysis particularly intractable for the purpose and ultimately not very meaningful.
>
> Cost estimation can be a relatively straightforward (if not always reliable) procedure once the elements of cost have been defined in a benefit-cost equation. The objective of the analysis will determine the degree of their inclusiveness. Thus, two major benefit-cost studies recently completed in the United States included on the cost side all expenditures associated with the development and operation of the Landsat space and ground segments because they sought to assess the total value of the system in a national endeavor . . . ."
>
> " . . . A growing literature describing completed projects that were based on remote sensing data provides figures comparing in each instance costs incurred using space derived data with prevailing costs using conventional sources. In this respect gain is simply the cost saving made possible by the substitution of one technique by another to get a certain job done. Such cost effectiveness is warranted in discrete tasks that allow the performance of alternative methods to be compared against a specific set of constraints and objectives . . . ."
>
> " . . . Benefit estimation in a more general sense, as would be occasioned for example by the prospective decision to create a national remote sensing user capability, presents problems of a wholly different order. If a remote sensing capability is to be viewed as an institutional resource, benefits must be placed

[1] *Remote Sensing from Space: Prospects for Developing Countries*, National Academy of Sciences, Commission on International Relations, 1977.

in a relatively spacious time frame that would allow the "learning curve" effects to manifest themselves. Moreover, benefits must be assessed not only in terms of cost savings or improved performance that might be obtained over current conventional data gathering functions, but also in terms of new functions that remote sensing uniquely might make possible. Distinction in the benefits also will need to be made as to whether they are tangible and quantifiable (clear economic returns) or tangible but not quantifiable (improved decision making) or intangible (educational or scientific values).

It will be seen that the results of any given study will be typically very sensitive to the particular set of assumptions that is made, both with regard to the projected technical performance of the remote sensing service facility in question, and with regard to the management decisions consequent upon the use of the facility's output . . . ."

" . . . In any application, the estimate of potential benefits can be a useful first step, because if they are large it suggests that the field is worth further investigation. Typically, in order to realize potential benefits, significant ancillary social and private investment may be required and, in some cases, an activity may have to be substantially restructured. The central point here is that remote sensing data as such are of no economic value. They take on value when they are translated into usable information that will actually affect the behavior of individuals and organizations so as, for example, to change the level of output, to reduce uncertainties, etc . . . ."

" . . . In the technologically advanced nations, there already exist information systems that "users" are familiar with and accustomed to integrating into their decisions and activities. To them, remote sensing data may often represent primarily a cost-reducing method for acquiring raw data, although it may be necessary to adapt the system and change certain institutional arrangements . . . ."

" . . . In contrast, in the developing world, especially in activities such as agricultural production, information systems are nonexistent or primitive, and potential users may be unfamiliar with how to integrate into their decision processes information of the sort that might become available through use of remote sensing and ancillary technology. In this situation, the potential benefits may be even larger than they are in the case of developed societies, but the realization of this potential may require profound changes in practice, institutions, and behavior . . . ."

A New Assessment

With these background remarks in mind, we shall now proceed to construct a broad summary of some aspects of benefits-to-cost analysis that you may wish to know before making a final judgment in this workbook on the efficacy of remote sensing as another technique for gathering information pertinent to your professional activities. No claims for validity, accuracy, and objectivity will be made for the examples given in the summary. Some points are derived from documentation available to the author. Others are largely subjective deductions or arbitrary calculations made by the author (who is not an economist nor especially knowledgeable in that field) from information supplied by colleagues. Thus, many of the provisos, qualified conclusions and nuances applied routinely by a cautious economist to a cost-benefits analysis are likely to be missing or inadequately represented in the assumptions made. Nevertheless, the author feels that the numbers generated and conclusions made from them are good "order of magnitude," "back-of-the-envelope" values, which establish the economic baseline to a first approximation.

Aerial Photography Versus Satellite Scanner Costs. Let us begin by performing a deceptively simple set of calculations to estimate the costs of producing a single ten-category Level I (and perhaps several categories of Level II) land use map of a *full* Landsat scene by (1) satellite remote sensing, and (2) conventional aerial photointerpretation methods. The key calculation is the unit cost per

image incurred with each data acquisition system. Many problems ensue in arriving at reasonable estimates. For both space and air platforms, costs depend on numerous factors that defy attempts to establish equivalency. For example, how does one apportion costs for equipment -- such as a receiving antenna or multipurpose aircraft -- not used exclusively in obtaining the desired product? Are quoted costs inclusive of manpower and overhead? Can a single Landsat image be considered equivalent to a photomosaic made from 4000 aerial photos taken at different dates, with much higher resolution, but without multispectral components? The list of inequalities is long, compounding any effort to normalize to a common base.

Cost Partitioning. Another fundamental problem with Landsat images is that of assigning total costs of the system ('costs to provide') versus actual costs to the users ('costs to purchase'). So far, Landsat has been essentially a subsidized federal program. The costs of *the data products purchased*[2] at the EROS Data Center do not reflect all real costs but are actually heavily discounted by the U.S. Government, partly to encourage the user community to "try out" the products before adopting and integrating Landsat technology into their activities. Some critics have advocated a more realistic approach that includes the major costs of data acquisition in any unit price. Thus, the costs of sensor development and fabrication, the spacecraft, launch, operational control, data retrieval (receiving stations), and all processing (both at Goddard and EDC) should be represented in the total operational costs. The argument favoring this view is that such costs would appear in the pricing structure if a Landsat-equivalent program were financed and operated entirely by private enterprise. Certainly, costs implicit in delivering a Landsat-sized area photomosaic made through conventional means by a commercial surveying firm would include prorated costs of the airplane, the cameras, the operating expenses in flight, film processing, rectification, and other procedural costs required to mosaic, manpower and overhead costs, and a profit margin.

The General Model. Taking these points into consideration, the author chooses to develop a simple model for comparing costs between Landsat and conventional photography to produce and interpret an image of the Earth's surface sized to Landsat dimensions. For Landsat, the cost per scene to a user will include most stated acquisition costs with the exception of some manpower costs, various program costs that are hard to prorate, and profits. This cost is just the total stated costs (estimated) for the Landsat program from the 1972 launch of Landsat-1 through operation of Landsat-3 up to April 1, 1980 (arbitrary cutoff date) divided by the total number of *usable* (but not necessarily used) scenes from operation of all three Landsats. The costs will also be reported in $/square mile and $/acre for classification and interpretation of a full scene. For conventional aircraft, the cost per scene will be derived from cost/square mile — converted to cost/acre — figures supplied to the author by personal communications with staff at the U.S. Geological Survey in Reston, Va., based on current programs to produce 7.5 orthophotoquads by using outside contractors to fly the photomissions. There are some hidden or ignored costs inherent to the estimates, so that the results are on the low side. Some simplifying assumptions justify these omissions. As you will shortly see, even if the Landsat costs are low by a factor of two and the aerial photo costs are high by the same factor, the differential still stongly supports the Landsat approach as long as one considers the two end products — Landsat image and aerial mosaic — to be used for the equivalent task of making a ten-category Level I classification.

For Landsat[3], the calculations run as follows:

[2] Prices as of 8/1/80 are $32 for a set of four (bands) of 1:1,000,000 black-and-white prints of a scene; $50 for a color composite of that scene (if not previously produced); and $15 for each additional print (if produced); and $200 for the CCT's covering the scene. The print costs include computer enhancement by EDIPS of any scene acquired after February 1, 1979.

[3] The numbers used here are not precise, sources of some are not official and the values used have been averaged over 1972-79 and then rounded off.

	Landsat Costs (in million of dollars)			
	1	2	3	All
(1) Sensor development; sensor/spacecraft fabrication		185	25	210
(2) Spacecraft management (OCC) (average of $1M × 8 yrs)				8
(3) Launch	5	5	5	15
(4) Receiving stations (3 in U.S. at operation costs of $1M/year/station for 8 years)				24
(5) Data processing at GSFC (average/year of $5M × 8 years)				40
(6) Data processing at EDC (average/year of $4M/year adjusted to income from user purchases, for 6 years)				24
(7) R&D program (principal investigators, NASA centers)				25
			SUM	$346M

(Note: Operational costs of foreign receiving stations and related expenses are not included in the above.)

A contingency cost of $54M, representiag an estimate of other, unaccounted-for costs, is arbitrarily added to the total, bringing the final value to $400M.

Through October 10, 1979, the total number of scenes in the United States inventory (mainly, United States territory and foreign scenes recorded on tape) acquired by Landsats-1, -2, and -3 are 149,610 + 150,870 + 42,660 = 343,140. This total is adjusted to 360,000 to carry through the first quarter of 1980. Total (additional) scenes in foreign inventories are 122,140 + 224,320 + 63,590 = 410,050, adjusted to 440,000. Assuming that the United States has some vested interest in the foreign imagery (based on a "good neighbor" policy implicit in the Landsat slogan "For the Good of all Mankind"), the total will be taken as 360,000 + 440,000 = 800,000 scenes. Now, only a few of these scenes are usable, owing largely to cloud cover obscuration. A conservative estimate of this fraction is 1/5 or 0.20. The number of total usable scenes is therefore 800,000 × 0.20 = 160,000.

Area-prorated Costs. It is now a straightforward matter to calculate a cost per (usable) scene as: $400,000,000/160,000 = $2500 per scene.[4] It is clear that this average cost will decrease over time as more scenes are obtained, since certain mission costs (spacecraft; launch) are one-time-only expenses.

To determine the cost per classified scene, the simplest approach is to add in the charges for a ten-category Level 1 classification of a full scene CCT

[4]Current estimate for the cost/scene for Landsat-D (based on one satellite operating for 3.5 years) is $4500. Some of this increase results from 1M costs and from higher processing costs.

data set, using typical prices in the data processing services industry. Those costs vary from company to company, but consultation with several such firms indicates that $3500 is a characteristic charge. Combining this cost with the scene acquisition costs, we obtain a value of $2500 + $3500 = $6000 as a representative cost per interpreted scene.

Keep in mind that the user is not now asked to pay this full cost. If a user elects to purchase a classification, then $3500 is an upper limit. Alternatively, the user (and his organization) may decide to conduct the classification in-house. This could be done by visual photointerpretation, with moderate accuracy, or by computer processing, with much greater accuracy. Initial equipment and facilities costs for computer processing can be as low as $5 to 10K for an ORSER-type system (software + terminal), or can be in excess of $500K for an IDIMS-type system. Whether the user decides to follow this route, and the extent of investment (level of processing) he commits himself to, will ultimately depend on the quantity of data he intends to analyze and on the value of the information produced. The latter requires some evaluation of the kinds of information needed, the details sought (mainly a function of spatial resolution), the sizes of areas to be classified, the number of such areas, the number of times each year for which up-to-date information is needed, the accuracy specified, the number and skill of personnel involved, and other factors.

The cost per scene data may be recast into cost per square mile or per acre, the units usually applied in estimating values to the U.S market. Taking 13,200 sq. miles as the area in a Landsat scene and 13,200 × 640 (acres/sq. mile) or 8,448,600 acres in the area, the unit costs become (in *cents*):

	$2500	$3500	$6000
Costs/sq. mile	20.0¢	26.5¢	46.5¢
Costs/acre	0.03¢	0.04¢	0.07¢

However, suppose the user must instead acquire a data base by aerial photography and photointerpretation. Here, two common options present themselves, namely low and high altitude photomissions. Although the same total "real estate" is involved, certain costs in processing, mosaicking, and interpretation will differ. Low altitude photomosaics should be more expensive (more individual flight lines; more photos to be rectified, etc.), but the extra costs are partly compensated by better resolution.

Low Altitude Photomosaic Costs. In 1972, the author had a photomosaic of an area in central Wyoming, approximately 175 km (110 miles) on each side, produced by a service corporation. The mosaic was made from a series of existing 15′ photoquadrangles put together from the central parts of more than 8000 individual large-scale aerial photos taken during a series of low altitude flights in the mid-1950's. The cost to NASA for this product was only $2000, since all requisite inputs existed and only minimal additional rectification of the geometrically corrected photoquads was necessary. However, the manager of the firm's photo lab estimated that the cost in 1972 dollars to reproduce the mosaic from "scratch" would be $250K (probably closer to $350K in 1980 dollars). This is for a one-time product consisting of black and white panchromatic photos with about 15 m resolution when reduced to a 1:400,000 scale. Comparison with a 1972 Landsat image of almost the same area of Wyoming at that scale shows the satellite product to be superior in tonal quality, geometrical fidelity, and image uniformity. The multiband and color IR images available from Landsat are an added advantage. Only in terms of resolution could the aerial photomosaic be judged notably better.

The adjusted price of $350,000 seemed too high at first glance, and so the author requested an independent cost estimate from another aerial survey firm. Much of the cost comes from the photoprocessing and rectification that goes into producing the orthophotoquads. Typical costs today for low altitude aerial photos (delivered to the customer) are $6 to 7 for black-and-white images and $7 to 8 for color. Depending on the scale, some 4000 to 8000 individual photos will be incorporated in a 21,000 km^2 (13,200 sq mile) Landsat-equivalent mosaic. The production costs of this mosaic quoted by the firm, would be (for 8000 black-and-white photos): $56,000 for the photomission + $200,000 for rectification +

$40,000 for assembling the mosaic = $296,000, or approximately $22.40/sq. mile.

A. F. H. Goetz estimates[5] the cost of processing a 10^{10} bits per second Landsat-type satellite data set through the usual computer manipulation and enhancement steps to be 100 times greater than the $3500 quoted for Landsat-D processing. This total of $350,000 provides a scene of Landsat dimensions having a resolution of 3 meters. Thus, for scenes of equivalent coverage area, scale, *and resolution*, the costs of satellite and conventional low altitude scenes are comparable at the present time.

High Altitude Mosaics. More and more orthophotoquads are being produced by high altitude photomissions. The U.S. Geological Survey currently produces 7.5′ quad sheets with a single photo per sheet (constituting 150 km^2 [57 sq. miles] on average). A mission is flown at $5.50/sq. mile (based on 1979 costs), in which a black-and-white photo at 1:40,000 and a color IR photo at 1:60,000 are acquired for each quad, but with additional photos obtained for stereo coverage.[6] This amounts to an acquisition cost of: 57 sq. miles multiplied by $5.50/sq. mile, or $315 per quad. This must be multiplied by 13,200/57 or 231 quads, that is $315 × 231 = $72,600 for enough black-and-white or color IR images to make, in principle, a Landsat-sized photomosaic. If the cost differential between color and black-and-white film is neglected, then the cost of each mosaic can be calculated as $72,000/2 = $36,000 (mainly for the input photos). However, in making a mosaic, the edges or outer parts of aerial photos are usually trimmed off to minimize distortion in unrectified images. Up to twice as many may be required; these can be taken from the stereo pairs. Costs of rectifying and joining 2 × 231 = 462 photo parts into a mosaic add about another $30,000 to each mosaic rendition. Thus, either a black-and-white or color IR photomosaic of Landsat dimensions costs on the order of $36,000 + $30,000 = $66,300.

Photointerpretation Costs. Costs of manual photointerpretation depend on the details (Levels) of classification sought. Figures cited by the U.S. Geological Survey are $1.50/sq. mile for Level II. Level I classification is not done in their Land Cover series but should cost less. A value of $1.00/sq. mile is assumed for this Level. A ten-class Level I map equivalent to a Landsat scene, made by standard photointerpretation procedures, would then be 13,200 × $1.00 = $13,200. This can be added to the $66,300 to give $79,500 as a "ball park" estimate for classifying a Landsat-sized scene by conventional methods (the costs might be notably higher if a low altitude photomosaic were used instead). Conversion of this value to cost/sq. mile yields $6.23, and to cost/acre gives $0.0103, or 1.03¢.

Some Trade-offs. On the face of it, then, a comparison of costs for a Landsat versus conventional classification map is $6000 versus $79,500 (high altitude), or $79,500/6000 = 13.3 times more expensive by aircraft. This compares all costs of the Landsat method with contract and in-house costs for conventional methods, using as the frame of reference a single equivalent task of classifying at a level of detail within the capability of both methods. However, this is certainly not the whole story—there are trade-offs and questions of data quality and sufficiency that favor each method for specific, and usually different, uses.

For example, Landsat has the advantage of repetitive coverage at a frequency so high that the costs of making seasonal observations by aircraft would be prohibitive. Landsat also provides near-instantaneous coverage for any one scene, while aircraft coverage of such a large area would extend over days or weeks. Landsat is, furthermore, a multispectral system, whereas most aerial photos are panchromatic (but can be multispectral at extra costs). Again, a Landsat image does not suffer from some of the usual mosaic problems (p. 77), and individual Landsat frames themselves may be effectively mosaicked. Also, the ready availability of Landsat data in computer compatible mode offers much more flexibility in data analysis and interpretation.

[5] On p. 684 of *Remote Sensing in Geology* (Siegal and Gillespie, editors), J. Wiley and Sons, 1980.

[6] Typical costs of $5 to $7 sq. mile are incurred in acquiring the 1:40,000 black-and-white photos for the ASCS (see Figure 6-9).

On the other hand, aerial photography has several key advantages. The main one is the much better resolution (less than 1 to 5-10 m) of aerial photos. There are many applications or tasks that can only be done with high resolution imagery – tree species identification; urban mapping at the street or house level; stratigraphic mapping in geology, to name a few. Landsat cannot currently compete for most such applications, and some will still not be possible even with future high resolution space systems such as the French SPOT. For many uses, Landsat can only be a supplemental tool, rather than a substitute system, for aerial surveillance as the prime instrument of information gathering. Aerial photography will always be a necessary data source. Aerial photomissions may also be scheduled to fly (if the weather is appropriate) to the right place at a particular time. Still another relevant factor is the common fact that many, perhaps a majority of the customary applications fall within areas much smaller than 21,000 km^2 (13,200 sq. miles). Aerial photography, in that sense, is selective and nonwasteful. A task is often accomplished by surveying, say, 800 km^2 (500 sq. miles), with all surrounding area being superfluous. This greatly reduces data acquisition and interpretation costs. Many organizational budgets cannot tolerate the spread of manpower and other resources over too wide an area at any one time.

It should be obvious now that Landsat is the superior approach under quite specific conditions, such as when:

1. large area or regional perspectives are required in a project;
2. the project needs input from many small, usually separated areas;
3. frequent repetitive coverage is necessary, or, at least, advantageous (e.g., crop growth);
4. monitoring environmental changes on a regional or even global scale (e.g., tropical deforestation; desertification) is important;
5. multispectral data improve the classification even more than increased resolution;
6. the nature and sizes of the features to be classified or mapped are within Landsat resolution capability;
7. accuracies for Level I classification at 75 to 95 percent (and 60 percent or less for Level II) are acceptable; these category-dependent accuracies may not be good enough for many needs.

The ultimate decision as to which system is best suited to your needs, of course, is yours. Your choice depends on your assessment of whether Landsat is sufficient to do your job. If it is, it will most probably be cost-effective as a replacement for most conventional methods.

Examples of Cost Savings

Before we leave this fascinating but obviously controversial topic of cost-benefits, we should evaluate some well-documented reports of real savings.

The costs for Landsat classification derived earlier are fairly consistent, although somewhat lower, with most such costs cited in the literature by Landsat investigators and users. These citations range from 10 to 50¢/sq. mile. Several typical examples are quoted in the *Proceedings of the Second Conference on the Economics of Remote Sensing*. Three such entries are:

1. land cover classification of 1,385,560 acres around Portland, Oreg., with Landsat = 20¢/sq. mile, or 0.04¢ per acre (p. 96 of Proceedings);
2. land use surveys by air and ground of 678,000 acres in the Sacramento-San Joaquin Delta of central California = 6.0¢/acre (p. 77);
3. airborne surveys (images only; no interpretation) (p.99); costs per square mile:

Resolution	1 m	3-5 m	80 m (extrapolated)
	$1.51	$0.57	$0.12

A very detailed cost analysis for making a land cover inventory of a small area (1786 or 3792 sq. miles) in southwestern Illinois compares ground surveys, aerial photointerpretation, and Landsat methods. The results are summarized in Table S-1.[7]

This cost per square mile for Landsat is much higher than values already given because of the smaller area involved and the dependence on manual (visual) rather than computer classification techniques. The main savings come from reduced manpower costs. No assessment of relative accuracies is given.

Now, consider three specific case studies of actual cost savings with Landsat. One such case involved the author personally, and represents probably the first documented operational use of Landsat by state agencies. Just two months after launch of Landsat-1, the author and colleagues from the University of Wyoming presented a review of Landsat capabilities to some 20 staff members from several state agencies at Cheyenne, Wyo. As a follow-up, one agency decided to experiment with Landsat imagery to learn how it might supplement a two-year project involving aerial photos and ground surveys to produce a series of land cover maps for the southern Powder River Basin. This basin has become one of the principal energy (oil and gas; coal; uranium) centers in the United States and was slated in 1972 for accelerated development. An up-to-date land cover map was requested by the state legislature prior to passing controlling and enabling legislation for systematic development. A budget of $500,000 was allotted to the map making. The agency "gambled" on the potential of Landsat by earmarking $50,000 to the University of Wyoming for specified products. The University delivered a set of Landsat-based maps in a folio less than three months later. After evaluation by the agency, it was decided that the Landsat maps met the main requirements for the project, and the remainder of the map project was cancelled, thus saving $450,000 and almost two years.

Table S-1

	Ground Survey	Aerial Photo Interpretation	Landsat
	8 Years	18 Months	6 Months
	40 Categories	5 Categories	16 Categories
	3 Counties	3 Counties	7 Counties
	1786 Sq. Miles	1786 Sq. Miles	3792 Sq. Miles
Maps, Photos or CCT	$130.90	$4,161.38	$400.00
Auto Travel Expense	570.90	Minimal	700.00
Inventory	55,000.00	17,056.00	3,792.00
Measure and Tabulate	30,000.00	8,528.00	3,700.00
Ground Checking			750.00
Map Preparation	20,000.00	5,969.00	5,615.00
Miscellaneous Supplies	500.00	135.00	1,000.00
TOTAL	$106,201.80	$36,049.38	$15,957.00
Per Square Mile	$59.46	$20.18	$4.20

[7] From *A Legislator's Guide to Landsat*, prepared by the National Conference of State Legislatures (NCSL) Remote Sensing Project.

The second example refers to an application already addressed several times in this workbook. The defoliation brought about by the gypsy moth in Pennsylvania alone affected more than 1,000,000 acres in that state in 1973 (and 1,500,000 acres throughout the northeast United States in 1977). Financial losses range from $4.60 per acre in pulpwood timber to $75.00 per acre in sawtimber stands in a given year. Pennsylvania officials estimated a loss, due to this moth, of $26,000,000 in timber production in 1973. Comprehensive monitoring would reduce these losses by guiding spraying (which costs the state an average $650,000 annually) to critical spreading areas and by determining those areas of extensive tree mortality where replanting could be undertaken. At this time, inflation-increasing costs (currently, limited to $50,000 a year) of aerial surveillance have restricted direct monitoring to selected areas rather than the whole state. Landsat-derived distribution of defoliated areas (easily found by visual interpretation of images) offers a very low cost method to estimate damage over the entire state.

A third example extends the scope of savings to the international level and also shows the magnitude of benefits that may be achieved. Bolivia has inaugurated an extensive program for Landsat applications under the direction of Dr. Carlos Brockman. By 1977, this program had produced a National Land Cover Map, a National Geologic Map, several regional soils and land use maps, a series of special purpose maps to aid in the national census, and an interpretation map leading to relocation of a railroad line (cutting off several years of surveying time and costs). Landsat-related costs accumulated in those projects were $689,000. Benefits are estimated to be in the millions of dollars. Two additional tasks led to specific savings estimates. As a result of using Landsat imagery at a cost of $2000, a gas pipeline was rerouted to shorten its length by 17 km, resulting in a savings of $12,000,000. A far greater potential payoff relates to the discovery of huge, rich deposits of lithium salts in several of the large saltpans in the dry, high desert of the Bolivian Altiplano. This discovery is directly attributed to computer-processed Landsat imagery (at a cost of $10,000), which reveals the presence and distribution of the salts, later confirmed by field exploration. As a consequence, a mining company has already invested $136,000,000 in leasing and development of the deposits.

This example attracts attention to the several ways in which Landsat observations can lead to some measure of benefits. One category of benefits is that of direct cost savings, i.e., performing a task or activity, now being done by other methods, in a faster and/or better way that is as efficient and effective. A second category is that of doing certain tasks that are not conducted at present because they are uneconomic or unfeasible; this is usually associated with a regional survey in which it was previously impractical to cover large areas in the allotted time. A third depends on the ability to monitor dynamic events or seasonal changes that necessitate frequent observations. A fourth way is more speculative, namely, discovery of a natural resource of large potential value (for instance, the Bolivian salt deposits), which might not have been found through current technological procedures or may have waited for many years before its surroundings were explored and it was located. The author, in an unpublished study of the benefits of Landsat-D to the mineral industry, noted that a Landsat-aided discovery of just one new giant oil or gas field—typically with market value of $2 to $5 billion—would, in a sense, pay for the entire Earth-observing satellite program to date.

Benefits of Advanced Systems

Our consideration of benefits will close by looking ahead to anticipated benefits from the many improvements planned for the Landsat-D system. Intensive studies were made by personnel at NASA Headquarters, Goddard Space Flight Center, Johnson Space Center, and other installations, working with a consulting firm, Econ, Inc. of Princeton, N.J., and with General Electric's Valley Forge Space Center.[8] The overall estimate

[8] Summarized in *A Cost-Benefit Evaluation of the Landsat Follow-on Operational System*, X-903-77-49, Goddard Space Flight Center, March, 1977.

(as a range) of annual benefits is presented in Table S-2 without comment, except to note that the cost-benefit evaluation did engender considerable debate and criticism, particularly from those who considered the values too high.

Table S-2

Annual Benefits of Landsat-D
(millions of FY 76 dollars)

	Benefits
Agricultural crop information	$294 - 581
Petroleum-mineral exploration	64 - 260
Hydrological land use	22
Water resources management	13 - 41
Forestry	7
Land use planning and monitoring	15 - 48
Soil management	5 - 9
SUM:	$420 - 968

TOTAL INFORMATION SYSTEMS

We turn now to the second topic to be treated in this closing section. This deals with the role of Landsat in a so-called Total Information Systems. A fundamental question must be posed: How are Landsat and other remotely sensed data best used to bring forth benefits (financial and otherwise) from the increasingly important role of satellites in observing, monitoring, and inventorying established natural and man-made resources, and in exploring for or developing new resources? In the preceding activities, we have seen two definite answers to this question. First, for many specific applications Landsat and other satellites are capable of being *stand-alone* systems. That is, some desired and acceptable information may be generated exclusively from satellite data. A Level I land cover classification, a map of rock alteration indicative of mineralization, an inventory of lakes, and a plot of defoliated trees are characteristic examples. Second, we also saw how the value of Landsat is often significantly expanded when its data and information products are integrated with other types and sources of data, usually as inputs to a Geographical Information System. In this approach, satellite data may be necessary but not self-sufficient as instruments of problem-solving for, or management of, the Earth's resources. In this view, Landsat is a component--commonly, but not universally, a necessary one--in a larger system of components dedicated to gathering, processing, archiving, interpreting, and applying information.

One concrete example should help to clarify this second point. In exploring for mineral and petroleum deposits, extensive use is made of various geophysical field surveys to develop information about subsurface rock materials and the three-dimensional structure of rock units. On first thought, integration of such data with Landsat data--which describe surface materials and structure (the latter actually concerns three-dimensional

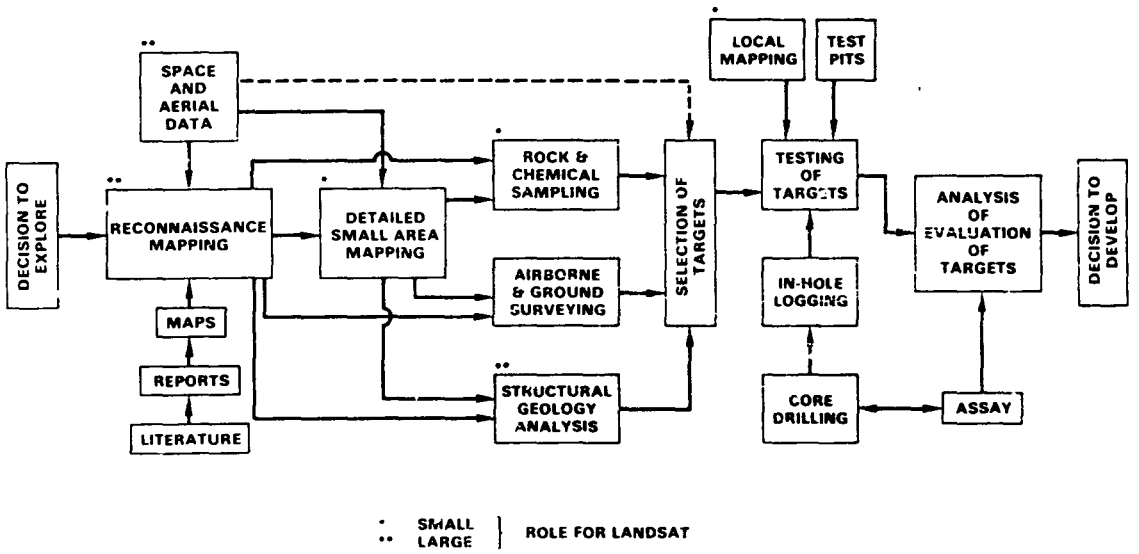

Figure S-1. Flow chart describing Mineral Exploration Model that utilizes remote sensing data.

topographical variation)—may not seem particularly meaningful. Yet, the surface conditions provide clues about shallow to deep subsurface conditions and conversely, subsurface states affect and control to varying extent development of surface states. Both geophysical and Landsat data are readily adapted to digital formats. Using some system like a GIS for integrating and comparing different types of data elements, any reasonable number of diverse types can be registered and correlated. The detection of interrelationships and the analysis of the implications of these are best executed by integration into a model which shows how each element influences the other(s) and how the analysis should proceed in a logical sequence. One such model for nonrenewable resources exploration which draws heavily upon remote sensing inputs is shown in Figure S-1.

Usually, the analyst starts by determining the associative or causative interrelation between two distinct (and sometimes disparate) elements. Consider, for example, gravity data that indicate the distribution of mass in the Earth's crust. The topographical data for surface shape can be cross-correlated to some extent because gravity highs often are associated with topographical highs, and lows with lows. Departure from a gravity-surface shape model points up significant anomalies. The anomalies themselves can become new data elements stored in the multi-element GIS data base.

Gravity data, commonly plotted as contours—typically, in units of milligals—can be readily converted into images that are made to resemble surfaces. Gravity data for the entire state of Pennsylvania have been presented as an image that looks very much like a 3-D topographical map (Figure S-2). This product, prepared from a computer program by Geospectra, Inc., is created by assigning different gray shades to different parts of the contoured gravity equipotential surface. The image can be made to appear like an airbrush-shaded relief map through projecting slanted illumination from an assumed light source (such as the Sun) located at different elevations and azimuths. This analog operation is, of course, simulated digitally on the computer. In Figure S-2, the "Sun" was placed to the southeast (top image) and the northeast (bottom) at an elevation of 30°. Even though the data are contained in 1-kilometer cells (coarse resolution), one can easily discern the major patterns of highs and lows and even some hints of discontinuities (lineament-related?). An obvious next step would be to compare in some way this gravity image with either a topographical image made with the same technique or directly with Landsat imagery (as, for example, a mosaic of the entire state).

Such is now being done. You have already been exposed to the merge of Landsat images with topographical data to produce a stereo-pair (p. 292;

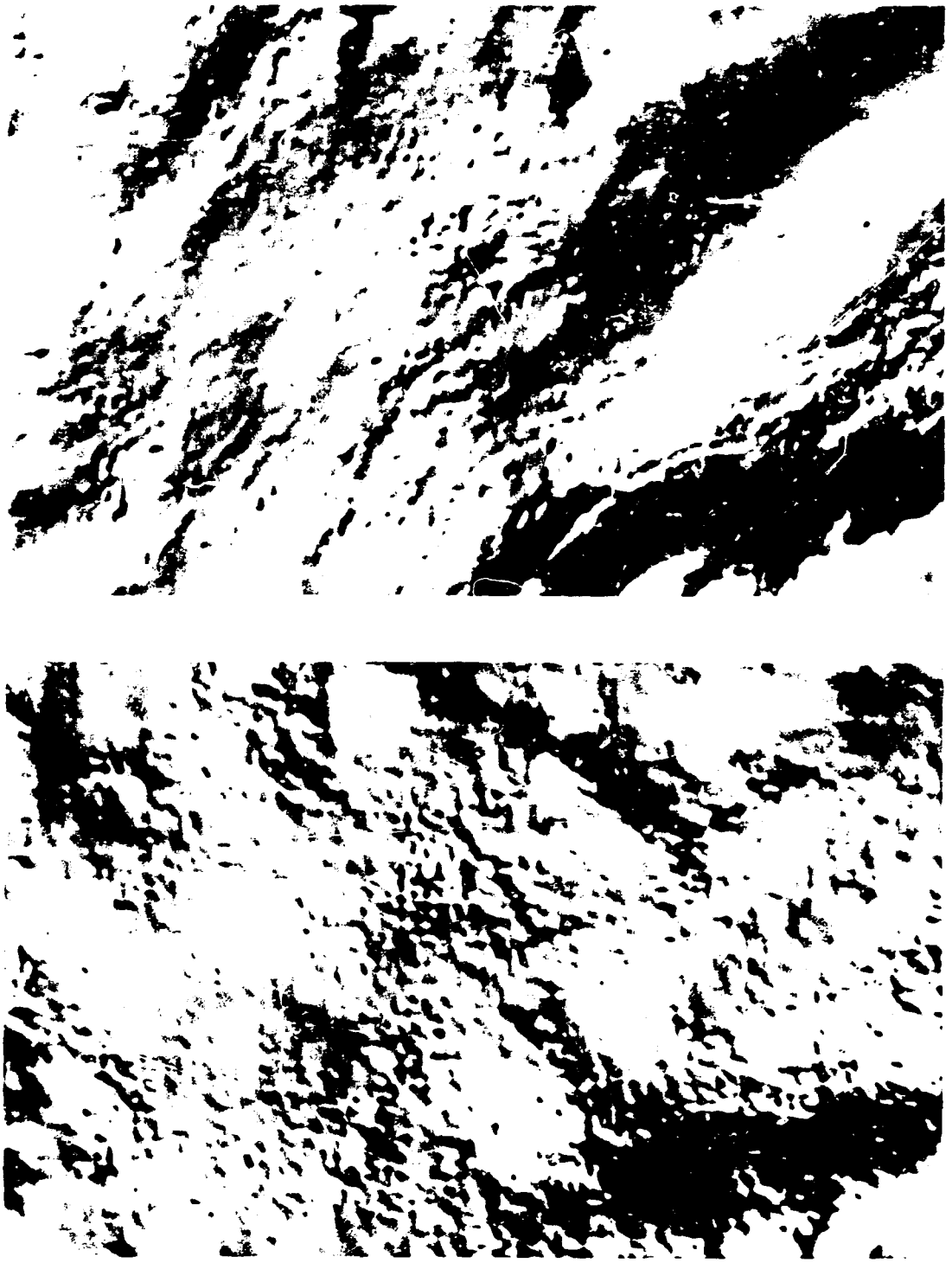

Figure S-2. Computer-generated image showing variations in directional gradient of gravity for the State of Pennsylvania (see text). Courtesy Geospectra, Inc., Ann Arbor, Mich.

images in back pocket). "Stereo" pairs, in which the three-dimensional image seen stereoscopically shows variations of gravity or magnetic field strength, or related parameters, have been prepared through computer processing by users in the mineral exploration community in the United States, Australia, and elsewhere. The results are often "mind-blowing," in that surface topographical features seen in the Landsat images are made to rise and fall in peculiar ways defying commonsense experience because of the surface data control. In some places strong visual correlations occur, such that some large surface landforms appear to rise in consort with a gravity high. At other positions streams seem to rise and fall abnormally (up hill and down, in effect) because the geophysical parameter may show no obvious control or relation. Thermal Night-IR data from HCMM have also been merged with Landsat images to depict variations in surface temperature with respect to surface materials and properties (p. 364). Exploration companies are finding these types of data overlay or merge quite exciting and are only now trying to learn how to interpret such visual aids in an effective manner.

The Information Management Cycle

In the next few paragraphs, we shall further examine some of the properties and implications of information systems that utilize satellite data as input. Figure S-3 is a classic illustration made early in the Landsat program, and one used frequently by many speakers in describing the role of remote sensing in a more general information system. The chart shows essentially a simple closed-loop, cyclic process, unencumbered by the various feedback loops that no doubt exist and are so typical of flow diagrams. The starting point, and the end point as well, is the segment labeled Information Requirements. This focuses on the ultimate driver of any information management system, the user, and his recurring needs. Various disciplines concerned with Earth resources are displayed and identified. The terrestrial globe in the background reminds us that the system should be worldwide in scope if it seeks to achieve optimum utility and benefits. The continent depicted is North America, where the principal efforts in a remote sensing program funded by the United States should be concentrated if the taxpayers of our nation are to reap the maximum returns.

Information requirements logically lead into user and customer demands. The best remote sensing system is the one most responsive to these demands, tempered by the stage of development or available state-of-the-art of the systems actually being operated. Proceeding through the loop, we see three such systems (in the mid-1970's): unmanned satellites, manned spacecraft, and aircraft. The first of these may be represented by Research and Development (R&D) systems (as was Landsat initially), quasi-operational systems (as Landsat has become), or truly operational systems (as will be decided by NOAA before the end of the 1980's decade). The spacecraft, shown here as Skylab but soon to be replaced by the Space Shuttle, not only allows limited, predetermined or target-of-opportunity observations for practical applications, but also testing of new sensors under the direct supervision of trained specialists. The aircraft plays a vital part in the program, to some extent as a platform for sensor tests, but mainly as a co-equal partner supremely suited to acquiring site-, time-, and resolution-dependent data from small sectors of the Earth's surface.

Data are recorded in a variety of formats; on film, as analog or digital signals, or in written or verbal forms from near-surface observations. These data are converted to convenient, flexible, and easily manipulated products that present the information in a readily understood and interpreted way. A goal at this point in the loop is to organize remote sensing data in formats compatible with other kinds and sources of ancillary data. Here, the concepts elicited in Activity 7 on Geographic Information Systems become interwoven with those exclusive to remote sensing analysis and interpretation. The thesis is clearly evident: remote sensing data must be part of a larger data base in which all data sources share a common denominator (normally, spatial or geographical location) and in

TYPICAL REMOTE SENSING SYSTEM

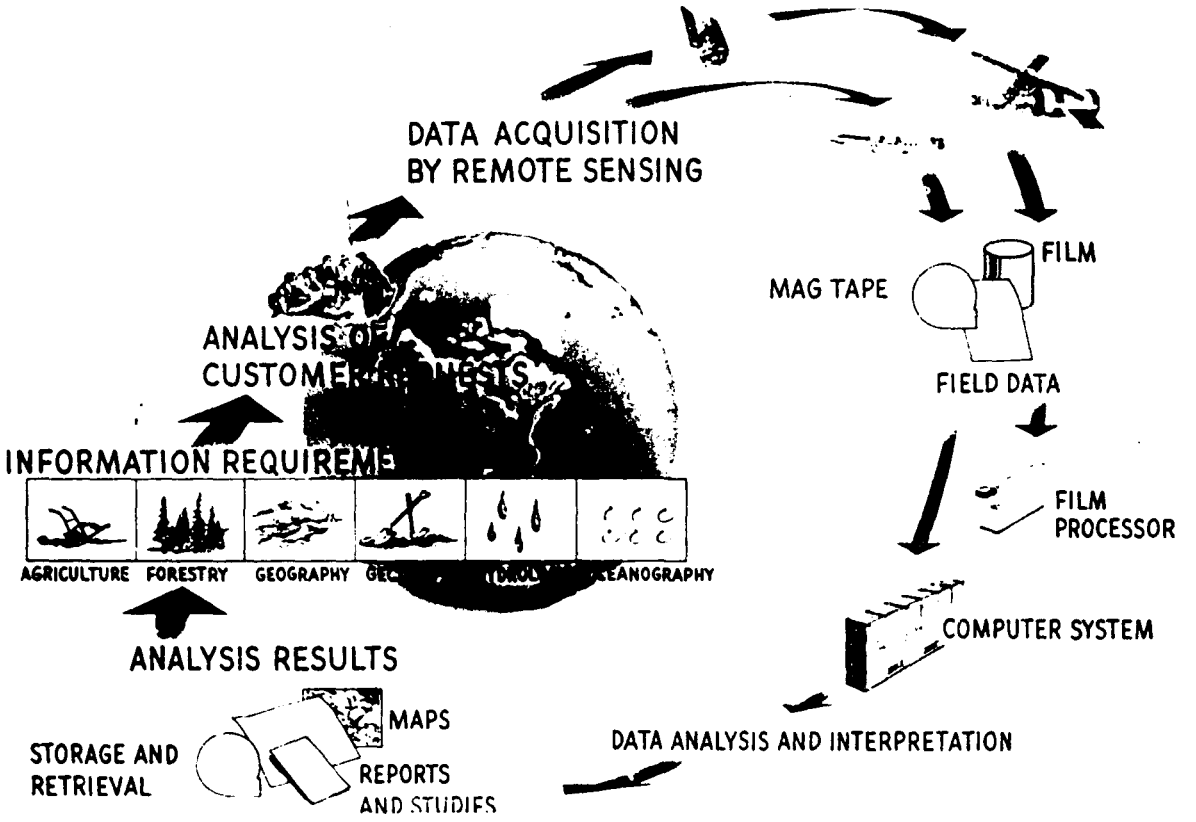

Figure S-3. The role of remote sensing in meeting information needs of the user community.

which the data can contribute to decision-making for a particular application by using appropriate relational models.

Some remotely sensed data are not needed immediately for a particular use but can have intrinsic value for future purposes. These data should be stored in such a way that they can be easily retrieved later. Other data are precisely those sought by the users, usually in near real-time, and should be delivered quickly for current applications. If the delivered products meet requested needs, the loop has closed and the process is re-initiated. If not, modifications may be introduced anywhere in the loop to improve the information quality until the user community is satisfied.

A Worldwide Information System: LACIE

We shall look next at another variant of an information system that leans heavily on satellite data in its functions. The LACIE (Large Area Crop Inventory Experiment) program was described briefly on page 219. This program has been the largest U.S. government-sponsored endeavor to use satellites in a global monitoring system for one practical application: in this instance

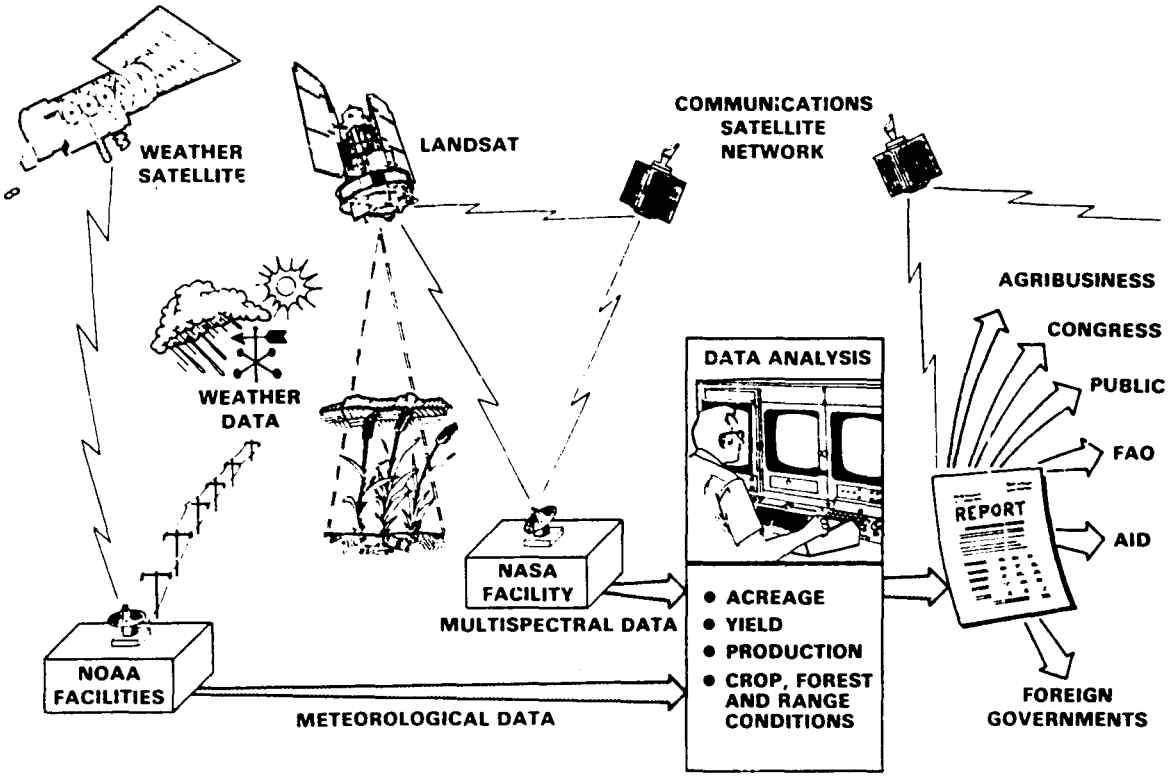

Figure S-4. System for inventory and monitoring global food and fiber.

predicting the production of a single crop—wheat—at a worldwide level.[9] Goals include faster assessments of yield (number of bushels per acre) on a pre- rather than post-harvest schedule, and estimates of annual productivity at least as good as, but preferably better than, current conventional methods of inventory (refer also to the 90/90 criterion given on p. 222).

In an agricultural applications-oriented system, the data used to predict productivity must come from several sources. This is illustrated in Figure S-4. Productivity is measured in terms of yield per acre x acreage. Obviously, even a satellite that produces images of all pertinent land surfaces throughout the globe is subject to limitations, the main one being the sheer magnitude of the data required. Millions of farms may be involved in growing just one crop; the number is compounded for all crops of interest. The strategy is, then, to take representative samples at several levels. This is analogous to the training site sampling philosophy expounded in Activities 5 and 6. A satellite must be able to find these training sites, verify that the crop within each is the type being inventoried, and make some quantitative judgment about yield. Yield data are dependent on adequate ground truth, acquired in the field and through reporting services.

Some spectral properties, such as reflectance (intensity), must correlate with meteorological or ground-based measurements of yield in the training sites at different times during a crop calendar cycle. Moreover, the trends in yield over the season can be predicted (and then verified) by using, among other data, meteorological input acquired daily from both satellites and ground stations. Once a yield function is determined for the training

[9] A good review of the LACIE program is found in *The Proceedings of Technical Sessions, The LACIE Symposium*, 1978, vols 1&2, Johnson Space Center Publication 16015, July 1979, 1123 pp.; See also McDonald and Hall, op. cit., p. 219.

samples, an estimate of total acreage given to that crop must be made by some extrapolation procedure. This is done through incorporation of data from selected sampling districts within the crop-producing regions. During its critical stages of growth, the pertinent crop is repeatedly monitored by an Earth resources satellite while climatic conditions affecting the growing cycle are simultaneously assessed by weather satellites. Yields for these sample acreages within districts are then extrapolated to a total for all relevant countries by assuming that the number, sizes, and characteristics of the districts are reasonable representations of the remainder of the agricultural regions contributing to production of the particular crop. Adjustments should be made to estimates to account for variations in productivity owing to crop conditions (damage, etc.). To be effective as a production estimate, large volumes of data must be acquired and interchanged rapidly (days or weeks at most) from widely separated parts of the world. This involves cooperation not only between American agencies, such as the Department of Agriculture, NOAA, and NASA, but also among government and private sources of crop data in this country and from many nations. A communications network, built around satellites, is a vital link in this comprehensive operation.

The LACIE program is now officially completed. Major research efforts in agricultural applications of satellite data are now being continued within the AgRISTARS (Agricultural and Resources Inventory Surveys through Aerospace Remote Sensing) program. This program is designed to determine the usefulness of remote sensing to improve the objectivity, reliability, and timeliness of such data for future U.S. Department of Agriculture (USDA) multi-crop information systems. In addition to the USDA as the lead agency, together with NASA and NOAA, other cooperating federal agencies now include the U.S. Department of the Interior (through its EROS program) and the Agency for International Development (AID). The announced objective of AgRISTARS is to evaluate remote sensing data, integrated with other data sources, as applied to:

- Early warning of changes affecting crop production (e.g., blight, drought, disease)
- Commodity production (multiple crops)
- Land-use monitoring
- Renewable resources (food and fiber) inventory
- Land productivity estimates
- Conservation practices assessment
- Pollution detection and influence

Commodity crops included in the global study are wheat, barley, rice, corn, and soybeans as grown both in the United States and participating foreign countries and, in addition, cotton, sorghum, and sunflowers in the United States alone.

Our final example is a step beyond the two cases just examined. Consider Figure S-5. This is a generalized outline of a global resources information program for the 1980's and beyond. There are four principal areas of applications: agriculture/range/forest (food and fiber); non-renewable resources (mainly energy and minerals); land use, hydrology, environment (land and water management); and geodynamics (areas of the geosciences that include gravity and magnetic fields; crustal dynamics; solid Earth investigations). Although this diagram is imperfect in its generality, it warrants your inspection because such a broad program serves as a model for development of federally-supported responses to an announced policy by the United States Government to provide information to all nations of the world.

A CLOSING CHALLENGE

You have at last reached the abrupt end of the main body of this workbook. We shall provide no florid exhortations to leave you exhilarated by prospects for the future. The closing will be your responsibility. To finish on an amusing note, look at Figure S-6. This pair of photos shows the famed pigeon platforms actually used in Europe in the early 1900's. The pigeons carried lightweight, automatic-advance cameras timed to produce a set of pictures in flight. One such

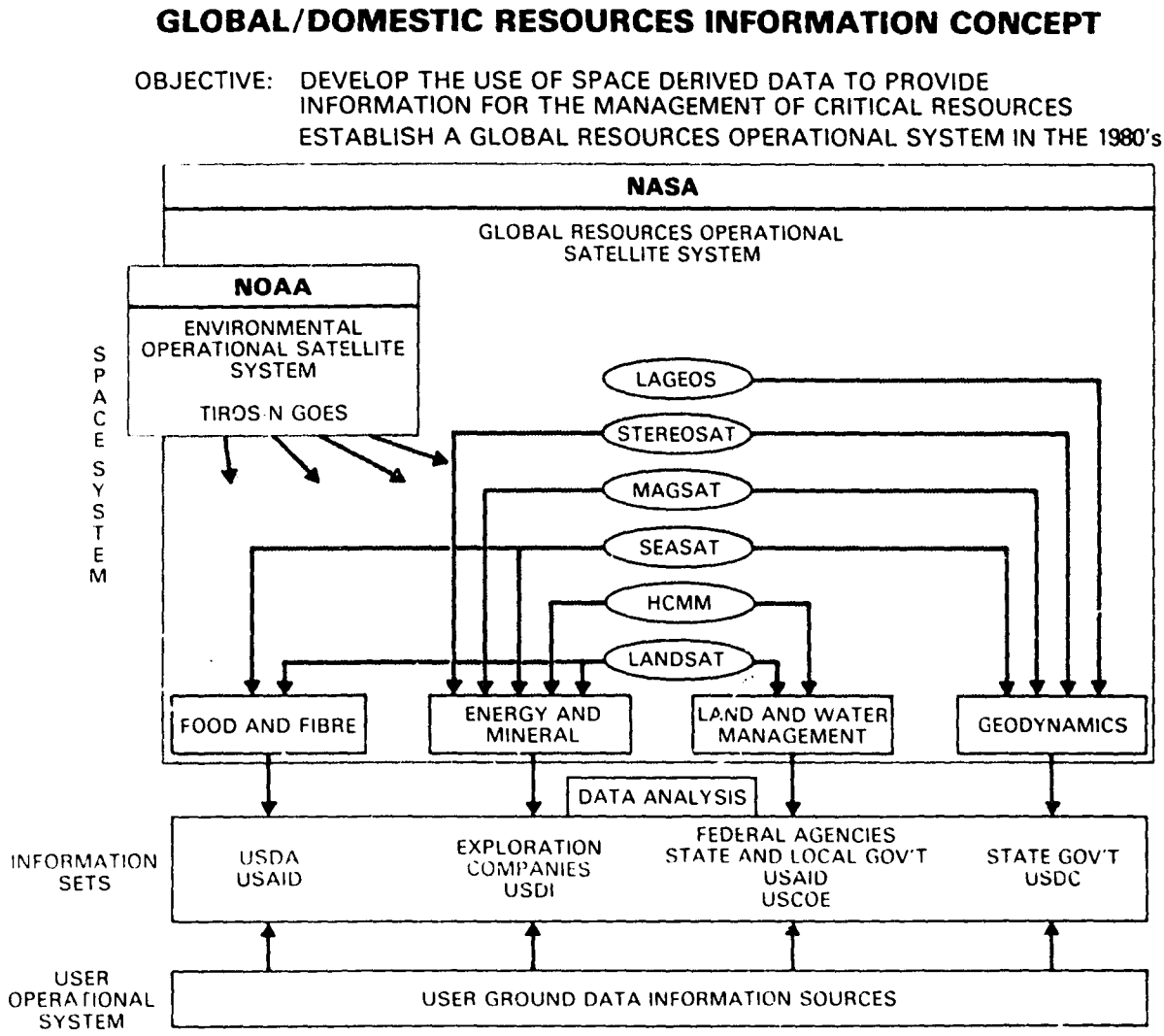

Figure S-5. The Global Resources Information System.

photo of a Bavarian castle is shown in the lower picture, note the wings (crudely analogous to the solar power panels on Landsat). Across the middle is a motto added to this display by the author. It may have many meanings, good or bad, depending on how one feels about remote sensing.

HOW DO YOU FEEL ABOUT THIS NEW FIELD?

In your notebook, write a summary outline, or a list of pluses and minuses for topics of your choice, that reveals your innermost feelings and attitude toward Landsat and remote sensing.

based on what you have learned and accomplished from this Workbook. (If you have grown weary of answering questions with written words, then at the least implant your views and thoughts in some hallowed niche in your mind.)

Remote Sensing is for the Birds!

Figure S-6. A mobile airborne platform with automated sensor and a resulting image of a Bavarian castle.

APPENDIX A
THE LANDSAT SYSTEM[1]

MISSION AND SYSTEM REQUIREMENTS

As initially defined in the late 1960's, the primary Landsat mission was to demonstrate the feasibility of multispectral remote sensing from space for practical Earth resources management applications. The overall system requirements were the acquisition of multispectral images, the collection of data from remotely located ground platforms, and the production of photographic and digital data in quantities and formats most helpful to potential users. In addition, it was required that these data be taken in a specific manner: namely, that repetitive observations be made at the same local time; that the images produced by the sensors be overlapping, both in and across the direction of flight; and that the images be correctly located to better than 3.7 km (2.3 miles). Periodic coverage of each area was to occur at least every 3 weeks. The operating lifespan of the spacecraft and its sensor systems was to be a minimum of 1 year. Finally, it was necessary to process and distribute all these data to investigators in a useful form and on a timely basis.

SPACECRAFT

To accomplish these goals, the Landsat spacecraft was designed and built by the Space Division of General Electric Company in Valley Forge, Pa. This spacecraft, an outgrowth of the Nimbus series of meteorological satellites, was designed to carry two remote sensing systems and a system for collecting data from sensors located in remote places on the Earth, the data collection system (DCS). Some of the more pertinent parameters of the spacecraft are given in Table A-1.

Table A-1
Landsat Spacecraft Characteristics

Weight	959 kg (2100 lb)
Size	3 by 1.5 m (10 by 5 ft); 4-m (13-ft) array
Power	550 W
Attitude control	±0.7°
Attitude measurement	±0.07°
Telemetry	912 points
Commands	520 commands
Thermal	20° C
Wideband videotape recorder	30-min recording capacity each (two recorders on board)
Orbit adiust	~80 m/s

[1]Part of this section was written by Dr. Stanley C. Freden, Chief, Missions Utilization Office, Goddard Space Flight Center, for use in *Mission to Earth: Landsat Views the World*, NASA SP-360.

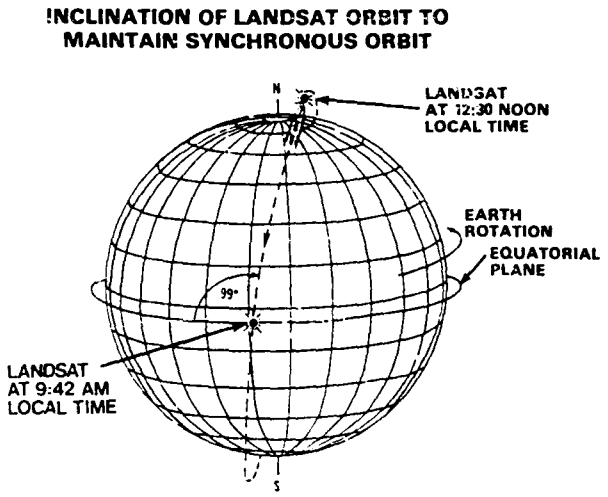

Figure A-1. Landsat spacecraft orbit.

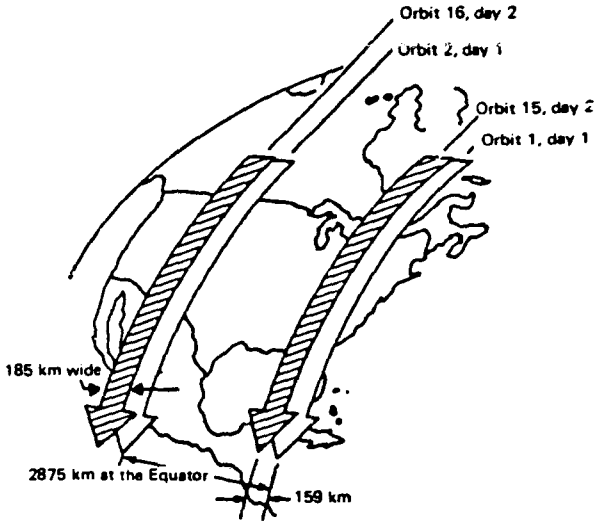

Figure A-2. Landsat ground coverage pattern. There are 14 revolutions per day; global coverage requires 18 days.

ORBIT

The Landsat-1 spacecraft was launched on July 23, 1972, and positioned in the orbit shown in Figure A-1 and Table A-2. Landsat-2 was launched on June 22, 1975, and Landsat-3 was launched on March 5, 1978. Currently, only Landsat-3 is operational. These satellites have a nominal altitude of 917 km (570 miles); 99° orbital inclination, which makes them nearly polar; and a Sun-synchronous orbit, which means that the orbit plane precesses about the Earth at the same angular rate that the Earth moves about the Sun. This feature enables the spacecraft to cross the Equator at the same local time (about 9:30 to 10:00 a.m.) on the sunlit side of the Earth. Each of the two sensing systems on Landsats-1 and -2, return beam vidicon (RBV) and multispectral scanner (MSS), views an area 185 km (115 miles) on a side. On Landsat-3 the RBV system was modified to improve the resolution. Figure A-2 indicates how the requirement for repeat coverage is met. From one orbit to the next, the subsatellite point moves 2875 km (1785 miles) at the Equator as the Earth rotates beneath the spacecraft. The next day, 14 orbits later, it is approximately back to its original location, with orbit 15 displaced westward from orbit 1 by 159 km (99 miles) at the Equator. This continues for 18 days, after which orbit 252 falls directly over orbit 1. As indicated in Figure A-2, there is sidelap of 26 km (16 miles) in coverage at the Equator from adjacent orbits on consecutive days. It is important to note that this sidelap increases with increasing latitude, to approximately 57 percent at 60°. Thus, at high latitudes, sidelap coverage is obtained on consecutive days over a large portion of an image. Sidelap coverage is essential for stereoscopic viewing; it also permits the monitoring of changes that occur over the 1-day period. It should be noted, however, that as the area of sidelap increases with latitude, the stereoscopic viewing angle decreases.

PAYLOAD

The sensors are mounted on the bottom of the spacecraft. The RBV system on Landsats-1 and -2 consists of three television-type cameras, each covering a different spectral region; images are obtained on a frame-by-frame basis. The spectral characteristics of the RBV system are shown in Table A-3. The time between picture sets is 25 s, and readout time is 3.5 s per camera. There are five exposure combinations, running from 4 to 16 ms: (1) 4, 4.8, and 6.4; (2) 5.6, 6.4, and 7.2; (3) 8, 8.8; (4) 12, 12, and 12; (5) 16, 16, and 16. Data are transmitted by the vidicon cameras at 3.5 MHz FM.

The three vidicon cameras are mounted on the base plate with their optical axes aligned. Fiducial marks, engraved into the photoconductor of

Table A-2
Landsat 1 Orbital Parameters

Parameter	Nominal	Initial correction	Current*
Altitude of apogee, km (miles)	917 (570)	912 (567)	919 (571)
Eccentricity	.0001	.0005	.0020
Apogee/perigee difference, km (miles)	1 (1.6)	9 (6)	22.7 (14.1)
Period, min	103.34	103.26	103.26
Inclination, deg	99.09	99.12	99.03
Descending node (a.m.)	9:30	9:42	9:38
Coverage cycle, days	18	18	18

*After 7 orbit corrections through February 4, 1974.

each camera, are used in the geometrical correction of the images on the ground. On Landsat-3 the three spectral RBV cameras were replaced by two panchromatic cameras giving side-by-side viewing at twice the spatial resolution (30-40 m).

Figure A-3 depicts both the concept of the MSS multidetector array and the scanning system. The scanning mirror oscillates through an angular displacement of ±2.89°. Because the angle of incidence is equal to the angle of reflection, the scanned beam is approximately 11° wide. Six parallel detectors in each of the four bands view the ground simultaneously. Thus, each mirror scan covers an along-track distance of approximately 480 m (1574 ft) on the ground.

Although the Instantaneous Field of View (IFOV) is 79 m^2 (67,143 sq ft), the ability to distinguish adjacent objects depends greatly on their shape and contrast. In fact, bridges over water and dirt roads passing through vegetation may be visible even if they are as narrow as 10 m (33 ft).

The DCS provides a mechanism for relaying data collected from remotely situated ground-based sensing platforms and retransmitting through the satellite to the receiving stations. These data are then quickly retransmitted to the data users. Each ground platform can have eight analog or digital inputs. The system has a high probability that data will be received from every platform within each 12-hour period. These sensing platforms are used to measure water flow in rivers, water level, water quality, seismic activity, and similar phenomena. Figure A-4, showing the geometry of the DCS, demonstrates that the spacecraft must be in view of both the platform antenna and the ground receiving antenna.

Table A-3 contains a summary of the Landsat payloads and the parameters of the three major payload systems.

MSS SCANNING ARRANGEMENT

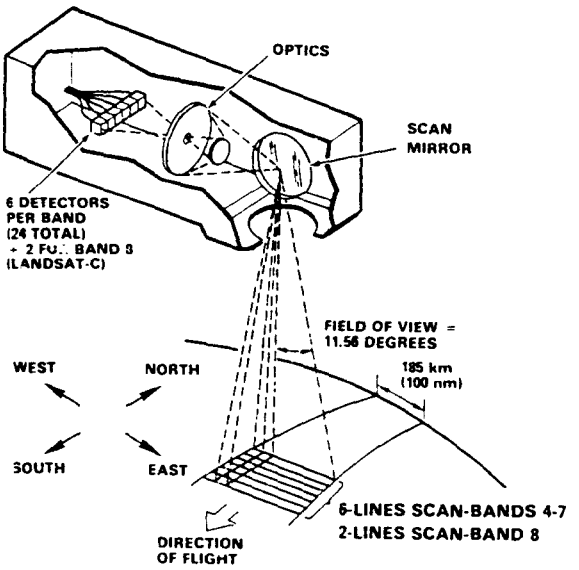

Figure A-3. Operation of the Landsat multispectral scanner (MSS).

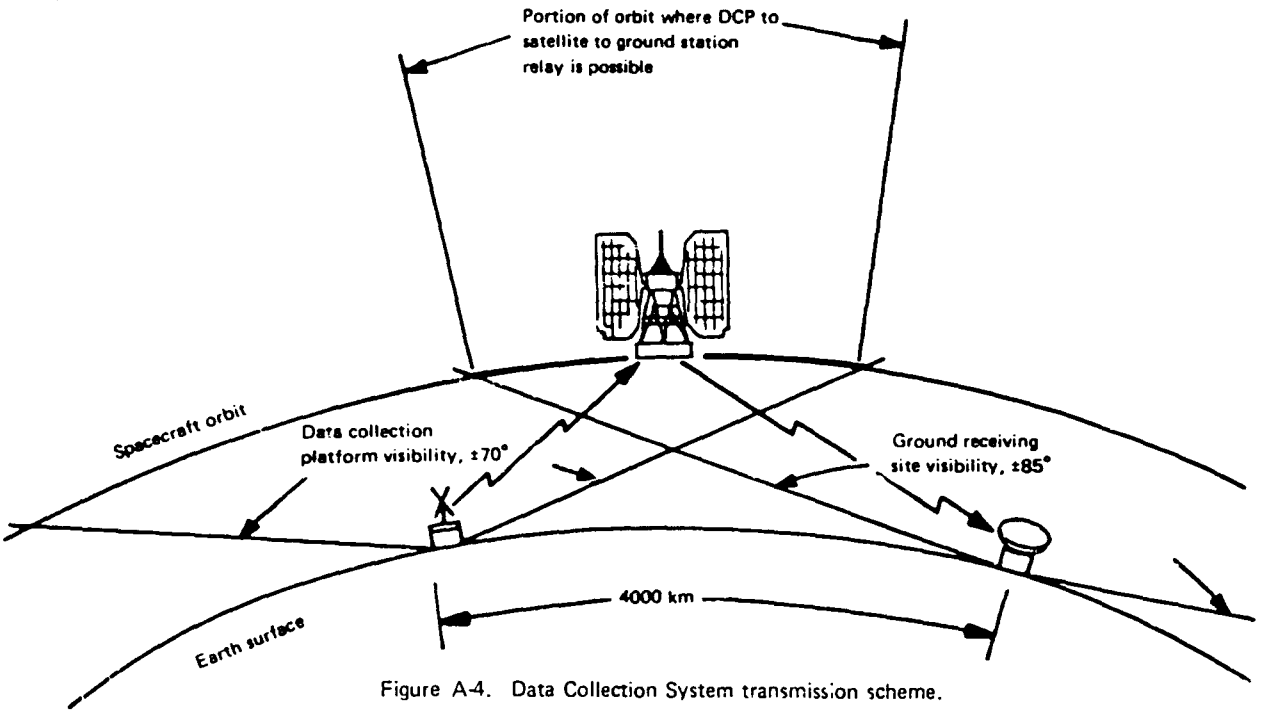

Figure A-4. Data Collection System transmission scheme.

Table A-3
Summary of Landsat 1 Payload Systems

High resolution TV (RBV) cameras:	
Coverage	185 by 185 km (100 n. mi.)
Spectral bands:*	
1	0.48 to 0.57 μm (Blue-Green)
2	0.58 to 0.68 μm (Yellow-Red)
3	0.70 to 0.83 μm (Red-IR)
Data	3.5 MHz video
4-channel MSS:	
Coverage	185 km (115 mi.) swath
Spectral bands:	
4	0.5 to 0.6 μm (Green)
5	0.6 to 0.7 μm (Red)
6	0.7 to 0.8 μm (IR)
7	0.8 to 1.1 μm (IR)
DCS:	
Ground platforms	Up to 1000
Ground platform input	8 analog or digital signals
Data	100 kHz digital

*The single band on the pair of RBV cameras on Landsat 3 extends from 0.505 to 0.750 μm (panchromatic).

GROUND DATA HANDLING

Processing History

In the early days of the Landsat program, all data were processed at Goddard Space Flight Center. A block diagram of the total Landsat data system then in operation is shown in Figure A-5. Video data from the sensors are telemetered to Earth and acquired at three data acquisition centers in the United States (Fairbanks, Alaska; Goldstone, Calif.; and Greenbelt, Md.). In addition, Canada, Brazil, Italy, Sweden, Japan, India and Australia have ground receiving stations for Landsat data, and several more countries are in the process of putting them into operation (Figure A-6). The data from the U.S stations are sent to the NASA Image Processing Facility (IPF), which is part of the Landsat Ground Data Handling System(GDHS) at the Goddard Space Flight Center. In the IPF, high density digital tapes are produced and sent to the EROS Data Center in Sioux Falls, S. Dak., where computer compatible tapes (CCT's) and film products are produced and distributed to the users. Requirements for coverage are fed into the Operations Control Center (OCC). The OCC is responsible not only for the housekeeping management of the spacecraft (for example, power budgeting), but also for command sequences that will activate and deactivate the sensors. Because both the recording capacity of the on-board video tape recorders and the power of the spacecraft are limited, the operation of the sensors must be scheduled very carefully.

The IPF must handle information from various sources, such as the video signals from the two instruments, the ephemeris (which is computed from the orbital tracking data), spacecraft performance (for example, attitude), and the DCS platform data. From these the IPF generates digital tapes of these images. The facility also processes data from up to 1000 data collection platforms (DCP's). The digital images are corrected, scaled, and also annotated with coordinates, gray scale, and geometrical and other identifications.

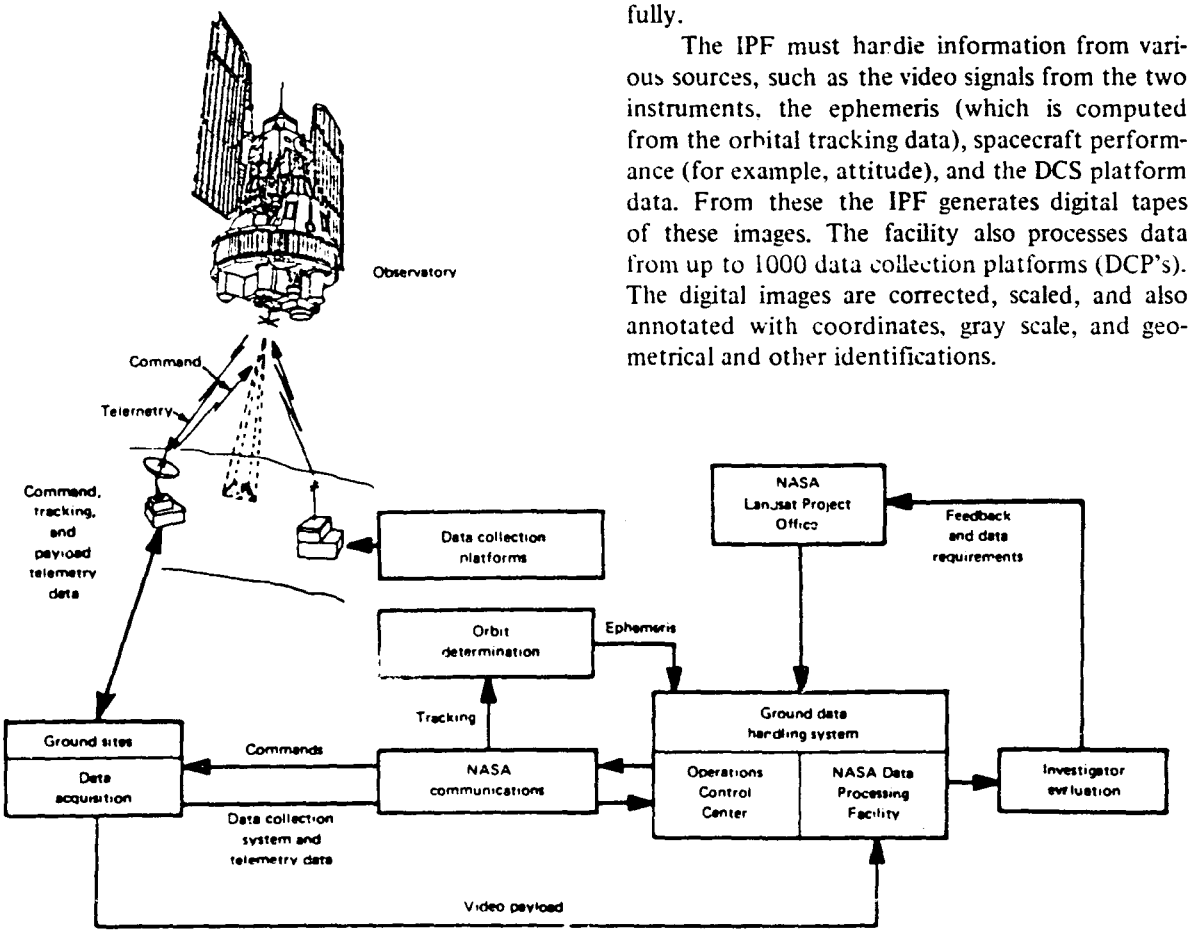

Figure A-5. Initial Landsat-1 data handling system.

CURRENT AND PROBABLE LANDSAT GROUND STATIONS

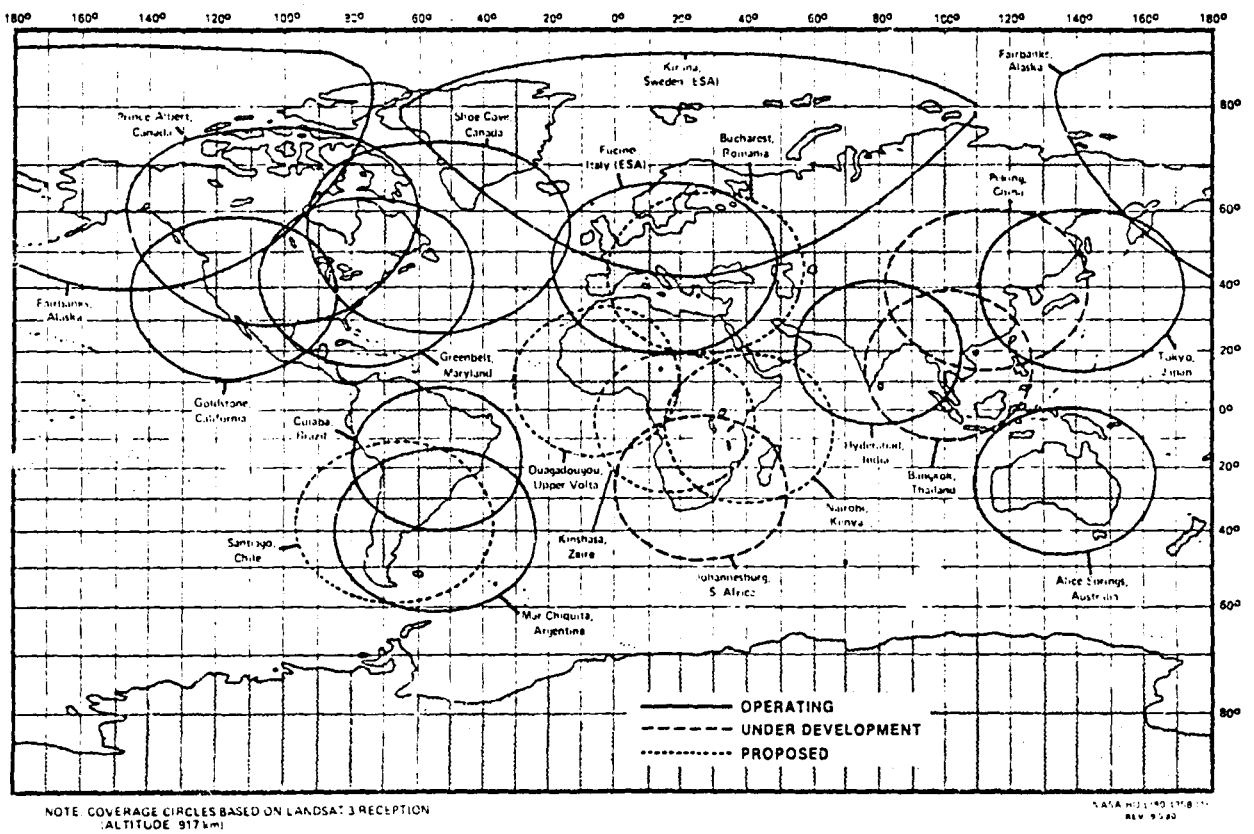

Figure A-6. Worldwide location of operating or proposed ground stations for reception of data transmitted by Landsat.

Current Processing Sequence

Since 1979, both Goddard and the EROS Data Center (EDC) have shared in the role of processing digital tapes, and EDC became the sole distributor of Landsat images and tapes for the U.S. Government. The major steps in the Landsat data handling plan as of 1980 are depicted in Figure A-7. The sequence of events and processing steps involved in producing a fully corrected standard image are described below, as extracted from the Landsat Data Users Notes, Issue 8, September 1979, published by EDC. Keep in mind that the 12-day time line represents somewhat idealized conditions and will likely be stretched out to longer than 2 weeks under many circumstances.

Days 1 and 2. Acquisition begins when the OCC at NASA/Goddard commands the MSS to acquire data over predetermined areas. If the satellite is within transmitting range of one of the three U.S. reception facilities (in Alaska, California, and Maryland) or any operated in foreign countries through agreements with NASA (Figure A-6), the data are transmitted immediately in real time. If the satellite is not within range, the data are recorded on onboard tape recorders for transmittal later when the satellite comes into range.

The receiving stations receive the data via tracking antennas and record it on wideband video tape. Each morning, the data received at the Alaskan and Californian stations are transmitted in wideband video form to NASA/Goddard, where processing of the data starts. A commercial domes-

tic communications satellite system (Domsat) serves as the link over which these transmissions are made.

Day 3 to Day 9. At NASA/Goddard, initial processing (preprocessing) consists of converting the wideband video data to digital form. At this time, the data are band interleaved by line. The output is a high density tape (HDT) known as an "F" tape.

Concurrently, an index tape called the Ancillary Data Tape (ADT) is prepared on the Goddard Sigma 5 computer. The ADT is used to create work order cards that control and schedule the processing of data at Goddard.

The preprocessing digital data are then processed through the Master Data Processor (MDP), which performs both radiometric and geometrical corrections. The geometrical corrections include corrections for band-to-band offset, line length, Earth rotation, and detector-to-detector sampling delay. In addition, the image data are mapped to the Hotine Oblique Mercator map projection, by using a geometrical model based on ground control points, or systematic data if ground control points are not available. A cubic convolution resampling technique is used in this process. The result is a high density tape denoted as a "P" tape.

The MDP also creates the annotation data (latitude/longitude tic marks, etc.) that will appear on each image when reproduced. The Sigma 5 computer creates a Goddard HDT Inventory Tape (GHIT) for use later at the EROS Data Center.

This processing by NASA/Goddard currently requires approximately 7 days if no problems are encountered.

Day 10. When processing at NASA/Goddard is complete, the corrected high density image tape data are transmitted, by using the Domsat communications link, to the EROS Data Center. The

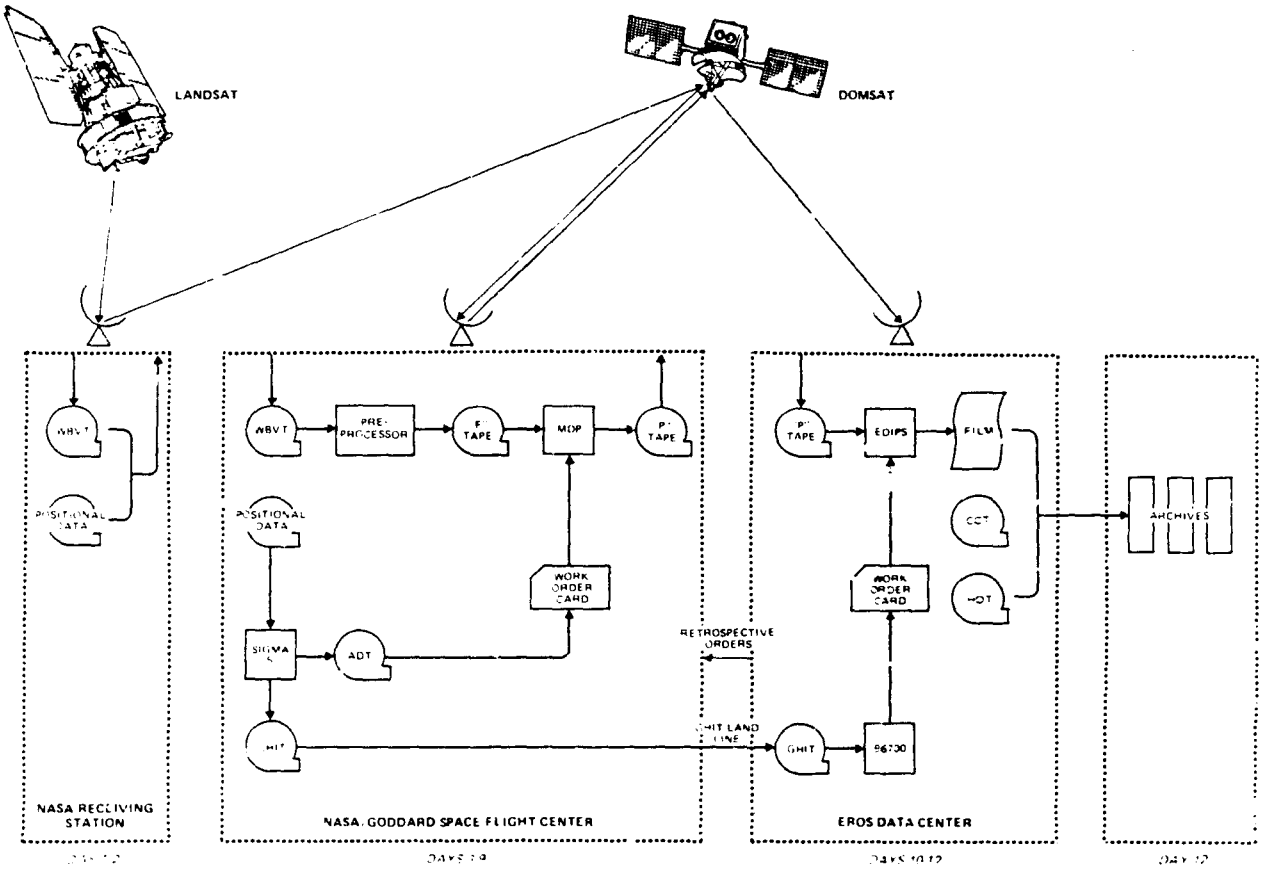

Figure A-7. The current data handling system for Landsat-1, -2, and -3 in operation since 1979.

digital data microwave transmissions are received by an antenna at EDC and rerecorded on high density tape. At this point, the data are ready for processing by the EDC Digital Image Processing System (EDIPS).

Concurrently, the Goddard-prepared GHIT is transmitted over a leased-line telecommunications link on the ground. The GHIT is used to prepare EDIPS work order cards for scheduling and control of image data processing at EDC.

Day 10 to Day 12. The high density image tapes are matched with the corresponding work order cards and both are input to EDIPS. As the tapes are read, a microprocessor generates a histogram of pixel values, computing the total number of pixels occurring at each of 128 digital levels of intensity. EDIPS then applies a haze removal algorithm and formats the digital data for input to an on-line laser beam recorder. Magnetic tape recorders are also on-line and can accept the formatted data and create computer compatible tapes (CCTs).

Once exposed, the film is delivered to the EDC Photographic Laboratories. It is developed, inspected, checked for density and scale, and assessed for image quality and cloud cover. After passing quality assurance, it is cut into individual images and archived.

Archival film and the fully processed high density tapes received from Goddard are maintained at EDC for product generation and dissemination. Computer compatible tapes are created, when needed, from the high density tapes in storage.

The processing that takes place at EDC requires approximately 3 days. If no major problems are encountered at any point from original acquisition by NASA to entry into the EDC archives, under optimum conditions a total processing time of 12 days could be expected. Any processing of orders from customers and dissemination of products would follow subsequently.

This nominal time line for processing of standard products may deviate widely if nonstandard products are involved. These would include products such as corrected data in different map projections, or uncorrected data. Such data products must be processed retrospectively through the system, and allowances for extra time should be made depending on the particulars of the nonstandard product ordered.

Landsat-D Data Handling Plan

The plans for handling the MSS and TM data from the Landsat-D series of spacecraft are still in a state of evolution, and some of the current decisions undergoing implementation are subject to change. As summarized by Dr. Vincent V. Salomonson, the Landsat-D program scientist, the major highlights and aspects of the Landsat-D program as of March 1981 are as follows:[2]

- Landsat-D to be launched by the third quarter of 1982 (target date: July 31, 1982)
- Landsat-D′ launch readiness to be achieved within 12 to 15 months after Landsat-D launch (target date: July 31, 1983)
- Tracking and Data Relay Satellite System (TDRSS) to be Landsat-D/D′ observatory to ground-segment communications network
- Ground Station Tracking and Data Network (GSTDN) will be employed until TDRSS becomes available
- Data to be transmitted directly to foreign ground stations
- Global Positioning System (GPS) to provide ephemeris data
- Predictive-fit ephemeris to be used until GPS becomes operational
- Protoflight thematic mapper to fly on Landsat-D, but will not cause delay of launch if not ready
- Angular displacement sensor to be flown on Landsats D and D′
- MSS data processing to begin at Landsat-D launch plus 14 days
- NASA to conduct TM evaluation at the 1-scene/day level during first year and TM R&D processing at the 12-scene/day level during the second year of Landsat-D mission life
- TM R&D quality data to be available on a limited basis beginning 1 year after Landsat-D launch

[2] Salomonson, V.V., Proc of SPIE Technical Symposium East '81, Society of Photo-optical Engineer, Apr 20-24, 1981, Washington, D.C.

- TM proves processing capability at the 12-scene high-density tape, 12-scene 241-mm film master, and 2-scene computer-compatible tape product level per day to be achieved by July 31, 1984
- TM processing capability at the 50-scene high-density tape, 50-scene 241-mm film master, and 10-scene computer-compatible tape product level per day to be achieved by January 31, 1985 (assuming that a TM will be launched by July 1983)

Ground segment performance and production requirements are shown in Tables A-4 and A-5. For the phase of data handling to be conducted at Goddard, the ground system components now planned for Landsat-D are compared in Figure A-8 with those developed for the earlier Landsats. Flow diagrams for the image generation process are given in Figure A-9 for the MSS (top) and TM (bottom) sensors. The output from both processes are high density tapes that are sent elsewhere for production of images and CCT's for the user community.

Table A-4
Landsat-D/D' Ground-Segment Image Performance Requirements

Function/Operation	Performance Objective
Turnaround	48 hours from collection of raw sensor data to generation of MSS archival products (worst-case averaged over 10 days)
Radiometric error correction (relative interdetector)	1 quantum level over full range
Geometric error correction (nominal conditions with GCP's)	0.5 sensor pixel (90% of the time) (with sufficient correlatable ground control points)
Temporal registration error	0.3 sensor pixel (90% of the time) (with sufficient correlatable control points)
Map projections supported	Space oblique mercator Universal transverse mercator/polar stereographic
Resampling algorithms supported	Cubic convolution Nearest neighbor

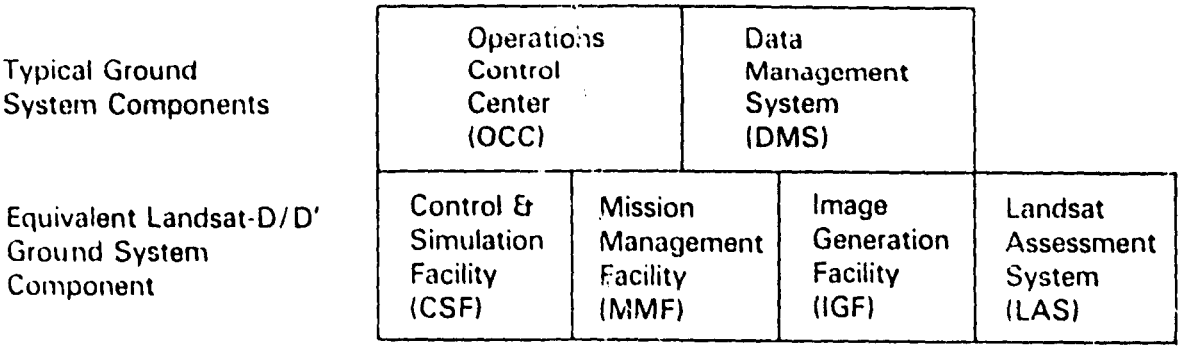

The MMF, the CSF and the IGF represent the logical extensions of the Operations Control Center and Data Management System concepts prevalent in the 1970s.

Figure A-8. Ground systems components at Goddard Space Flight Center for Landsat-1, -2, and -3 (top) and proposed for Landsat-D (bottom).

Table A-5
Landsat-D Production Requirements*

No.	Product	Quantity Required for NOAA (Scenes/Day)	When Available
1	MSS A tape (HDT) (user product) MSS 70-mm film (QC product) (one band)	200	a. Capability for 200 scenes/day at launch b. Turnover operational system to NOAA, 200 scenes/day at D launch plus 6 months
2	MSS CCT (A or P) (QC product)	2	At launch of Landsat-D
3	MSS 241-mm film (QC product)	4	a. At launch of Landsat-D: 2 scenes/day b. Launch + 90 days: 4 scenes/day
4	TM A tape (HDT) (user product)	100	a. In July 1983, 12 scenes/day with *a priori* jitter correction b. By April 1984, 12 scenes/day must be demonstrated* c. Turnover operational system to NOAA, 100 scenes/day, in January 1985*
5	TM P Tape (HDT) (user product)	50	a. In July 1983, 12 scenes/day with *a priori* jitter correction b. By April 1984, 12 scenes/day must be demonstrated** c. Turnover operational system to NOAA, 50 scenes/day in January 1985**
6	TM CCT (A or P) (user product)	10	a. In July 1983, 2 scenes/day b. By April 1984, 2 scenes/day must be demonstrated c. Turnover operational system to NOAA, 10 scenes/day in January 1985**

*Scenes/day are defined as output with a 48-hour turnaround averaged over a 10-day period.
**Assumes that a thematic mapper will be launched by July 1983.

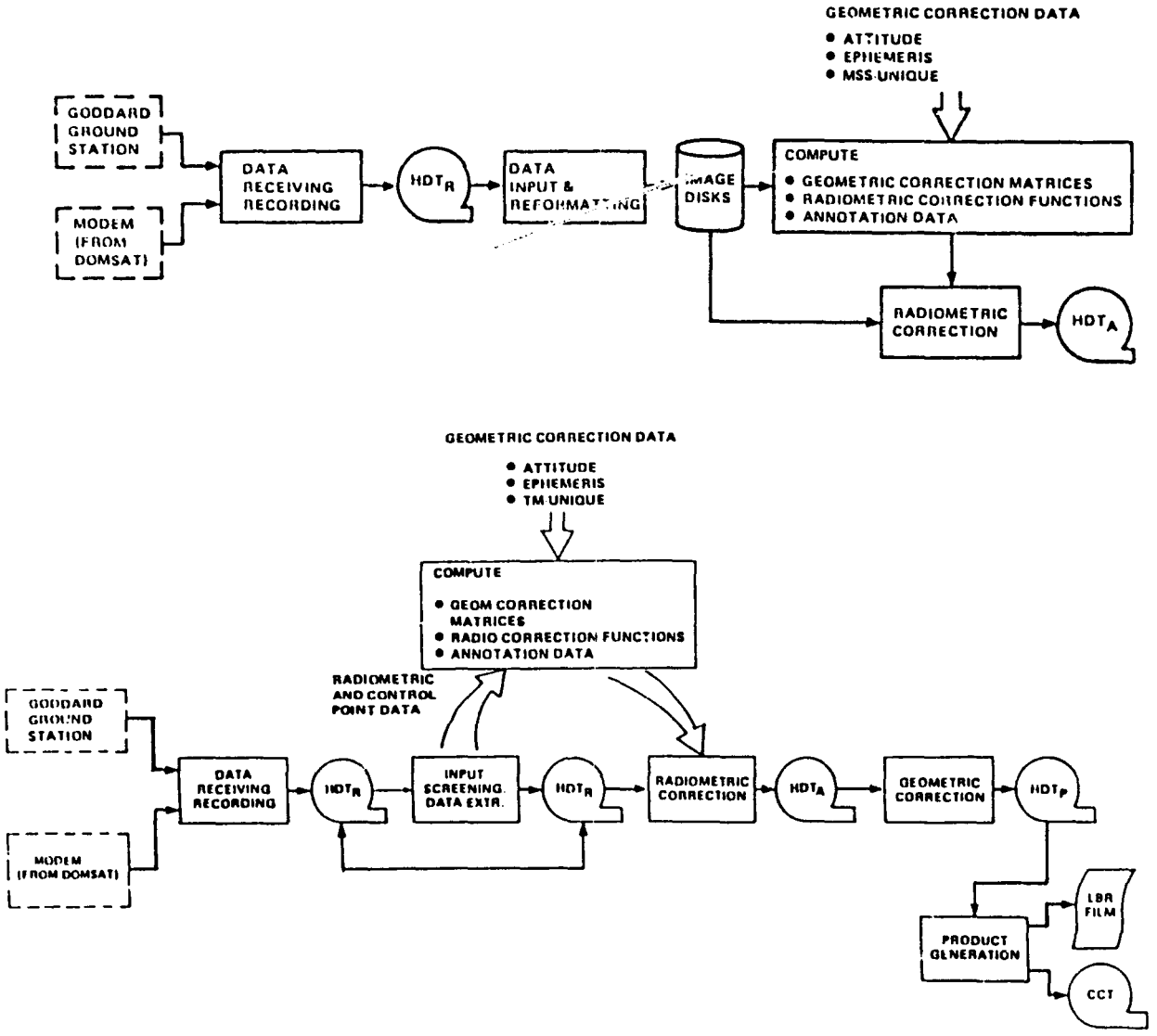

Figure A-9. Landsat-D image generation process flow for MSS (top) and TM (bottom) data.

N83
10470

UNCLAS

APPENDIX B

PRINCIPLES OF COMPUTER PROCESSING OF LANDSAT DATA

SOME GENERAL CONSIDERATIONS

The limitations to photointerpretation mentioned at the beginning of Activity 5 (p. 146) severely restrict the usefulness of the Landsat system for many much-needed applications. The computer, with its special capabilities, can overcome this deficiency by virtue of its volume capacity, its memory, its precision in measuring small differences, its flexibility, and its facility for carrying out complex mathematical operations and for numerous repetitions of the same processing steps. Specifically, computer processing facilitates extraction of information from every pixel by executing a variety of functional operations, called processing algorithms, in general or specialized routines. The best results are obtained when data from more than one multispectral band are used together.

Before reading on, it would be wise to consider the two tables on page 147, which outline the various ways in which computer processing assists in the interpretation and uses of satellite data for Earth resources applications. Remember that many of the techniques and resulting image displays discussed in the following pages have previously been documented visually in Activity 5. In presenting the specific principles and topics considered in this appendix, it is assumed that the reader has some basic understanding of digital or binary codes, of how computers operate as machines, and of the common concepts and terms that underlie today's computer technology. For an in-depth review of data processing built on a mathematical foundation, consult H. Moik, *Digital Processing of Remotely Sensed Data*, NASA SP-431, 1980, 330 pp. (Government Printing Office, Washington, D.C.)

STATISTICAL BACKGROUND

In addition to some awareness of computer fundamentals, a knowledge of statistical methods, with emphasis on multivariate analysis, would serve as a useful background for some of the concepts treated in this appendix, Activity 5, and parts of Activity 6. Pertinent topics in those sections of the workbook are presented with the presumption that the reader appreciates some basic terms in statistics, but familiarity with these terms is not always essential to understanding the remote sensing topics. The interested reader with mathematical inclinations may refer to Chapter 3 in *Remote Sensing: The Quantitative Approach,* by Swain and Davis (see reference in Appendix G), or, for a more general treatise, may consult Anderson, T.W., *An Introduction to Multivariate Statistical Analysis* (J. Wiley & Sons, New York), 1958.

For those with little experience in statistics, here are some key ideas in a nutshell.

Measurements of a particular parameter that are associated with a class will constitute a statistical *population* (a well-defined set of elements associated with representative individuals of a class). The values for a given sample of the elements will show variations due to natural differences and/or to errors of measurement. These values are usually distributed in some characteristic frequency of occurrence, such that one value (central value) occurs most often and other values less so in a systematic or random way. The frequency distribution is governed by appropriate rules of probability. The *normal* or *Gaussian* distribution appears as the familiar bell-shaped curve in which the central value corresponds to the *mean* (μ for population, $\bar{x}$ for sample), the arithmetic average, computed as the sum of all values x_i divided by the number of measurements n in the population or sample. The spread or dispersion of values about the mean is given by the *variance* (σ^2, for population; s^2 for sample subset; the sample variance is an efficient estimator of population if the samples are selected at random from a normal distribution), calculated as $\sigma^2 = \Sigma_{i=1}^{n} (x_i-\mu)^2 / n$ or $s^2 = \Sigma_{i=1}^{n} (x_i-\bar{x})^2 / n-1$, where each observed value x_i from 1 to n is differenced with respect to μ or $\bar{x}$, squared (thus changing any negative values to positive), and summed (Σ). The square root of the variance, as σ or s, is termed the *standard deviation*. For a normal distribution, some 68.3 percent of all observed (measured) values fall within $\pm 1\sigma$.

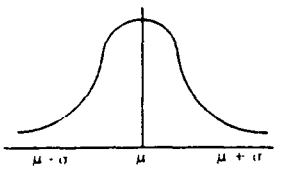

Covariance is a relevant property in the analysis of multivariate distributions. Several variables that describe a given population may or may not be related to each other. Covariance is a measure of such a relation between two variables. It is defined as

$$s_{ij} = \Sigma_{k=1}^{n} (x_{ik} - \bar{x}_i)(x_{jk} - \bar{x}_j) / n-1$$

where (x_{ik}, x_{jk}) are the values of variables x_i and x_j characterizing the k^{th} sample and $(\bar{x}_i, \bar{x}_j)$ are the means of these variables over the samples 1 through n. A high value of covariance indicates that the two variables are highly correlated, and it is therefore redundant to measure both variables. When handling multivariate distributions, it is convenient to arrange the covariance between all possible pairs of variables in a two-dimensional array called the variance-covariance matrix (commonly, shortened to covariance matrix). For a three-variable case, such a matrix would be as follows:

$$\begin{matrix} s_{11}^2 & s_{12} & s_{13} \\ s_{21} & s_{22}^2 & s_{23} \\ s_{31} & s_{32} & s_{33}^2 \end{matrix}$$

Note that s_{11}^2, s_{22}^2, s_{33}^2 are simply the variances of the individual variables. Also, $s_{31} = s_{13}$, etc., that is to say, the covariance matrix is "symmetrical."

In remote sensing, all pixels associated with any one class present in a scene constitute the sampled subset of the population of all values (of a specified property or parameter) for that class. Reflectance may be the variable to be considered; other variables could be chemical composition, density, etc., which may be closely tied to reflectance or may have no inherent relation. More commonly, the property (of reflectance) is expressed as two or more interrelated variables, such as intensity of reflected radiation and wavelength. For the Landsat MSS, each band (collection of wavelengths) may be considered as an independent variable which, in turn, has radiance (or radiant intensity) as a dependent variable. For a given surface class, the pixel DN's represent a series of dependent variable values as measured in each band. For any class, some spread of DN values (because of natural variation, the mix effect, errors) will occur within each band. When measurements on two different classes M and N are made in only one band, the spread of values for one class may be similar to that of a second class. This may also hold true for a second band considered independently (Figure B-1A). However, when the DN values for each and every pixel for both classes and both bands are plotted together (one against the other) on a simple *X-Y* diagram, a separation normally is achieved (Fig. B-1B).

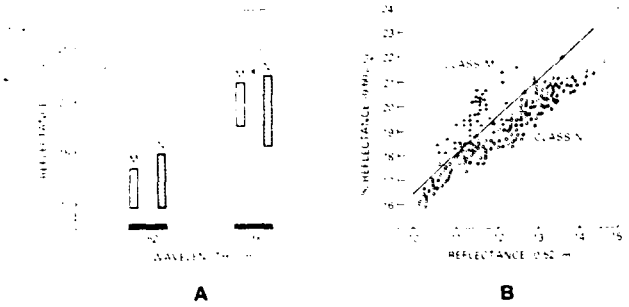

Figure B-1. Improvement in separability of two classes (M and N) by increasing measurement bands from one (A) to two (B) (modified from Swain and Davis, 1979).

Various statistical manipulations and tests are available to determine whether pixels belong to the same class (same population) or to different (and separable) classes. Other techniques can determine whether supposedly independent variables (e.g., two wavebands in different regions of the EM spectrum) are actually independent or are really correlated and hence redundant (so that measurement by either would suffice).

COMPUTER TAPE CHARACTERISTICS

Returning now to our consideration of computer processing, it will be instructive at the outset to highlight the characteristics of Landsat computer compatible tapes (CCT's). First, they are generated by conversion of the digital data recorded on wideband video tape at the various receiving stations in the United States and worldwide. For data acquired by U.S. receiving stations, the CCT's are produced by the Image Processing Facility (IPF; before mid-1978 this was known as NASA Data Processing Facility or NDPF) at Goddard Space Flight Center, and then sent to the Department of Interior's EROS Data Center (EDC) at Sioux Falls, S. Dak.

Each standard Landsat image (Figure B-2) is constructed from a sequence of 2256 scan lines and a variable number of pixels, set nominally at 3240.[1] In the CCT for the corresponding scene, the number of scan lines is fixed at 2340, and each line is adjusted to 3318 pixels by introduction of enough "bogus" pixels to fill a line so that its length is equivalent to a constant ground distance for a standard orbital altitude. Thus, for any given band, the total average number of pixels will be 3318 pixels/scan line × 2340 scan lines = 7,764,120. For the four bands the composite total of pixels is therefore 31,056,480.

In order for a computer to read a CCT, data on the tape must be arranged in a suitable format. Programs for conversion from one format to another are available. Information about data struc-

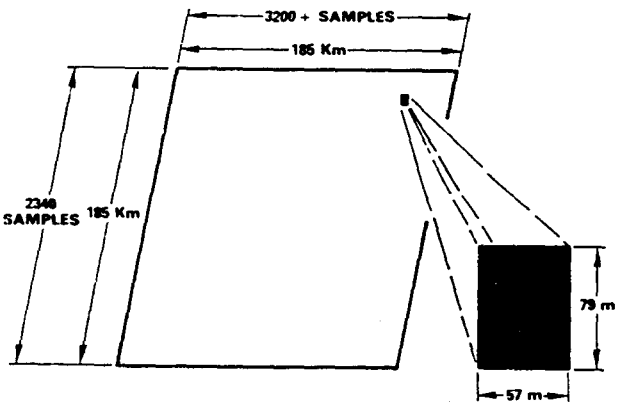

Figure B-2. The pixel makeup of a standard Landsat image.

[1] This number changes from scene to scene owing to variations in orbital altitude and mirror scan velocity.

ture and contents within files on a CCT are contained in header records. Three essential pieces of information are required.

1. *What are the number of tracks*? Since the DN's for a pixel are recorded on-board over a range of 0 to 63 (2^6 values), the minimum number of tracks needed on a CCT will be 6. One additional track is used for parity check. However, the DN range is commonly expanded to 0 to 255 (2^8 values), for which 8 tracks are required. Therefore, the data are normally recorded on either 7- or 9-track CCT's; the 9-track format is more frequently used today.
2. *What is the data density on a tape*? Until the launch of Landsat-3, the packing of data within each track was fixed at either 800 or 1600 bits per inch (BPI). While this CCT mode will continue to be furnished, after 1978 a high density digital tape (HDDT) containing up to 100 Landsat scenes on a large diameter reel will be an optional product available from the EROS Data Center for those equipped to handle this mode.
3. *How are the Landsat band data presented*? Two common options are *band sequential* and *band interleaved* (Figure B-3). In the first case, all data for a single band covering the entire scene are written on one file, usually on one 800 BPI tape. Thus, four standard (10-in diameter; 1-in width) tapes are needed (or one if the more efficient 1600 BPI packing is used). In the second case the data for the four bands are often written line by line on the same tape (there are other formats, such as interleaved pixel by pixel). For the 800 BPI density, each of four standard tapes will cover one-quarter of the Landsat data; for 1600 BPI all the data are included on one tape.

In working with the data sets in a CCT it is helpful to reference the locations within a scene according to some grid coordinate system that relates directly to the pixel distribution. Overlay 3 in the Back Pocket shows how this is done for a 1:1,000,000 scale image product. This skewed X-Y system simply uses the elements or pixels as X values and the scan lines as Y values; the origin or 0 point is here located in the upper left. When specifying the approximate location of an area of interest within a scene to be computer processed, these grid values may be quickly determined by placing such a transparent overlay on a Landsat image of the same scale.

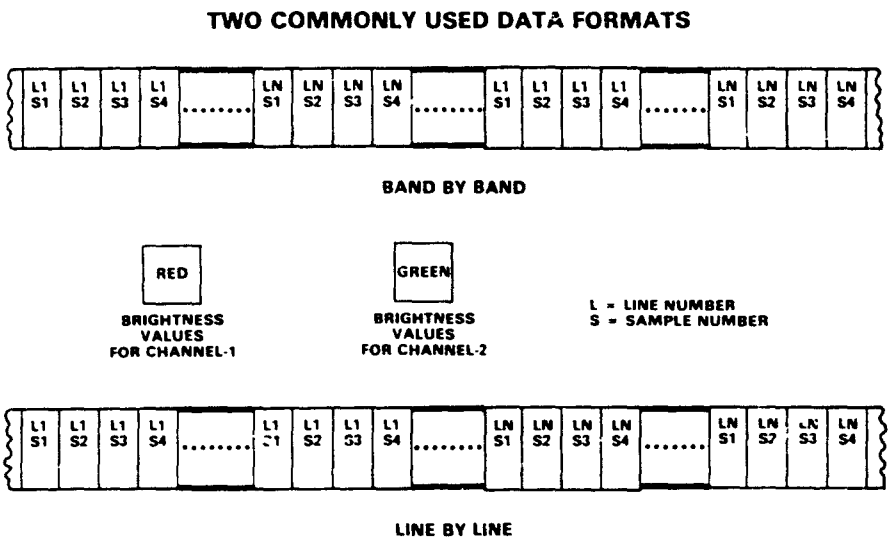

Figure B-3. Band by band and line by line data formats.

PROCESSING MODES

There are two basic approaches to computer-aided processing of Landsat data: (1) the batch mode, and (2) the interactive mode (usually with graphics and/or pictorial TV console display). In either processing mode, the user draws upon his knowledge of the areas being investigated and his experience in making interpretations and assessments according to the types of problems or data analysis. Ancillary information, in the form of maps, aerial photos, previous field trips, or general familiarity with the kinds of discipline-related results expected, are commonly integrated into the processing, as real inputs into the computer and/or as conceptual models in the user's mind.

In the batch mode a job or processing task is submitted through a terminal or card reader to a central processing unit and auxiliary hardware (e.g., an IBM 360/75) as one of many jobs run simultaneously. The desired output may be returned shortly if the computer is not under a heavy workload but, more frequently, will be produced some hours later, overnight, or occasionally later. For some computer systems the user generally relies on a programmer or "data tech" to define the best programs for the particular operations and to submit and retrieve the specific products. However, the user may instead select the precise algorithms and routines to be executed if reasonably familiar with the structure and content of the programs. An example is the VICAR system initially developed by the Jet Propulsion Laboratory (JPL) for processing data from lunar and Martian images, but since modified and expanded to handle terrestrial remote sensing data. Frequently, after suitable training, the user also becomes the operator and carries out the entire processing on a remote terminal. To some extent there is interaction with the processor, such that changes in parameters or choices of new training sites may be introduced until an optimum result based on user-set success criteria is reached.

In interactive graphics systems, the user has even more direct involvement with and close control over the operations being performed (usually on a minicomputer). Furthermore, he sees both intermediate and final results on a display unit almost immediately after taking appropriate processing steps. The user can thus make simultaneous decisions to improve the quality of these results and to check their validity. During normal operation, the user displays the scene (individual bands or color) on the TV screen and conducts processing on the terminal, the console controls, or in some systems with a series of buttons (switches) that access hardwired routines. Image enlargements (scaling) are common choices to define scene content more closely for further analysis. Full or subset scenes may be contrast stretched, ratioed, or otherwise enhanced by using applicable routines. Areas of interest can be blocked out with a movable light cursor whose dimensions and positions in the scene are controlled by a console joystick or a track ball.

Commercial interactive systems that have been applied to remote sensing data include General Electric's Image 100, the Bendix MDAS, the Electromagnetic Systems Laboratory IDIMS, International Imaging Systems' I²S, and Comtal Corporation's Series 9. In addition, interactive systems have been developed at several university and federal institutions, such as JPL's VICAR, the University of Kansas' KANDIDATS, and the NASA Earth Resources Laboratory's PATREC.

In either approach, the results sought must be documented as hard copy. This may have various forms (not all compatible with both approaches): chiefly, line printer output in pictorial (alphanumeric characters or shadeprints) or tabular formats, photographs of images from TV consoles, and data tapes in formats designed to produce pictures from such optical/photo computer-driven systems as electron and laser beam recorders and other film recorder units (for example, Dicomed; Optronics).

CHOICE OF SYSTEM

Choice of the approach and system is strongly dependent on the nature, scope, and volume of work to be performed, the level of financial support, the anticipated cost benefits, and the current availability of time-sharing opportunities. Batch systems may be developed at any institution possessing adequate hardware by purchasing suitable programs or software in the public domain from COSMIC[2] or from commercial suppliers. An investment of $10,000 to $100,000 is normally required, together with a period of 3 to 12 months to become operational. Table B-1 presents a list of Software Systems currently in use within the United States for analyzing multispectral data; some of these are available through COSMIC. Time on several batch systems, such as Purdue University's LARSYS and Pennsylvania State University's ORSER, may be rented at costs from a few hundred to several thousand dollars per month depending on the scope of work; terminals and printer/plotters may also be rented or purchased directly. Interactive systems are generally more expensive and have until now required outlays of about $50,000 to $500,000, depending on prior availability of basic computer components and the amount and sophistication of other hardware and software selected. However, less expensive systems will soon be on the market.

Aspects of both approaches may be contained in a system. The flow chart in Figure B-4 describes one such combination, as developed from JPL's VICAR software coupled with GE's Image 100 and other subsystems.

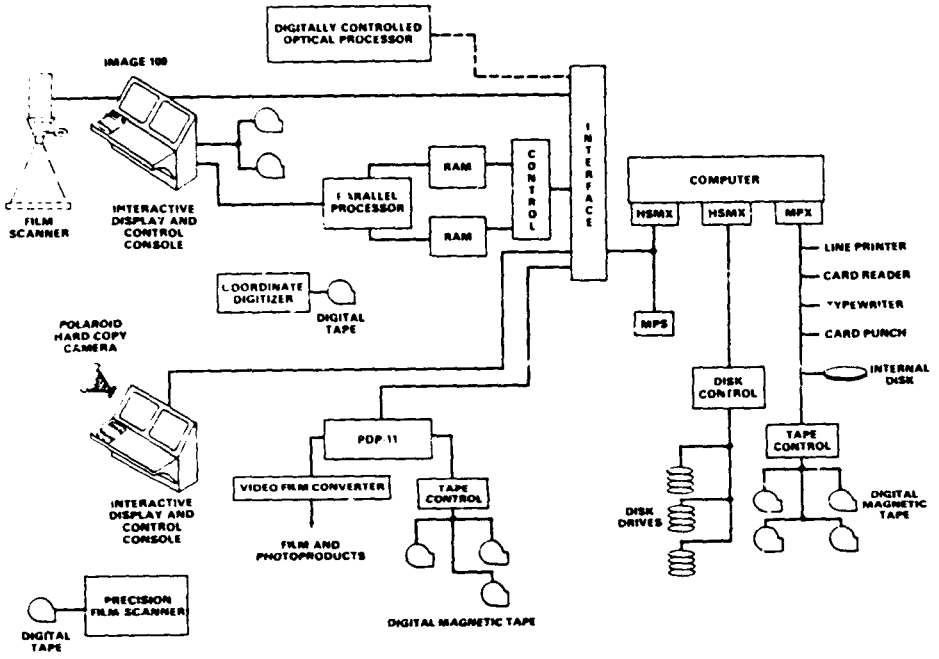

Figure B-4. The JPL hybrid interactive image processing system.

[2]COSMIC (Computer Software Management and Information Center) is a federally funded facility run by the University of Georgia, Athens, Ga., from which computer programs developed under government sponsorship may be purchased.

TABLE B–1

Software Systems
For
Multispectral Data Analysis

Acronym	Organization	Computers
---	University of Wisconsin	UNIVAC 1108, 1110
ARGOS	New Jersey/DEP	IBM 360, 370 UNIVAC 1108
ASTEP-II	JSC, GSFC	UNIVAC 1108, IBM 360
DAM	JSC	UNIVAC 1108
DIAL	GE	PDP 11
EDITOR	USDA/ESCS; WRAP	DEC-10
ELAS	ERL	VARIAN
ERDAS	ERDAS, INC	MICROCOMPUTER (Z-80 CPU)
ERIPS	JSC	IBM 360
GEOPIC	EARTHSAT	IBM 370
IMPAC	D. Egbert Assoc.	MICROPROCESSOR
ISURSL	Indiana State University	IBM 370
KANDIDATS	University of Kansas	PDP11, IBM, CDC
LARSYS	Purdue University	IBM 3031, DEC-10
LIGMALS	ERIM	AMDAHL 470
LIMAP	South Dakota SPB	IBM 360
ORSER (OCCULT)	Pennsylvania State University; ERRSAC	IBM 370
RIPPER	Stanford University	PDP10
UMIPS	University of Minnesota	CYBER 170 SERIES
VICAR	JPL, GSFC	IBM 360, PDP11
XPLOR	CDC	CYBER 170 SERIES

MAJOR OPERATIONS IN COMPUTER PROCESSING

We can summarize the main uses of computers in processing, interpreting, and applying Landsat data with these four descriptive categories: (1) pre-processing, (2) enhancement, (3) classification, and (4) multisource data correlation. The major elements of each will be reviewed in some detail in the following pages. Finally, in the remainder of this appendix, we shall illustrate several of the more common operations and products associated with both batch and interactive computer processing. Specific examples from IBM, EROS Data Center, VICAR, ORSER, and Image 100 processing systems have been presented for the New York scene, anthracite coal mining, and gypsy moth defoliation–topics introduced earlier in Activities 4 and 5.

Preprocessing

For many applications, especially those that may be conducted through direct viewing of images, probably the most essential first step in computer processing of Landsat data is that of "preprocessing." Embodied in this category is a series of corrective operations that remove or reduce radiometric and geometrical distortions, systematic or random noise, and other data imperfections. The corrections are needed to eliminate or compensate for the errors and anomalies in the raw data received from the satellite. Radiometric anomalies are introduced during sampling quantization and transmission of the sensed brightness levels for individual pixels. Geometrical errors result from variations in the sensor perspective (largely related to spacecraft attitude) of a naturally irregular surface. These various errors may be traced to four groups of effects, as follows:

Platform Effects

- Attitude (roll, pitch, yaw)
- Altitude variations
- Scan skew
- Spacecraft velocity changes

Sensor Effects

- Mirror scan nonlinearity
- Detector sampling delay
- Detector bias/gain
- Geometrical perspective
- Panoramic distortion

Scene Effects

- Earth rotation
- Earth curvature
- Earth elevation

Atmospheric Effects

- Attenuation
- Scattering

Much of the preprocessing is done routinely at Goddard's IPF. The preprocessed output is a digital tape that is used to generate images directly on an imaging device such as the electron beam recorder, or to produce a computer compatible tape (CCT). Thus, all images, regardless of subsequent history, will experience some radiometric and geometrical corrections. Since 1979 the preprocessing tapes sent to the EROS Data Center are subjected to further computer processing (haze removal and gray

level adjustments; pp. 432 and 433) before products are sent to the users. Most computer-oriented users accept the corrected CCT's as the starting point for their further processing, but some have requested "undoctored" tapes so that they can control all applied corrections without losing data that may otherwise be altered during Goddard preprocessing.

At Goddard, this preprocessing falls into five categories: (1) Rearrangment of the data stream into the 800 or 1600 BPI, 7- or 9-track tape formats. The raw data are uncalibrated (uncorrected), but radiometric calibration data are included in the CCT along with information on line lengths. (2) Expansion or decompression of the video signals for bands 4, 5, and 6 from an upper DN limit of 63 units to a new limit of 127. The range for band 7 is retained at 0 to 63. The expanded range must normally be recorded in the 9-track mode. (3) Reduction in variations of detector response: There are 6 detectors assigned to each of the 4 bands (giving a total of 24) which receive light during each MSS mirror scan. Although an extensive effort is made before launch to match these detectors to a uniform gain and offset response, their behavior in operation is invariably nonuniform. Thus, one or more lines in each array of 6 may, in any sweep, have higher or lower average radiance values over the entire line length, giving rise to an often noticeable striping (lighter or darker tones than neighbors) in individual band images. Procedures have been developed for normalizing the detector response variation to cut down on the brightness differences between these lines. However, further destriping is usually necessary to minimize this effect, and is applied at the option of the user. (4) Introduction of certain geometrical adjustments. These include correction for deviation of line of sight (MSS optics) from nadir owing to pitch, yaw, and roll of the spacecraft, standardization of scan line lengths, done usually by inserting synthetic pixels to reach a fixed number per line (3318), corrections for nonlinearity of mirror velocity, and an initial correction for Earth rotation, resulting in the skewed or parallelogram outline (Figure B-5) that is a trademark of Landsat images. Fractional band offsets, usually the result of false line starts, are also adjusted if

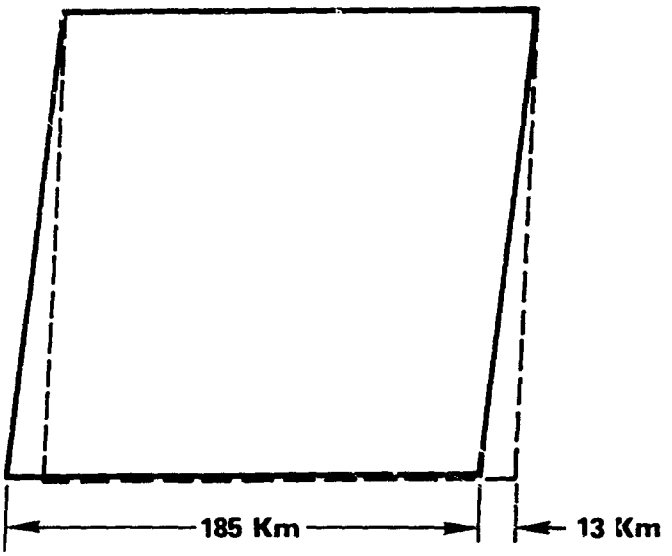

Figure B-5. The skew effect.

that problem occurs.[3] In addition, data on latitude and longitude (scene locators) and ground displacement errors (with respect to preselected ground control points) are provided in the tape. (5) Fitting to some standard map projection. The projection now being used is the Space Oblique Mercator (SOM) or Hotine Oblique Mercator (HOM). The Universal Transverse Mercator (UTM) was the base projection for Landsat products until 1978. Both that projection and Polar Stereographic (PS) for scenes above 65° N and below 65° S latitudes may be supplied instead upon special request as a retrospective order. The projection fitting is a mathematical operation analogous to the "rubber sheet stretching" procedures used in aerial photogrammetry, which interrelate tie points in an image to ground control points (GCP's) at the surface. Correction grids computed from spacecraft attitude and altitude data define an orthogonal plotting base of known dimensions and relation to the chosen projection. Pixels in the uncorrected image data array are then correlated with the GCP's located within the grid. This results in an output image data set with known pixel locations tied to a specific projection.

After receiving a preprocessed CCT, the user may elect to carry out further preprocessing prior to performing enhancements, classification, or other information extraction operations. This is normally done when an improved image product or display is sought. Certain steps or techniques may be omitted in some operations, especially if they tend to influence data values needed in spectroradiometric analysis.

Further preprocessing routines constitute an extensive and demanding topic that cannot be fully developed here. We shall end our survey of this subject by briefly considering these six important operations, several of which are now being done routinely during EDIPS processing by the EROS Data Center:

Rescaling. It has become common practice to further expand the DN limits from 0-127 to 0-255 (to the 8 bit or 2^8 single byte mode) to take advantage of the full dynamic range available on most CRT displays and film recorders. When this is done in the contrast stretching routine (see page 433), the result is a wider range of densities into which a given distribution of brightness values may be expanded. The expansion is accomplished simply by multiplying the numerical value of each DN by some factor (such as 2 in the 0-127 case above.)

Destriping. There are 24 detectors (6 per band) in the Landsat MSS that record the changing light intensities during each mirror sweep. Although closely matched in their ability to measure equal reflectances, there are actual differences in their responses, such that one or more detectors may produce consistently higher or lower voltage levels. If uncorrected, these variations will show up in a Landsat image as somewhat lighter or darker lines, which appear as distinctive stripes.

Although preprocessing at Goddard reduces the effects of nonuniform detector response, close inspection of standard Landsat prints reveals the persistence of noticeable striping. While this usually does not seriously hamper use of the imagery in photointerpretation, this striping is a distinct cosmetic blemish and may be distracting. Further, it may influence computer identification and classification of features by contaminating the statistical treatment of the DN's with anomalous or aberrant data values. Several methods for eliminating the stripes have been devised. The global method is illustrated in Figure B-6. In the histogram normalization method, the distribution of DN values measured by each detector in the group of 6 (per band of the MSS) is plotted in a histogram. The histogram data from a "bad" detector will appear significantly different (i.e., will show up as a deviation of its mean and variance) from those of "good" detectors. An edge test between line pairs is applied to identify bad lines that exceed some threshold criterion. A reference line in the group of 6 is then used to adjust or normalize deviant lines to new values that most closely approximate the proper DN's.

[3] This has proved especially troublesome in many Landsat-3 scenes. When scan line offset is corrected, useful data from as much as one-third of a scene may be compromised beyond retrieval.

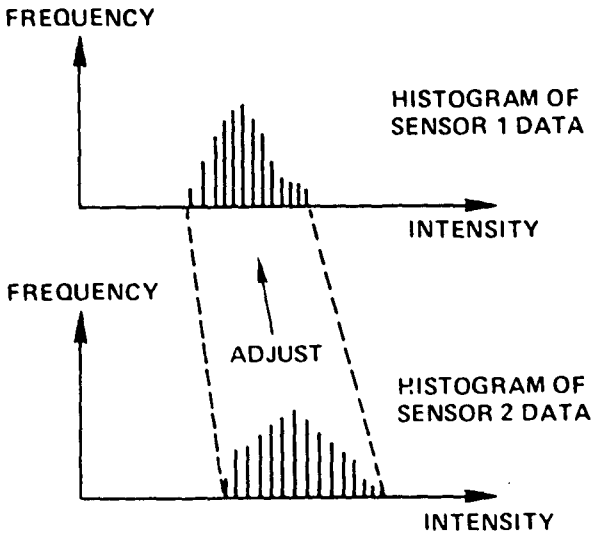

Figure B-6. The global destriping method.

Line Dropouts. Renditions of Landsat data (photoimages, printouts, displays) often show occasional individual or irregular groups of lines that are either dark or uniformly gray (in color composites some dominant color will prevail). This scanline dropout effect is usually related to momentary voltage fluctuations or loss of signals tied to the MSS electronics, or the data transmission system (on-board digitizer, radio transmitters, or receivers). The missing line data may be approximately restored by interpolation, in which DN values of adjacent pixels on either side of the dropout line are used to estimate (by averaging) the most probable value of the intermediate pixel. Another approach simply repeats the values of the preceding scan line and accepts the errors incurred. Regardless of method, the DN's constructed for the missing line are artificial but, nevertheless, may be included in the data sets involved in statistical tests without much damage to validity.

Resampling. Resampling is usually required whenever geometrical corrections are applied to an image data set and/or a data subset (part of a scene) is rescaled. After the various geometrical corrections or translations listed in previous pages have been applied, the net effect is that the resulting redistribution of pixels involves their spatial displacements to new, more accurate, relative positions. However, the radiometric values of the displaced pixels no longer represent the real world values obtained if this new and correct pixel array could be resensed by the scanner. Thus, the brightness value for a pixel shifted 100 m by geometrical rectification is not equivalent to the specific radiance value for that spectral band to be expected from this new section of the ground. The particular mixture of surface objects or materials (types and proportions) in the class assigned to the original pixel has changed somewhat. However, in most instances the recorded value is close to the true or expected value because of the high probability of features in the neighborhood of the original pixel position being similar in nature and characteristics. An estimate of the new brightness value or DN is made by some mathematical resampling technique, effectively, an interpolation procedure. Three resampling algorithms (Figure B-7A-C) are commonly used:

1. Nearest neighbor (A): the value of the closest input pixel to the corresponding one in the transformed output array is accepted as equal to the new one;
2. Bilinear interpolation (B): the average input value for the four pixels surrounding the transformed output pixel is assigned to the new one;
3. Cubic convolution (C): the average value for the 16 closest input pixels grouped around any new pixel is adopted.

Because of the increasing number of pixels used in the statistical calculation of new values for each output pixel, the accuracy of these values increases from (1) through (3). Resampling does compromise the original radiometry of the image to some extent. When applied to a subset expansion (enlargement), the cubic convolution procedure produces a sharper (less blocky) image with fewer edge abnormalities. The resampled image can take on even greater definition by application of a contrast stretch (see page 433).

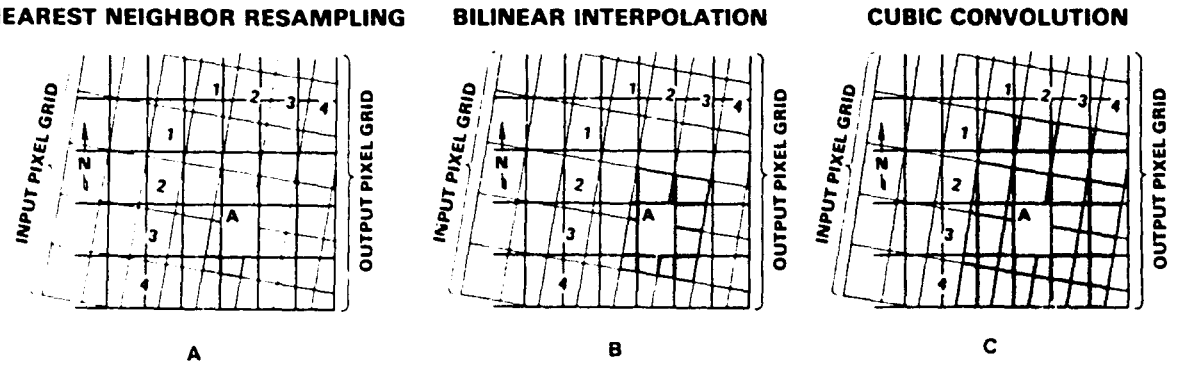

Figure B-7A-C. Three resampling options.

Atmospheric Correction. The interaction of light with atmospheric gases and particles can produce notable variations in the radiance levels recorded by a remote sensor. These interference effects are wavelength dependent. Both Rayleigh and Mie scattering processes give rise to an additional radiance from the atmosphere itself that increases the overall brightness level at shorter wavelengths. This contributes in part to the somewhat fogged or washed-out appearance of band 4 Landsat images, especially those taken on days of high relative humidity. The scattering decreases significantly at the wavelengths of bands 6 and 7, but absorption by water vapor increases, and hence attenuates the brightness of surface features as well as sky brightness induced by scattering. Removal of these atmospheric effects leads to more representative reflectance values and better quality images.

This removal is accomplished in several ways. Sophisticated techniques rely on direct meteorological measurements fed into models for calculating the expected atmospheric spectroradiances under specific weather conditions. This is nearly always impractical when working with a given scene, since contemporaneous weather data, even if available, are usually insufficient. In a far simpler approach, the presence of shadows (as from clouds or mountains) is used to approximate a zero base line for radiance. The lowest brightness value (DN) associated with shadows in seldom actually zero for band 4, although it may be near or at zero for band 7. Shadow-related values above zero in each band are assumed to be introduced solely from atmospheric radiance, and these are then subtracted from all other brightness values in the scene. In practice, the lowest value is usually determined from the histograms of brightness value distribution for each band, whenever these are computer-produced from the data sets. This works well in most scenes since some cloud- or topography-related shadows are nearly always present in most terrains, but the procedure may not be effective in flat desert scenes or polar regions.

Solar Illumination. If images taken at different times of the year are to be made into mosaics or compared for change detection, then the effect of seasonal changes in Sun elevation and azimuth should be adjusted or normalized. Several computer algorithms may be applied to accomplish this. The influence of Sun angle on bidirectional reflectances is a function of the cosine of that angle. Correction is made by dividing the DN's by the cosine of the elevation angle. The presence of topographical slopes complicates this correction, which assumes a flat Lambertian surface. This procedure may also be applied to the determination of absolute reflectances, which might be desired for referral to a reference file of standard spectral signatures. In practice, this is seldom done with Landsat data; more commonly, features are identified or classified by referring to field truth and training sites.

Enhancement

Although the various preprocessing routines are necessary to effective manipulation of data for information extraction, the several routines considered below under the functional heading of *enhancement* generally bring about the most dramatic improvements in the visual representation of these data. While trends toward classification and thematic mapping, and numerical and statistical analysis of both input and output data, are evident in current usage of Landsat data, the reliance on imagery (especially by geologists and geographers) remains at the core of much interpretive methodology. Enhanced "pictures" of the scenes of interest become powerful tools in the analytical approaches traditionally used in these disciplines. Agronomists, foresters, hydrologists, and others also continue to consult imagery in visualizing the relation between the alphanumeric, theme class, or tabulated outputs and their location within the real world.

"Cosmetic" Enhancement. This is a general (if somewhat colloquial) term that refers to the effects on image quality in carrying out several specific operations designed to improve the appearance of the scene. Typical steps in the enhancement include most of the preprocessing already discussed (particularly destriping, atmospheric corrections, and, if required, resampling), and other enhancements such as contrast stretch and or spatial filtering described in following paragraphs. These optional operations were normally not performed at Goddard or the EROS Data Center before 1979. Thus, in earlier imagery made by the Electron Beam Recorder (EBR), the photo products were degraded in sharpness and detail after passing through several positive-negative generations. In contrast, those made directly as first generation positives from a computer tape containing the enhanced data appear to have notably higher resolution, when in fact such images have simply realized all the clarity that was inherent to the original data but lost in the EBR processing sequence. Figure B-8A is a striking example of a high quality enhancement involving extended preprocessing and high bandpass filtering, made by Rupert Haydn of West Germany. This view of the San Francisco Bay region also makes use of a different combination of bands and filters: by matching band 5 with a red filter and band 7 with green, and modifying band 4 to simulate a blue band and projecting it through a blue filter, the image is given an approximate natural color balance. Figure B-8B shows a further enlargement of the San Francisco Bay subscene computer-generated by merging MSS bands 4, 5, and 7 with the same subscene as imaged by the Landsat-3 RBV. (see p. 178) This merged image was produced at the EROS Data Center. See also Figures 2-18, 4-3C, and 5-1B for other examples of "cosmetic" enhancement.

Density Slicing. One straightforward form of enhancement involves the combining ("lumping together") of DN's of different values, within a specified range, into a single value. The density slice method works best on single band images or digital data sets. This method is useful whenever any given surface feature has a unique and generally narrow spread of values. The new single value may be assigned some gray level density (or, an alphanumeric character in a printout) displayed on a photo or TV image, with all other values combined into a second level. If several features each have different (separable) values of means and spreads, then several gray level slices may be produced, each mapping the spatial distribution of its corresponding feature. The new sets of gray level slices may be assigned different colors on a display (Figure B-9). This may be done either on computer-processed renditions or on analog versions such as images scanned by a TV camera in an optical-electronic system.

Contrast Stretching. Both a casual viewer and an expert may easily be convinced by direct observation that altering the range of light and dark tones or gray levels in an image on a computer interactive display is often the single most revealing and informative operation performed on the scene. This process of modifying the tonal densities of a black and white image (on a TV screen or on photographs) is called contrast stretching (Figure B-10A-C). As carried out entirely in a photo-darkroom, the process involves techniques that shift the gamma (slope) or film transfer function of the plot of density versus exposure (H-D curve). This is brought about by changing one or more variables in the photographic process, as for example, the recording films, developer, paper contrast, etc.

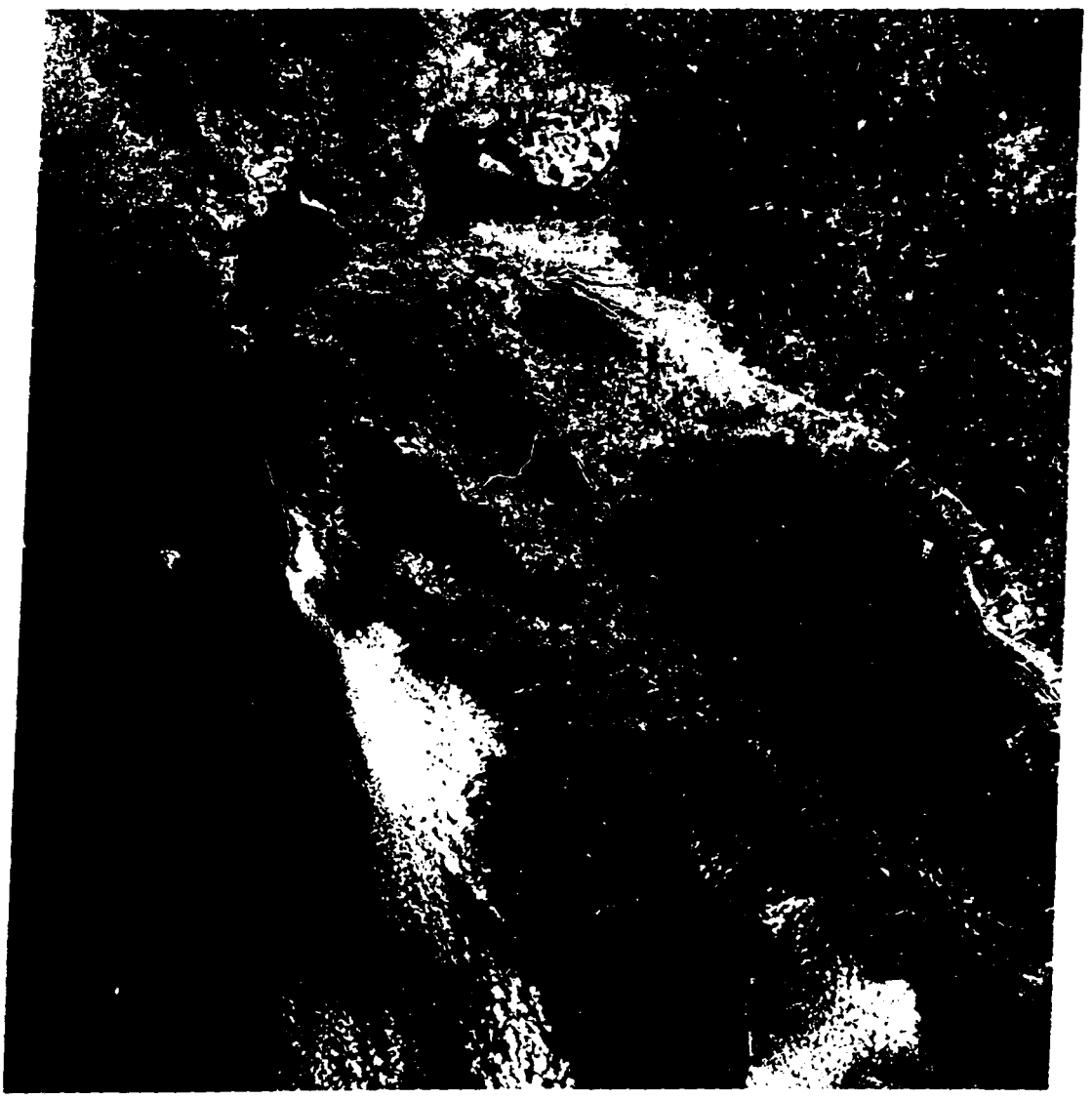

Figure B-8A. Enhanced Landsat subscene (February 1979) of San Francisco Bay.

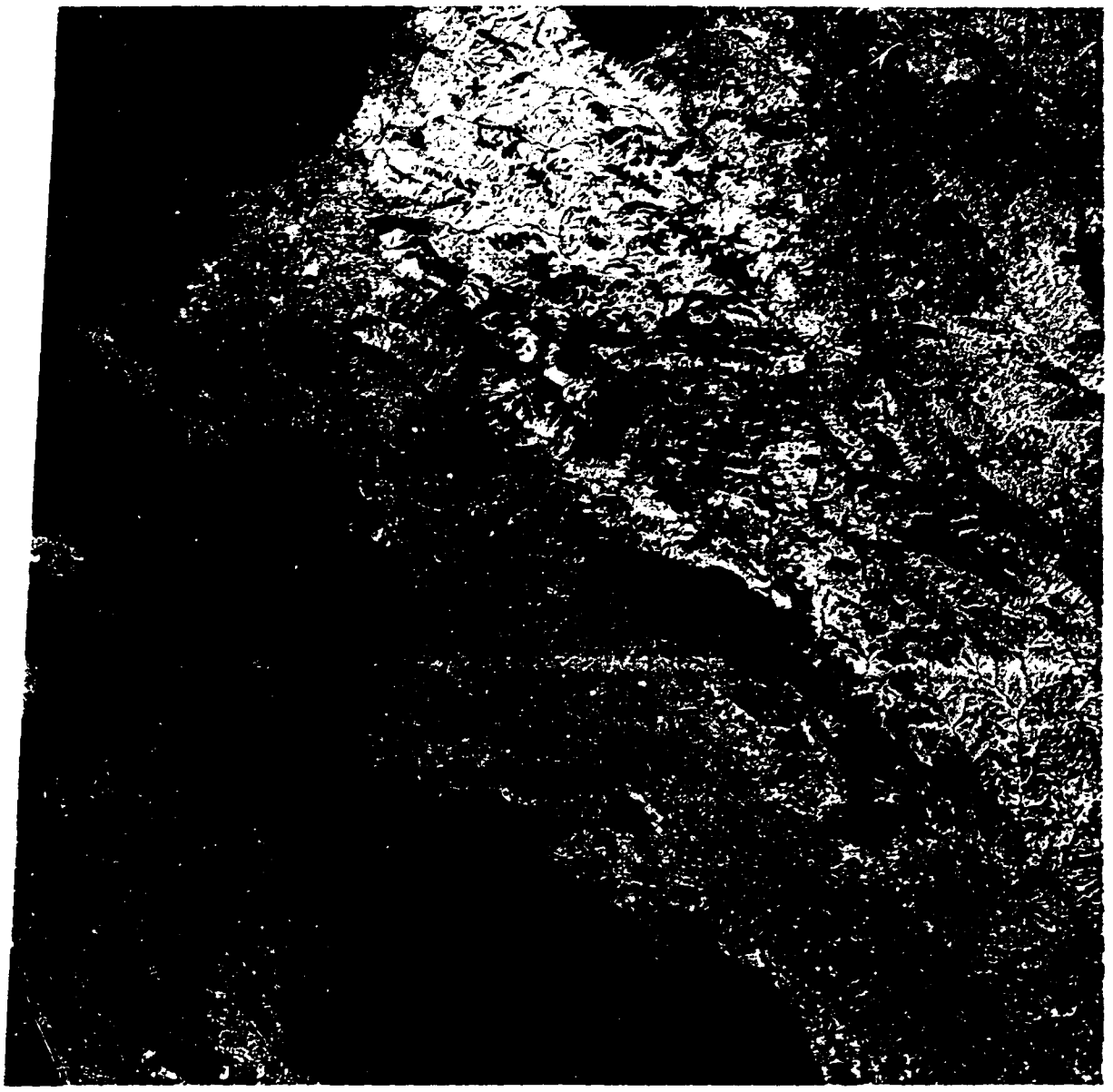

Figure B-8B. Enhanced Landsat subscene of the San Francisco Bay area, made by merging the September 5, 1975, MSS color composite (bands 4, 5, and 7) with the August 8, 1978, RBV panchromatic image.

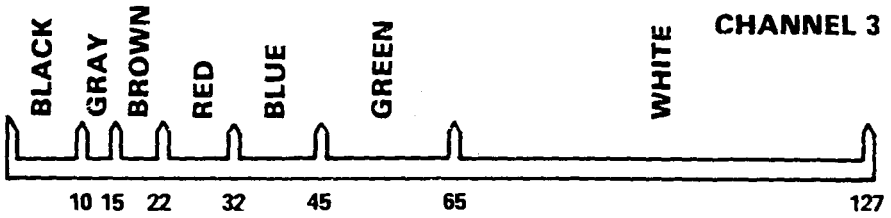

Figure B-9. A typical color assignment key for density slicing.

Frequently the result is a sharper, more pleasing picture, but certain information or expression in the scene may be lost in the trade-off if some higher or lower gray levels are "overdriven" into states that are too dark or too light.

Contrast stretching by computer is a routine operation, although some user skill is needed in selecting the specific techniques and new range limits applied to the stretch. For Landsat data, the DN range for each band in the entire scene or a subset is calculated and displayed in a table or a histogram. Frequently, the histogram distribution will be unimodal and Gaussian. Multimodal distributions (most commonly, bimodal) can result if a scene contains two or more dominant classes with distinctly different ranges of reflectance. For example, a region containing mostly forest cover and farmland would give rise to a Gaussian distribution of brightness, but if there were also numerous clear lakes (or playas), these features would produce "spikes" (peaks) in the histogram at low (high) values. Upper and lower limits of brightness values typically lie within only a part (30 to 60 percent) of the total available range. Furthermore, most values lie even further within this range. The few falling outside 1 or 2 standard deviations may usually be discarded (histogram trimming) without serious loss of prime data. This trimming allows the new, narrower limits to undergo even greater expansion to the full scale (0-255 for most Landsat image displays and film recorders). Linear expansion of the DN's into this full scale is a common option (Figures B-11A and B). When the full scale is matched with the widest range of densities (gray levels) inherent to the TV monitor (or output film), a significant broadening of contrast will occur. Care should be taken to hold the stretch to the straight line segment of the gray level dynamic range.

Other stretching functions are available for special purposes (Figure B-11C). These are mostly nonlinear functions that affect the precise redistribution of densities in different ways, such that some experimentation with any one may be required to optimize the result. These stretches are best made on an interactive display so that one can visually assess improvements and further adjust by trial and error. Commonly used nonlinear stretches include the following: (1) Piecewise Linear (Figure B-11D); (2) Gaussian; (3) Logarithmic; (4) Ramp Cumulative Distribution Function; and (5) Probability Distribution Function. These stretches tend to favorably expand some parts of the DN range at the expense of other parts (histogram equilization). If, for instance, most of the radiance variation has occurred over the lower range of brightness, these DN values may be selectively extended in greater proportion to higher (brighter) values.

Spatial Filtering. The enhancement techniques considered so far handle the data from each pixel independently of those from other pixels. However, the relations between neighboring pixel values may also be used in image enhancement. For example,

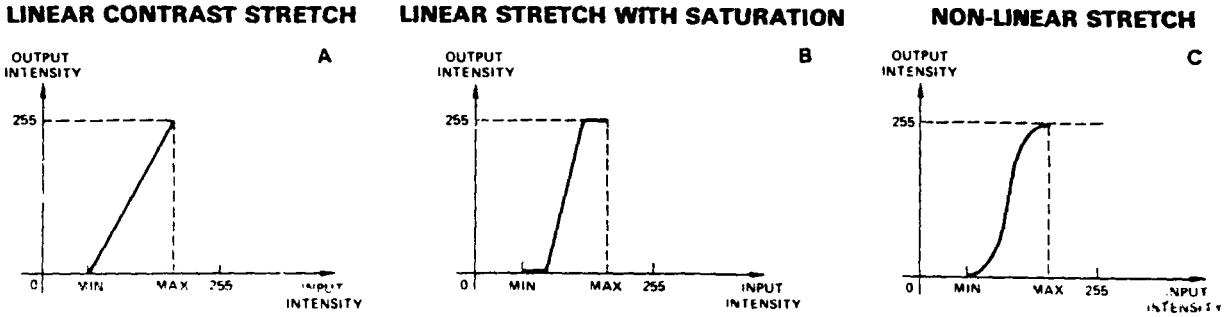

Figure B-10A-C. Three typical contrast-stretch functions.

an "edge" in an image is an abrupt change in value between two neighboring pixels. These boundary discontinuities may be sharpened by a spatial filtering technique commonly referred to as "edge enhancement".

The overall illumination of a scene will manifest itself as a slow change in pixel values over the entire image. This relation may be expressed in terms of "spatial frequencies." The spatial frequency is defined as the number of cycles of change in image value per unit distance (e.g., 10 cycles/mm) along a particular direction in the image. An image with only one spatial frequency consists of equally spaced stripes (for instance, a "blank" TV screen with the set turned on has horizontal stripes; this corresponds to zero frequency in the horizontal direction and a high spatial frequency in the vertical).

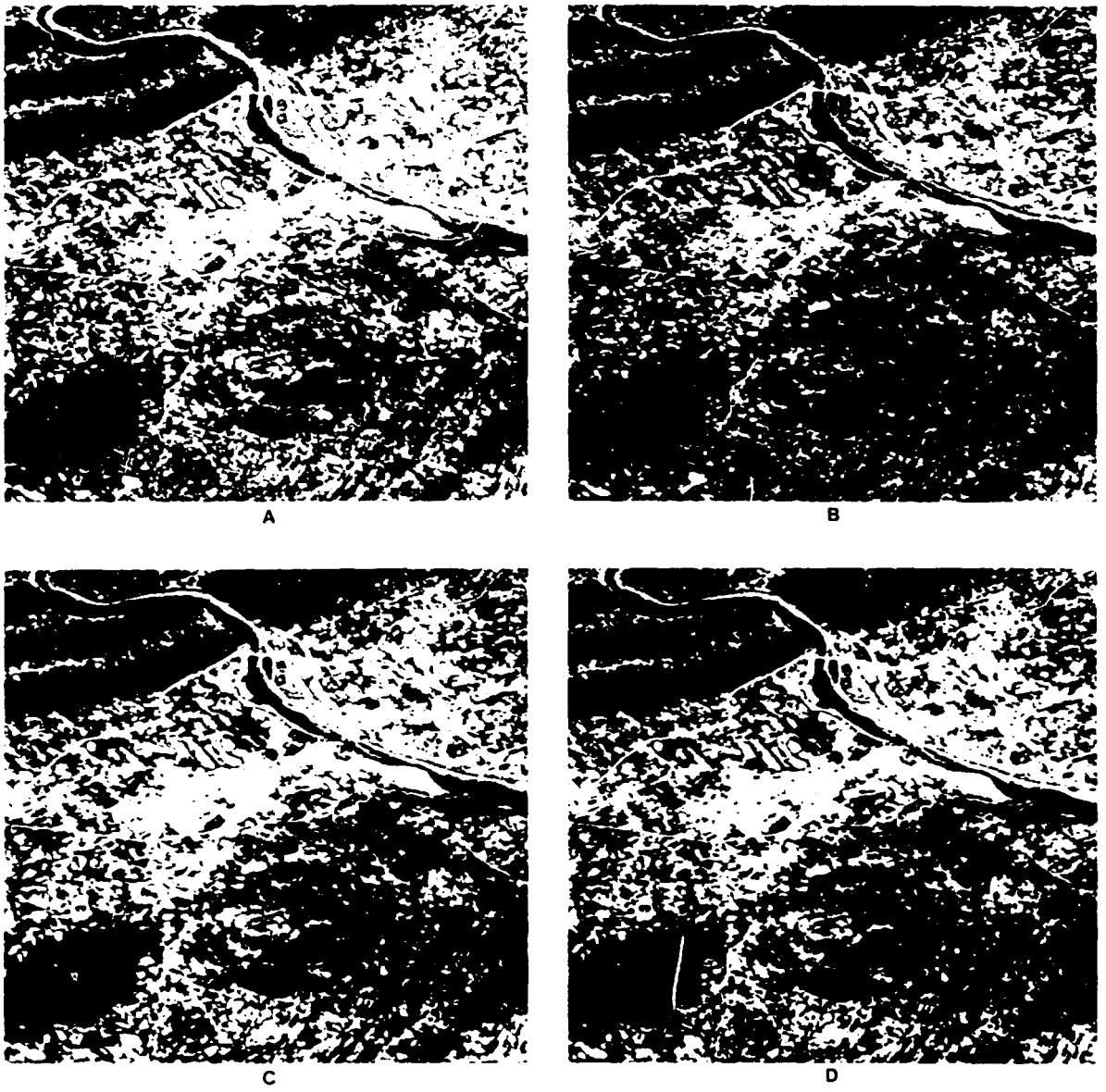

Figure B-11A-D. Example of contrast stretched images: A. "Raw" (unstretched); B. Linear stretch; C. Nonlinear; D. Piecewise linear.

In general, all images of any practical interest consist of several dominant spatial frequencies, occurring simultaneously. Clearly, fine detail in an image involves a larger number of changes per unit distance than the gross image features. The mathematical technique for separating an image into its various spatial frequency components is called Fourier Analysis. A quantitative discussion of Fourier Analysis is beyond the scope of this review; we shall only consider the application of Fourier Analysis to image enhancement.

After an image is separated into its component spatial frequencies (resulting in a "Fourier Transform" of the image), it is possible to emphasize certain groups (or "bands") of frequencies relative to others and recombine the spatial frequencies to produce an enhanced image. Algorithms to perform such enhancement are called "filters" because they suppress (or deemphasize) certain frequencies and pass (or emphasize) others. Filters that pass high frequencies, and, hence, emphasize fine detail and edges, are called highpass filters. Lowpass filters, which suppress high frequencies, are useful in "smoothing" an image with a "salt and pepper" appearance.

While the operation of spatial filters is conveniently described through the concept of Fourier Analysis, their implementation does not have to be through the Fourier Transform. "Convolution Filtering" is an equivalent method of implementing spatial filters. An especially simple particular case of this is a lowpass filter that generates moving averages over, say, 5 X 5 pixel square areas. Each pixel value in the image is replaced by the average over such a square area centered on that pixel. This tends to reduce deviations from local average and, hence, to smooth the image. A highpass filter is simply derived from this. The difference between the input image and the lowpass filtered image is the highpass filtered output.

Generally, spatially filtered images are contrast stretched to utilize the full range of image display (or recording) devices. With highpass filtering, boundaries such as farm borders, section lines, roads, streams, and rock strata and joints are brought into sharper forms (giving the impression of improved resolution). Edge enhancement can be particularly eye-catching for a terrain underlain by highly jointed rock strata in vegetation-sparse regions, as exemplified by the subimage of the Coconino Plateau in northern Arizona (Figure B-12A) processed by the Jet Propulsion Laboratory. A feeling of quasi-relief (somewhat akin to airbrush shading) can arise when viewing a topographically rugged region depicted in a spatially enhanced image. (Figure B-12B).

Ratioing. Still another method for image enhancement has been widely used by geologists because of its great utility in analyzing the spectral aspects of certain types of ground features. This is the *ratioing* of brightness values (BV) of corresponding pixels in any two bands. The DN of any one band pixel is simply divided by the DN of the equivalent pixel for any other band. The resulting quotient is a new number that can theoretically range between zero and infinity but in practice lies between about 0.3 and 3, or less, for the different combinations of band ratios. For the Landsat MSS a total of six ratios (4/5; 4/6; 4/7; 5/6; 5/7; 6/7) and their reciprocals are possible. From each ratio an image may be formed point by point from the pixel quotients in much the same way that an individual band image is produced by assigning gray levels to the DN's. Because of the narrower range of quotient values with respect to brightness values, these ratio numbers are usually expanded to some preset limit, such as the full scale of 0 to 255. It is then possible to combine any three ratio images in a color ratio composite by passing the individual ratio images as inputs through red, green, and blue filters.

Ratio images have two important properties not evident in the individual band images. First, strong differences in the intensities of the spectral response (signature) curves of different features may be accentuated by certain combinations of bands. Two examples here will illustrate this. In the first example, consider two distinctly different surface features, natural vegetation and camouflage netting, both of which may be predominantly green in the visible range. However, vegetation is distinctly brighter in the reflected infrared region (band 7) and shows low reflectances in the red (band 5) owing to chlorophyll absorption. A ratio of 7 to 5 will produce a notably higher value (steeper slope of the line joining the midpoints of the bars representing the 7 and 5 band radiance values) for the vegetation than the artificial material (characterized by lower band 7 and probably somewhat higher band 5 values). The difference in

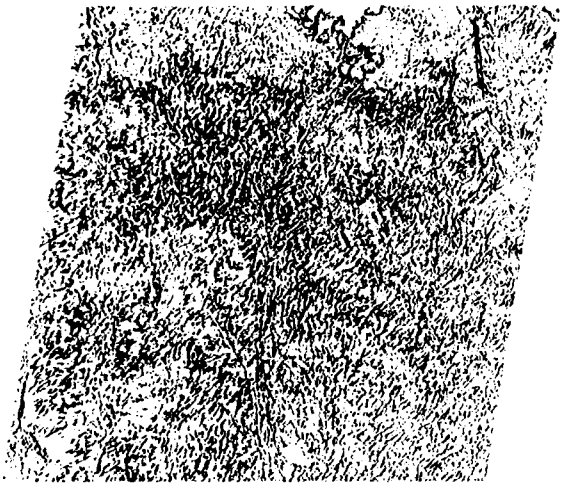

Figure B-12A. Bandpass filtered (edge-enhanced) image of terrain in central Arizona in which linear features are emphasized. (Produced by Image Processing Laboratory of the Jet Propulsion Laboratory.)

Figure B-12B. Edge-enhanced and contrast-stretched Landsat band 7 image of part of western Nevada (north of Reno) which strongly emphasizes the relief of the mountains. (Produced by Center for Astrogeology, U.S. Geological Survey.)

ratio values for the two feature types would be smaller for the 7 to 4 pairing because (a) both are green and (b) 4 and 7 values tend to rise together for vegetation. In the second example, consider a terrain containing scattered red soils or iron-rich (red to yellow) alteration products associated with mineralization. By ratioing bands 5 to 4 (red to green), this color difference from surrounding, less red, surfaces will be emphasized. This is demonstrated in Figure B-13, in which many of the light tones in the 5/4 ratio black and white image correspond to both reddish soil and rock units and to similar-colored alteration around the Gas Hills uranium district of Wyoming.

Second, ratios can remove differences in reflectance from surfaces composed of the same features brought about by topographical variations, shadowing, or seasonal changes in irradiance (sunlight intensity) levels (Figure B-14). If a rock surface is made up of a Sun-facing and a back slope (as along a ridge aligned normal to solar azimuth), the percentage reflectance or albedo will be reduced on the latter side. This reduction will, however, be proportionate in each band. Therefore, when the higher values for the more strongly illuminated slope in any two bands are ratioed, the quotient will be essentialiy the same as obtained for the ratio of values for the more shaded slope. The ratio is thus independent of irradiance at any instant, and becomes diagnostic of the particular feature or surface unit. Ratio images tend to smooth out intrinsic tonal contrasts related to topography, and appear at first glance to be without the details and variations in form so important to feature recognition in multiband or panchromatic images. Ratio images are, in effect, maps displaying the degree of autocorrelation or redundancy between MSS bands for the Earth terrain features sensed.

Two features with similar reflectance levels in one band may not be distinguishable (except by shapes) unless they show large reflectance differences in another band. A band ratio can accentuate these differences and is, in a sense, one way that features can be arranged in different *classes*. However, ratios eliminate the valuable distinction af-

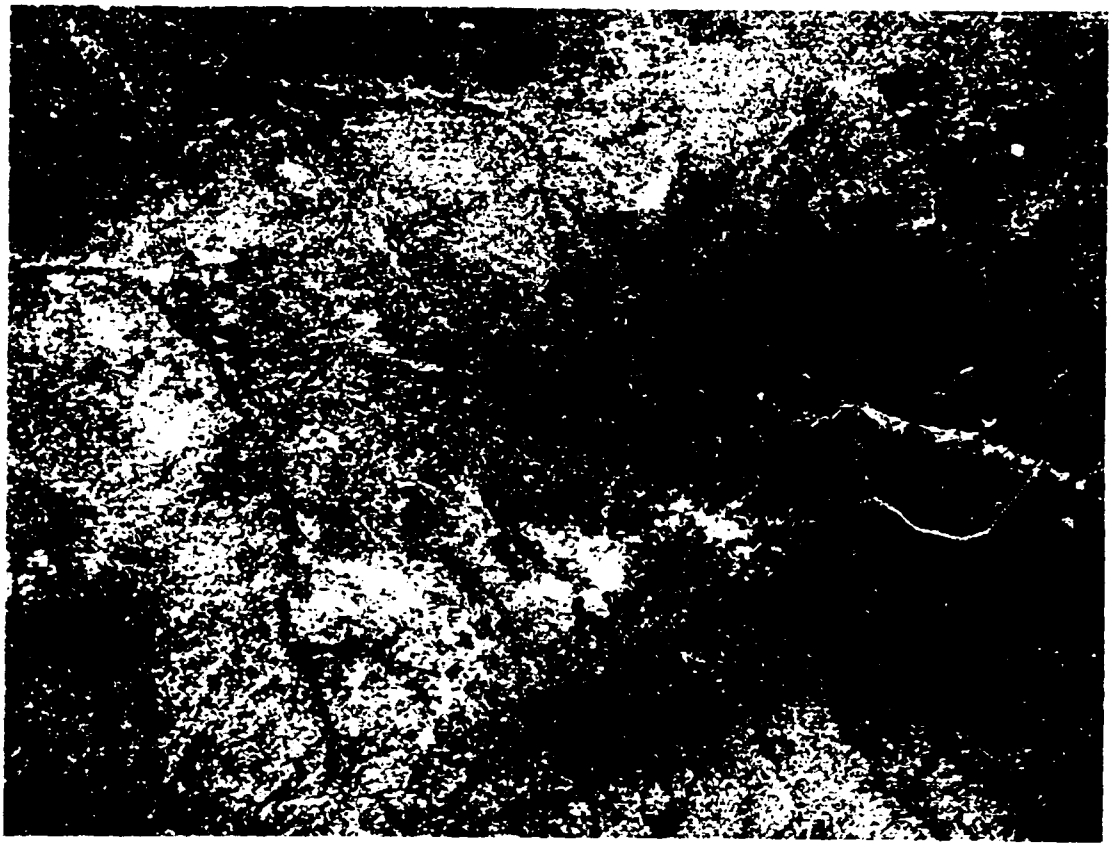

Figure B-13. Ratio image, MSS 5/MSS 4 of uranium-producing areas at the Gas Hills, Wy. Lighter tones usually associated with iron-rich rocks and alteration zones.

forded by albedo. Two unrelated materials with different reflectance values in two bands could give rise to the same ratio (e.g., A = 20(5), 30(7) and B = 40(5), 60(7), so that 5/7 for A and B is 20/30 = 0.67 and 40/60 = 0.67). By combining ratio images with a single band image (which contains albedo information), a *hybrid* color composite is produced with some of the distinguishing characteristics of both image types.

Data Transformations. The DN data for any spectral feature are usually plotted on multidimensional axes that represent the potential range of intensities (brightness) recorded for each channel (band) of a multispectral scanner. Thus, for multispectral scanner data, these axes are quantified by the full range of values for each channel. The axes may be designated by the channel wavelengths (usually the midpoint value for a spectral interval). These data normally scatter about their means in a broadly elliptical distribution in the two-dimensional (two axis) case. This spread of data, or variance, may be regarded loosely as an indication of the quantity of information along any arbitrary line passing through the center of the elliptical scatter plot. The initial measurement axes are not necessarily the best arrangement in multivariate space for expressing data variations and, hence, optimizing information content. The strategy is to find, by a prescribed procedure, a mathematical transformation (in effect, an axis rotation and translation) that redistributes all DN values with respect to a new set of axes. Each such axis will define a new dimension of information. One general procedure by which this transformation is executed is called Principal Component Analysis (PCA). In order to

EFFECTS OF RATIOING

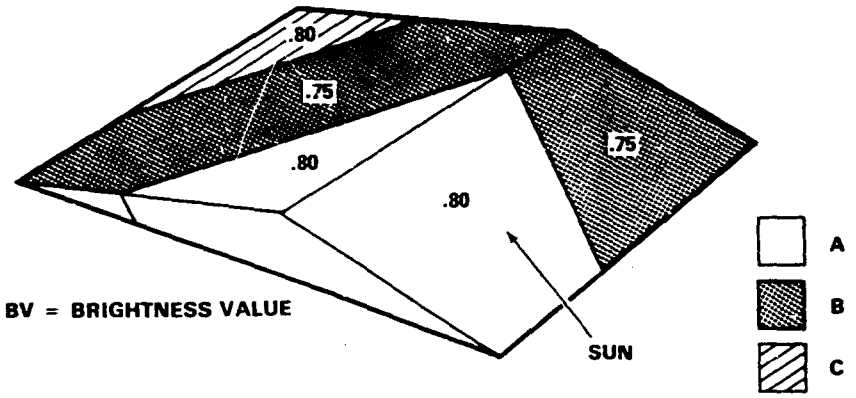

	BAND 4 (BV)	BAND (BV)	4/5 BAND RATIO
SLOPE FACING SUN			
UNIT A	20	25	.80
UNIT B	30	40	.75
SLOPE FACING AWAY FROM SUN			
UNIT A	16	20	.80
UNIT B	24	32	.75
UNIT C	32	40	.80

Figure B-14. Influence of slopes on ratio values.

gain some understanding of the mathematical basis of the PCA method, a summary[4] of the concepts and operations involved is provided in the next six paragraphs.

Consider the simplest case in which the data consist of measurements of two variables x_1 and x_2 (for example, length and width; in remote sensing, observed pixel radiances for two spectral bands). A plot of a set of bivariate measurements can be presented in a scatter diagram (Figure B-15A). Such a diagram shows how the two measurements are correlated. Numerical description of correlation comes from elementary statistics where "covariance matrices" are defined. The variance of a single variable measures the spread of its measurements about the mean; the covariance of two variables is a measure of the joint variation of their values about the respective means (see p. 422). The covariance matrix, S, of two variables is written as:

$$S = \begin{bmatrix} s_{11}^2 & s_{12} \\ s_{21} & s_{22}^2 \end{bmatrix}$$

where s_{11}^2 and s_{22}^2 are variances of variables x_1 and x_2 respectively and s_{12} (= S_{21}) is their covariance. With p variables, of course, S would be a p X p matrix (such a matrix is always symmetric about its main diagonal).

The covariance matrix S defines a set of concentric ellipsoids about the mean (Figure B-15A). If the mean is adjusted to zero (Figure B-15B), it is easy to imagine rotating the axes so that the first axis is coincident with the maximum amount of variation in the scattered data points (Figure B-15C). This axis is the first component and its variance is symbolized by λ_{11}.

The major and minor axes of an ellipsoid are called the Principal Components. The vectors a,

[4] Adapted from Davis, J.C., *Statistics and Data Analysis in Geology*, J. Wiley and Sons, Inc., New York, 550 pp. 1973.

which project the observations onto the principal components, are called eigenvectors (eigen, in German, means "characteristic"). If there are p linearly independent variables (e.g., spectral bands), then a set of p eigenvectors form a p X p matrix A such that $\Lambda = A' S A$, where A' is the transpose of A, S is the p X p covariance matrix, and Λ is a p X p diagonal covariance matrix whose elements λ_{ii}, called eigenvalues, are the variances of the i^{th} principal components, i = 1 to p. The λ_{ij} are all equal to zero and therefore can be ignored. For any given p X p covariance matrix, the maximum number of non-zero eigenvalues is p, and there are, at most, p eigenvectors as well. For a 4-band case, "hyperellipsoids" in higher dimensions are harder to imagine; however, the algebra extends, principal axes exist, their orientations are determined by the eigenvectors and their magnitudes by eigenvalues.

The original measurements (x_1, x_2 in our two-dimensional example) can be projected onto the eigenvectors or the principal axes to get a new set of values (say, y_1, y_2). These are "pseudo-measurements" which are linear combinations of these measurements. They comprise the principal components. In general, if a particular observation (e.g., pixel radiances) results in values $x_1, x_2, \ldots, x_p$ for the original variables, the principal components can be written as: $y_i = a_{i1} x_1 + a_{i2} x_2 + \ldots a_{ip} x_p$ where i can take on values 1 through p. For the two-dimensional case, $y_i = a_{11} x_1 + a_{22} x_2$ and $y_2 = a_{21} x_1 + a_{22} x_2$. The coefficients, a_{i1}, a_{i2}, etc., are the "elements" of the eigenvectors. They are also called "loadings." The y's are sometimes called the "scores." The principal components have variances equal to the corresponding eigenvalues.

If the variables on which the original observations are taken are highly correlated, most of the variation will be concentrated in the first few components. If, say, 90 percent of the variation is found in the first two components, then little information is lost by ignoring components 3 through p. This allows the investigator to reduce the number of dimensions, allowing him to better understand the patterns while losing a minimum of information.

A useful parameter characterizing a set of measurements is the variance of each measurement expressed as a percentage of the total variance. For the original set of measurements, the percentages are $100\ s_{11}^2/\Sigma\ s_{ii}^2$, $100\ s_{22}^2/\Sigma\ s_{ii}^2$, and so on. When data are scattered, as in Figure B-15A, the percentage variances defined above are approximately equal. However, if we derive the covariance matrix for the principal components y_i, the percentage variances are $100\ \lambda_1/\Sigma\ \lambda_i$, $100\ \lambda_2/\Sigma\ \lambda_i$, etc. For the example given in Figure B-15A, these new variances will be significantly different. It is

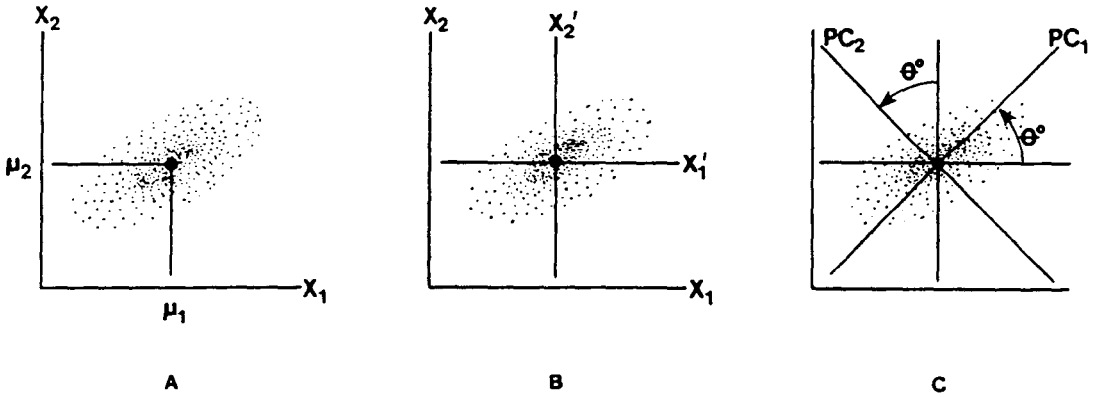

Figure B-15. Diagrams explaining rationale of Principal Components Analysis (PCA). A. Scatter plot of data points collected on two variables X_1 and X_2, with means μ_1 and μ_2; B. The new coordinate system found by shifting the axes to an X′ system. Values for the new data points are found by the transform relations $X_1' = X_1 - \mu_1$ and $X_2' = X_2 - \mu_2$; C. The X′ axis system is rotated about its origin (μ_1, μ_2 in the original system) so that the $\sigma^2_{PC_2}$ is a maximum. Since PC_2 must be perpendicular to PC_1, and there are only two dimensions, PC_2 is fixed. The PC axes are the Principal Components of this two-dimensional space.

customary to order the principal components in the descending order of eigenvalues. Since, in practice, most of the variance now resides in the first component, much less will be in the second component, and so forth.

Following this "crash course" in the concept of principal components, you may now better appreciate the utility of PCA in the processing of remote sensing data. For the Landsat MSS case (four bands or dimensions), the first, second, third, and fourth principal components contain successively less information (the first component usually contains about 85 to 90 percent and the fourth 1 to 2 percent, mostly noise contribution). Each component, however, contains inputs from all bands used. The precise linear transformations to be applied depend on the covariance matrix, calculated from the original data set.

The eigenvalue of each transformed data point (a pixel site, containing 4 values of x represented by the DN for each MSS band) can be used to produce a black and white image. An image for each principal component (4, for Landsat MSS data) can be produced. The first component image (containing most of the variance, combined from all 4 bands) most nearly resembles a standard Landsat image and, in fact, roughly approximates an albedo image covering the spectral interval from 0.5 to 1.1 μm. Second and third component images show quite different gray tone patterns and the fourth component image tends to be dominated by noise with little recognizable pattern, unlike contrast enhancement or band ratioing, ascribing a phenomenological attribute to an individual target or gray tone pattern is more difficult because the loadings that went into producing a given component depend on the total scene content rather than the contribution of individual classes making up the target/pattern.

These component images can be superimposed through color filters (or TV color guns) in much the same way as for band ratios to produce distinctive color composites. These bear strong pattern resemblances to standard 3-band color composites, but show many more subtle differences (color shading and distribution) that more effectively discriminate real variations among features—as well as defining new features on the surface.

Impressive image displays of transformed data frequently result from areas dominated by soils and rock units (geological scenes). In Figure B-16, each of the aircraft scanner images made from the first, second, third, and fourth principal components, respectively, reveals patterns of light to dark tones that correlate closely with different rock and alteration types exposed at the surface in this mineralized area near Medford, Utah (see also Figure 9-28). Examples of principal component images made from Landsat data for a heavily vegetated scene around Harrisburg, Pa., were included in Activity 5 (see Figures 5-15 and 5-16). Specific calculations of principal components for this scene are carried out on pp. 173-175).

The discussion above refers to one transformation technique, called Principal Components Analysis, which uses data from all features in all bands without regard to *a priori* knowledge of feature identities. A second transformation technique, called Canonical Analysis, employs user-supplied identity of certain features or categories (that is, depends on ground truth or computer-aided classification). The statistics characterizing each feature are determined, and from these an appropriate mathematical manipulation optimizes separability. Mathematically, the method produces a set of transformed variables based on maximizing the among-category covariance matrix and minimizing the within-category covariance matrix.

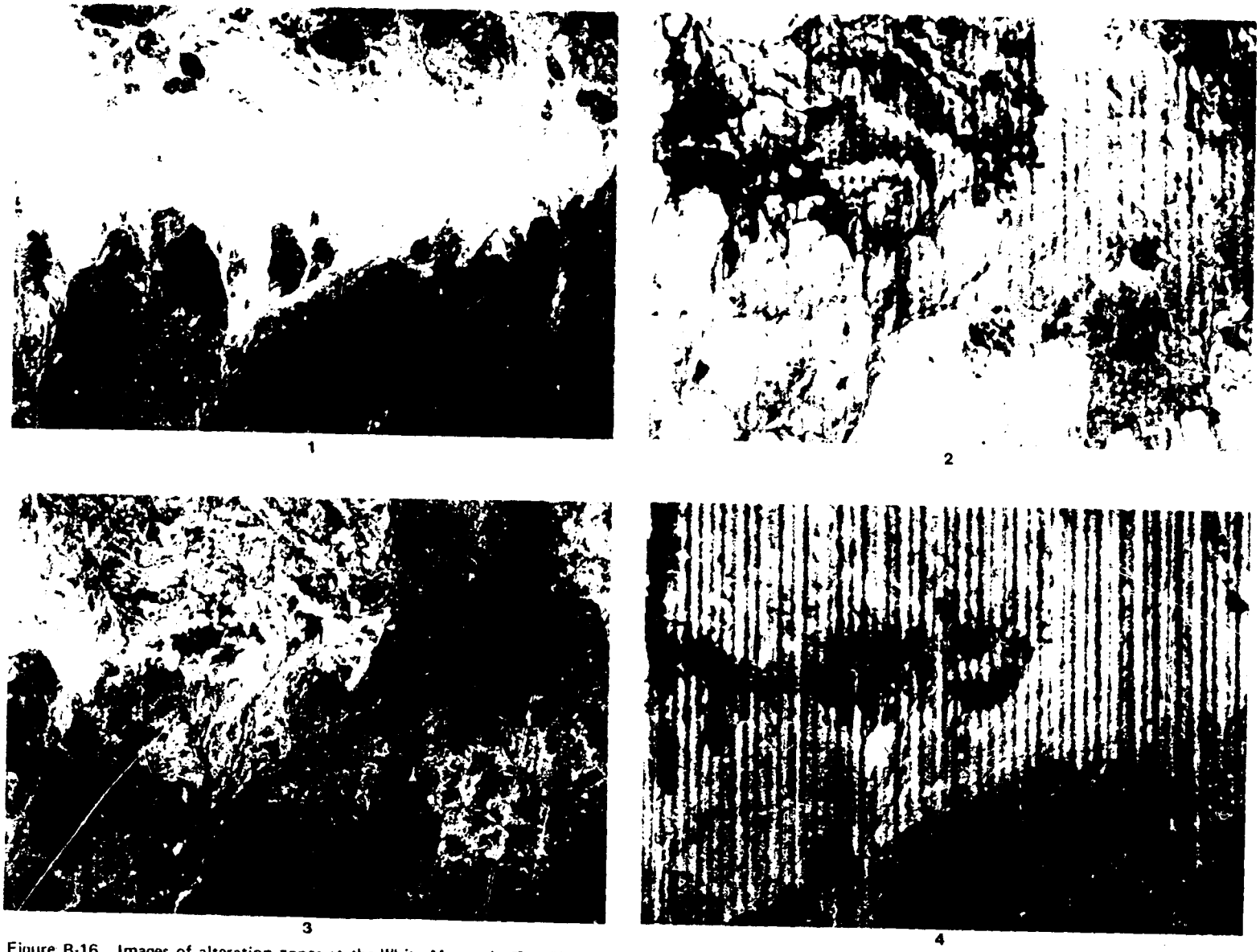

Figure B-16. Images of alteration zones at the White Mountain Test Site, Utah, representing principal components 1 through 4. Not shown are the two additional, noisier components 5 and 6. All six principal components were derived from six channels of the aircraft-mounted Bendix 24-channel scanner data.

Classification

Many applications dependent upon Landsat data require that the ground features of interest be located, identified, grouped into useful categories, and separated from extraneous objects within the scene. This requires definition of discrete classes on the basis of their spectral signatures and/or characteristics shapes and contextual relations. The general approach forms the basis of *pattern recognition*—an automated intelligence technique originally developed by the military for determining attack targets or defense positions and based on principles and methods that have been readily extrapolated to civilian remote sensing and to such special applications as fingerprint identification and automated reading of zip codes. As now adapted to Landsat data analysis, the recognition of land cover types or categories is accomplished mainly by *multispectral classification*.

Principles of Classification. The basis for classification of cover types is the correlation of different categories of interest with statistically separable groups of data as defined by their spectral properties in multidimensional space. The charts in Figure B-17 illustrate how this is done. In the upper left chart, spectral signatures for three common cover types are plotted from 0.4 to 14.0 μm, which includes the reflectance and emittance wavelength regions sensed by the MSS on Landsat-3. These curves show distinct differences in response (inten-

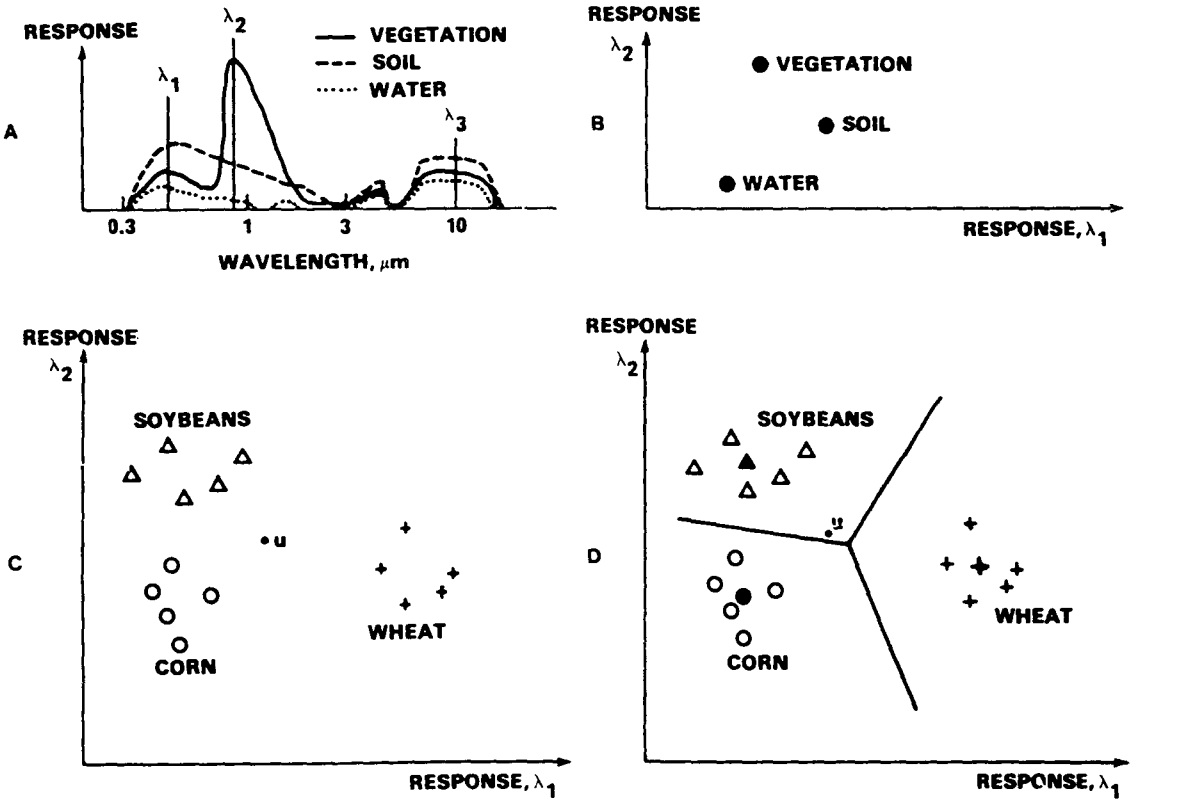

Figure B-17. Four schematic diagrams showing generalized spectral curves, values in two-dimensional space, sample spreads, and decision boundaries in classification (modified from Landgrebe, 1971).

sity) at many (but not all) discrete wavelengths. Consider the response values for each cover type at wavelengths λ_1, λ_2, λ_3. In this example, the three cover types can best be separated by value differences at λ_2, somewhat less so at λ_1, and least at λ_3. It is conceivable that some unnamed fourth cover type may have a response value at λ_1, similar to one of the three types shown, and might even be similar again at λ_2. It could therefore be confused with one of the three plotted types. However, the likelihood of this similarity recurring at some third wavelength would be much less if the fourth type were indeed different.

In the upper right chart of Figure B-17, the graph in two-dimensional (X, Y) space of the λ_1 versus λ_2 response values of the three cover types clearly shows their separability and distinctiveness. The separation distances become less when either λ_1 or λ_2 values are plotted with respect to the less varied λ_3 values. Any fourth cover type could be near any one of the three identified types for either λ_1 versus λ_2 or λ_2 versus λ_3 but, if of a different nature, will probably occupy an isolated position in three-dimensional (λ_1 - λ_2 - λ_3) space. Each distinct cluster of plotted points in multidimensional space (lower left and right) constitutes a spectrally separable *class*. For real features of unrelated character, efficient separability may be achieved by sampling at a minimum of two, but more commonly three, four, or five wavelengths or wavelength intervals (bands). The number and identity of wavelengths or bands that afford the best separation depend on the characteristic spectral signature of each distinct feature or class; different combinations of bands may be needed for different classes. Within a general class, say vegetation, differences among subclasses (for example, wheat, barley, rye, oats) may be much smaller but still measurable with precise, sensitive instruments and or narrower band widths.

The task of separation becomes somewhat more complicated as multiple measurements are made of the same feature or class distributed at different field locations. In the lower left chart of Figure B-17, replicate measurements of three crop types are plotted. A scatter of values is typical of each. This stems from natural variations among individual objects in a class, differences in background, coassociation of several unresolved classes (the mix problem, p. 83), sensor fluctuations, and other factors. An average value for the plotted position may be calculated for each cover type (see lower right chart of Figure B-17). Other values tend to *cluster* around each mean. When considered statistically as part of a multivariate population, each type is associated with a characteristic mean and variance (or standard deviation). Various statistical tests are available to establish quantitatively that the several data clusters meet significant difference criteria, that is to say, belong to different classes. Thus, separability criteria are specified, and decision boundaries (derived from discriminant functions and shown as dividing lines in the lower right chart) are set up between classes. Various *classifiers* may be employed to determine and validate separability. Among the most frequently used techniques are Bayesian methods (such as Maximum Likelihood), Nearest Neighbor, Piecewise Linear, and the Parallelepiped classifiers. The choice of a particular classifier or decision rule depends to some extent on the nature of the input data and the desired output (Table B-2).

Types of Classification. Multivariate classification may be performed by either of two methods: unsupervised and supervised.

In an *unsupervised* classification (Figure B-18A), identities of categories or cover types to be specified as classes within a scene are not generally known *a priori*, because appropriate ground truth is lacking or surface features within that scene are not well defined. The computer is asked to group (cluster) pixel data into different spectral classes distinguishable according to some statistically determined separability criterion. For Landsat data, these clusters are usually distributed in four-dimensional spectral space (bands 4-7). Any individual unknown point (pixel) u (see lower charts in Figure B-17) will occur somewhere in this space. The point is tested by the same separability criterion to determine whether it falls within a cluster and therefore belongs to the (still unknown) class defined by that cluster. If so, it is assigned to that class. If not, it is assigned to that, or another class, as determined by some decision rule (e.g., Nearest Neighbor). Thus, every data point will be identified with one of the separable classes, even if that point actually represents an unrecognized cover type. Natural class names must then be given to these spectral classes by associating the latter with char-

Table B-2
A Partial List of Classification Methods*

Classification Method	Categorization 1	Categorization 2	Comments
Bayes	Supervised	Parametric	Minimizes "average risk" of misclassification. Requires knowlege of a priori probabilities of occurrence of each class.
Maximum Likelihood	Supervised	Parametric	Minimizes average risk of misclassification when the probabilities of occurrence of each class are equal. When the conditional density functions are assumed Gaussian, this is a quadratic classifier used, for example, in IDIMS.
K Nearest Neighbor	Supervised	Nonparametric	Finds class assignments of K nearest neighbors and puts given samples in the majority class.
Prototype	Supervised	Nonparametric	Represents each class by a prototype and assigns a point to nearest prototype (e.g., minimum distance classifier used in ORSER).
Linear	Supervised	Nonparametric	Linear classifier is a general term to encompass techniques which use linear surfaces (hyperplanes) to separate classes. There are several iterative methods for deriving such hyperplanes.
Piecewise Linear	Supervised	Nonparametric	This is a generalization of linear classifiers. Useful when the classes are not separable by hyperplanes (either pairwise or individually from all other classes). The Parallelepiped Classifier is a particular case of this method.
Quadratic and Higher Order Polynomial	Supervised	Nonparametric	Use higher order surfaces for separating classes. The surfaces can be found using the same methods as for the Linear Classifier by suitable enlargement of the feature vectors.
Distance Based Clustering	Unsupervised	Nonparametric	There are several methods which use distance measures to group data into clusters. These are iterative methods and vary slightly from each other in the details of handling, initiation, and updating of clusters.
Density Based Clustering	Unsupervised	Parametric	Assuming form of probability density functions, find cluster assignments such that a measure of overlap is minimized.
Density Based Clustering	Unsupervised	Nonparametric	Approximate multivariate density by sample histograms or some other smooth functions and seek their local maxima (modes).
Table Look Up	Both	Both	Can be used to implement any decision rule obtained from any classification method.
Extraction and Classification of Homogeneous Objects (ECHO)	Both	Parametric	Spatial Classifier (as opposed to "per pixel"). Finds homogeneous spatial areas and then classifies all pixels in each such area into one class.
Layered	-	-	Hierarchical (decision tree) approach permitting selection of features, classes and classification method at each "node" (branch point).

*Parametric classifiers assume that samples from each class belong to a population modeled by a probability density function with a few parameters. Typically, a normal (Gaussian) density function is assumed. Nonparametric classifiers do not make such assumptions.

acteristic groups of surface features through referral to subsequent field observations, aerial photos, or, if suitable, spectral signature banks.

In a *supervised* classification (Figure B-18B), identities of the cover types of interest are already known, for small areas (training sites) within a larger scene, from field work, aerial photos, maps, personal experience, etc. The first step is to locate within the data set those areas of high spectral homogeneity likely to correspond to the dominant cover types within each training site. Appropriate multivariate statistical parameters (means, standard deviations, covariance, correlation matrices, etc.) are then calculated for each site and stored in the computer memory. For Landsat data, the four-band DN values for each cover type make up a specific class; each such class has its own characteristic multivariate parameters. Correct identification of every unknown point u outside the training sites becomes merely a matching of its multispectral properties to the known class with the closest similar properties, as tested by appropriate multivariate statistics.

For both methods, it is customary to view the classification at any intermediate stage as a printout using alphanumeric characters or a TV display using theme colors for the classes being set up. A certain fraction of unknown points (pixels) will have been misclassified, especially for classes with overlapping variances; this results in lower accuracies. Each version is checked against available ground truth to pick out these misclassified areas. Changes in the number of classes selected, statistics, etc., are made until misclassified points are reduced to a practical minimum; this will also cause shifts in boundaries and changes in size of already classified areas of the scene. A final classification is then accepted and documented in hard copy. If all relevant classes within a scene are properly specified, and both scene and training sites are reasonably homogeneous, the accuracy of a supervised classification can be quite high—up to 98 percent for three to five vegetation or crop classes when multitemporal Landsat data are combined.

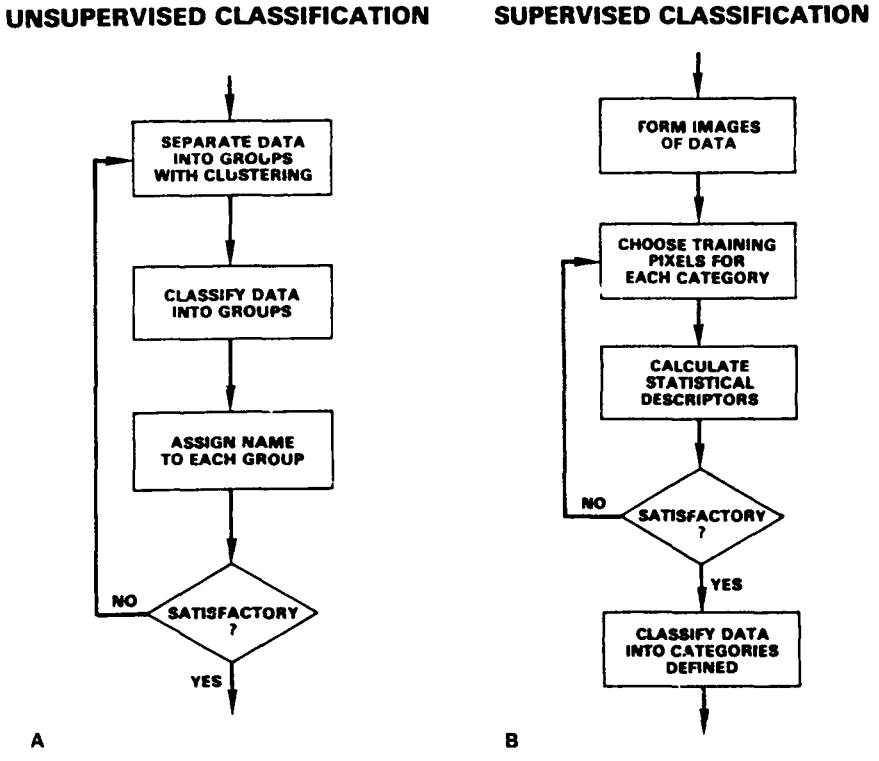

Figure B-18A-B. Generalized procedures, as flow diagrams for unsupervised and supervised classifications.

An Illustration of the Classification Process. The general procedures used to produce a classification map will be described step by step for one typical system. The processing routine executed by the ORSER system (Pennsylvania State University), shown by a flow diagram in Figure B-19, resembles most time-sharing systems (LARSYS, Purdue; RIPPER, Stanford) that operate in the Remote Job Entry (RJE) mode on Landsat data. The CCT's for the scenes to be analyzed are placed in the tape library at Penn State. To begin analysis, the user telephones the ORSER Computer Center to request that the data tape be entered into the active files. Thereafter the user communicates through his remote terminal.

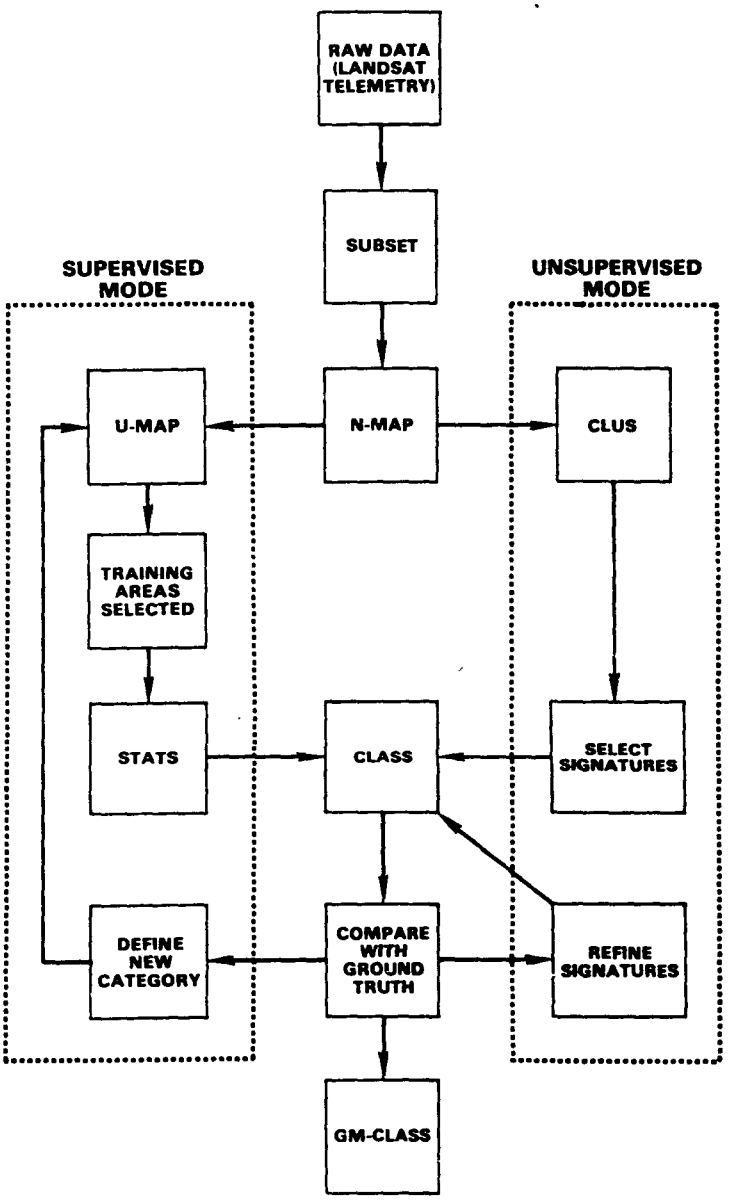

Figure B-19. Flow diagram for ORSER classification procedures.

The area to be classified is blocked out as a subset (Figure B-20), whose width is limited to a maximum of 810 samples (pixels), which is stored for recall on a separate tape. The first output is an *NMAP* print (upper left chart in Figure B-21). This product is just an alphanumeric map (three or more characters), made by grouping the subset DN's into several percentage brackets (analogous to density slices) that extend to the full range of brightness values present in some combination of one or all bands used. The purpose of NMAP is simply to provide a distinctive pattern, comparable to the gray tones in the band images, by which the user can ascertain that the correct subscene boundaries were chosen; if not, the limits are adjusted and a new subset is processed.

At this stage a decision must be made on whether to proceed with a supervised or unsupervised classification. Whenever feasible because of adequate ground truth or aerial photography, the supervised mode is preferred. The strategy is to seek out areas of high spectral homogeneity or uniformity that are likely to correspond to identifiable surface feature categories. A *UMAP* program uses a Euclidian distance measure to compare a pixel with near neighbors for degree of similarity. An example of the map developed by this algorithm appears in the upper right chart in Figure B-21; areas of greatest uniformity are designated by continuous patterns of U's. A number of training areas are picked on the basis of these patterns, and their boundaries are specified in line and element coordinates. Appropriate multivariate statistical parameters (means, standard deviations, variance-covariance and correlation matrices, and their eigenvalues) are then calculated for each training area by the *STATS* program, from which signatures characteristic of each training area are defined. The signature statistics are entered into one of several classifier programs, such as *CLAS*, to produce a first version of a classification map. The *LMAP* program converts this alphanumeric map to one with more conventional symbols (lower right chart, Figure B-21). This version is then matched against ground truth checks to pick out misclassified areas. Modifications are made through a feedback loop that reenters the procedure at UMAP.

Where appropriate ground truth is lacking or features are not well defined, an unsupervised classification routine must be followed. The *CLUS* program derives separable spectral space signatures from the subscene and then classifies each pixel according to the signature it most closely matches. An alphanumeric signature map (lower left chart, Figure B-21) is printed and the resulting patterns are compared with any ground truth or field check on hand. Signature refinement may be made until some subsequent version is accepted; this is usually converted to LMAP form (lower right chart, Figure B-21). Geometrical and scaling changes are incorporated through the DISPCM routine into the final map product, which is output on a plotter, a CRT display, or from a tape used to make gray tone or color prints.

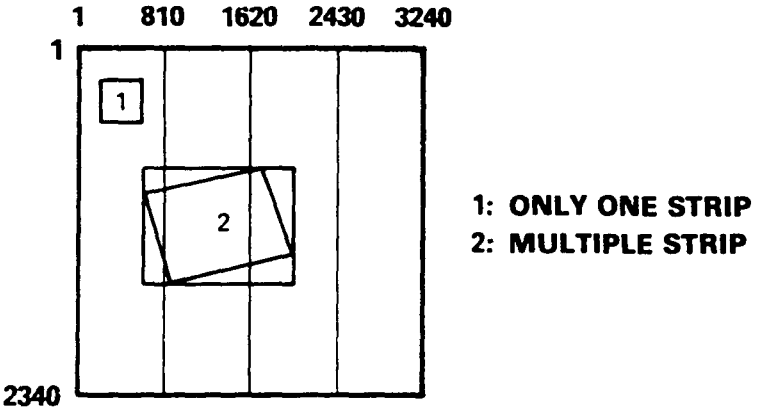

Figure B-20. Typical subset specification for data in a single or multiple image strips.

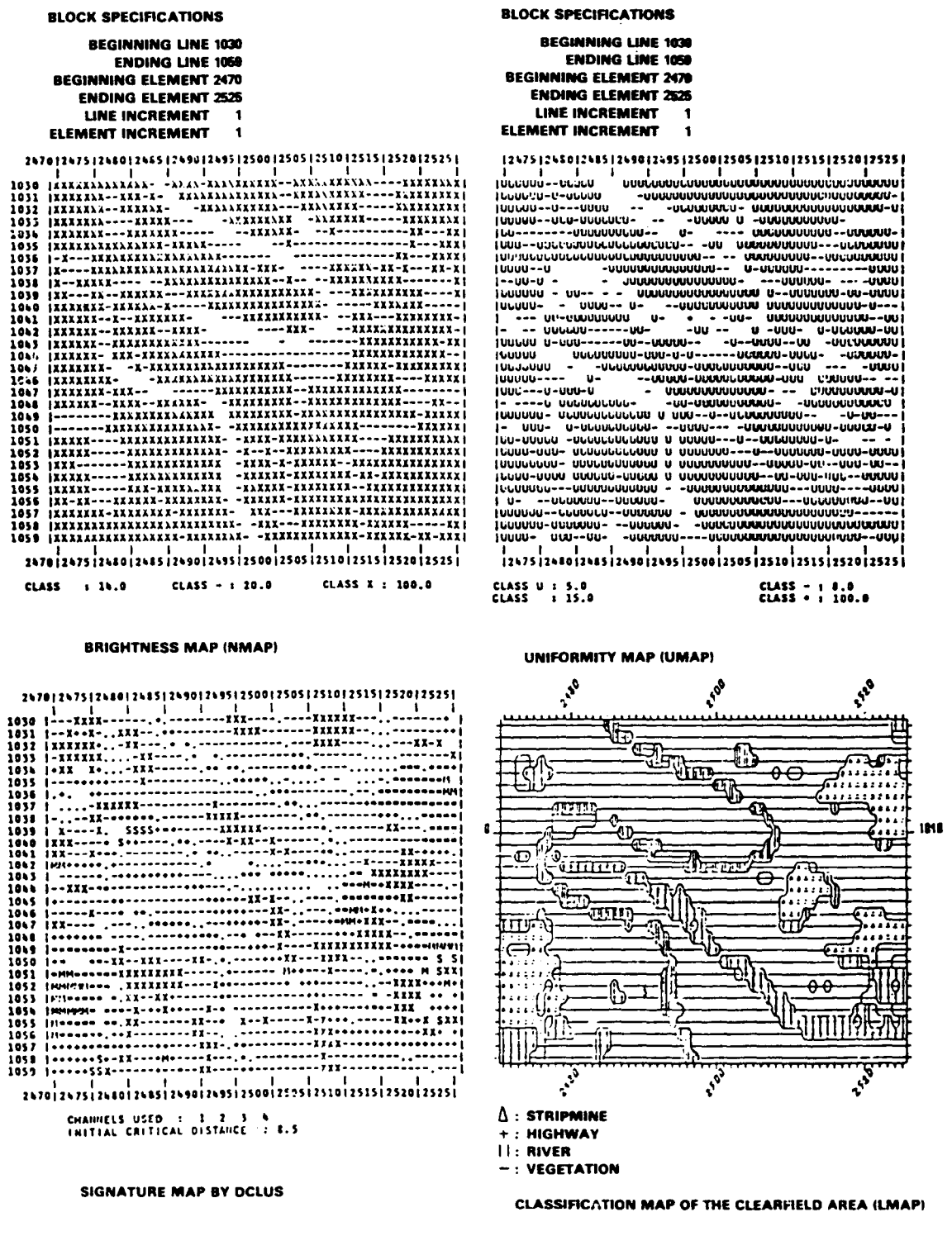

Figure B-21. Four characteristic ORSER output products.

Multisource Data Correlation

The development of computer-aided techniques for reliably identifying many categories of surface features within a Landsat scene, either by photointerpretation of enhanced images or by classification, is in itself an outstanding achievement. Numerous practical uses of such self-contained information are being made without strong dependence on other sources of complementary or supporting data. Thus, automatic data processing assists in recognizing and mapping major crop types, estimating their anticipated yields, and spotting early warning indicators of potential disease or loss of vigor. However, many other applications, particularly those involving control of dynamic growth or change systems, or decision making in management of natural resources, or exploration for nonrenewable energy and mineral deposits, among others, require a wide variety of input data of various kinds not intrinsic to Landsat.

Some data are essentially fixed or time-independent—slope aspect, rock types, drainage patterns, archaeological sites, etc.—in the normal span of human events. Other data come from measurements or inventories conducted by people on the ground or in the air—weather information, population censuses, traffic flow patterns, soil erodability, etc. However, many vital data are transient or ephemeral—crop growth stage, flood water extent, insect infestation, limits of snow cover, etc.—and must be acquired on a timely schedule. Pertinent Landsat data play a key role here, and, in fact, satellite monitoring is often the only practical and cost-effective way to acquire data frequently over a large region.

Geobased Systems. There is a rapidly increasing realization that the best future use of Landsat data will stem from correlating and interleaving this type of data with various other types that together are essential inputs to decision making and applications models. Remote sensing data constitute an integral element of a general Earth Survey Information System, as is exemplified in Figure B-22. The bulk of data in such systems have in common a geographical significance; that is, they are related to definite locations on the Earth's surface. In this sense, they make up a Geographic Information System (GIS; also known as geobased or geocoded systems). Because vast amounts of spatial or geographically referenced data must be collected, stored, analyzed in terms of their interrelations, and rapidly retrieved when required for day to day decisions, a geographic information system that accepts these data as prime input must be automated if it is to be efficiently utilized.

An automated GIS is built around a base composed of five elements: data encoding, input processing, data management, manipulative and analytical operation, and statistical and graphic output. Data are acquired in a variety of formats, including geographical entities, graphic data, nonspatial information in both printed and digital files, and digital spatial data tapes. Data will often require manual or automated preprocessing prior to encoding: for example, manual photointerpretation of aerial photography or automatic classification of Landsat data.

Each spatial data type is treated as a spatial data layer. Within each layer there are four types of geographical entities that must be encoded: (1) points, (2) lines, (3) area-enclosing lines or polygons, and (4) surfaces (for three-dimensional cases). These entities can be located as lying within cells referenced to a regular grid, or by their positions within an $X, Y, (Z)$ coordinate system. These locational data are encoded and, after input processing, stored as points, lines, networks, surfaces, or areas (polygons).

Ideally, an automated GIS should have data base management software to provide for the following: ability of the system to support multiple users, multiple data bases, efficient data storage, retrieval and update, data independence, security, integrity, and nonredundancy.

In general, analysis of data from multiple spatial data layers requires the processing of algorithms suited to manipulation of both grid and x,y coordinate-structured data, and for conversion from one structure to the other. Processing functions should provide for such operations as rota-

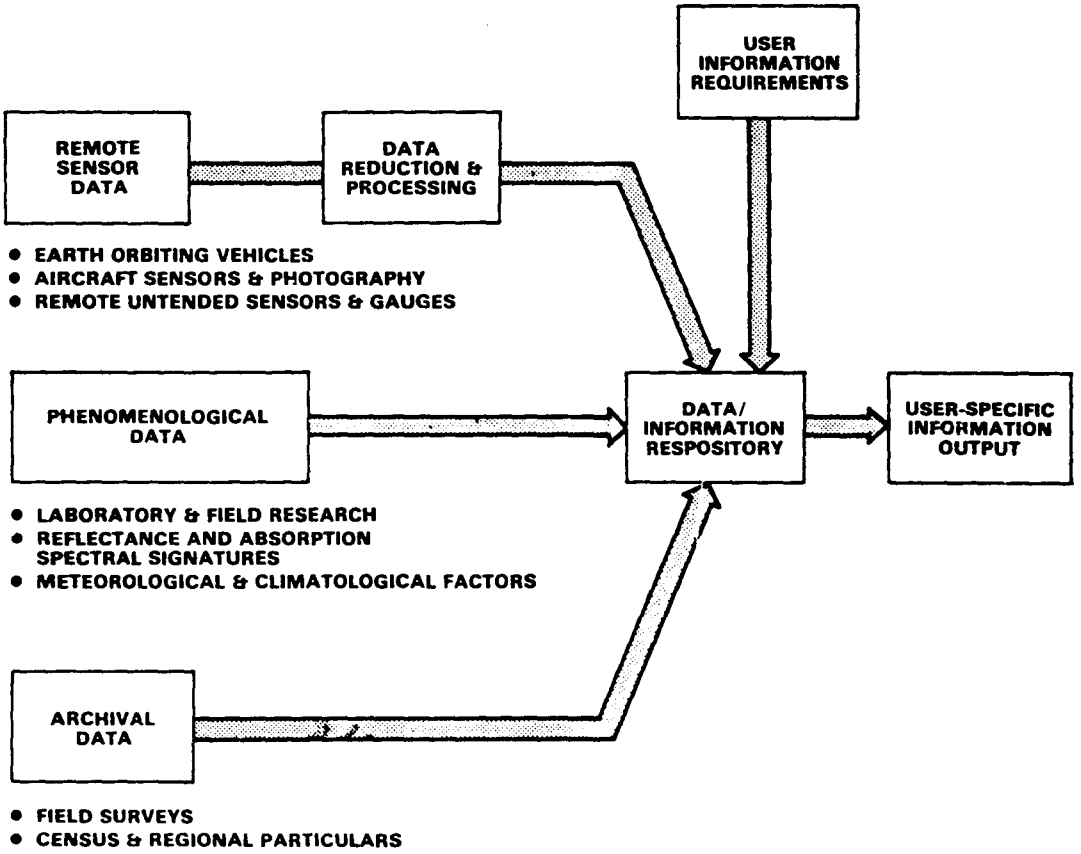

Figure B-22. A typical Earth Resources survey information system.

tion, translation, and scaling of coordinates, conversion from geographical coordinates to specified map projections; spatial analysis-statistical analysis; and modeling and measurement. Spatial analysis should include (1) overlay capability (in grid and x,y coordinates), (2) searches (proximity operations), (3) topographical analysis (calculation of slope, aspect, earthwork computations, visibility from a viewing point, route selection, etc.), and (4) spatial clustering (aggregation). An automated GIS should provide software for display of maps, graphs, and tabular information on a variety of output media.

Landsat data are being interfaced with existing geographical information systems in several ways. Where automated image processing techniques are not available (or not considered practical), the Landsat imagery is photointerpreted to derive the land cover information to be classified, encoded, and entered into the GIS. However, for optimal usage, Landsat digital tapes (both raw and classified) should be interfaced directly into the automated GIS.

In sum, Landsat data are now recognized as an important new component in automated geographical information systems because they are objective, up to date, cost effective, available in digital format, cover large areas, and have potential for temporal and spatial analysis by change detection techniques. Conversely, the other forms of data in these systems are often the key ancillary elements in better identification and interpretation of features in the Landsat images.

APPENDIX C

LANDSAT: A WORLDWIDE PERSPECTIVE

Assuming that you have completed, or at least attempted, the questions and exercises in Activities 1 through 9, you will no doubt have acquired considerable knowledge and skills in interpreting and utilizing Landsat data. However, if you have not studied satellite imagery from other parts of the world, you may well have developed a strongly biased or selective impression of the nature of the Earth's surface. Thus, you might think that Landsat color scenes are predominantly red, are dominated by folded mountains, and display forests as being severely damaged by gypsy moths. Actually, the world as seen by Landsat is a wonderfully varied and photogenic planet. This is evident from even a casual perusal of *Mission to Earth*—the picture book referenced at the very beginning of this tutorial workbook.

The New York City and Harrisburg, Pa., scenes used throughout the instructional sections of the workbook were chosen for two specific reasons. First, the workbook has been prepared under the auspices of the Eastern Regional Remote Sensing Applications Center (ERRSAC) for use in its training program, and so it was expedient to use imagery typical of the northeastern part of the United States. Second, with this constraint on general location, the selection of these two particular frames was based mainly on the diversity of terrain and cultural features and on the variety of applications inherent to each scene.

Your newly developed skills as a user of Landsat data would clearly be broadened and sharpened by coming into contact with a wider range of scenery and applications. The prime objective of this appendix is simply to enlarge your interpretive experience with Landsat by letting you examine images characteristic of other geographical regions. Twelve Landsat images are reproduced on the following pages. First, locate (by using geographical coordinates at bottom of image) the region represented in each image and make a note of (or sketch) the general terrain and cultural features you can identify with an appropriate atlas. Note, too, that for your convenience, specific features or areas considered within these images are referenced and located by the grid coordinates drawn on Overlay 1. Your task in this appendix is simply to answer a series of "leading" questions about these features. The questions appear at the bottom of each image. You are to answer them mentally or on a separate sheet if you so choose. The answers are given in Appendix H.

As an alternative to answering these questions, you may elect to write a caption of about 200 words with the format and typical content of the captions prepared for the plates in *Mission to Earth*. None of the 12 images used in Appendix C appears in that book, although some are located near certain plates in *Mission to Earth*.

You would be wise to make use of one or more atlases and geographical references in developing your answers. Consult the list of references given on p. vii of the preface of *Mission to Earth* for suggested sourcebooks.

ORIGINAL PAGE
COLOR PHOTOGRAPH

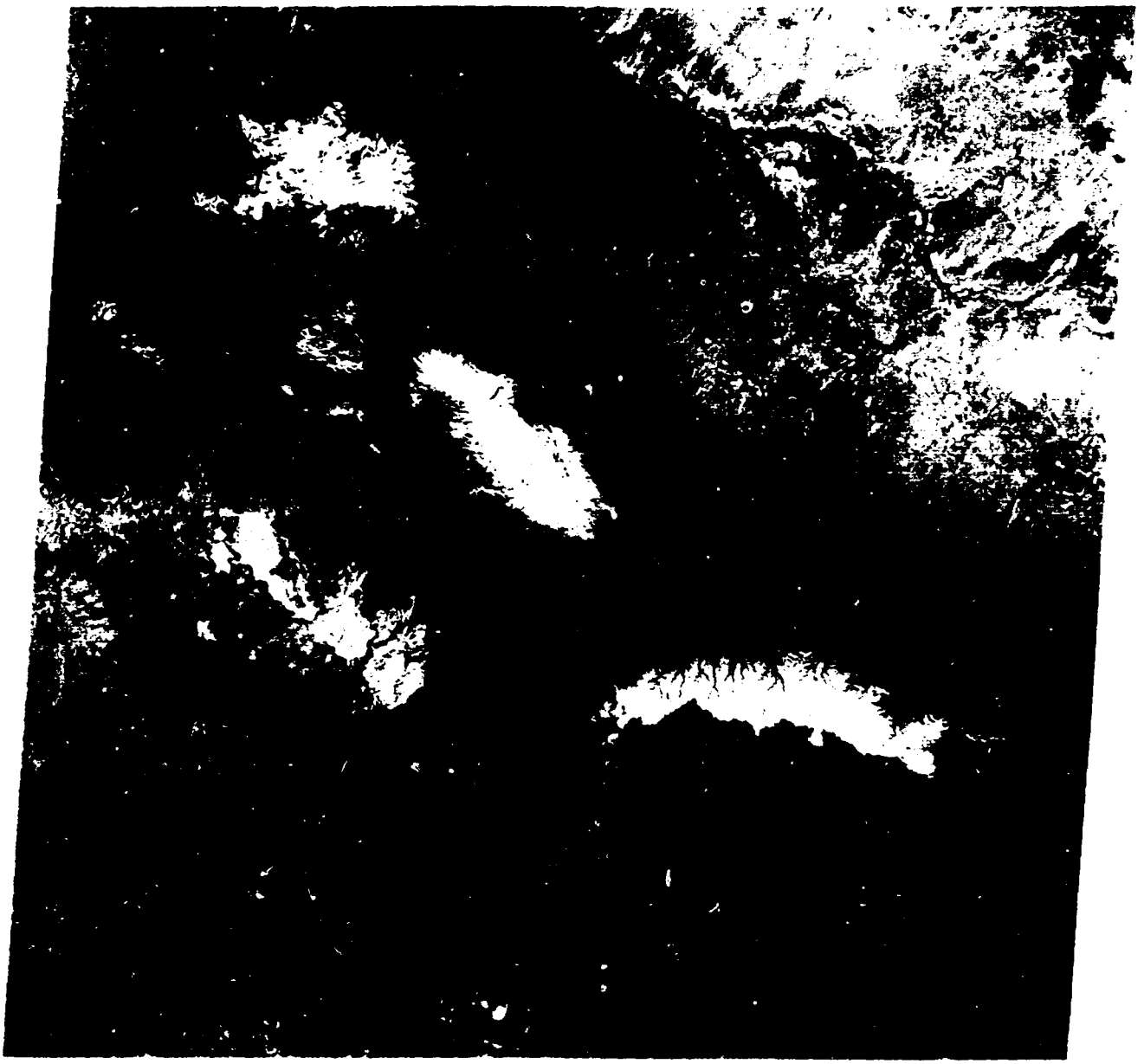

1N034-00 1W112-00 W111-301 W111-001
02MAY73 C N34-44/W111-27 N N34-43/W111-19 MSS 5 7 D SUN EL58 AZ121 190-3946-G-1-N-D-2L NASA ERTS E-1283-17332-5 01

Scene 1283-17332 **Location** _____ **Figure C-1**

1. What is the nature of the dark features clustered around I-3 and V-2? Name them geographically.
2. Identify the light spot within O-6. What is the long linear feature passing east-west about 10 km (6 miles) to the north?
3. Where is the largest town in this scene (estimate its population)? How does it appear? On the basis of color and tone, what is the most likely class (type) of trees occuring in the vicinity of this town?
4. What is the most likely class of vegetation shown around I-17 and southward? Where do farming activities seem to be concentrated? How large are these farms and what might they be growing?
5. Much of the area in the northeast quadrant is rendered in yellowish tints in this scene. Can you deduce the natural colors of the principal surface materials (guess their identity)? What natural feature passes northward through E-19?

Scene 1094-18231 **Location** _____ **Figure 6-2**

1. What are the terrain characteristics (topographical, geological) of the large region centered around H-9? What is the principal difference noted for terrain around P-7?
2. Identify the famous geological feature strongly expressed along the coastline at several points (e.g., C-11, G-14, M-20). What is the probable nature of the feature appearing at T-3?
3. There are various dark patches in forested hills, such as at I-14, M-4, P-9. Suggest a likely origin. What best explains dark areas at N-17, S-18, U-17? Indicate the most likely origin and use of lakes at J-7 and R-12.
4. Discuss the size distribution, stages of growth, and most plausible crop types (guess!) appearing as field patterns throughout the northeast section of the image. What famous products (imbibed!) are obtained from fields around O-15?
5. Locate and describe any metropolitan areas or other large works of man visible in this scene.

Landsat Mosaic of Oregon

Figure C-3

1. Identify the regional topographical units, and their geographical names, shown around the letters A, B, C and D.
2. On the basis of tone (relative grayness), speculate on the most probable vegetation cover types appearing on the terrains marked by A, B, C and D.
3. What is the nature and identity (geographical name) of the class of features to the right of letters E, F, G, and H? Why is the H feature dominantly dark whereas those at E, F, and G are associated with white patches?
4. Speculate on the identity of distinctive patterns of land use at I (regular, checkered) and J (irregular, rectangles). Look for similar patterns elsewhere. What practical uses can be found for monitoring changes in these patterns over time?
5. Locate several inland lakes in this scene. Why are some associated with light-toned terrain? What type of climate characterizes the regions containing these lakes and how might the lakes vary with season?

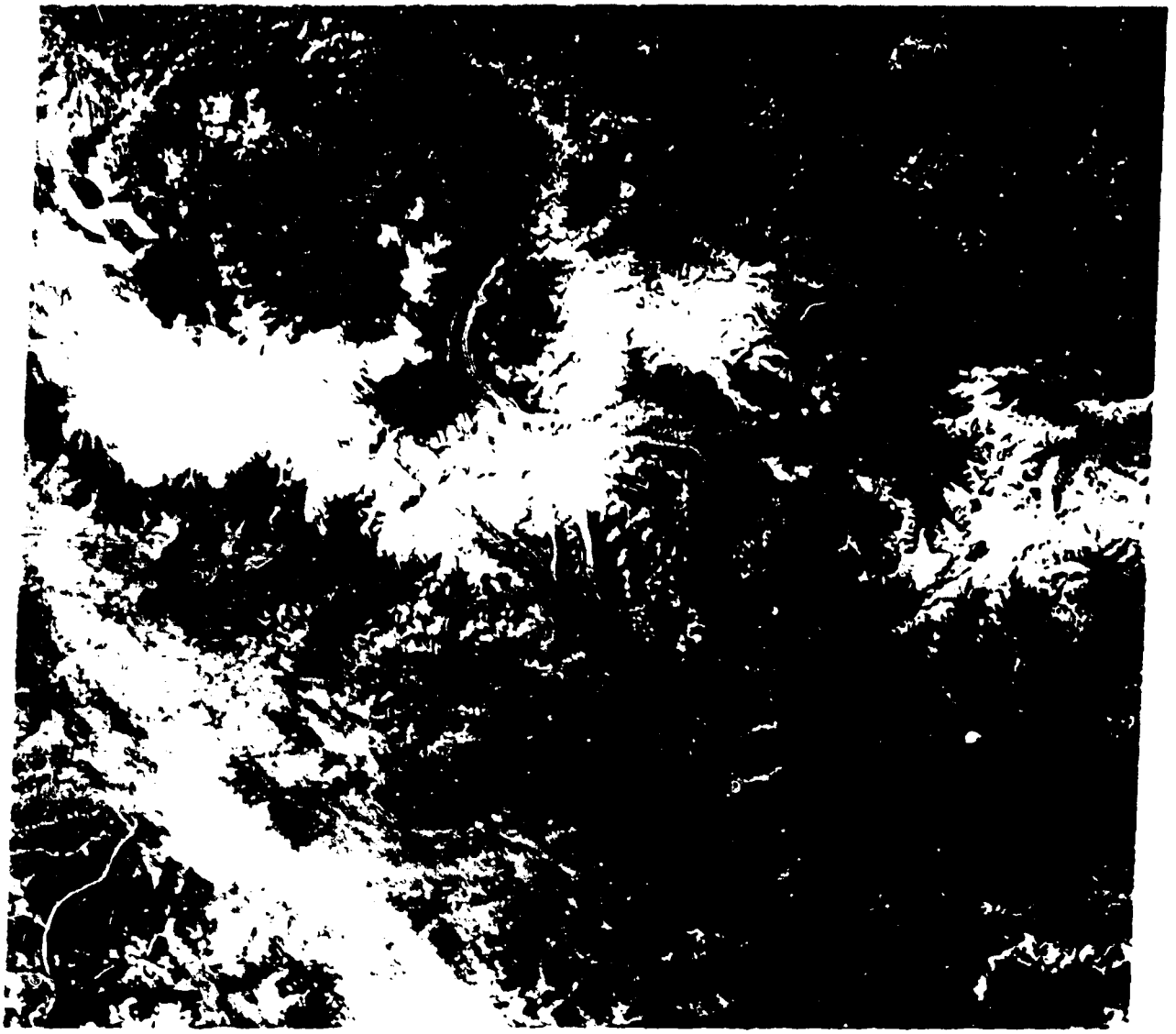

Scene 1026-20220 Location _____ Figure C-4

1. What is the nature of the large whitish area at I-13 and K-12? Is a similar area around C-10 the same or fundamentally different?
2. What are the large distinctive features evident at I-19, K-14, L-16 and elsewhere? What is the nature of the dark streaks contained therein? Are the features at R-18 and R-8, among others, different from those at I-9, etc?
3. Describe how the terrain at such places as Q-14 and Q-7 might appear to you if you were on the ground at some nearby point.
4. Why is the terrain considered at Q-14 in question 3 bluish in color, whereas terrain at places such as B-2, Q-7, and I-18 reddish? What general type(s) of vegetation can be expected in these reddish areas?
5. Offer an explanation for the origin of most of the small round lakes evident in much of the reddish-toned terrain.

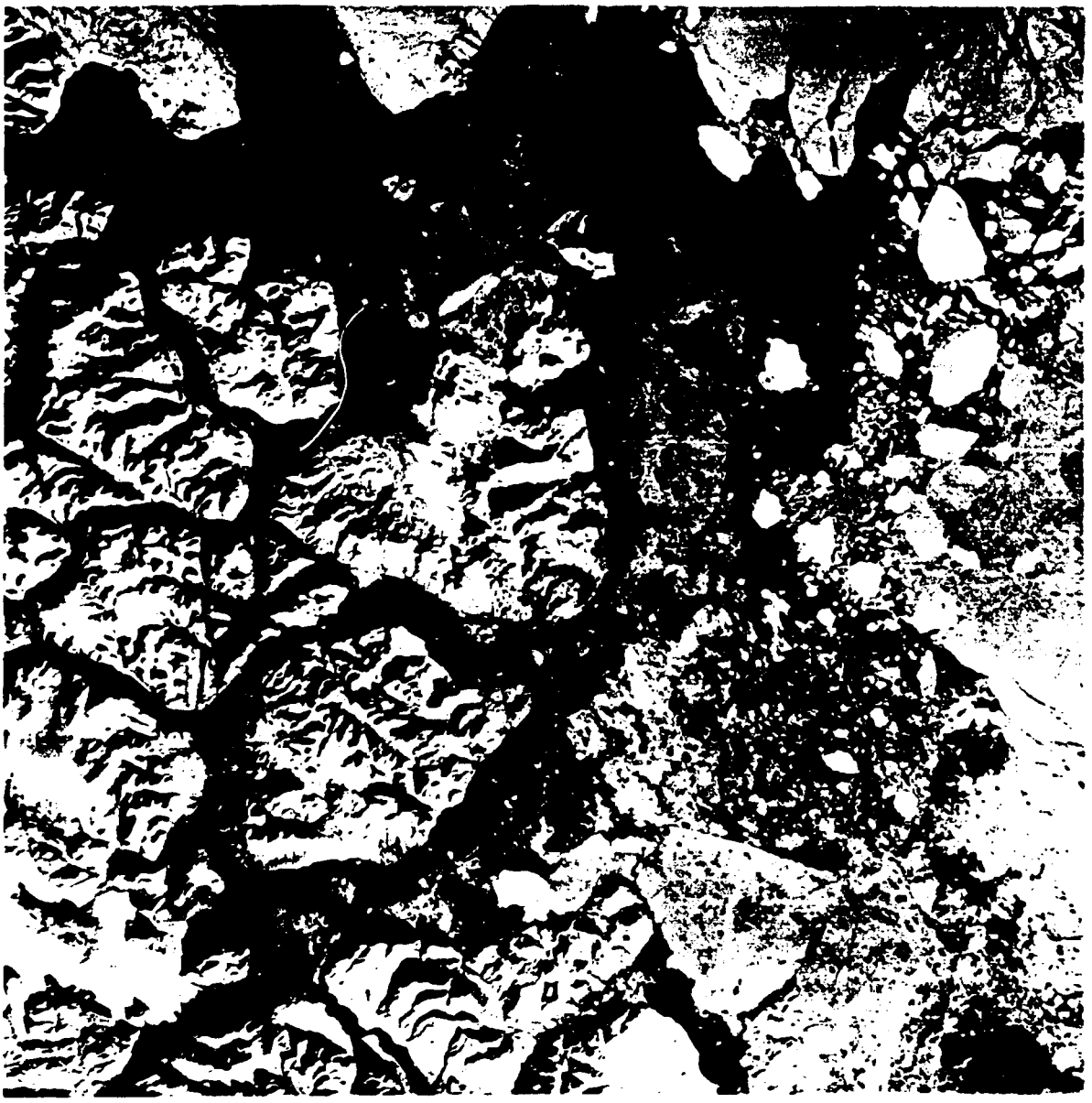

Scene 1079-13193 Location _____ Figure C-5

1. At what season was this image taken? What is the corresponding Sun elevation? What brings about the impression of topographical relief in the terrain on the left (west) side of this image?
2. Estimate the actual relief (difference in elevation) of the mountain group at H-20 (Hint: use the Sun angle and the shadow dimensions).
3. What is the natural feature occupying a valley area at C-20? The extension of the valley eastward into Gael Hamkes Bay is another common physiographical feature found particularly in high latitude mountainous terrain adjacent to the ocean; identify it.
4. What is the nature of the large irregular light-gra, objects occupying much of the right half of the image? Describe the state of the ocean surface at this time.
5. How might this kind of information about the sea's conditions as seen from Landsat be used in a practical way?

Scene 2453-09432 Location _____

Figure C-6

1. Speculate on the origin of the islands (C-7, F-5) north of the tidal marshes. Between these islands and the mainland is "apparent" terrain marked by a dark bluish-gray color; what is its nature? Do you think it is above or below sea level?
2. Identify by geographical coordinates the largest well-known cities (at least five) in this image. Two of these are connected by what river? Name the large river at C-2.
3. There are many thin linear features that appear black in this rendition. Many are interconnected and some extend into rivers. What are these features and how are they used?
4. In places, the border between the two countries depicted in this scene is sharply defined by a land-use pattern. Locate this border at that pattern (by coordinates). What are the principal land uses in this general region? There are many small dark brownish-black (with red tint) patches of irregular shapes but with straight to ragged edges; what are these?

1E060-0d E061-001 N053-301 E062-001
05JUL75 C N54-23/E061-33 N N54-22/E061-41 MSS R SUN EL53 AZ138 195-2200-N-1-N-D-?L NASA ERTS E-2164-06153-7 01

Scene 2164-06153 Location_____ Figure C-7

1. Discuss the apparent stages of growth of crops in the fields evident in the lower right corner of the image. What is the most likely crop type?
2. Most of the agricultural area (southeast) is characterized by dark tones (brownish-black). From your knowledge of this region, what accounts for this (consult a geography text if necessary)?
3. The upper and lower parts of the image, in particular, display colors indicative of extensive vegetation cover. Using a geographical reference book, as an information source, speculate on the types of natural vegetation present.
4. The lakes in this scene are numerous and have distinctive shapes and other attributes. Suggest an origin for these. Why do some contain reddish swirls–explain? What presumably has happened at J-7 and I-8? Why are some lakes marked by bluish-gray to whitish tones?
5. There are several prominent thin linear features in this image, as at L-14 and O-17. They seem also to have reddish tones. Speculate on their nature and origin.

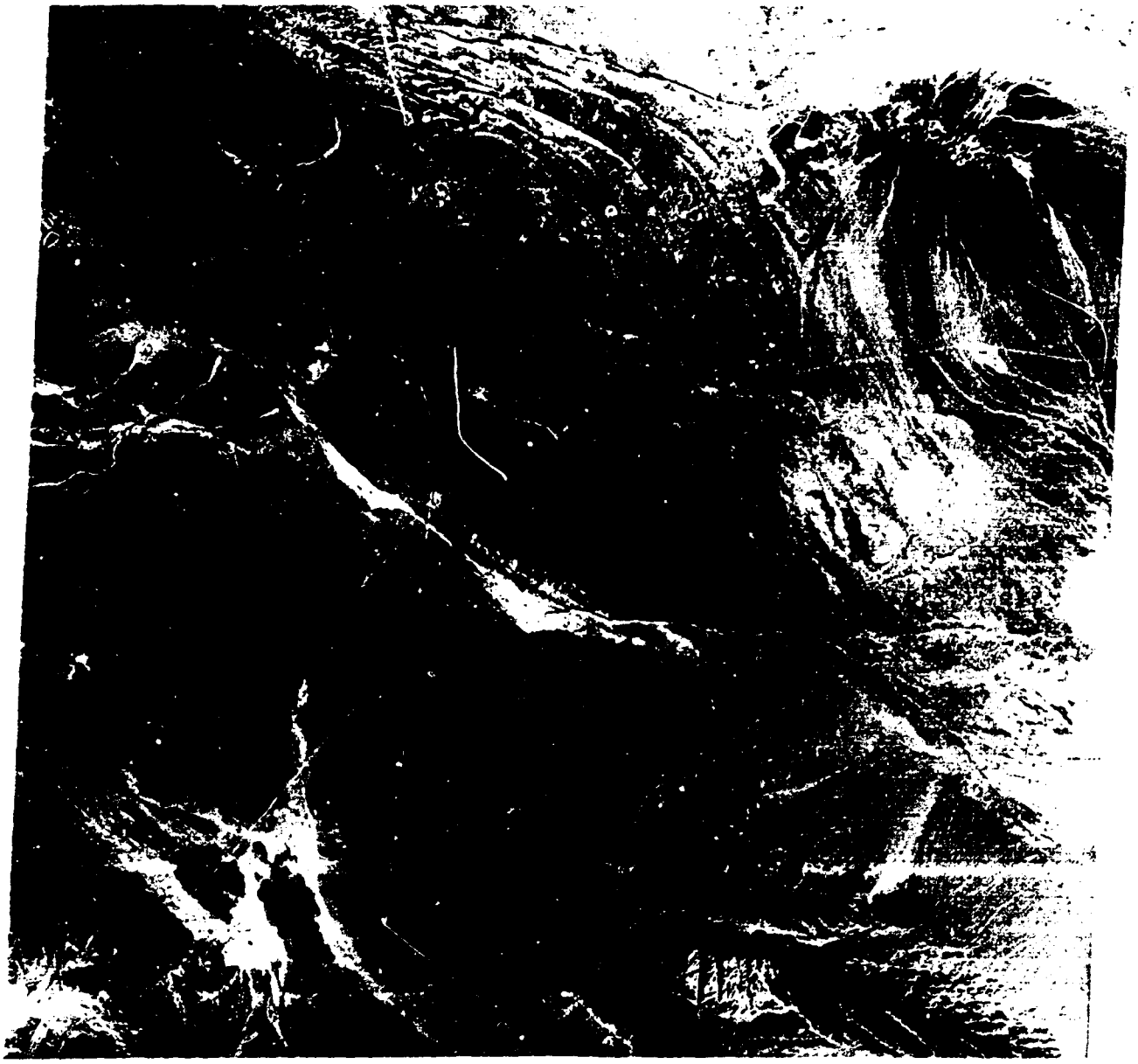

IN828-00 E861-301 E862-001 E862-301
25NOV72 C N28-42/E962-01 N N28-41/E062-03 MSS R SUN EL34 AZ150 190-1736-A-1-N-D-2L NASA ERTS E-1125-05545-4 01

Scene 1125-05545 Location _____

Figure C-8

1. What type of mountain is present at B-3 and again at S-3?
2. Name the physiographic features evident at and around L-3; identify another type of feature at H-12, K-15, and elsewhere.
3. Give the coordinates of at least one part of the mountain terrain in which sedimentary bedding units can be seen; again, note where well-developed jointing is exposed; and, locate parts of the basin where eroded folds are visible.
4. What is the likely nature of the long linear feature at J-18; what is a plausible explanation of the light-colored patch at O-21?
5. The overall color tone of this image is a greenish-blue; to what natural colors does this false color tone correspond; explain?
6. In this desolate terrain, can you find any evidence of man's activities?
7. An area known as Saindak lies at D-3 and D-4. This is the site of a porphyry copper mine valued in excess of a billion dollars. A Landsat investigator used computer classification to characterize the rock materials around the mine. Using the distinct reflectance classes for these rock and alteration zones as a standard, he sought, and found, similar classes elsewhere to the east. Can you spot any comparable class, or "anomaly" (cite coordinates)?

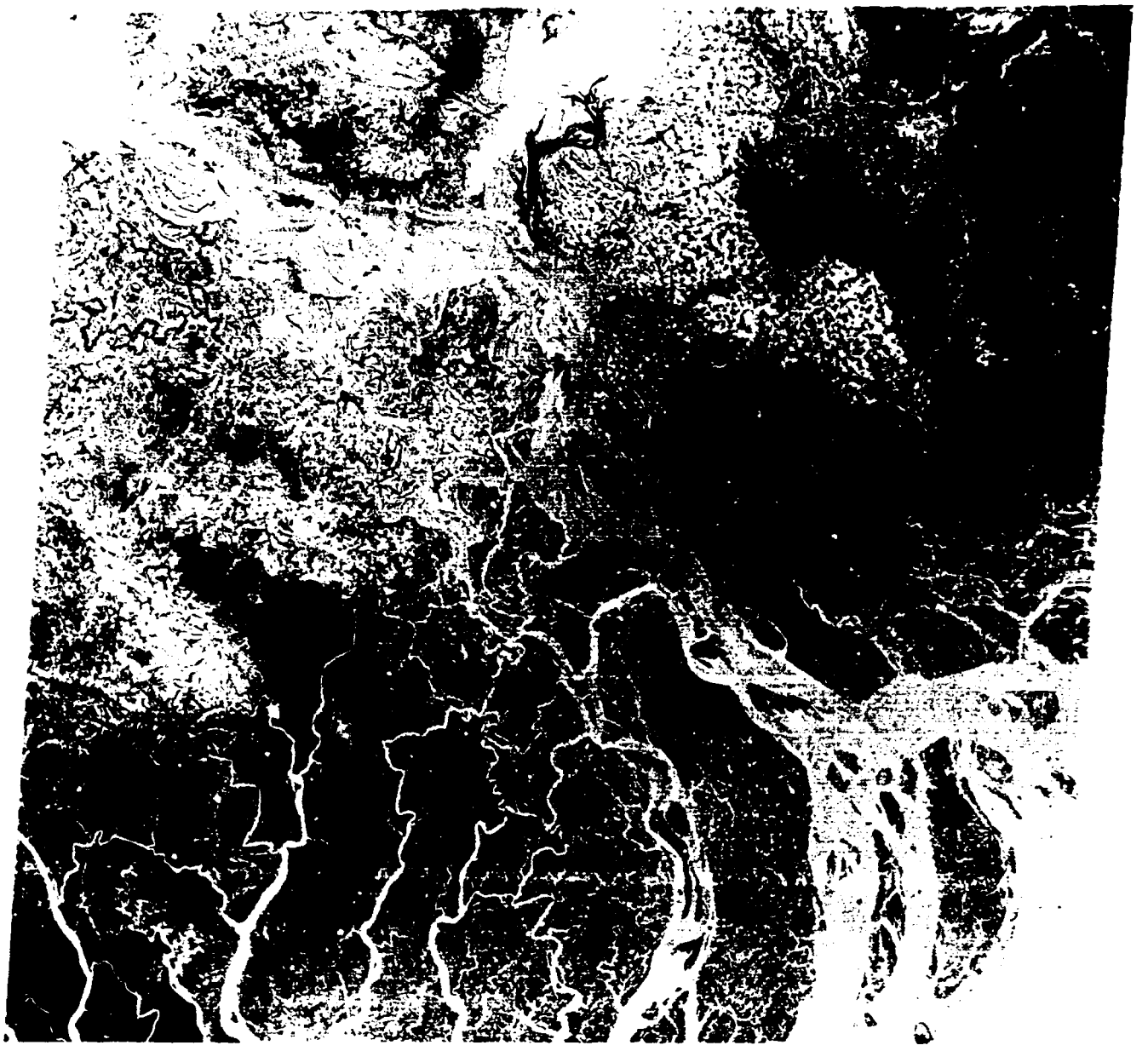

Scene 1122-03560 Location _____ Figure C-9

1. This scene covers only a part of a major geographical/geological terrain category. What is this large feature? Which two major rivers may be seen in this image (note: the ocean lies just to the south)?
2. Describe the nature of the water in the dominant river cutting across this scene, in terms of its reflectance as an indicator of the type of load it carries. What function is served by the numerous smaller streams flowing toward the bottom of the image?
3. What changes that can be monitored from Landsat could be expected for the islands in the southeastern part of the scene as a consequence of typhoons during the monsoon season? How may such observations be put to practical use?
4. Some of the different gray tones indicate varieties of vegetation communities. Speculate on the likely forest and on plant covers at B-21, T-4, G-19 and M-4.
5. Many distinctive patterns related to the history of development and change of the dominant terrain feature are well displayed, as at B-7, C-4, H-7, P-7, and elsewhere. Using appropriate references, offer some generalized explanation for this varied pattern.

Scene 1206-05000 Location _____

Figure C-10

1. From the sharpness of features displayed in this scene, suggest one or more factors responsible for this strong definition.
2. What is the nature (character and origin) of the ridges appearing at E-19, M-15, O-6, and elsewhere? What general class of rocks most probably makes up these topographical features? Do the mountainous areas at C-3 and I-6 appear different in rock type, geological structure and physiographical expression? Explain.
3. Trace at least one prominent fault evident in this scene.
4. What are the landform types prominently displayed at such points as I-10, K-13, S-7? How are they produced?
5. Speculate on the nature of the mottled tonal pattern at P-21, U-18, and other areas near the bottom of the image.

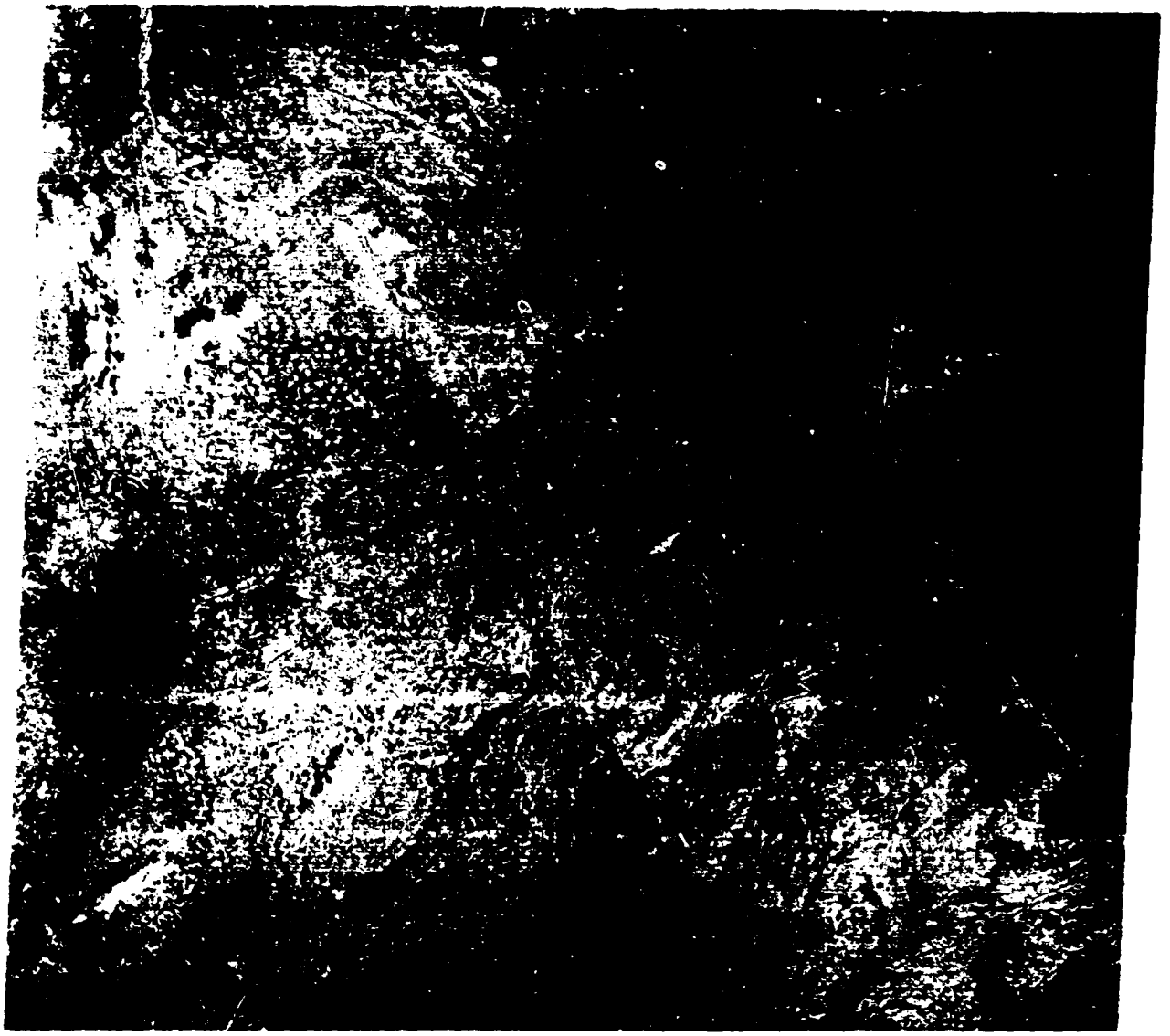

E116-081 E116-301 E117-081 N038-081
21AUG75 C N38-56/E116-53 N N38-55/E116-58 MSS 7 R SUN EL51 AZ125 191-2933-G-1-N-D-2L NASA ERTS E-2211-82122-7 81

Scene 2211-02122 Location _____ Figure C-11

1. Identify the large metropolitan areas in this scene at M-8 and B-1 (shown in part). What are the principal activities of man in this part of the world (consult an atlas or source-book)?
2. What is being grown at such places as C-14 and O-13? Where else? Describe the land patterns developed for other agricultural types, especially in terms of sizes, shapes, and distribution of farmlands.
3. What is a likely explanation for the large areas at R-11 and T-5 along the beach zones? What is produced there? Explain also the natural feature along the shoreline at T-15 and elsewhere.
4. What is the purpose of the many linear features, e.g., at P-4, O-11, and L-22, found throughout the scene?

ORIGINAL PAGE
COLOR PHOTOGRAPH

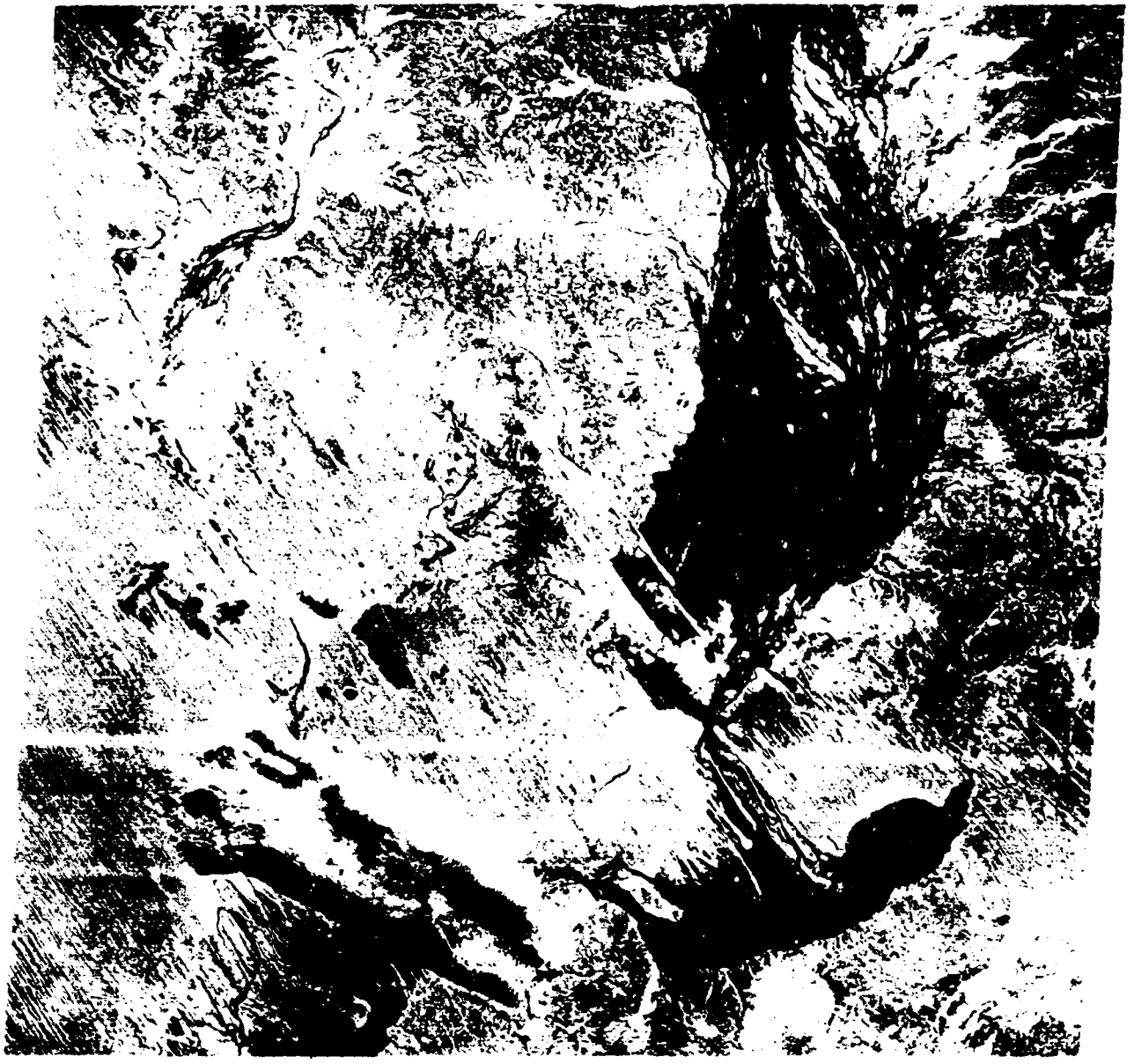

S025-001 E139-001 E139-301
26JUL73 C S24-15/E139-18 N S24-19/E139-23 MSS R SUN EL31 AZ045 189-5121-N-1-N-D-2L NASA ERTS E-1368-00081-5 01

Scene 1368-00081 Location _____ Figure C-12

1. Using an appropriate geography sourcebook, consider the region shown in this image. How well populated does it appear to be? How is the land used?
2. What are the linear features appearing prominently on the left (west) side of the image? Discuss their mode of origin.
3. What is the season in this part of the world? In particular, discuss the rainfall patterns that might occur during a typical year.
4. Account for the conspicuous areas of red that dominate parts of the scene. Note their association with bluish patterns. Can you reconstruct a recent weather history for the region?
5. Compare the cloud effects in this scene with those in 2211402122. What notable difference is evident? Why?

If you have put your mind to some of the questions dealing with the preceding 12 scenes, you should have nurtured a broadening perspective – or at least a "feel" – for satellite remote sensing as the mainstay of a global observing system. Before leaving this important appendix, we wish to further "condition" your opinion of and, hopefully, your admiration for Landsat by exposing your thoughts to several unusual but still characteristic kinds of applications (not demonstrated in the eastern U.S. scenes) being developed in the United States and worldwide. You will not be asked to respond to more questions; instead, just read on and appreciate three additional examples of the universality and adaptability of the technology we have been studying.

To set the stage for the first example, recall that in Activity 2 you learned that individual Landsat scenes can be effectively joined into mosaics often covering large regions. Mosaics have been made for each state in the U.S., the whole U.S., the entire North American continent, and many countries (e.g., England, France, Egypt, Iran, Pakistan, China, Thailand, Japan, New Zealand, Bolivia, among others) and regions (e.g., the Tibetan Plateau, the Mediterranean countries, parts of Africa, the Amazon Basin). In Activity 5 you also became familiar with the capability to classify selected subsets from a single Landsat scene into as many as 20 to 30 classes. Subsets, typically a few hundred to a few thousand square kilometers, are probably the most common classification product simply because of the practical size or volume limitations in handling large quantities of data, even in the computer. However, the potential value in classifying very large scenes – of mosaic dimensions – is nevertheless quite high, for obvious reasons, and in most instances would be worth the time and costs involved. The classification could be carried out by traditional photointerpretive methods, modified for the scale differences and sparsity of details at lower resolution, applied to mosaics and to their component scenes. This approach was used in several projects sponsored by organizations within the World Bank. W. Drewes, J. McKenna, and K. Willett of the Resource Planning Department of the World Bank, working with M. U. Chaudbury, A. Hakim, M. Munnaf and others of the Bangladesh Landsat Program have published (1979) a Land Use Association Map (scale 1:500,000) of the People's Republic of Bangladesh in which parts of 13 Landsat scenes served as the prime data base. The imagery was computer-enhanced by the Environmental Research Institute of Michigan (ERIM) and then printed on Cibachrome (a very fine-grained positive-to-positive color film capable of preserving a high level of detail) and mosaicked by Photoscience, Inc. Some computer-assisted classification was conducted but much of the actual classifying was performed by visual inspection of the Cibachrome mosaic, supported by reference to an earlier Land Use Map (1971) prepared by conventional methods and by some limited field checks. The current version of this map (too large to reproduce in this workbook) displays 21 cover types arranged in 7 general categories: Water; Wetlands; Saline Areas; Multiple Crop Area; Primarily Single Crop Area; Forests; and Other. The crop and forest types are further subdivided into 31 specialized classes, such as aus rice (early monsoon-grown); Rabi crops (dry season legumes, wheat, barley, mustard, etc.); mixed aus and deepwater aman rice (mainly monsoon season); guava orchards; pioneer grassland. Such information, updated as often as feasible, especially with Landsat on a seasonal schedule, can be invaluable, almost essential, to a developing nation which depends heavily on careful management of its food resources to avoid constant threats to staple supplies that can lead to dangers of starvation.

Closer to home, a splendid example of a large area classification is shown here as Figure C-13. This Cover Type Map of the State of California, made for the California Department of Forestry, drew upon Landsat-2 data contained in parts of 29 scenes acquired during August of 1976. A digital color mosaic was prepared from the data by the Jet Propulsion Laboratory. This mosaic was then subdivided into 30 ecozones within California that tend to be distinctive from one another, while internally similar, such as the Sierra Nevadas, the Mojave Great Desert, and the San Joaquin Valley. Each ecozone was classified as a separate entity through processing on the ILLIAC-Editor system, but the same theme colors and signature characteristics were carried through all scenes. Sixteen major resource types (classes) were established for this product. A cost per acre approaching 1/10th of 1 cent ($0.001) was achieved for a region consisting

ORIGINAL PAGE
COLOR PHOTOGRAPH

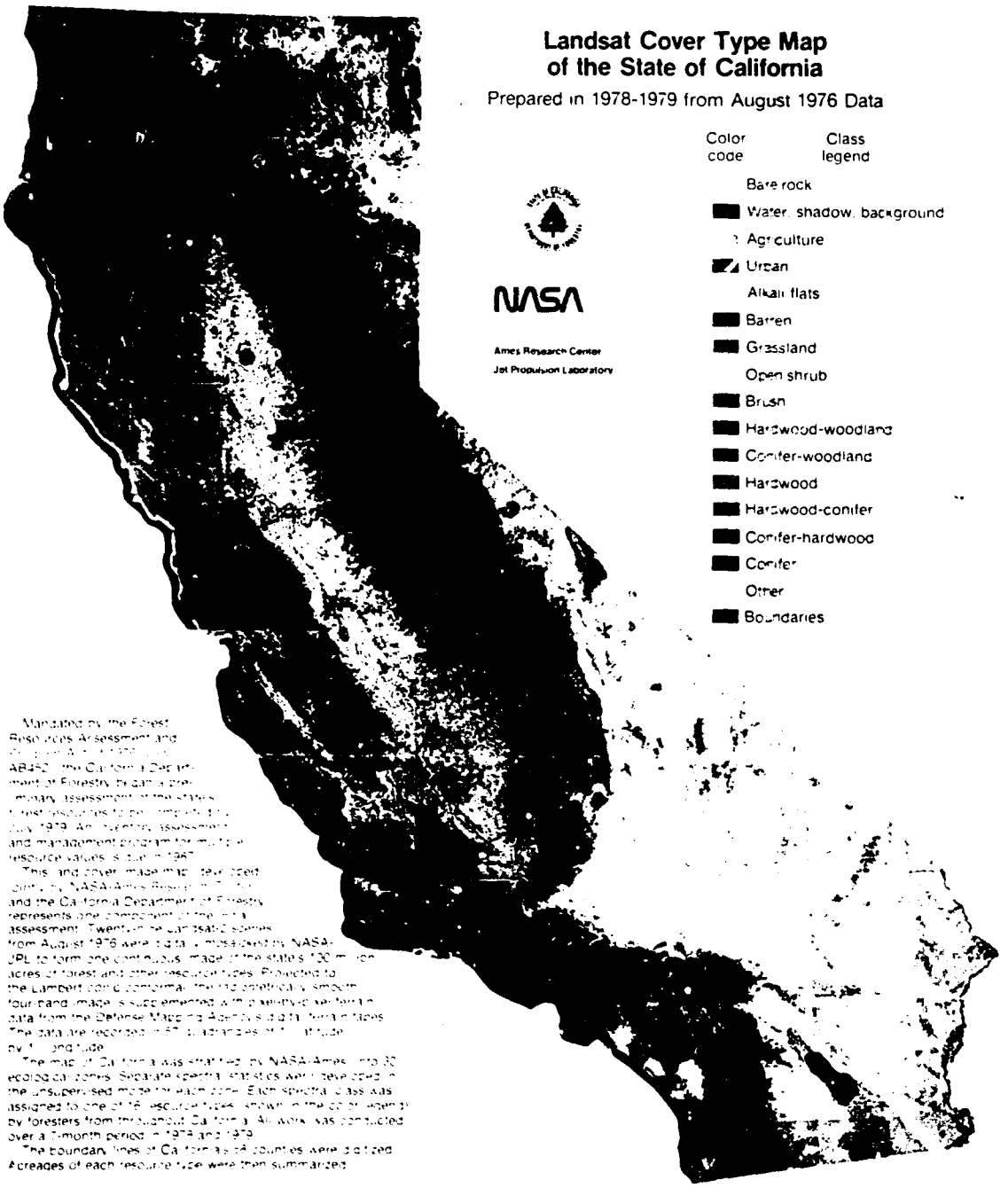

Figure C-13. Land Cover Type Map of California; the 57 rectangles connote the 1° X 1° topographic quadrangle sheets used as the mapping base.

of more than 100 million acres. This classification will be repeated in 1987.

Our second example heralds an event that frequently made headlines in 1980 and beautifully demonstrates the value of space imagery for disaster monitoring on a relatively short turnaround time. On May 18th, and several times thereafter, Mount St. Helens, in southern Washington State some 525 km north of Mt. Shasta in northern California, erupted violently for the first time in nearly 125 years. The May eruption was catastrophic, killing more than 50 people and causing greater than 1 billion dollars in damage. Aside from its newsworthy status, this eruption provided an exceptional opportunity for American volcanologists to instrument and investigate an active volcano in the confines of the 48 contiguous states. Remote sensing played a key role in documentation, analysis, and assessment of a series of events. Before, during,[1] and for months after the climactic eruption, aerial reconnaissance using photography, thermal infrared scanners, radar and other data collection systems provided outstanding images and other data sets. For example, pre-eruption thermal imagery revealed a few tell-tale "hot spots" along the flank of the main stratocone but these in themselves did not portend any impending event. After the May eruption, a large area of hot ash and flow debris ejected from near summit vents, as the peak slid and then was blasted away to form a kilometer-plus-wide amphitheater, showed up in thermal imagery as an extended high temperature anomaly. This anomaly was detected only once in HCMM images (see below) owing to the few passes over the area—mostly under cloudy conditions—between May and shutdown of the spacecraft's sensors; pre-eruption images show no abnormalities.

Landsat was more fortunate. Images were collected before the eruption. Afterwards, the western Cascade Range remained in morning clouds for nearly two months during each pass but by mid-July good looks at the area of damage occurred during some passes. Two superb views from Landsat appear in Figures C-14A and B. The first is a pre-eruption image dated September 11, 1979 that shows the symmetrical cone of Mt. St. Helens, located westward of the main line of Cascade volcanoes but still in the heavily forested (and clear cut) mountainous terrain. The second image was obtained on July 30, 1980 and graphically portrays the extent of the close-in ash flow, debris flow, mud and avalanche flow deposits, and the larger area of complete devastation marked by blowdown of trees and thick ashfall deposits. Other images to the east display more reflective (lighter toned) surfaces containing ashfall accumulations that are distributed across central and eastern Washington into neighboring states.

In Figures C-14C and D, the results from deriving an unsupervised and a supervised classification, respectively, indicate how well Landsat can compete with aerial photos as a mapping aid. The outer limit (solid white line) of deposits stemming from the ash cloud that hugged the slopes of the volcano and blast debris further out as mapped from high altitude (U-2) aerial photos can be almost exactly duplicated by the visible edges of these deposits as seen from Landsat. The unsupervised classification map delineates spectral classes set up by a clustering algorithm using a maximum likelihood classifier. The supervised classification is built from a set of classes (see caption) determined from field mapping, aerial photointerpretation, and published reports. While the areal extent of these deposits remains small enough (about 600 square kilometers) to be surveyed from aerial photos, one should not preclude use of space imagery to accomplish many of the same objectives; moreover, the setting of close-in deposits in relation to the extensive downwind deposits can best be described from the Landsat renditions.

The HCMM satellite passed over a cloud-free Mt. St. Helens area around 2:00 a.m. on June 19, 1980. The resulting Night IR image (Figure C-14E) clearly shows that the ash deposits filling the northward-trending valley leading to Spirit Lake were still quite warm (18 - 22°C at that surface) a month after the main eruption. A thermal scanner

[1] Photographers were on the ground at the time of eruption and obtained dramatic sequential pictures of the event. A scientist and a professional photographer were killed then; others taking pictures had to scurry to safety as the eruption clouds neared. Some sensational photos were obtained by individuals in several light aircraft; one plane passed across the path of the blast less than 20 seconds before its initiation. From space an extraordinary sequence of wide region images were taken 30 minutes apart by the GOES satellite. In this sequence the original blast wave (a compression) was spotted in two frames and the eastward spread of the ash cloud was followed into adjacent states for more than a day.

flown on an aircraft within 24 hours of this overpass confirmed in detail the observation made from HCMM.

The final example is a concise illustration of how Landsat can serve as an integral part in developing a timely, decision-oriented thematic map to be used in a crisis situation that continues over long periods.[2] A severe drought has beset extensive and widely separated sections of the African continent since the early 1970's. One of the more seriously affected regions is the Sahel in western Africa. Loss of water, forage for livestock, and basic crops have led to intense ecological damage that brought about countless thousands of deaths among the inhabitants. Large segments of the nomadic population have migrated almost aimlessly to different areas in search of relief, often not available, which simply futher exacerbated the conditions. In 1976, the Government of Upper Volta sought assistance from the International Development Association of the World Bank, through its West Volta Agriculture Development Project, in seeking to pinpoint possible favored areas for resettlement of the migrants. Because of the urgency of the situation, the decision was made to rely on available Landsat images as the source of current, far-reaching, and comprehensive data needed to update earlier studies rather than wait for the much later results from an aerial mission. The ancillary studies included a Soils Reconnaissance Series of maps done in 1969 and a Potential Land Use Map completed in 1976. Four Landsat scenes acquired in November of 1976 provide another critical data input. The areas chosen as most likely to meet resettlement needs lay in the southwestern portion of Upper Volta, along the Volta River. There, higher rainfall, a more suitable physical environment for agriculture, and lower population density all favored improved life-supporting conditions to which the migrants could be directed.

The Landsat scenes were digitally enhanced and classified to yield 15 distinct categories of surface state based on separable reflectances. These acted as base maps at a scale of 1:250,000, on which other map data were overlaid. Three color tones in the Landsat color composites were recognized as unfavorable to new agriculture: (1) Gray tones, representing sandstone and granite outcrops, (2) Reddish-yellow tones corresponding to areas unsuited to cultivation because of a thick, hard iron oxide crust overlying poorly developed lateritic soils, and (3) Whitish tones, marking shallow, barren soils containing iron shot or crust stones. Furthermore, absence of surface water and a high probability of deeper water tables were indicated by lack of natural vegetation evident in the Landsat imagery. Superimposed topographical data revealed inadequate terrain. This phase of the study succeeded in eliminating some 40 percent of the region from further consideration for resettlement.

Following appropriate field checks and, especially, detailed visits by helicopter to 19 areas of lower population and favorable agricultural potential, a map was prepared to show the terrain and ecological conditions along with the prime candidates for relocation. A section of this map is reproduced in Figure C-15. Rock outcrops are depicted in brown and iron-encrusted soils are shown in yellow. Blue along the Black Volta correlates with areas of alluvial soils where infestations causing river blindness would be likely. Concentrations of shrubs and trees, loosely called "forests," are indicated by a distinctive pattern. Rainfall zones are bounded by isohyet lines, such as the blue-dashed line at the 1200 mm position. The pink circles of varying radius on this map define the proportionate numbers (in black numerals) of more or less permanent inhabitants of settlements at the time of census. The uncolored areas (very light tan in this rendition) embrace areas considered more suited to developing new settlements. These areas are outlined in red and are rated as High (red crosses), Medium (red "rivets"), and Marginal (red dashes) Potential for Settlement, based on physical and human factors, and are generally surrounded by (or lie within) larger polygons (red dots) that could comprise an administrative zone.

Production of this map has fostered some firm decisions to implement relocation. Instead of an original 3.5 million hectares under consideration, now some 58,000 hectares have been singled out for more intensive examination, accompanied by detailed mapping. This "condensation" phase was completed in less than 6 months at a cost broken down as follows:

[2] Extracted from *Resource Sensing for Development: The World Bank Experience, 1972-1982*, by W. U. Drewes, in press.

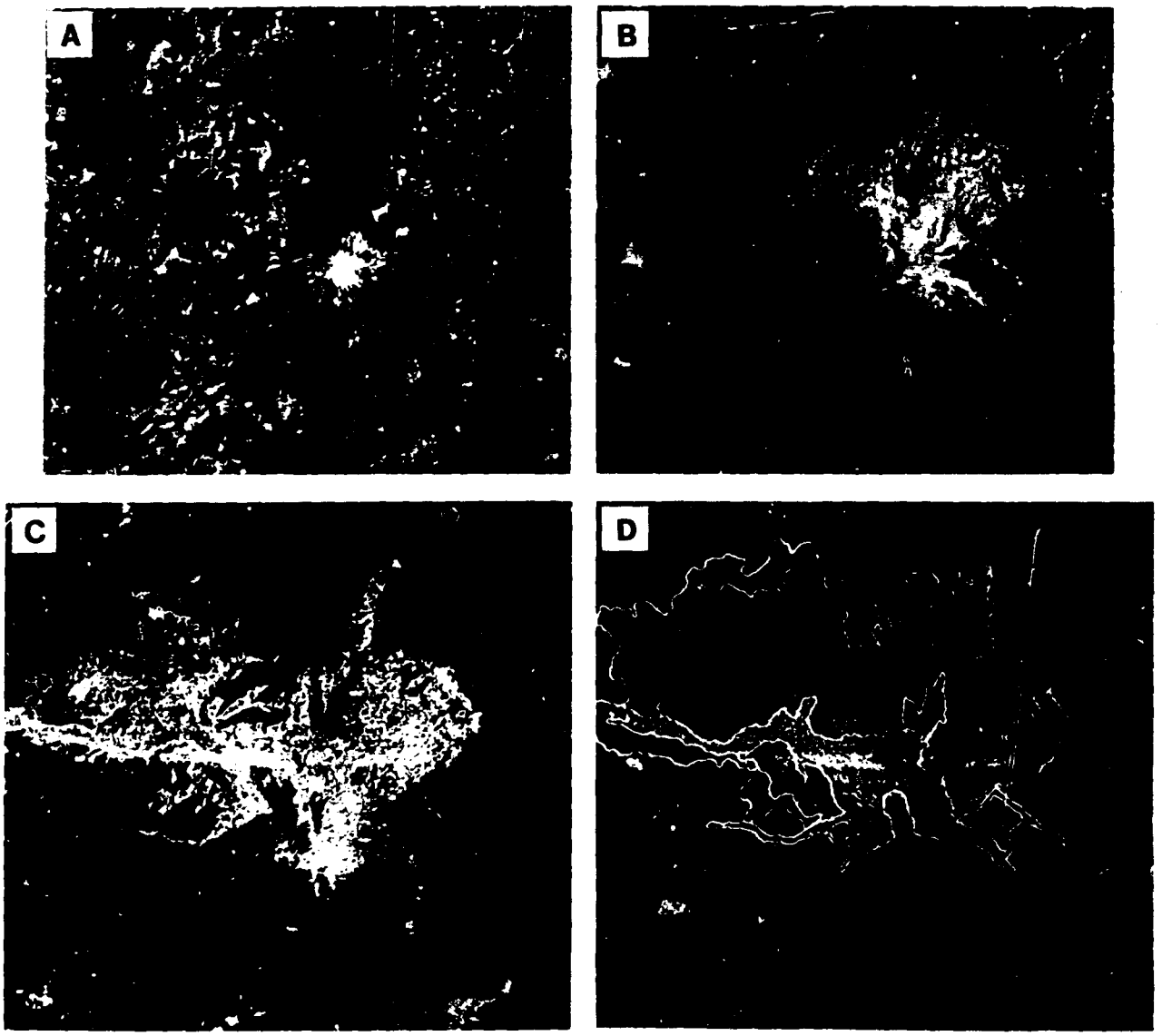

Figure C-14. A. Enlargement of Landsat image obtained on September 11, 1979 showing pre-eruption state of Mt. St. Helens. B. Ash deposits around Mt. St. Helens, as viewed from Landsat on July 31, 1980. C. Unsupervised classification of August 19, 1980 scene; the color themes (representing spectral classes) are interpreted as follows: Light Blue = Mud flow deposits; Dark Blue = Clear water; Gray = Ash-laden water; Brown and Yellow-brown = Ash flow, ash fall, mud flow deposits (undifferentiated); Orange-brown = Areas of extensive downed timber; Greenish-black = Forested areas (masked out); White = Clouds. D. Supervised classification of July 31, 1980 scene (using several published maps to select classes): Blue = Clear water; Gray = Silty (ash) water; Dark Green = Conifers; Light Green = Other vegetation (some conifers); Aqua = Ash-covered terrain, with trees down (also bare soil); Purple = Ash plus standing trees (de-needled); Yellow = Avalanche deposits; Orange = Mudflows; Red = Pyroclastics plus mudflows; Black = Pumice flow.

ORIGINAL PAGE
COLOR PHOTOGRAPH

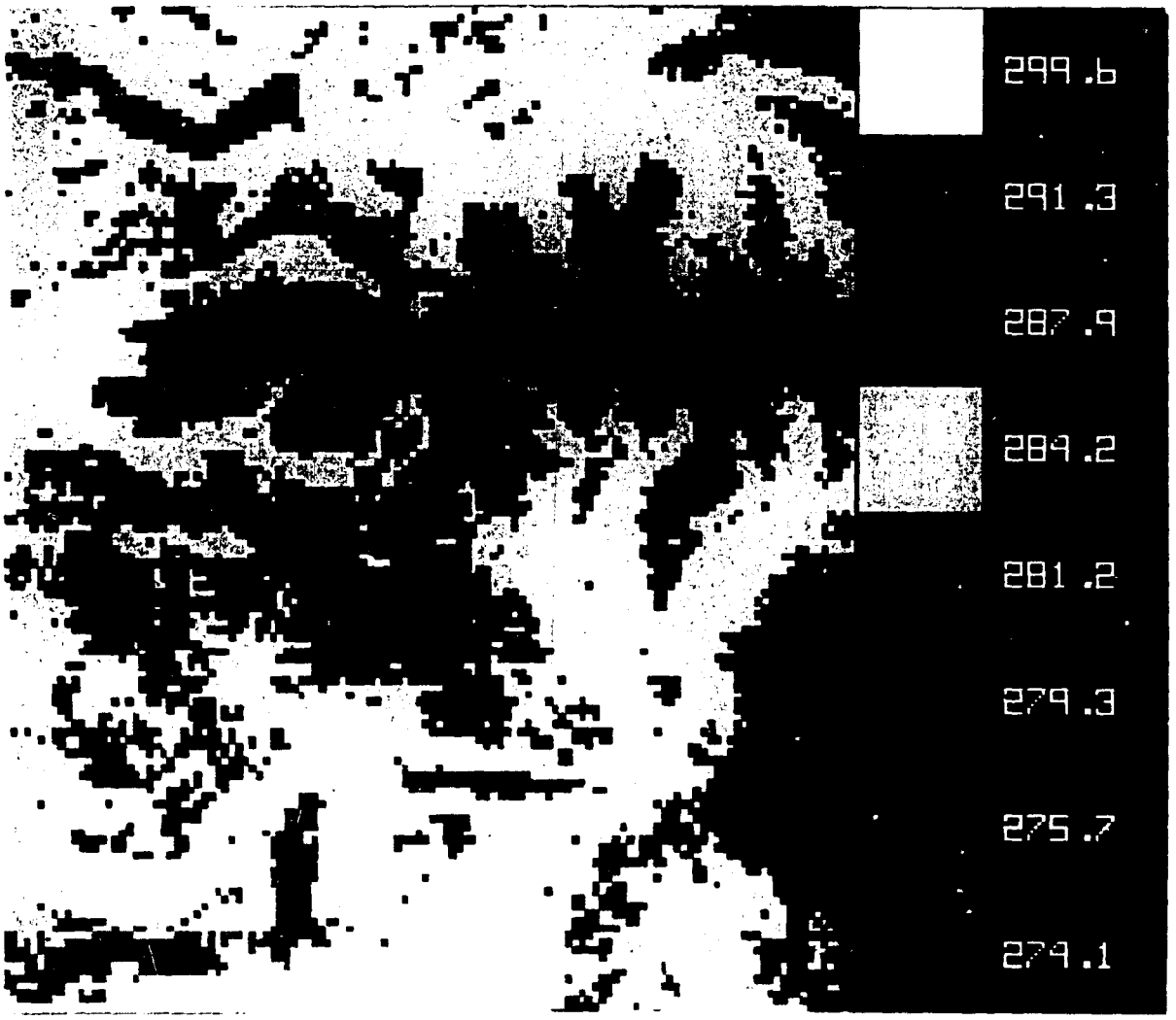

Figure C-14E. A color-coded density sliced image of the Mt. St. Helens volcano and environs produced from a subset of nighttime thermal IR data acquired by the Heat Capacity Mapping Mission (HCMM) satellite on June 19, 1980. The color-coded temperature scale on the right (in °K) is derived from DN values using a look-up table in the HCMM Users Handbook. The hottest zone (several white pixels) lies essentially near the top of the volcanic amphitheater formed when the north side of Mt. St. Helens slumped and then was blasted off on May 18, 1980. Red and orange colors define a tongue of hot ash, probably representing material emplaced from an eruption on June 12, 1980, that extends more than 8 km to the north. Much of the lofty volcano itself has relatively cold (purple and black) surface temperatures owing to its altitude. Coldwater Ridge to the northwest also shows up as cool (purple). The lakes both north and south of the eruption site are moderately warm (orange), as is characteristic of large water bodies at night because of their high thermal inertia (see p. 366).

ORIGINAL PAGE
COLOR PHOTOGRAPH

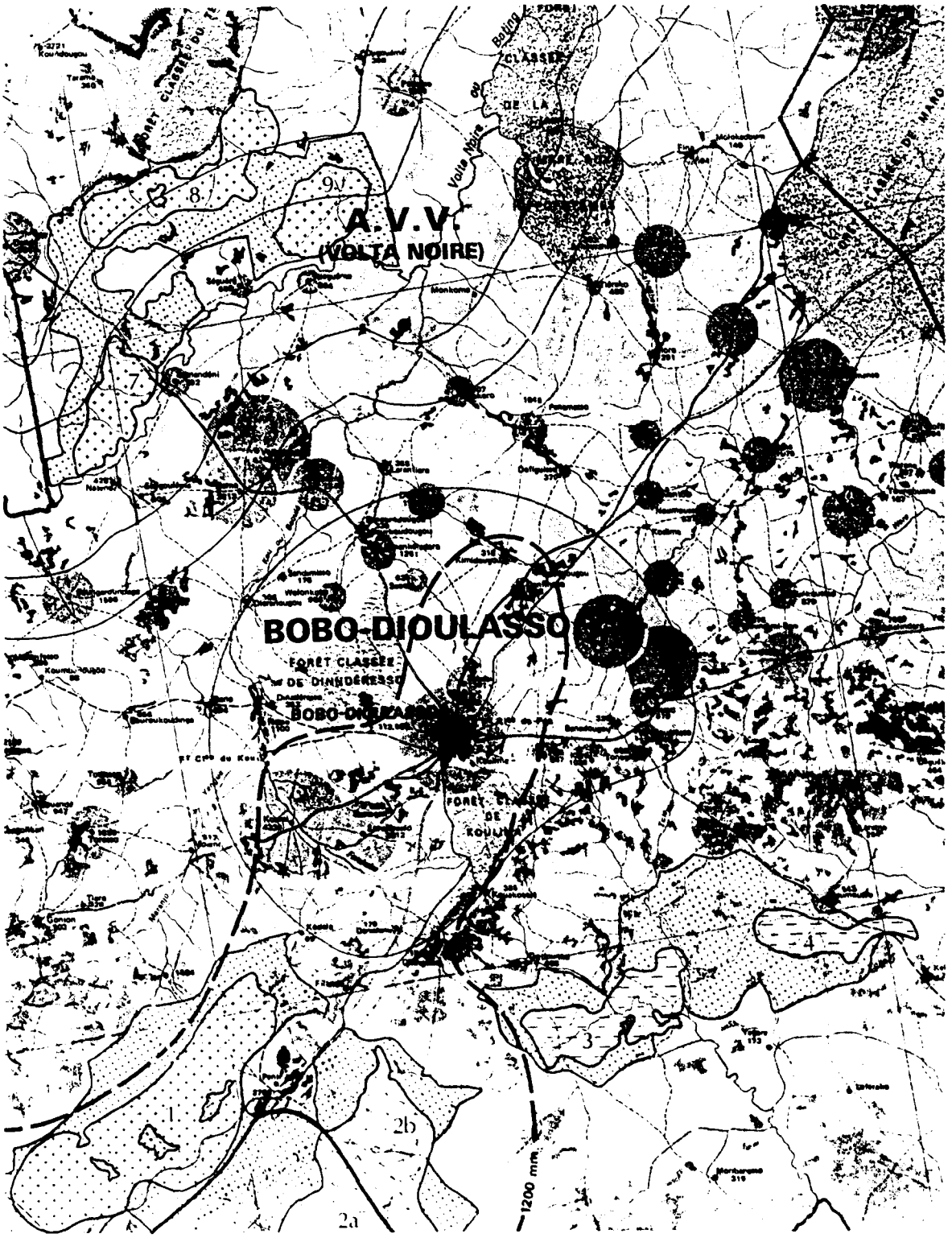

Figure C-15. Part of a Potential Settlement Areas Map of southwestern Upper Volta (see text for identification of themes), prepared by the World Bank. Base of map represents approximately 80 km.

Consultants	
Remote sensing (33 days)	$ 6,950
Soil survey (21 days)	3,150
Computer tape analysis	
Four scenes analyzed	12,000
Photo reproduction	1,400
Cartographic compilation	6,290
Map printing (500 copies)	1,900
	$31,690

Had the standard procedures using aerial photography been followed, the project would have required an estimated two years at a cost as follows:

Aircraft rental	$ 50,000
Aerial photos (13,095 frames at scale of 1:20,000)	65,475
Photo rectification	50,000
Photo mosaicking	130,095
Cartographic compilation	15,000
Photo reproduction	1,400
Map printing	1,900
Consultants, at 6 man-months	27,000
	$340,870

The only significant advantages of the aerial method would have been greater resolution and stereo-imagery.

Meanwhile, literally tens of thousands of lives remain at stake. This type of application strongly focuses on an aspect of the use of Landsat that is hard to quantify in precise, cut-and-dried terms but easy to defend and advocate in humanitarian terms.

The three examples just reviewed, together with those implicit in the previous 12 figures in this appendix, all point to one dominant fact. Namely, Landsat can be used anywhere by anyone for a wide range of purposes and at a cost which makes this use affordable by governments, commercial institutions, and even private individuals. To the developing Third World nations, as well as more affluent users in this country and across the globe, Landsat is almost certainly ratable as a "bargain" after making relatively modest initial investments in building up equipment and skilled personnel.

APPENDIX D
GLOSSARY OF TERMS[1]

Absorptance: A measure of the ability of a surface to absorb incident energy, often at specific wavelengths. (A)

Absorption: The process by which radiant energy is absorbed and converted into other forms of energy. (A)

Absorption band: A range of wavelengths (or frequencies) in the electromagnetic spectrum within which radiant energy is absorbed by a substance. (A)

Absorption spectrum: The array of absorption lines and absorption bands that results from the passage of radiant energy from a continuous source through a selectively absorbing medium cooler than the source. (A)

Absorptivity: The capacity of a material to absorb incident radiant energy. A special case of absorptance, it is a fundamental property of material that has a specular (optically smooth) surface and is sufficiently thick to be opaque. It may be further qualified as spectral absorptivity. The suffix (-ity) implies a property intrinsic with a given material, a limiting value. (A)

Accuracy: The success in estimating the true value. The closeness of an estimate of a characteristic to the true value of the characteristic of the population. (D)

Active system: A remote sensing system that transmits its own electromagnetic emanations at an object(s) and then records the energy reflected or refracted back to the sensor. (A)

Active microwave: Ordinarily referred to as a radar. (A)

Additive color process: A method for creating essentially all colors through the addition of light of the three additive color primaries (blue, green, and red) in various proportions through the use of three separate projectors. In this type of process, each primary filter absorbs the other two primary colors and transmits only about one-third of the luminous energy of the source. It also precludes the possibility of mixing colors with a single light source because the addition of a second primary color results in total absorption of the light transmitted by the first color. (A)

Aerial photograph, vertical: An aerial photograph made with the optical axis of the camera approximately perpendicular to the Earth's surface and with the film as nearly horizontal as is practicable. (A)

Aerial reconnaissance: The securing of information by aerial photography or by visual observation from the air. (A)

---

[1] Sources:
(A) Reeves (ed.) *Manual of Remote Sensing.*
(B) Swain and Davis, *Remote Sensing: The Quantitative Approach*
(C) Sabins, *Remote Sensing: Principles and Interpretation.*
(D) *Glossary of Statistical, Remote Sensing, and Image Processing Terms*, Esl, Ind. (unpublished).

Albedo: (1) The ratio of the amount of EMR reflected by a body to the amount incident upon it, often expressed as a percentage, e.g., the albedo of the Earth is 34 percent. (2) The reflectivity of a body as compared to that of a perfectly diffusing surface at the same distance from the Sun, and normal to the incident radiation. (A)

Algorithm: (1) A fixed step-by-step procedure to accomplish a given result; usually a simplified procedure for solving a complex problem; also a full statement of a finite number of steps. (2) A computer-oriented procedure for resolving a problem. (D)

Alphanumeric: A character set composed of letters, integers, punctuation marks, and special symbols. Usually the number of characters in a set varies between forty-eight and sixty-four. (D)

Analog: A form of data display in which values are shown in graphic form, such as curves. Also a form of computing in which values are represented by directly measurable quantities, such as voltages or resistances. Analog computing methods contrast with digital methods in which values are treated numerically. (A)

Ancillary data: In remote sensing, secondary data pertaining to the area or classes of interest, such as topographical, demographic, or climatological data. Ancillary data may be digitized and used in the analysis process in conjunction with the primary remote sensing data. (B)

Angle of depression: In SLAR usage, the angle between the horizontal plane passing through the antenna and the line connecting the antenna and the target. (C)

Angle of incidence: (1) The angle between the direction of incoming EMR and the normal to the intercepting surface; (2) In SLAR systems this is the angle between the vertical and a line connecting antenna and target. (C)

Angle of reflection: The angle that EMR reflected from a surface makes with the perpendicular (normal) to the surface. (A)

Angle of view: The angle subtended by lines that pass through the center of the lens to diametrically opposite corners of the plate or film used. (A)

Angstrom (Å): Unit of measurement, 10^{-10} m. (A)

Anomaly: An area on an image that differs from the surrounding normal area. For example, a concentration of vegetation within a desert scene constitutes an anomaly. (C)

Atmospheric windows: Those wavelength ranges in which radiation can pass through the atmosphere with relatively little attenuation; in the optical portion of the spectrum, approximately 0.3-2.5, 3.0-4.0, 4.2-5.0, and 7.0-15.0 μm. (B)

Attenuation: In physics, any process in which the flux density (or power, amplitude, intensity, illuminance) of a "parallel beam" of energy decreases with increasing distance from the energy source. (A)

Attitude: The angular orientation of a remote sensing system with respect to a geographical reference system. (C)

Azimuth: The geographical orientation of a line given as an angle measured clockwise from north. (C)

Background: Any effect in a sensor or other apparatus or system, above which the phenomenon of interest must manifest itself before it can be observed. (See background noise.) (A)

Background luminance: In visual-range theory, the luminance (brightness) of the background against which a target is viewed. (A)

Background noise: (1) In recording and reproducing, the total system noise independent of whether or not a signal is present. The signal is not to be included as part of the noise. (2) In receivers, the noise in the absence of signal modulation on the carrier. Ambient noise detected, measured, or recorded with the signal becomes part of the background noise. Included in this definition is the interference resulting

from primary power supplies, which separately is commonly described as hum. (A)

Backscatter: The scattering of radiant energy into the hemisphere of space bounded by a plane normal to the direction of the incident radiation and lying on the same side as the incident ray; the opposite of forward scatter. Also called backscattering. (A)

Band: (1) A selection of wavelengths. (2) Frequency band. (3) Absorption band. (4) A group of tracks on a magnetic drum. (5) A range of radar frequencies, such as X-band, Q-band, etc. (A)

Band-pass filter: A wave filter that has a single transmission band extending from a lower cutoff frequency greater than zero to a finite upper cutoff frequency. (A)

Bandwidth: (1) In an antenna, the range of frequencies within which its performance, with respect to some characteristic, conforms to a specified standard. (2) In a wave, the least frequency interval outside which the power spectrum of a time-varying quantity is everywhere less than some specified fraction of its value at a reference frequency. (3) The number of cycles per second between the limits of a frequency band. (A)

Base-height ratio: Air base (ground distance between centers of successive overlapping photos) divided by aircraft height. This ratio determines vertical exaggeration on stereo models. (C)

Batch processing: A method whereby items are coded and collected into groups and then processed sequentially. (D)

Beam: A focused pulse of energy. (C)

Blackbody, black body (symbol bb used as subscript): An ideal emitter which radiates energy at the maximum possible rate per unit area at each wavelength for any given temperature. A blackbody also absorbs all the radiant energy incident upon it. No actual substance behaves as a true blackbody, although platinum black and other soots rather closely approximate this ideal. In accordance with Kirchhoff's law, a blackbody not only absorbs all wavelengths, but also emits at all wavelengths and does so with maximum possible intensity for any given temperature. (A)

Blackbody radiation: The electromagnetic radiation emitted by an ideal blackbody; it is the theoretical maximum amount of radiant energy of all wavelengths that can be emitted by a body at a given temperature. The spectral distribution of blackbody radiation is described by Planck's law and related radiation laws. (A)

Brightness: (1) The attribute of visual perception in accordance with which an area appears to emit more or less light. (2) Luminance. (3) The luminous flux emitted or reflected per unit projected area per unit solid angle. The unit of brightness, the lambert, is defined as brightness of a surface which emits or reflects one/π lumen per square centimeter per steradian. (A)

Brightness temperature: (1) The temperature of a blackbody radiating the same amount of energy per unit area at the wavelengths under consideration as the observed body. Also called effective temperature. (2) The apparent temperature of a nonblackbody determined by measurement with an optical pyrometer or radiometer. (A)

Calibration: The act or process of comparing certain specific measurements in an instrument with a standard. (A)

Camera, multiband: A camera that exposes different areas of one film, or more than one film, through one lens and a beam splitter, or two or more lenses equipped with different filters, to provide two or more photographs in different spectral bands. (A)

Category: Each unit is assumed to be of one and only one given type. The set of types is called the set of "classes" or "categories," each type being a particular category. The categories are chosen specifically by the investigator as being the ones of interest to him. (D)

Cathode ray tube (CRT): A vacuum tube capable of producing a black-and-white or color image by beaming electrons onto a sensitized screen. As a component of a data-processing system, the CRT can be used to provide rapid, pictorial access to numerical data. (B)

Cell: An area on the ground from which EMR is emitted or reflected. (A)

Change-detection images: Images prepared by digitally comparing two original images acquired at different times. The gray tones of each pixel on a change-detection image portray the amount of difference between the original images. (C)

Chopper: A device, usually one that rotates, used to interrupt a continuous wave signal in a transmitter, receiver, or sensor. (A)

Class: A surface characteristic type that is of interest to the investigator, such as forest by type and condition, or water by sediment load. (D)

Classification: The process of assigning individual pixels of a multispectral image to categories, generally on the basis of spectral reflectance characteristics. (C)

Clustering: The analysis of a set of measurement vectors to detect their inherent tendency to form clusters in multidimensional measurement space. (B)

Color: That property of an object which is dependent on the wavelength of the light it reflects or, in the case of a luminescent body, the wavelength of light that it emits. If, in either case, this light is of a single wavelength, the color seen is a pure spectral color; but if light of two or more wavelengths is emitted, the color will be mixed. White light is a balanced mixture of all the visible spectral colors. (A)

Color balance: The proper intensities of colors in a color print, positive transparency, or negative, that give a correct reproduction of the gray scale (as faithful as can be achieved by photographic representation of the true colors of a scene.) (A)

Color composite (multiband photography): A color picture produced by assigning a color to a particular spectral band. In Landsat, blue is ordinarily assigned to MSS band 4 (0.5-0.6 μm), green to band 5 (0.6-0.7 μm), and red to band 7 (0.8-1.1 μm), to form a picture closely approximating a color-infrared photograph. (A)

Color infrared film: Photographic film sensitive to energy in the visible and near-infrared wavelengths, generally from 0.4-0.9 μm; usually used with a minus-blue (yellow) filter, which results in an effective film sensitivity of 0.5-0.9 μm. Color infrared film is especially useful for detecting changes in the condition of the vegetative canopy which are often manifested in the near-infrared region of the spectrum. Note that color infrared film is not sensitive in the thermal infrared region and therefore cannot be used as a heat-sensitive detector. (B)

Color temperature: An estimate of the temperature of an incandescent body, determined by observing the wavelength at which it is emitting with peak intensity (its color), determined by applying the Wien law. (A)

Computer-compatible tapes: Tapes containing digital Landsat data. These tapes are standard 19-cm (7½-in) wide magnetic tapes in 9-track or 7-track format. Four tapes are required for the four-band multispectral digital data corresponding to one Landsat scene. (D)

Continuous spectrum: (1) A spectrum in which wavelengths, wavenumbers, and frequencies are represented by the continuum of real numbers or a portion thereof, rather than by a discrete sequence of numbers. See absorption spectrum. (2) For EMR, a spectrum that exhibits no detailed structure and represents a gradual variation of intensity with wavelength from one end to the other, as the spectrum from an incandescent solid. (A)

Contrast stretching: Improving the contrast of images by digital processing. The original range of digital values is expanded to utilize the full contrast range of the recording film or display device. (C)

Coordinates, geographical: A system of spherical coordinates for describing the positions of points on the Earth. The declinations and polar bearings in this system are the latitudes and longitudes, respectively. (A)

Covariance: The measure of how two variables change in relation to each other (covariability). If larger values of Y tend to be associated with larger values of X, the covariance will be positive. If larger values of Y are associated with smaller values of X, the covariance will be negative. When there is no particular association between X and Y, the covariance value will approach zero. (D)

Cultural features: All map detail representing man-made elements of the landscape. (D)

Cursor: Aiming device, such as a lens with cross-hairs, on a digitizer or an interactive computer display. (D)

Data acquisition system: The collection of devices and media that measures physical variables and records them prior to input to the data processing system. (B)

Data bank: A well-defined collection of data, usually of the same general type, which can be accessed by a computer. (B)

Data dimensionality: The number of variables (e.g., channels) present in the data set. The term "intrinsic dimensionality" refers to the smallest number of variables that could be used to represent the data set accurately. (B)

Data processing: Application of procedures—mechanical electrical, computation, or other—whereby data are changed from one form into another. (A)

Data reduction: Transformation of observed values into useful, ordered, or simplified information. (A)

Decision rule (or classification rule): The criterion used to establish discriminant functions for classification (e.g., nearest-neighbor rule, minimum-distance-to-means rule, maximum-likelihood rule). (B)

Density (symbol, D): A measure of the degree of blackening of an exposed film, plate, or paper after development, or of the direct image (in the case of a printout material). It is defined strictly as the logarithm of the optical opacity, where the opacity is the ratio of the incident to the transmitted (or reflected) light or transmissivity, T, as $D = \log(1/T)$. (A)

Density slicing: The process of converting the continuous gray tone of an image into a series of density intervals, or slices, each corresponding to a specific digital range. (C)

Detection: A unit is said to be "detected" if the decision rule is able to assign it as belonging only to some given subset of categories from the set of all categories. Detection of a unit does not imply that the decision rule is able to identify the unit as specifically belonging to one particular category. (D)

Detector (radiation): A device providing an electrical output that is a useful measure of incident radiation. It is broadly divisible into two groups: thermal (sensitive to temperature changes), and photodetectors (sensitive to changes in photon flux incident on the detector), or it may also include antennas and film. Typical thermal detectors are thermocouples, thermopiles, and thermistors; the latter is termed a bolometer. (A)

Dielectric constant: Electrical property of matter that influences radar returns; also referred to as complex dielectric constant. (C)

Diffraction: The propagation of EMR around the edges of opaque objects into the shadow region. A point of light seen or projected through a circular aperture will always be imaged as a bright center surrounded by light rings of gradually diminishing intensity in the shadow region. Such a pattern is called a diffraction disk, Airy disk, or centric. (A)

Diffuse reflection: The type of reflection obtained from a relatively rough (in terms of the wavelength of the EMR) surface, in which the reflected rays are scattered in all directions. (A)

Diffuse reflector: Any surface that reflects incident rays in many directions, either because of irregularities in the surface or because the material is optically inhomogeneous, as a paint; the opposite of a specular reflector. Ordinary writing papers are good examples of diffuse reflectors, whereas mirrors or highly polished plates are examples of specular reflectors in the visible portion of the EM spectrum. Almost all terrestrial surfaces (except calm water) act as diffuse reflectors of incident solar radiation. The smoothness or roughness of a surface depends on the wavelength of the incident EMR. (A)

Diffuse sky radiation: Solar radiation reaching the Earth's surface after having been scattered from the direct solar beam by molecules or suspensoids in the atmosphere. Also called skylight, diffuse skylight, sky radiation. (A)

Digitization: The process of converting an image recorded originally on photographic material into numerical format. (C)

Discriminant function: One of a set of mathematical functions which in remote sensing are commonly derived from training samples and a decision rule, and are used to divide the measurement space into decision regions. (B)

Display: An output device that produces a visible representation of a data set for quick visual access; usually the primary hardware component is a cathode ray tube. (B)

Distribution function: The relative frequency with which different values of a variable occur. (D)

DN: Digital number. The value of reflectance recorded for each pixel on Landsat CCT's. (C)

Edge: The boundary of an object in a photograph or image, usually characterized by a rather drastic change in the gray shade value from the immediate interior of the boundary to the immediate exterior of the boundary. (D)

Edge enhancement: The use of analytical techniques to emphasize transition in imagery. (A)

Electromagnetic radiation (EMR): Energy propagated through space or through material media in the form of an advancing interaction between electric and magnetic fields. The term radiation, alone, is commonly used for this type of energy, although it actually has a broader meaning. Also called electromagnetic energy. (A)

Electromagnetic spectrum: The ordered array of known electromagnetic radiations extending from the shortest cosmic rays, through gamma rays, X-rays, ultraviolet radiation, visible radiation, infrared radiation, and including microwave and all other wavelengths of radio energy. (A)

Element: The smallest definable object of interest in the survey. It is a single item in a collection, population, or sample. (D)

Emission: With respect to EMR, the process by which a body emits EMR usually as a consequence of its temperature only. (A)

Emissivity: The ratio of the radiation given off by a surface to the radiation given off by a blackbody at the same temperature; a blackbody has an emissivity of 1, other objects between 0 and 1. (B)

Emittance: The obsolete term for the radiant flux per unit area emitted by a body, or exitance. (A)

Environment: An external condition, or the sum of such conditions, in which a piece of equipment or a system operates, as in temperature environment, vibration environment, or space environment. The environments are usually specified by a range of values, and may be either natural or artificial. (A)

Ephemeral data: Data that: (1) help to characterize the conditions under which the remote sensing data were collected; (2) may be used to calibrate the sensor data prior to analysis; (3) include such information as the positioning and spectral stability of sensors, Sun angle, platform attitude, etc. (B)

Equivalent blackbody temperature: The temperature measured radiometrically corresponding to that which a blackbody would have. Most natural objects including soil, plant leaves, and water have emissivities greater than 0.9 but less than 1.0. (A)

Exitance (symbol, M): The radiant flux per unit area emitted by a body or surface. (A)

False color: The use of one color to represent another; for example, the use of red emulsion to represent infrared light in color infrared film. (A)

Far range: Refers to the portion of an SLAR image farthest from the aircraft flight path. (C)

Feature: An n-tuple or vector with components which are functions of the initial measurement pattern variables or some subsequence of the measurement n-tuples. Feature n-tuples or vectors frequently have fewer components than the initial measurement vectors and are designed to contain a high amount of information about the discrimination between units of the types of categories in the given category set. Features often contain information about gray shade, texture, shape or context. Also, a cartographic type in digital form appearing as part of the descriptor in coded form (Feature Code). (D)

Feature extraction: The process in which an initial measurement pattern or some subsequence of measurement patterns is transformed to a new pattern feature. (D)

Field of view: The solid angle through which an instrument is sensitive to radiation. Owing to various effects, diffractions, etc., the edges are not sharp. In practice they are defined as the "half-power" points, i.e., the angle outwards from the optical axis, at which the energy sensed by the radiometer drops to half its on-axis value. (A)

Filter: (1, noun) Any material which, by absorption or reflection, selectively modifies the radiation transmitted through an optical system. (2, verb) To remove a certain component or components of EMR, usually by means of a filter, although other devices may be used. (A)

Filtering: In analysis, the removal of certain spectral or spatial frequencies to highlight features in the remaining image. (A)

Focus: The point at which the rays from a point source of light reunite and cross after passing through a camera lens. In practice, the plane in which a sharp image of any scene is formed. (A)

Format: The arrangement of descriptive data in descriptors, identifiers, or labels. The arrangement of data in bit, byte, and word form in the CPU. (D)

Frame: Complete tape of a single or multidate Landsat frame covering roughly an area about 100 nautical miles square. (D)

Frequency: Number of oscillations per unit time or number of wavelengths that pass a point per unit time. (D)

Frequency response: (1) Response of a system as a function of the frequency of excitations. (2) The portion of the frequency spectrum that can be sensed by a device within specified limits of amplitude error. (A)

Gain: (1) A general term used to denote an increase in signal power in transmission from one point to another. Gain is usually expressed in decibels. (2) An increase or amplification. (A)

Gamma: A numerical measure of the extent to which a negative has been developed, indicating the proportion borne by the contrast of the negative to that of the subject on which it was exposed. The numerical figure for gamma is the tangent of the straight-line (correct exposure portion of the curve resulting from plotting exposure against density. (A)

GCP: Ground control point. A geographical feature of known location that is recognizable on images and can be used to determine geometrical corrections. (C)

Geocoding: Geographical referencing or coding of location of data items. (D)

Geometrical transformations: Adjustments made in the image data to change its geometrical character, usually to improve its geometrical consistency or cartographic utility. (B)

Gray body: A radiating surface whose radiation has essentially the same spectral energy distribution as that of a blackbody at the same temperature, but whose emissive power is less. Its absorptivity is nonselective. Also spelled *grey* body. (A)

Gray scale: A monochrome strip of shades ranging from white to black with intermediate shades of gray. The scale is placed in a setup for color photograph and serves as a means of balancing the separation negatives and positive dye images. (A)

Grid line: One of the lines in a grid system; a line used to divide a map into squares. East-west lines in a grid sytem are x-lines, and north-south lines are y-lines. (A)

Ground data: Supporting data collected on the ground, and information derived therefrom, as an aid to the interpretation of remotely recorded surveys, such as airborne imagery, etc. Generally, this should be performed concurrently with the airborne surveys. Data as to weather, soils and vegetation types and conditions are typical. (A)

Ground range: The distance from the ground track (nadir) to a given object. (A)

Ground resolution cell: The area on the terrain that is covered by the instantaneous field of view of a detector. The size of the ground resolution cell is determined by the altitude of the remote-sensing system and the instantaneous field of view of the detector. (C)

Ground track: The vertical projection of the actual flight path of an aerial or space vehicle onto the surface of the Earth or other body. (A)

Ground truth (jargon): Term coined for data and information obtained on surface or subsurface features to aid in interpretation of remotely sensed data. Ground data and ground information are preferred terms. (A)

H-D (Hurter-Driffield) Curve: A graph showing the relationship of exposure to (photo) density, where the density is plotted against the logarithm of the exposure (also known as characteristic curve). (A)

Hardware: The physical components of a computer and its peripheral equipment. Contrasted with software. (D)

Histogram: The graphical display of a set of data which shows the frequency of occurrence (along the vertical axis) of individual measurements or values (along the horizontal axis); a frequency distribution. (B)

Hue: That attribute of a color by virtue of which it differs from gray of the same brilliance, and which allows it to be classed as red, yellow, green, blue, or intermediate shades of these colors. (A)

Illumination: The intensity of light striking a unit surface is known as the specific illumination or luminous flux. It varies directly with the intensity of the light source and inversely as the square of the distance between the illuminated surface and the source. It is measured in a unit called the lux. The total illumination is obtained by multiplying the specific illumination by the area of the surface covered by the light. The unit of total illumination is the lumen. (A)

Image: (1) The counterpart of an object produced by the reflection or refraction of light when focused by a lens or mirror. (2) The recorded representation (commonly as a photo-image) of an object produced by optical, electro-optical, optical mechanical, or electronic means. It is generally used when the EMR emitted or reflected from a scene is not directly recorded on film. (A)

Image Enhancement: Any one of a group of operations that improve the detectability of the targets or categories. These operations include, but are not limited to, contrast improvement, edge enhancement, spatial filtering, noise supression, image smoothing, and image sharpening. (D)

Image Processing: Encompasses all the various operations that can be applied to photographic or image data. These include, but are not limited to, image compression, image restoration, image enhancement, preprocessing, quantization, spatial filtering and other image pattern recognition techniques. (D)

Image Restoration: A process by which a degraded image is restored to its original condition. Image restoration is possible only to the extent that the degradation transform is mathematically invertible. (D)

Incident ray: A ray impinging on a surface. (A)

Infrared: Pertaining to energy in the 0.7-100 μm wavelength region of the electromagnetic spectrum. For remote sensing, the infrared wavelengths are often subdivided into near infrared (0.7-1.3 μm), middle infrared (1.3-3.0 μm), and far infrared (7.0-15.0 μm). Far infrared is sometimes referred to as thermal or emissive infrared. (B)

Infrared, photographic: Pertaining to or designating the portion of the EM spectrum with wavelengths just beyond the red end of the visible spectrum; generally defined as from 0.7 to about 0.1 μm, or the useful limits of film sensitivities. (A)

Insolation: Incident solar energy. (C)

Instantaneous field of view: (IFOV) A term specifically denoting the narrow field of view designed into detectors, particularly scanning radiometer systems, so that, while as much as 120° may be under scan, only EMR from a small area is being recorded at any one instant. (A)

Interactive image processing: The use of an operator or analyst at a console that provides the means of assessing, preprocessing, feature extracting, classifying, identifying, and displaying the original imagery or the processed imagery for his subjective evaluations and further interactions. (D)

Irradiance: The measure, in power units, of radiant flux incident upon a surface. It has the dimensions of energy per unit time (e.g., watts). (A)

Irradiation: The impinging of EMR on an object or surface. (A)

Kelvin: A thermometer scale starting at absolute zero (-273°C approximately) and having degrees of the same magnitude as those of the Celsius thermometer. Thus, 0°C = 273°K; 100°C = 373 °K; etc.; also called the absolute scale, thermodynamic temperature scale. (A)

Kinetic temperature: The internal temperature of an object, which is determined by the molecular motion. Kinetic temperature is measured with a contact thermometer, and differs from radiant temperature, which is a function of emissivity and internal temperature. (C)

Kirchhoff's Law: The radiation law which states that at a given temperature the ratio of the emissivity to the absorptivity for a given wavelength is the same for all bodies and is equal to the emissivity of an ideal blackbody at that temperature and wavelength. This important law asserts that good absorbers of a given wavelength are also good emitters of the wavelength. (A)

Lambertian surface: An ideal, perfectly diffusing surface, which reflects energy equally in all directions. (B)

Large scale: (1) Aerial photography with a representative fraction of 1:500 to 1:10,000. (2) Maps with a representative fraction (scale) greater than 1:100,000. (A)

Layover: Displacement of the top of an elevated feature with respect to its base on the radar image. The peaks look like flip-slopes. (A)

Light: Visible radiation (about 0.4-0.7 μm in wavelength) considered in terms of its luminous efficiency; i.e., evaluated in proportion to its ability to stimulate the sense of sight. (A)

Line, flight: A line drawn on a map or chart to represent the track over which an aircraft has been flown or is to fly. The line connecting the principal points of vertical aerial photographs. (A)

Lineament: A linear topographical or tonal feature on the terrain and on images and maps, which may represent a zone of structural weakness. (C)

Linear feature: A two-dimensional, straight to somewhat curved (usually) line, linear pattern, or alignment of discontinuous patterns evident in an image, photo, a map, which represents the expression of some degree of linearity of a single or diverse grouping of natural or cultural ground features. (Definition by N.M. Short.)

Look direction: Direction in which pulses of microwave energy are transmitted by an SLAR system. Look direction is normal to the azimuth direction. Also called range direction. (C)

Luminance: In photometry, a measure of the intrinsic luminous intensity emitted by a source in a given direction; the illuminance produced by light from the source upon a unit surface area oriented normal to the line of sight at any distance from the source, divided by the solid angle subtended by the source at the receiving surface. Also called brightness (luminance is preferred). (A)

Map: A representation in a plane surface, at an established scale, of the physical features (natural, artificial, or both) of a part of the Earth's surface, with the means of orientation indicated. (A)

Map, large-scale: A map having a scale of 1:100,000 or larger. (A)

Map, medium-scale: A map having a scale from 1:100,000, exclusive, to 1:1,000,000, inclusive. (A)

Map, small-scale: A map having a scale smaller than 1:1,000,000. (A)

Map, thematic: A map designed to demonstrate particular features or concepts. In conventional use this term excludes topographical maps. (D)

Maximum likelihood rule: A statistical decision criterion to assist in the classification of overlapping signatures; pixels are assigned to the class of highest probability.

Mie scattering: Multiple reflection of light waves by atmospheric particles that have the approximate dimensions of the wavelength of light. (C)

Micrometer (abbr. μm): A unit of length equal to one-millionth (10^{-6}) of a meter or one-thousandth (10^{-3}) of a millimeter. (A)

Micron (abbr. μ): Equivalent to and replaced by micrometer; 10^{-6} m. (A)

Microwave: Electromagnetic radiation having wavelengths between 1 m and 1 mm or 300-0.3 GHz in frequency, bounded on the short wavelength side by the far infrared (at 1 mm) and on the long wavelength side by very high-frequency radio waves. Passive systems operating at these wavelengths are sometimes called microwave systems. Active systems are called radar, although the literal definition of radar requires a distance-measuring capability not always included in active systems. The exact limits of the microwave region are not defined. (A)

Minimum distance classifier: A classification technique that assigns raw data to the class whose mean falls the shortest Euclidean distance from it.

Mosaic: An assemblage of overlapping aerial or space photographs or images whose edges have been matched to form a continuous pictorial representation of a portion of the Earth's surface. (A)

Mosaic, controlled: A mosaic that is laid to ground control and uses prints that have been rectified as shown to be necessary by the control. (A)

Mosaicking: The assembling of photographs or other images whose edges are cut and matched to form a continuous photographic representation of a portion of the Earth's surface. (A)

Multiband system: A system for simultaneously observing the same (small) target with several filtered bands, through which data can be recorded. Usually applied to cameras; may be used for scanning radiometers that use dispersant optics to split wavelength bands apart for viewing by several filtered detectors. (A)

Multichannel system: Usually used for scanning systems capable of observing and recording several channels of data simultaneously, preferably through the same aperture. (A)

Multispectral: Generally used for remote sensing in two or more spectral bands, such as visible and IR. (A)

Multispectral (line) scanner: A remote sensing device that operates on the same principle as the infrared scanner, except that it is capable of recording data in the ultraviolet and visible portions of the spectrum as well as the infrared. (A)

Multivariate analysis: A data-analysis approach that makes use of multidimensional interrelations and correlations within the data for effective discrimination. (B)

Nadir: (1) That point on the celestial sphere vertically below the observer, or 180° from the zenith. (2) That point on the ground vertically beneath the perspective center of the camera lens. (A)

Nautical mile (abbr. knot): A unit of distance used principally in navigation. For practical navigation it is usually considered the length of one minute of any great circle of the Earth, the meridian being the great circle most commonly used. Also called sea mile. (A)

Near range: Refers to the portion of an SLAR image closest to the aircraft flight path. (C)

Noise: Random or regular interfering effects in the data which degrade its information-bearing quality. (B)

Orbit: The path of a satellite around a body under the influence of gravity. (C)

Overlap: The area common to two successive photos along the same flight strip; the amount of overlap is expressed as a percentage of photo area. Also called endlap. (A)

Overlay: (1) A transparent sheet giving information to supplement that shown on maps. When the overlay is laid over the map on which it is based, its details will supplement the map. (2) A tracing of selected details on a photograph, mosaic, or map to present the interpreted features and the pertinent detail. (A)

Panchromatic: Used for films that are sensitive to broadband (e.g., entire visible part of spectrum) EMR, and for broadband photographs. (A)

Passive system: A sensing system that detects or measures radiation emitted by the target. Compare active system. (A)

Pattern: (1) In a photo image, the regularity and characteristic placement of tones or textures. Some descriptive adjectives for patterns are regular, irregular, random, concentric, radial, and rectangular. (2) The relations between any more-or-less independent parameters of a response, e.g., the pattern in the frequency domain of the response from an object. (A)

Pattern recognition: Concerned with, but not limited to, problems of:

1. pattern discrimination,
2. pattern classification,
3. feature selection,
4. pattern identification,
5. cluster identification,
6. feature extraction,
7. preprocessing,
8. filtering,
9. enhancement,
10. pattern segmentation,
11. screening. (D)

Perspective: Representation, on a plane or curved surface, of natural objects as they appear to the eye. (A)

Photogrammetry: The art or science of obtaining reliable measurements by means of photography. (A)

Photograph: A picture formed by the action of light on a base material coated with a sensitized solution that is chemically treated to fix the image points at the desired density. Usually now taken to mean the direct action of EMR on the sensitized material. Compare image. (A)

Photographic interpretation: The act of examining photographic images for the purpose of identifying objects and judging their significance. Photo interpretation, photointerpretation, and image interpretation are other widely used terms. (A)

Pitch: Rotation of an aircraft about the horizontal axis normal to its longitudinal axis, which causes a nose-up nose-down attitude. (C)

Picture: Representation of a scene by a photographic positive print or transparency, made from a negative, produced by the direct action of actinic (visible) light or EMR outside the visible part of the spectrum and converted into visible EMR by an optical-mechanical or wholly electronic scanner. (A)

Pixel: (Derived from "picture element.") A data element having both spatial and spectral aspects. The spatial variable defines the apparent size of the resolution cell (i.e., the area on the ground represented by the data values), and the spectral variable defines the intensity of the spectral response for that cell in a particular channel. (B)

Planck's Law: An expression for the variation of monochromatic emittance (emissive power) as a function of wavelength of blackbody radiation at a given temperature; it is the most fundamental of the radiation laws. (A)

Polarization: The direction of vibration of the electrical field vector of electromagnetic radiation. In SLAR systems polarization is either horizontal or vertical. (C)

Precision: A measure of the dispersion of the values observed when measuring a characteristic of elements of a population. The clustering of sample values about their own average. (D)

Pulse: (1) A variation of a quantity whose value is normally constant; this variation is characterized by a rise and a decay, and has a finite duration. (2) A short burst of EMR transmitted by the radar. (A)

Radar: Acronym for radio detection and ranging. A method, system or technique, including equipment components, for using beamed, reflected, and timed EMR to detect, locate, and (or) track objects, to measure altitude and to acquire a terrain image. In remote sensing of the Earth's or a planetary surface, it is used for measuring and, often, mapping the scattering properties of the surface. (A)

Radar beam: The vertical fan-shaped beam of EM energy produced by the radar transmitter. (A)

Radar shadow: A dark area of no return on a radar image that extends in the far-range direction from an object on the terrain that intercepts the radar beam. (C)

Radiance: The accepted term for radiant flux in power units (e.g., W) and not for flux density per solid angle (e.g., W cm^{-2} sr^{-1}) as often found in recent publications. (A)

Radiant flux: The time rate of the flow of radiant energy; radiant power. (B)

Radiant power: Rate of change of radiant energy with time. May be further qualified as spectral radiant power, at a given wavelength. (A)

Radiant temperature: Concentration of the radiant flux from a material. Radiant temperature is the product of the kinetic temperature multiplied by the emissivity to the one-fourth power. (C)

Radiation: The emission and propagation of energy through space or through a material medium in the form of waves; for example, the emission and propagation of EM waves, or of sound and elastic waves. The process of emitting radiant energy. (A)

Radiometer: An instrument for quantitively measuring the intensity of EMR in some band of wavelengths in any part of the EM spectrum. Usually used with a modifier, such as an IR radiometer or a microwave radiometer. (A)

Radiometric correction: Correcting gain and offset variations in MSS data. Procedure calibrates and corrects the radiation data provided by the Landsat sensor detectors.

Range direction: For radar images this is the direction in which energy is transmitted from the antenna and is normal to the azimuth direction. Also called look direction. (C)

Rayleigh-Jeans Law: An approximation to Planck's Law for blackbody radiation valid in the longer (microwave) wavelengths. It is almost always of sufficient accuracy for calculations in the radio and microwave regions of the spectrum. (A)

Rayleigh scattering: The wavelength-dependent scattering of electromagnetic radiation by particles in the atmosphere much smaller than the wavelengths scattered. (B)

Real-aperture radar: SLAR system in which azimuth resolution is determined by the physical length of the antenna and by the wavelength. The radar returns are recorded directly to produce images. Also called brute-force radar. (C)

Real time: Time in which reporting on events or recording of events is simultaneous with the events. For example, the real time of a satellite is the time in which it simultaneously reports its environment as it encounters it; the real time of a computer is the time during which it is accepting data and performing operations on it. (A)

Reflectance: The ratio of the radiant energy reflected by a body to that incident upon it. The suffix (-ance) implies a property of that particular specimen surface. (A)

Reflection (EMR theory): EMR neither absorbed nor transmitted is reflected. Reflection may be diffuse when the incident radiation is scattered upon being reflected from the surface, or specular, when all or most angles of reflection are equal to the angle of incidence. (A)

Reflectivity: A fundamental property of a material that has a reflecting surface and is sufficiently thick to be opaque. One may further qualify it as spectral reflectivity. The suffix (-ity) implies a property intrinsic with a given material, a limiting value. (A)

Refraction: The bending of EMR rays when they pass from one medium into another having a different index of refraction or dielectric coefficient. EMR rays also bend in media that have continuous variations in their indices of refraction or dielectric coefficients. (A)

Registration: The process of geometrically aligning two or more sets of image data such that resolution cells for a single ground area can be digitally or visually superposed. Data being registered may be of the same type, from very different kinds of sensors, or collected at different times. (B)

Remote sensing: In the broadest sense, the measurement or acquisition of information of some property of an object or phenomenon, by a recording device that is not in physical or intimate contact with the object or phenomenon under study; e.g., the utilization at a distance (as from an aircraft, spacecraft, or ship) of any device and its attendant display for gathering information pertinent to the environment, such as measurements of force fields, electromagnetic radiation, or acoustic energy. The technique employs such devices as the camera, lasers, and radio frequency receivers, radar systems, sonar, seismographs, gravimeters, magnetometers, and scintillation counters. (A)

Resolution: The ability of an entire remote sensor system, including lens, antennae, display, exposure, processing, and other factors, to render a sharply defined image. It may be expressed as line pairs per millimeter or meter, or in many other ways. In radar, resolution usually applies to the effective beam-width and range measurement width, often defined as the half-power points. For infrared line scanners the resolution may be expressed as the instantaneous field of view. Resolution may also be expressed in terms of temperature or other physical property being measured. (A)

Resolution cell: The smallest area in a scene considered as a unit of data. For Landsat-1 and -2 the resolution cell approximates a rectangular ground area of 0.44 hectares or 1.1 acres (see pixel, instantaneous field of view). (B)

Reststrahlen (residual) rays: The difference in intensities or radiance at certain frequencies (wavelengths) between the special signatures for the ideal (perfect blackbody) and actual emission curves of a substance.

Return beam vidicon (RBV): A modified vidicon television camera tube, in which the output signal is derived from the depleted electron beam reflected from the tube target. The RBV can be considered as a cross between a vidicon and an orthicon. RBVs provide highest resolution TV imagery, and are used in the ERTS (Landsat) series. (A)

Roll: Rotation of an aircraft about the longitudinal axis to cause a wing-up or wing-down attitude. (C)

Roughness: For radar images this term describes the average vertical relief of small-scale irregularities of the terrain surface. (C)

Sample: A subset of a population selected to obtain information concerning the characteristics of the population. (D)

Sampling rate: The temporal, spatial, or spectral rate at which measurements of physical quantities are taken. Temporally, sampling variables may describe how often data are collected or the rate at which an analog signal is sampled for conversion to digital format; the spatial sampling rate describes the number, ground size, and position of areas where spectral measurements are made; the spectral sampling rate refers to the location and width of the sensor's spectral channels with respect to the electromagnetic spectrum. (B)

Scale: The ratio of a distance on a photograph or map to its corresponding distance on the ground. The scale of a photograph varies from point to point because of displacements caused by tilt and relief, but is usually taken as f/H, where f is the principal distance (focal length) of the camera and H is the height of the camera above mean ground elevation. Scale may be expressed as a ratio 1:24,000; a representative fraction, 1/24,000; or an equivalence, 1 in. = 2,000 ft. (A)

Scan line: The narrow strip on the ground that is swept by the instantaneous field of view of a detector in a scanner system. (C)

Scanner: (1) Any device that scans, and thus produces an image. See scanning radiometer. (2) A radar set incorporating a rotatable antenna, or radiator element, motor drives, mounting, etc. for directing a searching radar beam through space and imparting target information to an indicator. (A)

Scanning radiometer: A radiometer, which by the use of a rotating or oscillating plane mirror, can scan a path normal to the movement of the radiometer. (A)

Scattering: (1) The process by which small particles suspended in a medium of a different index of refraction diffuse a portion of the incident radiation in all directions. (2) The process by which a rough surface reradiates EMR incident upon it. (A)

Scene: In a passive remote sensing system, everything occurring spatially or temporally before the sensor, including the Earth's surface, the energy source, and the atmosphere, that the energy passes through as it travels from its source to the Earth and from the Earth to the sensor. (B)

Sensitivity: The degree to which a detector responds to electromagnetic energy incident upon it. (C)

Sensor: Any device that gathers energy, EMR or other, converts it into a signal and presents it in a form suitable for obtaining information about the environment. (A)

Sidelap: The extent of lateral overlap between images acquired on adjacent flight lines. (C)

Signal: The effect (e.g., pulse of electromagnetic energy) conveyed over a communication path or system. Signals are received by the sensor from the scene and converted to another form for transmission to the processing system. (B)

Signal-to-noise ratio: The ratio of the level of the information-bearing signal power to the level of the noise power. Abbreviated as S/N.

Signature: Any characteristic or series of characteristics by which a material may be recognized in an image, photo, or data set. See also spectral signature. (A)

Signature analysis techniques: Techniques that use the variation in the spectral reflectance or emittance of objects as a method of identifying the objects. (A)

Signature extension: The use of training statistics obtained from one geographical area to classify data from similar areas some distance away; includes consideration of changes in atmosphere, and other geographical and temporal conditions that can cause differences in signal level for single classes of interest (see spectral signature). (B)

Smoothing: The averaging of densities in adjacent areas to produce more graduai transitions. (A)

Slant range: For radar images this term represents the distance measured along a line between the antenna and the target. (C)

Software: The computer programs that drive the hardware components of a data processing system; includes system monitoring programs, programming language processors, data handling utilities, and data analysis programs. (B)

Spatial filter: An image transformation, usually a one-to-one operator used to lessen noise or enhance certain characteristics of the image. For any particular (x, y) coordinate on the transformed image, the spatial filter assigns a gray shade on the basis of the gray shades of a particular spatial pattern near the coordinates (x, y). (D)

Spatial information: Information conveyed by the spatial variations of spectral response (or other physical variables) present in the scene. (B)

Spectral band: An interval in the electromagnetic spectrum defined by two wavelengths, frequencies, or wavenumbers. (A)

Spectral interval: The width, generally expressed in wavelength or frequency of a particular portion of the electromagnetic spectrum. A given sensor (e.g., radiometer or camera film) is designed to measure or be sensitive to energy received at the satellite from that part of the spectrum. Also termed spectral band. (A)

Spectral reflectance: The reflectance of electromagnetic energy at specified wavelength intervals. (C)

Spectral regions: Conveniently designated ranges of wavelengths subdividing the electromagnetic spectrum; for example, the visible region, X-ray region, infrared region, middle-infrared region. (B)

Spectral response: The response of a material as a function of wavelength to incident electromagnetic energy, particularly in terms of the measurable energy reflected from and emitted by the material. (B)

Spectral signature: Quantitative measurement of the properties of an object at one or several wavelength intervals. (A)

Spectrometer: A device to measure the spectral distribution of EMR. This may be achieved by a dispersive prism, grating, or circular interference filter with a detector placed behind a slit. If one detector is used, the dispersive element is moved so as to sequentially pass all dispersed wavelengths across the slit. In an interferometer-spectrometer, on the other hand, all wavelengths are examined all the time, the scanning effect being achieved by rapidly oscillating two, partly reflective, (usually parallel) plates so that interference fringes are produced. A Fourier transform is required to reconstruct the spectrum. Also called spectroradiometer. (A)

Specular reflection: The reflectance of electromagnetic energy without scattering or diffusion, as from a surface that is smooth in relation to the wavelengths of incident energy. Also called mirror reflection. (B)

Stefan-Boltzmann Law: One of the radiation laws stating that the amount of energy radiated per unit time from a unit surface area of an ideal blackbody is proportional to the fourth power of the absolute temperature of the blackbody. (A)

Steradian: The unit solid angle that cuts unit area from the surface of a sphere of unit radius centered at the vertex of the solid angle. There are 4π steradians in a sphere. (A)

Subtractive color process: A method of creating essentially all colors through the subtraction of light of the three subtractive color primaries (cyan, magenta and yellow) in various proportions through use of a single white light source. (A)

Supervised classification: A computer-implemented process through which each measurement vector is assigned to a class according to a specified decision rule, where the possible classes have been defined on the basis of representative training samples of known identity. (B)

Swath width (total field of view): The overall plane angle or linear ground distance covered by a multispectral scanner in the across-track direction. (B)

Synchronous satellite: An equatorial west-to-east satellite orbiting the Earth at an altitude of 34,900 km, at which altitude it makes one revolution in 24 h synchronous with the Earth's rotation. (A)

Synoptic view: The ability to see or otherwise measure widely dispersed areas at the same time and under the same conditions; e.g., the overall view of a large portion of the Earth's surface which can be obtained from satellite altitudes. (B)

System: Structured organization of people, theory, methods and equipment to carry out an assigned set of tasks. (D)

Target: (1) An object on the terrain of specific interest in a remote sensing investigation. (2) The portion of the Earth's surface that produces by reflection or emission the radiation measured by the remote sensing system. (B,C)

Thermal band: A general term for middle-infrared wavelengths which are transmitted through the atmosphere window at 8-14 μm. Ocasionally also used for the windows around 3-6 μm. (A)

Thermal capacity (symbol, C): The ability of a material to store heat, expressed in cal g^{-1} $°C^{-1}$ (C)

Thermal conductivity (symbol K): The measure of the rate at which heat passes through a material, expressed in cal cm^{-1} s^{-1} $°C^{-1}$. (C)

Thermal crossover: On a plot of radiant temperature versus time, this refers to the point at which the temperature curves for two different materials intersect. (C)

Thermal inertia (symbol, P): A measure of the response of a material to temperature changes, expressed in cal cm^{-2} $°C^{-1}$ $s^{-½}$. (C)

Thermal infrared: The preferred term for the middle wavelength range of the IR region, extending roughly from 3 μm at the end of the near infrared, to about 15 or 20 μm, where the far infrared begins. In practice the limits represent the envelope of energy emitted by the Earth behaving as a gray body with a surface temperature around 290°K (27 °C). (A)

Threshold: The boundary in spectral space beyond which a data point, or pixel, has such a low probability of inclusion in a given class that the pixel is excluded from that class. (D)

Tone: Each distinguishable shade of gray from white to black on an image. (C)

Training: Informing the computer system which sites to analyze for spectral properties or signatures of specific land cover classes; also called signature extraction.

Training samples: The data samples of known identity used to determine decision boundaries in the measurement or feature space prior to classification of the overall set of data vectors from a scene. (B)

Training sites: Recognizable areas on an image with distinct (spectral) properties useful for identifying other similar areas.

Transmissivity: Transmittance for a unit thickness sample. One may further qualify it as spectral transmissivity. The suffix (ity) implies a property intrinsic with a given material. (A)

Transmittance: The ratio of the radiant energy transmitted through a body to that incident upon it. The suffix (-ance) implies a property of that particular specimen. (A)

Ultraviolet radiation: EMR of shorter wavelength than visible radiation but longer than X-rays; roughly, radiation in the wavelength interval between 10 and 4000 Å.

Variance: Variance of a random variable is the expected value of the square of the deviation between that variable and its expected value. It is a measure of the dispersion of the individual unit values about their mean. (D)

Vidicon: (1) A storage-type electronically scanned photoconductive television camera tube, which often has a response to radiations beyond the limits of the visible region. Particularly useful in space applications, as no film is required. (2) An image-plane scanning device. See return beam vidicon. (A)

Vignetting: A gradual reduction in density of parts of a photographic image caused by the stopping of some of the rays entering the lens. (A)

Visible wavelengths: The radiation range in which the human eye is sensitive, approximately 0.4-0.7 μm. (B)

Wavelength (symbol λ): Wavelength = velocity/frequency. In general, the mean distance between maxima (or minima) of a roughly periodic pattern. Specifically, the least distance between particles moving in the same phase of oscillation in a wave disturbance. Optical and IR wavelengths are measured in nanometers (10^{-9} m), micrometers (10^{-6} m) and Angstroms (10^{-10} m). (A)

Wiens Displacement Law: Describes the shift of the radiant power peak to shorter wavelengths with increasing temperature. (C)

Window: A band of the electromagnetic spectrum which offers maximum transmission and minimal attenuation through a particular medium with the use of a specific sensor. (D)

Yaw: Rotation of an aircraft about its vertical axis, causing the longitudinal axis to deviate from the flight line. (C)

Zenith: The point in the celestial sphere that is exactly overhead; opposed to nadir. (A)

ACRONYMS AND ABBREVIATIONS

ADP: Automatic Data Processing
AEM: Applications Explorer Mission
AMS: Army Map Service
ASAP: Advanced Scientific Array Processor
ASCS: Agricultural Stabilization and Conservation Service
ATI: Apparent Thermal Inertia
ATS: Applications Technology Satellite

BPI: Bits per inch

CA: Canonical Analysis
C&D: Chesapeake and Delaware Canal
CCT: Computer Compatible Tape
CRT: Cathode Ray Tube
CZCS: Coastal Zone Color Scanner

DCA: Department of Community Affairs (New Jersey)
DCP: Data Collection Platform
DCS: Data Collection System
DIDS: Domestic Information Display System
DN: Digital Number
DWQ: Division of Water Quality (New Jersey)

EBR: Electron Beam Recorder
ED: Enumeration District
EDC: Eros Data Center (Sioux Falls, S. Dak.)
EDIPS: EDC Digital Image Processing System
EM: Electromagnetic
EMR: Electromagnetic Radiation
EPA: Environmental Protection Agency
ERE: Effective Resolution Element

ACRONYMS (CONT'D.)

ERIS: Earth Resources Inventory System
ERL: Earth Resources Laboratory (Bay St. Louis, Miss.)
EROS: Earth Resources Observing System
ERRSAC: Eastern Regional Remote Sensing Applications Center (Greenbelt, Md.)
ESMR: Electrically Scanned Microwave Radiometer
ESRI: Environmental Systems Research Institute

FOV: Field of View

GCP: Ground Control Point
GE: General Electric (Company)
GES: Geographic Entry System
GIS: Geographic Information System
GOES: Global Operational Environmental Satellite
GPS: Global Positioning System
GSFC: Goddard Space Flight Center

HDT: High Density Tape
Hg-Cd-Te: Mercury-Cadmium-Telluride (Detector)
HOM: Hotine Oblique Mercator
HRIR: High Resolution Infrared Radiometer

IBM: International Business Machines (Inc.)
IDIC: Image Dissector Camera System
IDIMS: Interactive Digital Image Manipulation System
IFOV: Instantaneous Field of View
IPF: Image Processing Facility
IR: Infrared
IRIS: Infrared Interferometer Spectrometer

JPL: Jet Propulsion Laboratory (Pasadena, Calif.)

LAPR: Linear Array Pushbroom Radiometer
LARS: Laboratory for Applications of Remote Sensing (W. Lafayette, Ind.)
LUDA: Land Use and Data Analysis (System)

MLA: Multilinear Array
MMS: Multi-Modular Satellite
MSS: Multispectral Scanner

NASA: National Aeronautics and Space Administration
NCIC: National Cartographic Information Center
NESS: National Earth Satellite Service
NIR: Near Infrared
NOAA: National Oceanic and Atmospheric Administration

OCS: Ocean Color Scanner
OMB: Office of Management and Budget
ORSER: Office of Remote Sensing of Earth Resources (Pennsylvania State University)

PCA: Principal Components Analysis
PFRS: Portable Field Reflectance Spectrometer
PP&L: Pennsylvania Power and Light (Company) (Allentown, Pa.)

RA: Rural Area
Radar: Radio Detection and Ranging
R&D: Research and Development
RBV: Return Beam Vidicon
RJE: Remote Job Entry

SAR: Synthetic Aperture Radar
SCMR: Surface Composition Mapping Radiometer
SEOS: Synchronous Earth Observations Satellite
SLAR: Side-Looking Airborne Radar
SMS: Synchronous Meteorological Satellite
SMSA: Standard Metropolitan Statistical Area
S/N: Signal to Noise
SOM: Space Oblique Mercator
SWIR: Short Wave Infrared

TDRS: Tracking and Data Relay Satellite
TIR: Thermal Infrared
TIROS: Television Infrared Observation Satellite
TM: Thematic Mapper

UA: Urban Area
USGS: United States Geological Survey
UTM: Universal Transverse Mercator
UV: Ultraviolet

VI: Vegetation Index
VICAR: Video Image Communication and Retrieval (System)

WRAP: Western Regional Applications Center (Moffett Field, Calif.)

ZTS: Zoom Transfer Scope

APPENDIX E
SOURCES OF DATA

The purpose of this appendix is simply to tell you where Landsat and other remote sensing data may be purchased and, in some cases, inspected beforehand. The information presented here is believed to be up to date through the middle of 1981.

Your best starting point is to request a 37-page booklet entitled *THE EROS DATA CENTER* by Allen H. Watkins. This booklet describes the EROS Data Center (EDC), now the exclusive U.S. Government outlet for data products from, among others, Landsat, Skylab, and Gemini-Apollo space missions and NASA and U.S. Geological Survey aerial photography. This booklet also contains a discussion of how to search for data in an area of interest, how to place an order for any of the data, and how to obtain other assistance and special services. When writing or phoning you should also ask for the information packet that contains order forms and current prices. Be advised that EDC supplies both Landsat images and computer compatible tapes (CCT's). As of February 1979, the Landsat imagery provided by EDC has first been computer-processed through their EDIPS routine (see p. 149) to make geometrically and/or radiometrically and otherwise enhanced products.

To establish contact with EDC, write or phone User Services EROS Data Center, Sioux Falls, SD 57198, Phone: 605-594-6511, x151, FTS: 784-7151.

The booklet also indicates the services and products available at the National Cartographic Information Center (NCIC) of the U.S. Geological Survey at Reston, Va. (addresses for NCIC offices at Reston, Rolla, Mo., Denver, Colo., and Menlo Park, Calif., are given on p. 5). Many kinds of maps (including the 1:250,000 National Topographic Maps and larger scale 7½′ and 15′ topographic sheets used or referred to in this workbook), aerial photos, and space imagery may be viewed at these NCIC facilities. In recent years, Landsat image viewing centers (sometimes referred to as Browse Libraries) have been established in many states.

Landsat data may also be obtained from a number of foreign sources, especially within those countries that operate Landsat Receiving Stations. Information about these sources is available from: Chief, International Programs Office, Mail Stop LID-18, NASA Headquarters, Washington, D.C. 20546.

Aerial photographs taken by ACSC (see p. 244) are available from: Aerial Photography Field Office, ACSC-USDA, P.O. Box 30010, Salt Lake City, UT 84125.

The black and white Landsat mosaics of the contiguous (48) United States and Alaska and Hawaii are sold in individual sheets (A through Q) at 1:1,000,000 scale and in other formats by: Cartographic Division Soil Conservation Service, Federal Center Building 1, Hyattsville, MD 20782.

The color (quasi-natural and color IR) mosaics of the United States are distributed by: National

Geographic Society, 17th & M Sts., NW, Washington, D.C. 20036.

Inquiries about images from the Heat Capacity Mapping Mission (HCMM) should be directed to: National Space Science Data Center NASA, Code 601, Goddard Space Flight Center, Greenbelt, Md. 20771.

A wide variety of space imagery, including some Landsat, Nimbus, and Seasat SAR, may be purchased from: National Climatic Center, Satellite Data Services Branch, World Weather Bldg., 5200 Auth Road, Washington, D.C. 20233.

A NASA-supported, university-based outlet for various types of space data, including 35 mm slides and other Landsat image products, is: Technology Applications Center, University of New Mexico, Albuquerque, NM 87131.

A growing number of universities and private commercial sources of remote sensing data processing and interpretation services, and image processing hardware and software systems suppliers, may be consulted for support in utilizing Landsat and other systems. A partial list of these organizations is maintained by the Applications Branch of the EROS Data Center.

Finally, if you wish to get in touch with personnel at any of NASA's three Regional Applications Centers, determine which federal region you reside in, and then write to:

Federal Regions I, II, III, and V:
Eastern Regional Remote Sensing Applications Center (ERRSAC)
Code 902.1 NASA
Goddard Space Flight Center
Greenbelt, MD. 20771

Federal Regions IV, VI, and VII:
NASA/Earth Resources Laboratory (ERL)
NSTL Station, Mississippi 39529

Federal Regions VIII, IX, and X:
Western Regional Applications Center (WRAP)
NASA/Ames Research Center
Mail Stop 242-2
Moffett Field, CA 94035

These field centers provide assistance in remote sensing technology transfer to state and local government agencies, and other users, including universities under certain conditions. Each center (as well as the EROS Data Center) publishes an informative Newsletter and offers training to selected groups.

A number of universities provide training, as workshops, short courses, and credit courses. Discussion of this type of instructional program is beyond the scope of this workbook. A list of educational institutions offering remote sensing courses is presented in:

Nealey, L.D., *Remote Sensing/Photogrammetry Education in the United States and Canada*, in Photogrammetric Engineering and Remote Sensing, vol. 43, no 3, March 1977, pp. 259-284

While comprehensive, the list has not been updated to record a number of new universities that have developed courses or centers for remote sensing since 1976. In particular, the article does not single out those university remote sensing centers, initiated and/or supported with NASA funds, that conduct specialized short courses and symposia open to individuals from outside the university community.

APPENDIX F[1]

THE REGIONAL APPLICATIONS PROGRAM

Each year, an increasing number of organizations—federal, state, and local government agencies, private industry, educational institutions, and foreign nations—are exploring operational use of the technology of satellite remote sensing. As the developer of Landsat, NASA seeks to work with potential users to help them to apply this technology to their resource assessment needs.

Toward that end, NASA's Office of Space and Terrestrial Applications has established the Regional Remote Sensing Applications Program. Its aim is to transfer the capability for using this technology by expanding awareness of Landsat's potential and by assisting users to evaluate the utility of the technology.

Designed to facilitate user assessment and adoption of Landsat technology, the Regional Remote Sensing Applications Program provides assistance primarily to state and local governments but is also available to representatives of federal agencies, universities, and private industry. The program includes the following:

- A liaison and awareness effort, which seeks to acquaint prospective users with the many opportunities for using remotely sensed data by means of briefings, workshops, conferences, and special publications.
- NASA-provided orientation and training in techniques of analyzing remotely sensed data.
- Cooperative user/NASA demonstration projects to show Landsat's capability as a resource management tool.
- Technical assistance to help users locate sources of services and systems, to help them apply the technology to their own projects, and to keep them informed on advances in technology.

The program draws upon the expertise and resources of all NASA centers, but it is concentrated in three NASA field installations, each covering a specific geographical area of the United States:

- The Eastern Regional Remote Sensing Applications Center (ERRSAC), Goddard Space Flight Center, Greenbelt, Md., which serves the northeast and north central states, plus Puerto Rico and the Virgin Islands.
- The Western Regional Applications Program (WRAP), Ames Research Center, Moffett Field, Calif., which serves the western states, including Alaska and Hawaii.
- The Earth Resources Laboratory (ERL) of the National Space Technology Laboratories, Bay St. Louis, Miss., which serves the southeast and south central states.

[1] Extracted from a brochure entitled *The Regional Remote Sensing Applications Program*, prepared and distributed by NASA Headquarters, Washington, D.C. 20546

All of NASA's Regional Remote Sensing Applications Centers use a variety of mechanisms to acquaint prospective and current users with developments in the remote sensing field and with the activities of the Regional Applications Program.

The Centers conduct workshops and orientation briefings for state and local officials, legislators, or state and local agency administrators on the benefits of Landsat for resource management. An annual symposium has been initiated to assess progress in the use of Landsat data and to build communication links between users and with the emerging service industry.

Cooperative demonstration projects, through which NASA joins with state and local governments in practical demonstrations of how Landsat technology may be applied to specific user needs, are key parts of the Regional Remote Sensing Applications Program. These projects are designed to give personnel of the user organization maximum involvement in the entire process of converting raw Landsat data to useful management information.

In these projects, users select their own priority applications and, where there is a match with available technology, join with NASA in developing a project plan. Users and NASA work together in processing remote sensing information and applying it in operational settings for selected test sites. Examples of demonstration projects already conducted with state agencies include general land cover classifications, assessments of agricultural and forestry resources, shoreline measurement for coastal zone studies, water resource inventories, and analyses of soil erosion hazards.

Cooperative projects in these and many other fields give users the opportunity to decide, on the basis of first-hand experience, to what extent remote sensing data can contribute to their informational needs and their decision-making process and if the use of remotely sensed data should be incorporated into their operational resource management programs.

If a user decides to build an independent capability to use Landsat data, NASA provides follow-on assistance for incorporating the technology into the user agency's operational system. Part of this assistance includes introducing the user to various hardware systems and services that are available from the private sector.

Each Center also disseminates information on a regular basis throughout its region through newsletters, brochures, and publications describing remote sensing applications or remote sensing products and services.

The content and duration of orientation and training programs vary in accordance with prospective user needs. Typically, the programs can include the following:

- Orientation briefings, lasting from a half a day to several days, which provide resource managers with a basic familiarization with remote sensing. These briefings also give state agency directors or other executive level personnel the opportunity to determine whether Landsat data can be employed to advantage in their particular areas.
- Basic technical training courses in which trainees from user organizations receive "hands-on" instruction in the fundamentals of computerized image analysis and data management to prepare them for participation in cooperative demonstration projects.
- Advanced courses that focus on the application of remote sensing to the user's specific sphere of interest. These are generally included as part of demonstration projects.

The intent is to help state governments and other users to apply remote sensing technology with confidence and to build the capability to conduct their own training program. A portion of the Regional Remote Sensing Applications Program is devoted to cooperative efforts with universities, involving training of professors and students through instructional courses, university symposia, and visits to NASA centers. NASA can also provide assistance to universities in developing curricula and discipline-oriented special publications.

In November 1979, the National Oceanic and Atmospheric Administration (NOAA) was assigned responsibility for all operational civilian remote sensing activities from space and has begun developing plans for moving to a fully integrated, satellite-based, land remote sensing program. The Department of Commerce, NOAA's parent organization, will seek ways to further private sector opportunities in civil land remote sensing activities; it will also coordinate programs among federal agencies and with state and local governments through representative organizations such as the National Governors Association (NGA) and the National

Conference of State Legislatures (NCSL). In supporting Congressional initiatives, the NCSL reviewed state government applications of Landsat data and found the results "impressive," urging Congress to make a firm commitment to ensure the operational status of the satellite-based system. Fully operational use of satellite data for managing the Earth's resources appears well on its way to becoming a reality.

APPENDIX G
SELECTED REFERENCES ON REMOTE SENSING[1]

Remote Sensing Books, Monographs, Etc.

Aggarval, J. K., R. O. Duda, and A. Rosenfeld, (eds.), *Computer Methods in Image Analysis*, IEEE Press, 1977.

Anderson, J., et al., *A Land Use and Land Cover Classification System for Use with Remote Sensor Data*, U.S.G.S. Prof. Paper 964, 1976.

Andrews, H. and B. Hunt, *Digital Image Restoration*, Prentice-Hall, 1977.

Barrett, E. and L. Curtis, *Introduction to Environmental Remote Sensing*, Halstead Press, 1978.

Bernstein, R., (ed.), *Digital Image Processing for Remote Sensing*, IEEE Press, 1978.

Brosius, C. A., F. C. Gervin, and J. M. Ragusu, *Remote Sensing and the Earth*, School Board of Brevard County, Rockledge, Florida, 1977.

Cehler, J., *Thermal Infrared Remote Sensing: A Bibliography*, Research Report 76-1, Canadian Center for Remote Sensing, Ottawa, 1976.

Claugh, J. and L. W. Morley, (eds.), *Earth Observation Systems for Resource Management and Environmental Control*, Plenum Press, New York, 1977.

Earth Photographs from Gemini 3, 4, and 5, NASA SP-129, 1967.

Estes, J. and L. Senger, (eds.), *Remote Sensing-Techniques for Environmental Analysis*, Hamilton Publishing Company, 1974.

General Electric Space Division, *Landsat 3: Reference Manual*, Valley Forge Space Center, Philadelphia, 1978.

Gierhoff-Emden, H. G., *Orbital Remote Sensing of Coastal and Offshore Environments: A Manual of Interpretation*, W. de Gouyter, New York, 1977.

Gonzalez, R. C. and P. Wintz, *Digital Image Processing*, Addison-Wesiey, Reading, Massachusetts, 1977.

Harper, D., *Eye in the Sky: Introduction to Remote Sensing*, Multiscience, Montreal, 1976.

Holz, R., (ed.), *The Surveillant Science*, Houghton Mifflin, 1973.

Johnson, P., (ed.), *Remote Sensing in Ecology*, University of Georgia Press, Athens, 1969.

[1] Adapted, updated, and expanded from Rudd, R. D., L. W. Bowden, R. N. Colwell, and J. E. Estes, *Textbooks and Technical References for Remote Sensing*, in Conf. of Remote Sensing Educators (CORSE-78), NASA Conf. Publication 2102, 1980, pp. 269-288.

Kroeck, D., *Everyone's Space Handbook*, Pilot Rock, Inc., 1976.

Krumpe, P., *The World Remote Sensing Bibliographic Index*, Tensor Industries, Inc., 1976.

Lebert, F., *Radargrammetry for Image Interpretations*, 2nd Ed., Internat. Inst. for Aerial Survey and Earth Sciences, Enschede, The Netherlands, 1978.

Lee, K., *Laboratory Manual for Study of Remote Sensing*, Colorado School of Mines, 1976.

Lillesand, T., *Fundamentals of Electromagnetic Remote Sensing*, S.U.N.Y., Syracuse, 1976.

Lillesand, T. M. and R. W. Kieffer, *Remote Sensing and Image Interpretation*, Wiley, New York, 1979.

Lintz, J., and D. Simonett, (eds.), *Remote Sensing of Environment*, Addison-Wesley Publishing Co., 1976.

Long, M. W., *Radar Reflectivity of Land and Sea*, Lexington Books, Lexington, Massachusetts, 1975.

Mathews, R., (ed.), *Active Microwave Workshop Report*, NASA SP-376, 1975.

NASA, *Landsat Data Users Handbook*, GSFC Document 76SDS-4258, Goddard Space Flight Center, 1976.

NASA, *Skylab Explores the Earth*, SP-380, Govt. Printing Office, Washington, D.C., 1977.

Nicks, O., (ed.), *This Island Earth*, NASA SP-250, 1970.

Pratt, W., *Digital Image Processing*, Wiley, 1977.

Reeves, R., *Electromagnetic Remote Sensing*, Amer. Geol. Institute, 1968.

Reeves, R., (ed.), *Manual of Remote Sensing* (Vols. I and II), Amer. Soc. of Photogrammetry, 1975.

Remote Sensing of Earth Resources, Committee on Science and Astronautics, U.S. House Repr., U.S.G.P.O., 1972.

Remote Sensing with Special Reference to Agriculture and Forestry, Nat'l. Acad. Sciences, 1970.

Richason, B., (ed.), *Introduction to Remote Sensing of the Environment*, Kendall/Hunt, 1978.

Rosenfeld, A. and A. C. Kak, *Picture Processing by Computer*, Academic Press, New York, 1976.

Rudd, R., *Remote Sensing: A Better View*, Duxbury Press, 1974.

Sabins, F., *Remote Sensing, Principles and Interpretation*, W. H. Freeman and Co., 1978.

Schanda, E., (ed.), *Remote Sensing for Environmental Sciences*, Springer-Verlag, New York, 1976.

Short, N., P. Lowman, S. Freden, and W. Finch, *Mission to Earth, Landsat Views the World*, NASA SP-360, 1976.

Siegal, B. S. and A. R. Gillespie, (eds.), *Remote Sensing in Geology*, J. Wiley & Sons, 1980.

Skolnik, M., (ed.), *Radar Handbook*, McGraw-Hill, 1970.

Smith, W., (ed.), *Remote Sensing Applications for Mineral Exploration*, Dowden, Hutchinson, and Ross, Stroudsburg, Pennsylvania, 1977.

Strahler, A. N., *Physical Geography*, Wiley, New York, 1975.

Swain, P. H. and S. M. Davis, (eds.), *Remote Sensing: The Quantitative Approach*, McGraw-Hill, New York, 1978.

Thomas, V., *Generation and Physical Characteristics of the Landsat 1 and 2 MSS Computer Compatible Tapes*, NASA GSFC Doc. X-563-75-233, 1975.

Thompson, K. P. B., R. K. Lane, and S. C. Csallany, *Remote Sensing and Water Management*,

Amer. Water Resources Assn., Urbana, Illinois, 1973.

Verstappen, H., *Remote Sensing in Geomorphology*, Elsevier, 1977.

Vezirogiu, T. N., *Remote Sensing: Energy-Related Studies*, Halsted Press, 1975.

Wheeler, G., *Radar Fundamentals*, Prentice-Hall, 1967.

Williams, R. and W. Carter, (eds.), *ERTS-1, A New Window on Our Planet*, U.S.G.S. Prof. Paper 929, 1976.

Photointerpretation Books, Monographs, Etc.

Aerial-Photo Interpretation in Classifying and Mapping Soils, USDA, SCS (Handbook 294), 1966.

Avery, T., *Interpretation of Aerial Photographs*, Burgess Publishing Co. (3rd edition), 1977.

Branch, M., *City Planning and Aerial Information*, Harvard University Press, 1971.

Denel, D., *Flights into Yesterday*, St. Martins Press, 1969.

Hammond, R., *Air Survey in Economic Development*, American Elsevier Publishing Co., 1967.

Howard, J. A., *Aerial Photo-Ecology*, American Elsevier Publishing Co., New York, 1973.

Jensen, N., *Optical and Photographic Reconnaissance Systems*, Wiley, New York, 1968.

Kodak, *Color as Seen and Photographed*, Eastman Kodak Co., 1962. (There are a number of inexpensive publications by Kodak on photography.)

Lattman, L., and R. Ray, *Aerial Photographs in Field Geology*, Holt, Reinhart and Winston, 1965.

Manual of Color Aerial Photography, American Soc. of Photogrammetry, 1968.

Manual of Photogrammetry (Vols. I and II), American Soc. of Photogrammetry, 1966.

Manual of Photographic Interpretation, American Soc. of Photogrammetry, 1960.

Miller, V., *Photogeology*, McGraw-Hill, 1961.

Mollard, J., *Air Photo Analysis and Interpretation*, Bellhaven House, Ltd., 1960.

Paine, D., *An Introduction to Aerial Photography for Natural Resource Management*, Oregon State Univ., 1975.

Ray, R., *Aerial Photographs in Geologic Mapping and Interpretation*, U.S.G.S. Prof. Paper 373, 1960.

Richter, G., *Dictionary of Optics, Photography, and Photogrammetry*, Elsevier Publishing Co., 1966.

Simon, J., *Infrared Radiation*, Van Nostrand Reinhold, 1966.

Spurr, S., *Photogrammetry and Photo-Interpretation*, Ronald Press, 1960.

Stimson, A., *Photometry and Radiometry for Engineers*, Wiley, New York, 1974.

Strandberg, C., *Aerial Discovery Manual*, Wiley, 1967.

Sully, G., *Aerial Photo Interpretation*, Bellhaven House, Ltd., 1970.

Wanless, H., *Aerial Stereo Photographs*, Hubbard Scientific Co., 1965.

Way, D., *Air Photo Interpretation for Land Planning*, Harvard University Press, 1968.

Way, D., *Terrain Analysis. A Guide to Site Selection Using Aerial Photographic Interpretation*, Dowden Hutchinson, and Ross, Inc., 1973.

Wenderoth, S., E. Yost, et al., *Multispectral Photography for Earth Resources*, West Hills Printing Co., 1972.

Wheeler, G., *Radar Fundamentals*, Prentice-Hall, 1967.

Wolf, P. R., *Elements of Photogrammetry*, McGraw-Hill, New York, 1974.

APPENDIX H

ANSWERS TO ACTIVITY QUESTIONS

You are reminded of the comments made on p. 6 that the answers given below are not always uniquely correct. Many answers are subjective in that they represent the particular choices made by the author. Your response may be different, yet equally valid. Many answers are probably longer than yours, either because added explanation is required or because an opportunity to teach certain concepts is seized.

Activity 1

#1-1: Key Words: acquisition, data, information, objects materials, targets, surface, atmosphere, sensors, platforms, multispectral measurements, effects of interactions, electromagnetic radiation, distance, noncontact.

#1-2: Shape; color, brightness, texture (internal), patterns, context (with surroundings), location, condition, stage of development, distribution, number present; composition, identity.

#1-3: Metropolitan; inner city suburbia; industrial, commercial, residential; transportation net, utilities, communications; warehouses, plants, shopping centers; amusement centers, schools, churches, apartments, townhouses, single dwellings, farms (incomplete list; order not necessarily hierarchical).

#1-4:

Temperature	*Clouds*	*Composition*
		Moisture
Pressure (indirect)	*Wind Patterns*	*Pollutants*

#1-5: 1000 nm μm; 10000 Å/μm

#1-6:

Visible-Near IR	*(0.4 - 2.3 μm)*
Mid IR	*(3 - 5 μm)*
Thermal IR	*(8 - 14 μm)*
Microwave	*(1 - 30 cm)*

(Note: The Far IR region window [20-90 μm] is not used in remote sensing.)

#1-7: Radiation is generally absorbed except where it passes through atmospheric windows; such radiation is absorbed, scattered, and reflected with loss of irradiant energy upon interacting with the atmosphere, then the surface, and then the atmosphere again.

#1-8: According to Figure 1-3 and also the function $I = I_0 \cos$, maximum reflectance from a surface occurs when the Sun is directly overhead (at zenith). The intensity of reflectance increases as the Sun's elevation on a given day increases to its maximum noon position at a given latitude and

then decreases as the Sun moves downward to the local sunset horizon. Another factor is the increasing path length of radiation passing through the atmosphere when the Sun is in its lower position (sunrise and sunset). This increased length leads to greater absorption and scattering. Scattering of course depends on wavelengths of the radiance. When the Sun is high, on looking up one sees a clear sky as blue because blue light (shorter wavelengths) is more efficiently scattered as irradiant skylight by atmospheric gases (Rayleigh scattering); thus skylight is dominated by the blue component. However, a sunrise or sunset appears red because of selective scattering of shorter wavelengths, which removes them from incoming white light leaving longer wavelength orange and red light to dominate. Scattering of light from the atmosphere provides a skylight glow as a source to illuminate the surface before a sunrise or after a sunset, even though the Sun is no longer directly visible. Sunglint or glitter is a highly directional reflected light effect evident when the observer is at or near the angle of reflection from a specular surface. Water, although of low intrinsic reflectivity, can function as a reflector when a water body surface is relatively calm. An observer on a hill could see a bright patch of reflected sunlight (glint) on the water if the Sun angle is appropriate to the observer's location. Glint is often a problem in aerial photographs made in the early morning or late afternoon.

#1-9: Illumination intensity, and hence the film exposure, decreases outward from the center (cosine effect), thus causing darkening or exposure fall-off. Film exposure is also affected by differential lens transmittance and by vignetting, a shadowing effect related to aperture setting and influence of the lens mount surface.

#1-10: Geometrical distortion (shape change) and scale (ground distance) increase outward.

#1-11: (1) 0.5 μm, (2) 4.8 μm, (3) 9.7 μm.

#1-12: (1) Visible, (2) Thermal IR (8 - 14 μm), (3) Mid IR (3 - 5 μm).

#1-13: (a) Visible (0.52 μm), (b) Near IR (may be second peak in visible), (c) Near IR (0.75 - 1.2 μm)

(Note: red rock/soil curve shows effect of moisture.)

#1-14: Highest = Rock/Soil; Lowest = Water.

#1-15: Rock and soil (note: some dark rocks, such as basalt and organic rock soils, could be less reflective than vegetation).

#1-16: Roughly: (a) 0.6 μm: V/R = 35/25 = 1.40, (b) 0.9 μm: V/R = 60/20 = 3.00, (c) 1.6 μm: V/R = 22/37 = 0.60. Maximum separation occurs at 0.9 μm. Remember, the abscissa in Figure 1-4 is plotted on log scale.

#1-17:

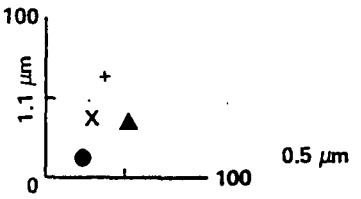

#1-18: Most probably rock or soil. To test for identity, first determine that the measurements are reproducible (some narrow range of values). Secondly, make measurements in other parts of available spectrum. Thirdly, compare the measured value with those for rocks and soils obtained as field data, from training sites, or as published spectral curves. Note, too, that there are statistical techniques for class identification, as discussed in Activities 5 and 6, and Appendix B.

#1-19:

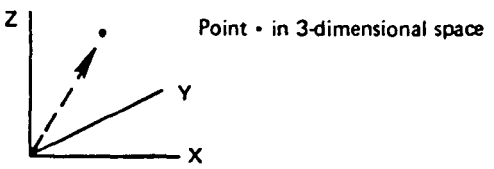

#1-20: Four or more wavelengths cannot be visually plotted in n-dimensional space, where $n > 3$. Treatment of multidimensional data plots for $n > 3$ requires mathematical (statistical) methods.

#1-21: Under these circumstances, spectral responses alone are insufficient. Information on shape, context (relation of features to surroundings), divergent changes over time, etc., may allow two features to be distinguished. Field patterns usually differ from forest patterns.

Activity 2

#2-1:

(a) 1079-15131 *(b) N40-17/W074-48*
(c) 38° *(d) October 10, 1972*
(e) 6

#2-2: (a) Path 16-Row 38; (b) 29-38; (c) 49-29, 45-30.

#2-3: Normally, four separate scenes, if the locality lies near a corner. Check the images used in making the mosaic described on p. 79 to satisfy your curiosity. Conceivably, for high latitudes (near polar), where sidelap approaches 85 percent, the same small area properly located in one image may appear in five others (images from paths on either side and adjacent rows).

#2-4:

New York City	*Q-3*
Newark, N.J.	*P-4*
Trenton, N.J.	*L-11*
Philadelphia, Pa.	*I-16*
Delaware River	*G-19*
Atlantic City	*S-22*
Pine Barrens, N.J.	*Q-17*
Long Island	*V-2*
Kittatinny Mtns.	*D-5*
New Jersey Coastline	*T-18*
Paterson, N.J.	*P-1*
Schuylkill River	*E-14*
Sandy Hook, N.J.	*S-6*
Reading, Pa.	*A-12*
Delaware Water Gap	*F-2*
Staten Island, N.Y.	*Q-5*
Wilmington, Del.	*F-20*
Pocono Mtns.	*C-2*
Barnegat Bay	*T-15*
Allentown, Pa.	*D-8*

#2-5: Band 4.

#2-6. Band 6 (in this printing; where the gray tone scale at the bottom is used to calibrate the printing, band 7 is usually lightest).

#2-7: Band 5.

#2-8: Water vapor and other atmospheric constituents generally absorb and scatter light more at the shorter wavelength end of the visible spectrum than at longer wavelengths. Thus, a haze effect occurs and the interference reduces intensity or brightness.

#2-9: Bands 6 and 7 (for both questions).

#2-10: Bands 6 and 7.

#2-11: This region is heavily vegetated. Vegetation is "brighter" in the infrared and will thus cause greater exposure of band 6 and 7 negatives, leading to lighter gray levels in the positive photo-images. Note also that the contrast between light-toned vegetation and shadows in topographically-rugged areas, (e.g., the mountains) accentuates the appearance of relief.

#2-12: Band 5. Vegetation, which tends to concentrate on these mountains as forests, appears noticeably darker in the red band image.

#2-13: It shows up in the color image but is cropped off in the black-and-white images.

#2-14: This is a tricky question, and not easily answered with certainty. Personal knowledge of an area, and its history, may be needed to make a correct interpretation. Both the Pennsylvania and the New Jersey Turnpikes were originally concrete, but parts have since been resurfaced with asphalt. Both also have been stained over the years with automobile wastes, etc., and thus the concrete behaves more like asphalt.

A few segments (mainly west of Philadelphia) of the Pennsylvania Turnpike may be picked out with difficulty in band 5 (but not in 7). However, the much newer Northeast Extension of this Turnpike (running northerly past Allentown) is especially evident (light line) in band 5.

What appears to be the New Jersey Turnpike shows up as light tones in band 5 and dark in 7 in the stretch from southeast of Philadelphia past Trenton. However, a new section of Interstate 95, numbered 295, is made of concrete and runs about parallel to the turnpike over this stretch. This is most probably what you are seeing.

Thus, these broad dual roadways do not stand out because of low spectral contrast with the surroundings. In the western United States, sometimes dirt roads only 10 m wide will be visible in a Landsat image if they contrast strongly with adjacent terrain (commonly sage-covered plains).

#2-15: Your choice of answer.

#2-16: Check the references on this.

#2-17: Very close fit. If the fit is made at the center, maximum discrepancies will occur at all edges. However, if, for example, the fit is made along the right-hand margin at the center, discrepancies will occur toward the top and bottom along that margin and increase even more toward the left. For small image subsets (e.g., 1/16th of a Landsat scene) discrepancies are almost negligible.

#2-18: In this instance, some minor blurring or fuzziness is evident. There is less contrast than desirable. Enlargement emphasizes the scan lines, but the individual pixels (see p. 54) are not yet discernible.

#2-19: This is obviously affected somewhat by initial image quality. A standard photo product starts to lose definition at a scale of about 1:200,000. Exceptional images hold definition to larger scales, but at 1:50,000 the quality loss exceeds the enlargement gain, and the pixels become noticeable.

#2-20: 13,300 sq. miles; 33,225 km^2; 8,512,000 acres.

#2-21: Only a small sliver in the upper left side of the photo is not present along the upper left edge of the Landsat image.

#2-22: Darker grayish tones in band 7 correspond to Jim Thorpe, Lehighton, and Slatington-Walnutport. Lehighton is most easily seen, partly because it contrasts sharply with lighter tones for the fields in the valley.

#2-23: Street patterns are not resolved in the satellite image.

#2-24: Band 7, color composite, band 5, decreasing in that order.

#2-25: See question 2-14. Concrete is a high reflector in the visible bands. It is also moderately bright in the infrared band images, but adjacent vegetation is even brighter, and so by contrast the road is darker.

#2-26: The longer ones, yes. The smaller ones, no, in general. Most of those are narrow, with little water in the channels (probably intermittent), and do not have enough effect on the topography to produce shadowing. Band 7 is the best.

#2-27: The fields are mostly small, irregular in shape, and arranged in irregular orientation and patterns. In February most fields were barren, although some show signs of active vegetative growth (red, probably winter wheat). A smaller number of fields were barren in October. A few of the barren fields stand out in the October Landsat image, but most are not resolvable as discrete individuals with discernible shapes. Band 5 best separates the field because of large tonal contrasts between those barren or plowed and those with crops. Although the estimate is subjective (yours may differ significantly from mine), it seems that about one-third of the individual fields may be picked out in the Landsat image. Beware: some fields are strip or contour-farmed, so that part is in crop and part is not.

#2-28:

	Recognize	Identify
(1)	+	+
(2)	+	-
(3)	-	-
(4)	-	-
(5)	-	-
(6)	+	+
(7)	+	-
(8)	-	-
(9)	+	-
(10)	+	+
(11)	+	-
(12)	+	+

"Recognize" is treated liberally here. By recognition is meant the ability to spot and single out in the Landsat image a gray tonal pattern that is also present in a similar way in the aerial photos. Details evident in the photos (because of high resolution which permits shapes to be defined) aid in identification of most of these patterns. Band 5 appears superior to 7 in the recognition process.

#2-29: Many of the buildings are indeed homes built and joined together side by side. Most have flat roofs that are covered with pitch or some other dark (low reflectance) material.

#2-30: Trees, trees, trees in these suburbs. The combination of trees, lawn grass, and many buildings tends to produce more pinkish hues.

#2-31: Judge your own answer.

#2-32: The scale, as printed, is 1:500,000.

#2-33: Again, a subjective answer.

#2-34: In this instance, the band 5 and RBV images show up as very similar. This is not unexpected because the spectral interval in band 5 covers much of the wider interval sensed in the panchromatic region. The terrain in early spring is not dominated by green from vegetation but instead is brownish overall thus contributing much light to band 5. However, band 7 responds quite differently, so that many features not sharply defined in 5 will stand out in 7—the Brooklyn and Queens boroughs in New York City are a case in point.

#2-35: Beware! Some of the differences are caused to some extent by photo processing differences. (Note variations in gray levels for equivalent steps.) However, real differences can be picked out. Overall drainage is best expressed in the winter and spring scenes. Still barren (soil-exposed) fields and early growth stages of some crops afford sharp contrasts in the spring image. A sharp, darker tonal discontinuity is evident above Allentown, Pa., up to a pronounced 180° river bend in the summer image. The fall image suggests the fields in this darker area are larger than those northward around Jim Thorpe. None of the small towns stand out well in any of the scenes, but Lehighton and Jim Thorpe show up as darker patches in the summer scene and as bluish tones in the spring scene color composite.

#2-36: The winter scene, 1205-15135. The low Sun angle (shadow effect) and lack of vegetation cover (trees are leafless; grasses dormant) contribute to this improved definition. Snow can also delineate topographical irregularities—it acts much like powder in "fingerprint dusting" (sporadic snow cover and ice produce this effect somewhat in the northwest corner of the February 1973 scene). The minor tributaries (insequent streams) north of the reservoir east of Lehighton show up well in both the February and April Landsat images but certainly not to the degree evident in the aerial photo.

#2-37: (1) Sun angle; (2) vegetation cover; (3) photo processing.

#2-38: This, again, depends on your choice of subscene. Those that show significant differences include (1) the Pine Barrens, (2) the agricultural areas of central New Jersey, (3) Philadelphia (note variations in the inner city, mainly in apparent area), and (4) the gray levels of the hills between Reading and Allentown. But remember that the difference results, to some extent, from overall image density variations. The gray scale at the bottom could have been used to calibrate densities by printing equivalent steps to the same densities.

#2-39: Your answer depends on your precise location. Obviously, 9-day coverage should increase the likelihood of obtaining scenes with less than 10 percent cloud cover by a factor of two (over an 18-day repeat cycle) on average.

#2-40: Those in Figure 2-3.

#2-41: Usually, the generation of the negative (if feasible, compare second and fifth generation prints). However, increasing contrast for any generation print usually improves image quality by sharpening tonal boundaries. These boundaries become fuzzier with increasing generation.

#2-42: Most probably you selected the transparency. Several factors make transparencies

appear sharper, with the back lighting effect being the most important. Light toned areas become especially bright in relation to darker (denser) areas, thus increasing contrast.

#2-43: If you did not rate the computer version as "tops," something is wrong with your eyesight.

#2-44: Again, you should clearly have favored the computer version.

#2-45: Mainly, the effect of extensive healthy vegetation, which can overwhelm some scenes with red. Of course, vegetation may be what you were looking for—it's your signal, but another person's noise. Also, summertime is humid in the eastern United States—atmospheric degradation is commonplace. High Sun angles likewise reduce shadow effects which, when strong, tend to emphasize relief.

#2-46: Most of the named features will have step values in the 4-6 range. Water is about 3. A few small areas may be 7. The coolest feature is the cloud (dark area near lower left corner), then the lakes. The brightest areas seem to be some barren areas and the coastal bars in eastern New Jersey. Normally, the large cities are also bright (warm), but in this unreprocessed image, the gray tones are not conspicuously lighter (e.g., New York metropolitan area). The Trenton, N.J., area shows two notably lighter toned areas.

#2-47: The fitting error is about 1 mm. This is quite small but still amounts to an offset of nearly 1 km (7 in on a side × 2.54 cm/in × 10 = 177 mm; a Landsat scene is 185 km on a side) If the same feature, near the midpoint, is exactly fitted, the maximum offset should be near one end of the join line. However, distortions away from nadir point, or any equivalent points on the join line, due to geometrical displacements should be minimal when matched.

#2-48: This mosaic pair will fit together well on a strictly point-by-point basis. However, the difference in scene content, owing to different seasons and years, will jar the eye. The overall tonal balance is off, too, because of much stronger atmospheric interference in the humid summer scene (1350-1519Ø). This same problem exists when aerial photos taken on widely separated dates are mosaicked. The distortions near the edges of aerial photos may be considerable owing to the increasing perspective angles away from nadir. For low-altitude photography, this distortion can be large. For Landsat, the scene width of 185 km relative to an orbital altitude of 970 km, when expressed as base to height ratio (185/970), ensures small perspective angles at the edge and thus little distortion.

#2-49: Images taken at different times of year will show different overall tonal densities related to seasonal variations in reflectances as the Sun elevation changes. The variations in atmospheric interference and in vegetation brightness, mentioned previously, also give rise to notable tonal differences in a full scene. In individual parts of an image, differences in field patterns as crop planting and harvest proceed, will also influence the harmony, especially where these patterns abut at the join lines.

#2-50: Obviously, obtain the images as close to the same time as possible in the same year. A magnificent color mosaic of all of California (42 scenes) was produced from Landsat by using August and September 1972 images. Join lines cannot be detected, first because the time interval was short and secondly because great care was taken in color photoprocessing. The next best thing is to take images in different years at about the same time period. With Landsat, this is possible because of the high frequency of repetition (20 times/year; images for the same seasons are now continuous from 1972 to 1980).

Finally, computer processing allows some adjustment of differences caused by illumination variations and variable atmosphere. However, natural vegetation differences through the seasons, and man-made changes, cannot be compensated for.

#2-51: Your decision.

#2-52: Regional planning; analysis of large physiographical and structural units in the crust; tracing of fault systems; recognition of regional differences in crop planting practices; state or re-

gionwide forest inventories; aiding geography students in obtaining an overview of a continent or a region; others.

#2-53: The sidelap is about 35 percent. This is not unusual for aerial photos, which may have up to 50 to 60 percent sidelap or overlap. The fraction varies with latitude for the same reason as the convergence of longitudinal lines. Examine a globe of the Earth to visualize this. The three-dimensional stereo effect with Landsat is one in which the vertical exaggeration (seeming abnormal rise or extension of such features as mountains above the general terrain level) is much less than usually encountered in aerial photos.

#2-54: Again, a subjective situation, but you will probably be surprised at the apparent stereo effect you see.

#2-55: Both the Sun elevation and azimuth will be significantly different on summer and winter dates. This, in a sense, is somewhat like looking at the same scene from separated perspective points. Differences in shadow lengths accentuate this effect.

#2-56: First, awareness of large changes in topography—seeing variations in slope, in height, etc., may often reveal subtle differences that aid in recognition and interpretation. Geologists, particularly, find that geological structures (fold limbs, faults) are more readily understood when the surface is visualized in three dimensions. In lowlands terrain, patterns that appear flat and undistinguished in a planar image are often revealed to be different in nature and origin by the low relief variations seen in stereo.

#2-57: The main modification would be to decrease the base-to-height ratio to accentuate (exaggerate) the topographical variability or relief. Stereo in overlap along the same orbit is preferable to sidelap along successive orbits a day apart. Check p. 385 to learn what is actually proposed for Stereosat.

Activity 3

#3-1: Yes, the corn field pixel in the upper left. Also, the bottom three pixels are nearly "pure." However, the corn pixel, and others, is really a multicomponent pixel. It consists of corn plantings plus soil, with other materials, including water (soil moisture), probably present. However, the radiances of this component are contributors, in their proportions, to the single pixel value for a feature specified as a corn field, which by definition is a multicomponent entity.

#3-2:

Band 5

1. (0.50) 30+(0.50)10=X
15 + 5 = 20

2. (0.35)30+(0.40)40+(0.25)50=X
10.5 + 16 + 12.5 = 37

3. (0.05) 10 +(0.30)30+(0.40)50
+(0.15)25+(0.10)15=X
0.5+9+12+22.5+1.5=45.5

Band 7

1. (0.50)55+(0.50)5 = X
27.5 + 2.5 = 30

2. (0.35)60+(0.40)60+(0.25)45=X
21 + 24 + 17.5 = 62.5

3. (0.05)5+(0.30)55+(0.40)45
+(0.15)40+(0.10)30 = X
0.25+16.5+18+6+3=48.75

Note: The areas (in parentheses) are "eyeball" estimates.

#3-3:

	Area (%)
Corn	*< 5*
Hardwood	*30*
Grasses	*45*
Rock	*15*
Shrubby meadows	*< 5*
Pine trees	*< 3*
Upper right	*>95 Hardwood*
Lower left	*100 Grassland*

Note that five components still remain in the lower right pixel.

#3-4: If components with dimensions equal to or greater than those of the sampling pixel are many and irregularly distributed or spaced, the probability that several will be within the pixel boundaries will decrease with decreasing pixel size. (There are several ways to state this rule.)

#3-5: Correlation with specific features is not good. The highway does not show up as a specific pattern. The tree areas west and southwest of the lake seem to be contributing to the reddish-toned pixels. The neighborhood homes to the north have some expression in the more gray-toned pixels.

#3-6: A microscope with multiple lenses, each having a different magnification.

#3-7: Your answer should include such points as these: A small-scale Landsat image shows regional patterns, trends, and interrelations. It is especially useful in portraying the contextual relations of large, first-order surface features. It allows measurements of distribution and changes in these factors with the seasons or over longer periods. If the application requires recognition of features of the order of a pixel or smaller in size, then aerial photographs ought to be part of the data gathering system.

#3-8: Band 7 has a band width of 0.3 μm whereas bands 4-6 are 0.1 μm wide; this greater width for 7 is necessary because of its lower detector sensitivity, and so more radiation must be admitted to provide a response that can be measured accurately.

#3-9: <u>Similarities</u>:

1. *They all show a rise in reflectance from 0.4 to 0.5 μm.*
2. *They all show a color peak in the visible.*
3. *The reflectance gradually tapers off at longer wavelengths.*
4. *All but water show at least two absorption bands.*

<u>Differences</u>:

1. *Water is much lower than the other three in total reflectance integrated over the 0.4 - 1.2 μm interval.*
2. *The two vegetation classes have their maximum reflectances in the infrared.*
3. *Rock-soil material is brightest in the visible range (not always the case; rock materials can be more reflectant in the near IR).*

#3-10: Regional or synoptic perspective, and frequent (repetitive) coverage.

#3-11:

	λ_1	λ_2	λ_3
Grass-Wheat	*0.65*	*0.80*	*1.20*
Concrete-Asphalt	*0.50*	*0.70*	*0.90*
Gravel-Shingles	*0.48*	*0.78*	*0.95*
Wheat Stubble-Fallow Field	*0.70(?)*	*poor*	
Sugar Beets-Gravel	*0.65*	*0.95*	*1.30*
Tree-Bare Soil	*0.65*	*0.95*	*1.30*

Vegetation/Non-Vegetation Differentiation in 0.3-0.4 and 1.2-1.3 μm intervals.

#3-12: The problem stems from the length of time (integrating time) needed to measure across broad spectral intervals. A laboratory grating spectrometer receiving reflected radiation from a standing target (such as a mounted sample) requires many seconds to a minute or more to sense across a continuous interval from 0.4 to 2.5 μm. Field spectrometers using diffraction gratings, filter wheels or wedges, or interferometer filters can scan comparable or smaller intervals in much shorter times. However, a moving target complicates the process—in effect, the field of view that is encompassed during a full scan is "stretched out" in

size, thus greatly reducing spatial resolution. The astronauts on Skylab compensated for this motion effect by visually tracking a ground target through an optical telescope attached to a mounted movable spectrometer that was continuously pointed and held on that target.

Techniques do exist to acquire quasi-continuous spectral curves from sensors on unmanned satellites. One is to use large numbers of narrow band detectors (e.g., 20 nm band width) that approximate a curve with these close-spaced continuous intervals. All such techniques experience limitations, as, for example, inadequate signal-to-noise ratios.

#3-13: Purple (red and blue).

#3-14: White (all three primary colors mixed equally).

#3-15: All patterns with no (less than 10 percent) transmission will yield black. Brown tones result from a combination of red, yellow (red and green), and black. Additive production of this with transparencies is difficult, as brown does not appear in the standard chromaticity diagram. A translucent gray filter will add some "blackness" to a yellow or orange projected color. A combination of red, some green, and black from a separate source gives brown in a color print made by the offset process.

#3-16: In B, red or white. In C, infrared radiation (by using a high band pass IR filter that does not admit visible light, as some do). A blue-sensitive filter is needed to pass light from a blue design. To a sense a yellow design, either a narrow band yellow filter or a filter with broader spectral coverage (e.g., an orange filter) than a red filter, is required. Infrared radiation must be transmitted through an infrared-sensitive filter and recorded on infrared-sensitive film.

#3-17: Variations in radiant intensity or in reflectance among most classes of vegetation are relatively small in the blue, green, and red wavelengths intervals but are notably larger in the 0.7 to 1.1 μm interval. Thus, the wider range of variations in that interval make it more sensitive to differences or changes.

#3-18: Purplish-blue.

#3-19: Sediment patterns, almost invisible in Figure 2-1, are readily seen in this version. The patterns strike the eye as having distinct definition, with detail and gradation now evident. No other features clearly stand out better in this blue-dominated version, but the suburban sections in metropolitan areas (e.g., Philadelphia) and even similar cities (e.g., Allentown) share some of the orange tones of the central sections.

#3-20: Figure 3-4 color predictions:

Cover type	*1*	*bluish (faint)*
	2	*blackish*
	3	*dark blue*
	4	*red*
	5	*dark gray ..-red*
	6	*red (with pink or orange tone)*
	7	*cream-white to light tan*
	8	*white*

These colors do not always appear as predicted in a false color composite (compare Figures 2-1, 2-6, and 4-4) because of differences in processing and other factors.

#3-21: Cover type 4	*Green (with bluish overtone)*
Cover type 7	*Cream-white (no real change from standard false color combination).*

#3-22: There is no blue-centered band on the MSS.

#3-23: The obvious answer: a blue band. Remember, though, that undesirable interactions between reflected radiation and the atmosphere are greater at shorter wavelengths; in other words, the blue band image will be degraded as though affected by a haze. This can add a bluish tone to a natural color image, as is often seen in aerial photos. Correction by digital processing can reduce this deleterious effect.

Activity 4

#4-1:	Harrisburg	H-13
	Chesapeake Bay	Q-22
	Interstate 80	I-10
	Allentown, Pa.,	R-6
	Juniata River	C-11
	Reading, Pa.,	O-10
	South Mountain	B-19
	Delaware River	U-19
	Sudbury, Pa.,	E-5
	Lycoming Creek	A-1
	Penn. Turnpike	I-14
	Gettysburg, Pa.,	D-20

#4-2: Other evident features include the Blue Mountain folded ridge north of Harrisburg, the Susquehanna River, the Schuylkill River, the Chesapeake and Delaware Canal, the towns of Hanover, York, Lancaster, Hershey, Lebanon, Williamsport, Pottsville, Hazleton, Wilmington, Interstates 83 and 95.

#4-3: A subjective answer—self evaluate! You should concur with the opinion that the spatial character of the computer image is sharper. Contrast is better and boundaries between surface features having different tone levels are crisper. Thus the fields in the farmlands, even though small, are more easily recognized if their crop cover varies (barren versus stubble versus unharvested crop).

#4-4: There may be several new features, but one that stands out (best in band 7) is a new reservoir west of Lehighton (coordinates N-2/3), described on p. 120.

#4-5: The tone or gray level in the October 1975 band 7 scene is darker for the mountains and for the scene as a whole. This results in part from lower photographic contrast (note that one or two more gray steps may be distinguished in the step bar scale at the bottom of 2274-15060). The slightly lower Sun elevation (33° versus 37°) reduces overall reflectance but is not a major factor. One might suspect that a difference in foliage is a primary cause. By October 23 most deciduous trees in this part of the country have turned orange and red. The false color composite (Figure 4-3B) shows more subdued red tones, typical of the signature of brilliant foliage in fall. However, the band 5 rendition of fall foliage usually also shows a brighter (lighter-toned) signature, while band 7 remains very light-toned (since cell structure of the leaves has not yet changed much). The EROS Data Center version of band 5 is abnormally dark and flat (more like a band 4 print). Still another factor may have been more moisture (humidity) in the atmosphere during the October 1975 overpass, which would reduce the reflectance.

#4-6: Again, subjective. However, you will almost certainly note the Landsat images as superior in terms of detail and, especially, color balance or effect. The blue dominance in some Skylab color IR photos is esthetically unappealing and distracting. The strong blue overtone is fairly typical of aerial color IR film (and less so in natural color film), especially when the scene is in a humid climate region. The blue results from Rayleigh scattering by the gas molecules in the air; this scattering is most efficient in the 0.45 to 0.52 μm spectral interval. The effect is strongest when the full column of atmosphere must be penetrated, as from a space platform.

#4-7: Roads, agricultural field patterns, tributary drainage channels show up better, or first appear, in the S-190B photo. Definition of detail within the towns is not significantly improved. The increase in resolution by more than a factor of 2 does not seem to produce a corresponding increase in information.

#4-8: Smoke from an industrial site.

#4-9: It could be industrial smoke but it is dispersed and thin. There is no obvious source (such as tracing a plume to its origin would pinpoint), and no large industrial town is nearby. Other possibilities include smoke from a forest fire

field burn, thin clouds, or dissipating morning g. Definitive evidence is lacking.

#4-10: Band 8. Particulates in smoke, or condensation droplets and mist in clouds, are more efficient reflectors (Mie scattering effect) at somewhat longer wavelengths. Thin, obscuring clouds or haze that reduce clarity in bands 4 and 5 images are commonly "penetrable" at the reflected IR wavelengths.

#4-11: Landsat can be and has been useful in monitoring air pollution, either of the point source variety (smoke stacks) or regional, as from a metropolitan area (see, for example, Plate 4b in "Mission to Earth")

#4-12: Lack of continuous coverage (although once every eighteen days even for a moment may often enough to catch occasional offenders). Low resolution also hampers detection of a specific source in many cases.

#4-13: The scene is not as "crisp" and is more washed-out or hazy. This is evident in band 5 and especially true for band 4 (not shown), which has an overall degraded look.

#4-14: The humidity on this July date was, about, high. The air may also have been "dirty" with pollutants that build up over much of the east during this season. Bands 4 and 5 are more degraded because of the higher skylight reflectance these wavelengths, in effect, every pixel receives small constant contribution to measured radiance from atmospheric reflectors, this tends to lessen differences in spectral responses from underlying surface features.

#4-15: There are several quantitative techniques for removing or reducing the effects of atmospheric radiance, they rely either on corrections from meteorological data or on systematic adjustments of pixel radiances by using a scene-dependent correction factor. Use of the computer to execute the correction, as described on page 43?, is almost mandatory; any other way would be a "brute force" effort.

#4-16: The winter scene has more immediate visual impact because many surface features, particularly the mountains, minor drainage, and the structural grain of the Piedmont, seem to stand out more in relief. This band 7 image shows more apparent contrast. The relief is more evident because of the light-dark patterns produced by shadows behind the ridges. This results from the low Sun angle (20°). The absence of vegetation also affects the gray levels of the hill slopes.

#4-17: The overall scene brightness is diminished owing to decreased reflectance as the Sun angle is lowered. This influences spectral signatures by reducing the intensity levels. Thus, differences in spectral response are subdued, leading to a smaller range of DN values and less radiometric sensitivity, which will diminish classification accuracies.

#4-18: In 1350-15190, Hazleton is located within V-?. Thus, and nearby towns, lie in the heart of the anthracite coal mining district.

#4-19: Band 5. Moderately dark gray. Band 7 almost black.

#4-20: Dark bluish-black. This and similar tonal patterns correspond to vast areas within the valleys now covered by surface "piles" of ground-up coal and other waste products from mine processing. The reddish tones around V are not the deep red of forests along the ridge slopes but in places represent less dense stands of younger trees and other vegetation growing on dumped coal refuse or in strip mined terrain now undergoing reclamation. See Figure 6-?B to visualize this.

#4-21: You should recognize a small, elongate body of water, which is some type of lake.

#4-22: This is the same lake, but it is distinctly longer. This could be a transient effect related to increased rainfall but is more probably a permanent result from gradual filling. The lake appears to be even smaller in the 19?? scene (Figure 4-1B), suggesting that a slow, long-term filling process was going on.

#4-23: This search takes very careful scrutiny and cross-comparisons on your part. The 19??

band 7 image shows three black spots in a row, all lying above another pattern: thus:  *. This arrangement is different in the 1973 image. The prominent spots are quite faint and only the lower pattern persists. Since this site was not visited, one can only speculate on identity. The 1977 upper spots appear to be bodies of water (small lakes or possibly large ponds). The 1973 upper spots look more like "open" areas, possibly cleared fields. The lower pattern resembles that of nearby coal wastes. These deductions, made entirely from band 7 images, are borne out by inspection of the 1973 color composite (Figure 4-7) and the 1977 color composite for 2904-14452. Check for yourself.*

#4-24: In the 1973 image, the area around each arrow is a medium dark gray, noticeably darker than the surroundings. In the 1977 image, the equivalent areas are light toned and do not differ from surrounding areas along the ridges.

#4-25: The tone is dark gray but not as dark as the surroundings in the 1973 image. These areas are just as dark as the very dark surroundings in the 1977 image.

#4-26: A grayish-red, somewhat speckled.

#4-27: The ridge surroundings are a rich red, typical of healthy vegetation. The gray level is not nearly as dark as parts of the coal areas, but there are spotty parts of those areas with gray levels about the same as the arrow-marked features. In the color image, some grayish-red tones are evident in the coal areas, but this in itself does not prove that the same feature is present on both ridge and coal areas.

#4-28: The 1973 feature noted on the ridges is not singled out in the July 1977 image at the same areas - which are a healthy red - but somewhat similar subdued reddish toned areas are noted in the ridges elsewhere, as well as in some of the coal waste areas.

#4-29: Narrow linear ridges, part of the folded sedimentary rock units in the Valley and Ridge province of the Appalachians.

#4-30: It is fairly widespread in the 1973 band 7 image and can also be seen, usually in different places, in the two 1977 band 7 images. The difference between areal distribution in the two 1977 images results in part from a disparity in the average gray level (and density range) related to processing.

#4-31: Your action!

#4-32: Almost no coincidence or overlap.

#4-33: Your choices!

#4-34: The feature appears to be further to the west in the 1977 scenes. Its distribution seems confined to the heavily wooded ridges. It occurs in patches, but the area within a patch is usually uniformly darker. Whatever causes this variation, as revealed on a following page, is transient, probably seasonal, and migratory, but selective as to ground class.

#4-35: Your action!

#4-36: Both defoliated areas and pinewoods tend to appear in darker gray tones than surrounding healthy forests in bands 6 and 7. However, the pinewoods should be quite dark (darker even than associated deciduous trees) in band 5, whereas defoliated areas are usually brighter than the forests because underlying soils, mostly browns and reds, can make a strong contribution to the reflectance. In a color composite, pinewoods generally show up as dark gray-red owing to their darker levels in all band images. Evergreens usually reflect less infrared radiation than most deciduous trees.

#4-37: Your map!

#4-38: You should produce a map in fairly good agreement with Figure 5-35, except that your map will have more classes. Estimate coincidence by confirming your comparison with equivalent classes: water, healthy foliage, defoliated areas (combined), coal wastes, and large towns. The level of classification of coal wastes is greater in the Figure 5-36 map than the single level you sought.

#4-39: Because of haze in summer, bands 4 and 5 images usually appear somewhat darker (which masks details) than do winter images. The shadow effect is emphasized in winter by lower Sun angles. Besides geomorphic features, fault lines are generally more easily detected in IR and winter images (unless the ground is snow covered). Lack of leafy vegetation may or may not improve detectability. However, in the infrared image the overall scene is brighter. Contrast between bright Sun-facing slopes and back slopes is greater for topographical features controlled by underlying geological units (such as ridges).

#4-40: Some of the linear features in the Piedmont (as at S-15 in 2088-14552) correspond closely to single stratigraphic units. These units, or soils derived from them, may be selective hosts to vegetation, for example, pine trees often concentrate on limey residual soils from carbonate rocks so that, if extensive, these trees may cause the units to appear darker gray. However, overall in this scene most individual rock units are not separable from others of different lithology.

The Valley and Ridge province is strikingly displayed in 2088-14552. The Piedmont is also highlighted, but its southeastern boundary is not sharply defined.

#4-41: The winter scene (2088-14552).

#4-42: For 2088-14552:

P: This seems to be associated with a slight ridge. It corresponds to tree-covered Cambrian mediscdimentary rocks on the north side of a granite intrusion. It fits well with these units, but it is not obvious why trees do not associate as well with the same units on the south and to the east. A large fault also closely fits this feature.

Q: South Mountain. This is an isolated mountain complex, having fairly high relief; it is anticlinal in structure with steep-dipping Cambrian and Ordovician metasedimentary rocks wrapped around older units, including crystalline rocks on the eastern side. Individual units are not visible. The boundary on the east side with lower relief Triassic rocks is fault-controlled; it shows in the imagery. (In band 5 images, it corresponds to a sharp increase in vegetation, appearing dark.)

R: These are steep ridges underlain by tight folds, consisting of Ordovician and Silurian sedimentary rock (ridges composed of hard sandstones). Younger (Devonian) rocks to the east across the river are weaker and form lowlands. This feature is a breached syncline. The fit is excellent; the oval area to the northwest, for example, closely corresponds to a breached anticlinal dome in which Ordovician carbonates are exposed.

S: This hilly area corresponds about exactly to a fault-bounded granite outlier. The steeper western side (shadowed) is held up by resistant Cambrian metasediments.

#4-43: The correspondence is less well expressed in the lowlands, especially in the Piedmont where the influence on relief and on vegetation is poor in many places. As examples of this, examine V-14 (the purple granite unit, g), Q-18 (the yellow and orange units, Xpc, Xwc, and Xwl), and H-19 (purple unit, Ocv). Note, too, that most thin dikes (Tr, red lines) fail to show up. Land use patterns often obliterate geologic boundaries in the lowlands.

#4-44: Only a few of the dikes plotted on the geological map seem to appear as discrete features in the imagery. Note particularly a pair of thin red (vegetation) lines in the color composite of 1350-1455. These may be dikes (but were not field checked). One seems to coincide with a continuous red line (on the map) that crosses the Susquehanna River. Studies elsewhere in the Triassic Lowlands and Piedmont of the eastern Appalachians indicate that these dikes seldom have any topographical effect (relief) but do produce different local, residual soils on which distinctive vegetation tends to congregate.

#4-45: Fence lines, transmission (power lines), oil pipe lines, airplane runways, roads, railway right-of-way, hedgerows.

#4-46: Many lineaments are zones of weakness, easily eroded to form valleys or linear depressions, others are associated with cliffs. Such topo-

graphical irregularities will be emphasized by shadows if they are oriented at high angles (45-90°) to the Sun azimuth direction. If parallel to the direction of illumination, opposing slopes in a depression will be equally irradiated (without shadow) and thus more difficult to see.

#4-47: Your map! Odds are, it is noticeably different from one I might draw.

#4-48: The December (winter) image should reveal more linear features because of lower Sun elevation. However, if you used the EDC computer-enhanced scene for October 1975 (Figure 4-3), it should show greater sharpness, which should lead to selection of linear features otherwise missed in a standard version.

Snow will tend to emphasize linear features because shadows will contrast even greater against a white background.

Leafless forests will remove the canopy effect, allowing a better view of the ground. At Landsat resolution, this may not greatly improve detection of lineaments.

#4-49: Most likely, less than half of your lineaments will coincide with the ORSER map. This underscores the inherent subjectivity in selection of bonafide linear features.

#4-50: If you are skeptical, keep this in mind: Searching for lineaments by conventional means (aerial photos; geophysics; ground mapping) is slow and costly (e.g., one mountain range in Wyoming was one-tenth mapped for structural features in five summers -fifteen man-months; the geologist completed the other nine-tenths, using only Landsat, in three hours). Many discontinuous but large lineaments are missed. Even if Landsat image interpretation produces many "false alarms," exploration geologists would rather accept the error than miss some critical ones otherwise undetected. It is easy to eliminate the erroneous ones, as well as to verify those of real identity, by checking out the (usually) smaller areas of interest in the field. Also, note this: In areas of greater relief, you would probably have more confidence in your decisions on locating structure-related lineaments. In flat areas, or those with subdued relief, many linear features turn out to be farm roads, transmission lines, etc.

#4-51: You are probably somewhat frustrated by this descriptive attempt. The fields are actually small and irregular in shape in this rolling terrain. They appear as blotches and spots in most scenes. Distribution patterns are hard to ascertain. You are pushing the limits of Landsat (1-3) resolution in trying to determine farm layout.

#4-52: By comparing band 5 images for the two months, you no doubt concluded that more fields were in crop, with more advanced growth, in July. This is indicated by a higher percentage of dark gray spots (fields with significant plant canopy) against a light-toned (reflective soils) background.

#4-53: Contour farming--plowing parallel with slope in rolling terrain. Fields tend to be curved, often with alternating strips of crop and barren ground.

#4-54: Those in the Coastal Plains in Delaware and Maryland are conspicuously larger and more homogeneous. They are usually more rectangular, but the orientations of neighboring fields are still rather haphazard.

#4-55: The corner of the June 1977 image may be somewhat overexposed. Nevertheless, most (more than 80 percent) of the fields appear fallow or in early stages of growth. Perhaps 50 percent or more of the fields in the same area show signs of active crops (mainly, further advanced in growth) five weeks later in mid-July, as one would expect.

#4-56: The aerial photos confirm most of what has been said in the past five questions. The fields around Lancaster are variably smaller, more divided by strips into alternate crops, and some are contour-plowed. The Delaware photo was taken in early October, two months after the Lancaster flight, and thus shows many newly plowed fields.

#4-57: Water is a strong absorber of radiation in the infrared. Most other common materials at the surface are not. Therefore, in bands 6 and 7, water will appear very dark, whereas nearly everything else is variably bright (some exceptions are cloud shadows, basaltic rocks, and some building materials).

#4-58: Four variables needed to predict snowmelt runoff are 1) areal extent, 2) thickness, 3) density (packing), and 4) rate of melting all of the snow cover itself. Landsat is effective in measuring only the areal extent. However, in most accessible regions, the thickness, density, and melting can be determined by measurements and observations at weather stations. Perhaps a minimum of 20 in a full Landsat scene are required for an adequate estimate.

#4-59: The snow seems thickest in the valleys of the folded ridge province. The snow line (visible) appears to run through Lebanon and other towns in the Piedmont. South of this boundary, snow cover appears insufficient to affect the reflectance, so that snow presumably has tapered off (or already melted) between the line and the coast. Examination of MSS bands 6 and 7 for this scene reveals a decrease in lighter tones (thus, lower reflectance) throughout the image, implying that the thickness of the snow blanket is probably less than 10 cm in most places and that the snow has begun to melt (producing absorbing water). The light tones in the Susquehanna river valley are from ice sheets (probably snow covered) where the river has frozen over.

#4-60: Runoff prediction is useful for estimating 1) potential flooding, 2) amount of water to be controlled by dams, and 3) water likely to be available for irrigation.

#4-61: Patches of snow in rugged terrain can resemble cumulus-type scattered clouds. The latter, however, usually have conspicuous shadows located northwest of the clouds themselves during the morning surveys by Landsat. If the clouds are low, some confusion can remain.

#4-62: In principle, a lake smaller than an acre could be detected by chance if it lies completely within a pixel when imaged during an overpass. The reflectance in band 7 is so low that it would contrast sharply with the higher reflectances of most surrounding materials (sand, grasses, etc.). However, more probably, the lake will be athwart several pixels (look at Figure 3-1 again) and the radiances from several features will mix. Under these conditions, spectral contrast with nonwater pixels further away may not be great, but a lake several pixels in dimension will dominate at least one or two of them and thus be readily detectable.

#4-63: From visual comparison only, one would select the October 1972 scene. Almost all reservoirs and lakes appear to have much larger surface areas than the 1975 scene. However, the rainfall data in footnote 3 seemingly contradicts this observation. One would assume that the heavy hurricane-related rains would have more than filled some reservoirs or, at least, produced surface areas comparable to 1972. Of course, some natural phenomenon or control by man could have moderated the stored volumes. However, an alternative explanation suggests a photographic artifact as an underlying cause. Note that the 1972 scene is characterized by water everywhere shown in black. In the 1975 scene, water is silty blue in many places. This different color pattern could be deceptive. It is also possible that the 1972 image might not be perfectly registered, causing a broadening of patterns, although other evidence for that is lacking and band 7 shows the same broad patterns. It is in cases such as this that recourse to digital data processing–pixel mensuration–becomes almost mandatory to resolve discrepancies or uncertainties.

#4-64: Marburg Reservoir – 40%; DeHart Reservoir – 50%; Unnamed Lake – 60%.

#4-65: Visually, 1975 storage is 50 percent that of 1972. However, at the end of October 1975, actual rainfall at Harrisburg was about 3.5 percent greater than 1972. Because of the late September hurricane, one would expect many full reservoirs. The dilemma remains unexplained.

#4-66: At first impression, the discernible water levels seem quite similar. However, at a second glance the river seems definitely to have more water in the June 1977 scene. Added support for this conclusion comes from estimating the areas of exposed land in islands throughout the river. Noticeably more of the reflecting land surface is evident at islands above the Juniata River and in the Three Mile Island group below Harrisburg. This is plausible. Early winter is usually a period of reduced rainfall in the East while spring is commonly a wet time.

#4-67: You are looking at the "infamous" Three Mile Island.

#4-68: This is the site of the Conowingo Hydroelectric Dam, over the top of which passes U.S. Route 1. Upstream the river backs up as a "lake," but downstream the water is normally so low that one can see the rocks from inclined strata extending right across the almost dry stream channel.

#4-69: Note that the blue streamer begins right at the confluence of the Juniata and Susquehanna Rivers. This blue results from reflectance from a heavy silt load, apparently in this instance being carried downstream along the right bank (west) of the Susquehanna. Note that the bodies of water from the two rivers are not mixing. The visible silt plume dies out just above Three Mile Island mainly because of the velocity check caused by the Yorkhaven Dam. This silt was probably derived as runoff from a rainstorm in the mountains drained by the Juniata.

This type of observation can be useful in tracking siltation patterns over a region as aids in determining complex runoff history and in noting distribution of silt transport and deposition, of interest to river and harbor engineers.

#4-70: The bluish tone again results from reflection of visible light from silt and clay and other particulates. This reflectance from rocklike material should occur at all Landsat wavebands except that only at the band 4 and, to a lesser extent, band 5 wavelengths does light penetrate water to any degree (that is to say, there is some transmission beyond the surface molecules to depths where silt is concentrated).

Most fish prefer clear, still waters. Silt implies some turbulence and/or moving currents. A certain amount of agitation is required to stir up nutrients but better fishing is usually associated with quiet waters.

#4-71: The Susquehanna appears milky blue over its entire visible length. The head of the Chesapeake Bay also is silt-laden. Other rivers are silty as well. These facts point to a heavy rainfall over the entire region, probably occurring several days earlier, to account for the uniform, widespread distribution of the silty load. Indeed, the footnote discloses persistent rains through October 21, only thirty-six hours before the Landsat pass.

#4-72: Marburg Reservoir shows little silt because (1) no large streams drain into it, and so less load is brought to it, and (2) its water is quite still, allowing rapid settling of any influx of silt.

#4-73: Bands 6 and 7.

#4-74: Mainly band 4; band 5 to a lesser degree.

#4-75: A dark grayish-red.

#4-76: Extensive water (absorbent; blackish in 6 and 7) mixed with tidal marsh and wetlands vegetation (reddish). Overall reflectance is reduced. The water is not easily seen from a ground position but would be obvious from a low flying airplane.

#4-77: Your action.

#4-78: Be wary of an optical illusion. The wetland-lagoonal water interface of the area south of Barnegat Bay, for example, is almost the same for the October 1972 and April 1978 scenes. Variations in this boundary from tidal differences, if any, are not resolvable. However, the wetland area (dark gray) in the 1972 scene looks to be much smaller than in the 1977 scene. In the 1977 scene this wetlands area is less dark in band 7 but appears continuous westward up to a straight boundary (an old beach ridge or strand line?) not visible in the 1972 scene, giving the impression of greater total area.

#4-79: Along the Mullica River.

#4-80: The gray levels for pinewoods and wetlands are both dark, probably somewhat darker for wetlands, in band 7. In the October color scene, the color hues and the darkness are also similar, so that if location and surroundings were not evident, the tonal signatures would make separation difficult. In the April color scene, the pinewoods appear a dark brownish-black and the wetlands a deep grayish-blue, a distinct difference.

#4-81: Your sketch.

#4-82: A weird cloud? A contrail? Something being trailed in the water?

#4-83: Your opinion!

#4-84: Off Cape May
Lagoons south of Ocean City
Choptank River
Maurice River Cove
Chincoteague Bay
Nanticoke River-Tangier Sound

#4-85: Delaware Bay; Nanticoke River; open Atlantic Ocean are the best display cases, but current flow patterns are evident within most of the water in the scene.

#4-86: Look at many scenes over the months and years, making maps of flow patterns (use arrows to show direction and magnitude); correlate with water measurements made from boats; sample silt loads.

#4-87: In order to enhance (bring out by emphasizing light tones) the sediment patterns, the image was printed "light," with a longer exposure and/or a shift in contrast.

Activity 5

#5-1: The IBM version gives the immediate impression of being "sharper," with more evident structure to the city, for two reasons. First, linear features and class boundaries, particularly street boundaries, have been edge-enhanced. Secondly, there is a superior color balance, related to computer processing that yields optimum contrasts in the black-and-white individual band prints, but even more, to careful, custom photo processing.

#5-2: The band 4 image has been "livened up" by atmospheric and other radiometric corrections. The print shows a greater range of lighter gray levels; this allows more blue light (with filter) to expose the film negative. The red colors, so conspicuous in Figure 5-1A, have been toned down. The overall result is to intensify the blues that characterize the usual false color appearance of building and road materials. However, the barren fields in rural areas take on an unnatural blue tone.

#5-3: More sections, and longer stretches, of several major highways mainly to the west of Washington and Baltimore are more easily seen in the IBM version. This is particularly true where these roads pass through forested country. You can find traces of some of these roadways in the equivalent areas of the photo-image, if you look hard, but they are certainly more conspicuous in the computer-enhanced image.

#5-4: Most probably you decided there was a substantial, although not dramatic, improvement in display of the Bridge in the IBM version. About three-quarters of the bridge span is visible in this version, compared with one-quarter in the GE image. A computer-enhanced enlarged print of this scene, published by the U.S. Geological Survey, reveals both side-by-side Bay Bridges (a second span was under construction in the early 1970's).

#5-5: The cross, or access, strips between parallel runways; also the grassy areas between them.

#5-6: The barren fields and those with unharvested crops or stubble are more readily separated. Field shapes and distribution patterns are more easily discernible. In a few larger fields, a suggestion of moisture variations is evident.

#5-7: Pinewoods.

#5-8: Check Plate 2 in "Mission to Earth" for an index of major landmarks in the central part of Washington. In Figure 5-2 you should be able to spot, but not necessarily identify:

The Capitol Building (Band 5)
The Mall (7)
Kennedy Center (5)
Jefferson Memorial (5)
RFK Stadium (5)
Pentagon (7)
and others

#5-9: The concrete paved roads (mainly highways) show up well in band 5 because of their high reflectance. Asphalt roads are more easily seen in band 7. The Capital Beltway (Interstate 495) is mostly concrete and can be clearly seen encircling Washington in band 5, except for a stretch (asphalt) in the northwest (Bethesda area) segment.

#5-10: To some extent you are still seeing the individual pixels, although blockiness was reduced by resampling and filtering procedures. Note, however, the offsets in the runway at Andrews Air Force Base (near center) and offsets and streaks in the Beltway. This results from slight displacements caused by nonuniform repeatability of the start of each scan mirror sweep through successive scan lines. Although this may be reduced by geometrical corrections, complete elimination is almost impossible without visual inspection and complicated shifts, which would require the use of an involved computer program.

#5-11: Yellow-green. The red band records the soils as "bright" and the IR band somewhat less so. Use of the green and red projection filters for bands 5 and 7 gives an additive mix of yellow, with a greenish excess.

#5-12: After developing experience with computer-processed enlargements, you can probably recognize the presence of large individual buildings if they have strong reflectance contrast with their surroundings. The large gleaming-white government buildings and monuments in the federal areas meet this condition. However, at this resolution, the shape and other details by which one might identify these structures are still too indistinct - they remain white "blobs."

#5-13: The White House has a flat, black-tarred roof, as does the Pentagon. Thus, both these white-sided buildings appear as dark patterns. The Jefferson Memorial is domed. The Lee Mansion has a sloping, rather dark roof and does not correspond to the white dot. The dot is the Memorial for the Unknown Soldier. (Fooled you! But this fooled me until I checked it in an aerial photo.)

#5-14: The Monument appears as a dark, elongate pattern slanting to the upper left (NW), in just the direction expected at 9:30 a.m.

#5-15: As you will learn later, a general, reasonably accurate map of the major first-order, or Level I, urban classes may be produced from Landsat data by computer classification techniques or even by photointerpretation of the enhanced imagery. Using older maps and other supporting data also, J. Wray and others of the Geography Division, U.S. Geological Survey, have produced just such a map from Landsat.

#5-16: You probably selected the Fourier Transform image as the best enhancement, with the snow-covered subscene a likely second. None of the versions is noticeably better than the others, although all are improvements over the unenhanced full scenes (question #4-17). Some of the linear features are obviously roads; these show up best in the winter scene because of high contrast between snow and road surfaces. Other linear features may be narrow stream courses; those that are long and straight are most likely fault- or joint-controlled (personal communication, Dr. Ida Hoos). The northeast-trending structural grain is evident in all versions since it is highlighted in part by vegetation; the winter scene suggests some topographical expression (relief caused by differences in rock erodability) emphasized more by shadowing than snow cover. The Cubic Convolution images display less detail than the Fourier Transform and snow cover images. Certain details stand out better in the Cubic Convolution image, more as a result of vegetation contrast than of computer-induced sharpening.

#5-17: A count of linear features is a subjective process. The author identified 10 apparently natural features trending generally NW in a 10-minute examination of the corresponding subset area within the full October 1975 enhanced scene. In another 10-minute period, he counted 30 northwest-trending features (many short; some dubious) in the Fourier Transform subscene. However, some of these additional features owe their detection to enlargement rather than enhancement.

A very dark feature within the darker gray pattern south of the Marburg Reservoir as seen in band 7 emerges with higher contrast in the June 1978 band 5 image. An analogous pattern change

does not occur in the hills north of Hanover when bands 5 and 7 are compared. A first reaction is to suspect a burn scar from a forest fire, except that such an effect should also show up as a strong contrast in band 7. Note that this specific pattern becomes general in the band 7 snow-covered subscene. A more likely explanation is to presume this dark pattern to be a stand of evergreens.

#5-18: Generally, the two versions should be in good agreement. The computer version, however, is better suited to boundary definition because of the strong contrast between black defoliation patterns and the red of healthy vegetation. Watch out, though, for confusion in separating the defoliation (a dull bluish gray-black) from anthracite waste (either bluish or a darker blue-black).

#5-19: As your intuition tells you, the boundaries outlined on the large-scale aerial photo are more exact and precise. However, the outlines drawn on the Landsat image should be broadly similar, and the areas enclosed by each outline, if you could conveniently calculate them by visual techniques, should be close. Once the defoliated area (in square meters) has been accurately classified by the computer, the area may be calculated by simply counting pixels in that class and multiplying by 79^2 or 6241 (meters). Note that in this case the few small clouds along the ridge in the Landsat image would prevent the entire defoliated area from being included in the count.

#5-20: Colorful as the three VI images are, no one of them does a better job of picking out and isolating the defoliated zones than the others. You may argue, convincingly, that the 1977 false color rendition in Figure 5-7 is superior to the specialized VI images.

#5-21: Confusion abounds! The colors associated with the defoliation are widespread throughout the subscene, recurring particularly in the valleys. Only when you, the interpreter, add the knowledge that these colors occur on the heavily forested ridges, which are otherwise marked by distinctive healthy vegetation colors, would you deduce some abnormality. There seems to be no unique defoliation signature in any of these VI images. A false color ratio composite, consisting of three sets of ratios instead of one, may result in more diagnostic ratio patterns and colors for some classes (particularly for rock materials where vegetation is sparse).

#5-22: These patterns can be misleading. They occur on the southeast side of each ridge and correspond to higher values (see color scale at top of each image) of each VI parameter. The most plausible interpretation is that they are brighter surfaces because of aspect (facing position relative to the Sun), in this case southeast-inclining slopes (with some bare rock?) oriented normal to the direction of the morning Sun's rays.

#5-23: Both classes have similar low ratio values (purples correspond to low DN's which, in turn, are assigned to ratios of less than 0.25). This may result from lower reflectances in band 7 than in 5. The reflectances for water are quite low in band 7 and moderately low in 5, so that ratios of 0.1 - 0.2 are characteristic. For urban classes, the band 7 reflectances are variably low (depending on amounts of vegetation intermixed with streets and buildings), and notably higher in 5, so that ratios again are low, but usually not as low as for water.

#5-24: The reflectances or brightness values of concrete (light toned roads in band 5) are high in 5 and low in 7. Therefore, a 7/5 ratio will approach zero. In Figure 5-11, the concrete roads show up, where still defined, as blue, but do not color-contrast with the blue tones that dominate the lowlands through which the roads pass.

#5-25: Broadly, the dark greens correlate with the southeast and the light greens with the northwest slopes along the ridges.

#5-26: On the ridges the purples and reds are associated with the defoliated areas, where the influence of rock and soil reflectances account for the diagnostic color effect. In the lowlands these colors tend to correlate with open and barren fields.

#5-27: All of the VI combinations share one thing in common - the importance of bands 7 (or 6) and 5 in the numerical calculations. As we have seen, band 7 is quite sensitive to the presence and variations of vegetation, and band 5 is particularly sensitive to rocks and soils. Almost any numerical

function that depends on the inverse relation between bands 7 and 5 (as vegetation radiances increase in band 7, the band 5 values for corresponding pixels will decrease) optimizes the ability to measure small but significant variations in such vegetation characteristics as species or types, proportions of different types, density (percentage ground or canopy cover), biomass and vigor. For example, where green-leaf vegetation increases beyond about one-third of the surface area, the ratio of 7 to 5 exceeds 1 and becomes increasingly higher; but, with increasing dominance of rock/soil, that ratio becomes progressively lower as the brightness of the inorganic fraction gradually overcomes the effect of the organic fraction.

Loss of chlorophyll and cellulose-rich leaves, exposing more of the non-vegetated part of the ground, causes an abrupt reversal in the relative contributions of vegetation and soil to band 7 and 5. Thus, defoliation among other healthy thick forest stands produces extreme differences in radiances within the 7 and 5 wavebands. The effects are so large that any of the VI combinations will yield sharply different values for vegetated and nonvegetated VI's. Inspection of each of the six combinations in Figures 5-12 and 5-13 indicates almost identical patterns (Linear VI being slightly different from the others). The nonforest mask eliminates most of the terrain hosting little or no vegetation, but some color patterns in the lowlands are most probably associated with fields containing emergent crops or stubble, or with small sparse woods.

#5-28: The band 5 difference image shows the normal forest cover on the ridges as dark but the same cover appears bright in bands 6 and 7 difference images. Approximately equal amounts of light from the 6 and 7 images, when projected through green and red filters, will combine as yellow.

#5-29: Defoliation patterns are bright in band 5 (DN 1977 > DN 1976, and +) and dark in bands 6 and 7 (DN 1977 < DN 1976, and –) difference images. If band 5 is projected through a blue filter, this pattern will receive only a blue light contribution.

#5-30: Those fields whose surfaces consisted of soil and small amounts of vegetation in June 1977 but had a thicker cover of crops or other vegetation later in the season, in July 1976, will behave much like the defoliated areas that prevailed in 1977.

#5-31: The first two components resemble individual Landsat bands. The first component is much like band 7; the second like band 5. However, some of the fields are bright in both components but would be bright or dark in the two bands. The third component contains very little of the independent (noncorrelated) information (see part 6 of Table 5-3), but its image is still recognizable. Noise, including scan line striping, begins to appear extensively in this rendition. Water shows as bright tones with no internal variation (as is revealed in the second component). The defoliated areas are rendered dark in all the first three components. The fourth component is even noisier, but the ridges and parts of the river may still be discerned.

#5-32:

$$\frac{108.267}{295.743} \times 100 = 36.6\%;$$

$$\frac{1.863}{395.743} \times 100 = 0.6\%$$

#5-33:

$$R_{22} = \frac{0.787 \times (108.267)^{1/2}}{(70.919)^{1/2}} = \frac{8.19}{8.42} = 0.971,$$

$$R_{14} = \frac{-0.279 \times (0.857)^{1/2}}{(56.116)^{1/2}} = \frac{0.259}{7.49} = -0.035.$$

Channels 3 and 4 contribute most to Principal Component 1, 1 and 2 to PC 2.

#5-34. The PCA color composite shows the forests as purplish red, owing to very light tones for the first component (red filter) and moderate tones for the third (blue filter). Water is blue because of its light tones in the third component. Some fields are yellow owing to comparable light tones in the first and second components. The defoliated area is blackish. The VI ratio image better separates strongly defoliated (red and black) from moderately defoliated (purple) from healthy (two

shades of green) ridge vegetation, but the mask has removed most of the lowlands information. The PCA composite retains and accentuates that information. In the lowlands, blue tends to be associated with much of the built-up urban areas, yellow with bright surfaces (large buildings, concrete roads, plowed fields), and red with forests or extensive crop cover.

#5-35: 7.50 km N-S × 7.84 km E-W equals 58 km² (22.6 square miles), approximately.

#5-36: Your action.

#5-37: Your action. The nonwater patterns are islands.

#5-38: The limit exceeds 32 percent.

#5-39: Your action.

#5-40: Railroad yards. On the east side of the Susquehanna, some H's correlate with similar train yards but other H's are associated with the high density of buildings in the central section of Harrisburg (see Figure 7-14). By themselves, therefore, the H's do not define a single class.

#5-41: Bright, reflective sediment load.

#5-42:

1977: (1) + :. ( ).
*(2) * = .*
*(3) * = +.*

#5-43: Overall, there are not many parts of either the 1973 or 1977 scenes that contain ten or more homogeneous symbols. The greatest homogeneity occurs in the river water and in the interstate roadway. Inhomogeneity is to be expected in this scene because of the wide diversity of land cover in a metropolitan area (many urban classes) that intermingles with agricultural lands, land under development, and forested slopes. Also, keep in mind that homogeneity in an NMAP does not imply comparable homogeneity in the data.

#5-44: 1973: 22-32 percent; 1977: 13-31 percent.

#5-45: NMAP

#5-46: Your action.

#5-47: Your guess. You are likely to have felt confident about several classes, such as water (0's and 1's), silty water (blanks, possibly E's), forest (3's, 5's), and concrete highways (blanks in linear patterns). But many patterns are ambiguous, almost a hodgepodge in distribution. The rail yards along the west bank of the Susquehanna do not stand out as obvious but may correspond to the long, thin grouping of 1's. The blank linear area northwest of the interstate highway is of uncertain identity but may well be a reflective ledge of sandstone along the Blue Mountain crest. Check these tentative identities against Figures 5-24 and 5-33.

#5-48 and 5-49: Your action.

#5-50: Your action.

#5-51. The CLAS map is clearly superior.

#5-52: Categories 3 through 9 are dominated by vegetation. Inspection of Figures 5-24 and 5-33 suggest that forests are certainly present in this part of the scene, not only along the ridge but in the lowlands. Some of the patterns appear to correspond to fields. Categories 11, 14, and 16 are less well correlated with vegetation, but in some areas could be clusters of trees or grass in residential areas or city parkland. Categorization may be simplified by lumping several of these classes together, showing them in single colors, and then by checking apparently misclassified patterns against good sources of ground truth (e.g., large-scale aerial photos).

#5-53: The blank symbol category 17 matches the interstate and another concrete highway, several large barren fields, and, seemingly, part of the water within the Susquehanna (on either side of the pattern of S's).

#5-54 and 5-55: Some of the blank areas coincide with areas that have reflectances greater than 31 percent. Had that single reflectance class been subdivided into two or more discrete classes and these then correlated with established ground

truth, the areas could have been given specific category names. If some of the blank area indeed ties in with silty water—a transient phenomenon—it may be difficult to establish a definite and meaningful class.

#5-56: Your action.

#5-57: Considering that Landsat was some 50 times higher than the aircraft when the two scenes were acquired, the ability of Landsat to recognize the principal land cover categories is remarkable. It is competitive when Level I features are sought. The forested ridges and hills are readily identified. Note, however, that the forests are dark blue instead of red in the color IR photo because the dominantly deciduous trees are leafless in this winter scene. Most major roads are visible in Landsat, especially if concrete, although a section of Interstate 81 remains uncompleted. Many of the larger crop fields are recognized as such, particularly if they bound fields with a different cultivation stage. The urban areas, including railroads, are easily detected. Several large industrial and factory sites are separated from their surroundings. Drainage patterns and land/water interfaces are clearly evident.

#5-58: Commercial; Residential; Transportation; Cropland and Pasture; Deciduous Forest Land; Gravel Pits.

#5-59: Your action.

#5-60: The foreshortening is vertical. The best clue to this deduction is the orientation of the Susquehanna River. It looks squashed towards the horizontal. Compare its orientation in Figure 5-27A with that in Figure 4-11 and imagine the rotation it would experience if the IDIMS images were stretched in a north-south direction.

#5-61: Make a photographic hard copy and stretch by varying the density-exposure relation (use high contrast paper or modify developing conditions). However, most such changes may be made interactively on the computer, by, for example, simply trimming more end value pixels in the DN range.

#5-62: The darker tones would remain fixed, i.e., would not get even darker. Contrast would increase, but the tonal expansion would move toward an overall lightening of all gray levels. Thus, a lighter, more contrasted image results.

#5-63: The main changes occur in the lowlands. The tones associated with urban classes become lighter gray. Barren fields become brighter (notably lighter gray) and stand in sharp contrast to vegetated areas (forest copses; crops). The bands of silty water in the Susquehanna are accentuated. Boundaries between classes are more easily picked out.

#5-64: Blue: clouds (the shadows seem to disappear).

Red: vegetation, mainly forests but apparently also crop fields and residential areas with trees.

Green: barren fields and defoliated forest.

(Note: blackish-green tones are also associated with defoliation and some residential areas.)

Conclusion: Density-slicing affords some general categorization but creates confusion by assigning a color slice to often quite disparate classes.

#5-65: Three classes—silty water; clear water; forested land—are lumped together.

#5-66: Generally, the classification seems to have correctly identified most of the Level 1 features, but some discrepancies at various places are evident. The forests have been properly classified wherever extensive and continuous areas are involved, but some small green patterns may be other features. Water was well-defined except for the meandering creek west of Harrisburg (see middle of p. 211). The railroad yards around Harrisburg are mislabeled industrial/commercial—a separate class could have been established. Red and yellow themes found on several islands in the Susquehanna are misleading; these islands consist of trees, bare rocks and cleared areas. Suburban housing developments in several places have been missed, being classed instead as open land. A thin red line

near the middle left edge of the classification map does not, on close inspection of the photo, seem to qualify as a residential urban strip. The barren lands are mostly correctly classified, but the crop and pasturelands are too generalized. Certain fields with extensive crop cover are shown either as cropland (not distinguished as a later stage of growth) or as unclassified (black). Open sandpits and several residential areas are also marked by black.

#5-67: The interstate, and similar concrete roads, have a spectral signature quite different from almost any other feature in the scene. No training pixels for this class were selected--although this could be done--because the roads are less than a pixel width and are combined with a variety of other features. When the computer classification algorithm was applied, no spectral cluster for roads had been entered and so road pixels were assigned to unclassified.

#5-68: 1977:

Silt in the River;
Defoliation in the forest;
Different proportion of industrial/commercial to residential;
Much more land classed as Medium Density Urban;
Much less barren/fallow land;
Different proportion and distribution of agricultural land.

Factors:
Different year (no defoliation in 1972);
Silt due to an earlier rainstorm;
Different part of the growing season;
Different criteria for defining medium density urban.

#5-69:
1. *Select subset(s) in Landsat scene(s).*
2. *Assemble ancillary data (photos, maps, etc.).*
3. *Choose training site samples.*
4. *Correlate with ground truth.*
5. *Check for homogeneity.*
6. *Select classifier.*
7. *Perform classification.*
8. *Establish accuracy level.*
9. *Evaluate classification accuracy*
10. *Rerun steps 4 (if necessary), 5, 7, and 8 until accuracy is reached.*
11. *Generate output (hard copy).*

#5-70: The LORES scene, density-sliced into six intervals, occupies about 35% of the five interval-sliced IDIMS scene. The density limits of the two sets of intervals are not the same, but the sequence of changing densities is similar. The densities corresponding to the river (two shades of blue in IDIMS; black in APPLEPIPS) define this water course in both renditions. The light green and dark green of the IDIMS version correspond reasonably well to the lavender and dark blue of the APPLEPIPS version. The red of IDIMS generally matches the distribution of some of the gray-blue interval of APPLEPIPS, but the latter is more continuous and uniform whereas the former may subdivide into light and dark green plus red. The brown and black (away from water) intervals of APPLEPIPS have no obvious counterparts in the IDIMS scene but are themselves a minority of patterns. The Conodoquinet Creek and railroad patterns are evident in the IDIMS density-sliced scene but not in APPLEPIPS.

The HIRES scene is best located by first finding it in the LORES scene and then consulting a map or aerial photo (Figures 5-19 and 7-14). Key geographical features are McCormick Island and the Interstate bridge. The scene lies along the northern end of Harrisburg. One characteristic of the HIRES image may strike you upon comparison. The image is "squashed" along the vertical, i.e., is foreshortened or compressed in aspect. For example, the island appears "flatter" and "snorter." The pixels have not been reformatted (expanded) in this routine, so that geometrical rectification is lacking.

The HIRES scene fits in the NMAP print approximately between the NMAP line numbers 1144 to 1184 and sample numbers 1010 to 1050. The NMAP and APPLEPIP scenes are for the same date so that there is some general correspondence in the pattern of varying norms and densities. You can convince yourself of this by outlining the NMAP norm values in Figure 5-20B and then comparing that pattern with the color square patterns in Figure 5-34B.

Interpretation of the APPLEPIPS scene is difficult. The two aerial photos (Figures 5-23 and

7-14) are the best guide, but neither is equivalent to a band 7 rendition. The dark green seems to follow the railroad yards. The beige and olive patterns broadly correlate with residential areas (olive relating to neighborhoods with more trees). Browns in several places are related to open areas. Light blue-gray on the island and near the upper right corner can be tied to wooded areas. However, many patterns are confusing; the considerable variation in density across the Interstate bridge is surprising (anomalous?). Overall, this simple density slice is of limited utility in classification. Work is now in progress in adapting APPLEPIPS to a multiband classification routine.

#5-71: You probably decided that the I-100 classification map was much easier to "read" than the photo-enlargement, mainly because the themes or classes are displayed in distinctly different colors, which cause sharp separation. Thus, blue and yellow provide a far better visual separation for the mine refuse and defoliation classes than the two shades of dark blue used in the EROS product.

#5-72: The maroon pixels or conflict class. Also, some of the smaller patches of defoliation (blue) may be mine waste or open fields.

#5-73: The largest cluster of conflict pixels correlates with the town of Hazleton (near upper left corner). Some of the other maroon pixels might be villages or groups of buildings. However, most maroon pixels are scattered and isolated, and most probably represent variants of the ground features surrounding them; in other words, they have spectral properties similar to, but outside, the cluster boundaries for the surrounding class.

#5-74: The I-100 classification did not set up two classes of water, nor was a special category of swamp vegetation established. Several lakes in I-100 are identified as refuse/silt in the ORSER classification; conversely, ORSER recognizes at least one small body of clear water not in the I-100 map. The I-100 map shows considerably more coal waste—note more yellow patterns on the right and bottom of the ORSER equivalent area.

#5-75: This is, in effect, a mask in which other categories (mostly vegetation) are eliminated by thresholding. This allows concentration on the classes of interest in this subscene, namely coal refuse, water, and swamp vegetation.

#5-76: All these coal-related categories have in common the presence of coal and dark shale refuse. On site in the field the several types of refuse may be distinguished by use, shape, associated re-vegetation and other criteria, but the spectral characteristics of each are much too similar to the others to differentiate them with acceptable reliability.

#5-77: Reclaimed land will show varying degrees of newly established vegetation usually mixed with soil. This class should appear as a pinkish gray-blue in the valleys containing the refuse.

#5-78: A few of the small lavender patterns correlate with farm villages or grouped buildings (crop storage or industrial), but most are false alarms associated with roads or with fields containing vegetation in the early stages of growth.

#5-79: Part of this is illusory. Upon rigorous analysis there are fewer rectangular fields than assumed from first inspection. Some fields are triangular and others have straight segmented boundaries but with irregular polygonal shapes. This results from the way in which the original land was developed. Instead of establishing farms along section lines, as is common in the Great Plains, large areas were cleared of forest and subdivided within plantations (in the 17th and 18th centuries) as convenient rather than from some master plan. As estates diminished in size and ownership was diversified, unusual field shapes emerged.

In the classification map, many actual straight boundaries become "ragged" because of mixed pixel effects at the juncture of two crop or field types. One pixel may be classed as A and a second neighboring one as B because both straddle two crop types but contain different proportions of A and B.

#5-80: In the listing below, G refers to measurements made on the ground and RS to aircraft and/or spacecraft remote sensing observations.

Variables include:

Soil types (G, RS)
Soil moisture (G, RS)
Seasonal rainfall (G)
Temperature history (G)
Number of sunshine days (G)
Location of major producing areas (G, RS)
Average field size (G, RS)
Regional crop types (G, RS)
Proportions of crops in training areas (G, RS)
Crop calendar data (planting times and growth stages) (G)
Crop vigor/crop diseases (G, RS)
Productivity (actual yields) (G, RS)
Spectral signatures as function of time (RS)

Various flow diagrams are possible. One simple linear example is:

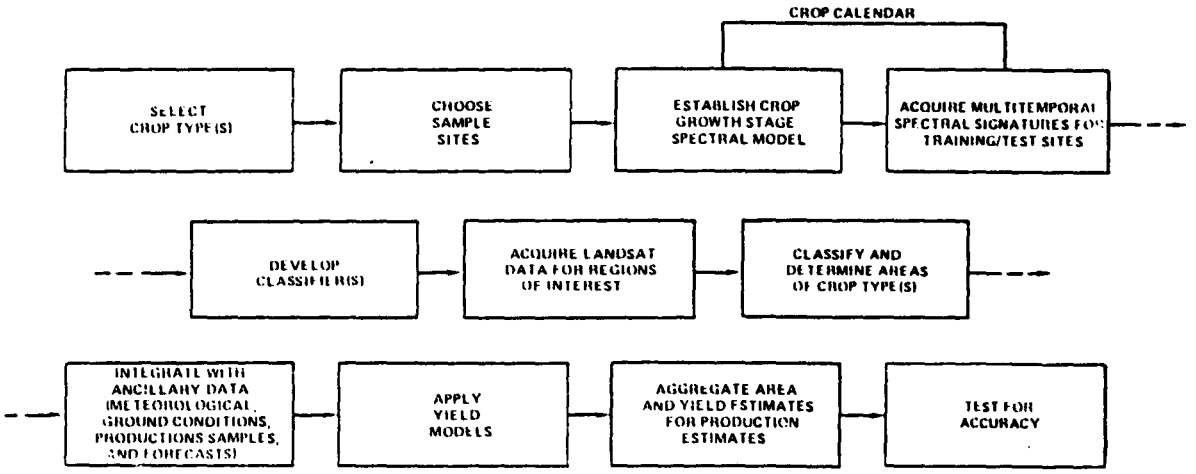

#5-81: By looking now at the coded classes, you should improve your detection and separation of open water, wetlands, agriculture, and beach/sandpit classes. You can probably also better recognize the evergreen stands but cannot visually differentiate between cedar and pitch pine or separate these from mixed forest, as is done effectively by the computer. The computer classification also picks out developed and urban land, which proves difficult in the photo-images.

#5-82: Answered in 5-81.

#5-83. (a) High Density Urban/Industrial,
(b) Mixed Industrial, High-Medium Density Urban; Open Land,
(c) Forest/Grass/Park/Water,
(d) Industrial/Open,
(e) High Density Urban,
(f) Mostly Industrial/Commercial,
(g) High Density Urban,
(h) Mostly Industrial/Some Open.

#5-84: The overall classification appears quite believable, but there are some discrepancies. The general distribution of maximum industrialization in the central city, progressing to high, medium, and low density urban zones arranged in broadly concentric patterns outward, so typical of a large metropolitan region, is evident for Philadelphia. On the basis of the author's personal knowledge of this city, the area assigned to industrial (red) seems low but is properly located for the most part. The several medium density urban (purple) patches in the central city may be anomalous but, at least near the river, may represent some redeveloped areas. Some open land area (gray) may be misclassified. The level of accuracy of this classifica-

tion is probably too low to be competitive with high altitude photography if the desired product is a detailed land use or urban unit map.

#5-85: The signature developed for rail yards is simply not unique for Landsat data. Rail yards are characterized by rolling stock (locomotives and rail cars) that resemble buildings, road beds (ties and cinders), dirt and soil, and scattered structures (round houses, switching towers, etc.). In high resolution aerial photos, these features are distinctive, especially where tracks and rights-of-way are visible. At Landsat resolution, this assemblage resembles other collections of buildings, making up other categories, all showing similar spectral signatures. The misclassification might be reduced by identifying the nonrailroad white-shaded features, determining whether they have signatures separable from the rail yards, and setting them up as new classes.

#5-86: The advantage of Landsat-type observations lies in the high frequency of simultaneous coverage of the entire region. Updates in population shifts and land use changes may be made at least once a year. More frequent checks would be unnecessary since such growth is not all that rapid. The most prominent modifications of the land tend to concentrate at the rural/suburban boundary—the fringe zone. An effective way to monitor this is to set up about 5 small control areas along the fringe for which accurate variations in population and land development are checked periodically on the ground. These changes are correlated with gradual, consistent alterations in the corresponding spectral signatures. The control areas become training sites to extrapolate the growth data to the larger comparable areas along the fringe.

Activity 6

#6-1: Your action.

#6-2: The main valley south of Blue Mountain and the South Mountain hills on the horizon are readily recognized. The low hills in the middle ground are not evident in the image. The curvilinear tree rows delineate streams. These are not evident in Figure 6-3 but may show up poorly in band 5 images of the Harrisburg scenes. The lowlands are about 19 to 23 km (12 to 14 miles) wide.

#6-3: You are on the west side of the I-83 bridge across the Susquehanna looking slightly east of north towards the railroad bridge and downtown Harrisburg.

#6-4: The individual fields are rectangular with a width of 30 to 60 m (100 to 200 ft) and length ranging from 150 to 300 m (500 to 1000 ft). This strip pattern, with different crops in alternating plots, is characteristic of farming in the rolling Piedmont of Pennsylvania Dutch country.

These fields are typically only 2 or 3 pixels in area. The pixels probably cut across crop boundaries, thus becoming mixed pixels having little contrast with neighbors. Only the largest fields are discernible in the standard image. The computer enlargement (Figure 6-4) shows a number of discrete fields, mainly because of contrasts in stages of crop growth and interspersion with fallow plots. However, elongate fields are not prominent. Most fields seem irregular in shape. Mixed pixel effects, which will produce irregular boundaries, offer at least a partial explanation.

#6-5: The size of Mahoney City (more than 40 pixels) and its brightness (light-colored frame buildings) indicate that this town should be visible in, say, Figure 6-3. This town shows high visible contrast with the coal-strewn surface of the valley and the trees in the ridges and hills. However, evidence for the town in band 7 imagery is inconclusive. The town lies approximately on a line joining the 2b and 2c arrowheads, at the point about 1 cm (0.4 in) to the right of 2b. There are mottled dark and light patterns in the immediate vicinity relating to the coal surfaces scattered among woods. To the west, the town of Frackville is easily recognized as the dark gray spot about 0.5 cm (0.2 in) SE of the 2b arrowtip. A similar pattern for Mahoney City is missing.

#6-6: It is very difficult to locate yourself. There are two clues, but both are somewhat am-

biguous. The coal on the surface in the foreground can place you almost anywhere along the south side of Reservoir Lake, which is adjacent to surface mining activities in the hills just to the south. However, note the large cleft or valley on the hill in the background. It appears to curve to the left or westward. A second depression further west seems to trend to the east. There are two thin dark lines (stream channels?), just left of the 2c arrowtip in Figure 6-3, whose orientations fit this pattern. The camera, then, was located on the south side of the east end of the reservoir.

#6-7: The bloom would show up as somewhat lighter tones in all bands, particularly in 6 and 7 and would be bright red in a color composite. Normally, to be seen, the bloom should be widespread in a fairly large lake (see Figure 23b in Mission to Earth).

#6-8: Steps:

1. *Define the classes to be included in classification;*
2. *Determine the sources of information;*
3. *Procure suitable ancillary information (maps, photos, tabular data);*
4. *Make Landsat enlargements of the regions containing sites;*
5. *Locate potential sites in imagery and assess detectability and homogeneity;*
6. *Consult with local experts and residents on specific feature identities, characteristics, and accessibility;*
7. *Identify features on Landsat enlargements, using ancillary and consultant inputs;*
8. *Make on-site observations to check identification, and new sites, and ensure that each site is suitable in terms of the five factors in site selection;*
9. *Record degrees of homogeneity within sites, and otherwise describe;*
10. *Document sites in ground photos.*

#6-9:

1. *Different crops are planted in the same fields in different years or as a second crop in a given year.*
2. *Different tonal patterns result from different stages of development during the growing season.*
3. *The same field may be subdivided for two or more crops in a different manner in successive seasons.*
4. *The farmer may elect to keep a field fallow during one or more years.*

#6-10: The two race tracks in the color aerial photo are located about 3.2 cm (1.25 in) up from a point just to the left of the center of the bottom margin of the U-2 photo. Look for the pattern of the woods just to the east of these tracks. The bottom parts of the woods patterns in the upper right corner of the aerial photo are just to the right of the central fiducial mark at the bottom of the ASCS photo.

#6-11: The lower (more southern) race track may be readily seen in Figure 6-8 at a position slightly to the right of a point about 5 cm (2 in) up from the center point on the bottom margin. The other track is faint but visible.

#6-12: Sources of Error:
Variable scanning mirror velocity
Detector response (striping bias)
Irregular detector sampling
False line start
Atmospheric interference
Map projection
Variable spacecraft velocity
Shifting orbit (altitude)
Attitude changes (pitch; roll; yaw)
Perspective (off-nadir) distortion
Earth curvature
Earth rotation
Scan skew
The net effect of these errors is that individual pixels will not be located in the precise array represented by initial sampled areas on the ground, and radiometric intensities measured at the sensor are not equivalent to those leaving the target areas. Resampling and other techniques for correction are needed.

#6-13: In the overall classification, the accuracy is simply calculated as the sum of the number of correct identifications for each class as a per-

centage of the total number of units (pixels), which consists of the sum of the correctly identified pixels for a class plus the pixels representing errors of commission and omission associated with that class. These errors may significantly increase the denominator to numbers greater than the actual total for any one class.

#6-14: An error of commission is a measure of the ability to discriminate within a class and occurs when the classifier incorrectly commits pixels of the class being sought to other classes. In the agricultural example, the commission error for corn stems from improperly calling other classes corn, so that seven pixels labeled as corn are really a composite of other classes. An error of omission measures between class discrimination and results when one class on the ground is misidentified as other classes(es) by the observing sensor. Thus, Landsat fails to recognize and correctly identify all 43 pixels of corn as such, and labels 18 of these pixels as other classes.

#6-15:
- *Training site mislocated*
- *Inadequate training samples*
  - *number too low and or sites*
  - *non-uniform (inhomogeneous)*
- *Mixed pixel effect*
- *Class improperly defined*
- *Ground truth inaccurate*
- *Signature extension invalid*
- *Stage of growth not considered*
- *Temporal difference between ground truth and satellite data*

#6-16:
- *Movement of glaciers*
- *Eruption of volcanoes*
- *Deposition of sand*
- *Growth stages of vegetation*
- *Storm damage*
- *Influx of pollutants*

#6-17:
- *Identification of most cover types (classes)*
- *Identity and distribution of urban subclasses*
- *Location of lakes*
- *Advance of strip mining*

#6-18:
- *Silt load in streams*
- *Point source pollution*
- *Insolation (irradiance)*
- *Relative humidity (at calibration site)*

#6-19: The distortions result mainly from a combination of irregular, often erratic motions (yaw, pitch, and roll; variations in speed and altitude) and off-nadir or perspective distortions (scan elements or pixels tend to lengthen away from ground track).

#6-20: The most likely explanation is that crops consisting of corn, soybeans, and small grains produced in 1971 had largely been harvested by October 21. Fields were either bare or contained corn stubble and other crop refuse. The histograms associated with these crops actually represent the underlying soil. Also, these crops, if still present, are in senescence and are likely experiencing decreases in characteristic IR reflectance levels.

#6-21: Percent reflectance. Some rocks are much "brighter" than others.

#6-22: Frontier Green Sandstone. Its reflectance signature shows a distinct peak around 0.55 μm.

#6-23: Chugwater: Reddish; steep spectral response curve between 0.6 and 0.7 μm.

Thermopolis Shale: Blackish; uniform, flat spectral reflectance through the visible; low intensity.

#6-24: Absorption bands at 1.5 and 1.9 μm are tied to normal atmospheric H_2O (water bands). The band at 2.3 μm relates to CO_3 in carbonate (in limestone or in calcite cement in sandstones) or OH^- in clays, an atmospheric CO_2 band near 2.8 μm is beyond the wavelengths measured.

#6-25: Both surfaces have almost the same spectral response in the 0.4 to 0.6 μm interval, but the natural surface of the Muddy Sandstone shows significantly higher reflectance (0.1 0.2 reflectance units) than the sawed (smooth) surface. Two factors account for this: (1) the smooth surface

approaches specular reflectance whereas the natural surface is diffuse and scatters more radiation to the detector, and (2) the natural surface was covered by light-colored alteration products (clays) that have higher reflectances.

#6-26:

Viewing conditions can be controlled;
Reflectances can be quantified, using calibration targets;
Different surfaces can be examined to get average values;
Measurements can be repeated under the same or other conditions;
Targets can be sampled directly to determine composition and other properties affecting reflectances.

#6-27: Variations introduced by illumination differences etc., influence both calibration and target surfaces in the same way. Referencing to a standard (in this case by dividing or ratioing) eliminates the variations (reflectance values for both surfaces might rise proportionately as the Sun appears from behind a thin cloud; division produces the same percentage reflectance as obtained when cloud obscures sunlight, since values for both surfaces then decrease proportionately).

#6-28: The normalization applied to the field spectra removes the external influences, such as atmospheric absorption, and provides a "truer" indication of the natural reflectances of the material.

#6-29: For detecting vegetation, bands at 0.67 and 0.87 μm; these show the maximum spectral contrast and thus most sharply separate vegetation from soil. Variations among vegetation species and conditions show the largest differences at 0.87 μm. A third channel at 0.56 μm is sensitive to "greenness."

For detecting vegetation changes related to stage of development, monitoring with MSS bands 6 and 7 are best (A. Park, pers. comm.) By taking the ratio of 7 to 6, as plant growth stops, the rate of change itself changes. If plant stress occurs, the ratio value may flip. Vegetation changes related to moisture stress can best be monitored by MSS 5 and 7. When moisture stress occurs, the absorption by chlorophyll detected by band 5 will change, and the plant turgidity expressed in band 7 also changes. Radiance levels in these bands are very sensitive to these shifts and may even provide previsual evidence of stress in individual or groups of plants.

#6-30: None is too effective. The bands at 1.42, 1.77, and 1.94 μm relate both to atmospheric moisture and to plant water absorption. At 1.94 μm there is also absorption associated with the wet bare soil. At that wavelength, the reflectances from vegetation are noticeably lower, so that their contribution is reduced relative to soil. Absorption at ca. 0.98 μm and 1.18 μm in the vegetation is caused mainly by plant water.

Perhaps a better strategy is to measure the differences in water content between dry and wet soil at the wavelength of maximum reflectance difference. This is again located at 1.94 μm, for these samples at least.

#6-31: Candidates for rejection are 1.22 or 1.27 μm (redundant and not particularly indicative), 1.42 μm, and 1.77 μm (covariant and affected by atmospheric moisture), and 2.22 or 2.25 μm (redundant); 0.985 μm may be ambiguous.

#6-32:

0.40 μm (measures blue)
0.56 μm (sensitive to green)
0.67 μm (chlorophyll absorption)
0.87 μm (maximum biomass reflectance; contrast)
1.25 μm (moderately good separation)
2.25 μm (separates soils from vegetation; sensitive to CO_3, and OH in soils/rocks)

All but one of these were selected for Landsat-D; a case may be made for 1.66 μm, also on Landsat-D.

#6-33: These troughs correspond to atmospheric absorption bands and also to absorption bands resulting from water in the form of leaf moisture. The spectrometer used to obtain these curves effectively measures these peaks and provides a quantitative estimate of moisture content. However, a radiometer (or scanner with bands) flown in space would experience two problems: (1) the signal from a narrow spectral band centered on an absorption band would be weaker, and (2) atmos-

pheric absorption would interfere with (mask) the effects of plant water absorption by additively intensifying the decrease in reflectance.

#6-34: Band 6, centered at 2.2 μm.

#6-35: 0.66 μm and 0.77 μm.

#6-36: The TM band 2 sensitivity is peaked at 0.56 μm or the green. Its band width is designed to accept visible light ranging from blue-green through yellow-orange. Because soils usually have a yellow color component, they also contribute to band 2 and spectral contrast between soil and vegetation is reduced.

#6-37:

	(a)	(b)	(c)
4/5	$\frac{23\%}{31\%} = 0.72$	$\frac{30\%}{26\%} = 1.15$	$\frac{56\%}{21\%} = 2.66$
4/1	$\frac{23\%}{8} = 2.88$	$\frac{30\%}{4} = 7.50$	$\frac{56\%}{2\%} = 23.0$

The systematic changes in these ratio values suggest that it may be feasible to estimate the percentage of the vegetation component in a mixed pixel representing a two-component (vegetation; soil) surface.

#6-38: Curve E correlates ND with a series of events in the growing cycle. Once this curve is established observationally, the values of ND can indicate which major stage has been, or will be, reached. However, there are normally two ND's with the same value. Some idea of the relation of the time of observance with the relative time (early to late) within the crop calendar must be obtained from independent sources. Curve F shows that ND increases up to the time of maximum yield; thereafter, it presumably reduces as the plants age (curve E), while the yield should continue to be constant until harvest. Successive observations will establish the ND trends so that the maximum may be picked and correlated with a yield curve established by a regression plot. The effect of wheat water stress will show up as a trough or downward spike in the plots of IR radiance, IR/red ratio, or ND as a function of observation (Julian) dates.

#6-39: The pointable imager, when looking off to the side, will cause an image distortion much like that characteristic of aerial oblique photos. In effect, square pixels (at nadir) will become increasingly elongate in the direction of side-looking, with those in the foreground less stretched than those further out towards the horizon. (This effect occurs with the MSS on Landsat, but the relatively narrow field of view [11.56°] makes this distortion rather small.)

The changing angles in this side viewing also influence the radiometric signals in several ways: (1) the angle of reflectance changes, (2) the ground area measured by one pixel (detector) increases, and (3) the length of the atmospheric path increases.

Activity 7

#7-1: Management of range lands; wildlife habitat input; petroleum exploration; disaster assessment.

#7-2: Present highway locations, ease of excavation, tax rates; zoning laws; current cost of available land.

#7-3: Entries 2, 3, 6, 7, 10, 11 (?) to varying effectiveness.

#7-4: Depth to bedrock; depth to groundwater; groundwater yield rate, etc.

#7-5: The spatial component would be the water supply network. Available surface water which is prone to seasonal fluctuations meets the temporal dimension requirement, and amounts of water consumption in a high density area would satisfy the thematic requirement.

In a non-GIS data base, the data elements would not be georeferenced. For example, the available surface water supply is available by acre feet on a month-by-month account. The high density resident use is filed by district in most water companies. This information is in chart or tabular form not by the georeferenced method of a GIS.

#7-6: The following is not an exhaustive list; rather it represents the more popular boundaries used in today's decision making.

- National
- Regional
- State
- County
- Town
- Section
- Range
- Township
- Watersheds
- Ecological communities
- Forest stands
- Topological (mountains)
- Water bodies
- Climatological, etc.

These boundaries could be coded in the standard coding scheme, such as:

- Presence absence
- Percentage of cell occurrence
- Ordinal or nominal scale
- Polygon, etc.

The mutually exclusive layers are less than or equal to the total number of possible boundary layers.

#7-7: Four other methods are: (1) Ordinal Ranking, (2) Nominal Ranking, (3) Corner Designation: Records data values at each corner of a grid cell, or at some one corner (e.g., NW corner); (4) Comparative Values: measures amount of a particular data item within a data element, compared with other items within the same element.

#7-8: One could argue for any of the formats on the basis of the following considerations:

Grid - All values could be encoded to the center point of the grid cell, which represents the property ownership. This saves encoding time and cost but loses geographical details.

Polygon - If property boundaries must be defined or if the grid cell size is either greater or less than the property size, then this format is the one to choose.

Mixed - Allows for both advantages in that grid cost and manipulations savings can be recognized and then converted to polygon for real-world display.

#7-9: This would depend on your organization, but the particulars are essentially the same as put forth in this section.

#7-10: List the preprocessing actually used. This is important because the preprocessing will influence the information contained on the tape (e.g., geographical location, mixing of spectral signatures, atmospheric effects, etc.), and therefore will affect your classification.

The standard preprocessing is to correct for geometric, radiometric, and skew distortions and sometimes rotation to true north.

#7-11: Aesthetic considerations, federal and state regulations, property values, local political considerations. The weighting would be subjective, although some economist might argue that a financial value should be put on all factors in the decision making.

As with any type of site analysis, a large variety of variables should be incorporated into the analysis.

#7-12:

1. Fall tilling could be included under land use or soil. If it were included under land use, it would create one more class of land use, but any changes in or effects due to the estimated probability would be clear.

2. Data could be collected by remote sensing, or by asking the farmers.

3. Field test data would be needed to calibrate the model.

4. Farmers could be encouraged to use new practices through information circulated in Soil Conservation Service bulletins or university agricultural extension service pamphlets.

5. The model would be run with all farmers using no fall tillage or all farmers using complete fall tillage. This would show by difference which practice would best meet the model objective.

#7-13: As with any system, a certain degree of confidentiality is necessary to ensure data consistency and accuracy.

A variety of ways will work, such as user password, account specific, limited access, file security, write data to tape, and physically secure it.

#7-14: Reread the geocoding section of this chapter. Obviously the larger the grid cell size, the less accurate will be a given specific geographical location.

The categories that would be most seriously affected would be linear features (highways, railroad, etc.) and any special feature such as points (historic sites or service facilities).

#7-15: The broad land cover pattern evident in the PP&L map is effectively duplicated in the Landsat classification. The big differences are in details, levels of classification, and accuracy – Landsat being much more specific for some classes. Thus, for convenience, the PP&L map combines several urban categories that are subdivided into three well-defined classes in the Landsat map. However, the PP&L map contains several classes, such as forested and nonforested wetlands, that were chosen from ground surveys for specialized purposes not considered important in the Landsat classification. One big reason for differences between the two maps is the coarse mapping "resolution" adopted for the PP&L map: 22.9 acres compared with 1.1 acres for Landsat. The differences also result from arbitrary class selection and intended use. The PP&L choices tended to lump some diverse natural features into a general category determined from ground inspection; the Landsat map is more an indication of real spectral classes that also correspond to land cover classes.

#7-16: The industrial areas (red) appear somewhat underclassified and/or misclassified (large office and government buildings in central Harrisburg are classed as industrial; a group of warehouses south of the airport are considered heavy urban). The medium density urban areas (violet) are too broad a class – some areas west of the city seem to have a building density similar to high density urban, but many areas even further west (around Carlisle, Pa.), colored violet, are almost certainly rural and farmland.

The PP&L classification would certainly be more useful if the urban areas were better subdivided. That should be an important category of subclasses (sublayers) to a utility company. The PP&L barren land unit is possibly too indefinite or transient to be called out as a separate sublayer. Instead, the general sublayer for agriculture could be reorganized to include major agricultural classes such as fallow land.

#7-17: Assuming some qualitative equivalence in accuracy between the two maps, one is tempted to choose the Landsat classification over the PP&L map. The Landsat map is current for the particular date used in the classification. However, in this instance, the extensive defoliation in summer of 1977 introduces a class that would not be relevant under most circumstances to a long-standing PP&L data set; it would be misleading to update the PP&L map with this transient class.

Although most users would normally favor a detailed classification (1.1 acre Landsat) for many applications, too much detail might be confusing for some purposes. Thus, in placement of transmission lines, agricultural land is sufficient in the designation of land cover; knowledge of crop type and status is not relevant to the decision. By coding cover type in a coarse cell size (23 acres), the amount of computer time in a GIS analysis will be significantly reduced.

Activity 8

#8-1: Section 208 - Water Quality Management Planning was a federal mandate, and as such its juridiction covered all watersheds in the United States, not just the designated areas. The concept of "Designated Areas" was to highlight high risk watersheds. As a result, the state spent most of its federal 208 monies on the designated areas, leaving little additional funds to complete the job.

#8-2: The Supreme Court decision on 208 mandated state responsibility for water quality planning in the "nondesignated areas." This placed

an unanticipated financial, managerial and administrative workload on the state government. To cope with this new task, now required by law, most of the water quality planning work was done by state councils of government, or water quality planning boards, or the local municipalities. However, much of the state water quality planning could only be done by the Department of Environmental Protection.

#8-3: Soil erosion—Owing primarily to poor agricultural practices coupled with unfavorable weather, large amounts of topsoil are lost each year. Other causes are large-scale construction and loss of ground cover due to forest or brush fires. Waterborne sediment can be observed directly by Landsat, particularly in the near infrared bands.

Acid rain—Although the atmospheric sulphur compounds that are responsible for acid rain are formed by a point source (usually coal burning power plants), the rain itself can be seen as a nonpoint pollutant. Landsat cannot see acid rain directly. The probability of detecting the effects of acid rain is also small. However, by looking at the changes in lake clarity over several years, it may be possible to see the indirect effects of acid rain in extreme cases. Acid rain lowers the pH of water and kills most of the living organisms, making the water clearer as the lake dies.

Agricultural chemicals such as nitrogen and phosphorus—As a secondary consequence of soil erosion, chemical fertilizers find their way into rivers and streams. Their effects can be viewed by Landsat indirectly. As fertilizers, nitrogen and phosphorus promote the growth of algae, which can be detected directly, usually in the near infrared.

Heavy metals, mercury, lead, cadmium—These result from industrial pollution by direct dumping, a point source, or atmospheric pollution which, through rain, becomes a nonpoint source. An interesting pollutant is cadmium, used in automobile tires; as the tires wear out, the rubber is deposited on roads and highways. This is eventually washed away and finds its way into water supplies. Heavy metal pollutants seldom kill plant life or animals in sufficient numbers likely to be visible to Landsat even indirectly.

#8-4: We know that most nitrogen and phosphorus are used as an agricultural fertilizer that finds its way into rivers, lakes, and streams through the process of soil erosion. Phosphorus is also an urban waste used in detergents. Therefore, the extent of agriculture and urban development in a watershed should theoretically be directly related to the severity of the pollution. A multiple regression model can be developed to relate dissolved nitrogen or phosphorus to the total land area in urban and agricultural uses.

#8-5: The results of the pollution can be detected indirectly by looking at water clarity over time. This is unreliable with Landsat because of many intervening factors such as spatial resolution (the inability to see many streams); spectral resolution (the inability to separate polluted water from shallow water), and so on. However, use of Landsat to determine the extent of agriculture and urban development is a good application of the technology; it is mainly a Level I Land Use Classification.

#8-6: You might want to combine topographical information to predict runoff rates from different land covers, given a particular slope. Distances to water bodies could be calculated if their locations were known, also increasing the model's sophistication. Finally, much of the pollution can find its way to water bodies through ground water transport, so percolation rates and distance to bedrock could be used to gauge this means of transport.

#8-7: The entire state is imaged during a single orbit, with three consecutive Landsat frames. Total imaging time is less than 75 seconds north to south.

#8-8: The model requires information about the extent of land in urban and agricultural uses; all other land covers are irrelevant. With crops at the height of their vigor, a single summer scene is best. Also, extensive cloud cover is not as frequent as in the spring or fall.

#8-9: Certain agricultural crops, particularly forage crops (clover, sorghum, hay), may be confused with fallow fields or low brush. This could be a serious problem. When fields support two crops in one season, preparation for a second crop (plowing) may be confused with urban land. Since the

model uses the percentage of land in urban use plus the percentage of land in agriculture, the confusion between urban and agriculture does not matter.

#8-10: In most cases, the analysis by a trained remote sensing specialist uses raw Landsat data whenever possible and geocorrection is done after classification. This method resamples the data only after classification, a procedure many think is preferable. DCA decided to geocorrect and therefore resample the raw data prior to classification. The reason was that many people who will be doing the analysis are not highly trained remote sensing specialists but are intimately familiar with what is on the ground. By working from geocorrected raw data, they can find their ground locations and can choose training sites more effectively.

#8-11: A raw Landsat pixel is a rectangle 56 m × 79 m in size so that the ratio of height to width is roughly the same as a line printer character 1/10 in by 1/8 in. Also, if a character of that size is used to represent one pixel, the resulting map approaches a scale of 1:24000, so not much resampling has to be done.

#8-12: The U.S. Geological Survey 7.5 minute quadrangle maps, state maps and much aerial photography are at that scale.

#8-13: Central Park in New York City is mostly forest and open space but is classified as an urban land use, a park. A golf course and a sod farm look similar from the air, but one is urban recreational while the other is agricultural. Beaches and sand quarries have the same land cover—sand—but dissimilar land uses.

#8-14: Many tree species grow in consort with one another; foresters call this a species association. On the east coast a common association is oak and hickory or oak and maple. In the arid southwest a common association is pinon pine and juniper. Of course, the age of a stand of trees and the devising of the stand should also be noted in any forest cover classification. Your strategy, then, is to recognize a class as an association, which gives you some information about the species within it, even though the percentage of each cannot be reliably estimated.

#8-15: Unlike forest vegetation, salt marsh vegetation usually occurs in pure stands. The type of vegetation present depends on the amount of water available to the plants. In a coastal area this is tidally influenced. In many cases Landsat can be used effectively to identify individual species or salt marsh vegetation because of its single species nature. In fact if a particular marsh grass is growing at the limits of its environment (too much or too little water), its vigor will be affected. In some cases Landsat has been used to look at a single species and identify indications of high and low vigor.

Activity 9

#9-1: (1) Vignetting occurs in individual photos (darker toward edges); (2) Distortions occur toward edges; (3) There are seasonal differences (most mosaics consist of images taken weeks, months, or even years apart). Also, (4) There are atmospheric variations for different photos; (5) There are different shadow directions; (6) Clouds are erratically distributed; (7) Flight lines may be nonparallel; and (8) There are high costs for large mosaics.

#9-2: (1) Structural and geomorphic features are seen in regional context; (2) Effects of regional cultural/urban changes may be observed coherently; (3) Agricultural practices and production trends can be examined over wide areas; (4) Land use patterns can be seen in synoptic unity; (5) Widespread pollution effects are evident; (6) Restrictions of political boundaries are overcome; (7) Frequent repeat coverage is possible; and (8) Large area mosaics are possible.

#9-3: Resolution.

#9-4: Meteorological conditions; oceanographic phenomena.

#9-5: (1) Floods can be monitored in progress; (2) Damage from volcanic eruptions can be assessed; (3) Air pollution over large areas can be tracked; (4) Soil moisture patterns and changes (drying) may be noted; (5) Ice movements in oceans can be observed; and (6) Oil spills can be monitored.

#9-6: Barren fields in the Piedmont and Coastal Plains. The soils tend to display reddish tones but the film response overemphasizes this.

#9-7: (1) Shifts in desert sands (North Africa); (2) Effects of a drought (Sahel); and (3) Annual inland flooding (e.g., Niger River inland delta).

#9-8: Ice in the north polar regions shows a brightness temperature range from 195 to 230° K. This is higher than the open water temperatures because the emissivity ϵ of ice is notably greater than the ϵ of water. Note that the brightness temperatures of both materials are below 0° C.

#9-9: The spills may often extend for many miles and are thus difficult to document by aerial photos. The full dispersal over time may be followed through periodic satellite coverage, allowing some prediction of further spread trends so that advanced warnings can aid in preparations for blockage or clean-up. Such an observational history may serve as evidence in court when claims are filed.

#9-10: This distortion is caused mainly by the panoramic effect resulting from the Earth's curvature (it may be considerable when a surface extending over ten or more degrees of latitude and longitude is imaged) and also the perspective effect caused by angular displacements toward the edges of the field of view.

#9-11: Clouds; the land is cooler.

#9-12: The water temperatures are 10 to 20° K higher than temperatures on the United States mainland. Coolest water temperatures occur along the coast. Temperatures increase towards open water in the Gulf and south Atlantic and southward past Cuba, which itself is about 10° K warmer than Florida.

#9-13: Assuming that higher chlorophyll a means more plankton ("fish food"), the best fishing seems to be off the west coast of Florida.

#9-14:

	04:00 h	10:00 h	13:00 h	21:00 h
Rock/Soil	d. gray	l. gray	l. gray	m. gray
Vegetation	l. gray	m. gray	d. gray	m. gray
Water	l. gray	d. gray	black	l. gray

d = dark; m = medium; l = light.

#9-15: Typically, around 2:00 p.m. (14:00 h) and between 2:00 a.m. and just before dawn. The best times to fly are about one hour before dawn (this permits the plane to land in some daylight) and in the early afternoon. Times around 8:00 a.m. and 5:00 to 6:00 p.m. should be avoided, as thermal contrasts are low. This is when the radiant temperature of one material approaches that of another; when the relatively higher-lower temperatures of two materials reverse, a thermal crossover has occurred.

#9-16: Water: 08:00 h; 10:59 h; land: 10:59 h; interior: 08:00 h. However, the images were processed to emphasize thermal differences in the water while subduing the land response, so that this set of pictures is not typical. Normally the best thermal contrast between land and water is around 1400 h (see Figure 9-7).

#9-17: The high tide image shows more contrast, but maximum contrast should have occurred around 14:20 h. However, in the processing of the images the thermal patterns in the water have been printed darker in the ebb tide image at the expense of brightness and details on the land.

#9-18: Steam generator units; cooling towers.

#9-19: Waste hot water carried by a pipe under water to a near surface outlet for discharge.

#9-20: The operators of this power plant were concerned about ambient temperatures in the

vicinity of the discharge. Regulations require that the discharge-produced temperature rise does not exceed 1° C at a specified distance from the outlet. Temperature monitors placed at several points in the river channel provide some indication of temperature distribution, but calibrated thermal data from aircraft flights integrate the temperature variations into a two-dimensional thermal map that better complies with regulations.

The Delaware River is flowing downstream from north to south (right to left in the illustration). Normally, the current flow would carry discharge downstream, but this may reverse during flood and high tides generating some upstream flow. This tidal influence would be greatest in slack water. At flood tide, the warm discharge is carried upstream in slack water, but this discharge does enter into the small bay behind the point of land, where some possible ecological damage might occur. Just about high tide, the discharge begins to move downstream but is turned aside by waning upstream tidal currents, even as cooler water from the bay heads past the point and then downstream. At ebb tide, downstream movement dominates, as both river and tidal current flow southward. The seemingly anomalous upstream flow during low tide results from a transitional condition in which currents in slack water near the shore carry the discharge against the prevailing downstream flow.

The interpretations presented here clearly show why remote sensing data must usually be coupled with other kinds of information in order to understand anomalous observations.

#9-21: To compute surface brightness temperatures, corrections for the input from air temperatures must be made, since the air is interposed between target and sensors.

#9-22: It is hard to tell without comparing with a planimetric photo or image, but the bent street blocks in A and the curved or rhombic fields in B show evident distortions, although not as pronounced as in many other scanner images.

#9-23: Either A or D, but the light tones may be influenced by photoprocessing, and perhaps also by scan direction versus Sun angle. Without calibration, this is a subjective judgment.

#9-24: On the right side. Look at the ridge and nearby lake near the top of D. The bright (warm) side of the ridge is away from the lake, whereas the dark, shadowed side is next to the lake.

#9-25: The barren fields are warmer and thus have a lighter tone. Evapotranspiration during daylight cools leafy vegetation so that most field crops appear in darker tones. This is reversed at night, because heat is effectively radiated away from bare soils while the plant canopy acts as an insulator.

#9-26: Many road materials (especially asphalt) develop higher radiant temperatures than adjacent usually porous soils during the day. Asphalt, is particular, has a lower albedo and higher emissivity than concrete or soils and thus experiences greater heating by absorption (see curves B and C of Figure 9-10). Vegetation cover further reduces the radiant temperatures in the countryside, bringing about a larger thermal contrast to the roads.

#9-27: Soil water, or even water released from shallow aquifers, will concentrate along lower slopes leading into a stream channel. The cooler soil-water zone will appear darker, thus better delineating a stream. Also, vegetation (with its cooling effects) commonly concentrates along streams.

#9-28: These reasons are evident: (1) The thermal sensitivity (NEΔT) for the thermal band 8 is about 1.5°C, several times poorer than most aircraft scanners; (2) The 9:30 a.m. time of Landsat overpass is not yet at the thermal contrast maximum; (3) The low resolution (240 m) results in some smoothing of temperature differences; and (4) The image has not been stretched or otherwise enhanced by computer processing (see Figure 2-19B).

#9-29.

	Stainless Steel	Basalt	Soil	Water
P =	0.168	0.053	0.024	0.038

Sample Calculation:

$$P = ([3 \times 10^{-2}]/[1.2 \times 10^{-1}]/[7.8 \times 10^{0}])^{1/2}$$

$$= (281 \times 10^{-4})^{1/2} = 16.8 \times 10^{-2}$$

$$= 0.168 \text{ cal cm}^{-2} \text{ s}^{-1/2} \text{ °C}^{-1}.$$

Soil should show the largest day-night temperature changes.

#9-30: (a) Cooler (darker) than soils during the midday heating; the overall gray levels will usually be lighter for all common land features during the daytime. (b) Basalt would appear warmer (thus lighter-toned) than soil materials associated with it, when viewed at midnight.

These deductions must be tempered by the large differences in albedo for basalt and soil. Basalts have albedos around 0.1 and those of soils tend to be about 0.2 to 0.4. This would raise basalt temperatures relative to soil both at day and night. The statements (a) and (b) apply more aptly to granite and sandy soils, as both of those have similar thermal inertias and albedos.

#9-31: $ATI = \dfrac{1000 \times 1.516\,(1 - 0.20)}{310 - 280} =$

$$\frac{1516 \times 0.8}{30} = 40.4$$

#9-32:

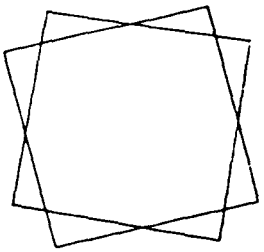

#9-33: Mainly in the upper left and left center of the map. The clouds appear very dark gray (almost black) in Figure 9-12, and in colors ranging from black through purple to blue and then green.

#9-34: The central part of the Gulf Stream is shown in two shades of green. It is warmer than surrounding waters because the Stream results from tropically heated waters that flow northward away from a convergent zone where waters from the western Atlantic meet those from the Gulf of Mexico.

#9-35: These are a series of cities in North Carolina and include Winston-Salem, Greensboro, Durham, and Raleigh. They show up as orange spots in Figure 9-13.

#9-36: These three large metropoli, along with Washington and Richmond, are urban heat islands whose temperatures are several degrees higher than surrounding rural areas. They appear as lighter gray tones in Figure 9-12 and as prominent white spots (warmest features) in Figure 9-13.

#9-37:

	Day	*Night*
Atlantic Ocean	*very d. gray*	*very l. gray*
Susquehanna River	*very d. gray*	*very l. gray*
Baltimore/Philadelphia	*l. gray*	*l. gray*
Pine Barrens	*m. gray*	*d. gray*
Blue Mountain	*l. to m. gray*	*l. gray*
Valleys	*l. gray*	*d. gray*
Delmarva	*m. gray*	*m. gray*

d = dark; m = medium; l = light.

#9-38: The clouds.

#9-39: Dark gray (cool) in day image; light gray (warm) at night.

#9-40. The cities are warmer than the rural areas during the day, and warmer again at night, because much of the heat is derived internally and surficially from activities of the inhabitants.

#9-41: Day: Most of the valleys in which coal mining is or was active appear in light gray tones.

Night: Much of the same area now shows as very dark gray, almost blackish. Note that other areas in the Appalachians are similarly dark (for other reasons).

#9-42: This is an excellent example of the blackbody effect. The very dark ground surface

(both from coal wastes and from dark shales) absorbs more thermal energy from the Sun and re-radiates this outward during the day. The heat is readily lost at night, resulting in cooler surfaces. In the ATI formula, the high (1 - a) term would keep the numerator large but the large ΔT would also increase the denominator, so that a low to moderate ATI would result. A low value of k and relatively low ρ would offset a somewhat higher value of C, and so again the thermal inertia P should be on the low side.

#9-43: The thermal inertia behavior of vegetation is not well known. A vegetated surface will receive thermal contributions from the vegetation itself as well as from underlying rock and soil and surface water therein. The ATI for such a complex surface is probably higher than that for soil alone, suggesting that P is higher for vegetation than for soil. In the land south of Albermarle Sound, the clearing of forest cover exposes dark soils with low thermal inertia. Such materials experience greater day-night thermal differences than the forests and grasslands.

#9-44: These ridges are largely forest-covered. In the daytime, the forests should be cooler (darker) because of the cooling effects of evapotransportation. At night, the insulating effect of the foliage keeps the heavily vegetated ridges warm (light), while the lower valleys are relatively cooler because of the sinking of cold air. The south-facing slopes will be more directly heated during the day than north-facing ones. Thus, these southern slopes might be expected to appear even warmer.

#9-45: The same arguments as developed in #9-43 apply here. The valleys are less heavily vegetated, with a higher proportion of exposed soils.

#9-46: The lighter tones near shore suggest warmer water. One or more factors may interplay: more nearshore turbulence and upward convection, keeping the temperatures more uniform and high; more impurities (e.g., silt); surface runoff of warmer water from the land; influx of ground water (temperatures may be lower). The sharp boundary between the two gray levels in the lake may coincide with the thermal barrier between two unmixed bodies of water of differing density.

#9-47: The clouds appear dark (low ΔT) in the ΔT image. Clouds should not vary much in temperature within the atmosphere regardless of time of day. Since these clouds have lower temperatures than most features on the land, they will show only small ΔT values. The clouds are also cooler than the surface below in the night image. But, when the night temperatures of the cloud pixel are subtracted from the day temperatures of the land underneath (assuming no cloud cover over those areas, as is the case here), the ΔT is larger, and the clouds are expressed in somewhat lighter gray tones. The fringing areas along the ridges are relatively warmer than their surroundings in the night thermal IR image and relatively cooler in the day IR image. However, the absolute radiant temperatures of these fringes are likely to be higher in the day. The ΔT is therefore small but positive. This same argument holds for the ocean and estuarine waters (as well as for rivers and lakes), as has been explained in some detail on p. 351. While there is some drop in water temperature from mid-afternoon to dawn, the change can be moderately to quite small and, conversely, the rise in temperature during the day also does not keep pace with either air or thermometer temperatures (which accounts for the feeling of warmth in a swimming pool relative to cool night air but a feeling of chill in that pool on a sunny morning after a cold front has passed).

#9-48: (a) In HCMM Harrisburg is difficult to spot as a city if its location were not known (its dark tones abut against the dark river), but Lancaster stands out dark against a light-toned background in both HCMM and Landsat; (b) The linear grain so evident in Landsat is obscured in HCMM except for a few long linear features of unknown nature; (c) In both image types, the major folds are readily distinguishable against a lighter-toned background (valleys). Although HCMM images lack fine detail, they have enough resolution to adequately display regional structures of this magnitude; (d) Larger tributaries are visible if one knows where to look. The Juniata River is evident north of Harrisburg, but the smaller Conodoquinet Creek to the west is not.

#9-49: These dark areas coincide with distinct whitish areas in the Day VIS image. They are almost

certainly due to snow-covered ground; much cooler snow, if thick enough, shows up as a lower temperature signature relative to the background. The dark gray tones probably represent lower ground temperatures in the Appalachian uplands relative to warmer surfaces in the Piedmont and Coastal Plains owing to snow and/or lower near-surface temperatures at the higher elevations.

#9-50: Pittsburgh is represented by several small lighter-toned patches at the confluence of the Allegheny, Monongahela, and Ohio Rivers. The larger gray patch several hundred kilometers to the west is Columbus, Ohio. The two distinct light gray tones in the Baltimore area correspond closely to the patterns of warmer surfaces observed with Landsat Band 8. The western patch is the city proper, while the smaller eastern patch corresponds to an industrial zone (mostly steel mills) around Sparrows Point.

#9-51: The evidence is lacking. Snowfall had not yet become general in early November. The black patches correspond to active coal mining districts (anthracite in eastern Pennsylvania; bituminous in western Pennsylvania and W. Virginia) and presumably result from waste and strip mining effects.

The rolling topography of the Piedmont, in contrast to the flatter Coastal Plains, is revealed by variations in gray tones resulting from differential heating of Sun-facing and more sheltered hillslopes.

#9-52: A number of elongate, generally straight dark thin lines extend for distances up to about 50 km in the physiographical regions occupied by the Plateau and the Catskills. These are clearly the loci of stream drainage. Soil water and high water table, associated vegetation, and slope sheltering probably account for the cooler temperatures in the valleys traversed by the streams. Many of the straight stream courses are controlled by fault zones. This is confirmed by field studies in a similar topographical region—the Adirondack Mountains to the north (top of image), where fault lines and joints strongly influence major drainage.

#9-53: Most of the smaller whitish patterns are associated with cities and large towns. Philadelphia, New York, Buffalo, Rochester, and Syracuse are readily picked out. Harrisburg, Lebanon, Allentown-Bethlehem, Altoona, Erie, Binghamton, Elmira, and Utica are among the smaller metropolitan areas that stand out in contrast to darker surrounding tones. The lenticular light pattern southwest of Scranton, dark in the Day-VIS, once again correlates with the anthracite belt. The diffuse light tones both east and west of South Mountain-Catoctin Mountain are not readily explained. Another area of light patterns along the left margin of Figure 9-19B is probably correlated with industrial sites and higher population density just east of Pittsburgh.

#9-54: Rather suprisingly, not too well, although the outlines of Harrisburg and the towns across the river are discernible as lighter tones (but not lighter than some areas in the mountains). There is no obvious explanation for this, except the smaller size of Harrisburg, the scarcity of heavy industry, and its openness in a river valley, with cooling night winds, might account for the thermal differences in comparison with Philadelphia and other urban heat island cities.

#9-55: The northern end of the South Mountain—a topographical high. This is heavily forested terrain; the trees serve as a thermal insulator (blanket).

#9-56: There are several patches of darker gray squares near the right side of D. These seem to lie in valleys and probably represent coal waste.

#9-57: As stated on p. 369, most of the reflected pulses have the same polarization as the transmitted pulses, so that the energy represented in the returned signal is greater for the like polarization mode.

#9-58: The resolution is difficult to ascertain except in a qualitative way. However, individual buildings and secondary roads may be distinguished. Since these are typically of the order of 10-15 m (35-50 ft), a resolution of ca. 15 m is a reasonable estimate.

#9-59: The look direction is left to right or west to east. This is indicated by the somewhat greater brightness (lighter tones) of the northwest

and southwest slopes of the folded ridges and by the image compression in the near range direction.

#9-60: Compared with radar images of more rugged topography, this image does not show pronounced layover or shadowing effects. Lower depression angles and/or lower flight altitudes increase shadow lengths. Those same conditions may or may not produce stronger layover, depending on the orientation of facing slopes relative to the wavefront curvature of the incoming (transmitted) radar pulses.

#9-61: There is compression in the near slant range. Other geometrical distortions persist throughout the image but are not immediately obvious until locality-by-locality comparisons are made with a planimetric map or photo. Examine the U.S. Navy warehouse facility (cluster of parallel, elongated buildings just south of the Conodoguinet Creek) in the aerial photo (Figure 7-14) and in the HH radar image. The square pattern of this facility has been distorted to a rhomb in the radar image. Erratic distortions from aircraft motions are minimal in this image. Some side-lobe banding, a light and dark set of bands parallel to the flight direction caused by periodic signal reenforcement from secondary pulses, is evident in the near range, especially in the HV image.

#9-62: The pattern has a distinct "graininess" (small, mottled light and dark specks) resulting from interaction of the 0.86 cm wavelength beam with the thick forest canopy (leaves and twigs) along the ridges.

#9-63: The HV image is darker overall than the HH image, and tonal contrast is less.

#9-64: Feature by feature, the tonal patterns in both HH and HV images are similar in this image. Dark fields (crops) are dark in both and light are light. Contrast is less in the HV image, but whether this represents a distinct signature difference is not known. In the HV image, buildings in the built-up areas of small towns show distinctly fewer point or corner reflections, but several roads are more sharply displayed.

#9-65: Slope brightness and layover foreshortening favor the right or east side of ridges, indicating a look direction to the west.

#9-66: Elongate shadowing, which tends to emphasize relief, is not developed in the images because of the high depression angles of the SAR.

#9-67: The bright bands caused by layover serve (in an analogous way to shadowing) to improve the expression of relief by increasing contrast. Those ridges oriented at high angles to the look direction (E → W) are the main beneficiaries of this effect.

#9-68: Small obsequent (slope-following) streams are emphasized by the layover and slope aspect effects. There seems to be some angular distortion in the patterns formed by these streams since many are arranged in slanted positions along the slopes rather than at right angles (following maximum slope inclination) to the crests.

#9-69: Except for the layover effect, distortions in the Seasat SAR images seem to be less than in typical radar images. The stability of the satellite platform (no pronounced pitch, yaw or roll) and the high depression angles account for this. However, comparison of certain features (e.g., islands in the river) in Figure 9-22 with the low altitude photo in Figure 7-14 indicates some "broadening" of dimensions parallel to the look direction.

#9-70: Harrisburg contains numerous small buildings with corner reflectors that send strong signal returns to the SAR. Even at the resolution achieved by digital processing, the clustering of buildings produces a saturation or clutter which prevents individual structures from being resolved. Note in Figure 9-22 that some isolated buildings outside the central city stand out as discrete "blips," usually with distorted shapes.

#9-71: The orientation of the major streets shifts more to the northeast. This has the effect of rotating and aligning buildings along the streets into a different general position. The contribution from corner reflections presumably diminishes.

#9-72: At first glance you might be tempted to correlate these regularly spaced lines with the base supports on both sides of each arch of the Interstate 83 bridge and parallel bridges. However,

there are more than 40 such supports on the railroad bridge seen in Figure 6-1D and less than 20 dark lines in the radar image. Inspection of the aerial photo in Figure 7-14 reveals a similar number of objects with the same spacing in the several bridges in that group. These appear to be light standards for the road bridges and power line stanchions for the rail line bridges.

#9-73: Bands 1, 2, and 3.

#9-74: 900 m^2 0.241 m^2 or 0.144. When calculated in acres, the results are: (1) 3.25 ft/m × 30 m = 97.5 ft; (2) $(97.5)^2$ = 9475 sq ft; (3) 9475 sq ft 43560 sq ft per acre = 0.218 acres or 0.218 acres 2.4 hectares per acre = 0.090 hectares.

#9-75: 25 × 0.090 ≈ 2.25 hectares.

#9-76: The quantity of data returned from the TM will be much greater than for the MSS in the earlier Landsats. As calculated on p. 423, there are 7,764,120 (not exact) pixels/band in a Landsat MSS image. There will be approximately 6167 × 6320 or 38,975,440 pixels/band for TM. This is about 5 times more. Each TM pixel will represent a radiometric (DN) range of 2^8, compared with 2^6 for the MSS. The data rates transmitted to receiving stations are 15 and 85 megabits/s for MSS and TM respectively. All these numbers imply noticeable increases in data handling and processing requirements.

#9-77: Among many applications that should be improved and become more effective because of TM are these typical examples: Better identification of different crop types; Better estimates of crop yields (smaller fields can be examined); Better assessment of forest clearcutting and replanting; Improved detection of faults and alteration products associated with ore bodies; Smaller bodies of water detectable in stock pond inventories; More precise mapping of wetlands and their boundaries; More accurate separation of urban fringe categories; and More Level II land use classes identifiable.

Appendix C

C-1 The location is north-central Arizona around Flagstaff. Volcanic cones and flows occur near I-3 and butte-like volcanic pipes near V-2. The light spot at O-6 is Meteor Crater, an impact-generated depression. Highway 66 passes to its north. Flagstaff, shown as a dark gray-blue elongate pattern near H-6, looks large enough to house 50,000 people (but western towns spread out). The dark red tones nearby suggest evergreens (conifers, in fact). The redder tone of vegetation around F-17 indicates a higher proportion of deciduous trees (oaks are common, particularly from F-17 southward). Farming is evident around F-12 and the nearby river; hay and other cattle feed products are the likely crops. Desert soils and sands abound in the northeast quadrant. They are typically reddish in natural color. E-19 lies along a tight fold (monocline) with some faulting. Note Oak Creek Canyon just to the east.

C-2. The scene is located in northern California. H-9 lies in the heart of rugged mountains making up the Coast Range. F-7, along the flank of this range, marks rocks arranged in more orderly elongate folds. The San Andreas Fault runs along M-20 to C-11 and then passes out to sea at Bodega Bay. It is expressed as a linear valley in places. At F-3 is Marysville Butte, an eroded volcano. The dark patches at I-14 and elsewhere are forest fire scars, partly revegetated. Very dark areas at N-17 and other locations near the San Pablo Bay are water-inundated wetlands. The farmlands in the Sacramento Valley are dominated by large fields in which such cash crops as sugar beets, tomatoes, barley, rice, and cotton are grown. The region around O-15 is the Napa Valley, home of some of the finest California wines. The large metropolitan area around F-22 contains some of the East Bay cities -Berkeley, Richmond, San Pablo–north of Oakland.

C-3: Letter A refers to the Oregon Coast ranges, covered with a mix of deciduous and evergreen forests; B is the Willamette Valley, a large agricultural region; C marks the Cascades, extensively covered by conifers; D lies near the west edge

of the Great Desert, sparsely covered by sage and other arid climate vegetation; E lies between Mount St. Helens on the west and Mount Adams; F is next to Mount Hood; G is adjacent to Crater Lake (Old Mount Mazama)—all active/dormant or extinct volcanoes mantled by snow. H is the volcanic Newberry caldera, a large collapsed volcanic complex now heavily forested. Around I, extensive timber clearcutting is taking place; its progress, and reforestation, are easily monitored from Landsat. J denotes regions of extensive wheat farming in the Palousse country south of the Columbia and Snake Rivers. Lakes in varying degrees of fill are scattered over much of the Great Desert of central and east Oregon, a region of low rainfall. Some of these lakes are semi-dry and are approaching a playa condition as the heat of summer ensues.

C-4: This is the Wrangell Mountains region of southeastern Alaska. The areas around K-12 and T-13 are snow-covered mountainous terrain, whereas clouds cover the C-10 area (also snow-coated). Glaciers abound at I-19, K-14 and elsewhere. The dark streaks are surface moraines. Silt and extensive water spread over braided streams in valleys at R-8 and R-18. At Q-14 you would be on a mountain ridge looking into a steep-walled valley, but at Q-7 you are in low rolling terrain. The bluish terrain at Q-14 is bare rock coated with snow in places. The reddish terrain is marshy and tundra terrain, heavily vegetated in summer with grasses and low bush. The ovoid lakes are glacial in origin, most being kettle lakes in outwash deposits.

C-5: This region is the east-central coast of Greenland and the Greenland Sea. The image was acquired in early fall of 1972 when the Sun was only 8° above the horizon at this latitude. The low Sun angle, and resulting large shadows, strongly emphasizes the relief. The range of mountains around H-20 casts shadows into the ice-covered marine embayment to the north (at sea level). The largest shadow is about 6.5 km in length (scale it: the 17 cm up-down dimension of the image represents 185 km on the ground). The height a of the highest mountain casting that shadow is a/b = tan θ, where θ is the Sun elevation angle, or a = 6.5 × tan 8° = 6.5 × 0.1405 = 0.91 km or about 3000 ft. A glacier extends westward from C-20 and enters a marine embayment to the east, which is almost certainly a fjord. Numerous ice flows, many 10-30 km in maximum dimension, cover much of the Sea. Some flows are probably multi-year ice slabs (formed in previous years, then breaks off, and refreezes), but first-year ice is forming in open waters near shore, especially within the northernmost embayment. The Landsats can effectively monitor this sea ice on a continuing basis to provide invaluable information regarding hazards (icebergs; ice-locked areas) for any shipping in the region.

C-6: The image covers northeastern Holland and West Germany, west of the Jutland Peninsula. The East Frisian Islands are essentially offshore bars produced by deposition off a shoreline of emergence. These barrier islands have been breached and modified by tidal and nearshore currents. The dark bluish area between the mainland and the islands is a series of tidal flats submerged at this time in very shallow water. Among major towns visible in the scene are Groningen (A-14), Wilhelmshaven (K-7), Bremerhaven (N-6), Bremen (Q-11), and Oldenburg. Bremen and Bremerhaven are on the east bank of the Weser River. A small segment of the Elbe appears in the upper right hand corner. Most of the linear features are man-made canals used for transportation, irrigation, and flood control. In one area the border runs west of the Elms River and seemingly coincides with a straight northerly line (G-17) defined by a tonal contrast. The land surface to the west appears blackish—the signature resembles that of standing water but may instead represent dark organic soils. Most of the region is given to dairy farming and agricultural practices. Many of the dark patches are thick woods left as large forest copses after land clearing.

C-7: This image shows a region in the southern Soviet Union, just east of the city of Magnetorgorsk and the Urals. This is part of the great wheat belt that extends from the Ukraine and the Volga in European Russia to western Siberia. Many of the large fields in this image are fallow in July after winter wheat harvest or before spring wheat reaches a mature stage. Soils in southwestern Siberia tend to be rich in dark organic matter (chernozems). Vegetation in these steppe plains includes grasslands, grassy marshes, wet meadows and bogs, with some birch and aspen forest. The lakes may result from deflation of glacial loess or silt deposits or other

glacial activity, along with poor drainage in the flatlands. The reddish swirls consist of algal blooms. Some lakes are gradually drying out over the years (I-8) and many are filling with salt-encrusted silt (whitish tones) in this semi-arid region. The thin red lines mark irrigation canals with vegetation in and along them.

C-8: This region lies along the northwestern end of Pakistan, where that country meets the tip of Afghanistan and the Baluchistan Ranges of Iran. The two large mountains are huge dissected volcanoes that rise to 2500 m above sea level. Extensive sand dunes develop around L-3 in the Chagai Hills and alluvial fans at H-12 and elsewhere occur at the base of the Baluchistan Mountains. Sedimentary bedding is evident at D-7, K-21, and other places; joints are especially visible at K-21 and Q-21, and folds can be seen at I-11. The linear feature at J-18 is an eroded fault trace covered with sand deposits. The light materials at O-21 probably make up an igneous intrusion (granite?). The greenish-blue false colors correspond to a dominant yellow or yellow-brown on the natural surfaces. One work of man stands out: a highway across the desert (R-8). Alteration anomalies similar to the Saindak deposits are presumably present at L-7 and elsewhere, but the evidence from this image alone is insufficient.

C-9: The scene depicts the great Ganges River delta in southern Bangladesh. Near the image top, the Jamuna (Brahmaputra) River joins the Ganges. The Ganges is obviously choke-laden with silt, in contrast to the much clearer water of the Jamuna. Numerous distributaries carry water from the main course of the Ganges into the Bay of Bengal. Typhoons can completely inundate or drastically erode many of the low, vulnerable coastal islands. Landsat is helpful in assessing gross damage, remapping the new shapes and locations of islands, and indicating conditions that imply instability in future storms. Dense mangroves and other salt water forests occur at B-21. Vegetation typical of a lowlands subtropical delta extends beyond G-19, while mountain forests are evident at T-4. Vegetation is sparse in drier grasslands at M-4. The varied ground patterns at B-7 and elsewhere result from a combination of natural shifts in the Ganges channels and the influence of a dense population that has stripped off most forest cover in converting the land to rice, jute, and other crop staples.

C-10: The image shows part of the western Takla Maklan desert in the Sinkiang Province of westernmost China. Excellent images are obtained by Landsat from this part of the world where the air is clear and dry over the higher elevations (here, about 2000 m). The southwest-trending ridges consist of sedimentary (layered) rocks that are strongly folded and perhaps block-faulted. Mountains at C-3 and elsewhere appear to be underlain largely by crystalline (igneous-metamorphic) rocks that give rise to more uniformly dissected terrain with narrow valleys and sharp divides. A prominent fault passes northward through D-15; another is present at H-13. Alluvial fans (many coalescing into bolsons) occur at I-10 and other places as intermittent streams carry materials from the ranges into lower landlocked basins. The mottled pattern presumably represents an alluvial plain developed in lower terrain where ephemeral streams wander about, eroding in places and depositing elsewhere. Although not clear from the band 7 rendition alone, this pattern suggests variable vegetation growth, possibly swampy in places.

C-11: This image touches the Hopeh Province of northeastern China southeast of Peking. Tienching is a major city (M-8) near the Gulf of Chihli. The southern environs of Peking itself are just visible at B-1. Apart from these metropolitan industrial areas, most of the countryside is given to farming of various kinds. Rice is grown in water-filled paddies at C-14 and Q-13, and also at M-4 and S-16. In general, the land patterns of farms away from these rice-rich areas are characterized by small, irregular plots that lack the sharp boundaries so typical of American farms in the Great Plains. Vast salt evaporating basins occur at R-11 and T-5. Canals used both for irrigation and transportation appear at P-4 and other places.

C-12: This is part of east central Australia near the southwestern corner of Queensland. The area appears desolate as though devoid of any population. A roadway runs north from Birdsville (off the bottom of the image) through several settlements not visible in the image. Cattle grazing is the main

activity on the land. Longitudinal dunes (aligned parallel to prevailing winds) mark the eastern end of the Simpson Desert. This July scene is taken during the winter season in the southern hemisphere. This is normally a dry period in a region that gets less than 20 in. of rainfall per year. Floods during summer (February) are common and cover large stretches of the low plains for weeks or more. Following this, extensive mulga vegetation—grasses, acacias, and shrubs—flourish and persist in the moist gound (vast red areas), and depressions like Lake Machattie (S-18) can remain filled to shallow depths for some months. Note the cloud bank at J-18. It is casting its shadow to the southwest, as expected in the southern hemisphere; at this time the Sun's rays slant in from the northeast.

INDEX

(Note: In general, this index omits individual persons' names when cited, most localities imaged or described in the text, and references to the terms appearing in Appendix H. Many of the entries below are also defined in the Glossary of Appendix D.)